Advances in Palladium-Catalyzed Allylation, Propargylation, and 1,3-Dienylation of Acetonitrile Pronucleophiles

By

Theresa Marie Locascio

Submitted to the graduate degree program in Chemistry and the Graduate Faculty of the University of Kansas in partial fulfillment of the requirements for the degree of Doctor of Philosophy

_____
Chairperson, Jon A. Tunge

_____
Paul R. Hanson

_____
Apurba Dutta

_____
Michael D. Clift

_____
Helena C. Malinakova

July 25, 2016

The Dissertation Committee for Theresa M. Locascio
certifies that this is the approved version of the following dissertation:

Advances in Palladium-Catalyzed Allylation, Propargylation, and 1,3-Dienylation of Acetonitrile Pronucleophiles

_____

Dr. Jon A. Tunge

Date Approved: July 28th, 2016

Abstract

Theresa M. Locascio and Jon A. Tunge

Department of Chemistry, July 2016

University of Kansas

Presented herein is the development and application of palladium-catalyzed methods for allylation, propargylation and 1,3-dienylation of acetonitrile pronucleophiles. The developed methods focus on optimizing both atom- and step-economy during product formation thus resulting in a minimal production of waste. Further, ligand-controlled regiodivergent strategies are also presented which provide efficient access to various functionalities through a change in reaction mechanism controlled by the denticity of the coordinating ligand.

In regards to the developed methods for the propargylation and 1,3-dienylation of acetonitrile pronucleophiles, the presented work provides access to these functionalities using propargylic electrophiles that were rarely observed using previously known methods. In chapter 1, a brief review of commonly employed propargylation methods is presented which often occur under harsh reaction conditions or result in a large amount of byproduct formation. Further, few exceedingly difficult palladium-catalyzed propargylation strategies are also reported that overcome the large bias for the allenyl isomer or products arising from dinucleophilic addition.

Alternatively, in chapter 2, we present our ligand-controlled regiodivergent strategy for the propargylation and 1,3-dienylation of acetonitrile pronucleophiles. Specifically, we report the first palladium-catalyzed coupling of a butadiene synthon to generate 1,3-dienylated products. Further, each method provides significant advantages over commonly employed strategies to access such functionalities such as optimizing step-economy and avoiding the necessity for prefunctionalized starting materials.

In chapter 3 of this dissertation, we present our ongoing efforts to expand the substrate scope of the developed regiodivergent method to nitriles possessing a pK_a >17. To achieve this goal, decarboxylative cross-coupling is employed to access the reactive intermediate *in situ* via irreversible decarboxylation thus generating CO_2 as the only byproduct. Once again, selective propargylation or 1,3-dienylation is ligand-controlled and can occur though changing the ligand from monodentate to bidentate, respectively.

Lastly, in chapter 4 we present a method for the *in situ* activation of allylic alcohols using CO_2 for the allylation of nitroalkanes, nitriles, and aldehydes. The developed method provides several advantages over commonly employed allylation strategies: (a) avoids the pre-activation of allylic electrophiles for successful cross-coupling, (b) avoids the use of additives for allylic alcohol activation, and (c) generates base *in situ* for pronucleophile activation thus providing an atom-economic alternative for allylic cross-coupling.

Dedicated to my parents, Saverio and Diane Locascio,

for their unconditional love and support.

Table of Contents

Chapter 1. Synthetic Methods for Propargylation and Propargylic Electrophile Reactivity

Chapter 2. Palladium-Catalyzed Regiodivergent Substitution of Propargylic Carbonates

Chapter 3. Palladium-Catalyzed Decarboxylative Propargylation and 1,3-Dienylation

Chapter 4. Activation of Alcohols with Carbon Dioxide: Intermolecular Allylation of Weakly Acidic Pronucleophiles

Abbreviations

AcOH	Acetic acid
$AgBF_4$	Silver tetrafluoroborate
$AgSbF_6$	Silver hexafluoroantimonate(V)
$[(allyl)PdCl]_2$	Allylpalladium(II) chloride dimer
aq.	Aqueous
$AuCl(PPh_3)$	Chloro(triphenylphosphine)gold(I)
Azocane	Heptamethyleneimine
BuLi	Butyl lithium
Bu_2NH	Dibutylamine
$B(O\text{-}iPr)_3$	Triisopropyl borate
CDI	1,1′-Carbonyldiimidazole
CH_2Cl_2	Dichloromethane
CH_3NO_2	Nitromethane
Cs_2CO_3	Cesium carbonate
CsF	Cesium fluoride
CO_2	Carbon dioxide
$Co_2(CO)_6$	Dicobalt hexacarbonyl
Cp	Cyclopentadienyl
CpRuCl(cod)	Chloro(pentamethylcyclopentadienyl)(cyclooctadiene) ruthenium(II)
Cp_2TiCl	Titanocene dichloride

$CrCl_2$	Chromium(II) chloride
CuI	Copper(I) iodide
$Cu(OTf)_2$	Copper(II) Triflate
CyJohnPhos	(2-Biphenyl)dicyclohexylphosphine
DBPC	2,6-Di-*tert*-butyl-4-methylphenol
DCE	Dichloroethane
DMEDA	*N,N′*-Dimethylethylenediamine
DMF	Dimethylformamide
DMSO	Dimethyl sulfoxide
Dppb	1,4-Bis(diphenylphosphino)butane
Dppe	1,2-Bis(diphenylphosphino)ethane
Dppf	1,1′-Ferrocenediyl-bis(diphenylphosphine)
Dppm	Bis(diphenylphosphino)methane
Dppp	1,3-Bis(diphenylphosphino)propane
Et_3B	Triethylborane
EtOAc	Ethyl acetate
EtOH	Ethanol
GC/MS	Gas chromatography mass spectroscopy
HBr	Hydrogen bromide
H_2O	Water
I_2	Iodine
$InBr_3$	Indium(III) bromide

iPr_2NEt	*N*-*N*-Diisopropylethylamine
iPr_2NH	Diisopropylamine
JohnPhos	(2-Biphenyl)di-*tert*-butylphosphine
K_2CO_3	Potassium carbonate
K_2HPO_4	Dibasic potassium phosphate
KIE	Kinetic isotope effect
KOH	Potassium hydroxide
K_3PO_4	Potassium phosphate tribasic
L	Ligand
LIC-KOR	Schlosser's base
LiO-*t*Bu	Lithium *tert*-butoxide
MeCN	Acetonitrile
MeOH	Methanol
MeONa	Sodium methoxide
MePhos	2-Dicyclohexylphosphino-2′-methylbiphenyl
Mesitol	2,4,6-Trimethylphenol
Mg	Magnesium
$MgSO_4$	Magnesium sulfate
Mn	Manganese
N_2	Nitrogen
Na	Sodium
NaH	Sodium hydride

$NaHCO_3$	Sodium bicarbonate
Na_2SO_4	Sodium sulfate
$Na_2S_2O_3$	Sodium thiosulfate
NaO_2CCF_2Br	Sodium bromo(difluoro)acetate
NH_4BF_4	Ammonium tetrafluoroborate
NHC	*N*-Heterocyclic carbene
NH_4PF_6	Ammonium hexafluorophosphate
$Ni(dppp)Cl_2$	[1,3-Bis(diphenylphosphino)propane]dichloronickel(II)
NMP	*N*-methyl-2-pyrrolidone
NMR	Nuclear magnetic resonance
Nu	Nucleophile
[O]	Oxidant
PCy_3	Tricyclohexylphosphine
$Pd(acac)_2$	Palladium(II) 2,4-pentanedionate
$PdCl_2$	Palladium(II) chloride
$PdCl_2(MeCN)_2$	Bis(acetonitrile)dichloropalladium(II)
$P(2\text{-furyl})_3$	Tri(2-furyl)phosphine
$Pd_2(dba)_3$	Tris(dibenzylideneacetone)dipalladium(0)
$Pd(dba)_2$	Bis(dibenzylideneacetone)palladium(0)
$Pd_2(dba)_3 \bullet CHCl_3$	Tris(dibenzylideneacetone)dipalladium(0)-chloroform adduct
$Pd(dmdba)_2$	Bis(3,5,3′,5′-dimethoxydibenzylideneacetone)palladium(0)
$Pd(OAc)_2$	Palladium(II) acetate

$Pd(PPh_3)_4$	Tetrakis(triphenylphosphine)palladium(0)
Ph_3B	Triphenylborane
PhONa	Sodium phenoxide
PhZnBr	Phenylzinc bromide
PPh_3	Triphenylphosphine
Propofol	2,6-Bis(1-methylethyl)phenol
PTS	*p*-Toluenesulfonic acid
rac-BINAP	(±)-2,2′-Bis(diphenylphosphino)-1,1′-binaphthalene
rt	Room temperature
SET	Single electron transfer
SMe_2	Dimethyl sulfide
$SnCl_4$	Tin(IV) chloride
SPhos	2-Dicyclohexylphosphino-2′,6′-dimethoxybiphenyl
(*S*)-TRIP	(S)-3,3′-Bis(2,4,6-triisopropylphenyl)-1,1′-binaphthyl-2,2′-diyl hydrogenphosphate
TBAF	Tetrabutylammonium fluoride
TBD	1,5,7-Triazabicyclo[4.4.0]dec-5-ene
*t*BuMePhos	2-Di-*tert*-butylphosphino-2′-methylbiphenyl
*t*Bu	*tert*-butyl
t-BuOK	Potassium *tert*-butoxide
THF	Tetrahydrofuran
Ti	Titanium
TLC	Thin-layer chromatography

TMS	Trimethylsilyl
TMSCl	Chlorotrimethylsilane
XPhos	2-Dicyclohexylphosphino-2′,4′,6′-triisopropylbiphenyl
XantPhos	4,5-Bis(diphenylphosphino)-9,9-dimethylxanthene
$Yb(OTf)_3$	Ytterbium(III) trifluoromethanesulfonate
$ZnBr_2$	Zinc bromide
$Zn(OTf)_2$	Zinc triflate

Chapter 1. Synthetic Methods for Propargylation and Propargylic Carbonate Reactivity.

1.1 Introduction to Propargylation Methods

The alkyne functional motif lies at the center of many synthetic efforts due to its ability to serve as a precursor to a diverse variety of functional group transformations.[1,2] This characteristic leads to the broad application of alkynes as synthetic intermediates in both the development of synthetic methods and syntheses of biologically active compounds.[3,4] Further, alkynes themselves are prevalent in many natural products, pharmaceuticals, and fine chemicals, which contributes to their overall chemical significance.[5,6]

Electrophilic propargylation is one highly utilized method for alkyne incorporation into molecular scaffolds. In the most straightforward transformation, direct electrophilic propargylation can be achieved via S_N2 substitution of a propargylic halide.[7,8] Although this method can be attractive in terms of simplicity, it often suffers from some inherent drawbacks such as low regioselectivity, poor reagent availability, toxicity of propargylic halides, and the lack of potential for an asymmetric variant.[7,8,9] As an alternative, less reactive but more readily available propargyl alcohols, acetates, and carbonates can be employed in the presence of transition metals to promote selective propargylation while minimizing reagent toxicity. Further, transition metal controlled propargylation would also allow the use of chiral, non-racemic ligands as a potential source of asymmetric induction.

Scheme 1.1: Regioselective Nucleophilic Attack of Propargylic Electrophiles

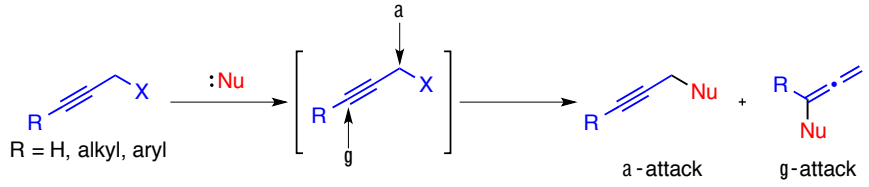

Unlike addition into allylic electrophiles, which yield alkene products,[10] transition metal-catalyzed additions to propargylic electrophiles are much more complex since they can result in alkyne, allene, or cyclized products and therefore have been underdeveloped in comparison.[11] As alluded to previously, one characteristic that significantly contributes to the complexity of these reactions is the issue of regioselectivity. Similar to a transition metal-catalyzed allylation reaction, nucleophilic attack of a propargylic electrophile has the potential to occur at the α-carbon to the leaving group, to yield propargyl products, or at the γ-carbon, to yield allenyl products (Scheme 1.1**)**. However, unlike allylation reactions that proceed through a similar metal-bound intermediate, propargylic electrophiles have the potential to generate numerous types of metal-bound intermediates, which substantially increases the difficulty in controlling product selectivity.

1.2 Lewis and Brønsted Acid Catalyzed Propargylation Reactions

Classically, the Nicholas reaction has been highly utilized as a reliable method to control regioselective addition to the α-carbon of propargyl alcohols (Scheme 1.2).[12,13] Compatible nucleophiles include: alcohols, amines, thiols, ketones, silyl enol ethers, and electron-rich aromatic rings.[13] However, the reaction lacks both step and atom-economy with the requirement of preformed, organometallic reagents using $Co_2(CO)_6$, Lewis or Brønsted acid additives, and the need for a subsequent oxidative demetallation to obtain the desired propargylated product. Necessarily, these reactions also result in the production of a significant amount of metal waste.

Scheme 1.2: Classic Nicholas Reaction Sequence.

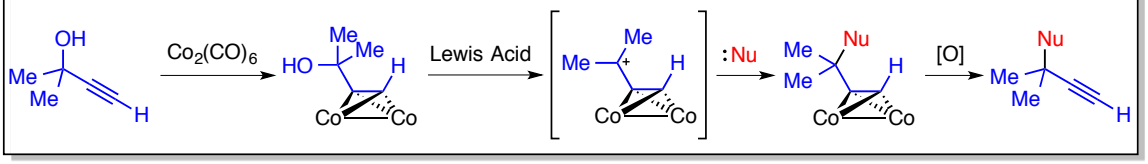

Alternatively, in attempt to provide a "greener" and more cost effective propargylation method, recent attention has focused on the development of Lewis or Brønsted acid catalysis to activate propargyl alcohols directly for S_N1 propargylic substitution and avoid the necessity for preformed organometallic compounds. For example, in 2007 Sanz and coworkers reported the use of *p*-toluenesulfonic acid monohydrate (PTS) in the Brønsted acid-catalyzed propargylation of 1,3-dicarbonyl compounds with internal propargylic alcohols resulting in water as the only byproduct (Scheme 1.3).[14] Under the optimized reaction conditions, acyclic β-diketone nucleophiles underwent successful propargylation at room temperature and resulted in moderate isolated yields of the propargylated product. However, a decrease in yield was observed when the nucleophile was altered to cyclic β-diketones and even more so when β-ketoesters were employed. Further, the reaction was only tolerant of mono-substitution at the propargylic position of the starting propargyl alcohols. For tertiary alkynols, selective formation of the allenylated products was observed. Lastly, refluxing reaction conditions were required for the propargylation of 1,3-dicarbonyl compounds using singly activated, terminally unsubstituted propargyl alcohols.

Scheme 1.3: Bronsted Acid Catalyzed Propargylation of 1,3-Dicarbonyl Compounds

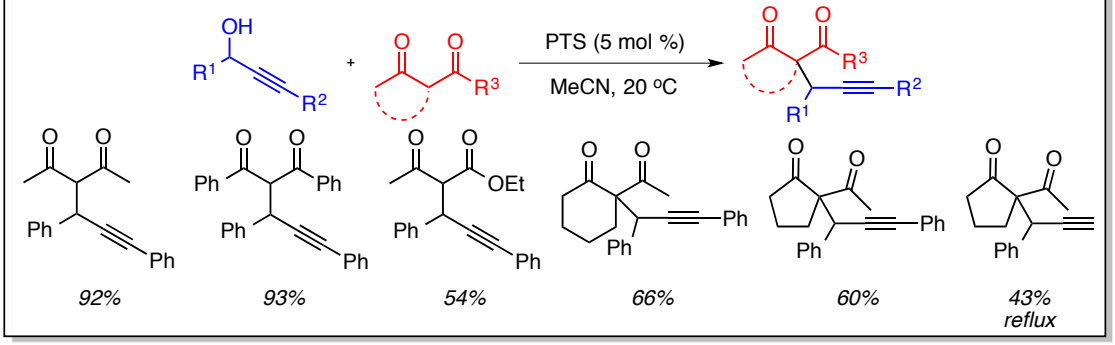

Shortly after Sanz's report in 2007, Zhou and coworkers reported the use of $Yb(OTf)_3$ in the Lewis acid-catalyzed propargylation of 1,3-dicarbonyl compounds at room temperature (Scheme 1.4).[15] In addition to successful propargylation of acyclic β-diketones with internal propargylic alcohols, Zhou's method also tolerated cyclic β-diketones, β-ketoesters and the use of

terminal propargylic alcohols under the optimized reaction conditions without a significant decrease in product yield. However, the reaction remained intolerant of disubstituted alkynols, which again resulted in selective formation of the allenyl isomers. Further, in the report by Sanz, propargylic alcohol starting materials were still limited to those with aryl substitution at the propargylic position presumably to stabilize the forming cation and facilitate ionization for S_N1 substitution.

Scheme 1.4: Lewis Acid-Catalyzed Propargylation of 1,3-Dicarbonyl Compounds

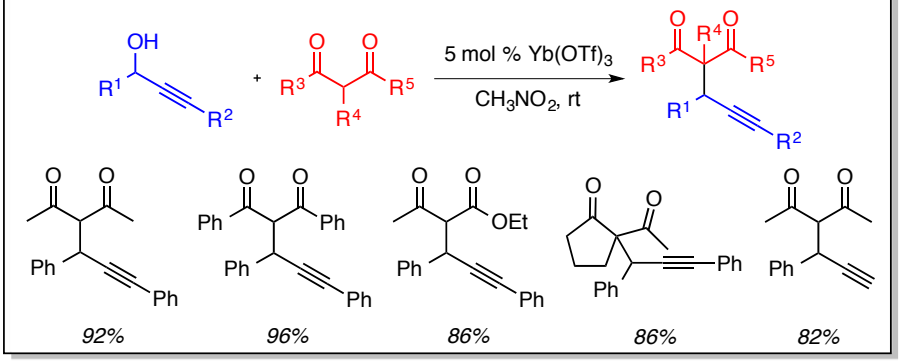

Recently, in 2015, Díez-González and coworkers reported the use of inorganic acid HBF_4 in the propargylation of oxygen-, nitrogen-, and carbon- nucleophiles with propargylic alcohols at room temperature (Scheme 1.5).[16] Contrary to Lewis or organic Brønsted acid catalysts, inorganic Brønsted acids can be easily removed from the reaction media and are typically more stable to air and reagent-grade solvents. Despite being successful for the propargylation of oxygen-, nitrogen-, and carbon- nucleophiles using both terminal and internal propargylic alcohols, the developed method was restricted to electron-rich 1-aryl propargyl alcohols. However, when the reaction temperature and catalyst loading were both increased, the reaction scope could be expanded to a few substrates with alkyl or electron-poor aryl substituents and products were obtained in moderate yield. Surprisingly, a similar increase in reaction temperature and catalyst loading also lead to the successful propargylation from tertiary alkynols, which under the previously discussed methods lead to selective formation of the allene isomer. Lastly, in addition to β-diketones, the

scope of carbon nucleophiles was extended to both electron rich aryl and heteroaryl moieties to yield the products of Friedel-Crafts –type substitution.

Scheme 1.5: Inorganic Bronsted Acid-Catalyzed Propargylation Reactions.

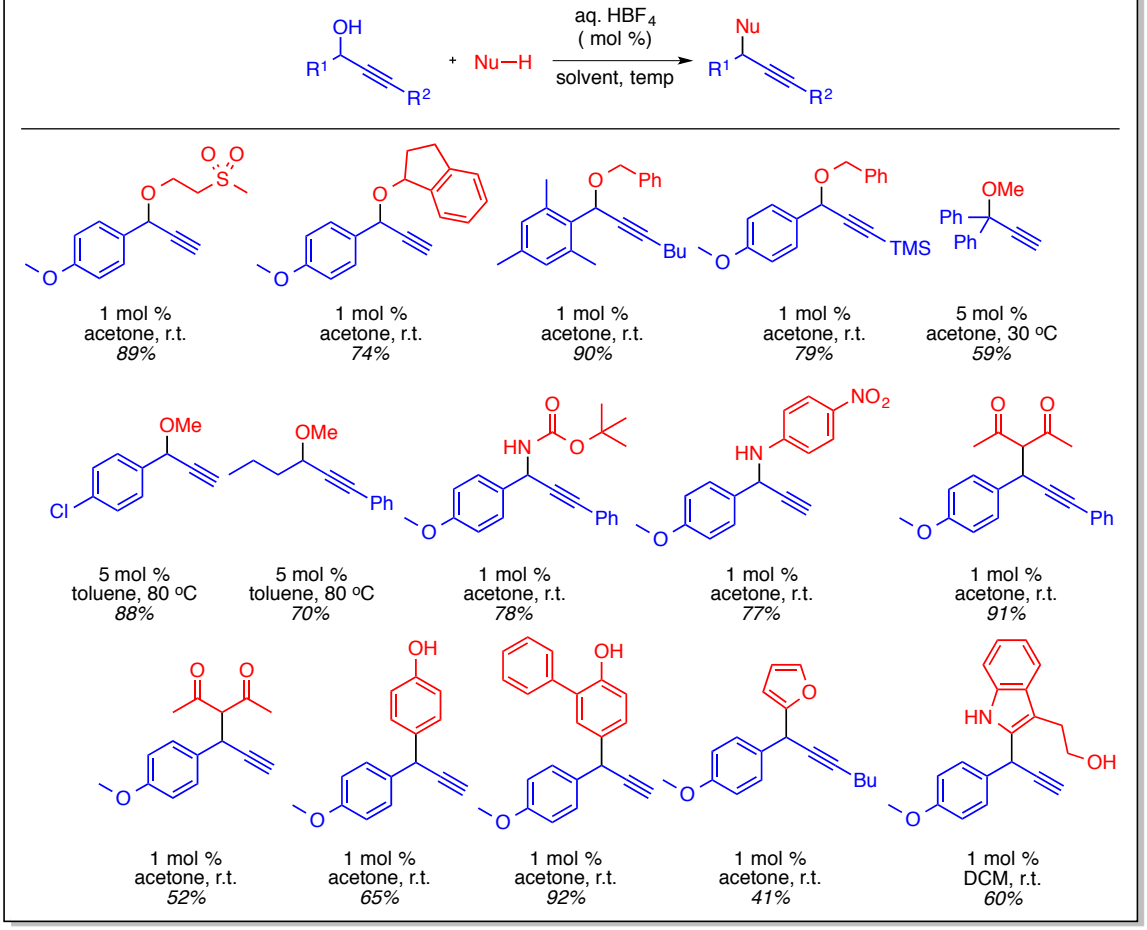

As illustrated above, both Lewis and Brønsted acid-catalysis can be a highly efficient method for the propargylation of various nucleophiles. However, the current methods are largely dependent on both the electronic and steric environment surrounding the starting materials. Further, the extended application of Lewis or Brønsted acid catalysis in larger, more structurally complex systems can lead to complications with chemoselectivity with other sensitive functionalities.[17] As an alternative, transition metal-catalyzed propargylation methods have been employed as an attempt to tune the reactivity of the starting propargylic electrophile in order to

develop more generalized reaction methods. For conceptual simplicity, the following transition metal-catalyzed propargylation methods have been divided into sections according to the metal catalyst.[18,19]

1.3 Ruthenium-Catalyzed Propargylation Reactions

Beginning in 2000, Nishibayashi, Hidai, Uemura and coworkers began developing methods for the propargylation of various nucleophiles with propargylic alcohols using thiolate-bridged ruthenium (III,III) dimers.[20] Over the course of their studies, methods have been developed for the propargylation of carbon-,[21,22,23] oxygen-, phosphonate-, thiols-, and nitrogen-nucleophiles.[20, 24 , 25 , 26] Following initial coordination, rearrangement and dehydration, regioselective nucleophilic addition is reportedly controlled through formation of cationic ruthenium allenylidene intermediates, which undergo selective nucleophilic attack at the γ-carbon (Scheme 1.6).

Scheme 1.6: Mechanism of Diruthenium-Catalyzed Propargylation

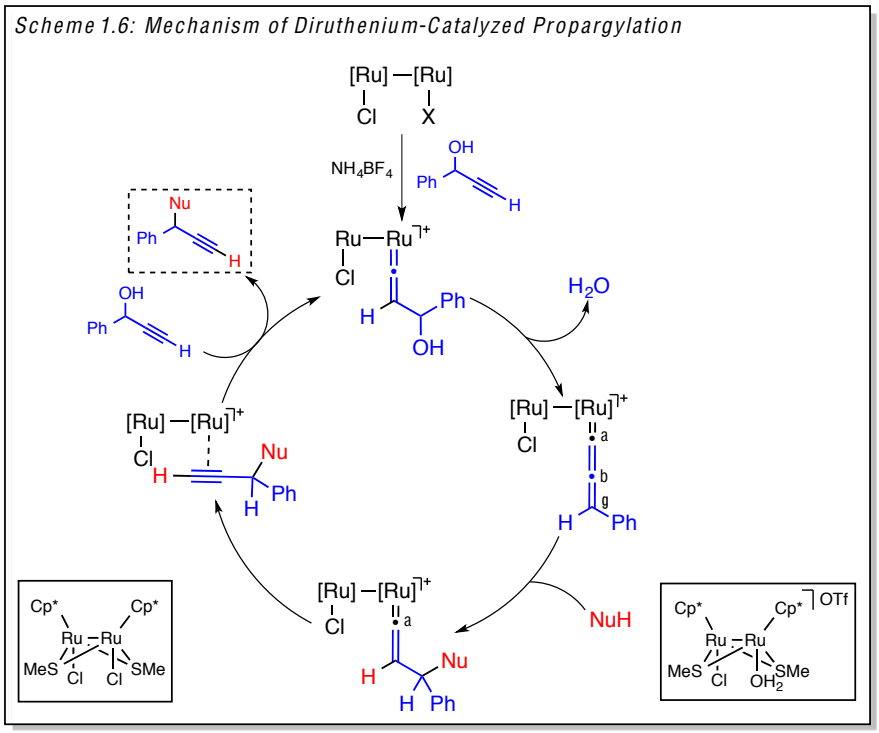

Prior investigation of ruthenium allenylidene complexes conducted by Valerga,[27] Esteruelas and López[28] have demonstrated that cationic ruthenium allenylidene complexes are highly electrophilic in contrast to their neutral counterparts. Further, the allenylidene ligand itself has unique characteristics including electrophilic character at C_α and C_γ and nucleophilic character at C_β of monometallic species (Scheme 1.7). By tuning the basicity of the metal center through the choice of coordinating ligands, regioselective nucleophilic addition could favor either the C_α (weakly basic metal centers) or Cγ (strongly basic metal centers) position. However, when the cationic monometallic complexes were applied to selective propargylation in the presence of propargylic alcohols, the complexes were found to be inactive.[27,28,29] This observation motivated Nishibayashi, Hidai, Uemura and coworkers to evaluate other types of ruthenium catalysts (beyond monometallic species) for the activation of propargylic alcohols. Specifically, thiolate-bridged diruthenium catalysts were screened based on prior observations of their success in catalyzing the head-to-head dimerization of terminal alkynes[30] and ability to promote selective propargylation of various nucleophiles without any allene formation. However, due to the requirement of a ruthenium-allenylidene intermediate, the substrate scope and overall synthetic application was significantly restricted by the need for terminal propargylic alcohol starting materials.

Scheme 1.7: Reactivity of the Allenylidene Ligand on Ruthenium.

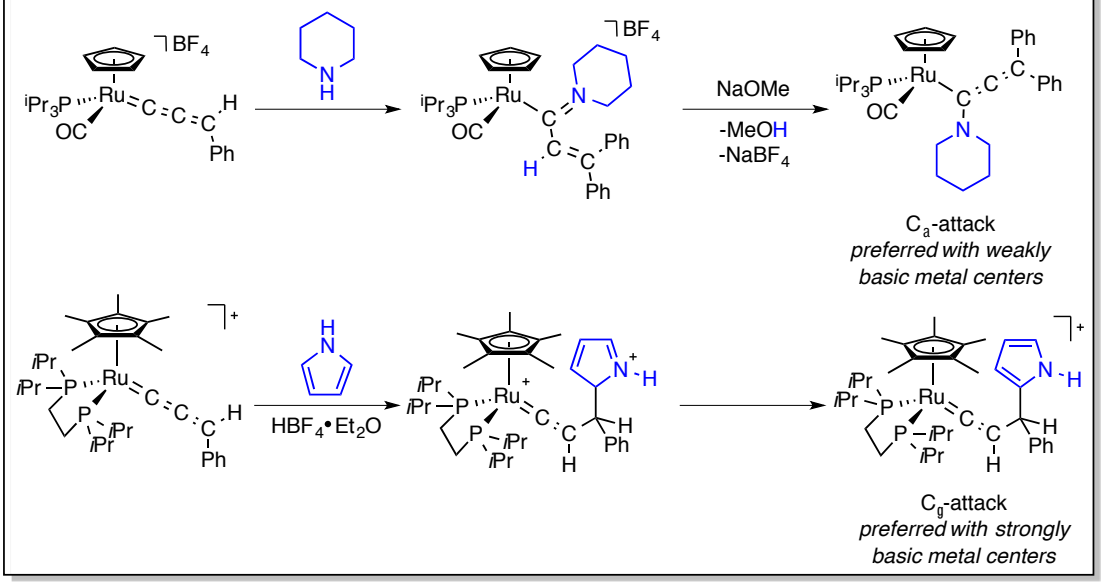

In attempt to overcome the restricted synthetic application to terminal propargylic electrophiles using diruthenium catalysts, some attention has been devoted toward the development of a mononuclear variant. Unfortunately, the developed methods continue to suffer from severe drawbacks. For example, in 2002 Mitsudo and coworkers were able to demonstrate that thio- nucleophiles underwent successful propargylation when propargylic carbonates were employed in the presence of 10 mol % CpRuCl(cod) (Scheme 1.8).[31] However, the reaction was only successful in the presence of *N*-methylpiperidine as a solvent (necessary to retain catalyst activity) and at elevated reaction temperatures of 100 °C. Further, terminal propargylic electrophiles were unsuccessful and the reaction was intolerant of substitution at the propargylic position.

Scheme 1.8: Mononuclear Ruthenium Catalyzed Propargylation of Thiols.

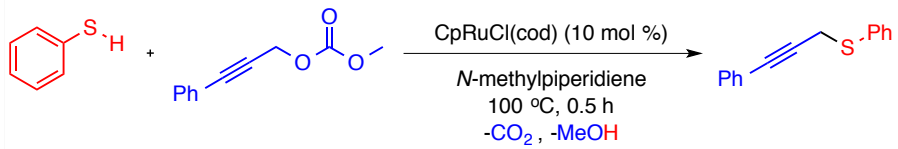

1.4 Copper-Catalyzed Propargylation Reactions

Similarly, a number of groups including Hennion and Hanzel,[32] Murahashi,[33] Caporusso[34] and van Maarseveen[35] have developed methods for the copper(I)-catalyzed propargylation of various nucleophiles in which the regioselectivity determining step is proposed to occur through nucleophilic attack of a copper allenylidene intermediate (Scheme 1.9).[36] However, contrary to the diruthenium-catalyzed rearrangement and subsequent condensation of propargylic alcohols to generate a ruthenium-acetylidene intermediate, the use of copper(I) catalysts requires a stoichiometric or super stoichiometric amount of base to deprotonate the alkyne proton and generate a copper-acetylide or copper acetylidene intermediate. This mechanistic requirement of a metallic-acetylidene intermediate once again limits the synthetic utility of the copper(I)-catalyzed method to terminal propargylic electrophiles.

Scheme 1.9: Copper(I)-Catalyzed Propargylation of 2°-Amines

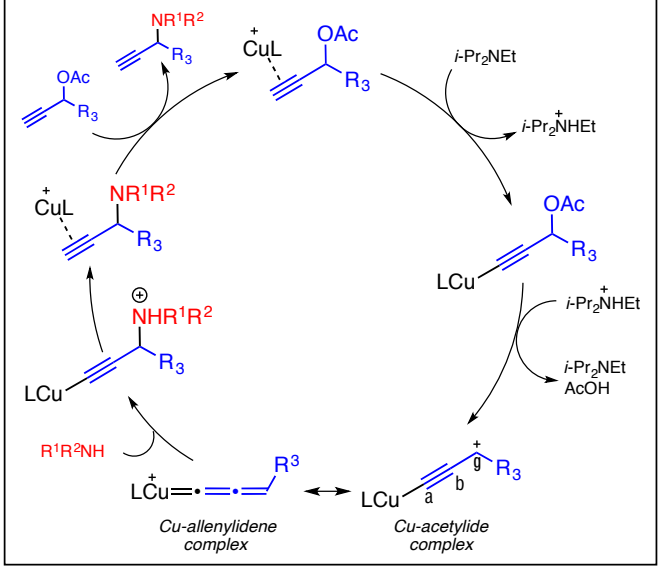

Despite the synthetic limitation of copper(I)-catalyzed propargylations using terminal propargylic electrophiles, Hu and coworkers were recently able to expand the scope of carbon nucleophiles to β-ketoesters which had only been mildly successful under previously developed transition metal-catalyzed methods (Scheme 1.10). Further, the use of propargylic carbonates as

their source of the propargylic electrophile allowed for *in situ* generation of ketone enolate equivalents rather than requiring preformation prior to subjection to the propargylation reaction conditions.

As an alternative to copper(I)-catalyzed propargylations, Zhan[37,38] and coworkers have also explored the use of copper(II) in the S_N1 substitution of propargyl acetates (Scheme 1.11). However, similar to the substrate restrictions found in section 1.1.2, the developed reaction was sensitive to substitution on the starting propargylic electrophile. As typically found in the transition metal-catalyzed reactions covered thus far, an aryl substituent was required at the 1-position of the starting propargyl alcohol, but 1,1-diaryl substituted alcohols were found to preferentially form the allene isomer as opposed to the propargyl product.

Scheme 1.10: Copper(1)-Catalyzed Decarboxylative Propargylation

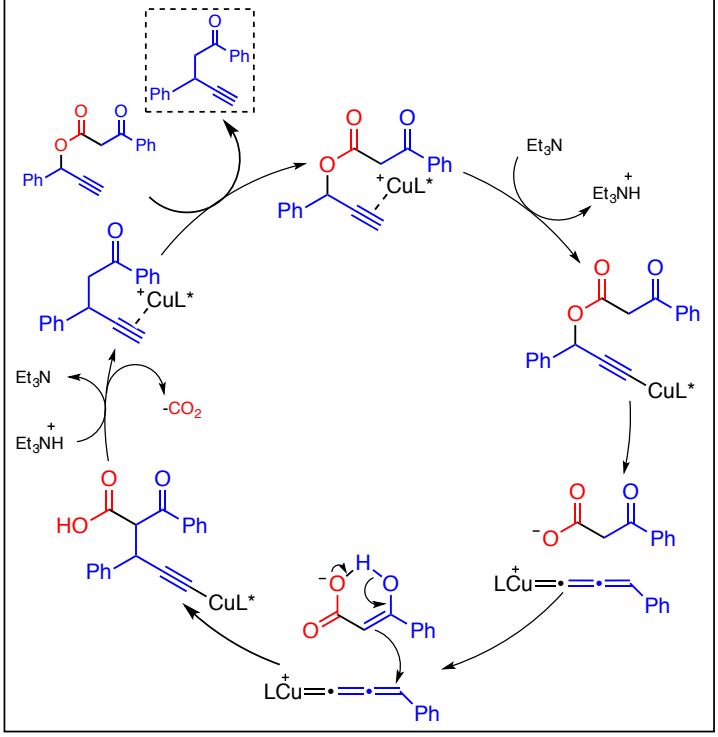

Scheme 1.11: Copper(II)-Catalyzed Propargylation

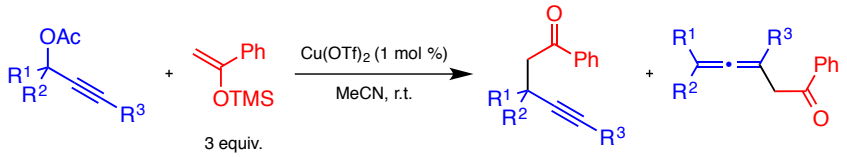

R^1, R^2, R^3	propargyl:allene
Ph, H, Ph	88% : 0%
Ph, H, H	84% : 0%
Ph, Ph, Ph	38% : 52%

1.5 Rhenium-Catalyzed Propargylation Reactions

In order to avoid the formation of metal allenidene intermediates and bypass the limitation of terminal propargylic electrophiles, Toste[39,40,41] and Takai[42] reported the use of a rhenium metal-oxo complex to promote the propargylation of carbon-, oxygen- and nitrogen nucleophiles (Scheme 1.12).[18] The mechanism by which propargylation occurs, utilizes a known [3,3]-rearrangement of the metal-oxo species to form an allenolate intermediate. Next, S_N2' nucleophilic attack occurs to yield the propargylated product.

Scheme 1.12: Rhenium-Oxo-Catalyzed Propargylation Reactions.

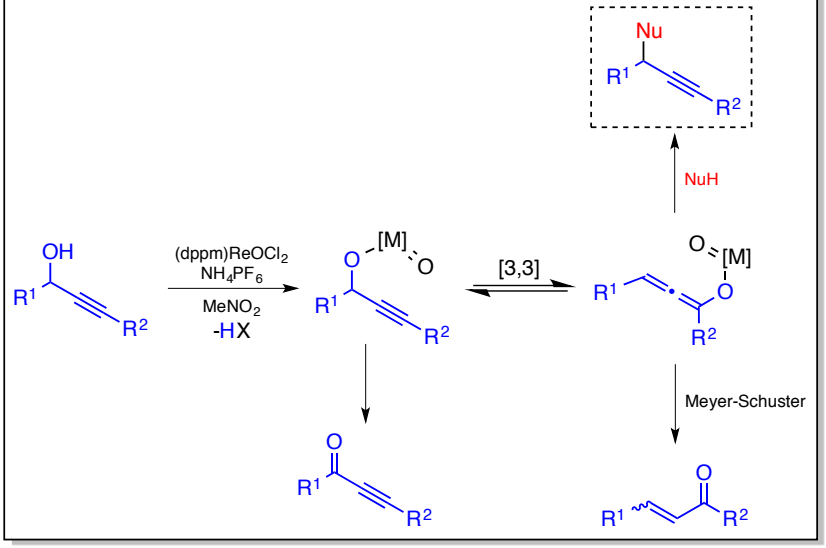

The use of a rhenium metal-oxo complex as a catalyst was found to produce moderate to good yields of the propargylated nucleophiles from secondary propargylic alcohols, although there was again a requirement for an aryl moiety at the propargylic position. Further, tertiary propargylic alcohols were unsuccessful, presumably due to steric hindrance between to the two allenyl substituents and the incoming nucleophile in the transition state. Importantly, propargylation reactions with the rhenium-oxo catalyst were successful for alkyl, aryl and silyl terminally substituted propargylic alcohols without any effect on product yield.

1.6 Palladium-Catalyzed Reactions with Propargylic Electrophiles

Despite significant contributions involving transition metal-catalyzed propargylation reactions by other metals, palladium-catalyzed reactions with propargylic electrophiles possess unique reactivity owed to its ability to yield several different types of products. Bias toward formation of a specific product is known to arise through the tuning of various palladium-coordinated intermediates and the hard/soft character of the active nucleophile. Both will be discussed in the following.

In 1999, Tsutsumi, Ogoshi, Kurosawa and coworkers conducted thorough studies on the synthesis and characterization of various palladium complexes resulting from the reaction of propargylic halides with $Pd(PPh_3)_4$.[43] It was observed that when $Pd(PPh_3)_4$ was added in a stoichiometric amount to either a propargyl halide or an allenyl halide, two isomeric products formed following initial oxidative addition of the halide—carbon bond: the η^1-allenylpalladium complex and the η^1-propargylpalladium complex. Preference for either of the η^1-palladium-coordinated intermediates was dependent on competitive steric hindrance at the internal and terminal positions of the starting material (Scheme 1.13) however; both starting materials generated the same palladium-bound intermediates. It is important to realize that the nature of the

counterion on the palladium complex significantly contributes to its preferred configuration. For example, when both the η^1-allenyl and η^1-propargylpalladium complex were simultaneously treated with silver tetrafluoroborate, ligand exchange between the coordinating chloride ligand and the non-coordinating BF_4^- counterion lead to exclusive formation of a cationic η^3-propargylpalladium complex (Scheme 1.14).

Scheme 1.13: Stoichiometric Addition of Palladium(0) to Propargylic Halides:

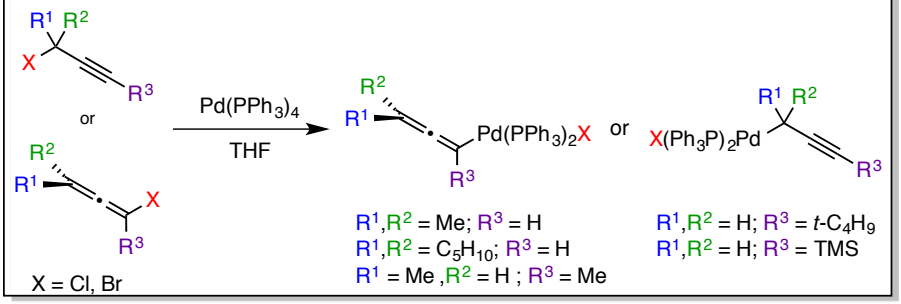

Scheme 1.14: h^1-h^3-Propargylpalladium Interconversion Based on Counterion

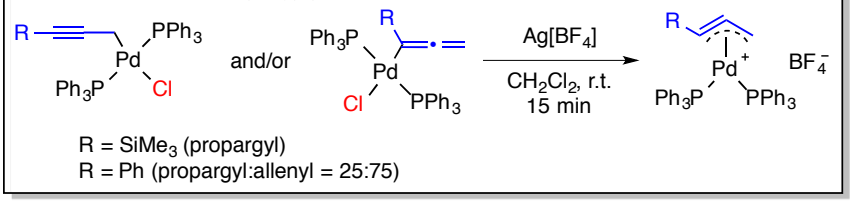

Further, when the cationic η^3-propargylpalladium complex was subjected to a series of NMR solvent studies, it was found that the polarity of the solvent also had a significant effect on the preferred coordination mode of the palladium-bound complex (Scheme 1.15).[43] When polar solvents were employed, such as $CDCl_3$ or DMF-d_7, the cationic η^3-propargylpalladium complex was largely favored over the neutral η^1-allenylpalladium complex. In contrast, when non-polar C_6D_6 was used, exclusive formation of the neutral η^1-allenylpalladium complex was observed. Therefore, the η^1-allenylpalladium complex is preferred in the presence of coordinating counterions, such as chloride ions as well as in non-polar, aprotic solvents. Alternatively, in addition to the presented studies, subsequent reports have revealed that the η^3-propargylpalladium

complex is preferred in the presence of bidentate phosphine ligands, hard or non-coordinating counterions, and in polar solvents.[43,44,45,46]

Scheme 1.15: Solvent Effects on Palladium-Complexes

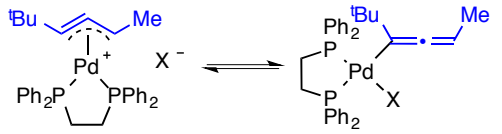

7a: X = Cl
7b: X = Br

8a
8b

Run	X	Solvent	**7**/**8**[a]
1	Cl	$CDCl_3$	75/25
2	Cl	DMF-d_7	89/11
3	Cl	C_6D_6	0/100
4	Br	$CDCl_3$	68/32

[a] Ratios of **7** and **8** calculated by integrations of respective ^{1}H NMR signals at 25 °C.

In addition to the evaluation of reaction conditions that favor either a neutral η^1-palladium or cationic η^3-palladium complex, a large amount of work has been conducted by Chen,[47] Kurosawa,[48,49] Ogoshi,[48,49] Wojcicki,[50] and Tsuji[11] that has provided invaluable information regarding the reactivity of these palladium-bound intermediates with various nucleophiles. For the purpose of this review, only carbon nucleophiles will be discussed. In general, palladium-catalyzed nucleophilic substitution of propargylic electrophiles can be categorized into four different types (Scheme 1.16).[11,51] Typically, when considering nucleophilic additions of type I or type II, an η^1-allenylpalladium complex is generated (largely biased through the lack of steric hindrance at the terminal position of the propargylic electrophile along with the soft-character of the palladium-catalyst). The intermediate complex can then undergo either insertion with a compatible alkene (type I) or transmetallation with an organometallic carbon nucleophile (type II), both of which result in allene products. Alternatively, soft-carbon nucleophiles (type III) are known to regioselectively attack the center carbon of a cationic η^3-propargylpalladium complex. After subsequent protonation to yield a π-allyl palladium intermediate, these species can undergo a second attack either intermolecularly, to yield an alkene

product, or intramolecularly to yield a cyclization product and regenerate the active palladium(0) complex. Lastly, although very rare, type IV nucleophilic additions arise from the formation of an η^1-propargylpalladium complex. In general, the η^1-propargylpalladium complex can be biased when a bulky substituent is located at the terminal position of the allene thus promoting the palladium catalyst to proceed via oxidative addition of the carbon—halide bond rather than S_N2' displacement of the leaving group to generate the η^1-allenylpalladium complex. Similar to the type I and type II additions, once the η^1-propargylpalladium complex is formed, either insertion of an alkene or nucleophilic attack of an organometallic carbon nucleophile could occur to yield the respective alkene or propargyl product.

Scheme 1.16: Palladium-Catalyzed Nucleophilic Addition to Propargylic Electrophiles.

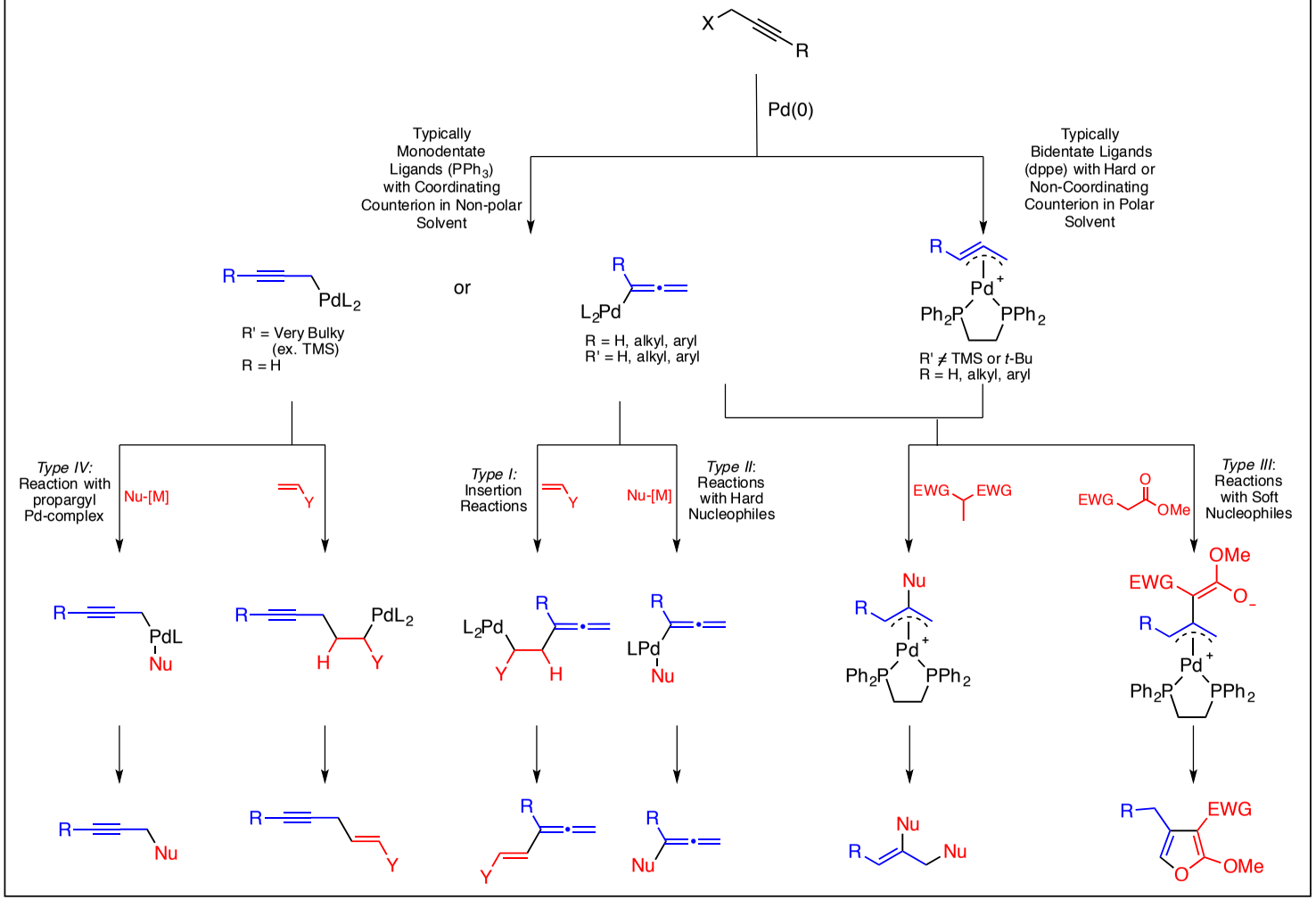

1.7 Reactivity of η^3-Propargylpalladium Complexes

As mentioned in the previous section, addition to an η^3-propargylpalladium complex has been shown to occur exclusively at the center carbon.[52] In 1995, Ogoshi and Kurosawa reported that a phenyl substituted η^3-propargyl ligand on palladium was not linearly coordinated to palladium with an angle of 154°.[53] Further, the η^3-propargylpalladium ligand was located in approximately the same plane as the monodentate phosphine ligands to form a planar tetracoordinate palladium complex.[53,54] Additional studies contributed by Delbecq and Sinou,[54] along with previous reports,[52] revealed that in the η^3-propargylpalladium, palladium is bound to the terminal carbons of the propargyl moiety through orbital overlap analysis. However the bond distances are not equal. A slightly longer bond distance exists between palladium and the substituted carbon (in this case 2.35 Å) compared to the unsubstituted terminal carbon (2.19 Å). Although no overlap population exists between C_2 and palladium (indicating no bond), the distance from the palladium center was found to be short (2.19 Å). Importantly, DFT calculations have suggested that the central carbon is positively charge whereas the terminal carbons of the propargyl ligand are negatively charged.[54] Further examination of orbital overlap populations were found to be highest at the center carbon of the propargyl ligand when NH_3 or MeO^- were employed as nucleophiles. Therefore, selective nucleophilic attack the center carbon of η^3-propargylpalladium complexes is proposed to occur under both orbital and charge-control at the central carbon.

Of additional importance are the characteristics of the phosphine ligand. Specifically, the P-Pd-P angle[55] which has a direct affect on the bent angle of the η^3-propargyl ligand. In 2014, Anderson and Paton reported that the charge distribution on each of the carbon atoms of the η3-propargyl moiety are not affected with an increase or decrease in the bite angle of the phosphine ligand.[56] However, the energy of the molecular orbitals changes significantly. Through DFT

calculations it was found that bidentate ligands with larger bite angles cause an elongation, or bond lessoning, between palladium and the terminal carbons of η^3-propargyl ligand. As a result, a flattening of the η^3-propargyl moiety occurs which lowers the LUMO of the terminal carbons to resemble an allenyl cation. The lowered LUMO orbitals promote favored attack at the unsubstituted terminal carbon as opposed to the center carbon of the η^3-propargyl moiety as is commonly observed. Therefore, bidentate ligands possessing small bite angles are optimal for regioselective nucleophilic attack at the center carbon of η3-propargylpalladium complexes.

1.8 Palladium-Catalyzed Propargylation Reactions from Propargylic Electrophiles

As discussed in sections 1.1 – 1.5 of this chapter, current methods for selective propargylation of carbon nucleophiles often suffer from poor atom-economy, reagent toxicity, or, most importantly, selectivity among a diverse class of propargylic electrophiles or nucleophiles. Further, despite the advantages of palladium-catalyzed reactions with propargylic electrophiles, section 1.6 demonstrated that soft carbon nucleophiles most commonly lead to products of dinucleophilic addition or cyclization as opposed to propargyl products. Therefore, development of a palladium-catalyzed method that selectively yields propargylated soft carbon nucleophiles would significantly advance the realm of palladium-catalyzed reactions with propargylic electrophiles. However, reactions of this type remain scarce to date.

In 2015, Iazzetti and coworkers reported the successful propargylation of Meldrum's acid derivatives in the presence of 5 mol% $Pd(OAc)_2$, 20 mol% P(2-furyl)$_3$, in refluxing THF (Scheme 1.17).[57] It was found that both alkyl and aryl substitution was tolerated at the terminal and internal position of the propargyl carbonate starting materials without a significant effect yield. However, nucleophiles were strictly limited to highly stabilized, monosubstituted Meldrum's acid derivatives. When 2-methylcyclohexandione was employed instead, exclusive

formation of the dinucleophilic addition product was observed, clearly displaying the limitation of this method (Scheme 1.18).

Scheme 1.17: Palladium-Catalyzed Propargylation of Meldrum's Acid Derivatives

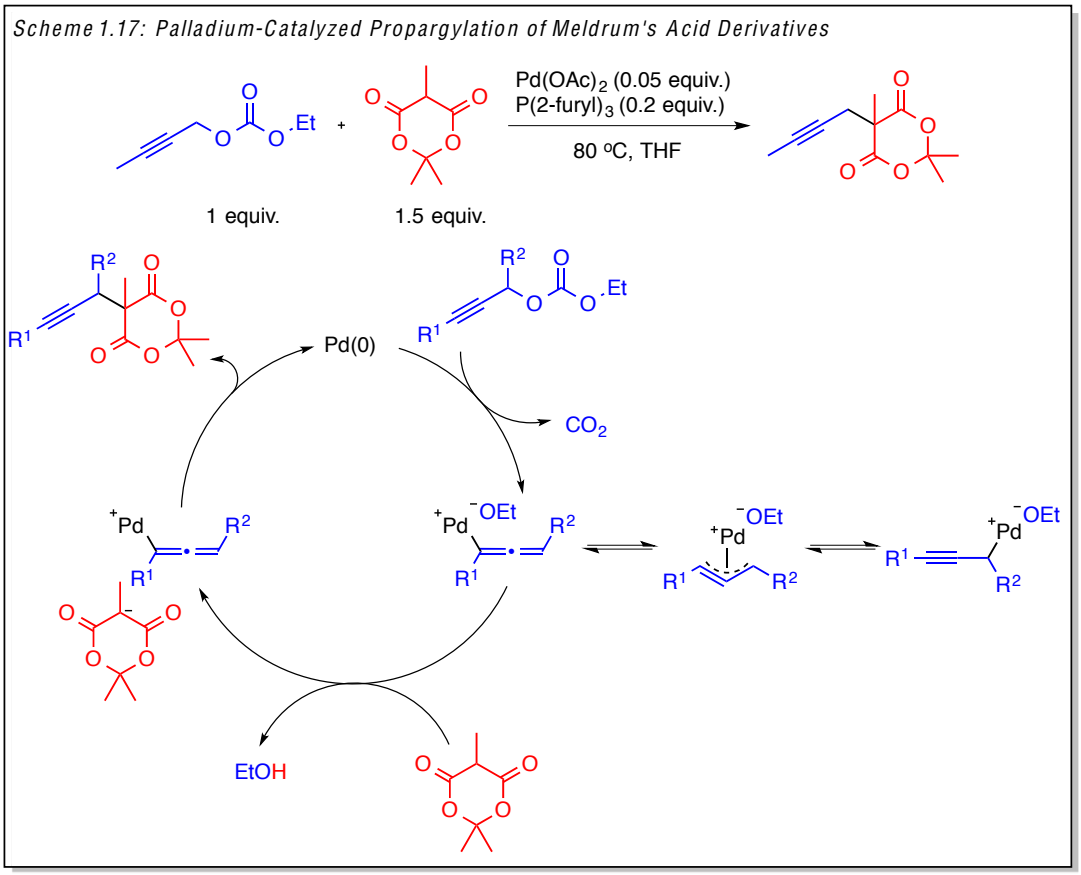

Scheme 1.18: Palladium-Catalyzed Reaction of 1,3-Dione

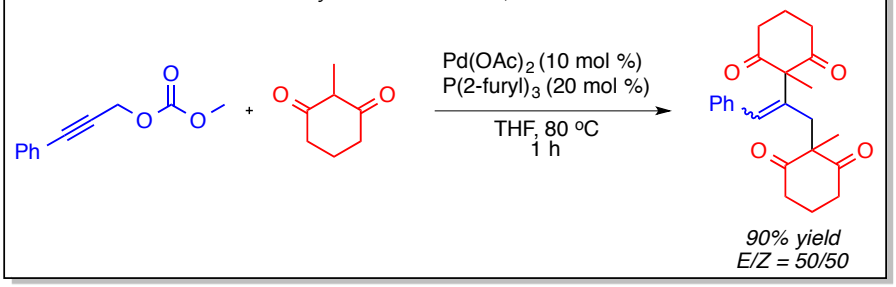

Due to the difficulty associated with direct nucleophilic addition of palladium-bound intermediates to yield propargyl products, Morken and coworkers designed a palladium-catalyzed cross-coupling reaction with allyl boronates where a 3,3'-reductive elimination yields a

propargylated product (Scheme 1.19).[58] Upon optimization of reaction conditions, it was found that allylation of various propargyl acetates proceeded stereospecifically with respect to the starting propargyl acetate. Further, mono- and disubstitution was tolerated at the propargylic position of the starting acetate materials, without a significant effect on product yields or contamination by the allene isomer. However, the reaction was intolerant of substitution at the terminal position of the propargyl acetate starting materials and also required three equivalents of CsF as an additive. Lastly, due to the mechanistic constraints of the developed reaction, only allyl moieties were sufficient coupling partners to obtain the propargylated products.

Scheme 1.19: Palladium-Catalyzed Cross-Coupling of Allyl Boronates

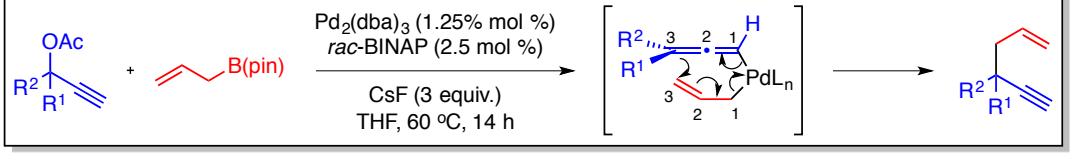

As one last alternative, in 2011, Álvarez de Cienfuegos and Cuerva reported a dual-catalytic system consisting of palladium and titanium for the nucleophilic propargylation of aldehyde and ketone moieties (Scheme 1.20).[59] As found in typical palladium-catalyzed reactions with propargylic electrophiles, the first suggested step in the mechanistic sequence was the oxidative addition of propargyl carbonate to palladium(0) will undergo oxidative addition into the propargyl carbonate to yield an η^1-allenylpalladium complex (in equilibrium with the η^1-propargyl and η^3-propargylpalladium complexes). Subsequent fragmentation of the palladium(II) complex is then promoted by a single-electron transfer (SET) from the super-stoichiometric addition of Cp_2TiCl to yield an allenyltitanocene intermediate. Next, coordination of the electrophilic carbonyl compound occurs which undergoes regioselective nucleophilic attack to yield the resulting propargyl alcohol after an acid work-up. Although this method utilized a palladium(0) catalyst to promote initial activation of the propargylic carbonate, significant

drawbacks include the requirement of super-stoichiometric amounts of titanium and the limitation to carbonyl electrophiles to yield propargylation products.

Scheme 1.20: Titanium/Palladium-Mediated Propargylation of Ketones

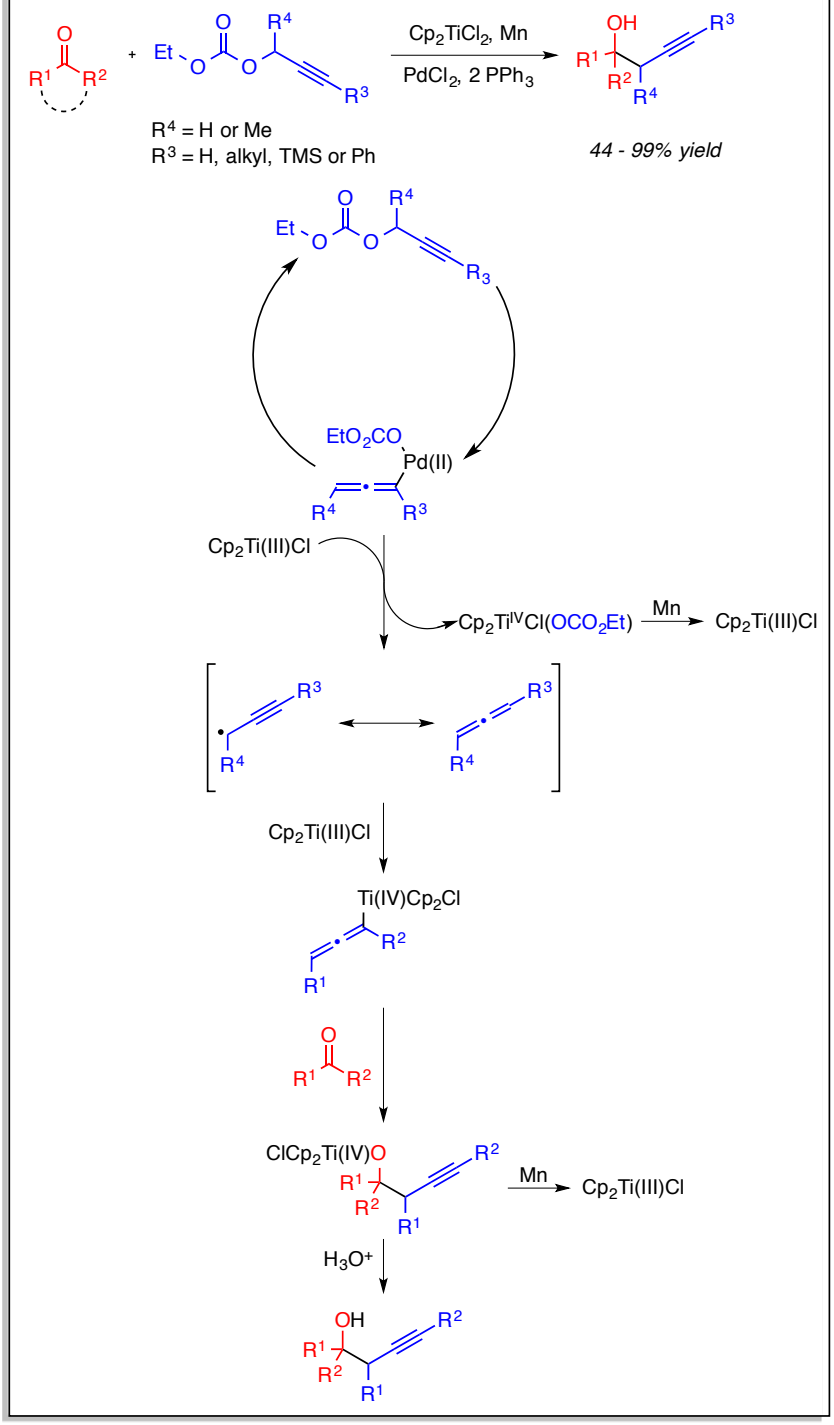

1.9 Conclusion:

Throughout chapter 1, numerous methods have been presented that catalyze the propargylation of carbon-centered nucleophiles including the Nicholas reaction, Lewis acids, Brønsted acids, and transition metal catalysis. However, known propargylation methods still suffer from a limited substrate scope of substituted propargylic electrophiles and lack generality for a diverse class of carbon-centered nucleophiles. Additionally, in regard to palladium-catalyzed reactions, only a handful of methods exist that are able to override the large bias for the allenyl isomer or products arising from dinucleophilic addition to palladium-bound intermediates in favor of propargylation. Therefore, a more generalized atom-economical propargylation method would significantly advance the field of propargylation chemistry. Specifically, the method should expand the scope of carbon nucleophiles and provide access to propargylation reactions using substituted propargylic electrophiles.

1.10 References for Chapter 1:

[1] Alabugin, I. V.; Gold, B. "Two Functional Groups in One Package': Using Both Alkyne π-Bonds in Cascade Transformations." *J. Org. Chem.* **2013**, *78*, 7777-7784.

[2] Trost, B. M.; Li, C-J. *"Modern Alkyne Chemistry: Catalytic and Atom-Economic Transformations"* New York: John Wiley & Sons, Inc. 2016.

[3] Tron, G. C.; Pirali, T.; Billington, R. A.; Canonico, P. L.; Sorba, G.; Genazzani, A. A. "Click Chemistry Reactions in Medicinal Chemistry: Applications of the 1,3-dipolar Cycloaddition Between Azides and Alkynes." *Med. Res. Rev.* **2008**, *28*, 278-308.

[4] Gil, C.; Bräse, S. "Solid-Phase Synthesis of Biologically Active Benzoannelated Nitrogen Heterocycles: An Update." *J. Comb. Chem.* **2009**, *11*, 175-197.

[5] Thompason, A. S.; Corley, E. G.; Huntington, M. F.; Grabowski, E. J. J. "Use of an Ephedrine Alkoxide to Mediate Enantioselective Addition of an Acetylide to a Prochiral Ketone: Asymmetric synthesis of the Reverse Transcriptase Inhibitor L-743,726." *Tetrahedron Lett.* **1995**, *36*, 8937.

[6] Wright, J. L.; Gregory, T. F.; Kesten, S. R.; Boxer, P. A.; Serpa, K. A.; Meltzer, L. T.; Wise, L. D.; Espitia, S. A.; Konkoy, C. S.; Whittenmore, E. R.; Woodward, R. M. "Subtype-Selective *N*-Methyl-D-Aspartate Receptor Antagonists: Synthesis and Biological Evaluation of 1-(Heteroarylalkynyl)-4-benzylpiperidines." *J. Med. Chem.* **2000**, *43*, 3408-3419.

[7] Florio, S.; Granito, C.; Ingrosso, G.; Troisi, L. "Wittig Rearrangements of (Heteroaryl)alkyl Propargyl Ethers – Synthesis of Allenic and Propargylic Alcohols." *Eur. J. Org. Chem.* **2002**, 3465-3472.

[8] Shavrin, K. N.; Gvozdev, V. D. "Reactions of 1-(alk-1-ynyl)-1-chlorocyclopropanes with arenethiols and alkanethiols in dimethyl sulfoxide in the presense of KOH." *Russ. Chem. Bull. Int. Ed.* **2009**, *58*, 2431-2436.

[9] Tsuji, J. "*Overview of the Palladium-Catalyzed Carbon–Carbon Bond Formation via π-Allylpalladium and Propargylpalladium Intermediates*." Ed. Ei-ichi Negishi. New York: John Wiley & Sons, Inc. 2002. 1680-1686. Online.

[10] Tsuji, J. "*Overview of the Palladium-Catalyzed Carbon–Carbon Bond Formation via π-Allylpalladium and Propargylpalladium Intermediates*." Ed. Ei-ichi Negishi. New York: John Wiley & Sons, Inc. 2002. 1669-1679. Online.

[11] Tsuji, J.; Mandai, T. "Palladium-Catalyzed Reactions of Propargylic Compounds in Organic Synthesis." *Angew. Chem. Int. Ed.* **1995**, *34*, 2589-2612.

[12] Nicholas, K. M. "Chemistry and Synthetic Utility of Cobalt-Complexed Propargylic Cations" *Acc. Chem. Res.* **1987**, *20*, 207-241.

[13] Teobald, B. J. "The Nicholas reaction: the use of dicobalt hexacarbonyl-stabilised propargylic cations in synthesis." *Tetrahedron*. **2002**, *58*, 4133-4170.

[14] Sanz, R.; Miguel, D.; Martínez, A.; Álvarez-Gutiérrez, J. M.; Rodríguez, F. "Brønsted Acid Catalyzed Propargylation of 1,3-Dicarbonyl Derivatives. Synthesis of Tetrasubstituted Furans." *Org. Lett.* **2007**, *9*, 727-730.

[15] Huang, W.; Wang, J.; Shen, Q.; Zhou, X. "Yb(OTf)3-catalyzed propargylation and allenylation of 1,3-dicarbonyl derivatives with propargylic alcohols: one-pot synthesis of multi-substituted furocoumarin." *Tetrahedron.* **2007**, *63*, 11636-11643.

[16] Barreiro, E.; Sanz-Vidal, A.; Tan, E.; Lau, S-H.; Sheppard, T. D.; Díez-González, S. "HBF_4-Catalysed Nucleophilic Substitutions of Propargylic Alcohols." *Eur. J. Org. Chem.* **2015**, 7544-7549.

[17] Bauer, E. B. "Transition-Metal-Catalyzed Functionalization of Propargylic Alcohols and Their Derivatives." *Synthesis*. **2012**, *44*, 1131-1151.

[18] Detz, R. J.; Hiemstra, H.; van Maarseven, J. H. "Catalyzed Propargylic Substitution." *Eur. J. Org. Chem.* **2009**, 6263-6276.

[19] Nishibayashi, Y. *Synthesis*. **2012**, *44*, 489-503.

[20] Nishibayashi, Y.; Wakiji, I.; Hidai, M. "Novel Propargylic Substitution Reactions Catalyzed by Thiolate-Bridged Diruthenium Complexes via Allenylidene Intermediates." *J. Am. Chem. Soc*. **2000**, *122*, 11019-11020.

[21] Nishibayashi, Y.; Wakiji, I.; Ishii, Y.; Uemura, S.; Hidai, M. "Ruthenium-Catalyzed Propargylic Alkylation of Propargylic Alcohols with Ketones: Straightforward Synthesis of γ-Keto Acetylenes." *J. Am. Chem. Soc*. **2001**, *123*, 3393-3394.

[22] Nishibayashi, Y.; Yoshikawa, M.; Inada, Y.; Hidai, M.; Uemura, S. "Ruthenium-Catalyzed Cycloaddition between Propargylic Alcohols and Cylic 1,3-Dicarbonyl Compounds via an Allenylidene Intermediate." *J. Org. Chem.* **2004**, *69*, 3408-3412.

[23] Inada, Y.; Yoshikawa, M.; Milton, M. D.; Nishibayashi, Y.; Uemura, S. Ruthenium-Catalyzed Propargylation of Aromatic Compounds with Propargylic Alcohols." *Eur. J. Org. Chem.* **2006**, 881-890.

[24] Nishibayashi, Y.; Milton, M.D.; Inada, Y.; Yoshikawa, M.; Wakiji, I.; Hidai, M.; Uemura, S. "Ruthenium-Catalyzed Propargylic Substitution Reactions of Propargylic Alcohols with Oxygen-, Nitrogen-, and Phosphorus-Centered Nucleophiles." *Chem. Eur. J.* **2005**, *11*, 1433-1451.

[25] Inada, Y.; Nishibayashi, Y.; Hidai, M.; Uemura, S. "Ruthenium-Catalyzed Propargylic Substitution Reaction of Propargylic Alcohols with Thiols: A General Synthetic Route to Propargylic Sulfides." *J. Am. Chem. Soc*. **2002***, 124*, 15172-15173.

[26] Nishibayashi, Y.; Uemura, S. "Ruthenium-Catalyzed Novel Carbon-Carbon Bond Forming Reactions via Ruthenium-Allenylidene Complexes." *Curr. Org. Chem.* **2006**, *10*, 135.

[27] Bernad, D. J.; Esteruelas, M. A.; López, A. M.; Modrego, J.; Puerta, M. C.; Valerga, P. "Addition of Secondary and Primary Amines to the Allenylidene Ligand of [Ru(η5-C5H5)(C=C=CPh2)(CO) (P*i*Pr$_3$)BF$_4$: Synthesis of Azoniabutadienyl, Aminoallenyl, and Azabutadienyl Derivatives of Ruthenium (II)." *Organometallics.* **1999**, *18*, 4995-5003.

[28] Bustelo, E.; Jiménez-Tenorio, M.; Mereiter, K.; Puerta, M. C.; Valerga, P. "Reactivity of the Electron-Rich Allenylidene-Ruthenium Complexes [Cp*Ru{=C=C=C(R)Ph}-(dippe)][BPh4] (R = H, Ph). X-Ray Crystal Structure of a Novel Dicationic Ruthenium Carbyne (Cp* = C5Me5; dippe = 1,2-bis(diisopropylphosphine)ethane)." *Organometallics.* **2002**, *21*, 1903-1911.

[29] Cadierno, V.; Conejero, S>; Gamasa, M. P.; Gimeno, J. "Efficient Synthetic Routes to Terminal γ-Keto-Alkynes and Unsaturated Cyclic Carbene Complexes Based on Regio-

and Diastereoselective Nucleophilic Additions of Enolates on Ruthenium(II) Indenyl Allenylidene." *Organometallics.* **2001**, *20*, 3175-3189.

[30] Nishibayashi, Y.; Yamanahi, M.; Wakiji, I.; Hidai. "Cyclization of Terminal Diynes Catalyzed by Thiolate-Bridged Diruthenium-Complexes: A Simple Synthetic Route to *endo*-Macrocyclic (Z)-1-En-3-ynes." *Angew. Chem. Int. Ed.* **2009**, *39*, 2909-2911.

[31] Kondo, T.; Kanda, Y.; Baba, A.; Fukuda, K.; Nakamura, A.; Wada, K. Morisaki, Y.; Mitsudo, T-a. "Ruthenium-Catalyzed *S*-Propargylation of Thiols Enables the Rapid Synthesis of Prpargylic Sulfides." *J. Am. Chem. Soc.* **2002**, *124*, 12960-12961.

[32] Hennion, G. F.; Hanzel, R. S. "The Alkylation of Amines with *t*-Acetylenic Chlorides. Preparation of Sterically Hindered Amines." *J. Am. Chem. Soc.* **1960**, *82*, 4908-4912.

[33] Imada, Y.; Yuasa, M.; Nakamura, I.; Murahashi, S.I. "Copper(I)-Catalyzed Amination of Propargyl Esters. Selective Synthesis of Propargylamines, 1-Alken-3-ylamines, and (Z)-Allylamines." *J. Org. Chem.* **1994**, *59*, 2282-2284.

[34] Geri, R.; Polizzi, C.; Lardicci, L. Caporusso, A. M. "Reactions of Nitrogen Nucleophiles with 1-Bromoallenes: regioselective Synthesis of Propargylamines." *Gazz. Chim. Ital.* **1994**, *124*, 241-248.

[35] Detz, R. J.; Delville, M. M. E.; Hiemstra, H.; van Maarseveen, J. H. "Enantioselective Copper-Catalyzed Propargylic Amination." *Angew. Chem. Int. Ed.* **2008**, *47*, 3777-3780.

[36] Zhang, D-Y.; Hu, X-P. "Recent Advances in Copper-Catalyzed Propargylic Substitution." *Tetrahedron Lett.* **2015**, *56*, 283-295.

[37] Zhan, Z-p.; Wang, S-p; Cai, X-b.; Liu, H-j.; Yu, J-l.; Cui, Y-y. "Copper(II) Triflate-Catalyzed Nucleophilic Substitution of Propargylic Acetates with Enoxysilanes. A Straightforward Synthetic Route to Polysubstituted Furans." *Adv. Syn. Catal.* **2007**, *349*, 2097-2102.

[38] Pan, Y.; Zhao, Ji, W.; Zhan, Z. "One-Pot Synthesis of Substituted Furans Using Cu(OTf)2-Catalyzed Propargylation/Cycloisomerization Tandem Reaction." *J. Comb. Chem.* **2009**, *11*, 103-109.

[39] Sherry, B.; Radosevich, A. T.; Toste, F. D. "A Mild C–O Bond Formation Catalyzed by a Rhenuim-Oxo Complex." *J. Am. Chem. Soc.* **2003**, *125*, 6076-6077.

[40] Kennedy-Smith, J.; Young, L. A.; Toste, F. D. "Rhenium-Catalyzed Aromatic Propargylation." *Org. Lett.* **2004**, *6*, 1325-1327.

[41] Luzung, M. R.; Toste, F. D. "Rhenium-Catalyzed Coupling of Porpargyl Alcohols and Ally Silanes." *J. Am. Chem. Soc.* **2003**, *125*, 15760-15761.

[42] Kuninobu, Y.; Ueda, H.; Takai, K. "Rhenium-catalyzed Coupling of 2-Propynyl Alcohols and Several Nucleophiles via Dehydration." *Chem. Lett.* **2008**, *37*, 878-879.

[43] Tsutsumi, K.; Kawase, T.; Kakiuchi, K.; Ogoshi, S.; Okada, Y.; Kurosawa, H. "Synthesis and Characterization of Some Cationic η^3-Propargylpalladium Complexes." *Bull. Chem. Soc. Jpn.* **1999**, *72*, 2687-2692.

[44] Su, C-C.; Chen, J-T.; Lee, G-H.; Wang, Y. "Direct Approach to Palladium-Mediated Cycloaddition. First Single-Crystal Structure and Convenient Synthesis of Zwitterionic η^3-Timethylenemethane-Palladium form Nucleophilic Addition of Carbanions to an Allenyl Complex." *J. Am. Chem. Soc.* **1994**, *116*, 4999-5000.

[45] Tsutsumi, K.; Yabukami, T.; Fujimoto, K.; Kawase, T.; Morimoto, T.; Kakiuchi, K. "Effects of a Bidentate Phosphine Ligand on Palladium-Catalyzed Nucleophilic Substitution Reactions of Propargyl and Allyl Halides with Thiol." *Organometallics.* **2003**, *22*, 2996-2999.

[46] Tsutsumi, K.; Ogoshi, S.; Nishiguchi, S.; Kurosawa, H. "Synthesis, Structure, and Reactivity of Neutral η^3-Propargylpalladium Complexes." *J. Am. Chem. Soc.* **1998**, *120*, 1938-1939.

[47] Huang, T-M.; Chen, J-T.; Lee, G-H.; Wang, Y. "A Versatile Route to the β-Substituted π-Allyl Complexes via Addition to a Cationic η3-Propargyl Complex of Platinum." *J. Am. Chem. Soc.* **1993***, 115*, 1170-1171.

[48] Kurosawa, H.; Ogoshi, S. "Structure-reactivity relationship in allyl and 2-propynyl complexes of Group 10 metals relevant to homogeneous catalysis." *Bull. Chem. Soc. Jpn.* **1998**, *71*, 973-984.

[49] Tsutsumi, K.; Ogoshi, S.; Kakiuchi, K.; Nishiguchi, S.; Kurosawa, H. "Cross-coupling reactions proceeding through η1-propargyl/allenyl-palladium(II) intermediates." *Inorganica Chimica Acta.* **1999**, *296*, 37-44.

[50] Blosser, P. W.; Schimpff, D. G.; Gallucci, J. C.; Wojcicki, A. "Interconversion of η1-Allenyl, and η^3-Propargyl/Allenyl Ligands on Platinum. Synthesis, Structure, and Reactivity of [(Ph3P)2Pt(η3-CH2CCPh)]O3SCF3." *Organometallics.* **1993**, *12*, 1993-1995.

[51] Kalek, M.; Stawinski, J. "Novel, Stereoselective and Stereospecific Synthesis of Allenyl-phosphonates and Related Compounds *via* Palladium-Catalyzed Propargylic Substitution." *Adv. Synth. Catal.* **2011**, *353*, 1741-1755.

[52] Graham, J. P.; Wojcicki, A.; Bursten, B. E. "Molecular Orbital Description of the Bonding and Reactivity of the Platinum η^3-Porpargyl Complex [(η3-CH2CCPh)-Pt(PPh3)2]+." *Organometallics.* **1999**, *18*, 837-842.

[53] Ogoshi, S.; Tsutsumi, K.; Kurosawa, H. "Synthesis and structure of cationic η^3-allenyl/propargylpalladium complexes." *J. Organomet. Chem.* **1995,** *493*, C19-C21.

[54] Labrosse, J-R.; Lhoste, P.; Delbecq, F.; Sinou, D. "Palladium-Catalyzed Annulation of Aryl-1,2-diols and Propargylic Carbonates. Theoretical Study of the Observed Regioselectivities." *Eur. J. Org. Chem.* **2003**, 2813-2822.

[55] Kamer, P. C. J.; Van Leeuwen, P. W. N. M.; Reek, J. N. H. "Wide Bite Angle Diphosphines: Xantphos Ligands in Transtion Metal Complexes and Catalysis." *Acc. Chem. Res.* **2001**, *34*, 895-904.

[56] Daniels, D. S. B.; Jones, A. S.; Thompson, A. L.; Paton, R. S.; Anderson, E. A. "Ligand Bite Angle-Dependent Palladium-Catalyzed Cylcization of Propargylic Carbonates to 2-Alkynyl Azacycles or Cyclic Dienamides." *Angew. Chem. Int. Ed.* **2014**, *53*, 1915-1920.

[57] Ambrogio, I.; Cacchi, S.; Fabrizi, G.; Goggiamani, A.; Iazzetti, A. "Palladium-Catalyzed Nucleophilic Substitution of Propargylic Carbonates and Meldrum's Acid Derivatives." *Eur. J. Org. Chem.* **2015**, 3147-3151.

[58] Ardolino, M. J.; Morken, J. P. "Construction of 1,5-Enynes by Stereospecific Pd-Catalyzed Allyl-Propargyl Cross-Coupling." *J. Am. Chem. Soc.* **2012**, *134*, 8770-8773.

[59] Millán, A.; Álvarez de Cienfuegos, L.; Martín-Lasanta, A.; Campaña, A. G.; Cuerva, J. M. "Titanium/Palladium-Mediated Regioselective Propargylation of Ketones using Propargylic Carbonates as Pronucleophiles." *Adv. Synth. Catal.* **2011**, *353*, 73-78.

Chapter 2. Palladium-Catalyzed Regiodivergent Substitution of Propargylic Carbonates.

2.1 Introduction:

Chapter 1 of this dissertation was a review of electrophilic propargylic substitution to yield propargylated carbon-centered nucleophiles. Specifically, attention was focused on methods such as the Nicholas reaction or those mediated by, Lewis acids, Brønsted acids, and catalysts using various transition metals. However it was stated that, in general, the developed methods suffer from detrimental drawbacks that prevent their widespread application including: (a) limited substrate scope, (b) limit to highly stabilized carbon-centered nucleophiles, or (c) production of a large amount of waste.

Chapter 1 also covered the unique reactivity of palladium-catalyzed substitutions of propargylic electrophiles and it was demonstrated that palladium has the potential to generate structurally diverse metal-bound intermediates (Scheme 2.1). As a result, various products can be selectively accessed by altering the reaction conditions to favor one of the metal-bound intermediates, along with judicious choice of the activated nucleophile. However, palladium-catalyzed propargylation of carbon-centered nucleophiles is rare.

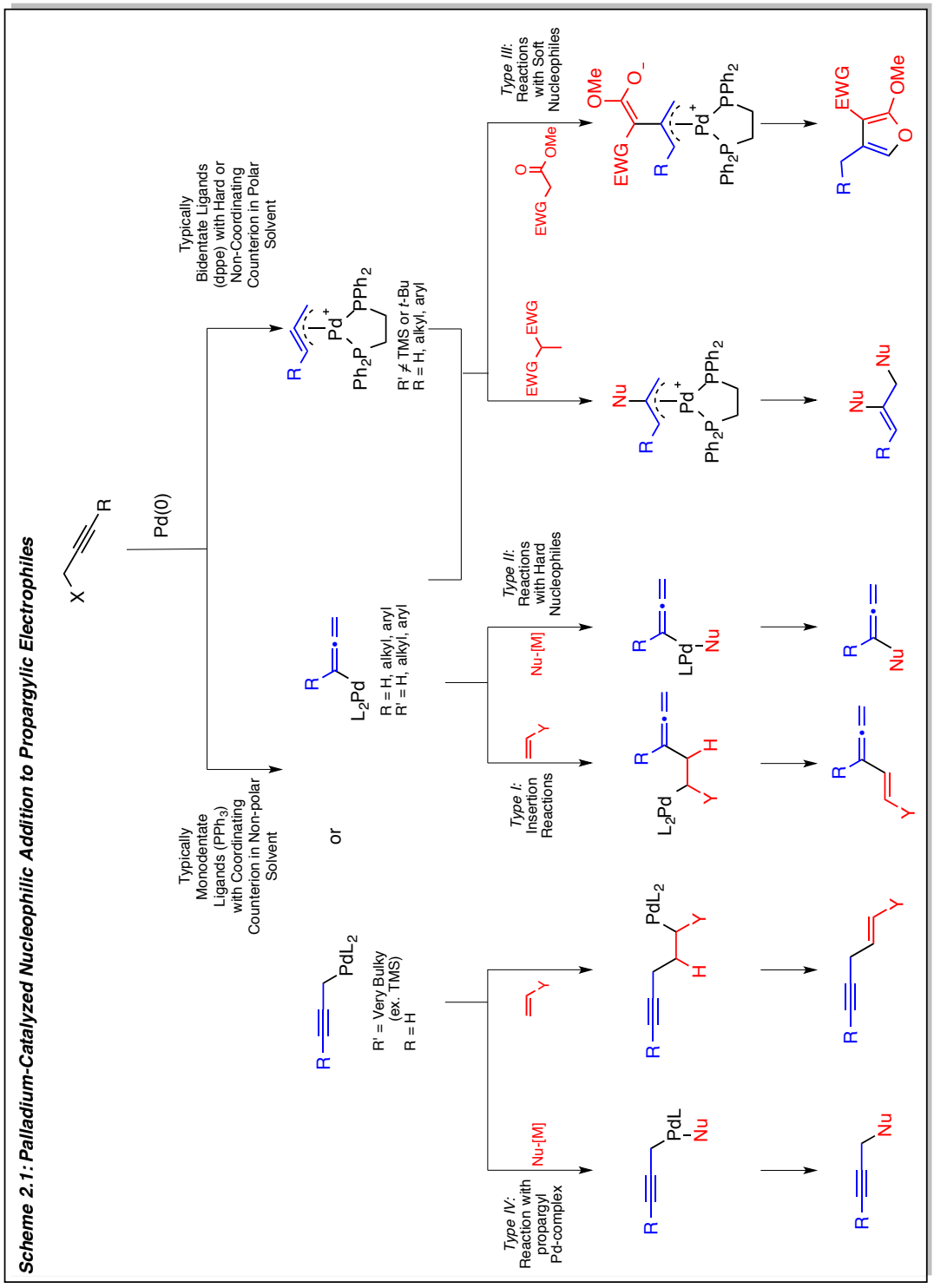

To briefly reiterate the typical reaction patterns of palladium-catalyzed substitutions of propargylic electrophiles, use of non-stabilized carbon nucleophiles (pK_a > 20) yield allene

products (Scheme 2.2). In contrast use of stabilized nucleophiles, such as malonates, commonly leads to *bis*-addition products, while selectivity for propargylic substitution is much more rare.[1,2,3,4] Additionally, only under select circumstances, primarily controlled through cyclization, have diene products arisen from the substitution of propargyl electrophiles.

Scheme 2.2: Potential Substitution Products.

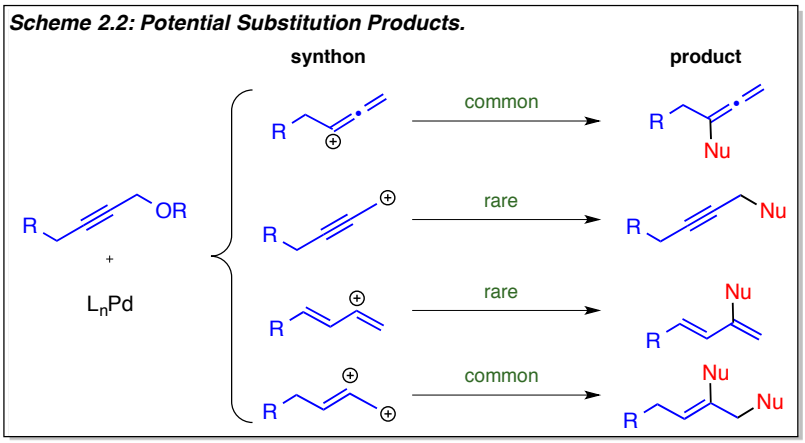

Based on the material presented above, palladium-catalyzed substitution of propargylic electrophiles offer the potential to develop a regiodivergent strategy to access functionally diverse products from a single class of starting materials. Chapter 2 of this dissertation will detail our contribution toward the development of a palladium-catalyzed, ligand-controlled, regiodivergent strategy to access both the rarely observed propargyl and dienyl isomers resulting from palladium-catalyzed propargylic substitution (Scheme 2.3). Further, in order to optimize the atom efficiency of the reaction, propargylic carbonates were employed as the electrophilic propargyl species to access both the activated electrophile and nucleophile *in situ*.

Scheme 2.3: Regiodivergent Substitution of Propargylic Carbonates.

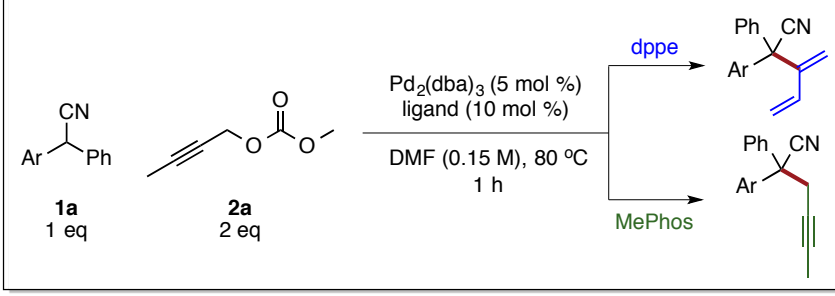

2.2 Ligand-Controlled Regiodivergent Strategies:

A major endeavor in the development of transition metal-catalyzed reactions typically entails the mass screening of various ligands for optimized reaction selectivity. Although effective, this protocol usually results in the optimized formation of one product class or bond-type. Occasionally, however, regiodivergent strategies arise in which orthogonal selectivity is observed for two or more products simply by changing the characteristics of the metal-coordinated ligand. Such examples optimize method development through production of various products with minimal reaction modification. However, development of ligand-controlled regiodivergent strategies is difficult since they must circumvent both steric and electronic properties of the substrate that typically govern product regioselectivity. In the following, a brief summary of recent regiodivergent strategies will be presented.

In 2016, Jiang and coworkers reported the gold-catalyzed, ligand-controlled regiodivergent hydroarylation of alkynes to access both *ortho*- and *para*-substituted cyclized products (Scheme 2.4).[5] Selectivity was controlled through electronic variations at the gold-center through employment of either electron-deficient tris(2,4-di-*tert*-butylphenyl)phosphine or electron-rich XPhos as the ligand source. When electron-deficient tris(2,4-di-*tert*-butylphenyl)phosphine was employed, selective formation of the *ortho*-substituted product was observed. Due to the electron-deficient metal center, along with the weakly coordinating $^{-}$OTs counterion, it was proposed that the gold catalyst would "pull" the coordinated alkyne toward the methoxyl amide directing-group resulting in the *ortho*-cyclized product.[6,7,8] Alternatively, employment of bulky, electron-rich XPhos would disfavor amide coordination through unfavorable steric interactions and "push" the coordinated alkyne away from the directing group resulting in the *para*-cyclized product.

Scheme 2.4: Au(I)-Catalyzed, Ligand Controlled Regiodivergent Cyclization.

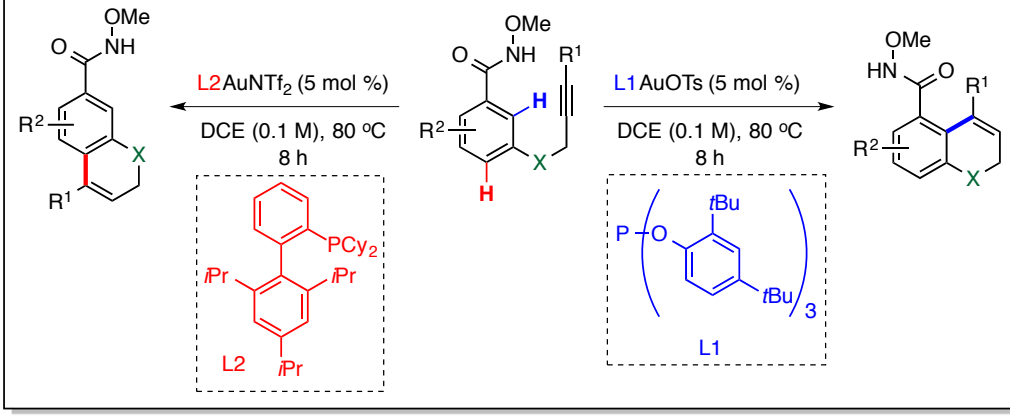

Alternatively, in regards to palladium-catalyzed regiodivergent methods, Cárdenas and coworkers reported the selective synthesis of allylboronates and alkenylboronates controlled by the coordinating strength of the employed ligand (Scheme 25).[9] It was proposed that cyclization to generate the alkenylboronate could be favored with weaker, more labile trialkylphosphine ligands (path a) that enable a free coordination site on the metal center upon dissociation. The empty coordination site could allow coordination of the alkyne followed by transmetalation and reductive elimination to yield the alkenylboroante product. Alternatively, more strongly coordinating, non-labile NHC ligands prevent cyclization by perturbing alkyne coordination and thereby promote direct transmetalation resulting the allylboronate product.

Scheme 2.5: Palladium-Catalyzed Regiodivergent Synthesis of Allylboronates and Alkenylboronates.

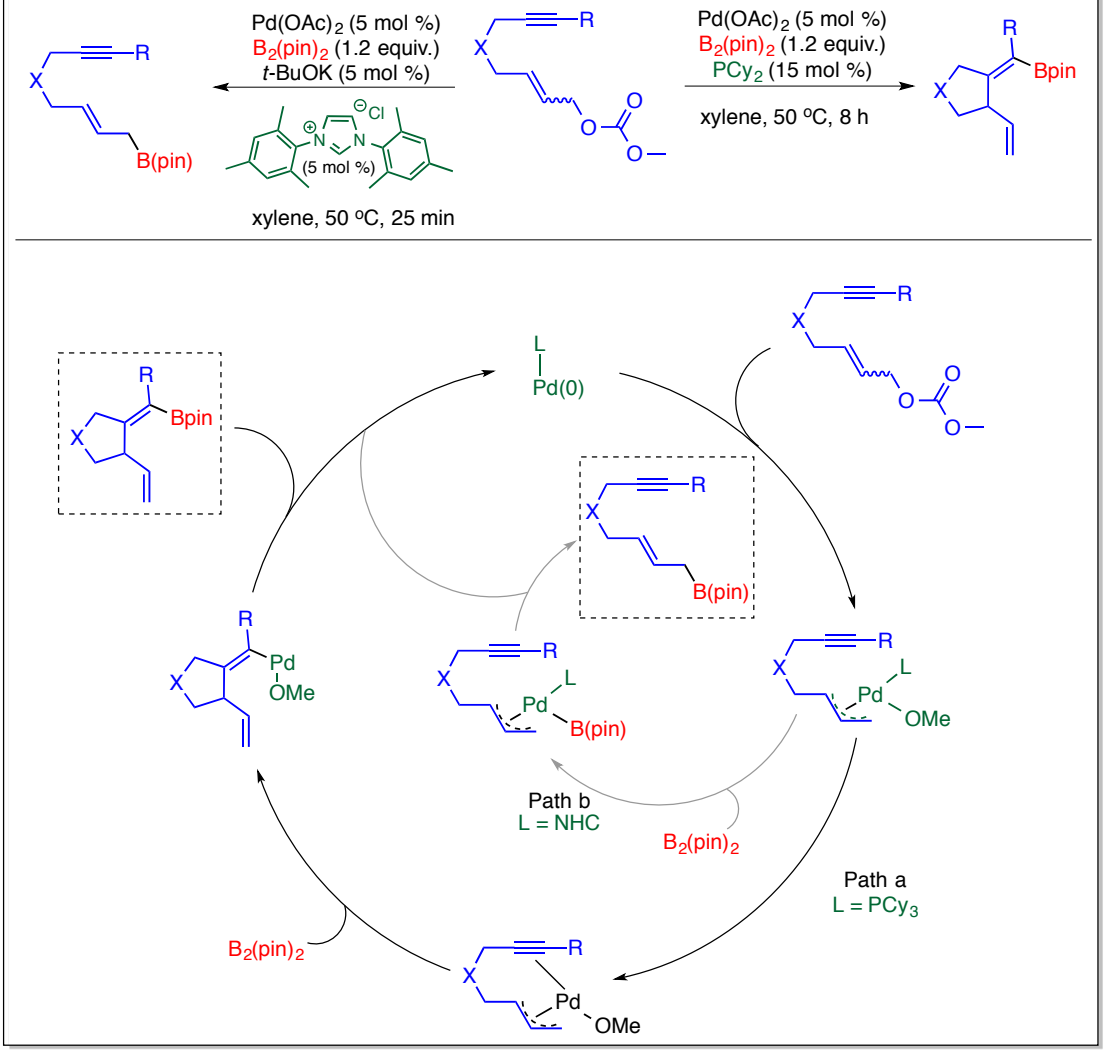

In 2014, and subsequent reports in 2015, Hall and coworkers reported a regiodivergent Suzuki-Miyaura cross-coupling to produce 2- and 4-substituted dihydropyrans and dehydropiperidines (Scheme 2.6).[10,11] As reported by Cárdenas, regioselective product formation was again attributed to the strength and steric environment about the coordinating ligand. For phosphine-based ligands, it was previously reported that the S_E' pathway is favored to generated intermediate **2.2 B**.[12,13] Further, use of more weakly coordinating trialkylphosphine ligands was reported to promote the σ-π-σ interconversion from intermediate **2.2 B** to the more stabilized

heteroatom conjugated σ-bond palladium(II) species **2.2 D** prior to reductive elimination to form the α-arylated product.[10] In contrast, more electron-rich and sterically bulky SPhos promotes rapid reductive elimination of the arylated palladium intermediate **2.2 B** to yield the γ-arylated product.

Scheme 2.6.: Regiodivergent Suzuki-Miyaura Cross-Coupling to Yield α- or γ-Arylated Heterocycles.

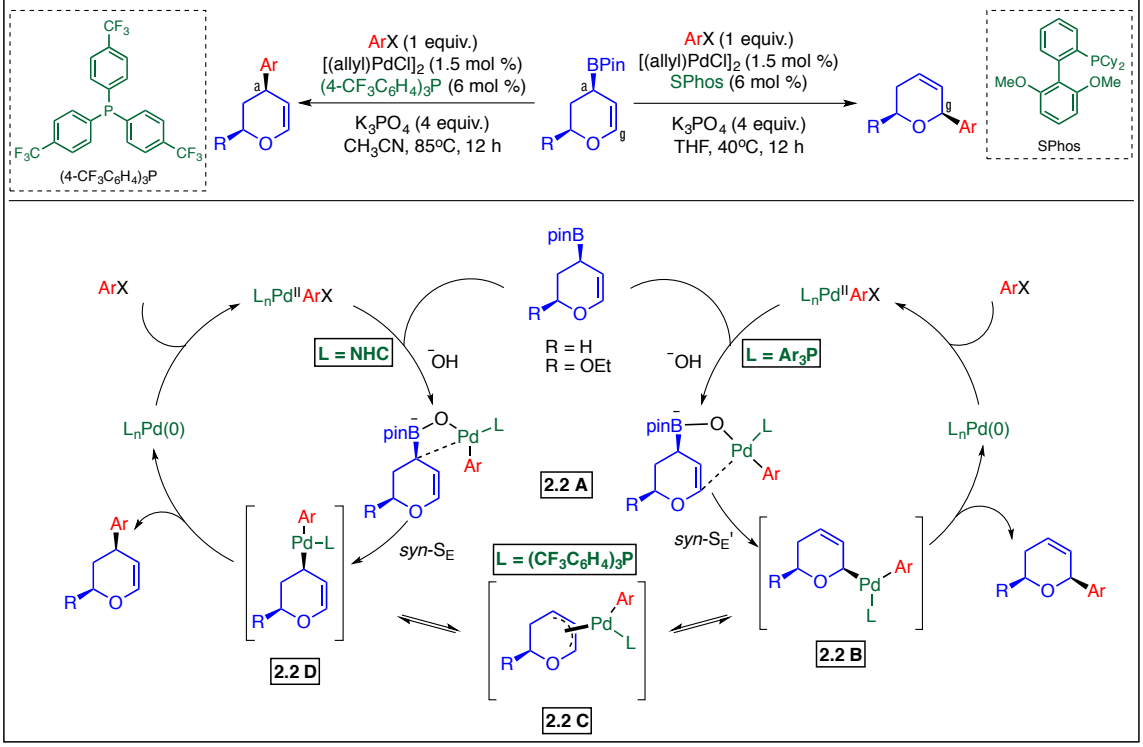

Lastly, most recently in 2016, Buchwald further expanded the known methods of regiodivergent Suzuki-Miyaura cross-coupling reactions to yield both substituted linear and branched prenyl functionalities (Scheme 2.7).[14] Initially, it was proposed, and eventually supported, that optimal product selectivity could be achieved by minimizing the σ-π-σ interconversion of palladium-bound intermediates through the employment of strongly coordinating ligands. Further, bias for a 6-membered transition-state could be favored with smaller ligands to yield the branched product while more sterically bulky ligands would disfavor the 6-membered transition-state to yield the linear isomer.

Scheme 2.7: Palladium-Catalyzed, Regiodivergent Suzuki-Miyaura Cross-Coupling.

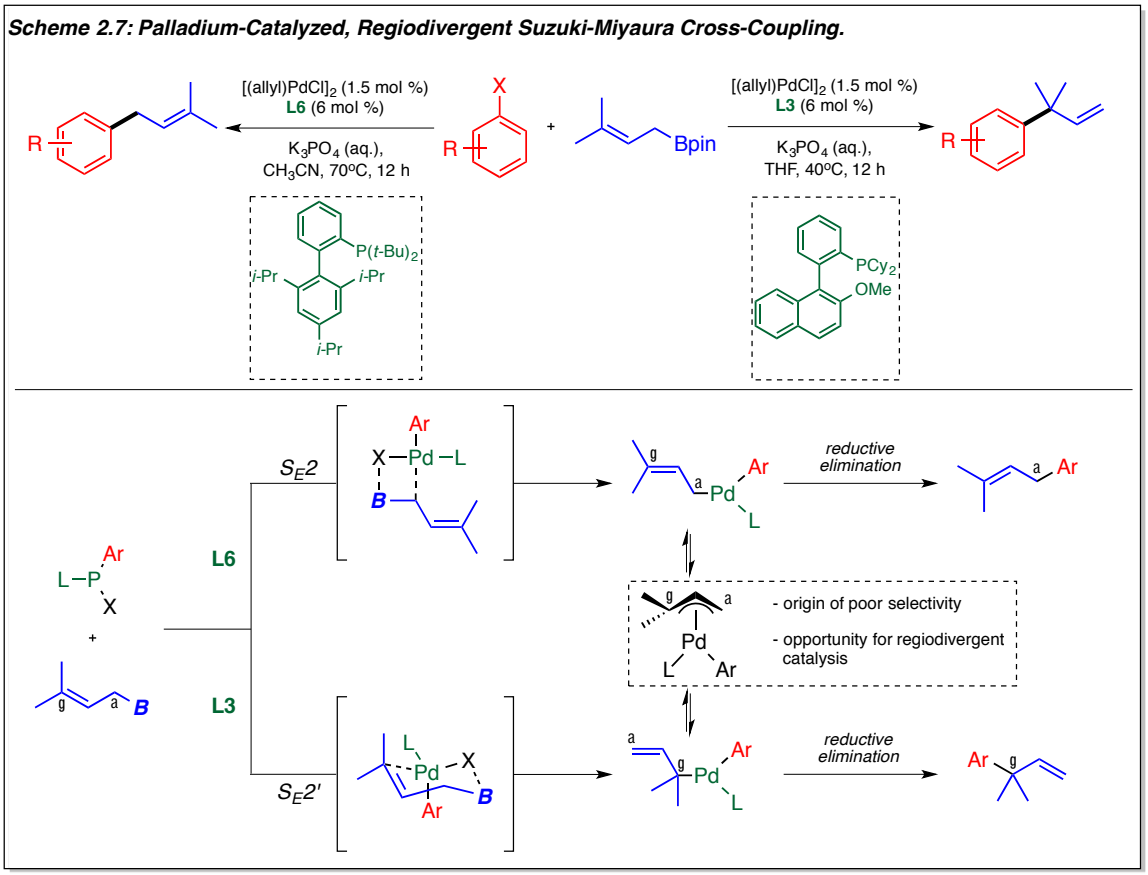

The above examples display methods in which both steric and electronic characteristics of the ligand are utilized to promote selective product formation. Such strategies can be invaluable to further predict substrate reactivity and potentially reveal alternative reaction pathways for new product formations.

2.3 Synthetic Significance and General Synthetic Methods that Yield 1,3-Butadiene Motifs:

Conjugated butadiene motifs are highly valuable synthetic targets for organic chemists. Much of their significance stems from their use as functional handles in total syntheses,[15,16] syntheses of biologically active compounds[17] and complex molecule syntheses.[18,19] Specifically, conjugated butadienes are known to undergo versatile and highly utilized synthetic transformations such as

inter- and intramolecular Diels-Alder reactions,[20,21,22,23] cycloadditions,[24,25,26] hydrogenations,[27] Sharpless epoxidation,[28,29] etc. Further, 1,3-dienes themselves are prevalent sub-structural motifs in natural products,[30,31,32] biologically active pharmaceuticals,[33] and materials.[34]

In general, current synthetic methods to synthesize 1,3-dienes rely heavily on transition metal-catalyzed cross-coupling reactions,[35] transformations from allene derivatives,[36] olefination reactions,[37] or cyclization reactions.[38] However, very few methods utilize the direct cross-coupling of butadiene synthons for diene incorporation. Furthermore, methods that report direct butadiene cross-coupling often require pre-formed organometallic or organoborane reagents and produce a large amount of waste. A brief summary of butadiene coupling methods will be presented in the following.

In 1981, Nunomoto, Kawakami, and Yamashita reported the dienylation of aryl and alkyl iodides with palladium tetrakis and copper iodide respectively (Scheme 2.8).[35g] However, the presented method suffered from a very limited substrate scope of both alkyl and aryl iodides. Further, the method also suffered from low to moderate isolated yields and some substrate dependent polymerization was also reported. Lastly, the presented methods were limited to aryl or alkyl-iodides and were incompatible with bromo- and chloro- derivatives.

Scheme 2.8: Pd(0) and Cu(I)-Catalyzed Dienylation.

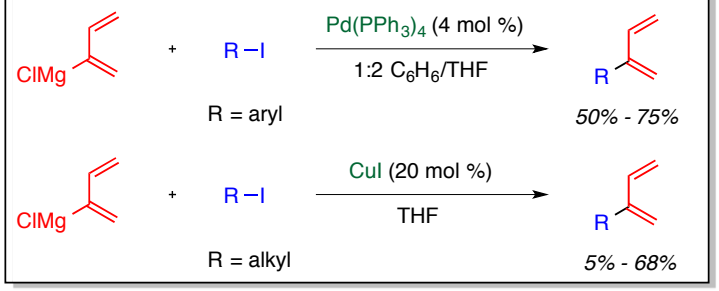

Two-years later in 1983, Shea and Pham reported an expansion of the substrate scope of 1,3-dienylation to selective 1,4-addition of α,β-unsaturated ketones along with cross-coupling of alkyl bromides and alkyl tosylates (Scheme 2.9).[35h] Unlike previous observations, the authors

report that selective dienylation occurred without contamination by the allene isomer. However, in general, product yields remained low to moderate and extended reaction times of 24-48 hours were required for successful 1,3-dienylation of alkyl bromides or tosylates.

Scheme 2.9: Copper-Catalyzed 1,4-Addition of 1,3-Butadiene.

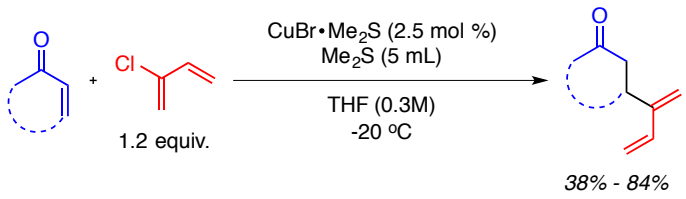

Alternatively, in 1999, Hatakeyama and coworkers reported the use of tributylstannylbuta-1,3-diene in the dienylation of aldehyde derivatives (Scheme 2.10).[35i] Although the reaction appeared to be selective, high yielding and could be conducted at room temperature, a stoichiometric amount of $SnCl_4$ was required to generate the homoallenyl intermediate required for subsequent 1,3-dienylation. Further, along with the narrow scope of alkyl and aryl aldehydes, tin reagents are toxic which promotes the development of more amiable reaction conditions.

Scheme 2.10: Buta-1,3-Dienylation of Aldehydes.

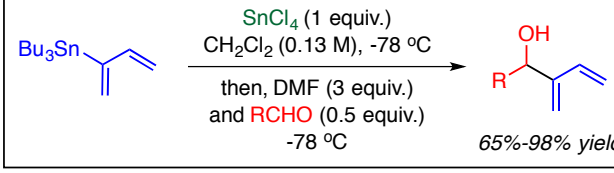

As an alternative, subsequent studies conducted by Venturello revealed that 1,3-dienylboronate esters could be used in the Suzuki cross-coupling of aryl or alkenyl iodides, bromides, chlorides and triflates (Scheme 2.11).[35d] In general, the developed method produced the 1,3-dienylated aryl species in moderate yields except for reactions of aryl chlorides which produced low yields of products.

Scheme 2.11: Suzuki Cross-Coupling of 1,3-dienylboronate Esters:

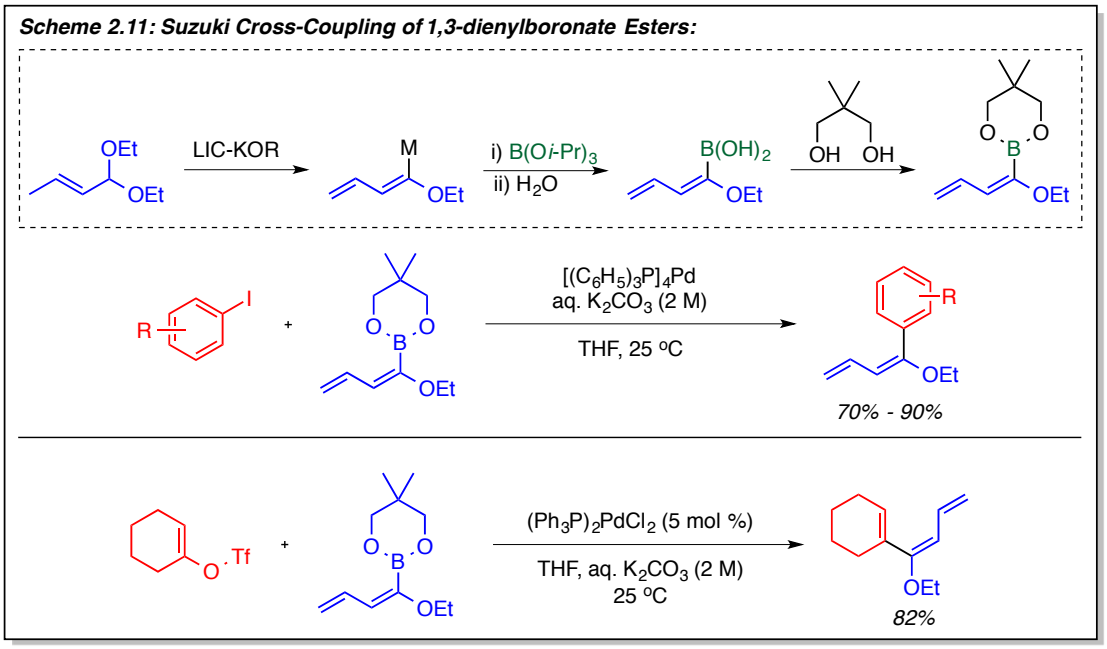

Similarly, Sherburn and Paddon-Row reported the utility of both the Kumada-Tamao-Corriu reaction and the Negishi reaction in the coupling of 1,3-dienes to efficiently synthesize dendralene hydrocarbons (Scheme 2.12).[35f] Specifically, these coupling methods provided a synthetic route to produce branched hydrocarbons in moderate yields and high selectivity as opposed to previously utilized methods. However, despite the obvious importance of these coupling reactions, one drawback lies in the production of a stoichiometric amount of metal waste along with the necessity for preformed organometallic species.

Scheme 2.12: 1,3-Butadiene Coupling to Yield Branched Hydrocarbons.

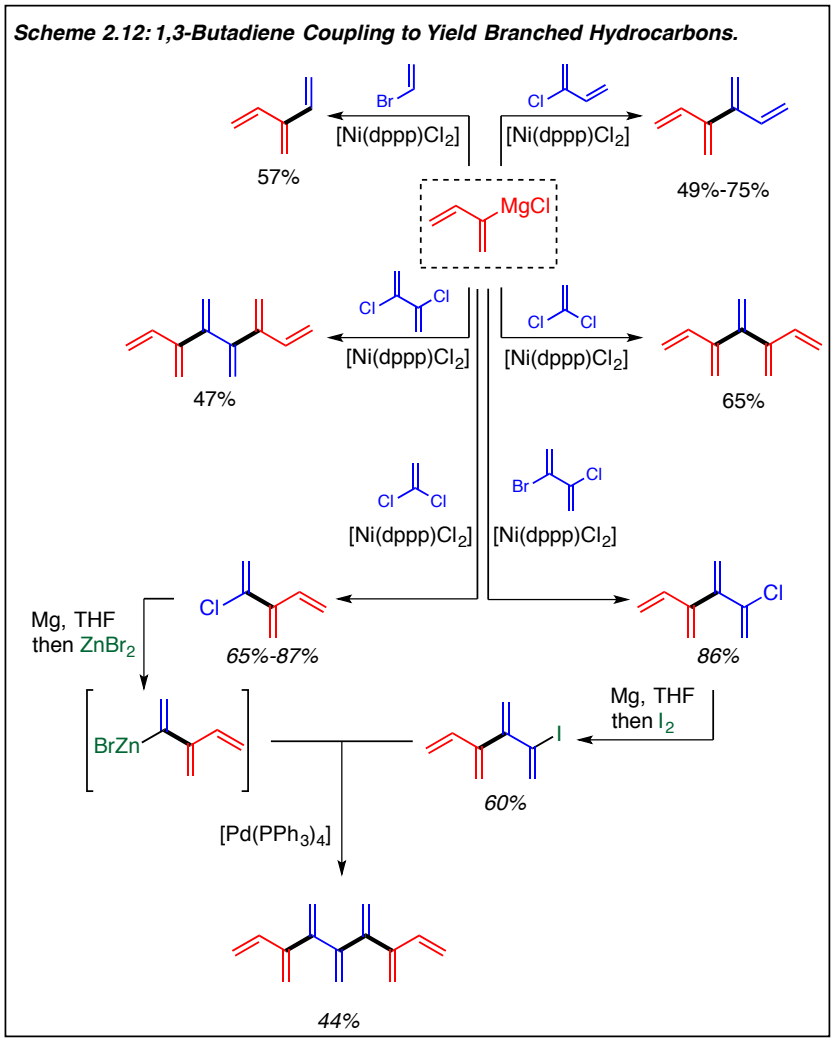

In attempt to circumvent the requirement of preformed organometallic compounds and expand the functional group tolerance of 1,3-dienylation methods, Connell and coworkers reported the asymmetric 1,3-dienylation of aldehyde derivatives from propargylic halides (Scheme 2.13).[36a] However, the method suffers from numerous inefficiencies compared to the previous presented methods. Although it does not require preformed organometallic compounds, successful dienylation occurs over a two-step process in which stoichiometric and super-stoichiometric amounts of numerous additives are employed. Further, attempts to develop a one-pot procedure resulted in low yields of the desired product.

Scheme 2.13: One-Pot Asymmetric 1,3-Dienylation of Aldehydes.

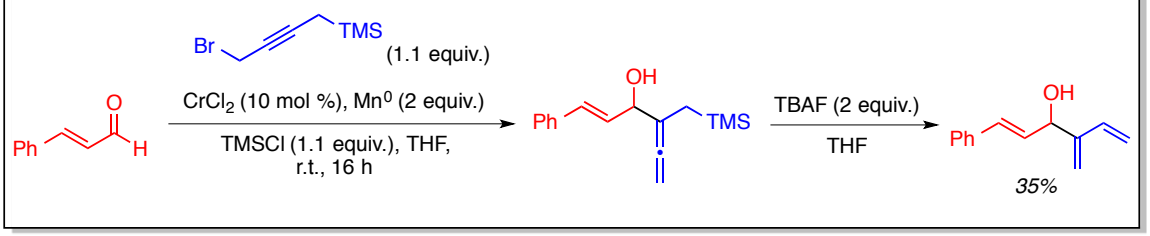

Alternatively, in 2013 Yu and coworkers reported the use of cyclopropylmethyl *N*-tosylhydrazones as butadiene surrogates in the palladium(0)-catalyzed 1,3-dienylation of aryl and heteroaryl motifs (Scheme 2.14).[35c] Their protocol bypasses the need for pre-formed organometallic species and occurs in one-step with moderate to high overall yields of the desired product. However, the method is limited to unsubstituted cyclopropyl rings and requires super-stoichiometric amounts of base. Further, in general, isolated products are formed with poor E/Z selectivity.

Scheme 2.14: Cross-coupling of Cyclopropylmethyl N-Tosylhydrazones as a Source of 1,3-Butadiene

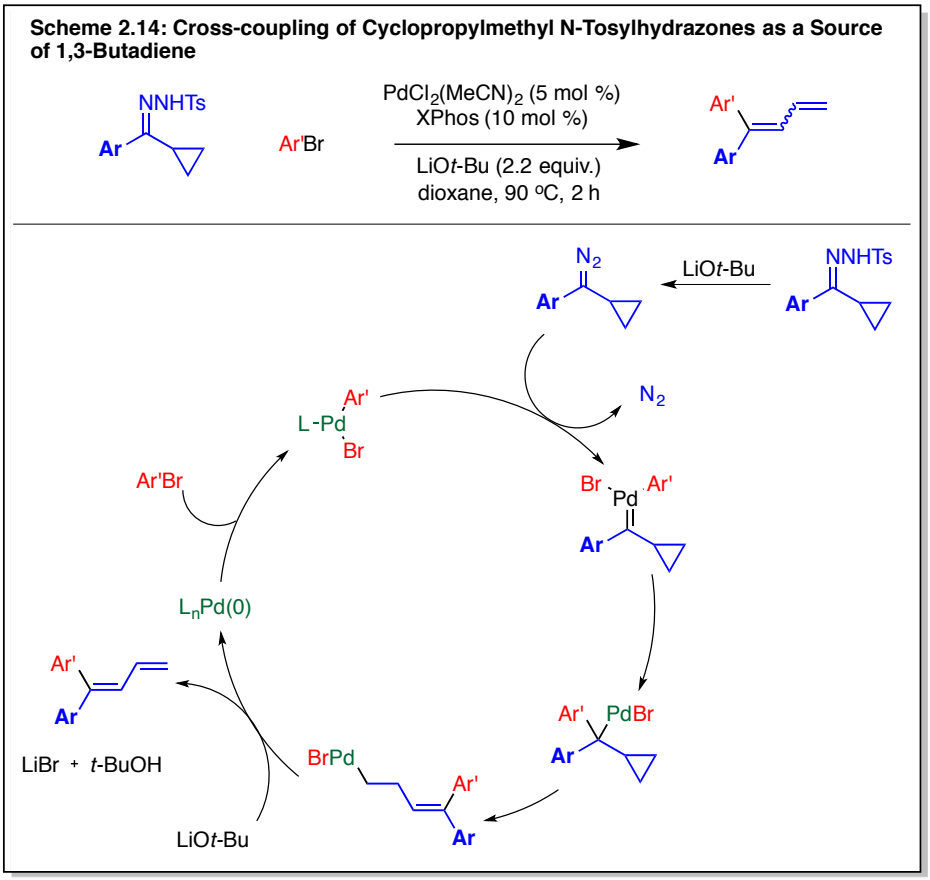

2.4 Development of Regiodivergent Synthesis of 1,3-Dienes

Current synthetic methods that achieve the direct cross-coupling of butadiene synthons rely heavily on pre-formed organometallic or organoborane reagents. Consequently, these methods lack step-economy and produce a significant amount of waste. Therefore, it would be useful to develop alternative methods to cross-couple 1,3-dienyl motifs via reaction of readily available starting materials under mild reaction conditions, while minimizing overall byproduct formation. To address this need, we hypothesized that propargyl carbonates could serve as diene electrophiles if, after mono-substitution to generate a palladium π-allyl intermediate,[39,40,41] elimination occurred instead of the more common attack by a second nucleophile (Scheme 2.15).[42] This method would provide facile access to 1,3-dienes in an atom and step economic

fashion via the formal coupling of an electrophilic 1,3-diene synthon. To the best of our knowledge, the use of a propargyl carbonate as a source of butadiene electrophile for cross-coupling has not been reported.[43]

Scheme 2.15: Proposed Synthetic Route to 1,3-Dienes.

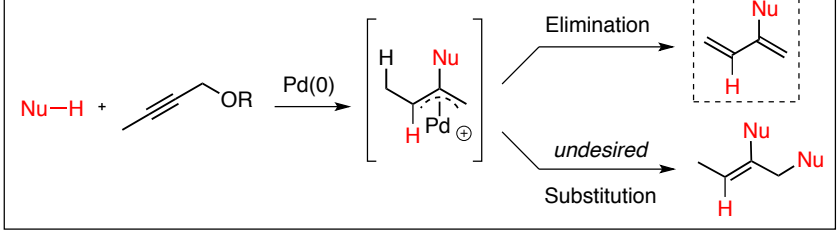

Given our experience with allylic alkylations of acetonitriles,[44] our optimization studies began by examining the effects of palladium catalyst, ligand, and solvent on the cross-coupling of methyl propargyl carbonate with commercially available diphenyl acetonitrile (Table 2.1). Initially, reaction conditions that previously provided high yields for allylation of tertiary acetonitriles with allylic alcohols were employed (entry 1).[44b] Under these conditions, GC/MS analysis revealed the formation of three isomeric products. Upon isolation and characterization of each product, it was confirmed that the major products were the 1,3-dienyl and propargyl isomers, with only minor formation of the allene. In order to optimize reaction conversion, we next conducted a solvent screen, which revealed that polar, aprotic solvents provided optimal conversion (entry 1, 3) compared to non-polar solvents (entries 2, 17, 18). In an attempt to determine the ligand effect on product ratios, several bidentate ligands were examined (entries 4-9). Excitingly, (diphenylphosphino)ethane (dppe) displayed optimal selectivity for the 1,3-diene product (entry 5). This result was in sharp contrast to previous accounts that report cyclization,[43] *bis*-addition,[42] or allenylation [45] as the major products arising from palladium-catalyzed substitution of propargylic carbonates using bidentate ligands.[45m,46]

Table 2.1: Optimization of Reaction Conditions:

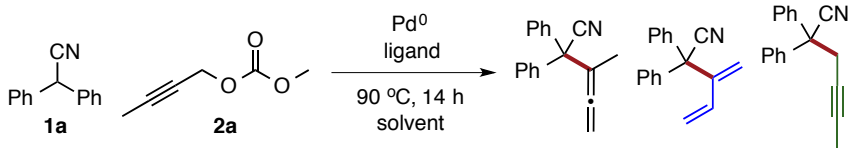

entry[a]	catalyst	ligand	solvent	**1a**[b]	allene[b]	diene[b]	propargyl[b]
1	$Pd(PPh_3)_4$	--	DMSO	26	3	40	31
2	$Pd(PPh_3)_4$	--	THF	62	1	15	22
3	$Pd(PPh_3)_4$	--	DMF	3	0	55	39
4	$Pd_2(dba)_3$	dppm	CH_3CN	28	4	42	27
5	**$Pd_2(dba)_3$**	**dppe**	**CH_3CN**	**3**	**0**	**94**	**3**
6	$Pd_2(dba)_3$	dppp	CH_3CN	5	0	87	8
7	$Pd_2(dba)_3$	dppb	CH_3CN	2	0.2	85	13
8	$Pd_2(dba)_3$	dppf	CH_3CN	1	0.5	74	24
9	$Pd_2(dba)_3$	XantPhos	CH_3CN	1	11	7	31
10	$Pd_2(dba)_3$	rac-BINAP	CH_3CN	4	0.5	70	24
11[c]	$Pd_2(dba)_3$	JohnPhos	CD_3CN	45	20	2	33
12[c]	$Pd_2(dba)_3$	tBu-MePhos	CD_3CN	22	29	2	47
13[c]	$Pd_2(dba)_3$	Cy-JohnPhos	CD_3CN	56	4	15	25
14[c]	$Pd_2(dba)_3$	MePhos	CD_3CN	11	3	19	67
15[c]	$Pd_2(dba)_3$	MePhos	DMSO-d_6	51	5	9	35
16[c]	**$Pd_2(dba)_3$**	**MePhos**	**d-DMF**	**43**	**3**	**7**	**47**
17[c]	$Pd_2(dba)_3$	MePhos	toluene-d_8	87	6	0.3	6
18[c]	$Pd_2(dba)_3$	MePhos	1,4-dioxane	87	5	1	8
19	$Pd_2(dba)_3$	MePhos	DMF	10	3	6	81
20	$Pd_2(dba)_3$	dppe	DMF	3	0	95	2
21	$Pd_2(dba)_3$	MePhos	DMF	10	3	6	81
22[d]	$Pd_2(dba)_3$	dppe	DMF	9	0	91	0
23[e]	$Pd_2(dba)_3$	dppe	CH_3CN	3	0	95	2
24[f]	**$Pd_2(dba)_3$**	**dppe**	**CH_3CN**	**1**	**0**	**98**	**1**
25[g]	**$Pd_2(dba)_3$**	**MePhos**	**DMF**	**1**	**3**	**6**	**90**
26[f,g]	$Pd_2(dba)_3$	--	DMF	--	--	--	--

a) diphenylacetonitrile (0.3 mmol), carbonate (0.3 mmol), catalyst (2.5 mol %), ligand (5 mol%), 0.15 M, 90 °C, 14 h. b) % conv. determined by GC/MS. c) diphenylacetonitrile (0.1 mmol), carbonate (0.1 mmol), reaction monitored by ^1H NMR spectroscopy. d) isolated yield 24%. e) 0.3 M f) 80 °C g) 0.6 mmol carbonate

With the optimized reaction conditions established for 1,3-dienylation of diphenylacetonitrile, we next evaluated the scope of α,α-diaryl acetonitrile derivatives in the substitution of methyl propargyl carbonate to synthesize 1,3-dienes (Scheme 2.16).[47] A variety of unsymmetric diarylacetonitrile reactants with electron-donating or withdrawing substituents provided product in good to excellent yields (**3b**, **3c**, **3h**, **3m**). Further, *meta*-chloro and *para*-bromo substituted arenes, which can be prone to other coupling reactions, were well tolerated (**3g**,

3e). Notably, a variety of substitution patterns were tolerated and even increased steric bulk at the *ortho*-position did not hinder product formation (**3c**, **3f**, **3h**). Unfortunately, basic heteroaryl moieties, while requiring reduced reaction time, lead to poor isolated yields (**3i**, **3j**). In contrast, the non-basic heteroaromatic 1,5-(dimethyl)pyrrole reactant provided product in good yield, as did arene substituents that contained extended conjugation (**3d**, **3f, 3k**). Lastly, styrene and benzoxazole derivatives were unsuccessful and only degradation of the starting material was observed (**3n, 3o**).

Scheme 2.16: Acetonitrile Scope of 1,3-Diene

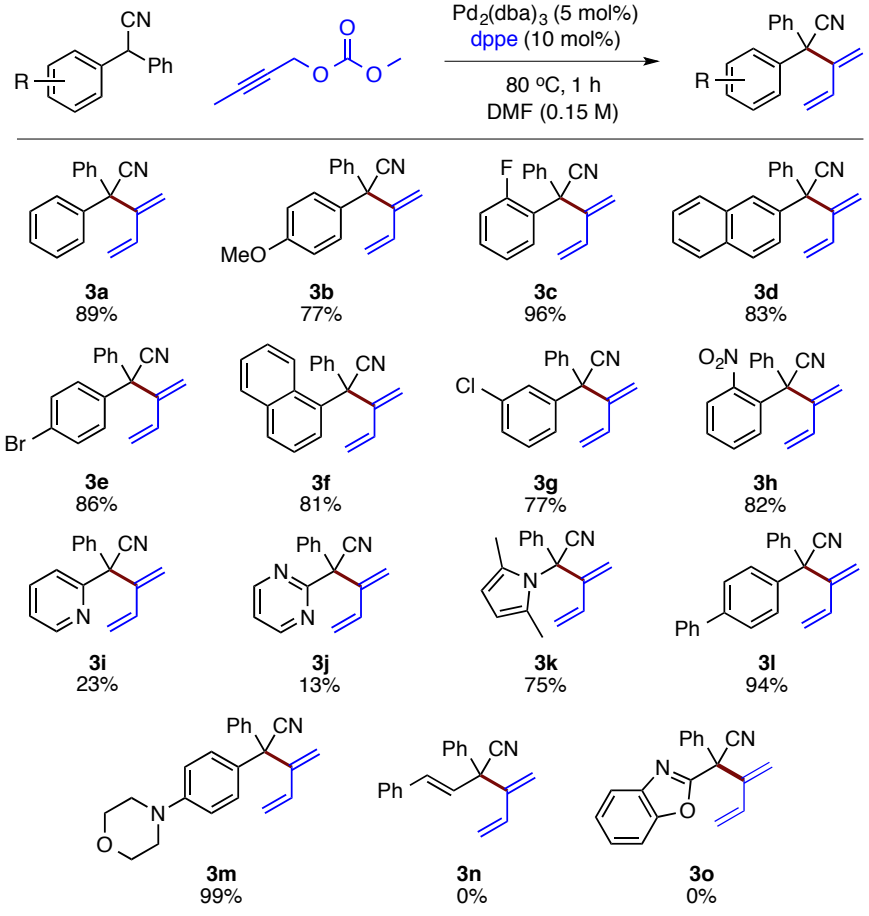

a) nitrile (0.3 mmol), carbonate (0.6 mmol), palladium (5 mol %), dppe (10 mol%), DMF (2 mL), 80 °C, 1 h. Isolated yields are reported.

With the functional group tolerance evaluated for the acetonitrile reaction component, other propargylic carbonates were examined to see if they could be used to form substituted diene products (Scheme 2.17). It was found that nucleophilic substitution of a terminally substituted ethyl or heptyl propargylic carbonate resulted in decreased isolated yields (**4b**, **4c**) compared to the model substrate **3a**. However, terminally substituted benzyl propargylic carbonate produced the substituted 1,3-diene product in moderate yield (**4d**). In attempt to access more intricate triene functionalities, an allyl substituent was utilized at the terminus of the propargylic carbonate, and the resulting triene was isolated in good yield (**4e**). Unfortunately, both terminal carbocyclic substituents along with internal alkyl substituents on the propargylic carbonate significantly hindered product formation (**4f-4g**).

Scheme 2.17: Scope of Substituted 1,3-Dienes.

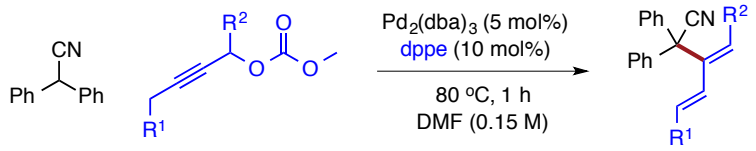

entry	carbonate	product	yield[b]	diene:propargyl[c]
4b	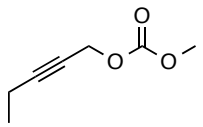	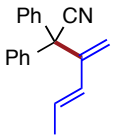	42%	>20:1
4c	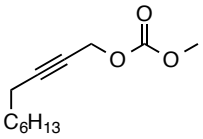	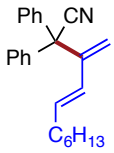	41%	9:1
4d	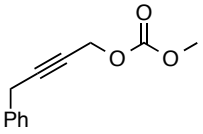	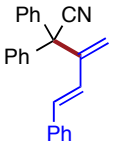	70%	>20:1
4e	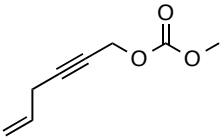	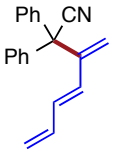	74%	9:1
4f	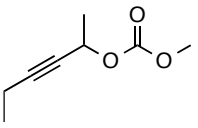	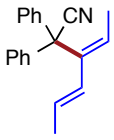	14% conversion[d]	nd
4g	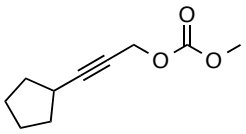	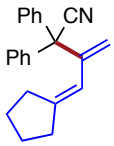	51%	1:1.2

a) nitrile (0.3 mmol), carbonate (0.6 mmol), palladium (5 mol %), dppe (10 mol%), DMF (2 mL), 80 °C, 1 h, isolated yields are reported. b) isolated yield. c) determined by ^{1}H NMR spectroscopy. d) determined by GC/MS

Fueled by the selective formation of the terminal 1,3-diene analogues, we next examined the potential pathways that could give rise to dienylation. It has been reported that palladium catalysts, in the presence of bidentate ligands, favor oxidative addition to form an η^3-propargyl

palladium intermediate.[41,48] Further, outer-sphere nucleophilic attack of η^3-propargyl palladium species often occurs exclusively at the center carbon.[49] Therefore, we envisioned that 1,3-dienylation could arise via two potential mechanistic pathways (Figure 2.1). In both cases, initial oxidative addition of the propargylic carbonate and subsequent loss of CO_2 would yield an η^3-propargyl palladium intermediate along with methoxide. Next, deprotonation of the pronucleophile would promote nucleophilic attack at the center carbon of the palladium intermediate to generate the corresponding palladacyclobutene (**B**).[50] If the mechanism proceeds via *path a*, protonation could occur from either methanol or nitrile, leading to π-allyl palladium intermediate **C**. Base-induced elimination would regenerate the palladium(0) catalyst and yield the 1,3-diene product.[51,52] Alternatively, β-hydride elimination from the palladacycle **B** could produce intermediate **E** followed by reductive elimination of the 1,3-diene product.

Figure 2.1. Potential Pathways for 1,3-Dienylation.

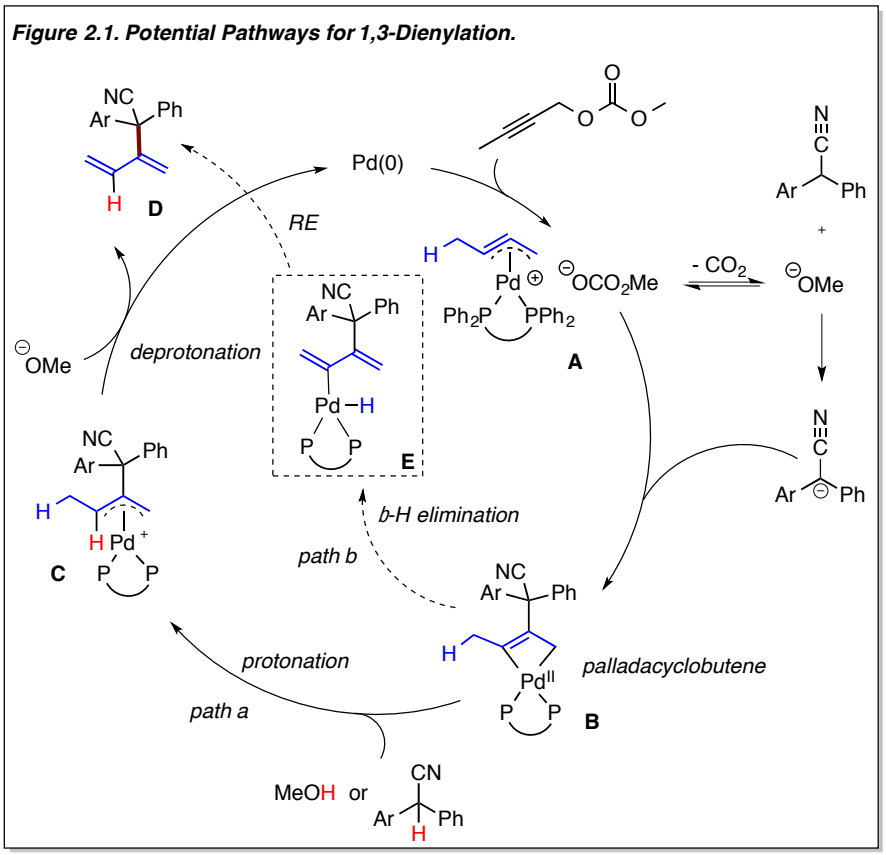

To determine which pathway is more likely, two isotopic labeling experiments were performed (Scheme 2.18). The terminally deuterated propargylic carbonate produced product with an 8.1:1.0 H/D ratio at the internal carbon of the diene as determined by ^{1}H NMR spectroscopy (Scheme 2.18a). A similar reaction that coupled deuterated diphenyl acetonitrile with protio methyl propargyl carbonate resulted in an H/D ratio of 1.2/1.0 (Scheme 2.18b). The differing ratios result from a primary KIE for protonation combined with the competitive protonation from nitrile and liberated methanol. These results are inconsistent with a mechanism involving β-hydride elimination/reductive elimination. Thus, we favor *path a* which involves protonation of the palladacyclobutene to form π-allyl palladium intermediate **C**.

Scheme 2.18: Deuterium Labeling Studies.

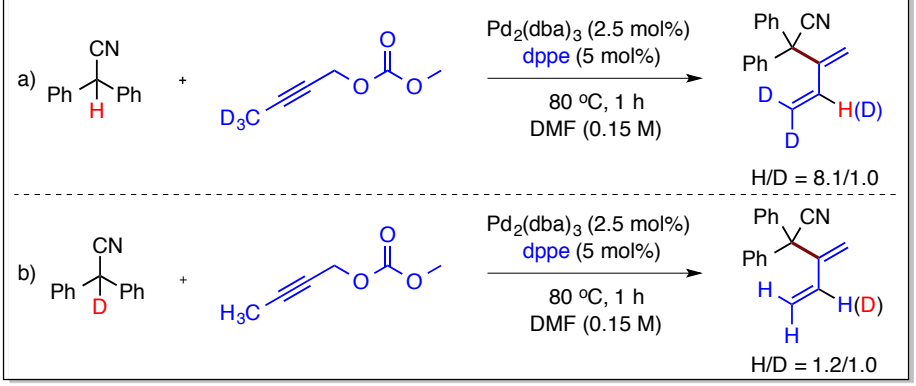

In attempt to trap a putative π-allyl intermediate, the palladium-catalyzed acetonitrile cross-coupling was performed with a propargylic carbonate that was unable to undergo elimination (Scheme 2.19). The observation of bis-substituted 1,3-diene product in 93% yield supports the kinetic feasibility of the formation of a π-allyl palladium intermediate required for *path a*.

Scheme 2.19: Trapping of Palladium p-Allyl Intermediate.

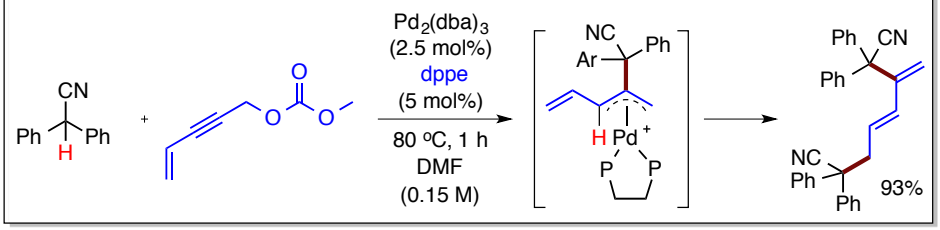

2.5 Development of Regiodivergent Synthesis of Propargylated Diaryl Acetonitrile Derivatives

As discussed previously, palladium-catalyzed substitution of methyl propargyl carbonate with α,α-diaryl acetonitrile pronucleophiles selectively forms 1,3-dienyl products in the presence of bidentate ligand dppe. During our reaction optimization studies, a change from bidentate (dppe) to monodentate (MePhos) ligand was accompanied by a switch in selectivity from the 1,3-dienyl isomer to the propargyl isomer under otherwise identical reaction conditions (Table 2.1). The development of palladium-catalyzed substitution of propargylic carbonates to selectively yield propargylated nucleophiles would not only expand on the limited strategies known for catalytic propargylation from internal propargylic electrophiles,[53] but also allow for a regiodivergent synthesis of 1,3-dienyl and propargyl acetonitrile derivatives solely by altering the denticity of the coordinating ligand.

Classically, the Nicholas reaction has been utilized as a method for propargylation utilizing propargylic alcohol reactants. Despite this, its utility has been limited by the requirement for stoichiometric organometallic reagents.[54] Recent focus on propargylation has been concentrated on the development of alternative methods using catalytic transition metals. For example, propargylic alkylation using internal propargylic carbonates was only recently reported by Iazzetti in 2015.[55] However, the reaction is limited to highly stabilized Meldrum's acid-like nucleophiles. Most other cases report palladium-catalyzed nucleophilic substitution of

propargylic carbonates that result in cycloaddition[42b,56] or formation of allene[45] derivatives. The method outlined herein aims to expand the scope of palladium-catalyzed propargylation to weakly acidic α,α-diaryl acetonitrile motifs that give rise to functionalized quaternary diarylmethane products.

Beginning with the same optimized reaction conditions developed for the 1,3-dienylation method, we merely changed the coordinating ligand from bidentate dppe to monodentate MePhos and evaluated the scope of diarylacetonitriles that undergo propargylation (Scheme 2.20). Analogous to results of 1,3-diene syntheses, the propargylation of acetonitriles containing 1-naphthyl, 2-naphthyl and *para*-substituted biphenyl derivatives provided very good yields without being influenced by steric hindrance (**5a**, **5d**, **5f**, **5l**). When *para*-methoxy, *ortho*-fluoro and *meta*-chloro-substituted phenyl rings were screened, all corresponding products were obtained in moderate-good isolated yields (**5b, 5c, 5g**). Altering the *ortho*-substituent to a nitro moiety resulted in an excellent isolated yield of 94% (**5h**). In contrast to their poor reactivity for dienylation, heterocyclic pyridine and pyrimidine derivatives were tolerated under the general reaction conditions and resulted in good isolated yields (**5i, 5j**). However, when the heterocycle was changed to a benzoxazole functionality, a dramatic decrease in yield was observed (**5o**, Scheme 8). A styrene derivative proceeded smoothly to the propargylated product albeit slightly lower yield compared to the polycyclic and bicyclic analogues (**5n**). Lastly, a *para*-morpholine substituted acetonitrile failed to undergo reaction (**5m**).

Scheme 2.20: Propargylation of Acetonitrile Derivatives.

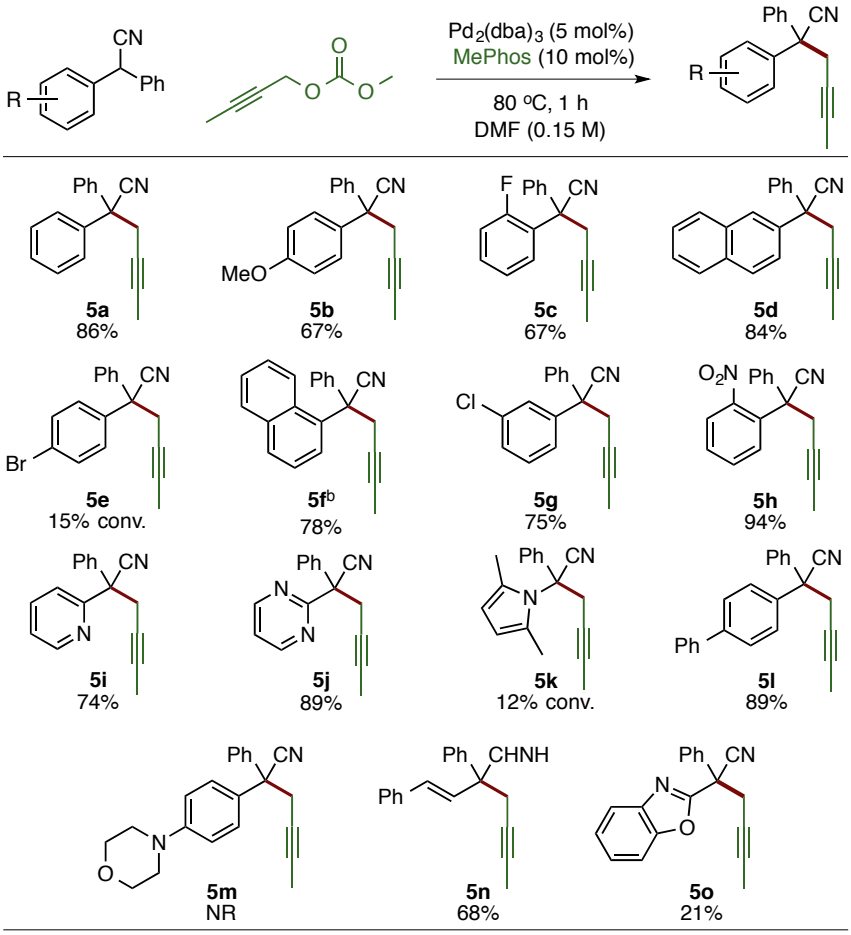

a) nitrile (0.3 mmol), carbonate (0.6 mmol), palladium (5 mol %), MePhos (10 mol%), DMF (2 mL), 80 °C, 1 h, isolated yields are reported. b) isolated with 10% allene and 7% bis addition product.

With the propargylation of various diaryl acetonitrile substrates examined, we next sought to apply our propargylation method to substituted propargylic carbonates (Scheme 2.21). Nucleophilic substitution of terminally substituted ethyl or heptyl propargylic carbonates was well tolerated (**6b**, **6c**). However, a decrease in isolated yield was observed with using a benzyl propargylic carbonate (**6d**). Gratifyingly, excellent isolated yields were obtained from propargylic carbonates that are terminally substituted by carbocycles (**6e-6g**). Further, allyl and internally substituted methyl and ethyl propargylic carbonates resulted in moderate-high isolated yields of

the propargylated products (**6h**, **6i**, **6j**, **6k**). Unfortunately, vinyl and phenyl propargylic carbonates were not well-tolerated under the standard reaction conditions (**6l, 6m**).

Scheme 2.21: Propargylation with Substituted Carbonates.

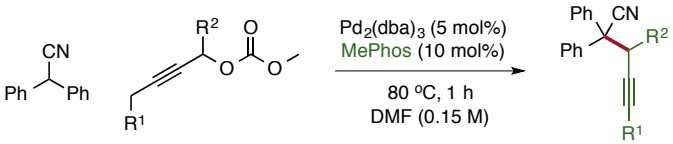

carbonate	product	carbonate	product
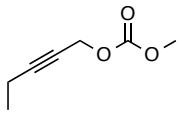	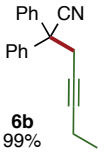 **6b** 99%	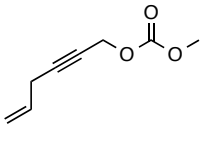	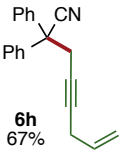 **6h** 67%
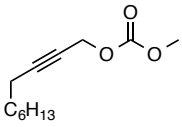	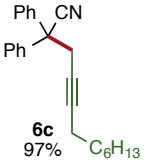 **6c** 97%	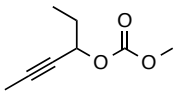	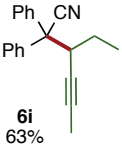 **6i** 63%
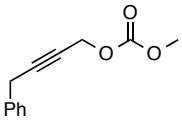	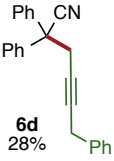 **6d** 28%	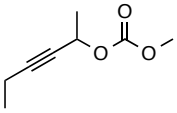	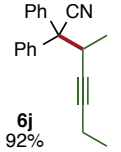 **6j** 92%
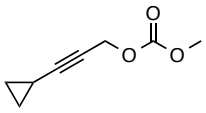	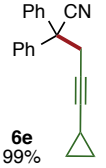 **6e** 99%	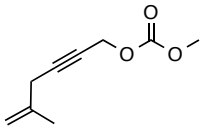	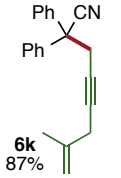 **6k** 87%
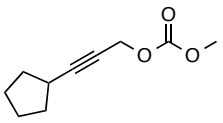	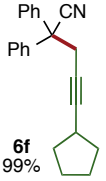 **6f** 99%	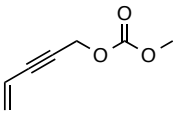	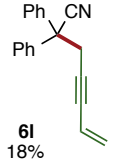 **6l** 18%
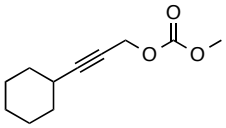	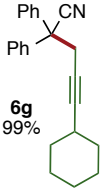 **6g** 99%	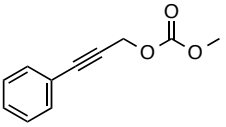	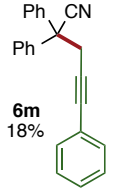 **6m** 18%

a) diphenylacetonitrile (0.3 mmol), carbonate (0.6 mmol), palladium (5 mol %), MePhos (10 mol%), DMF (2 mL), 80 °C, 1 h. Isolated yields are reported.

Having studied the synthetic scope of the dienylation and propargylation reactions, we aimed to convert our observation of denticity-dependent regioselectivity into a more formal mechanistic hypothesis. Beginning with Pd(0) and monodentate MePhos, we propose that oxidative addition of the propargylic carbonate would initially favor a cationic η^3-propargyl palladium intermediate **E** similar to intermediate **A** in the dienylation pathway (Figure 2.22). Contrary to bidentate ligand dppe, which forces outer-sphere nucleophilic attack of the activated nitrile, we propose that the mono-coordination of the MePhos ligand provides an open coordination site for binding of the activated nitrile.[44a,57] Binding of an anionic ligand has been observed to typically favor the η^1-allenyl species (in this case **G**).[41,48,52] Subsequent inner-sphere nucleophilic attack at the terminal allenyl carbon could then occur to provide the propargylated product.[44a,57]

Figure 2.22: Proposed Pathways for Regiodivergent Synthesis of 1,3-Dienes and Propargyl Derivatives.

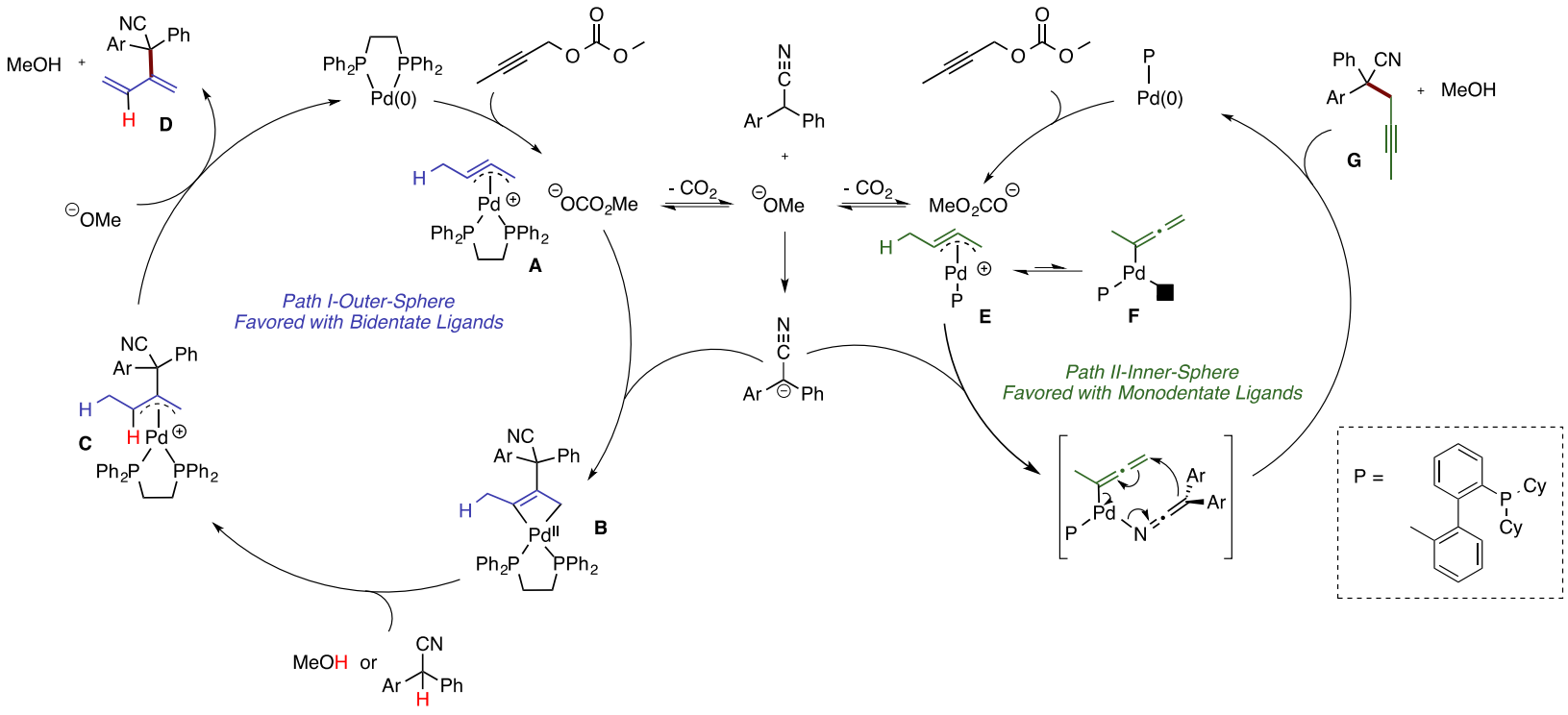

2.6 Conclusion

In conclusion, we report the regiodivergent synthesis of substituted 1,3-dienyl and propargyl quarternary diaryl methanes. We propose that regioselective nucleophilic substitution to palladium-bound intermediates occurs through two distinct reaction mechanisms that are controlled by the denticity of the ligand. Bidentate ligands block coordination of the nitrile nucleophile, favoring outer-sphere attack of the nucleophile, leading to dienylation. In contrast, a monodentate ligand allows coordination of the nucleophile to palladium, resulting in propargylation via inner sphere nucleophilic attack.

2.7 References for Chapter 2

[1] Tsuji, J.; Mandai, T. *Metal-Catalyzed Cross-Coupling Reactions*, (Eds.: F. Diedrich and P. J. Stange), Wiley-VCH, New York, **1998**, pp. 455.

[2] Tsuji, J. *Palladium(0)-Catalyzed Reactions of Propargyl Compounds. Palladium Reagents and Catalysis: New Prospectives for the 21st Century*, John Wiley & Sons Ltd, England, **2004**, pp. 543.

[3] Tsuji, J.; Mandai, T. "Palladium-Catalyzed Reactions of Propargylic Compounds in Organic Synthesis." *Angew. Chem. Int. Ed.* **1995**, *34*, 2589-2612.

[4] Kalek, M.; Stawinski, J. "Novel, Stereoselective and Stereospecific Synthesis of Allenyl-phosphonates and Related Compounds *via* Palladium-Catalyzed Propargylic Substitution." *Adv. Synth. Catal.* **2011**, *353*, 1741-1755.

[5] Ding, D.; Mou. T.; Feng, M.; Jiang, X. "Utility of Ligand Effect in Homogenous Gold Catalysis: Enabling Regiodivergent π-Bond-Activated Cyclization." *J. Am. Chem. Soc.* **2016**, *138*, 5218-5221.

[6] Luo, Y.; Ji, K.; Li, Y.; Zhang, L. "Tempering the Reactivities of Postulated α-Oxo Gold Carbenes Using Bidentate Ligands: Implication of Tricoordinated Gold Intermediates and the Development of an Expedient Bimolecular Assembly of 2,4-Disubstituted Oxazoles." *J. Am. Chem. Soc.* **2012**, *134*, 17412.

[7] Gualco, P.; Mallet-Ladeira, S.; Kameo, H.; Nakazawa, H.; Mercy, M.; Maron, L.; Amgoune, A.; Bourissou, D. "Coordination of a Triphosphine-Silane to Gold: Formation of a Trigonal Pyramidal Complex Featuring Au^{+} Si Interaction." *Organometallics*, **2015**, *34*, 1449.

[8] Yang, H.; Gabbaï, F. P. "Activation of a Hydroamination Gold Catalyst of a Redox-Noninnocent Clorostibine Z-Ligand." *J. Am. Chem. Soc*. **2015**, *137*, 13425.

[9] Martos-Redruejo, A.; Lópex-Durán, R.; Buñuel, E.; Cárdenas, D. J. "Ligand-controlled divergent formation of alkenyl- or allylboronates catalyzed by Pd, and synthetic applications." *Chem Commun*. **2014**, *50*, 10094.

[10] Ding, J.; Rybak, T.; Hall, D. G. "Synthesis of chiral heterocycles by ligand-controlled regiodivergent and enatiospecific Suzuki Miyaura cross-coupling." *Nat. Commun*. **2014**, 5:5474.

[11] Rybak, T.; Hall, D. G. "Stereoselective and Rigiodivergent Allylic Suzuki-Miyaura Cross-Coupling of 2-Ethoxydihydropyranyl Boronates: Synthesis and Conformation of Absolute Stereochemistry of Diospongin B." *Org. Lett.* **2015***, 17*, 4156-4159.

[12] Yamamoto, Y.; Takada, S.; Miyaura, N.; Iyama, T.; Tachikawa, H. "γ-Selective Cross-Coupling Reactions of Potassium Allyltrifluoroborates with Haloarenes Caalyzed by a Pd(0)/D-t-BPF or Pd(0)/Josiphos ((R,S)-CyPF-t-Bu) Complex: Mechanistic Studies on Transmetalation and Enatioselection." *Organometallics*. **2009**, *28*, 152-160

[13] Chausset-Boissarie, L.; Ghozati, K.; LaBine, E.; Chen, J. L.-Y.; Aggarwal, V. K.; Crudden, C. M. "Enantiospecific, Regioselective Cross-Coupling Reactions of Secondary Allylic Boronic Esters." *Chem. – Eur. J.* **2013**, *19*, 17698-17701.

[14] Yang, Y.; Buchwald, S. L. "Ligand-Controlled Palladium-Catalyzed Regiodivergent Suzuki-Miyaura Cross-Coupling of Allylboronates and Aryl Halides." *J. Am. Chem. Soc.* **2016**, *135*, 10642-10645.

[15] Dounay, A. B.; Overman, L. E. "The Asymmetric Heck Reaction in Natural Product Synthesis." *Chem. Rev*. **2003**, *103*, 2945-2963.

[16] Routier, S.; Mérour, J.-Y.; Dias, N.; Lansizux, A.; Bailly, C.; Lozach, O.; Meijer, L. "Synthesis and Biological Evaluation of Novel Phenylcarbazoles as Potential Anticancer Agents." *J. Med. Chem.* **2006**, *49*, 789-799.

[17] Erb, W.; Zhu, J. "From natural product to marketed drug: the tiacumicin odyssey." *Nat. Prod. Rep*. **2013**, *30*, 161-174.

[18] Johnson, W. S.; Telfer, S. J.; Cheng, S.; Schubert, U. "Cation-Stablizing Auxiliaries: A New Concept in Biomimetic Polyene Cyclization." *J. Am. Chem. Soc.* **1987**, *109*, 2517.

[19] Schreiber, S. L.; Kiessling, L. L.; "Synthesis of the Bicyclic Core of the Esperamicin/Calichemicin Class of Antitumor Agents." *J. Am. Chem. Soc.* **1988**, *110*, 631-633.

[20] Bear, B. R.; Sparks, S. M.; Shea, K. J. "The Type 2 Intramolecular Diels-Alder Reaction: Synthesis and Chemistry of Bridgehead Alkenes." *Angew. Chem. Int. Ed.* **2001**, *40*, 820-849.

[21] Pham, H. V.; Paton, R. S.; Ross, A. G.; Danishefsky, S. J.; Houk, K. N. "Intramolecular Diels-Alder Reactions of Cycloalkenones: Stereoselectivity, Lewis Acid Acceleration, and Halogen Substituent Effects." *J. Am. Chem. Soc.* **2014**, *136*, 2397-2403.

[22] Danishefsky, S.; Kahn M. "Regiospecificity in the Diels-Alder Reactions of an Enedione." *Tetrahedron Lett.* **1981**, *22*, 489-492.

[23] Pollini, G. P.; Bianchi, A.; Casolari, A.; Risi, C. D.; Zanirato, V.; Bertolasi, V. "An efficient approach to chiral nonracemic *trans*- and *cis*-decalin scaffolds for drimane and labdane synthesis." *Tetrahedron: Asymmetry*. **2004**, *15*, 3223-3231.

[24] Mamane, V.; Gress, T.; Krause, H.; Fürstner, A. "Platinum- and Gold-Catalyzed Cycloisomerization Reactions of Hydroxylated Enynes." *J. Am. Chem. Soc.* **2004**, *126*, 8654-8655.

[25] Patel, R. M.; Argade, N. P. "Palladium-Promoted [2 + 2 + 2] Cocyclization of Arynes and Unsymmetrical Conjugated Dienes: Synthesis of Justicidin B and Retrojusticidin B." *Org. Lett.* **2013**, *15*, 14-17.

[26] Roversi, E.; Vogel. P "Competition between hetero-Diels-Alder and chelotropic additions of sulfur dioxide to 2-substituted 1,3-butadienes. Synthesis of 2-(1-napthyl)-and 2-(2-naphthyl)-1,3-butadiene." *Helv. Chim. Acta*. **2002**, *85*, 761-771.

[27] Boaz, N. W. "Asymmetric Hydrogenation of Acyclic Enol Esters." *Tetrahedron Lett.* **1998**, *39*, 5505-5508.

[28] Hatakeyama, S.; Yoshida, M.; Esumi, T.; Iwabuchi, Y.; Irie, H.; Kawamoto, T.; Yamada, H.; Nishizawa, M. "A Novel Enantioselective Synthesis of (+)-Myriocin Based on the Chemistry of 1-Trimethylsilylbuta-2,3-dienes." *Tetrahedron Lett.* **1997**, *38*, 7887-7890.

[29] Yanagimoto, D.; Kawano, K.; Takahashi, K.; Ishihara, J.; Hatakeyama, S. "Enantioselective Route to Aryl(1,3-butadien-2-yl)methanols: Formal Synthesis of (-)-Sporochnol A." *Heterocycles.* **2009**, *77*, 249-253.

[30] Prakash, C. V. S.; Hoch, J. M.; Kingston, D. G. I. "Structure and Stereochemistry of New Cytotoxic Clerodane Diterpenoids form the Bark of *Casearia lucida* from the Madagascar Rainforest." *J. Nat. Prod.* **2002***, 65*, 100-107.

[31] Ohtsu, H.; Tokuda, H.; Nishino, H.; Matsunaga, S.; Tanaka, R. "Anti-tumor Promoting Diterpenes from the Stem Bark of *Thuja standishii* (Cupressaceae)." *Bioorg. Med. Chem.*, **2001**, *9*, 1911-1921.

[32] Peters, L.; Koenig, G. M. Terlau, H.; Wright, A. D. "Four New Bromotryptamine Derivatives from the Marine Bryozoan *Flustra foliacea*." *J. Nat. Prod.* **2002**, *65*, 1633.

[33] Wnuk, S. F.; Ro, B.-O.; Valdez, C. A.; Lewandowska, E.; Valdez, N. X.; Sacasa, P. R.; Yin, D.; Zhang, J.; Borchardt, R. T.; Clercq, E. D. "Sugar-Modified Conjugated Diene Analogues of Adenosine and Uridine: Synthesis, Interaction with *S*-Adenoxyl-L-homocysteine Hydrolase, and Antiviral and Cytostatic Effects." *J. Med. Chem.* **2002**, *45*, 2651-2658.

[34] Biermann, U.; Bornscheuer, U.; Meier, M. A. R.; Metzger, J. O.; Schaefer, H. J. "Oils and Fats as Renewable Raw Materials in Chemistry." *Angew. Chem. Int. Ed.* **2011**, *50*, 3854-3871.

[35] (a) Han, L.-B.; Ono, Y.; Yazawa, H. "Nickel-Catalyzed Addition of P(O)-H Bonds to Propargyl Alcohols: One-Pot Generation of Phosphinoyl 1,3-Butadienes." *Org. Lett.* **2005**, *7*, 2909-2911.

(b) Negishi, E.-I.; Huang, Z.; Wang, G.; Mohan, S.; Wang, C.; Hattori, H. "Recent Advances in Efficient and Selective Synthesis of Di-. Tri-, and Tetrasubstituted Alkenes via Pd-Catalyzed Alkenylation-Carbonyl Olefination Synergy." *Acc. Chem Res.* **2008**, *41*, 1474-1485.

(c) Yang, Q.; Chai, T.; Yu, Z. "Palladium-Catalyzed Cross-Coupling of Cyclopropylmethyl N-Tosylhydrazones with Aromatic Bromides: An Easy Access to Multisubstituted 1,3-Butadienes." *Tetrahedron Lett.* **2013**, *54*, 6485-6489.

(d) Tivola, P. B.; Deagostino, A.; Prandi, C.; Venturello, P. "A New Synthesis of Butadienyl- and Styrylboronic Esters: Highly Reactive Intermediates for Suzuki Cross-Coupling." *Org. Lett.* **2002**, *4*, 1275-1277.

(e) Ogasawara, M.; Ikeda, H.; Hayashi, T. "π-Allylpalladium-Mediated Catalytic Synthesis of Functionalized Allenes." *Angew. Chem. Int. Ed.* **2000**, *39*, 1042-1044.

(f) Payne, A. D.; Bojase, G.; Paddon-Row, M. N.; Sherburn. M. S. "Practical Synthesis of the Dendralene Family Reveals Alternation in Behavior." *Angew. Chem. Int. Ed.* **2009**, *48*, 4836-4839.

(g) Nunomoto, S.; Kawakami, Y.; Yamashita, Y. "Synthesis of 2-Substituted 1,3-Butadienes by Cross-Coupling Reaction of 2-(1,3-Butadienyl)magnesium Chloride with Alkyl or Aryl Iodides." *Bull. Chem. Soc. Jpn.* **1981**, *54*, 2831-2832.

(h) Shea, K. J.; Pham, P. Q. "Reactions of Organocopper Reagents Derived from Cloroprene. Conjugate Addition and Nucleophilic Substitution." *Tetrahedron Lett.* **1983**, *24*, 1003-1006.

(i) Luo, M.; Iwabuchi, Y.; Hatakeyama, S. "Regioselective Buta-1,3-dienylation of Aldehyde via Transmetallation of 2-Tributylstannylbuta-1,3-diene." *Synlett.* **1999**, 1109-1111.
(j) Xia, Y.; Xia, Y.; Liu, Z.; Zhang, Y.; Wang, J. "Palladium-Catalyzed Cross-Coupling Reaction of Diazo Compounds and Vinyl Boronic Acids: An Approach to 1,3-Diene Compounds." *J. Org. Chem.* **2014**, *79*, 7711-7717.

[36] (a) Durán-Galván, M.; Connell, B. T. "Asymmetric Synthesis of (1,3-Butadien-2-yl)methanols from Aldehydes via [1-(Silylmethyl)allenyl]methanols." *Eur. J. Org. Chem.* **2010**, 2445-2448.

(b) Huang, Y.; Yang, X.; Lv, Z.; Cai, C.; Kai, C.; Pei, Y.; Feng, Y. "Asymmetric Synthesis of 1,3-Butadienyl-2-carbinols by the Homoallenylboration of Aldehydes with a Chiral Phosphoric Acid Catalyst." *Angew. Chem. Int. Ed.* **2015**, *54*, 7299-7302.

(c) Djahanbini, D.; Cazes, B.; Gore, J. "Reactivite D'Esters α-Alleniques. Synthese Regiospecifique de Diesters γ-Alleniques et de Dienes-1,3." *Tetrahedron Lett.* **1984**, *25*, 203-206.

(d) Wu, L.; Huang, H.; Liang, Y.; Cheng, P. "Regio- and Stereoselective Synthesis of 2-Amino-dienes via Decarboxylative Amination of 4-(Ethoxycarbonyl-2,3-allenols by TsNCO." *J. Org. Chem.* **2014**, *79*, 11264-11269.

(e) Horváth, A.; Bäckvall, J.-E. "Palladium(II)-Catalyzed SN2' Reactions of α-Allenic Acetates. Stereoconvergent Synthesis of (*Z,E*)-2-Bromo-1,3-dienes." *J. Org. Chem.* **2001**, *66*, 8120-8126.

(f) Chen, Y.-Z.; Zhang, L.; Lu, A.-M.; Yang, F.; Wu, L. "α-Akkebtk Ethers as Starting Materials for Palladium Catalyzed Suzuki-Miyaura Couplings of Allenylphosphine Oxides with Arylboronic Acids." *J. Org. Chem.* **2015**, *80*, 673-680.

(g) Fu, C.; Ma, S. "Highly Regio- and Stereoselective Synthesis of 2(*E*),4-Alkadienoates via the Pd(0)-Catalyzed Reaction of Aryl Halides with 3,4-Alkadienoates." *Org. Lett.* **2005**, *7*, 1707-1709.

(h) Buzas, A. K.; Istrate, F. M.; Gagosz, F. "Gold(I)-Catalyzed Isomerization of Allenyl Carbinol Esters: An Efficient Access to Functionalized 1,3-Butadien-2-ol Esters." *Org. Lett.* **2007**, *9*, 985- 988.

(i) Yu, F.; Lian, X.; Ma, S. "Pd-Catalyzed Regio- and Stereoselective Cyclization-Heck Reaction of Monoesters of 1,2-Allenyl Phosphonic Acids with Alkenes." *Org. Lett.* **2007**, *9*, 1703-1706.

(j) Deng, Y.; Jin, X.; Ma, S. "Studies on Highly Stereoselective Addition-Elimination Reactions of 3-(Methoxycarbonyl)-1,2-allen-4-ols with MX. An Efficient Synthesis of 3-(Methoxycarbonyl)-2-halo-1,3(*Z*)-dienes." *J. Org. Chem.* **2007**, *72*, 5901-5904.

(k) Deng, Y.; Jin, X.; Fu, C.; Ma, S. "Efficient Highly Selective Synthesis of Methyl 2-(thynyl)alk-2(*E*)-enoates and 2-(1'-Chlorovinyl)alk-2(*Z*)-enoates from 2-(Methoxycarbonyl)-2,3-allenols." *Org. Lett.* **2009**, *11*, 2169-2172.

(l) Sabbasani, V. R.; Mamidipalli, P.; Lu, H.; Xia, Y.; Lee, D. "Subtle Electronic Effects in Metal-Free Rearrangement of Allenic Alcohols." *Org. Lett.* **2013**, *15*, 1552-1555.

(m) Xu, S.; Zhou, L.; Zeng, S.; Ma, R.; Wang, Z.; He, Z. "Phosphine-Mediated Olefination between Aldehydes and Allenes: An Efficient Synthesis of Trisubstituted 1,3-Dienes with High *E*-Selectivity."

(n) Naodovic, M.; Xia, G.; Yamamoto, H. "TBOxCrIIICl-Catalyzed Enantioselective Synthesis of 1,3-Butadien-2-ylcarbinols." *Org. Lett.* **2008**, *10*, 4053-4055.

(o) Hampton, C. S.; Harmata, M. "Regiodivergent Synthesis of 1- and 2-Arylsulfonyl 1,3-Dienes." *Org. Lett.* **2014**,*16*, 1256-1259.

Reviews:

(p) Ma, S. "Some Typical Advances in the Synthetic Applications of Allenes." *Chem. Rev.* **2005**, *105*, 2829-2871.

(q) Zimmer, R.; Dinesh, C. U.; Nandanan, E.; Khan, F. A. "Palladium-Catalyzed Reactions of Allenes." *Chem. Rev.* **2000**, *100*, 3067-3125.

[37] a) Wang, Y.; West, F. G. "A Convenient Method for the Synthesis of Terminal (*E*)-1,3-Dienes." *Synthesis*, **2002**, *1*, 99-103.

b) Negishi, E-i.; Huang, Z.; Wang, G.; Mohan, S.; Wang, C.; Hattori, H. "Recent Advances in Efficient and Selective Synthesis of Di-, Tri-, and Tetrasubstituted Alkenes via Pd-Catalyzed Alkenylation-Carbonyl Olefination Synergy." *Acc. Chem. Res.* **2008**, *41*, 1474.

c) Billard, F.; Robiette, R.; Pospíšil, J. "Julia-Kocienski Reaction-Based 1,3-Diene Synthesis: Aldehyde-Dependent (*E*,*E*/*E*,*Z*)-Selectivity." *J. Org. Chem.* **2012**, *77*, 6358.

[38] a) Nemoto, T.; Zhao, Z.; Yokosaka, T.; Suzuki, Y.; Wu. R.; Hamada, Y. "Palladium-Catalyzed Intramolecular *ipso*-Friedel-Crafts Alkylation of Phenols and Indoles: Rearomatization-Assisted Oxidative Addition." *Angew. Chem. Int. Ed.* **2013**, *52*, 2217.

b) Weinstabl, H.; Gaich, T.; Mulzer, J. "Application of the Rodriguez-Pattenden Photo-Ring Contraction: Total Synthesis and Configurational Reassignment of 11-Gorgiacerol and 11-Epigorgiacerol." *Org. Lett.* **2012**, *14*, 2834.

c) Inada, Y.; Nishibayashi, Y.; Uemura, S. "Ruthenium-Catalyzed Asymmetric Propargylic Substitution Reactions of Propargylic Alcohols with Acetone." *Angew. Chem. Int. Ed.* **2005**, *44*, 7715.

d) Tsuji, J.; Watanabe, H.; Minami, I.; Shimizu, I. "Novel Palladium-Catalyzed Reactions of Propargylic Carbonates with Carbonucleophiles under Neutral Conditions." *J. Am. Chem. Soc.* **1985**, *107*, 2196.

e) Duan, X-h, Liu, X-y.; Guo, L-n, Liao, M-c., Liu, W-M, Liang, Y-m. "Palladium-Catalyzed One-Pot Synthesis of Highly Substituted Furans by a Three-Component Annulation Reaction." *J. Org. Chem.* **2005**, *70*, 6980.

f) Ambrogio, I.; Cacchi, S.; Gabrizi, F.; Prastaro, A. "3-(o-Trifluoroacetamidoaryl)-1-propargylic esters: common intermediates for the palladium-catalyzed synthesis of 2-aminomethyl-, 2-vinylic, and 2-alkylindoles." *Tetrahedron*. **2009**, *65*, 8916.

g) Daniels, D. S. B.; Jones, A. S.; Thompson, A. L.; Paton, R. S.; Anderson, E. A. "Ligand Bite Angle-Dependent Palladium-Catalyzed Cyclization of Propargylic Carbonates to 2-Alkynyl Azacycles or Cyclic Dienamides." *Angew. Chem. Int. Ed.* **2014**, *53*, 1915.

[39] Ma, S. "Pd-Catalyzed Coupling Reactions Involving Propargylic/Allenylic Species." *Eur. J. Org. Chem.* **2004**, 1175-1183.

[40] Tsuji, J.; Mandai, T. "Palladium-Catalyzed Reactions of Propargylic Compounds in Organic Synthesis." *Angew. Chem. Int. Ed. Engl.* **1995**, *34*, 2589-2612.

[41] Su, C-C.; Chen, J-T.; Lee, G-H.; Wang, Y. "Direct Approach to Palladium-Mediated Cycloaddition. First Single-Crystal Structure and Convenient Synthesis of Zwitterionic η^3-Trimethylenemethane Palladium from Nucleophilic Addition of Carbanions to an Allenyl Complex." *J. Am. Chem. Soc.* **1994**, *116*, 4999-5000.

[42] For selected examples of dinucleophilic substitution of propargylic carbonates see:

(a) Guo, L-N.; Duan, X-H.; Bi, H-P.; Liu, X-Y.; Liang, Y-M. "Palladium-Catalyzed Carboannulation of Propargylic Carbonates and Nucleophiles to 2-Substituted Indenes." *J. Org. Chem.* **2007**, *72*, 1538-1540.

(b) Ren, Z-H.; Guan, Z-H.; Liang, Y-M. "Highly Regioselective Synthesis of Benz[a]anthracene Derivatives via Pd-Catalyzed Tandam C-H Activation/Biscyclization Reaction." *J. Org. Chem.* **2009**, *74*, 3145-3147.

(c) Bi, H-P.; Guo, L-N.; Gou, F-R.; Duan, X-H.; Liu, X-Y.; Liang, Y-M. "Highly Regio- and Stereoselective Synthesis of Indene and Benzo[b]furan Derivatives via a Pd-Catalyzed Carboannulation of propargyl Carbonates with Nucleophiles." *J. Org. Chem.* **2008**, *73*, 4713-4716.

(d) Yoshida, M.; Nakagawa, T.; Kinoshita, K.; Shishido, K. "Regiocontrolled Construction of Furo[3,2-c]pyran-4-one Derivatives by Palladium-Catalyzed Cyclization of Propargylic Carbonates with 4-Hydroxy-2-pyrones." *J. Org. Chem.* **2013**, *78*, 1687-1692.

(e) Nibbs, A. E.; Montgomery, T. D.; Zhu, Y.; Rawal, V. H. "Access to Spirocyclized Oxindoles and Indolenines via Palladium-Catalyzed Cascade Reactions of Propargyl Carbonates with 2-Oxotryptamines and Tryptamines." *J. Org. Chem.* **2015**, *80*, 4928-4941.

For reviews:

(f) Yoshida, M. "Development of Palladium-Catalyzed Transformations using Propargylic Carbonates." *Chem. Pharm. Bull.* **2012**, *60*, 285-299.

[43] (a) Nemoto, T.; Zhao, Z.; Yokosaka, T.; Suzuki, Y.; Wu. R.; Hamada, Y. "Palladium-Catalyzed Intramolecular ipso-Friedel-Crafts Alkylation of Phenols and Indoles: Rearomatization-Assisted Oxidative Addition." *Angew. Chem. Int. Ed.* **2013**, *52*, 2220.

(b) Weinstabl, H.; Gaich, T.; Mulzer, J. "Application of the Rodriguez-Pattenden Photo-Ring Contraction: Total Synthesis and Configurational Reassignment of 11-Gorgiacerol and 11-Epigorgiacerol." *Org. Lett.* **2012**, *14*, 2834-2837.

(c) Inada, Y.; Nishibayashi, Y.; Uemura, S. "Ruthenium-Catalyzed Asymmetric Propargylic Substitution Reactions of Propargylic Alcohols with Acetone." *Angew. Chem. Int. Ed.* **2005**, *44*, 7715-7717.

(d) Tsuji, J.; Watanabe, H.; Minami, I.; Shimizu, I. "Novel Palladium-Catalyzed Reactions of Propargyl Carbonates with Carbonucleophiles under Neutral Conditions." *J. Am. Chem. Soc.* **1985**, *107*, 2196-2198.

(e) Duan, X-h.; Liu, X-y.; Guo, L-n.; Liao, M-c.; Liu, W-M.; Liang, Y-m. "Palladium-Catalyzed One-Pot Synthesis of Highly Substituted Furans by a Three-Component Annulation Reaction." *J. Org. Chem.* **2005**, *70*, 6980-6983.

(f) Ambrogio, I.; Cacchi, S.; Gabrizi, F.; Prastaro, A. "3-(o-Trifluororacetamidoaryl)-1-propargylic Esters: Common Intermediates fo the Palladium-Catalyzed Synthesis of 2-aminomethyl-, 2-vinylic, and 2-alkylindoles." *Tetrahedron*. **2009**, *65*, 8916-8929.

(g) Daniels, D. S. B.; Jones, A. S.; Thompson, A. L.; Paton, R. S.; Anderson, E. A. "Ligand Bite Angle-Dependent Palladium-Catalyzed Cyclization of propargylic Carbonates to 2-Alkynyl Azacycles or Cyclic Dienamides." *Angew. Chem. Int. Ed.* **2014**, *53*, 1915-1920.

[44] (a) Recio, A.; Tunge, J. A. "Regiospecific Decarboxylative Allylation of Nitriles." *Org. Lett.* **2009**, *11*, 5630-5633.

(b) Lang, S. B.; Locascio, T. M.; Tunge, J. A. "Activation of Alcohols with Carbon Dioxide: Intermolecular Allylation of Weakly Acidic Pronucleophiles." *Org. Lett.* **2014**, *16*, 4308-4311.

(c) Maji, T.; Ramakumar, K.; Tunge, J. A. "Retro-Claisen Benzylation: Direct Use of Benzyl Alcohols in Pd-Catalyzed Couplings with Nitriles." *Chem. Commun.* **2014**, *50,* 14045-14048.

(d) Ariyarathna, Y.; Tunge, J. A. "Multicomponent Decarboxylative Allylations." *Chem. Commun*. **2014**, *50*, 14049-14052.

[45] For reports of allene syntheses from palladium-catalyzed reactions with propargyl carbonates:

(a) Shu, W.; Jia, G.; Ma. S. "Palladium-Catalyzed Regioselective Cyclopropanating Allenylation of (2,3-Butadienyl)malonates with Propargylic Carbonates and Their Application to Synthesize Cyclopentaenones." *Org. Lett.* **2009**, *11*, 117-120.

(b) Shu, W.; Ma, S. "Palladum-Catalyzed Synthesis of 1,3,4-alkatrien-2-yldihydrofurans from 2,3-allenylacetylacetates and Propargylic Carbonates and Their Application to Synthesize Polysubstituted Dihydrofurylcyclopentenones." *Tetrahedron*. **2010**, *66*, 2869-2874.

(c) Kalek, M.; Johansson, T.; Jezowska, M.; Stawinski, J. "Palladium-Catalyzed Propargylic Substitution with Phosphorus Nucleophiles: Efficient, Stereoselective Synthesis of Allenylphosphonates and related Compounds." *Org. Lett.* **2010**, *12,* 4702-4704.

(d) Chen, G.; Zhang, Y.; Fu, C.; Ma, S. "A Facile Synthesis of β-Allenyl Furanimines via Pd-Catalyzed Cyclization of 2,3-allenamides with Propargylic Carbonates." *Tetrahedron*. **2011**, *67*, 2332-2337.

(e) Ye, J.; Li, S.; Ma, S. "Palladium-Catalyzed Cyclization Reactions of 2,3-Allenyl Amines with Propargylic Carbonates." *Org. Lett.* **2012**, *14*, 2312-2315.

(f) Wang, Y.; Zhang, W.; Ma, S. "A Room-Temperature Catalytic Asymmetric Synthesis of Allenes with ECNU-Phos." *J. Am. Chem. Soc*. **2013**, *135*, 11517-11520.

(g) Yoshida, M.; Ohno, S.; Namba, K. "Synthesis of Substituted Tetrahydrocyclobuta[b]benzofurans by Palladium-Catalyzed Substitution/[2+2] Cycloaddition of Propargylic Carbonates with 2-Vinylphenols." *Angew. Chem. Int. Ed.* **2013**, *52*, 13597-13600.

(h) Ye, J.; Ma, S. "Palladium-Catalyzed Cyclization Reactions of Allenes in the Presence of Unsaturated Carbon-Carbon Bonds." *Acc. Chem. Res.* **2014**, *47*, 989-1000.

Cu:

(i) Ito, H.; Sasaki, Y.; Sawamura, M. "Copper(I)-Catalyzed Substitution of Propargylic Carbonates with Diboron: Selective Synthesis of Multisubstituted Allenylboronates." *J. Am. Chem. Soc*. **2008**, *130*, 15774-15775.

(j) Zhong, C.; Sasaki, Y.; Ito, H.; Sawamura, M. "The Synthesis of Allenes by Cu(I)-Catalyzed Regio and Stereoselective Reduction of Propargylic Carbonates with Hydrosilanes." *Chem. Commun*. **2009**, 5850-5860.

(k) Deutsch, C.; Lipshutz, B. H.; Krause, N. "(NHC)CuH-Catalyzed Entry to Allenes via Propargylic Carbonates S_N2'-Reductions." *Org. Lett.* **2009**, *11*, 5010-5012.

Rh:

(l) Ohmiya, H.; Ito, H.; Sawamura, M. "General and Functional Group-Tolerable Approach to Allenylsilanes by Rhodium-Catalyzed Coupling Between Propargylic Carbonates and a Silylboronate." *Org. Lett.* **2009**, *11*, 5618-5620.

For reviews:

(m) Tsuji, J.; Mandai, T. "Palladium-Catalyzed Reactions of Propargylic Compounds in Organic Synthesis." *Angew. Chem. Int. Ed. Engl.* **1995**, *34*, 2589-2612.

[46] Su, W.; Gong, T-J.; Lu, X.; Xu, M-Y.; Yu, C-G.; Xu, Z-Y.; Yu, H-Z.; Xiao, B.; Fu, Y. "Ligand-Controlled Regiodivergent Copper-Catalyzed Alkylboration of Alkenes." *Angew. Chem. Int. Ed.* **2015**, *54*, 12957-12961.

[47] Note that extended reaction time resulted degradation of the 1,3-diene products.

[48] (a) Tsutsumi, K.; Yabukami, T.; Fujimoto, K.; Kawase, T.; Morimoto, T.; Kakiuchi, K. "Effects of a Bidentate Phosphine Ligand on Palladium-Catalyzed Nucleophilic Substitution Reactions of Propargyl and Allyl Halides with Thiol." *Organometallics*. **2003**, *22*, 2996-2999.

(b) Tsutsumi, K.; Ogoshi, S.; Nishiguchi, S.; Kurosawa, H. "Synthesis, Structure, and Reactivity of Neutral η3-Propargylpalladium Complexes." *J. Am. Chem. Soc*. **1998**, *120*, 1938-1939.

(c) Tsutsumi, K.; Kawase, K.; Kakiuchi, K.; Ogoshi, S.; Okada, Y.; Kurosawa, H. "Synthesis and Characterization of Some Cationic η3-Propargylpalladium Complexes." *Bull. Chem. Soc. Jpn.* **1999**, *72*, 2687-2692.

[49] (a) Blosser, P. W.; Schimpff, D. G.; Gallucci, J. C.; Wojcicki, A. "Interconversion of η1-Propargyl, η1-Allenyl, η3-Propargyl/allenyl Ligands on Platinum. Synthesis, Structure, and Reactivity of [(Ph3P)2Pt(η3-CH2CCPh)]O3SCF3." *Organometallics*. **1993**, *12*, 1993-1995.

(b) Kurosawa, H.; Ogoshi, S. "Structure-Reactivity Relationship in Allyl and 2-Propynyl Complexes of Group 10 Metals Relevant to Homogeneous Catalysis." *Bull. Chem. Soc. Jpn*. **1998**, *71*, 973-984.

(c) Tsutsumi, K.; Ogoshi, S.; Kakiuchi, K.; Nishiguchi, S.; Kurosawa, H. "Cross-Coupling Reactions Proceeding Through η1- and η3-Propargyl/Allenyl-Palladium(II) Intermediates." *Inorganica Chimica Acta*. **1999**, *296*, 37-44.

(d) Huang, T-M.; Chen, J-T.; Lee, G-H.; Wang, Y. "A Versatile Route to the β-Substituted π-Allyl Complexes via Addition to a Cationic η3-Propargyl Complex of Platinum." *J. Am. Chem. Soc*. **1993***, 115*, 1170-1171.

[50] (a) Casey, C. P.; Nash, J. R.; Yi, C. S.; Selmeczy, A. D.; Chung, S.; Powell, D. R.; Hayashi, R. K. "Kinetic Addition of Nucleophiles to η3-Propargyl Rhenium Complexes Occurs at the Central Carbon to Produce Rhenacyclobutenes." *J. Am. Chem. Soc*. **1998**, *120*, 722-733.

(b) Labrosse, J-R.; Lhoste, P.; Delbecq, F.; Sinou, D. "Palladium-Catalyzed Annulation of Aryl-1,2-diols and Propargylic Carbonates. Theoretical Study of the Observed Regioselectivities." *Eur. J. Org. Chem.* **2003**, 2813-2822.

[51] (a) Xia, Y.; Xia, Y.; Liu, Z.; Zhang, Y.; Wang, Z. "Palladium-Catalyzed Cross-Coupling Reaction of Diazo Compounds and Vinyl Boronic Acids: An Approach to 1,3-Diene Compounds." *J. Org. Chem.* **2014**, *79*, 7711-7717.

(b) Fu, C.; Ma, S. "Highly Regio- and Stereoselective Synthesis of 2(E),4-Alkadienoates via the Pd(0)-Catalyzed Reaction of Aryl Halides with 3,4-Alkadienoates." *Org. Lett.* **2005**, *7*, 1707-1709.

(c) Hampton, C. S.; Harmata, M. "Regiodivergent Synthesis of 1- and 2-Arylsulfonyl 1,3-Dienes." *Org. Lett.* **2014**, *16*, 1256-1259.

[52] Kalek. M.; Stawinski, J. "Novel, Stereoselective and Stereospecific Synthesis of Allenylphosphonates and Related Compounds via Palladium-Catalyzed Propargylic Substitution." *Adv. Synth. Catal.* **2011**, *353*, 1741-1755.

[53] (a) Nakamura, E.; Hatakeyama, T.; Ito, S.; Ishizuka, K.; Ilies, L.; Nakamura, M. *Iron-Catalyzed Cross-Coupling Reactions. Organic Reactions, Vol. 83. (*Ed.: Scott E. Denmark et al.), John Wiley & Sons, Inc, Hoboken, **2014**, pp. 25-31.

(b) Schneider, U.; Kobayashi, S. "Low-Oxidation State Indium-Catalyzed C-C Bond Formation." *Acc. Chem. Res.* **2012**, *45*, 1331-1344.

(c) Bandini, M.; Cozzi, P.G.; Melchiorre, P.; Tino, R.; Umani-Ronchi, A. "Chemo- and Enantioselective Catalytic Addition of propargyl Chloride to Aldehydes Promoted by [Cr(Salen)] Complexes." *Tetrahedron: Asymmetry*. **2001**, *12*, 1063-1069.

(d) Lee, P. H.; Shim, E.; Lee, K.; Seomoon, D.; Kim, S. "Pd-Catalyzed Substitution Reactions with Organoindium Reagents *in situ* Generated from Indium and Allyl or Propargyl Halides." *Bull. Korean Chem. Soc.* **2005**, *26*, 157-160.

[54] Lockwood, R. F.; Nicholas, K. M. "Regioselective Conversion of O-Protected Glycidols to Fluorohydrins Catalyzed by Tetrabutylammonium Dihydrogentrifluoride Under Solid-Liquid PTC Conditions." *Tetrahedron Lett.* **1977**, *48*, 4163-4166.

[55] Ambrogio, I.; Cacchi, S.; Fabrizi, G.; Goggiamani, A.; Iazzetti, A. "Palladium-Catalyzed Nucleophilic Substitution of Propargylic Carbonates and Meldrum's Acid Derivatives." *Eur. J. Org. Chem.* **2015**, 3147-3151.

[56] For reports of palladium-catalyzed cyclizations with propargyl carbonates:

(a) Ambrogio, I.; Cacchi, S.; Fabrizi, G. "2-Alkylindoles via Palladium-Catalyzed Reductive Cyclization of Ethyl 3-(o-trifluoroacetamidophenyl)-1-propargyl Carbonates." *Tetrahedron Lett.* **2007**, *48*, 7721-7725.

(b) Yoshida, M.; Higuchi, M.; Shishido, K. "Highly Diastereoselective Synthesis of Tetrahydrobenzofuranones by Palladium-Catalyzed Reaction of Propargylic Carbonates with 2-Substituted Cyclohexane-1,3-diones." *Tetrahedron Lett.* **2007**, *49*, 1678-1681.

(c) Guan, Z-H.; Ren, Z-H.; Zhao, L-B.; Liang, Y-M. "Palladium-Catalyzed Synthesis of Indene Derivatives via Propargylic Carbonates with *in situ* Generated Organozinc Compounds." *Org. Biomol. Chem.* **2008**, *6*, 1040-1045.

(d) Yoshida, M.; Higuchi, M.; Shishido, K. "Stereoselective Construction of Substituted Chromans by Palladium-Catalyzed Cyclization of Propargylic Carbonates with 2-(2-Hydroxyphenyl)acetates." *Org. Lett.* **2009**, *11*, 4752-4755.

(e) Yoshida, M.; Higuchi, M.; Shishido, K. "Highly Diastereoselective Synthesis of Tetrahydrobenzofuran Derivatives by Palladium-Catalyzed Reaction of Propargylic Esters with Substituted β-dicarbonyl Compounds." *Tetrahedron*. **2010**, *66*, 2675-2682.

(f) Gao, R-D.; Liu, C.; Dai, L-X.; Zhang, W.; You, S-L. "Pd(0)-Catalyzed Alkenylation and Allylic Dearomatization Reactions between Nucleophile-Bearing Indoles and Propargyl Carbonates." *Org. Lett.* **2014**, *16*, 3919-3921.

(g) Montgomery, T. D.; Nibbs, A. E.; Zhu, Y.; Rawal, V. H. "Rapid Access to Spirocyclized Indolenines via Palladium-Catalyzed Cascade Reactions of Tryptamine Derivatives and Propargylic Carbonate." *Org. Lett.* **2014**, *16*, 3480-3483.

[57] a) Ardolino, M. J.; Morkin, J. P. "Construction of 1,5-Enynes by Stereospecific Pd-Catalyzed Allyl-Propargyl Cross-Couplings." *J. Am. Chem. Soc.* **2012**, *134*, 8770.

b) Recio III, A.; Heinzman, J. D.; Tunge, J. A. "Decarboxylative Benzylation and Arylation of Nitriles." *Chem. Commun*. **2012**, *48*, 142-144.

Chapter 2. Appendix

Experimental Methods and Spectral Analysis for Chapter 2 Compounds

Table of Contents

General Information:

Purified compounds, unless otherwise stated, were obtained by column chromatography using 60 Å porosity, 230 x 400 mesh standard grade silica gel from Sorbent Technologies. TLC analysis was preformed on silica gel HL TLC plates w/UV254 from Sorbent Technologies. Gas chromatography/mass spectrometry data was obtained using a Shimadzu GCMS-QP2010 SE. NMR spectra were obtained on a Bruker Advance 500 DRX equipped with a QNP cryoprobe. ^{1}H and ^{13}C spectra were normalized using residual undeuterated solvent signals as a reference ($CDCl_3$ = 7.28 ppm for ^{1}H and 77.36 ppm for ^{13}C).[1] ^{19}F NMR spectra were referenced to α,α,α-trifluorotoluene (purchased from Sigma Aldrich) at -62.7 ppm.

N,*N*-Dimethylformamide (DMF) and nitromethane were purchased from Sigma Aldrich and stored in a glove box. Dichloromethane (DCM), tetrahydrofuran (THF), and toluene were either purified by an Innovative Technology Pure Solv™ solvent purification system or purchased from Sigma Aldrich and stored in a glove box. Tris(dibenzylideneacetone)dipalladium(0) ($Pd_2(dba)_3$) was purchased from Strem as were ethylenebis(diphenylphosphine) (dppe) and 2-dicyclohexylphosphino-2'-methylbiphenyl (MePhos). All were stored in a glove box. Diphenylacetonitrile was purchased from Sigma Aldrich and used without further purification.

Synthesis of Starting Materials

Acetonitrile 2.1b,[2,3] **2.1c**, **2.1d**,[4] **2.1e**,[2] **2.1f, 2.1g and 2.1l:**

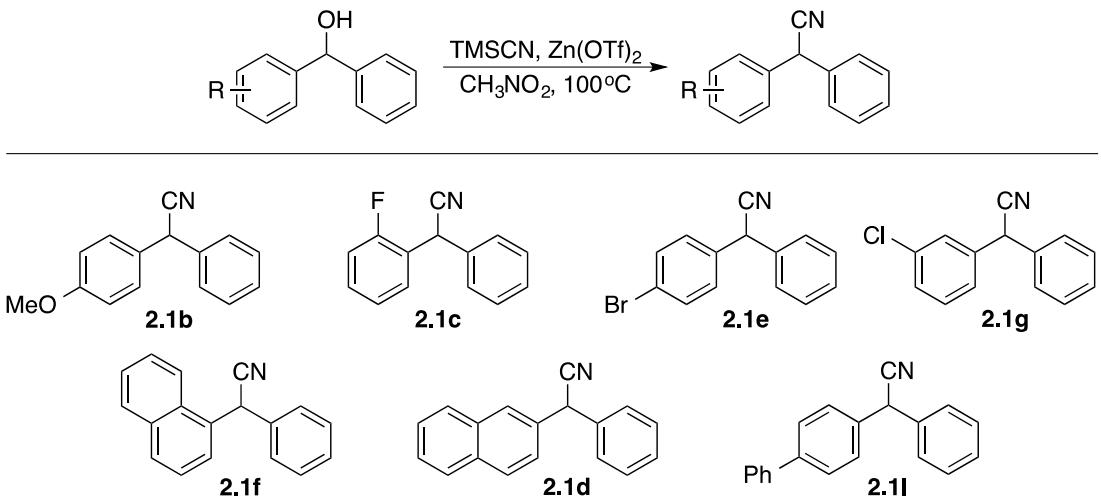

General Procedure for direct cyanation of benzylic alcohols in the synthesis of diaryl nitriles 2.1b-2.1g and 2.1i[2]: In a glove box under an argon atmosphere, an oven or flame dried 20 mL Biotage microwave vial (#355458) equipped with a magnetic stir bar was charged with benzylic alcohol (2 mmol), $Zn(OTf)_2$ (0.11 g, 0.3 mmol, 15 mol %), and CH_3NO_2 (20 mL, 10 M) then sealed and removed. TMSCN (0.24 g, 2.4 mmol, 1.2 eq) was then added using a syringe before heating the vessel at 100 °C overnight. The mixture was diluted with distilled water (100 mL) and extracted into ethyl acetate (50 mL x 2) and washed with brine (20 mL). The organic layer was dried over sodium sulfate and concentrated before purification by column chromatography in a gradient of 5% - 10% ethyl acetate in hexanes.

Characterization of 2.1c:

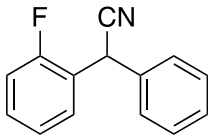

2.1c

Yield: .36 g, 1.7 mmol, 85%

Appearance: off-white solid

^{1}H NMR Spectra (500 MHz, $CDCl_3$): δ 7.77 (td, *J* = 7.6, 1.8 Hz, 1H), 7.68 (m, 6H), 7.51 (td, *J* = 7.5, 1.2 Hz, 1H), 7.42 (ddd, *J* = 9.7, 8.2, 1.2 Hz, 1H), 5.77 (s, 1H).

^{13}C NMR Spectra (126 MHz, $CDCl_3$): δ 160.00 (d, *J* = 248.5 Hz), 135.01, 130.72 (d, *J* = 8.2 Hz), 129.60 (d, *J* = 2.7 Hz), 129.55, 128.70, 127.83 (d, *J* = 1.3 Hz), 125.28 (d, *J* = 3.6 Hz), 123.78 (d, *J* = 13.9 Hz), 119.19, 116.37 (d, *J* = 21.2 Hz), 36.42 (d, *J* = 4.0 Hz).

^{19}F NMR Spectra (376 MHz, $CDCl_3$): δ -117.2 (s, 1F).

HRMS: $[M-H]^-$ calcd for $C_{14}H_{10}FN$: 210.0719. Found: 210.0740.

IR: 3087, 3064, 3031, 2246, 1589, 1492, 1456, 1236, 1093, 1031, 804, 756, 725, 696cm^{-1}

Characterization of 2.1f:

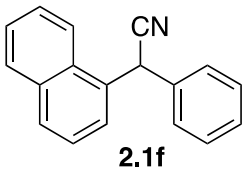

2.1f

ref. 5

Yield: 0.48 g, 1.97 mmol, 98%

Appearance: white solid

^{1}H NMR Spectra (500 MHz, $CDCl_3$): δ 7.92 (m, 3H), 7.66 (m, 1H), 7.53 (m, 3H), 7.36 (m, 5H), 5.86 (s, 1H).

^{13}C NMR (126 MHz, $CDCl_3$): δ 135.58, 134.47, 131.11, 130.64, 129.89, 129.53, 129.49, 128.61, 128.12, 127.51, 127.38, 126.56, 125.77, 123.38, 120.08, 77.61, 40.25.

HRMS: $[M]^+$calcd for $C_{18}H_{13}N$: 243.1048. Found: 243.1052.

IR: 3085, 3062, 2962, 2927, 2904, 2632, 2416, 2358, 2331, 2241, 1681, 1650, 1625, 1598, 1512, 1494, 1454, 1396, 1159, 1029, 862, 796, 775, 750, 725, 696, 642, 561 cm^{-1}

Characterization of 2.1g:

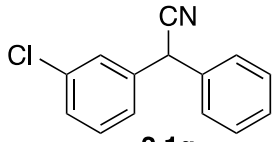

2.1g

ref. 6

Yield: 26 mg, 1.12 mmol, 28%

Appearance: dark yellow oil

^{1}H NMR Spectra (500 MHz, $CDCl_3$): δ 7.37 (m, 9H), 5.13 (s, 1H).

^{13}C NMR Spectra (126 MHz, $CDCl_3$): δ 137.82, 135.18, 130.54, 129.46, 128.66, 128.65, 127.98, 127.79, 125.98, 119.15, 42.30.

HRMS: $[M+H]^+$ calcd for $C_{14}H_{10}ClN$: 228.0580. Found: 228.0598.

Characterization of 2.1l:

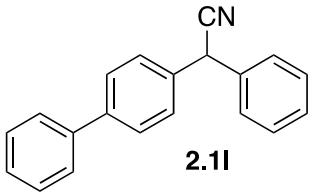

2.1l

Yield: 0.38 g, 1.4 mmol, 48%

Appearance: white solid

^{1}H NMR Spectra (500 MHz, $CDCl_3$): δ 7.60 (m, 4H), 7.43 (m, 10H), 5.21 (s, 1H).

^{13}C NMR (126 MHz, $CDCl_3$): δ 141.61, 140.49, 136.16, 135.16, 129.60, 129.20, 128.66, 128.48, 128.24, 128.09, 128.00, 127.44, 119.99, 42.66.

HRMS: $[M+H]^+$ calcd for $C_{20}H_{15}N$: 270.1283. Found: 270.1307.

Preparation 2.1h:[7]

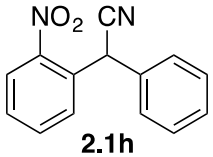

2.1h

To a 50 mL round bottom flask equipped with a magnetic stir bar, 1-fluoro-2-nitrobenzene (0.7 g; 5 mmol), benzyl cyanide (0.6 g; 5 mmol), tetrabutylammonium bromide (1.6 g; 5 mmol), and toluene (21 mL) were added and allowed to stir for 10 min. Next, 50% w/w NaOH (2 mL, 2.5 M) was added to the solution and the mixture was stirred overnight at 50 °C. The mixture was diluted with toluene (15 mL) and washed with distilled water (50 mL x 3) and brine (20 mL) then dried using Na_2SO_4. The purified product was obtained after column chromatography in 10 % - 20% ethyl acetate:hexane. Yield 0.42 g (35%). ^{1}H NMR (500 MHz, $CDCl_3$): δ 8.09 (dd, J = 8.2, 1.4 Hz, 1H), 7.74 (m, 2H), 7.58 (m, 1H), 7.37 (m, 5H), 6.20 (s, 1H). ^{13}C NMR (126 MHz, $CDCl_3$): δ 148.02, 134.51, 134.43, 131.31, 130.91, 130.05, 129.69, 129.08, 128.24, 126.15, 118.98, 38.66.

Synthesis of 2.1i,[8,9] 2.1j,[9] and 2.1o:[10]

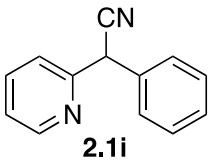

2.1i

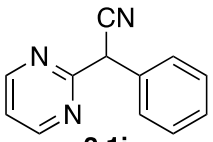

2.1j

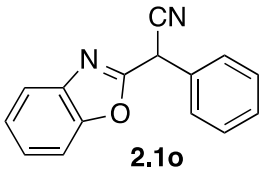

2.1o

General procedure for aryl chloride coupling with benzyl cyanide in the synthesis of 2.1i, 2.1j, 2.1o:[6] In a 10 mL oven or flame dried Schlenk flask purged with argon, potassium hydroxide (KOH) (1.2 g, 20 mmol) and dimethyl sulfoxide (DMSO) (2.5 mL) were added and stirred for 30 minutes. In a separate flask, benzyl cyanide (7.5 mmol, 0.89 g) was diluted with DMSO (1 mL) and the solution was added dropwise via syringe to the KOH mixture then stirred for 30 minutes. Aryl chloride was then added in portions and the mixture was stirred at room temperature overnight. Upon reaction completion, the vessel contents were poured into ice water (20 mL) and extracted into ethyl acetate (20 mL x 2) and washed with brine. The organic layer was dried over sodium sulfate and concentrated before purification by column chromatography with a gradient of 5%, 10%, 15% ethyl acetate:hexanes.

Synthesis of 2,5-dimethyl-α-phenyl-1*H*-Pyrrole-1-acetonitrile:[11]

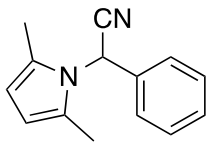

2.1k

In a 50 mL round bottom flask, 2-amino-2-phenylacetonitrile (2.6 mmol, 0.34 g), hexane-2,5-dione (3.1 mmol, 0.35 g), and THF (13 mL) were added and stirred at room temperature for 5 minutes. Iodine (0.26 mmol, 0.076 g) was added to the solution and stirred overnight. The mixture was then diluted with ethyl acetate (30 mL) and washed with saturated $Na_2S_2O_3$ (20 mL) then $NaHCO_3$ (20 mL) and brine. The organic layer was then dried over sodium sulfate and concentrated. The crude product was purified by column chromatography in a gradient of 5% - 10% ethyl acetate:hexanes. Yield 77% (0.42 g). ^{1}H NMR (500 MHz, $CDCl_3$): δ 7.41 (m, 3H), 7.17 (m, 2H), 6.35 (s, 1H), 5.90 (s, 2H), 2.19 (s, 6H). ^{13}C NMR (126 MHz, $CDCl_3$): δ 133.82, 129.62, 129.37, 128.80, 125.80, 166.61, 108.05, 48.72, 13.30. HRMS: $[M+H]^+$ calcd for $C_{14}H_{14}N_2$: 211.1235. Found: 211.1233.

General procedure for the synthesis of Acetonitrile 2.1m and 2.1n:[3]

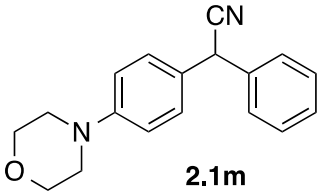

2.1m

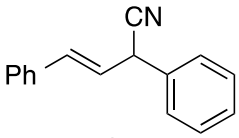

2.1n

In an oven or flame dried 25 mL Schlenk flask a solution of indium(III) bromide (0.17 mmol, 0.06 g) and TMSCN (3.4 mmol, 0.33 g) in DCM (4 mL) was stirred for 30 minutes. In a separate flask, the alcohol (1.7 mmol) was diluted with DCM (4 mL) and the solution was added dropwise to the $InBr_3$ mixture and stirred overnight. The reaction was quenched with distilled water (20 mL) and diluted with DCM (20 mL). The organic layer washed with distilled water (2 x 20 mL) then brine (20 mL). The crude product was dried over sodium sulfate and concentrated before purification by column chromatography in 5%, 10%, 15% ethyl acetate:hexane.

Characterization of 2-(4-morpholinophenyl)-2-phenylacetonitrile **2.1m**:

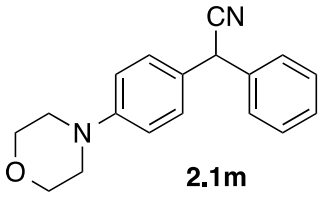

2.1m

Yield: 53% (25 mg).

Appearance: orange solid

^{1}H NMR (500 MHz, $CDCl_3$): δ 7.37 (m, 5H), 7.25 (m, 2H), 6.90 (m, 2H), 5.10 (s, 1H), 3.87 (m, 4H), 3.17 (m, 4H).

^{13}C NMR (126 MHz, $CDCl_3$): δ 151.34, 136.65, 129.45, 128.94, 128.43, 127.98, 127. 13, 120.30, 116.13, 67.14, 49.21, 42.14,

HRMS: [M+H] calcd for $C_{18}H_{18}N_2O$: 279.1497. Found: 279.1498.

IR: 2966, 2856, 2835, 2358, 1643, 1596, 1446, 1284, 1118, 923, 833, 740, 703, 644 cm^{-1}

Synthesis and Characterization of Propargyl Carbonates:

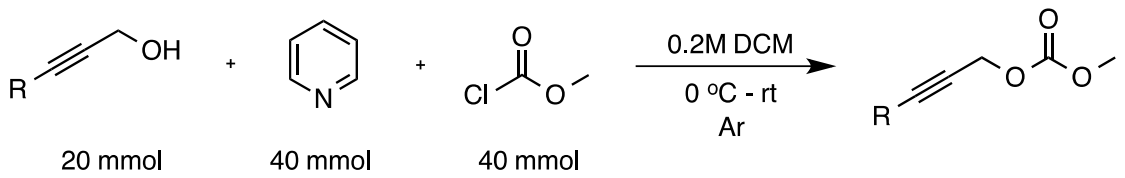

A 200 mL flame dried Schlenk flask was placed under an argon atmosphere and charged with propargyl alcohol (20 mmol) and DCM (100 mL) then stirred for 5 minutes at room temperature. Next, pyridine (3.3 mL, 40 mmol) was added to the solution and the mixture was stirred for 15 minutes. The solution was then cooled to 0 °C using an ice water bath followed by the dropwise addition of methyl chloroformate (3.3 mL, 40 mmol) over ten minutes. The resulting mixture was allowed to stir for 1 hour at 0 °C then warmed to room temperature and stirred for an additional hour. The reaction was quenched with a saturated solution of ammonium chloride (50 mL) and extracted into DCM (100 mL) and washed with water (50 mL x 3) then brine (100 mL x 1). The crude product was dried over sodium sulfate and concentrated before purification by column chromatography in 2-10% ethyl acetate in hexane. **2.2a**,[12,14] **2b**,[12] **2i**,[13] **2j**,[14] **2m**.[15]

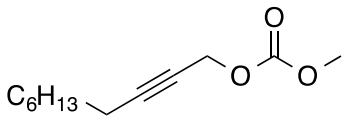

2.2c

ref. 16

Yield: 0.25 g, 1.2 mmol, 60%

Appearance: clear liquid

^{1}H NMR (500 MHz, $CDCl_3$): δ 4.74 (t, *J* = 2.2 Hz, 2H), 3.82 (s, 3H), 2.23 (tt, *J* = 7.3, 2.2 Hz, 2H), 1.53 (m, 2H), 1.32 (m, 8H), 0.90 (t, *J* = 6.9 Hz, 3H).

^{13}C NMR (126 MHz, $CDCl_3$): δ 155.66, 88.96, 73.64, 56.65, 55.36, 32.05, 29.13, 29.12, 28.67, 22.97, 19.09, 14.44.

GC/MS: *m/z* $[M+H]^+$ calcd for $C_{12}H_{20}O_3$: 213.1; found: 213.1.

IR: 2956, 2929, 2858, 2235, 1755, 1444, 1377, 1261, 1151, 950, 790 cm^{-1}

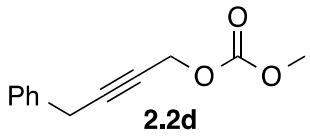

2.2d

Yield: 18 mg, 1 mmol, 33%

Appearance: clear liquid

^{1}H NMR (500 MHz, $CDCl_3$): δ 7.35 (m, 4H), 7.27 (m, 1H), 4.82 (t, *J* = 2.2 Hz, 2H), 3.83 (s, 3H), 3.67 (t, *J* = 2.2 Hz, 2H).

^{13}C NMR (126 MHz, $CDCl_3$): δ 155.51, 136.14, 128.74, 128.08, 126.93, 85.98, 75.83, 56.31, 55.24, 25.25.

GC/MS: *m/z* $[M]^+$ calcd for $C_{12}H_{12}O_3$: 204.1; found 204.1.

IR: 3062, 3029, 3008, 2956, 2235, 2202, 1747, 1731, 1703, 1600, 1583, 1494, 1444, 1421, 1377, 1267, 1203, 1143, 948, 902, 790, 732, 696 cm^{-1}

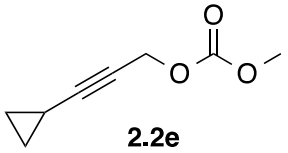

2.2e

Yield: 0.77g, 5 mmol, 45%

Appearance: clear liquid

^{1}H NMR (500 MHz, $CDCl_3$): δ 4.71 (d, *J* = 2.1 Hz, 2H), 3.82 (s, 3H), 1.28 (m, 1H), 0.76 (m, 4H),

^{13}C NMR (126 MHz, $CDCl_3$): δ 155.63, 91.92, 69.00, 56.64, 55.34, 8.62, -0.22.

GC/MS: *m/z* $[M]^+$ calcd for $C_8H_{10}O_3$: 154.1; found: 154.1.

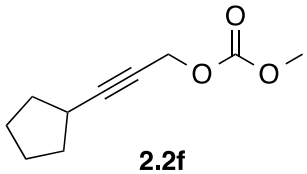

2.2f

Yield: 55 mg, 3 mmol, 60%

Appearance: clear liquid

^{1}H NMR (500 MHz, $CDCl_3$): δ 4.75 (d, *J* = 2.1 Hz, 2H), 3.82 (s, 3H), 2.64 (qt, *J* = 7.6, 2.1 Hz, 1H), 1.93 (m, 2H), 1.73 (m, 2H), 1.60 (m, 4H).

^{13}C NMR (126 MHz, $CDCl_3$): δ 155.64, 93.01, 73.13, 56.74, 55.34, 33.85, 30.40, 25.31.

GC/MS: *m/z* $[M]^+$ calcd $C_{10}H_{14}O_3$: 182.1; found: 182.1.

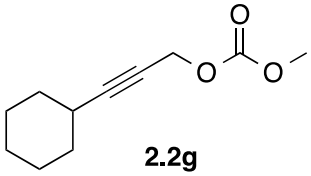

2.2g

Yield: 1.76 g, 9.0 mmol, 83%

Appearance: clear liquid

^{1}H NMR (500 MHz, $CDCl_3$): δ 4.76 (d, *J* = 2.1 Hz, 2H), 3.82 (s, 3H), 2.41 (m, 1H), 1.80 (m, 2H), 1.70 (m, 2H), 1.47 (br m, 3H), 1.30 (m, 3H).

^{13}C NMR (126 MHz, $CDCl_3$): 155.63, 92.81, 73.54, 56.70, 55.33, 32.63, 29.38, 26.12, 25.14.

GC/MS: *m/z* $[M]^+$ calcd for $C_{11}H_{16}O_3$: 196.1; found: 196.1.

IR: 2931, 2854, 2235, 1755, 1446, 1375, 1265, 1157, 1020, 948, 900, 790 cm^{-1}

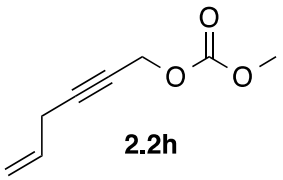

2.2h

Yield: 2 g, 13 mmol, 70%

Appearance: clear liquid

^{1}H NMR (500 MHz, $CDCl_3$): δ 5.81 (m, 1H), 5.33 (dq, *J* = 17.1, 1.8 Hz, 1H), 5.14 (dq, *J* = 10.0, 1.6 Hz, 1H), 4.78 (t, *J* = 2.2 Hz, 2H), 3.83 (s, 3H), 3.03 (dp, *J* = 6.0, 2.0 Hz, 2H).

^{13}C NMR (126 MHz, $CDCl_3$): δ 155.63, 132.02, 116.86, 85.19, 76.09, 56.43, 55.40, 23.38.

GC/MS: *m/z* $[M]^+$ calcd for $C_8H_{10}O_3$: 154.1: found: 154.1.

IR: 3016, 2983, 2958, 2358, 2341, 1747, 1714, 1444, 1421, 1377, 1263, 1149, 1107, 1020, 993, 950, 919, 900, 790, 648 cm^{-1}

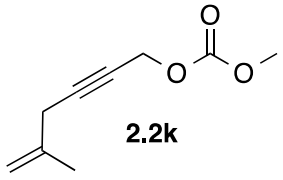

2.2k

Yield: 1.7 g, 10.1 mmol, 56%

Appearance: clear liquid

^{1}H NMR (500 MHz, $CDCl_3$): δ 5.00 (br m, 1H), 4.86 (br m, 1H), 4.78 (t, 2H), 3.83 (s, 3H), 2.96 (m, 2H), 1.80 (m, 3H).

^{13}C NMR (126 MHz, $CDCl_3$): δ 155.64, 140.14, 112.36, 85.65, 76.03, 56.47, 55.40, 27.82, 22.40.

GC/MS: *m/z* $[M]^+$ calcd for $C_9H_{12}O_3$: 168.1; found: 168.1.

IR: 2958, 2887, 2858, 2235, 1755, 1652, 1444, 1375, 1261, 1228, 1149, 948, 900, 790 cm^{-1}

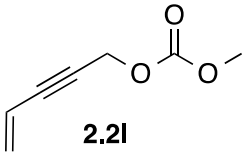

2.2l

Yield: 1.3 g, 9 mmol, 62%

Appearance: clear liquid

^{1}H NMR (500 MHz, $CDCl_3$): δ 5.83 (ddt, *J* = 17.6, 11.0, 1.9 Hz, 1H), 5.71 (dd, *J* = 17.5, 2.2 Hz, 1H), 5.56 (dd, *J* = 11.0, 2.2 Hz, 1H), 4.87 (d, *J* = 2.0 Hz, 2H), 3.84 (s, 3H).

^{13}C NMR (126 MHz, $CDCl_3$): δ 155.58, 128.86, 116.52, 86.14, 83.15, 56.40, 55.49.

GC/MS: *m/z* $[M]^+$ calcd for $C_7H_8O_3$: 140.0; found: 140.1.

IR: 3014, 2958, 2235, 1749, 1712, 1602, 1444, 1413, 1375, 1263, 1199, 1168, 1107, 1018, 950, 900, 792 cm^{-1}

Ligand Screen:

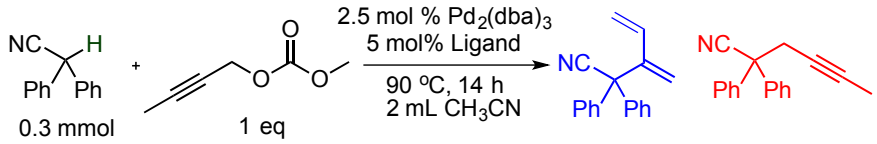

entry	Ligand	starting material	allenylation	dienylation	propargylation
1	XantPhos	2%	22%	14%	62%
2	**dppe**	**3%**	**0%**	**94%**	**3%**
3	dppm	28%	4%	42%	27%
4	dppb	2%	0%	85%	13%
5	dppp	5%	0%	87%	8%
6	dppf	1%	1%	74%	24%
7	(*R*)-SEGPHOS	5%	0%	76%	23%
8	tri-otolylphosphine	48%	3%	41%	9%
9	rac-BINAP	4%	1%	70%	24%
10	(*R*)-C_3-tunephos	1%	0%	86%	13%
11	XPhos	11%	1%	36%	53%
12	**dppbz**	**3%**	**0%**	**93%**	**3%**
13[b]	SPhos	13%	2%	24%	60%
14[b]	(*R*)-DM-BINAP	3%	1%	80%	17%
15[b]	tri-1-nap phosphine	52%	3%	37%	9%
16[b]	Ligand 1	44%	1%	48%	7%
17[b]	JohnPhos	45%	20%	2%	33%
18[b]	Cy-JohnPhos	56%	4%	15%	25%
19[b]	tBu-MePhos	22%	29%	2%	47%
20[b]	tBu-XPhos	43%	18%	7%	37%
21[b]	MePhos	11%	3%	19%	67%
22	**MePhos**	**10%**	3%	**6%**	**81%**

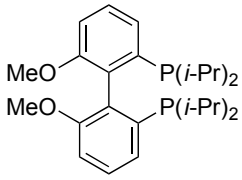

Ligand 1
1,1'-[(1*S*)-6-6'-dimethoxy[1,1'-biphenyl]-2,2'diyl]bis[1,1'bis(methylethyl)-phosphine

[a] Determined by GC/MS analysis.
[b] NMR Scale - 0.078 mmol, 80 °C, 0.5 mL CD_3CN

Solvent Screen:

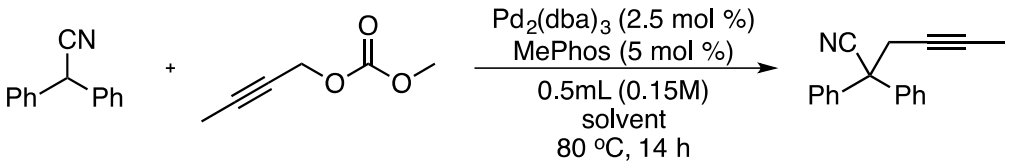

entry	solvent	starting material	allene	dienylation	propargylation
1	CD_3CN	11%	3%	19%	67%
2	DMSO-d_6	51%	5%	9%	35%
3	toluene-d_8	87%	6%	0%	6%
4	d-DMF	43%	3%	7%	47%
5	MeOD-d_4	90%	1%	2%	5%
6	1,4-dioxane-d_8	87%	5%	1%	8%

References:

1) Gottlieb, H. E.; Kotlyar, V.; Nudelman, A. *J. Org. Chem.* **1997**, *62*, 7512.

2) Theerthagiri, P.; Appaswami, L. *Tetrahedron Lett.* **2012**, *53*, 5535.

3) Chen, G.; Wang, Z.; Wu, J.; Ding, K. *Org. Lett.* **2008**, *10*, 4573.

4) Wang, J-C.; Masui, Y-I.; Onaka, M. *ACS Catal.* **2011**, *1*, 446.

5) Avramoff, M.; Sprinzak, Y. *J. Org. Chem.* **1961**, *26*, 1284-1286.

6) Moffett, R. B.; Aspergren, B. D.; Speeter, M. E. *J. Am. Chem. Soc.* **1957**, *79*, 4451.

7) Bonnet, B.; Campo, B.; Raveglia, L.; Riccaboni, M. *PCT Int. Appl.,* **2008**, WO 2008117175.

8) Kawano, T.; Kurimoto, M.; Hatanaka, M.; Ueda, I. *Chem. Pharm. Bull.* **1992**, *40*, 3067.

9) Hermann, C. K. F.; Sachdeva, Y. P.; Wolfe, J. F. *J. Heterocyclic Chem.* **1987**, *24*, 1061.

10) Yamanaka, H.; Ohba, S.; Sakamoto, T. *Heterocycles*. **1990**, *31*, 1115.

11) Banik, B. K.; Samajdar, S.; Banik, I. *J. Org. Chem.* **2004**, *69*, 213.

12) Minami, I.; Yuhara, M.; Watanabe, H.; Tsuji, J. *Organomet. Chem.* **1987**, *334*, 225.

13) Kalek, M.; Stawinski, J. *Adv. Synth. Catal.* **2011**, *353*, 1741.

14) Zhao, T. S. N.; Yang, Y.; Lessing, T.; Szabó, K. *J. Am. Chem. Soc.* **2014**, *136*, 7563.

15) Ma, S.; Zhang, A. *J. Org. Chem.* **2002**, *67*, 2287.

16) Tsuji, J.; Sugiura, T.; Minami, I.; *Tetrahedron Lett.* **1986**, *27*, 731.

Experimental Procedure for the dienylation and propargylation of tertiary nitriles:

In an oven or flamed dried Biotage microwave reaction vial (part no. 354624) equipped with a magnetic stir bar, catalyst ($Pd_2(dba)_3$, 0.0137 g, 5 mol %), ligand (dppe, 0.012 g, 10 mol % or MePhos, 0.011 g, 10 mol %), and diaryl acetonitrile (0.3 mmol if solid) were added under an argon atmosphere in a glovebox. The solid mixture was dissolved in 2 mL anhydrous DMF followed by addition of diaryl acetonitrile (0.3 mmol if liquid) and propargyl carbonate (0.6 mmol). The vessel was sealed, removed from the glovebox, and placed in a preheated oil bath at 80 ^{o}C for 1 hr. After reaction completion, the vessel was unsealed and solid lithium hydroxide (0.6 mmol) was added to the solution followed by 1 mL distilled water. The resulting mixture was stirred for an additional hour. The crude product was diluted with DCM (50 mL) and the organic layer was washed with distilled water (50 mL x 3) then brine (50 mL) before being dried over sodium sulfate. The organic phase was concentrated via rotary evaporation and purified via column chromatography in 0-5% ethyl acetate in hexane.

Characterization of Dienylated and Propargylated Tertiary Nitriles:

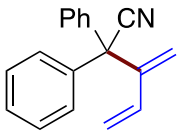

2.3a

Yield: 66 mg, 0.27 mmol, 89%

Appearance: yellow oil

^{1}H NMR (500 MHz, $CDCl_3$): δ 7.48 (m, 10H), 6.46 (dd, *J* = 17.6, 11.2 Hz, 1H), 5.79 (s, 1H), 5.55 (d, *J* = 17.5 Hz, 1H), 5.33 (d, *J* = 11.2 Hz, 1H), 4.82 (s, 1H).

^{13}C NMR (126 MHz, $CDCl_3$): δ 145.87, 138.35, 135.07, 128.99, 128.91, 128.51, 122.39, 120.51, 118.55, 56.94.

GC/MS: *m/z* $[M]^+$ calcd for $C_{18}H_{15}N$: 245.1; found: 245.2.

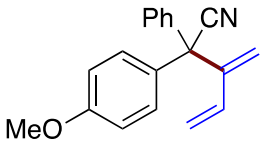

2.3b

Yield: 64 mg, 0.23 mmol, 77%

Appearance: yellow oil

^{1}H NMR (500 MHz, $CDCl_3$): δ 7.38 (m, 5H), 7.26 (m, 2H), 6.91 (m, 2H), 6.35 (m, 1H), 5.67 (s, 1H), 5.45 (d, *J* = 17.5 Hz, 1H), 5.23 (d, *J* = 11.2 Hz, 1H), 4.72 (s, 1H), 3.83 (s, 3H).

^{13}C NMR (126 MHz, $CDCl_3$): δ 159.59, 146.11, 138.67, 135.10, 130.30, 130.11, 128.95, 128.81, 128.43, 122.55, 120.21, 118.45, 114.27, 56.28, 55.61.

GC/MS: *m/z* $[M]^+$ calcd for $C_{19}H_{17}NO$: 275.1; found: 275.2.

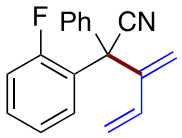

2.3c

Yield: 76 mg, 0.29 mmol, 96%

Appearance: yellow oil

^{1}H NMR (500 MHz, $CDCl_3$): δ 7.42 (m, 6H), 7.14 (m, 2H), 6.95 (td, *J* = 7.9, 1.7 Hz, 1H), 6.36 (dd, *J* = 17.5, 11.2 Hz, 1H), 5.70 (s, 1H), 5.52 (d, *J* = 17.5 Hz, 1H), 5.25 (d, *J* = 11.1 Hz, 1H), 4.83 (s, 1H).

^{13}C NMR (126 MHz, $CDCl_3$): δ 160.75 (d, *J* = 252.4 Hz), 144.05, 136.89, 134.77, 131.06 (d, *J* = 8.5 Hz), 130.57 (d, *J* = 2.2 Hz), 129.15, 128.79, 128.60, 126.36 (d, *J* = 11.3 Hz), 124.43 (d, *J* = 3.7 Hz), 120.81, 119.25, 118.49, 117.00 (d, *J* = 21.7 Hz), 52.94.

GC/MS: *m/z* $[M]^+$ calcd for $C_{18}H_{14}FN$: 263.1; found: 263.1.

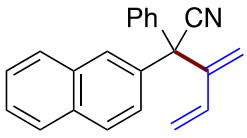

2.3d

Yield: 74 mg, 0.25 mmol, 83%

Appearance: yellow oil

^{1}H NMR (500 MHz, $CDCl_3$): δ 7.87 (m, 2H), 7.80 (m, 2H), 7.52 (m, 3H), 7.40 (m, 5H), 6.39 (dd, *J* = 17.5, 11.2 Hz, 1H), 5.73 (s, 1H), 5.48 (d, *J* = 17.5 Hz, 1H), 5.24 (d, *J* = 11.2 Hz, 1H), 4.77 (s, 1H).

^{13}C NMR (126 MHz, $CDCl_3$): δ 145.77, 138.35, 135.72, 135.13, 133.29, 133.09, 129.08, 129.05, 128.86, 128.70, 128.62, 128.16, 127.91, 127.20, 126.97, 126.52, 122.41, 120.74, 118.70, 57.12.

GC/MS: *m/z* $[M]^+$ calcd for $C_{22}H_{17}N$: 295.1; found: 295.2.

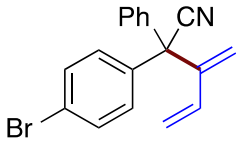

2.3e

Yield: 84 mg, 0.26 mmol, 86%

Appearance: yellow oil

^{1}H NMR (500 MHz, $CDCl_3$): δ 7.53 (m, 2H), 7.38 (m, 5H), 7.24 (m, 2H), 6.33 (dd, *J* = 17.5, 11.2 Hz, 1H), 5.69 (s, 1H), 5.44 (d, *J* = 17.5 Hz, 1H), 5.24 (d, *J* = 11.2 Hz, 1H), 4.71 (s, 1H).

^{13}C NMR (126 MHz, $CDCl_3$): δ 145.44, 137.82, 137.56, 134.79, 132.17, 130.64, 129.15, 128.78, 128.75, 122.84, 121.91, 120.80, 118.89, 56.50.

GC/MS: *m/z* $[M]^+$ calcd for $C_{18}H_{14}BrN$: 323.0. Found: 323.1.

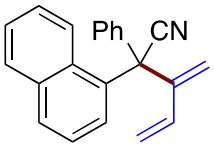

2.3f

Yield: 72 mg, 0.24 mmol, 81%

Appearance: yellow oil

^{1}H NMR (500 MHz, $CDCl_3$): δ 8.15 (m, 1H), 7.91 (m, 2H), 7.47 (m, 8H), 7.13 (m, 1H), 6.43 (dd, *J* = 17.4, 11.1 Hz, 1H), 5.80 (s, 1H), 5.63 (d, *J* = 17.5 Hz, 1H), 5.28 (d, *J* = 11.1 Hz, 1H), 4.87 (s, 1H).

^{13}C NMR (126 MHz, $CDCl_3$): δ 145.33, 138.25, 135.22, 134.88, 133.84, 130.89, 130.43, 129.33, 129.20, 128.99, 128.79, 128.65, 126.57, 126.48, 126.16, 124.90, 122.21, 119.70, 118.30, 55.91.

GC/MS: *m/z* $[M]^+$ calcd for $C_{22}H_{17}N$: 295.1; found: 295.2.

IR: 3087, 3060, 3029, 2925, 2248, 2239, 1591, 1487, 1448, 1398, 1076, 1010, 914, 815, 757, 734, 698, 649, 538 cm^{-1}

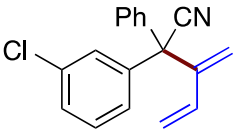

2.3g

Yield: 75 mg, 0.23 mmol, 77%

Appearance: yellow oil

^{1}H NMR (500 MHz, $CDCl_3$): δ 7.38 (m, 8H), 7.28 (m, 1H), 6.33 (dd, *J* = 17.5, 11.2 Hz, 1H), 5.70 (s, 1H), 5.44 (d, *J* = 17.6 Hz, 1H), 5.25 (d, *J* = 11.2 Hz, 1H), 4.72 (s, 1H).

^{13}C NMR (126 MHz, $CDCl_3$): δ 145.35, 140.43, 137.66, 135.09, 134.77, 130.24, 129.18, 129.03, 128.87, 128.81, 127.21, 121.84, 120.91, 118.92, 56.63.

GC/MS: *m/z* $[M]^+$ calcd for $C_{18}H_{14}ClN$: 279.1; found: 279.2.

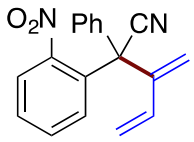

2.3h

Yield: 71 mg, 0.25 mmol, 82%

Appearance: orange oil

^{1}H NMR (500 MHz, $CDCl_3$): δ 7.82 (m, 1H), 7.47 (m, 2H), 7.29 (m, 5H), 7.17 (m, 1H), 6.18 (dd, *J* = 17.4, 11.1 Hz, 1H), 5.60 (s, 1H), 5.35 (d, *J* = 17.4 Hz, 1H), 5.11 (d, *J* = 11.1 Hz, 1H), 4.75 (s, 1H).

^{13}C NMR (126 MHz, $CDCl_3$): δ 150.00, 144.88, 136.96, 134.53, 132.85, 132.36, 131.32, 130.30, 129.21, 128.90, 128.37, 126.38, 119.70, 119.47, 118.97, 55.33.

GC/MS: *m/z* $[M]^+$ calcd for $C_{18}H_{14}N_2O_2$: 290.1. Found: $[M^+] - NO_2$: 245.1.

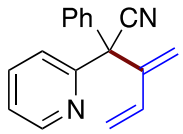

2.3i

Yield: 17 mg, 0.070 mmol, 23%

Appearance: orange-red oil

^{1}H NMR (500 MHz, $CDCl_3$): δ 8.72 (ddd, *J* = 4.8, 1.9, 0.9 Hz, 1H), 7.72 (td, *J* = 7.8, 1.9 Hz, 1H), 7.39 (m, 6H), 7.28 (m, 1H), 6.36 (dd, *J* = 17.6, 11.2 Hz, 1H), 5.69 (s, 1H), 5.39 (d, *J* = 17.6 Hz, 1H), 5.20 (d, *J* = 11.2 Hz, 1H), 4.73 (s, 1H).

^{13}C NMR (126 MHz, $CDCl_3$): δ 157.66, 150.07, 145.30, 137.51, 137.39, 135.06, 129.09, 128.85, 128.67, 123.52, 123.27, 121.53, 120.67, 118.45, 59.39.

GC/MS: *m/z* $[M]^+$ calcd for $C_{17}H_{14}N_2$: 246.1; found: 246.2.

IR: 3085, 3058, 3006, 1585, 1571, 1492, 1463, 1448, 1431, 1153, 1031, 995, 918, 777, 750, 698, 667 cm^{-1}

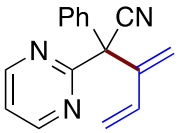

2.3j
major isomer

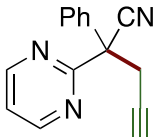

2.5j
minor isomer

Yield: 9.6 mg, 0.04 mmol, 13%

Appearance: orange-red oil

^{1}H NMR (500 MHz, $CDCl_3$) *major isomer*: δ 8.85 (d, *J* = 4.9 Hz, 2H), 7.52 (m, 2H), 7.39 (m, 4H), 6.38 (dd, *J* = 17.6, 11.3 Hz, 1H), 5.70 (s, 1H), 5.31 (d, *J* = 17.6 Hz, 1H), 5.17 (d, *J* = 11.3 Hz, 1H), 4.85 (s, 1H).

^{13}C NMR (126 MHz, $CDCl_3$) *major isomer*: δ 167.30, 158.13, 144.90, 136.43, 135.05, 129.04, 128.80, 128.76, 120.78, 120.53, 120.29, 118.03, 60.83.

GC/MS: *m/z* $[M]^+$ calcd for $C_{16}H_{13}N_3$: 247.1; found: 247.1.

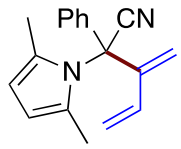

2.3k

Yield: 59 mg, 0.23 mmol, 75%

Appearance: orange oil

^{1}H NMR (500 MHz, $CDCl_3$): δ 7.44 (m, 3H), 7.32 (m, 2H), 6.51 (dd, *J* = 17.6, 11.3 Hz, 1H), 5.88 (s, 2H), 5.72 (s, 1H), 5.63 (d, *J* = 17.5 Hz, 1H), 5.39 (d, *J* = 11.2 Hz, 1H), 4.68 (s, 1H), 2.11 (s, 6H).

^{13}C NMR (126 MHz, $CDCl_3$): δ 144.35, 136.94, 134.35, 131.55, 129.78, 129.22, 128.77, 120.69, 119.77, 118.76, 109.86, 66.92, 16.76.

GC/MS: *m/z* $[M]^+$ calcd for $C_{18}H_{18}N_2$: 262.1; found: 262.2.

IR: 3099, 3062, 3029, 2960, 2927, 2898, 1712, 1593, 1523, 1492, 1450, 1375, 1271, 1186, 1064, 985, 923, 898, 756, 698 cm^{-1}

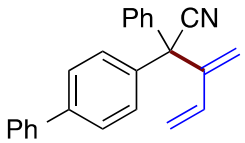

2.3l

Yield: 91 mg, 0.28 mmol, 94%

Appearance: yellow oil

^{1}H NMR (500 MHz, $CDCl_3$): δ 7.64 (m, 5H), 7.45 (m, 10H), 6.40 (dd, *J* = 17.5, 11.2 Hz, 1H), 5.73 (s, 1H), 5.50 (d, *J* = 17.5 Hz, 1H), 5.27 (d, *J* = 11.1 Hz, 1H), 4.80 (s, 1H).

^{13}C NMR (126 MHz, $CDCl_3$): δ 145.80, 141.32, 140.31, 138.30, 137.34, 135.04, 129.35, 129.17, 129.05, 128.89, 128.57, 127.99, 127.62, 127.37, 122.35, 120.55, 118.65, 56.70.

GC/MS: *m/z* $[M]^+$ calcd for $C_{24}H_{19}N$: 321.2; found: 321.2.

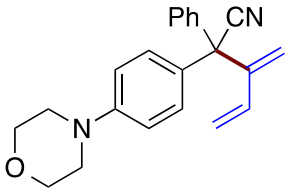

2.3m

Yield: 99 mg, 0.3 mmol, 99%

Appearance: orange-red oil

^{1}H NMR (500 MHz, $CDCl_3$): δ 7.37 (m, 5H), 7.22 (m, 2H), 6.90 (m, 2H), 6.35 (dd, *J* = 17.5, 11.2 Hz, 1H), 5.66 (s, 1H), 5.45 (d, *J* = 17.5 Hz, 1H), 5.21 (d, *J* = 11.2 Hz, 1H), 4.73 (s, 1H), 3.87 (m, 4H), 3.20 (m, 4H).

^{13}C NMR (126 MHz, $CDCl_3$): δ 150.94, 146.10, 138.73, 135.11, 129.73, 128.99, 128.87, 128.78, 128.33, 122.54, 120.05, 118.32, 115.29, 67.05, 56.21, 48.89.

GC/MS: *m/z* $[M]^+$ calcd for $C_{22}H_{22}N_2O$: 330.2; found: 330.2.

IR: 2962, 2910, 2893, 2854, 2827, 2235, 1608, 1514, 1490, 1448, 1380, 1263, 1238, 1184, 1122, 1051, 927, 819, 759, 730, 700, 648, 547 cm^{-1}

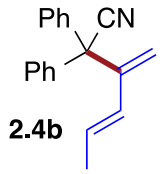

2.4b

Yield: 33 mg, 0.13 mmol, 42%

Appearance: light yellow oil

^{1}H NMR (500 MHz, $CDCl_3$): δ 7.37 (m, 10H), 6.03 (m, 1H), 5.94 (dq, *J* = 15.8, 6.5 Hz, 1H), 5.54 (s, 1H), 4.53 (s, 1H), 1.73 (dd, *J* = 6.4, 1.5 Hz, 3H).

^{13}C NMR (126 MHz, $CDCl_3$): δ 145.70, 138.64, 130.31, 129.41, 128.97, 128.93, 128.41, 122.66, 118.37, 57.33, 18.91.

GC/MS: *m/z* $[M]^+$ calcd for $C_{19}H_{17}N$: 259.1; found: 259.2.

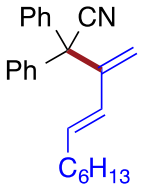

2.4c
9:1
diene:propargyl isomer

Yield: 41 mg, 0.12 mmol, 41%

Appearance: yellow oil

^{1}H NMR (500 MHz, $CDCl_3$) *major isomer***:** δ 7.37 (m, 10H), 6.00 (m, 1H), 5.90 (dt, *J* = 15.8, 6.8 Hz, 1H), 5.55 (s, 1H), 4.56 (s, 1H), 2.04 (m, 2H), 1.25 (m, 8H), 0.88 (t, *J* = 7.2 Hz, 3H).

^{13}C NMR (126 MHz, $CDCl_3$) δ 145.80, 138.69, 135.96, 129.00, 128.90, 128.38, 128.14, 122.64, 118.47, 57.28, 33.31, 31.96, 29.23, 28.96, 22.91, 14.43.

GC/MS: *m/z* $[M]^+$ calcd for $C_{24}H_{27}N$: 329.2; found: 329.2**.**

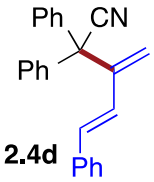

2.4d

Yield: 49 mg, 0.21 mmol, 70%

Appearance: yellow oil

^{1}H NMR (500 MHz, $CDCl_3$): δ 7.22 (m, 15H), 6.69 (d, *J* = 16.2 Hz, 1H), 6.60 (d, *J* = 16.2 Hz, 1H), 5.68 (s, 1H), 4.63 (s, 1H).

^{13}C NMR (126 MHz, $CDCl_3$): δ 145.55, 138.49, 136.82, 132.85, 129.06, 128.99, 128.88, 128.57, 128.40, 127.05, 126.75, 122.53, 119.83, 57.40.

GC/MS: *m/z* $[M]^+$ calcd for $C_{24}H_{19}N$: 321.2; found: 321.2**.**

IR: 3082, 3060, 3028, 2927, 2250, 2237, 1639, 1633, 1598, 1492, 1448, 1334, 1074, 1031, 962, 912, 750, 734, 698, 648 cm^{-1}

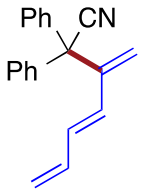

2.4e
9:1
diene:propargyl isomer

Yield: 60 mg, 0.22 mmol, 74%

Appearance: yellow oil

^{1}H NMR (500 MHz, $CDCl_3$): δ 7.35 (m, 10H), 6.48 (dd, *J* = 15.6, 10.5 Hz, 1H), 6.32 (dt, *J* = 17.0, 10.3 Hz, 1H), 6.19 (d, *J* = 15.6 Hz, 1H), 5.70 (s, 1H), 5.24 (d, *J* = 16.9 Hz, 1H), 5.15 (d, *J* = 9.9 Hz, 1H), 4.68 (s, 1H).

^{13}C NMR (126 MHz, $CDCl_3$): δ 145.34, 138.44, 136.94, 133.60, 130.76, 129.03, 128.98, 128.56, 122.46, 119.54, 119.46, 57.35.

GCMS: *m/z* $[M]^+$ calcd for $C_{20}H_{17}N$: 271.1. Found: 271.2.

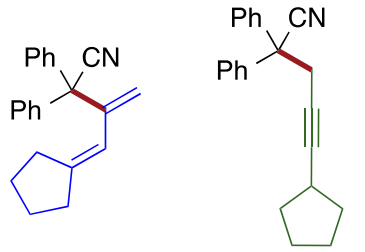

2.4g *minor isomer* **2.6f** *major isomer*

1:1.2 diene:propargyl isomer

Yield: 45 mg, 0.15 mmol, 51%

Appearance: yellow oil

^{1}H NMR (500 MHz, $CDCl_3$): product **5f** only: δ 7.38 (m, 10H), 5.82 (m, 1H), 5.43 (s, 1H), 4.85 (s, 1H), 2.43 (m, 2H), 2.33 (m, 2H), 1.74 (m, 2H), 1.62 (m, 2H).

^{13}C NMR (126 MHz, $CDCl_3$): product **5f** only: δ 151.24, 145.39, 138.68, 129.05, 128.85, 128.38, 122.79, 118.61, 118.25, 59.29, 35.49, 32.11, 27.01, 25.77.

GC/MS: *m/z* $[M]^+$ calcd for $C_{22}H_{21}N$: 299.2; found: 299.2.

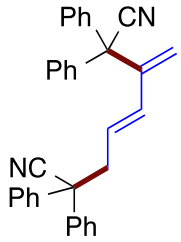

Yield: 63 mg, 0.14 mmol, 93%

Appearance: off-white solid

^{1}H NMR (500 MHz, $CDCl_3$): δ 7.31 (m, 20H), 6.20 (d, *J* = 15.8 Hz, 1H), 5.78 (dt, *J* = 15.9, 7.2 Hz, 1H), 5.56 (s, 1H), 4.64 (s, 1H), 3.14 (dd, *J* = 7.3, 1.4 Hz, 2H).

^{13}C NMR (126 MHz, $CDCl_3$): δ 144.73, 139.76, 138.19, 133.45, 129.12, 129.00, 128.83, 128.42, 128.17, 127.91, 127.20, 122.27, 122.00, 121.11, 56.83, 52.03, 43.69.

GCMS: *m/z* $[M]^+$ calcd for $C_{33}H_{26}N_2$: 450.2; found: 450.3.

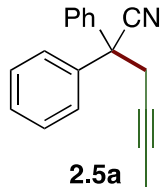

2.5a

Yield: 64 mg, 0.26 mmol, 86%

Appearance: yellow oil

^{1}H NMR (500 MHz, $CDCl_3$): δ 7.39 (m, 10H), 3.21 (q, *J* = 2.5 Hz, 2H), 1.76 (t, *J* = 2.51 Hz, 3H).

^{13}C NMR (126 MHz, $CDCl_3$): δ 139.62, 129.05, 128.40, 127.40, 122.30, 81.08, 73.56, 51.94, 31.54, 3.86.

GC/MS: *m/z* $[M]^+$ calcd for $C_{18}H_{15}N$: 245.1; found: 245.2.

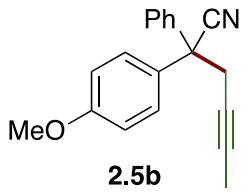

2.5b

Yield: 55 mg, 0.20 mmol, 67%

Appearance: yellow oil

^{1}H NMR (500 MHz, $CDCl_3$): δ 7.38 (m, 7H), 6.91 (m, 2H), 3.82 (s, 3H), 3.17 (q, J = 2.5 Hz, 2H), 1.76 (t, J = 2.5 Hz, 3H).

^{13}C NMR (126 MHz, $CDCl_3$): δ 159.49, 139.98, 131.62, 129.01, 128.66, 128.33, 127.33, 122.50, 114.32, 81.00, 73.68, 55.60, 51.27, 31.72, 3.89.

GC/MS: *m/z* $[M]^+$ calcd for $C_{19}H_{17}NO$: 275.1; found: 275.2.

IR: 3002, 2956, 2920, 2839, 2237, 1608, 1583, 1512, 1494, 1461, 1448, 1299, 1255, 1184, 1033, 912, 827, 732, 698, 594, 543 cm^{-1}

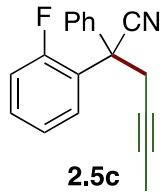

2.5c

Yield: 53 mg, 0.20 mmol, 67%

Appearance: yellow oil

^{1}H NMR (500 MHz, $CDCl_3$): δ 7.63 (td, J = 7.9, 1.7 Hz, 1H), 7.37 (m, 6H), 7.25 (td, J = 7.6, 1.3 Hz, 1H), 7.07 (ddd, J = 11.5, 8.2, 1.3 Hz, 1H), 3.28 (m, 2H), 1.75 (t, J = 2.5 Hz, 3H).

^{13}C NMR (126 MHz, $CDCl_3$): δ 160.64 (d, *J* = 251.1 Hz), 138.79, 130.91 (d, *J* = 8.7 Hz), 129.02, 128.91 (d, *J* = 2.8 Hz), 128.49, 126.76, 126.42 (d, *J* = 10.8 Hz), 124.51 (d, *J* = 3.6 Hz), 120.94, 117.13 (d, *J* = 21.7 Hz), 81.35, 73.31, 48.92, 30.50 (d, *J* = 2.2 Hz), 3.86.

^{19}F (376 MHz, $CDCl_3$): δ -108.8 (s, 1F).

GC/MS: *m/z* $[M]^+$ calcd for $C_{18}H_{14}FN$: 263.1; found: 263.2.

IR: 3062, 2920, 2854, 2241, 1612, 1598, 1581, 1490, 1450, 1226, 1112, 1035, 810, 757, 732, 698, 514 cm^{-1}

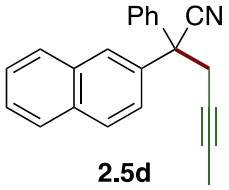

2.5d

Yield: 74 mg, 0.25 mmol, 84%

Appearance: yellow oil

^{1}H NMR (500 MHz, $CDCl_3$): δ 8.02 (d, *J* = 2.1 Hz, 1H), 7.87 (m, 3H), 7.55 (m, 2H), 7.42 (m, 6H), 3.31 (q, *J* = 2.5 Hz, 2H), 1.75 (t, *J* = 2.5 Hz, 3H).

^{13}C NMR (126 MHz, $CDCl_3$): δ 139.60, 136.80, 133.26, 133.03, 129.16, 129.12, 128.68, 128.54, 127.93, 127.57, 127.12, 127.03, 126.37, 125.26, 122.30, 81.32, 73.55, 52.12, 31.48, 3.96.

GC/MS: *m/z* $[M]^+$ calcd for $C_{22}H_{17}N$: 295.1; found: 295.2.

IR: 3058, 2920, 2852, 2239, 1598, 1494, 1448, 1434, 1274, 1124, 910, 815, 748, 734, 698, 478 cm^{-1}

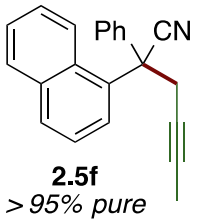

2.5f
> 95% pure

Yield: 68 mg, 0.23 mmol, 78%

Appearance: yellow oil

^{1}H NMR (500 MHz, $CDCl_3$): δ 7.89 (m, 4H), 7.59 (t, *J* = 7.8 Hz, 1H), 7.35 (m, 7H), 3.43 (dq, *J* = 16.4, 2.5 Hz, 1H), 3.28 (dq, *J* = 16.4, 2.5 Hz, 1H), 1.80 (t, *J* = 2.5 Hz, 3H).

^{13}C NMR (126 MHz, $CDCl_3$): 140.70, 135.03, 132.71, 130.69, 130.51, 129.37, 129.11, 128.27, 126.65, 126.61, 126.04, 125.90, 125.80, 124.94, 121.96, 81.60, 73.67, 50.37, 33.63, 3.94.

GCMS: *m/z* $[M]^+$ calcd for $C_{22}H_{17}N$: 295.1. Found: 295.2.

IR: 3085, 3055, 3029, 2918, 2237, 1600, 1510, 1490, 1448, 1434, 1398, 1161, 1031, 910, 796, 777, 761, 732, 700, 640, 565, 513 cm^{-1}

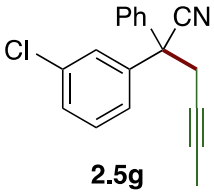

2.5g

Yield: 64 mg, 0.23 mmol, 75%

Appearance: yellow oil

^{1}H NMR (500 MHz, $CDCl_3$): δ 7.37 (m, 9H), 3.18 (p, *J* = 2.5 Hz, 2H), 1.76 (t, *J* = 2.5 Hz, 3H).

^{13}C NMR (126 MHz, $CDCl_3$): δ 141.62, 138.94, 135.08, 130.32, 129.30, 128.78, 128.76, 127.79, 127.38, 125.79, 121.80, 81.63, 73.14, 51.72, 31.53, 3.90.

GC/MS: *m/z* $[M]^+$ calcd for $C_{18}H_{14}ClN$: 279.1; found: 279.2.

IR: 3062, 3029, 2920, 2852, 2239, 1593, 1573, 1492, 1475, 1448, 1421, 1190, 1168, 1089, 999, 879, 783, 740, 717, 696, 669, 416 cm^{-1}

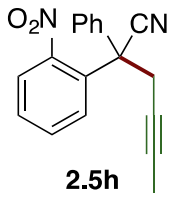

2.5h

Yield: 81 mg, 0.28 mmol, 94%

Appearance: orange oil

^{1}H NMR (500 MHz, $CDCl_3$): δ 8.00 (dd, *J* = 8.0, 1.3 Hz, 1H), 7.74 (m, 2H), 7.58 (td, *J* = 7.7, 1.3 Hz, 1H), 7.32 (m, 5H), 3.40 (m, 2H), 1.76 (t, *J* = 2.5 Hz, 3H).

^{13}C NMR (126 MHz, $CDCl_3$): δ 150.17, 137.55, 132.52, 131.49, 130.89, 130.19, 128.98, 128.78, 126.96, 126.15, 120.40, 82.40, 73.05, 50.31, 32.30, 3.85.

GC/MS: *m/z* $[M]^+$ calcd for $C_{18}H_{14}N_2O_2$: 290.1; found: 290.1.

IR: 3062, 2920, 2852, 2241, 1749, 1600, 1577, 1535, 1492, 1448, 1440, 1359, 1031, 912, 854, 781, 732, 698, 649, 416 cm^{-1}

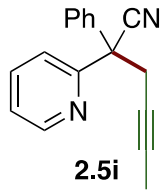

2.5i

Yield: 54 mg, 0.22 mmol, 74%

Appearance: orange-red oil

^{1}H NMR (500 MHz, $CDCl_3$): δ 8.55 (m, 1H), 7.39 (m, 8H), 3.33 (m, 2H), 1.61 (m, 3H).

^{13}C NMR (126 MHz, $CDCl_3$): δ 157.52, 149.58, 138.71, 137.47, 129.06, 128.45, 126.96, 123.28, 122.80, 121.80, 80.30, 73.95, 54.42, 30.55, 3.87.

GC/MS: *m/z* $[M]^+$ calcd for $C_{17}H_{14}N_2$: 246.1; found: 246.1.

IR: 3058, 2920, 2854, 2241, 1587, 1573, 1494, 1467, 1448, 1431, 1298, 1153, 1054, 1033, 993, 777, 757, 746, 698, 619, 538, 416 cm^{-1}

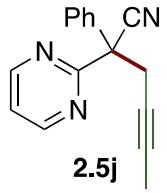

2.5j

Yield: 67 mg, 0.27 mmol, 89%

Appearance: red oil

^{1}H NMR (500 MHz, $CDCl_3$): δ 8.79 (d, *J* = 4.9 Hz, 2H), 7.56 (m, 2H), 7.32 (m, 4H), 3.61 (dq, *J* = 16.5, 2.5 Hz, 1H), 3.32 (dq, 16.4, 2.5 Hz, 1H), 1.70 (t, *J* = 2.5 Hz, 3H).

^{13}C NMR (126 MHz, $CDCl_3$): δ 166.79, 158.01, 137.59, 129.15, 128.67, 126.66, 120.88, 120.40, 80.25, 73.69, 56.75, 30.42, 3.88.

GC/MS: *m/z* $[M]^+$ calcd for $C_{16}H_{13}N_3$: 247.1; found: 247.2.

IR: 3087, 3060, 3039, 3960, 2920, 2854, 2244, 1566, 1494, 1450, 1434, 1409, 1058, 1033, 912, 811, 757, 730, 698, 634 cm^{-1}

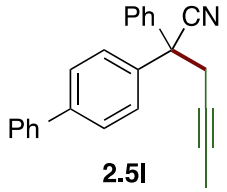

2.5l

Yield: 87 mg, 0.27 mmol, 89%

Appearance: yellow oil

^{1}H NMR (500 MHz, $CDCl_3$): δ 7.62 (m, 4H), 7.44 (m, 10H), 3.26 (q, J = 2.5 Hz, 2H), 1.78 (t, J = 2.5 Hz, 3H).

^{13}C NMR (126 MHz, $CDCl_3$): δ 141.28, 140.38, 139.61, 138.60, 129.17, 129.14, 128.50, 127.97, 127.90, 127.73, 127.44, 127.39, 122.31, 81.22, 73.58, 51.76, 31.57, 3.92.

GC/MS: *m/z* $[M]^+$ calcd for $C_{24}H_{19}N$: 321.2; found: 321.2.

IR: 3058, 3029, 2918, 2239, 1598, 1487, 1448, 1434, 1407, 1006, 910, 833, 763, 730, 696, 675, 649, 563, 520 cm^{-1}

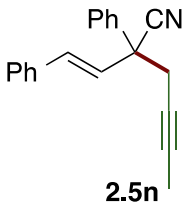

2.5n

Yield: 54 mg, 0.20 mmol, 68%

Appearance: dark yellow oil

^{1}H NMR (500 MHz, $CDCl_3$): δ 7.55 (m, 2H), 7.44 (m, 4H), 7.37 (m, 3H), 7.32 (m, 1H), 6.91 (d, J = 16 Hz, 1H), 6.39 (d, J = 16 Hz, 1H), 3.02 (q, J = 2.5 Hz, 2H), 1.80 (t, J = 2.5 Hz, 3H).

^{13}C NMR (126 MHz, $CDCl_3$): δ 138.38, 135.95, 132.76, 129.27, 129.02, 128.72, 128.65, 127.78, 127.14, 126.78, 120.99, 81.10, 73.08, 49.38, 31.91, 3.91.

GC/MS: *m/z* $[M]^+$ calcd for $C_{20}H_{17}N$: 271.1; found: 271.1.

IR: 3060, 3028, 2918, 2852, 2239, 1714, 1577, 1494, 1448, 1434, 1157, 1072, 1029, 966, 748, 694, 416 cm^{-1}

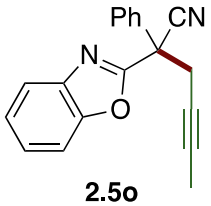

2.5o
> 91% pure

Yield: 18 mg, 0.063 mmol, 21%

Appearance: orange oil

^{1}H NMR (500 MHz, $CDCl_3$) *major isomer*: δ 7.83 (m, 1H), 7.55 (m, 3H), 7.42 (m, 5H), 3.62 (dq, *J* = 16.6, 2.5 Hz, 1 H), 3.34 (dq, *J* = 16.6, 2.5 Hz, 1H), 1.76 (t, 3H).

^{13}C NMR (126 MHz, $CDCl_3$) *major isomer:* δ 161.44, 151.52, 140.81, 135.09, 129.52, 129.50, 126.54, 126.37, 125.32, 121.06, 118.03, 111.50, 81.51, 72.30, 49.55, 31.17, 3.95.

GC/MS: *m/z* $[M]^+$ calcd for $C_{19}H_{14}N_2O$: 286.1; found: 286.2.

IR: 2956, 2921, 2852, 2243, 1610, 1560, 1492, 1452, 1238, 1166, 1002, 761, 748, 696 cm^{-1}

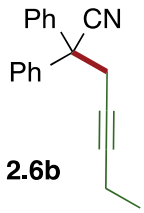

2.6b

Yield: 78 mg, 0.3 mmol, 99%

Appearance: clear yellow oil

^{1}H NMR (500 MHz, $CDCl_3$): δ 7.40 (m, 10H), 3.22 (t, *J* = 2.4 Hz, 2H), 2.12 (qt, *J* = 7.4, 2.3 Hz, 2H), 1.06 (t, *J* = 7.5 Hz, 3H).

^{13}C NMR (126 MHz, $CDCl_3$): δ 139.61, 128.99, 128.38, 127.46, 122.26, 87.19, 73.91, 51.95, 31.54, 14.04, 12.65.

GC/MS: *m/z* $[M]^+$ calcd for $C_{19}H_{17}N$: 259.1; found: 259.2**.**

IR: 3060, 2975, 2935, 2920, 2237, 1598, 1585, 1494, 1448, 1319, 1033, 1002, 754, 698, 651, 624, 538 cm^{-1}

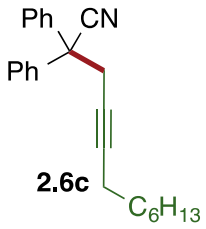

2.6c

Yield: 96 mg, 0.29 mmol, 97%

Appearance: yellow oil

^{1}H NMR (500 MHz, $CDCl_3$): δ 7.39 (m, 10H), 3.24 (t, *J* = 2.4 Hz, 2H), 2.11 (tt, *J* = 7.0, 2.4 Hz, 2H), 1.31 (m, 10H), 0.92 (t, *J* = 7.2 Hz, 3H).

^{13}C NMR (126 MHz, $CDCl_3$): δ 139.64, 129.01, 128.37, 127.48, 122.30, 85.93, 74.51, 52.02, 32.03, 31.63, 29.09, 28.87, 28.84, 22.96, 18.92, 14.43.

GC/MS: *m/z* $[M]^+$ calcd for $C_{24}H_{27}N$: 329.2; found: 329.2.

IR: 3060, 2954, 2927, 2856, 2237, 1598, 1494, 1465, 1448, 1434, 1330, 1033, 1002, 754, 698, 651, 624, 538 cm^{-1}

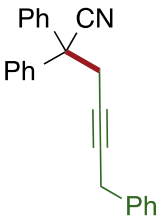

2.6d
85% pure with 15% allene isomer

Yield: 27 mg, 0.084 mmol, 28%

Appearance: yellow oil

^{1}H NMR (500 MHz, $CDCl_3$): δ 7.33 (m, 15H), 3.56 (t, J = 2.4 Hz, 2H), 3.33 (t, J = 2.4 Hz, 2H).

^{13}C NMR (126 MHz, $CDCl_3$): δ 139.48, 136.80, 129.15, 128.67, 128.49, 128.12, 127.50, 126.73, 122.31, 83.09, 76.98, 51.97, 31.75, 25.33.

GC/MS: *m/z* $[M]^+$ calcd for $C_{24}H_{19}N$: 321.2; found: 321.2.

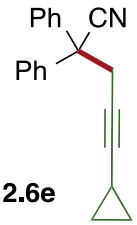

2.6e

Yield: 81 mg, 0.3 mmol, 99%

Appearance: yellow oil

^{1}H NMR (500 MHz, $CDCl_3$): δ 7.39 (m, 10H), 3.20 (d, J = 2.0 Hz, 2H), 1.15 (m, 1H), 0.68 (m, 2H), 0.55 (m, 2H).

^{13}C NMR (126 MHz, $CDCl_3$): δ 139.56, 128.97, 128.38, 127.44, 122.19, 88.98, 69.63, 51.96, 31.58, 8.33, -0.23.

GC/MS: *m/z* $[M]^+$ calcd for $C_{20}H_{17}N$: 271.1; found: 271.2.

IR: 3089, 3060, 3026, 2918, 2237, 1598, 1494, 1448, 1359, 1053, 1031, 877, 754, 698, 624 cm^{-1}

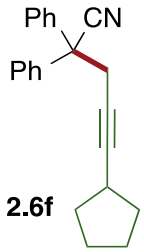

2.6f

Yield: 90 mg, 0.3 mmol, 99%

Appearance: yellow oil

^{1}H NMR (500 MHz, $CDCl_3$): δ 7.39 (m, 10H), 3.23 (d, J = 2.2 Hz, 2H), 2.56 (m, 1H), 1.79 (m, 2H), 1.63 (m, 2H), 1.51 (m, 4H).

^{13}C NMR (126 MHz, $CDCl_3$): δ 139.64, 128.95, 128.35, 127.51, 122.26, 90.42, 74.19, 52.04, 33.89, 31.65, 30.38, 24.97.

GC/MS: *m/z* $[M]^+$ calcd for $C_{22}H_{21}N$: 299.2; found: 299.2.

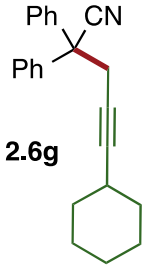

2.6g

Yield: 93 mg, 0.3 mmol, 99%

Appearance: yellow oil

^{1}H NMR (500 MHz, $CDCl_3$): δ 7.39 (m, 10H), 3.24 (d, J = 2.2 Hz, 2H), 2.34 (br m, 1H), 1.65 (br m, 2H), 1.57 (br m, 2H), 1.31 (m, 6H).

^{13}C NMR (126 MHz, $CDCl_3$): δ 139.62, 128.97, 128.36, 127.53, 122.29, 90.05, 74.71, 52.09, 32.63, 31.65, 29.04, 26.15, 24.68.

GC/MS: *m/z* $[M]^+$ calcd for $C_{23}H_{23}N$: 313.2; found: 313.3.

IR: 3060, 3029, 2929, 2852, 2237, 1731, 1598, 1494, 1448, 1317, 1033, 754, 698, 624, 538 cm^{-1}

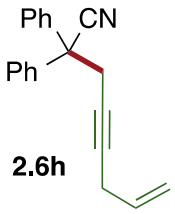

2.6h

Yield: 54 mg, 0.20 mmol, 67%

Appearance: yellow oil

^{1}H NMR (500 MHz, $CDCl_3$): δ 7.41 (m, 10H), 5.73 (m, 1H), 5.16 (dq, *J* = 16.9, 1.8 Hz, 1H), 5.04 (dq, *J* = 10.0, 1.7 Hz, 1H), 3.29 (t, *J* = 2.3 Hz, 2H), 2.91 (dp, *J* = 4.3, 2.1 Hz, 2H).

^{13}C NMR (126 MHz, $CDCl_3$): δ 139.51, 132.43, 129.10, 128.47, 127.46, 122.26, 116.36, 82.08, 77.13, 51.93, 31.64, 23.23.

GC/MS: *m/z* $[M]^+$ calcd for $C_{10}H_{17}N$: 271.1; found: 271.2.

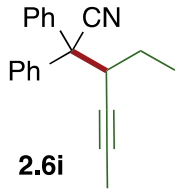

2.6i

Yield: 52 mg, 0.19 mmol, 63%

Appearance: clear yellow oil

^{1}H NMR (500 MHz, $CDCl_3$): δ 7.49 (m, 2H), 7.27 (m, 8H), 3.24 (m, 1H), 1.65 (d, J = 2.3 Hz, 3H), 1.46 (m, 2H), 1.00 (t, J = 7.3 Hz, 3H).

^{13}C NMR (126 MHz, $CDCl_3$): δ 139.68, 139.37, 129.13, 128.71, 128.12, 128.03, 127.92, 127.25, 121.56, 82.22, 77.54, 57.70, 42.42, 25.37, 12.71, 3.92.

GC/MS: *m/z* $[M]^+$ calcd for $C_{20}H_{19}N$: 273.2; found: 273.2.

IR: 3064, 2964, 2921, 2877, 2239, 1596, 1494, 1450, 1326, 1031, 767, 754, 734, 698, 536 cm^{-1}

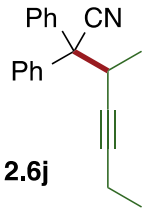

2.6j

Yield: 77 mg, 0.28 mmol, 92%

Appearance: clear light yellow oil

^{1}H NMR (500 MHz, $CDCl_3$): δ 7.51 (m, 2H), 7.38 (m, 2H), 7.26 (m, 6H), 3.52 (qt, J = 6.8, 2.2 Hz, 1H), 2.01 (m, 2H), 1.23 (d, J = 6.9 Hz, 3H), 0.93 (t, J = 7.5 Hz, 3H).

^{13}C NMR (126 MHz, $CDCl_3$): δ 139.45, 139.11, 129.09, 128.62, 128.16, 128.05, 127.99, 127.31, 121.26, 87.21, 79.39, 58.13, 34.75, 18.61, 14.05, 12.66.

GC/MS: *m/z* $[M]^+$ calcd for $C_{20}H_{19}N$: 273.2; found: 273.2.

IR: 3060, 3033, 2977, 2937, 2918, 2877, 2237, 1598, 1494, 1450, 1377, 1319, 1033, 1002, 914, 765, 750, 698, 657, 540 cm^{-1}

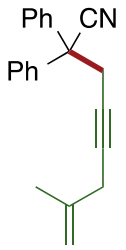

2.6k

Yield: 74 mg, 0.26 mmol, 87%

Appearance: clear yellow oil

^{1}H NMR (500 MHz, $CDCl_3$): δ 7.40 (br m, 10H), 4.84 (m, 1H), 4.76 (m, 1H), 3.28 (t, J = 2.4 Hz, 2H), 2.84 (m, 2H), 1.67 (m, 3H).

^{13}C NMR (126 MHz, $CDCl_3$): δ 140.68, 139.55, 129.13, 128.48, 127.48, 122.31, 111.92, 82.66, 76.86, 51.98, 31.70, 27.80, 22.32.

GC/MS: *m/z* $[M]^+$ calcd for $C_{21}H_{19}N$: 285.2; found: 285.2.

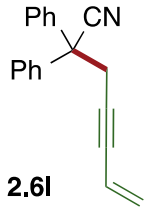

2.6l

Yield: 14 mg, 0.054 mmol, 18%

Appearance: clear yellow oil

^{1}H NMR (500 MHz, $CDCl_3$): δ 7.40 (br m, 10H), 5.71 (ddt, J = 17.5, 11.0, 2.0 Hz, 1H), 5.55 (dd, J = 17.6, 2.2 Hz, 1H), 5.43 (dd, J = 11.1, 2.2 Hz, 1H), 3.38 (d, J = 2.0 Hz, 2H).

^{13}C NMR (126 MHz, $CDCl_3$): δ 139.41, 129.15, 128.58, 127.68, 127.47, 122.08, 117.05, 84.65, 84.12, 51.73, 32.08.

GC/MS: *m/z* $[M]^+$ calcd for $C_{19}H_{15}N$: 257.1; found: 257.2.

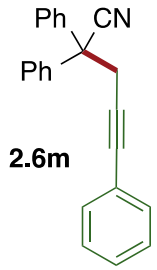

Yield: 16 mg, 0.054 mmol, 18%

Appearance: clear yellow oil

^{1}H NMR (500 MHz, $CDCl_3$): δ 7.40 (m, 15H), 3.49 (s, 2H).

^{13}C NMR (126 MHz, $CDCl_3$): δ 139.44, 131.96, 129.14, 128.59, 128.53, 128.48, 127.53, 123.08, 122.13, 85.53, 84.17, 51.80, 32.17.

GC/MS: *m/z* $[M]^+$ calcd for $C_{23}H_{17}N$: 307.1; found: 307.2

IR: 3060, 3031, 2954, 2923, 2852, 2239, 1596, 1583, 1490, 1448, 1313, 1031, 912, 756, 694, 655, 626, 541, 532 cm^{-1}

^{1}H and ^{13}C NMR Spectra:

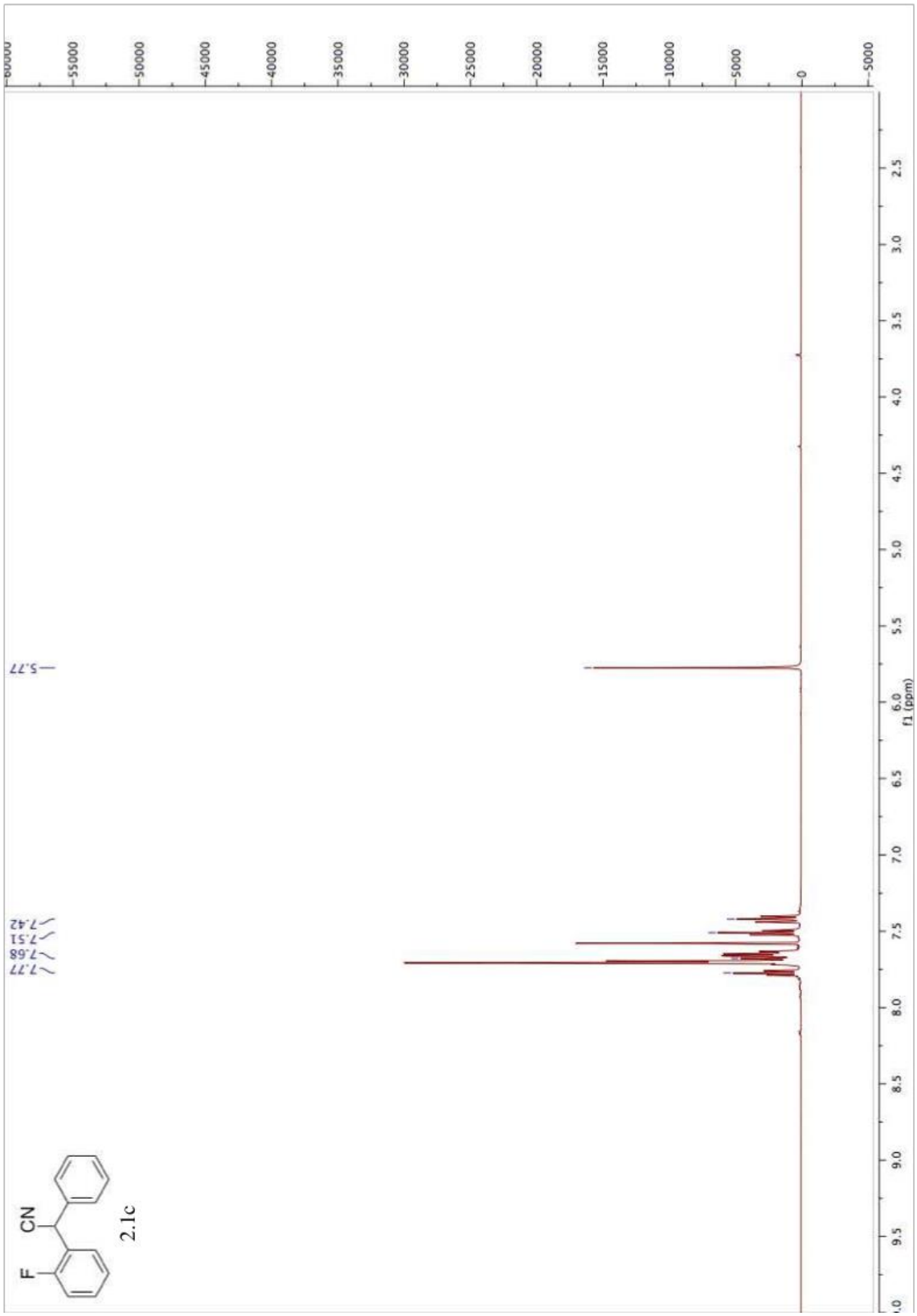
5.77
7.77
7.68
7.51
7.42
CN
F
2.1c
f1 (ppm)

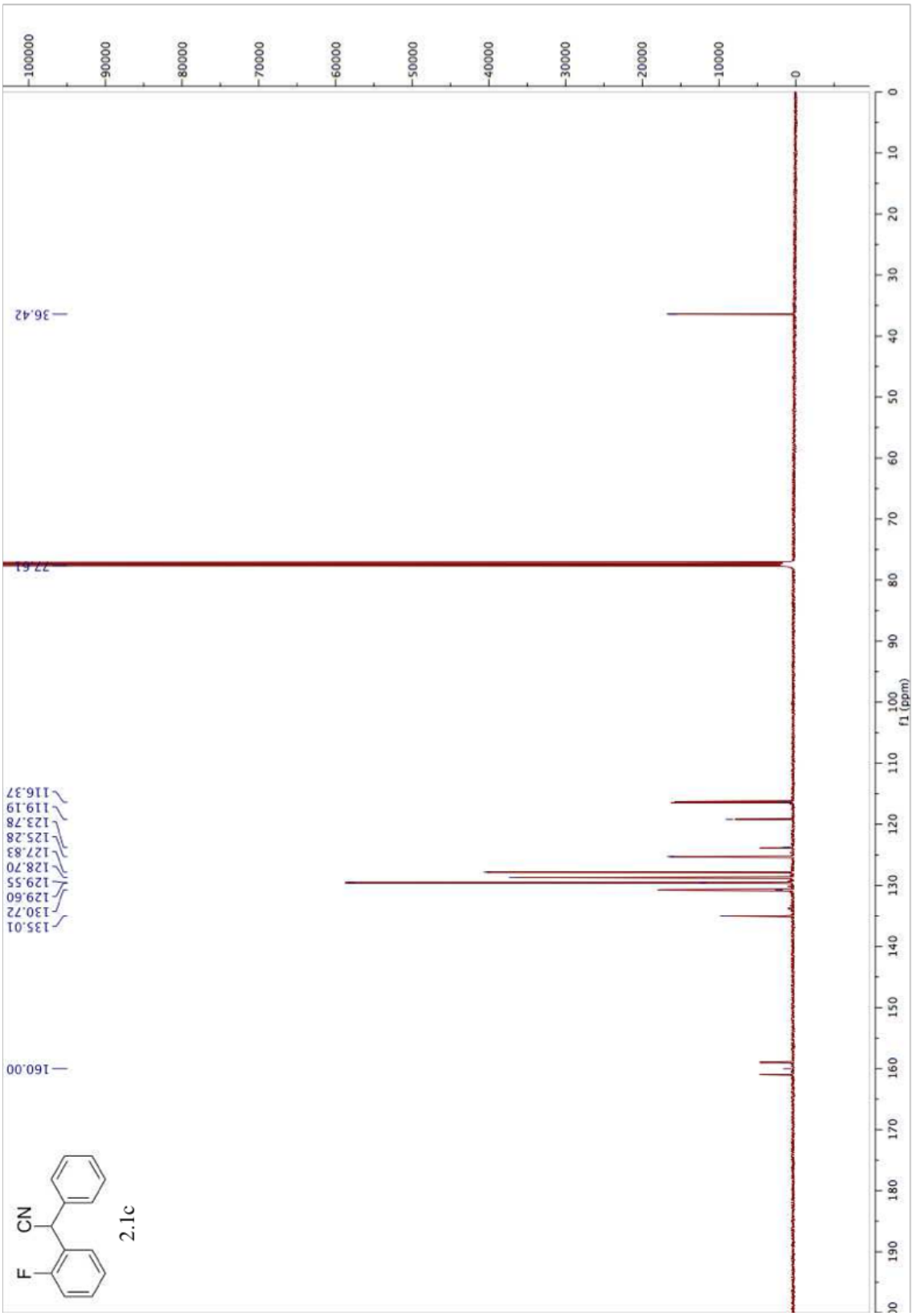
36.42
77.61
116.37
119.19
123.78
125.28
127.83
128.70
129.55
129.60
130.72
135.01
160.00
CN
F
2.1c
f1 (ppm)

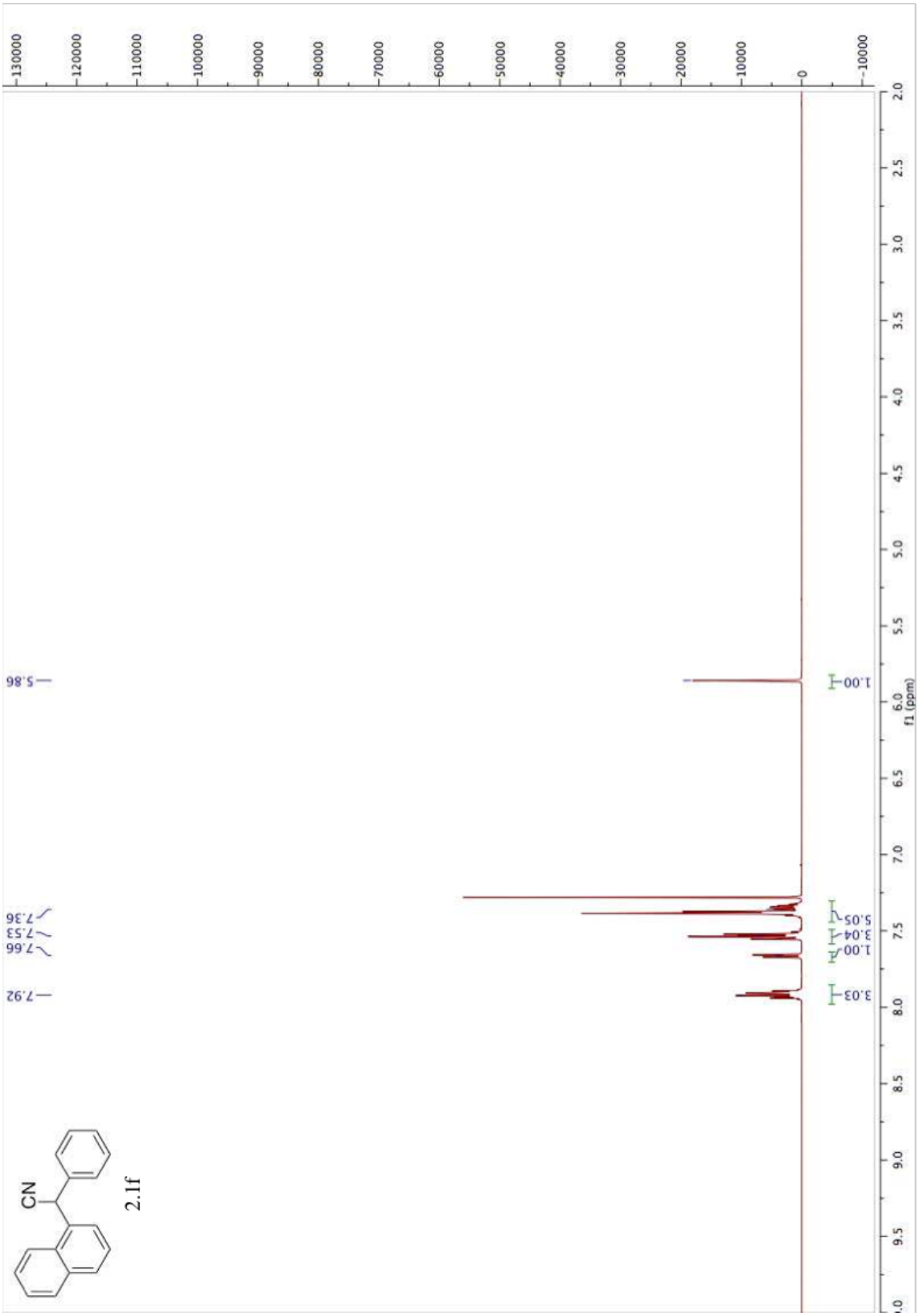
5.86
7.92
7.66
7.53
7.36
1.00
3.03
1.00
3.04
5.05
f1 (ppm)
CN
2.1f

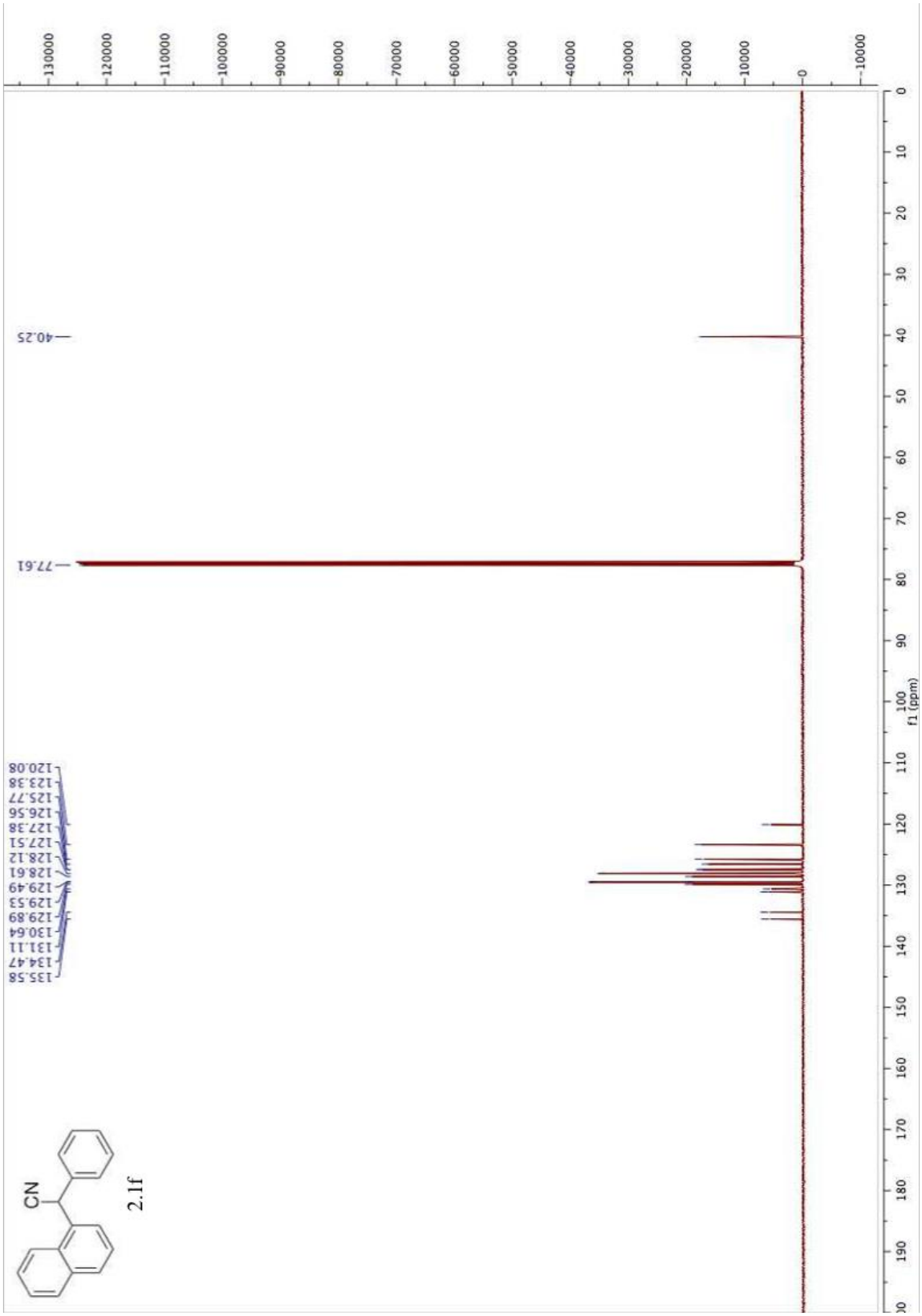
40.25
77.61
135.58
134.47
131.11
130.64
129.89
129.53
129.49
128.61
128.12
127.51
127.38
126.56
125.77
123.38
120.08
CN
2.1f
f1 (ppm)

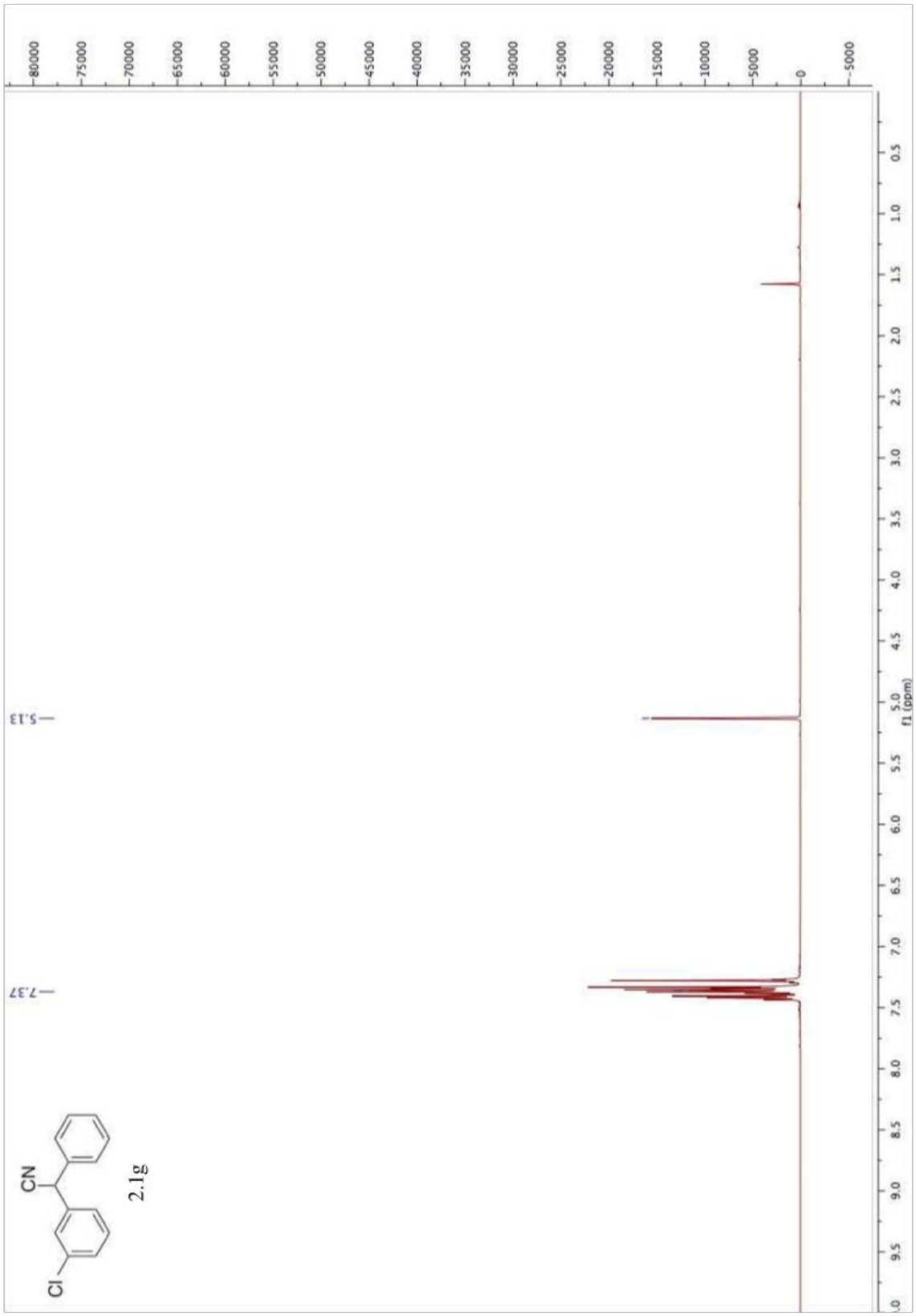
5.13
7.37
f1 (ppm)
CN
Cl
2.1g

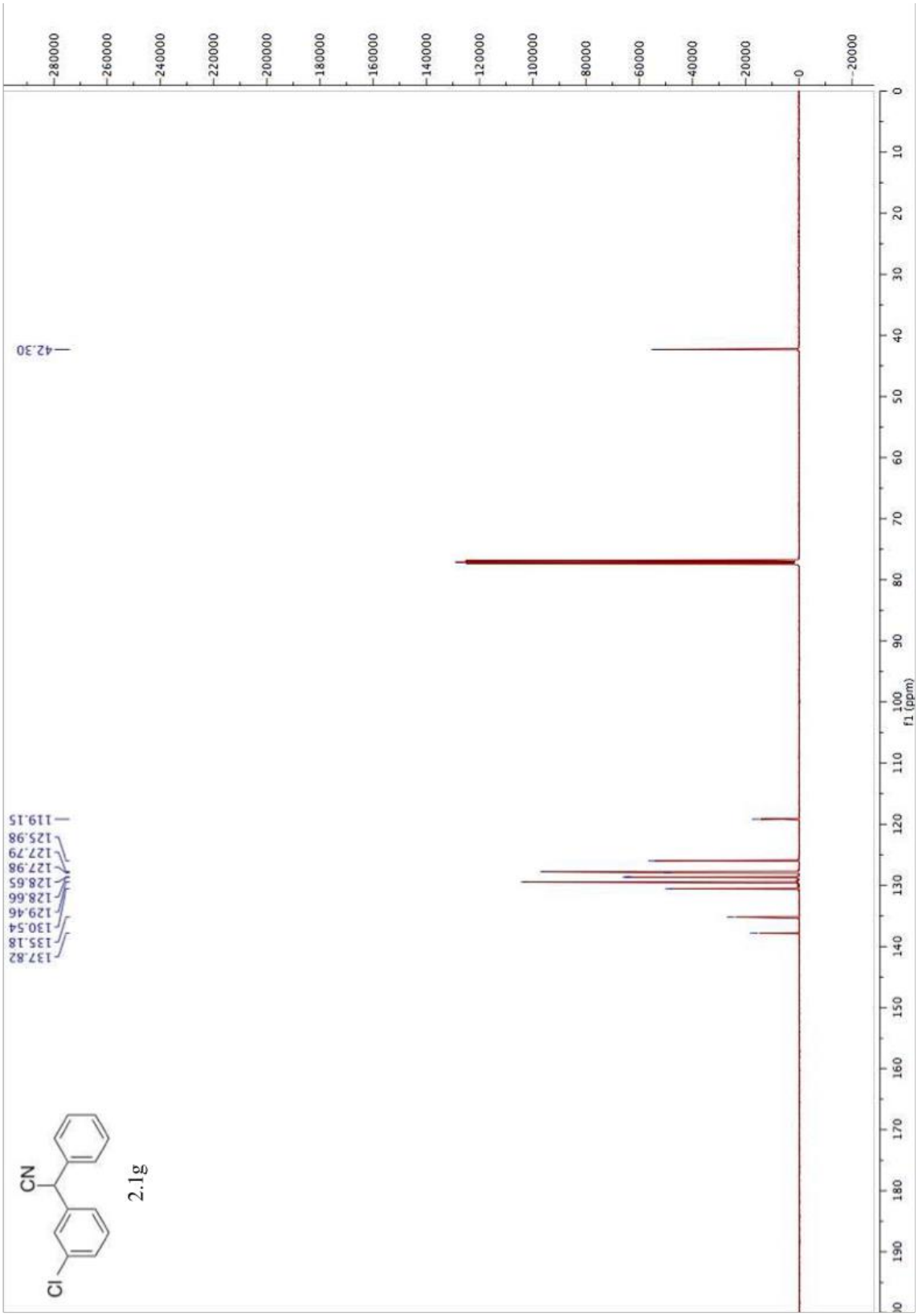
42.30
119.15
125.98
127.79
127.98
128.65
128.66
129.46
130.54
135.18
137.82
CN
Cl
f1 (ppm)

2.1g

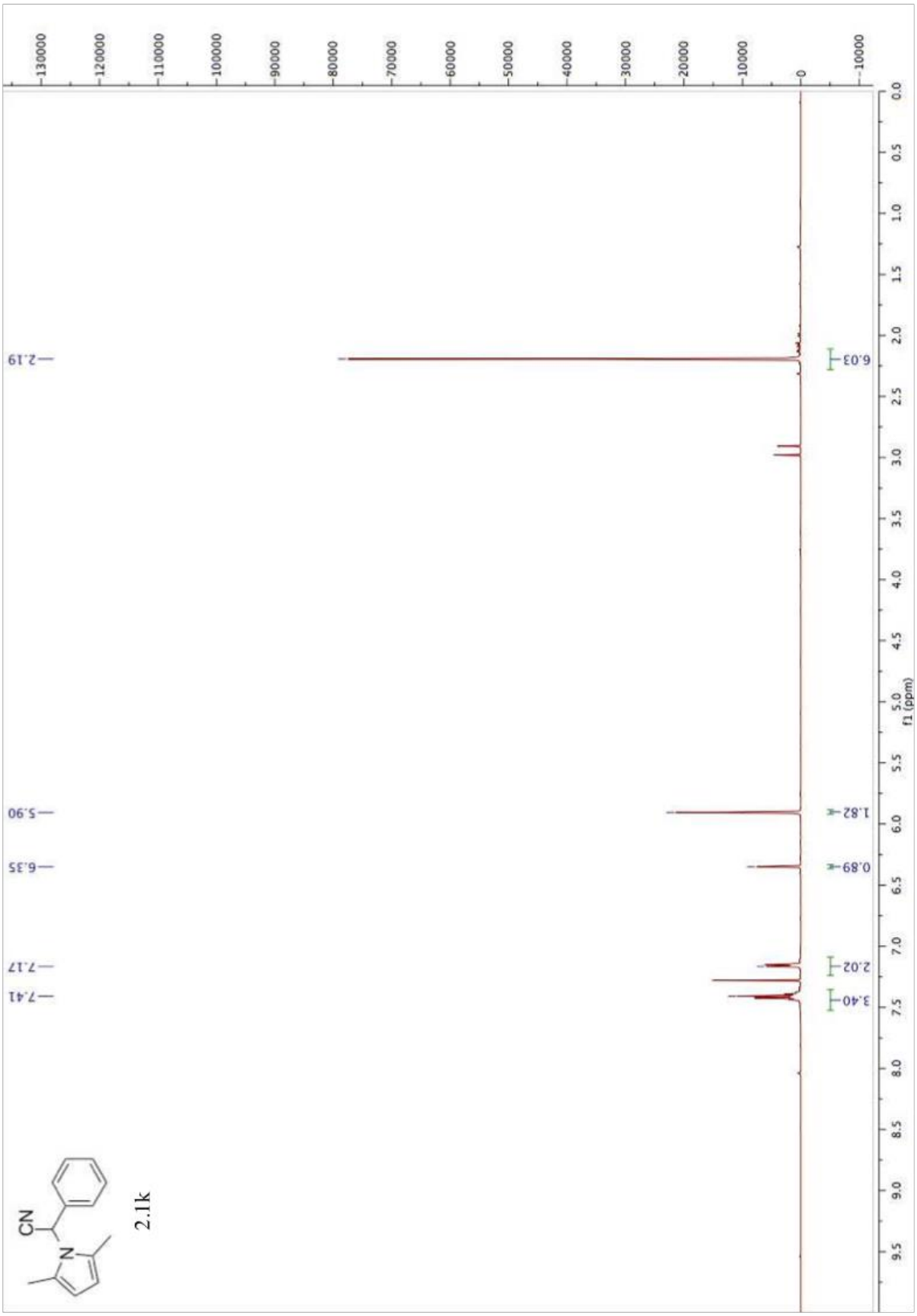
2.19
5.90
6.35
7.17
7.41
6.03
1.82
0.89
2.02
3.40
f1 (ppm)
CN
N
2.1k

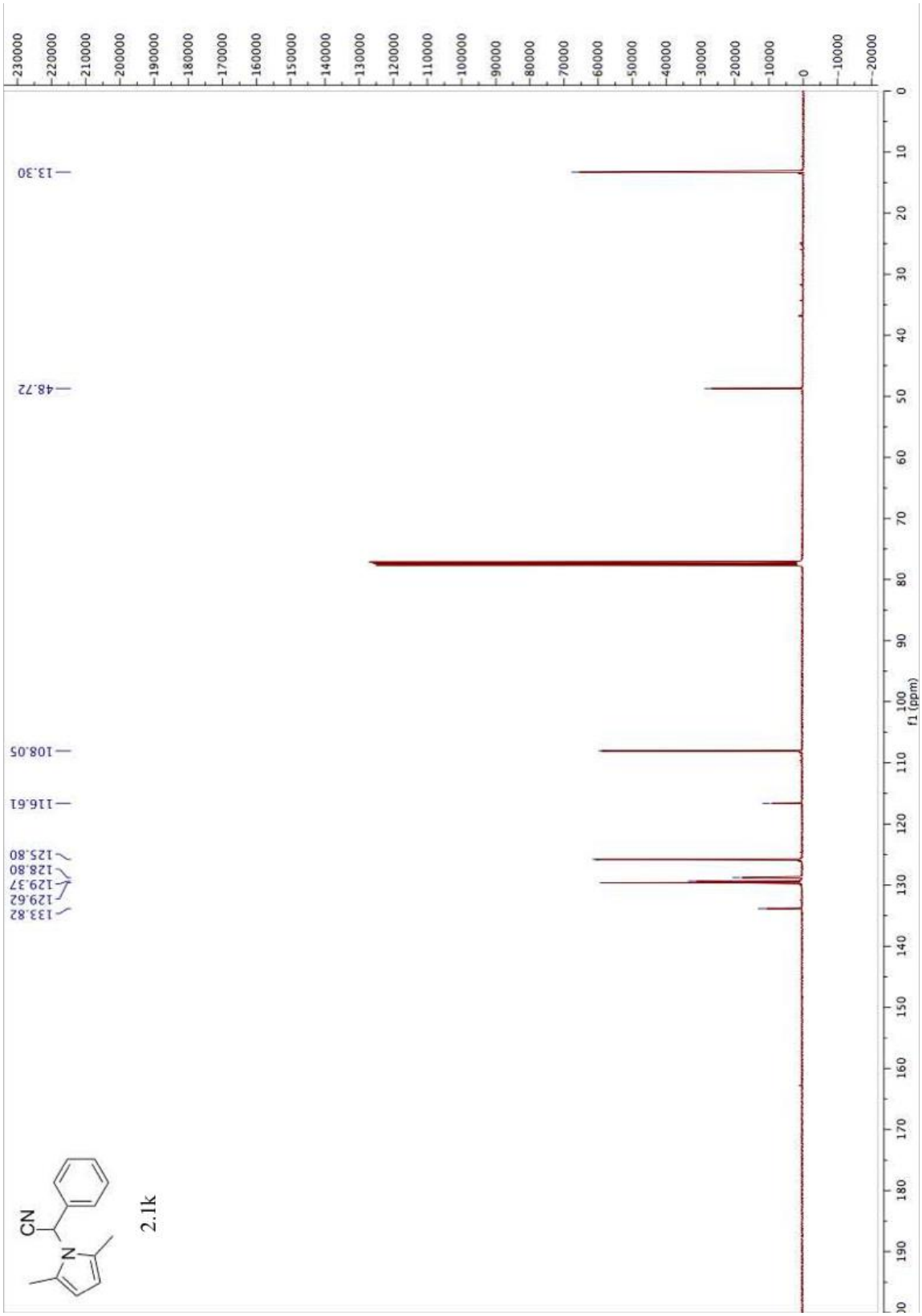
13.30
48.72
108.05
116.61
125.80
128.80
129.37
129.62
133.82
CN
N
2.1k
f1 (ppm)

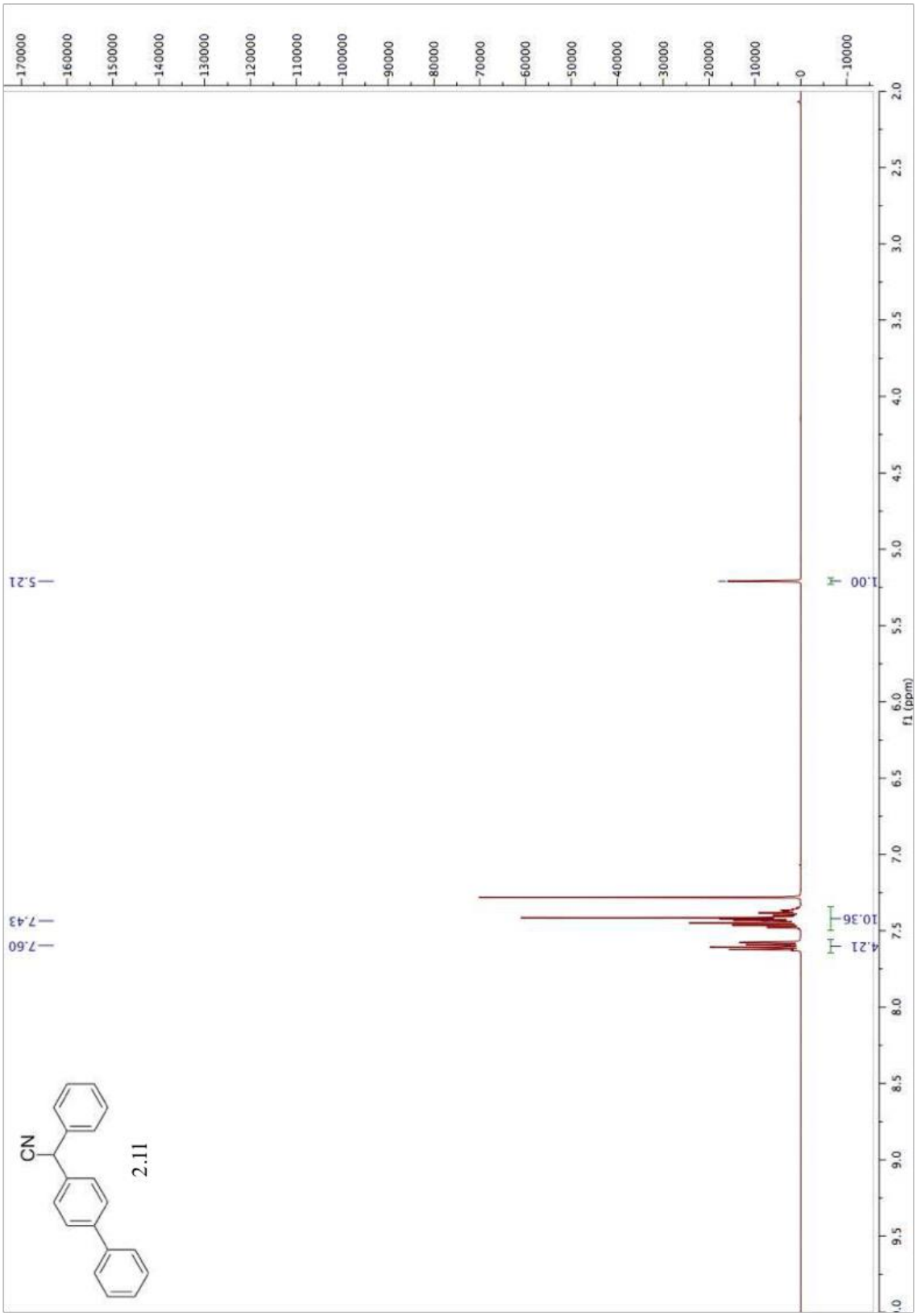
5.21
7.43
7.60
1.00
10.36
4.21
f1 (ppm)
CN
2.11

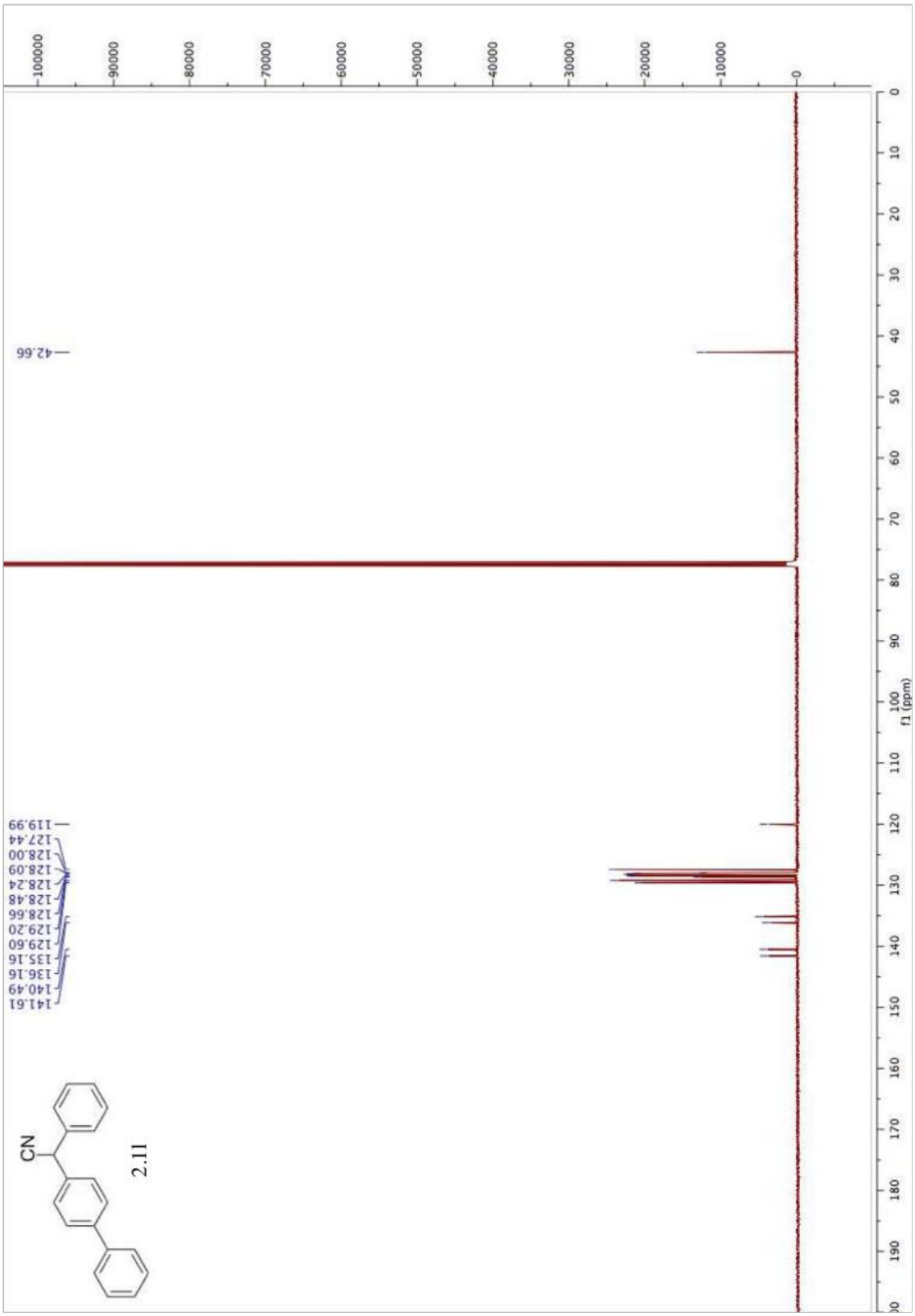
42.66
141.61
140.49
136.16
135.16
129.60
129.20
128.66
128.48
128.24
128.09
128.00
127.44
119.99
CN
2.11
f1 (ppm)

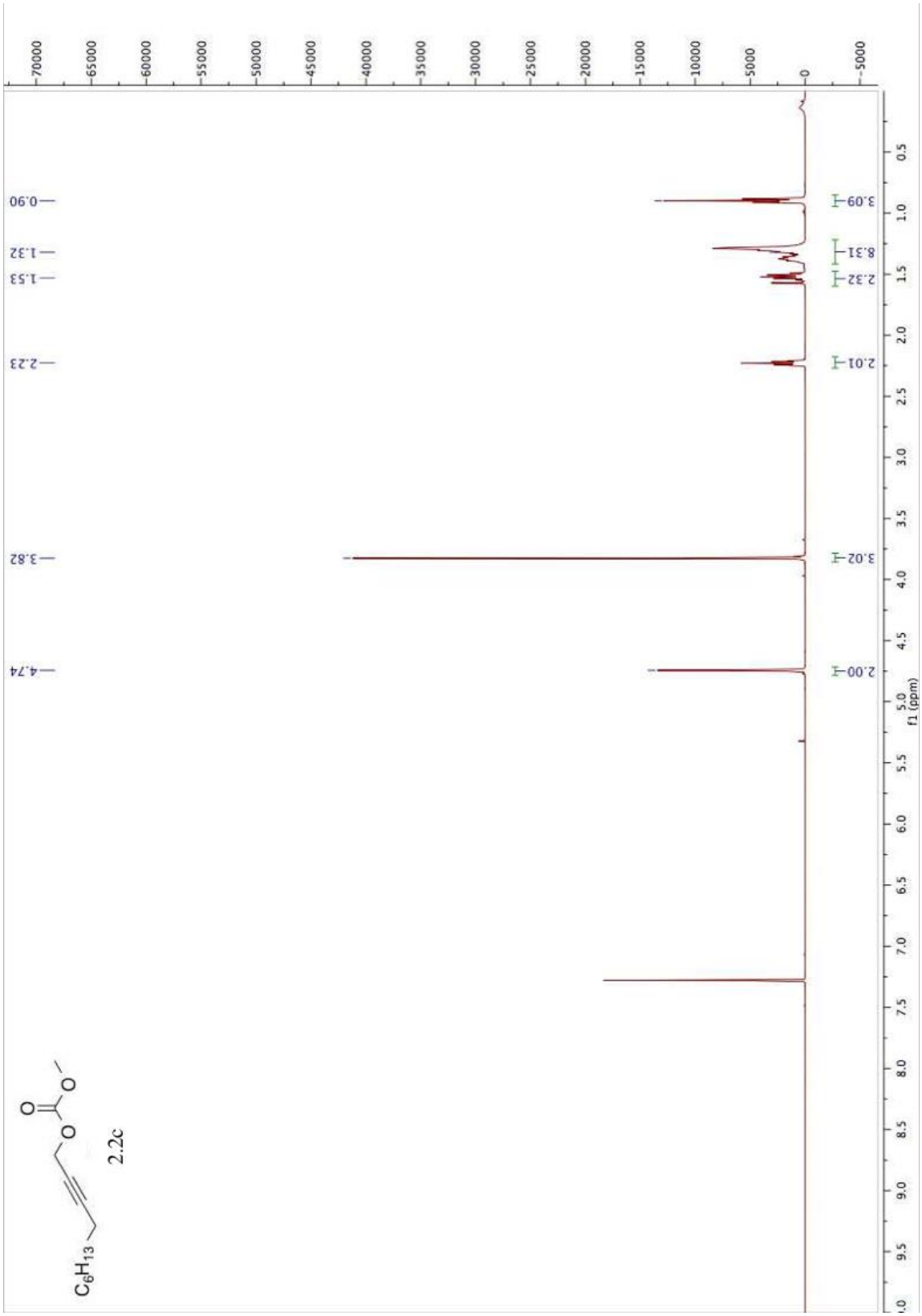
0.90
1.32
1.53
2.23
3.82
4.74
3.09
8.31
2.32
2.01
3.02
2.00
f1 (ppm)
2.2c

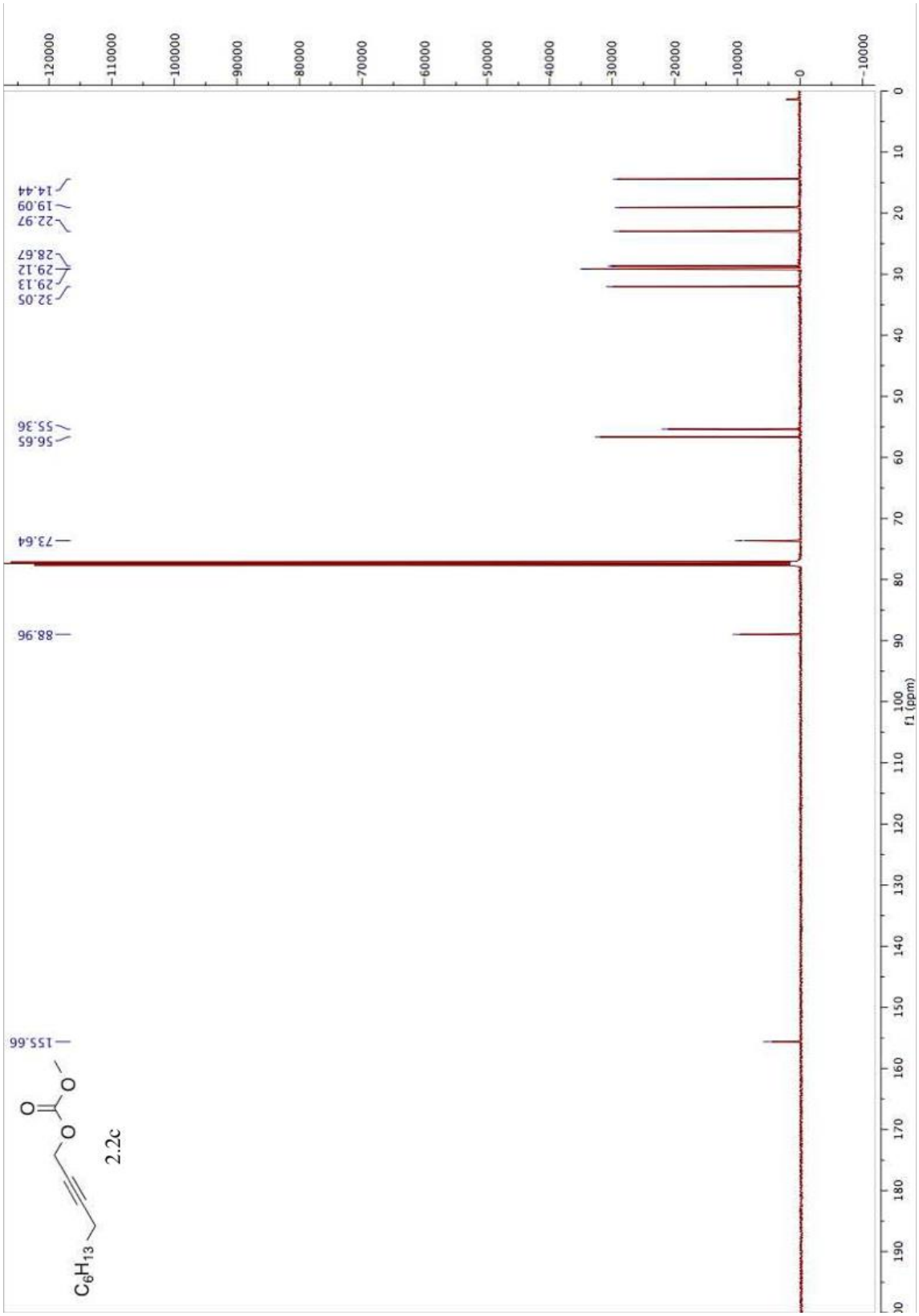
155.66
88.96
73.64
56.65
55.36
32.05
29.13
29.12
28.67
22.97
19.09
14.44
f1 (ppm)
2.2c

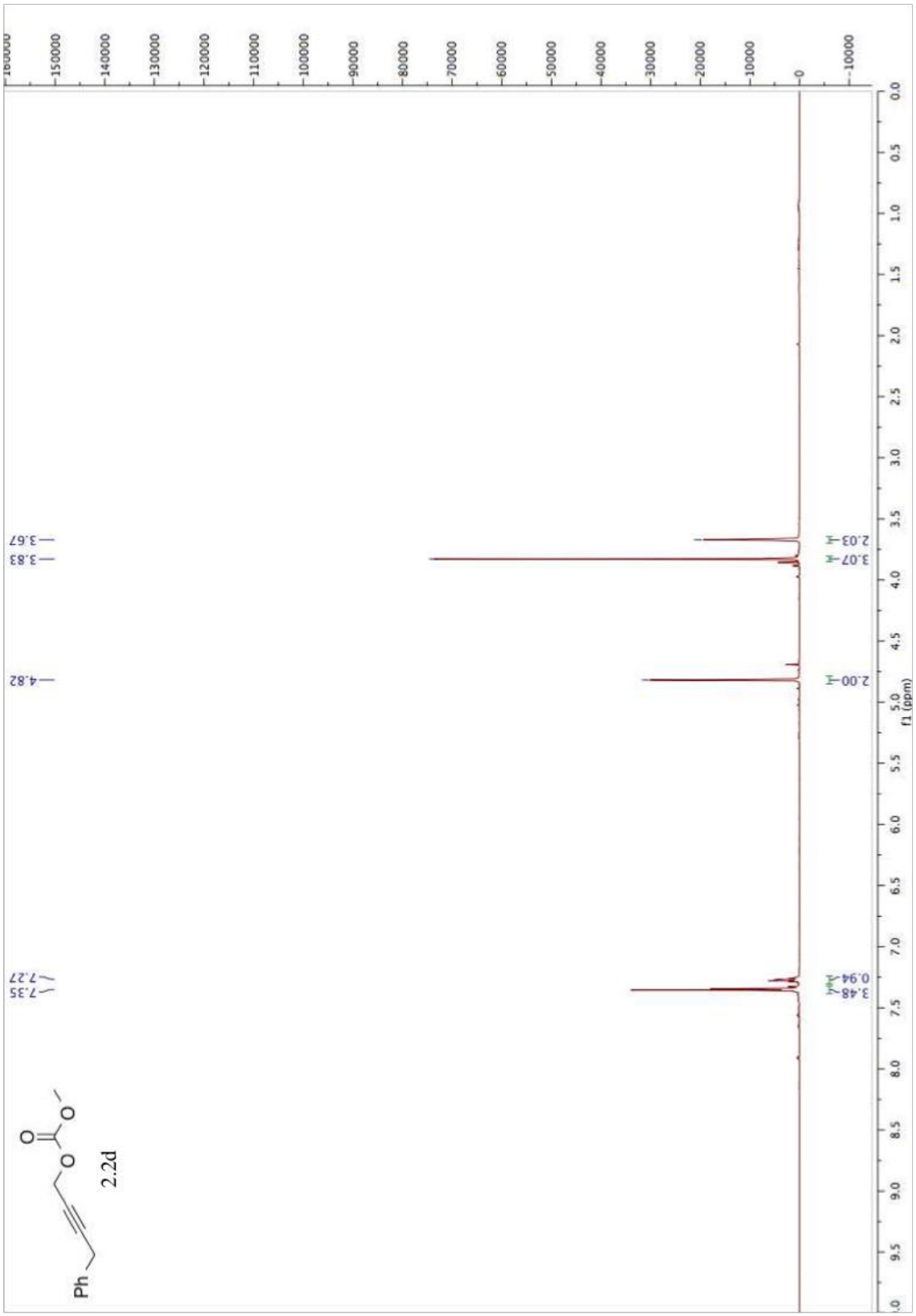
Ph
2.2d
7.35
7.27
4.82
3.83
3.67
3.48
0.94
2.00
3.07
2.03
f1 (ppm)

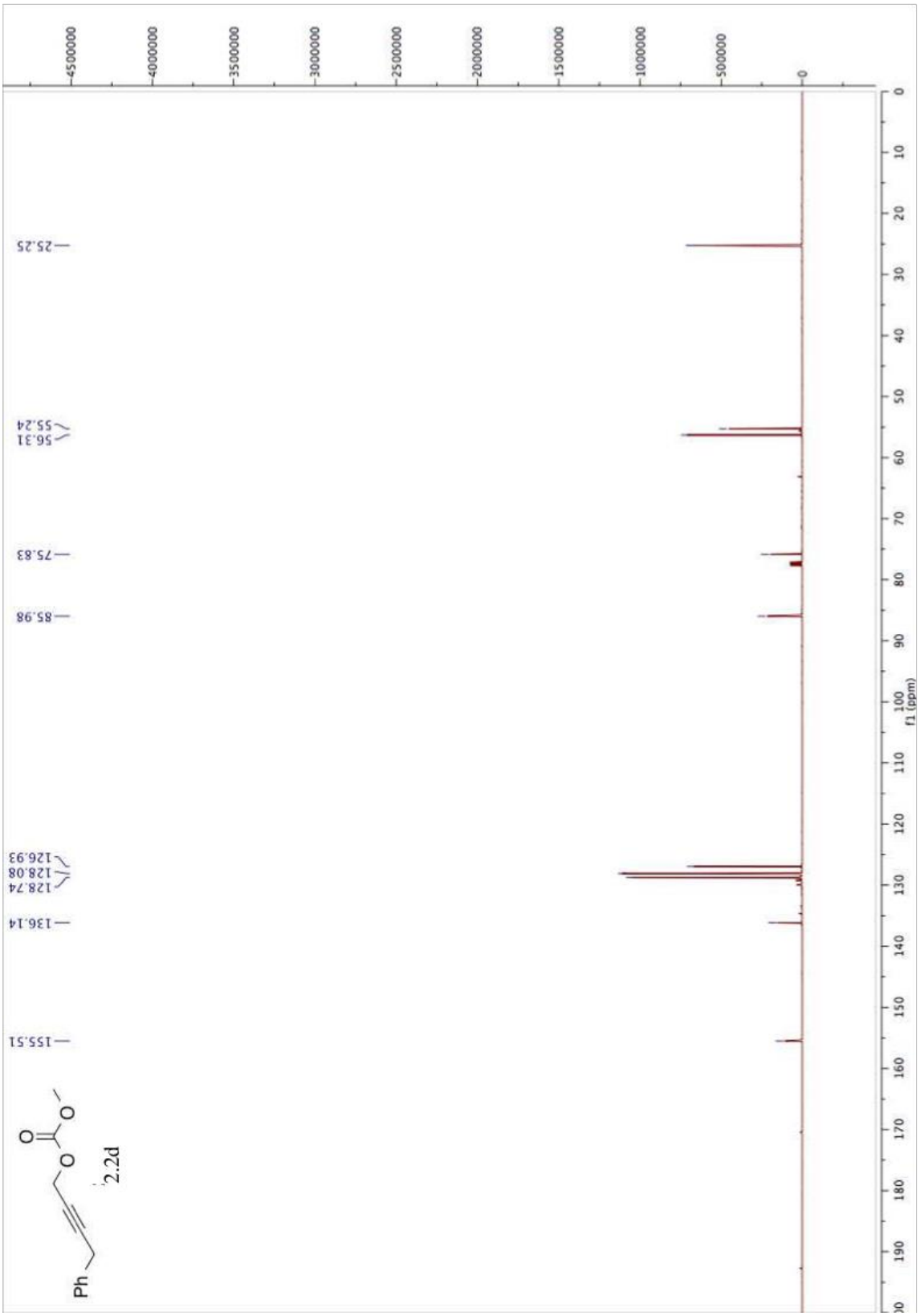
155.51
136.14
128.74
128.08
126.93
85.98
75.83
56.31
55.24
25.25
f1 (ppm)
Ph
O
O
O
2.2d

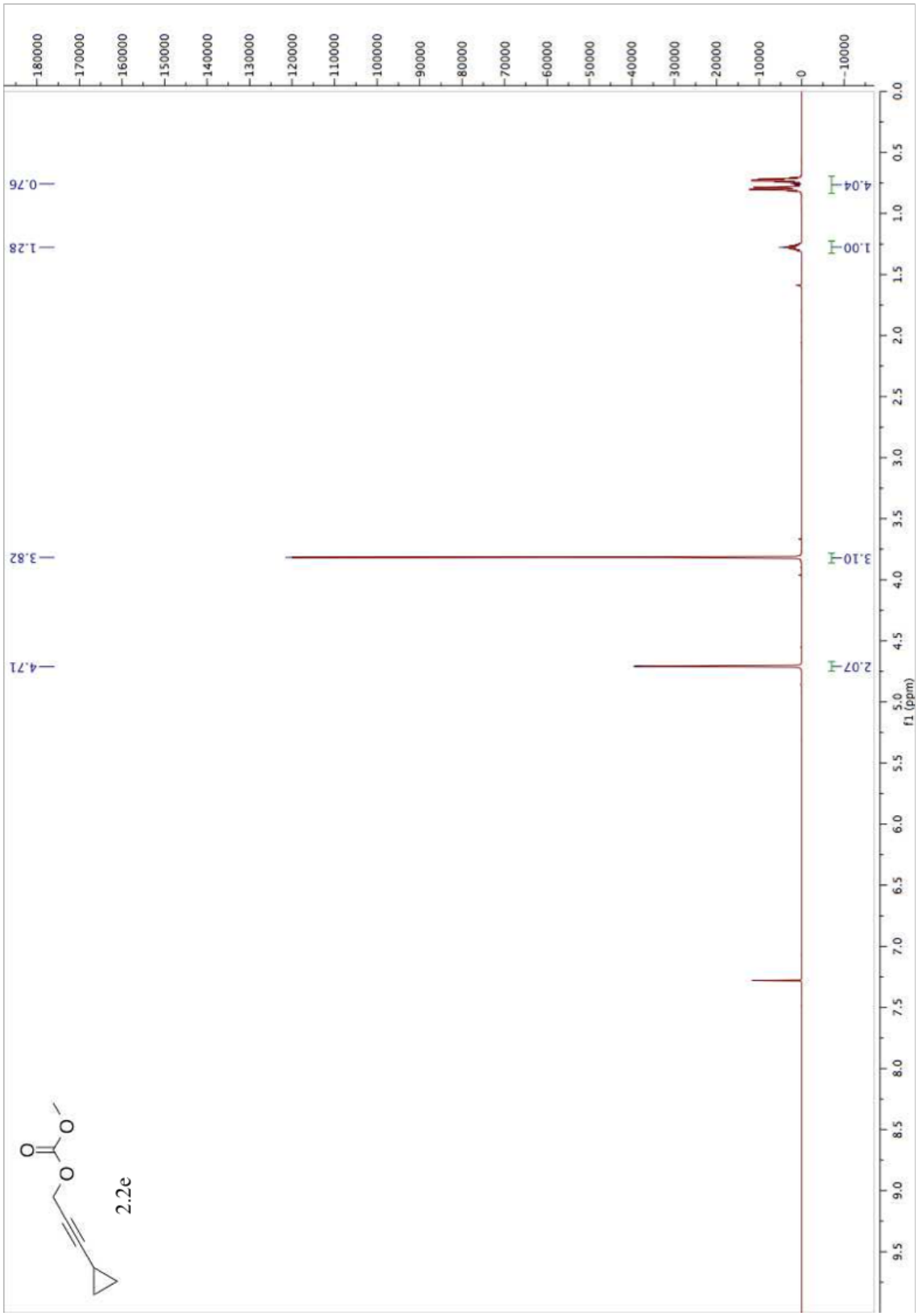
0.76
1.28
3.82
4.71
4.04
1.00
3.10
2.07
f1 (ppm)
2.2e

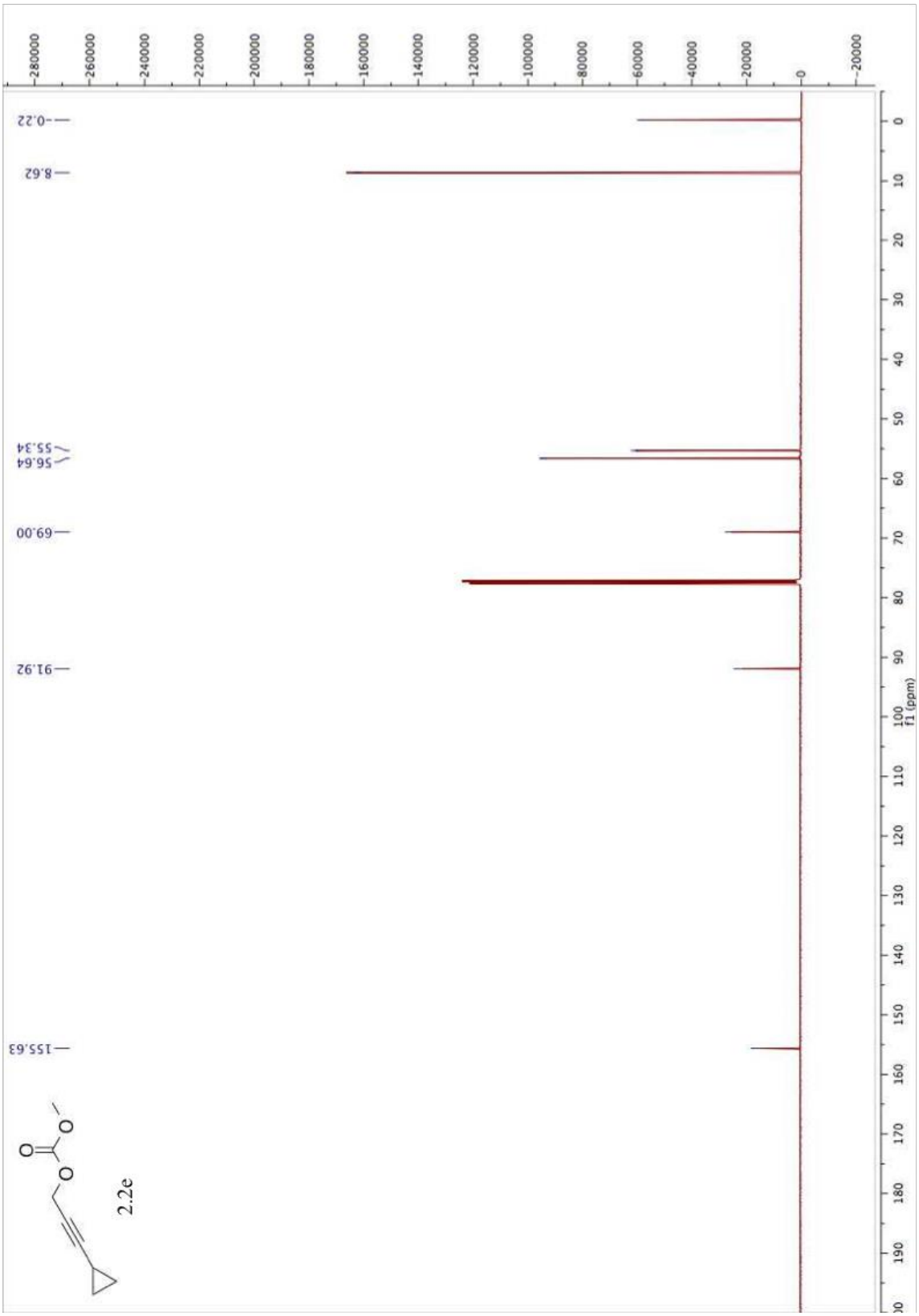
-0.22
8.62
55.34
56.64
69.00
91.92
155.63
2.2e
f1 (ppm)


2.2f
4.75
3.82
2.64
1.93
1.73
1.60
2.05
2.98
1.00
1.99
2.02
4.18
f1 (ppm)

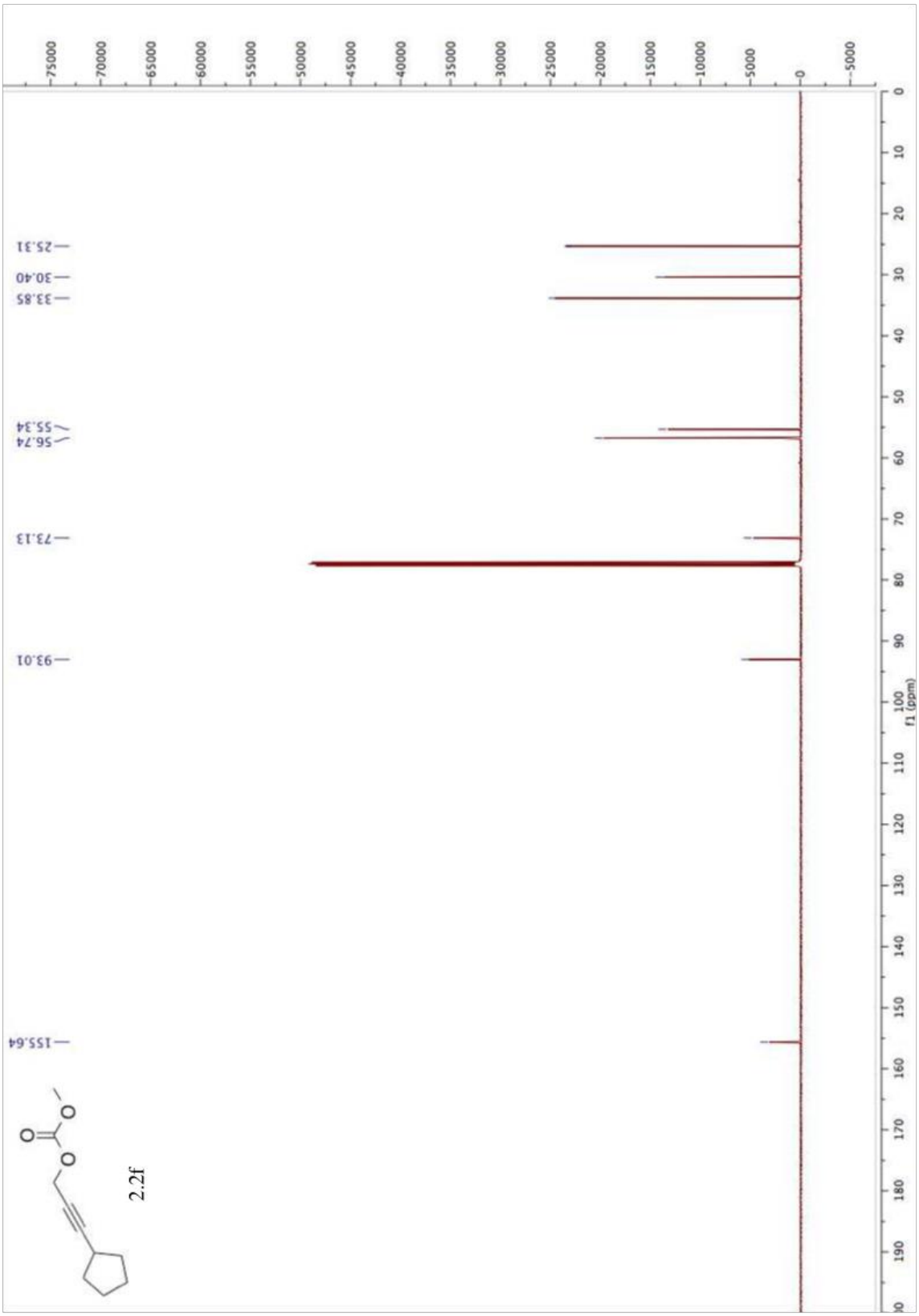

2.2f

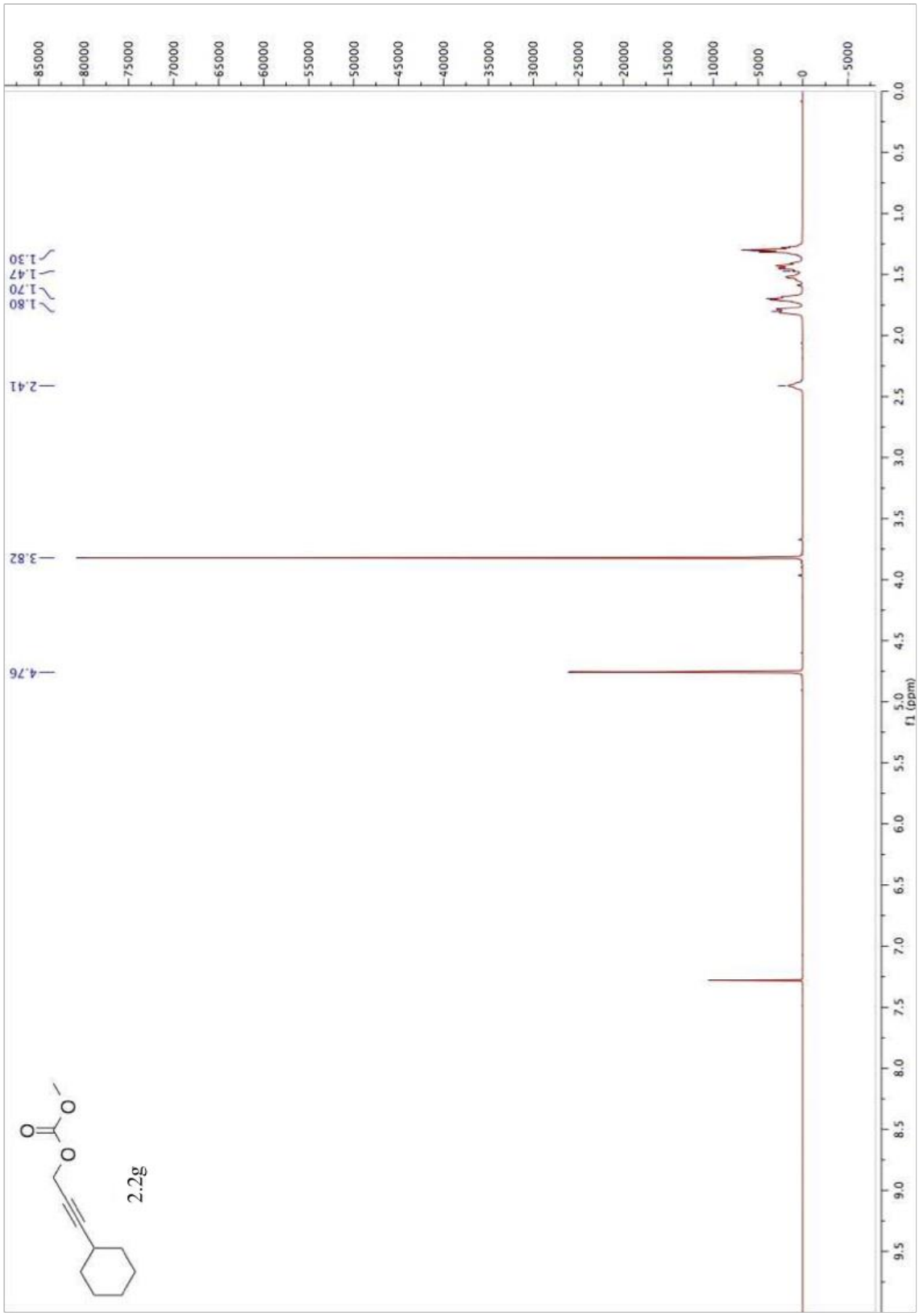

2.2g

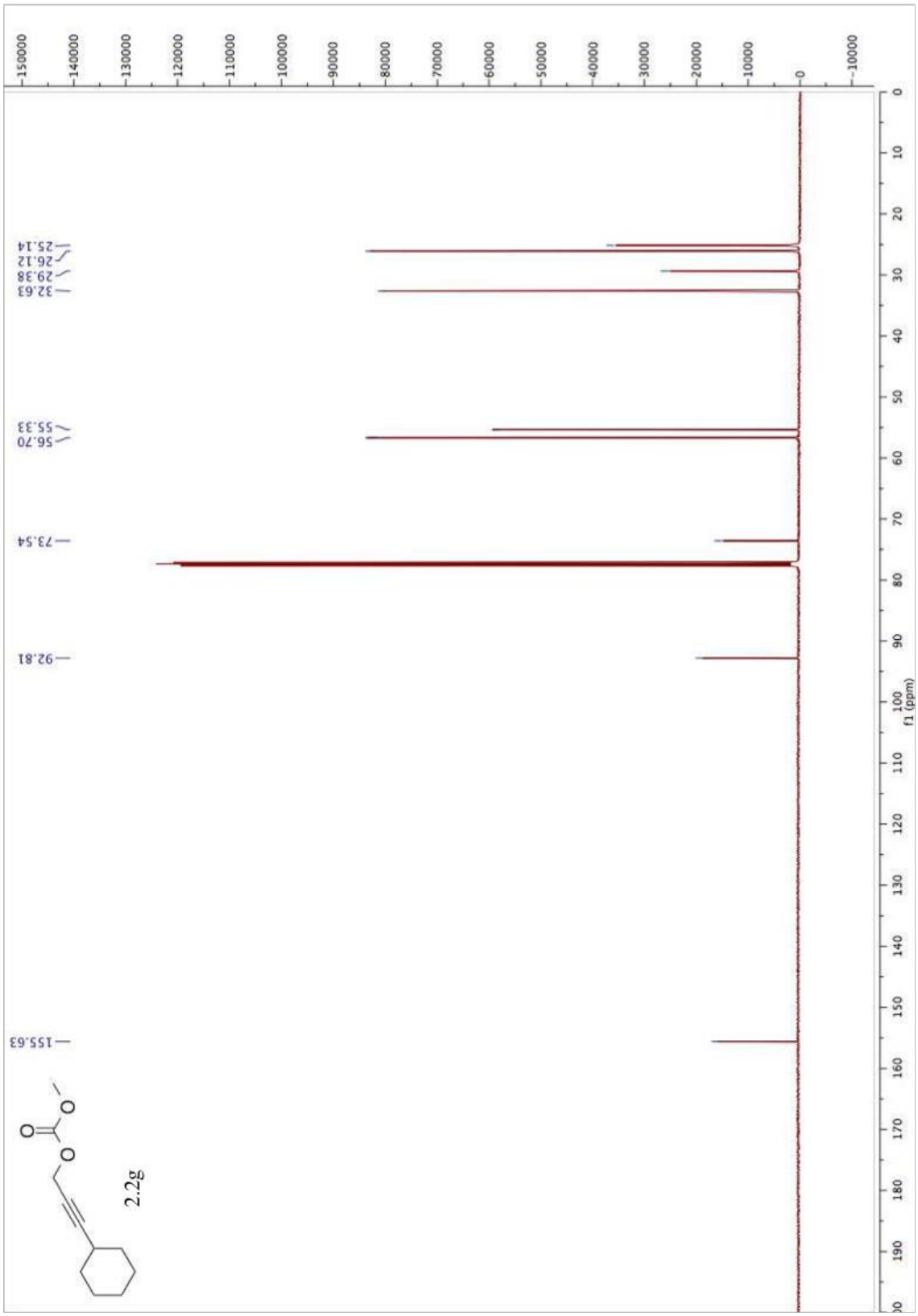
155.63
92.81
73.54
56.70
55.33
32.63
29.38
26.12
25.14
f1 (ppm)
2.2g

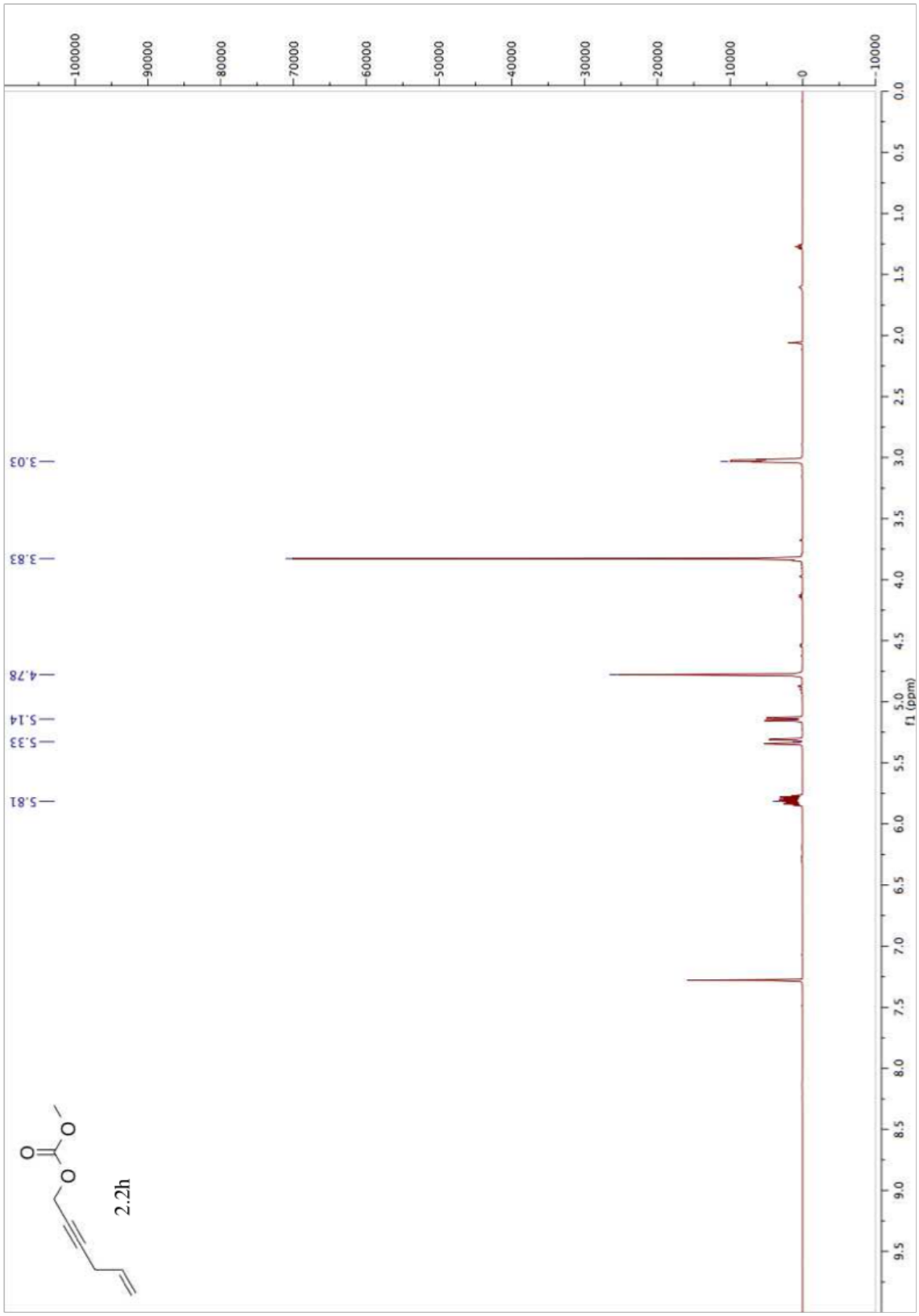
3.03
3.83
4.78
5.14
5.33
5.81
f1 (ppm)
2.2h

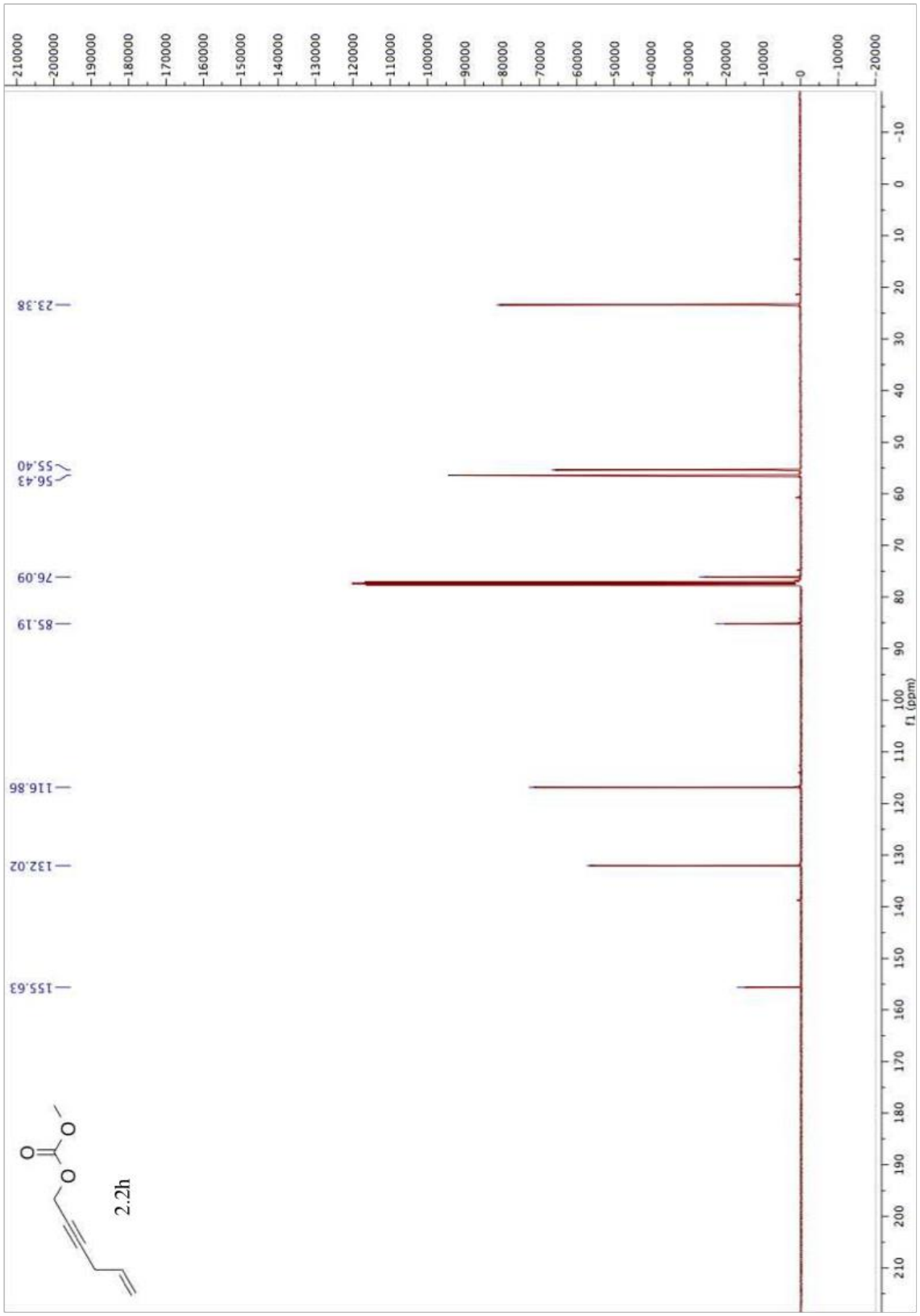
23.38
55.40
56.43
76.09
85.19
116.86
132.02
155.63
2.2h
f1 (ppm)

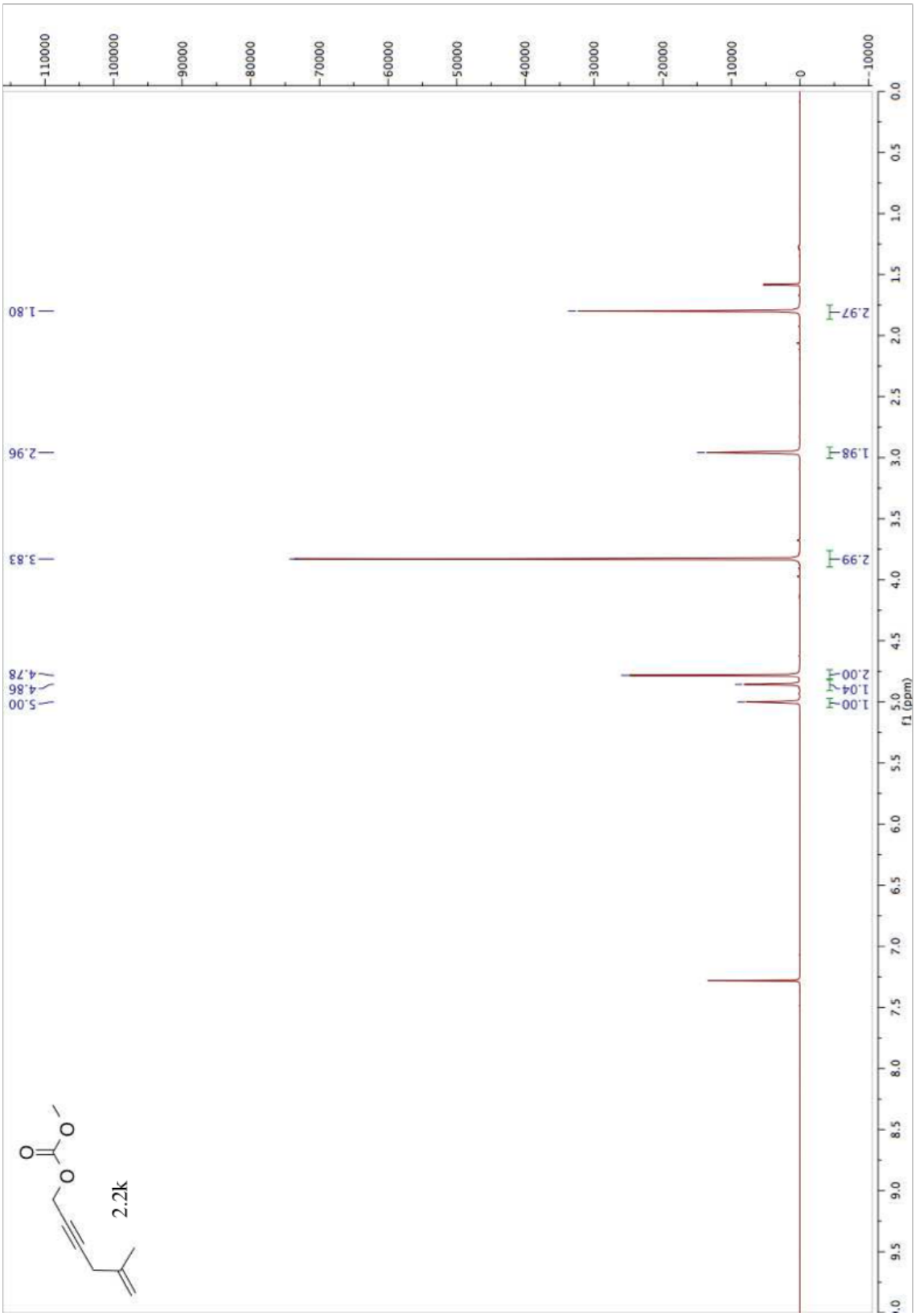
1.80
2.96
3.83
4.78
4.86
5.00
2.97
1.98
2.99
2.00
1.04
1.00
f1 (ppm)
2.2k

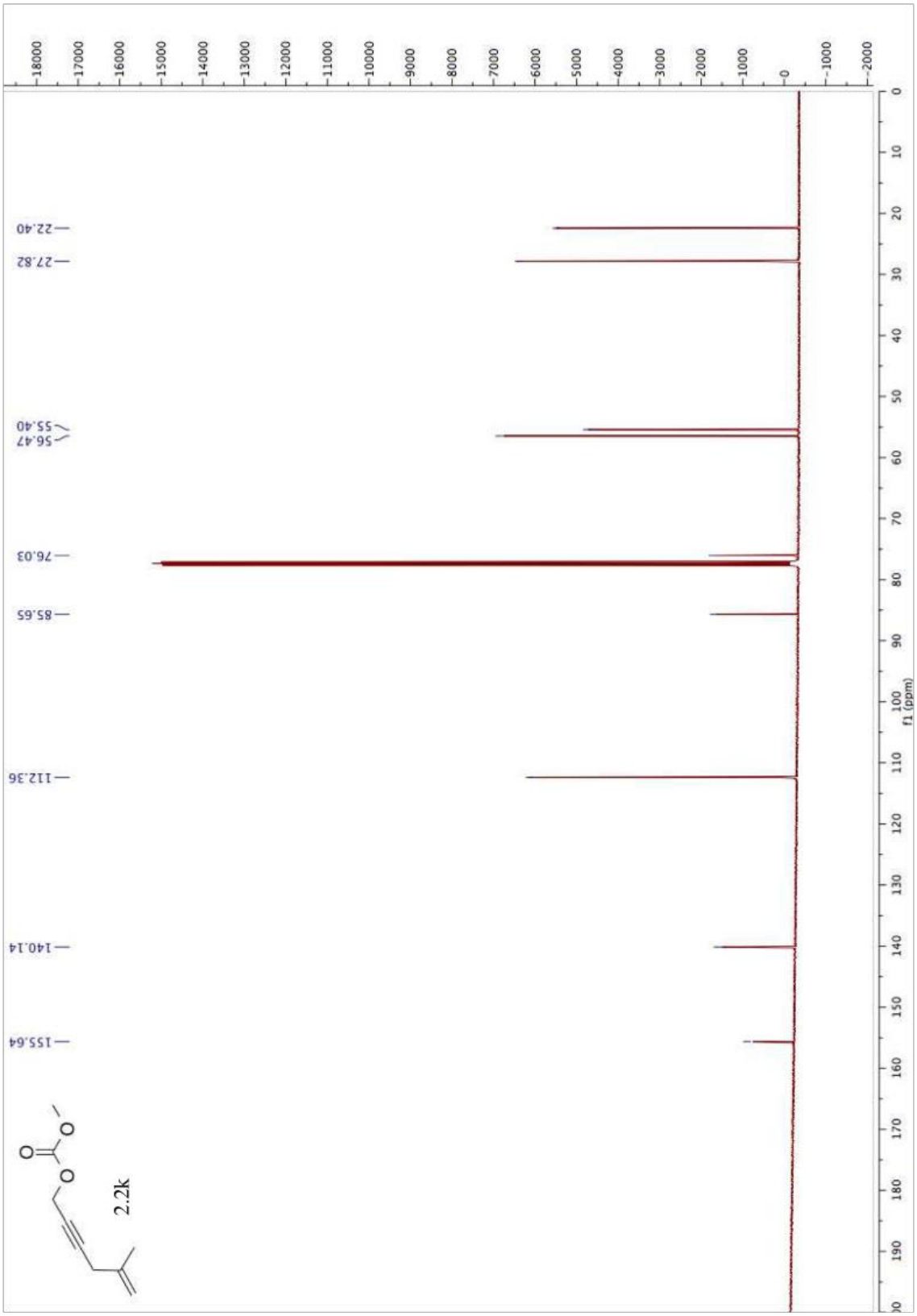
22.40
27.82
55.40
56.47
76.03
85.65
112.36
140.14
155.64
2.2k
f1 (ppm)

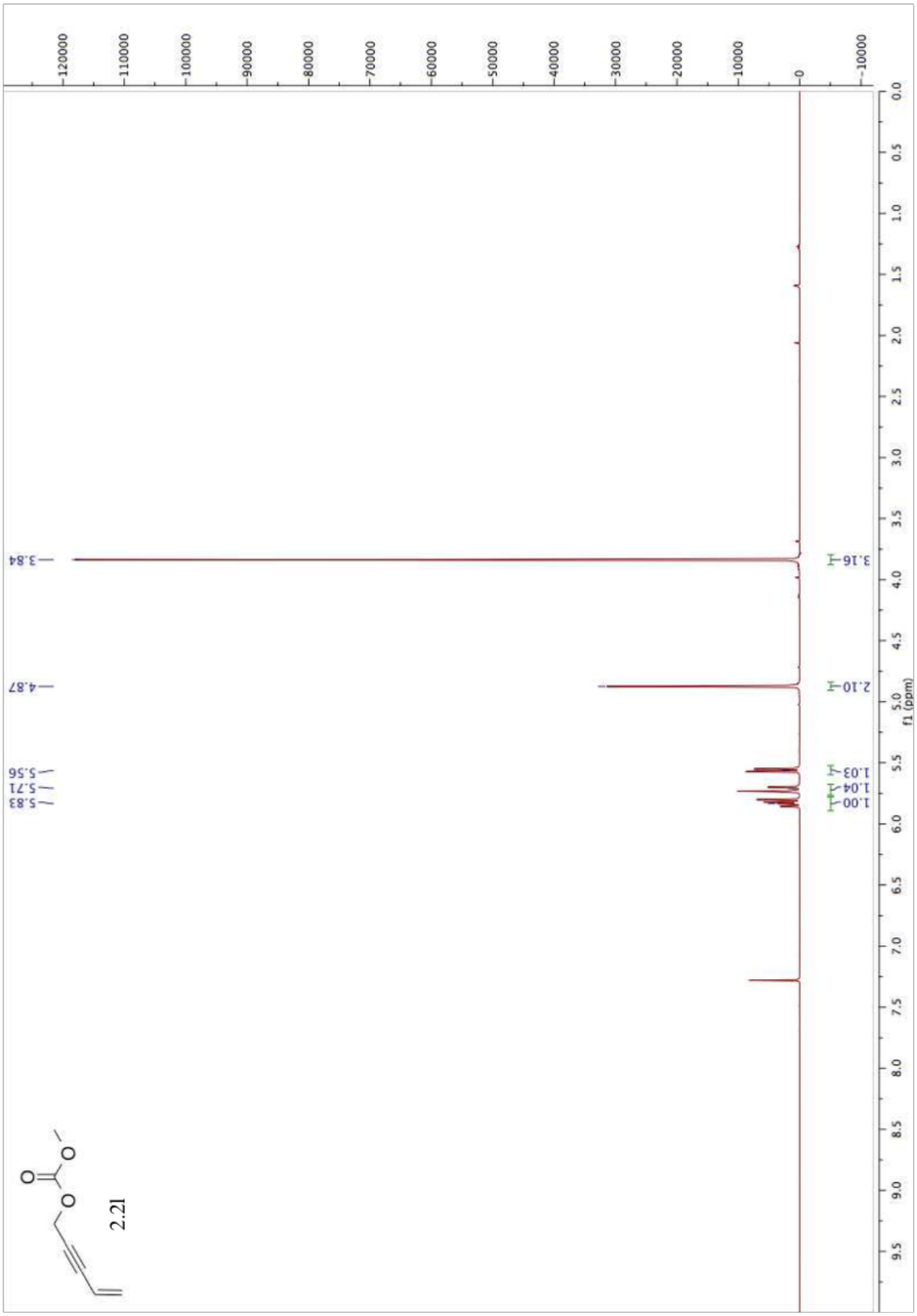
3.84
4.87
5.83
5.71
5.56
3.16
2.10
1.03
1.04
1.00
f1 (ppm)
2.21

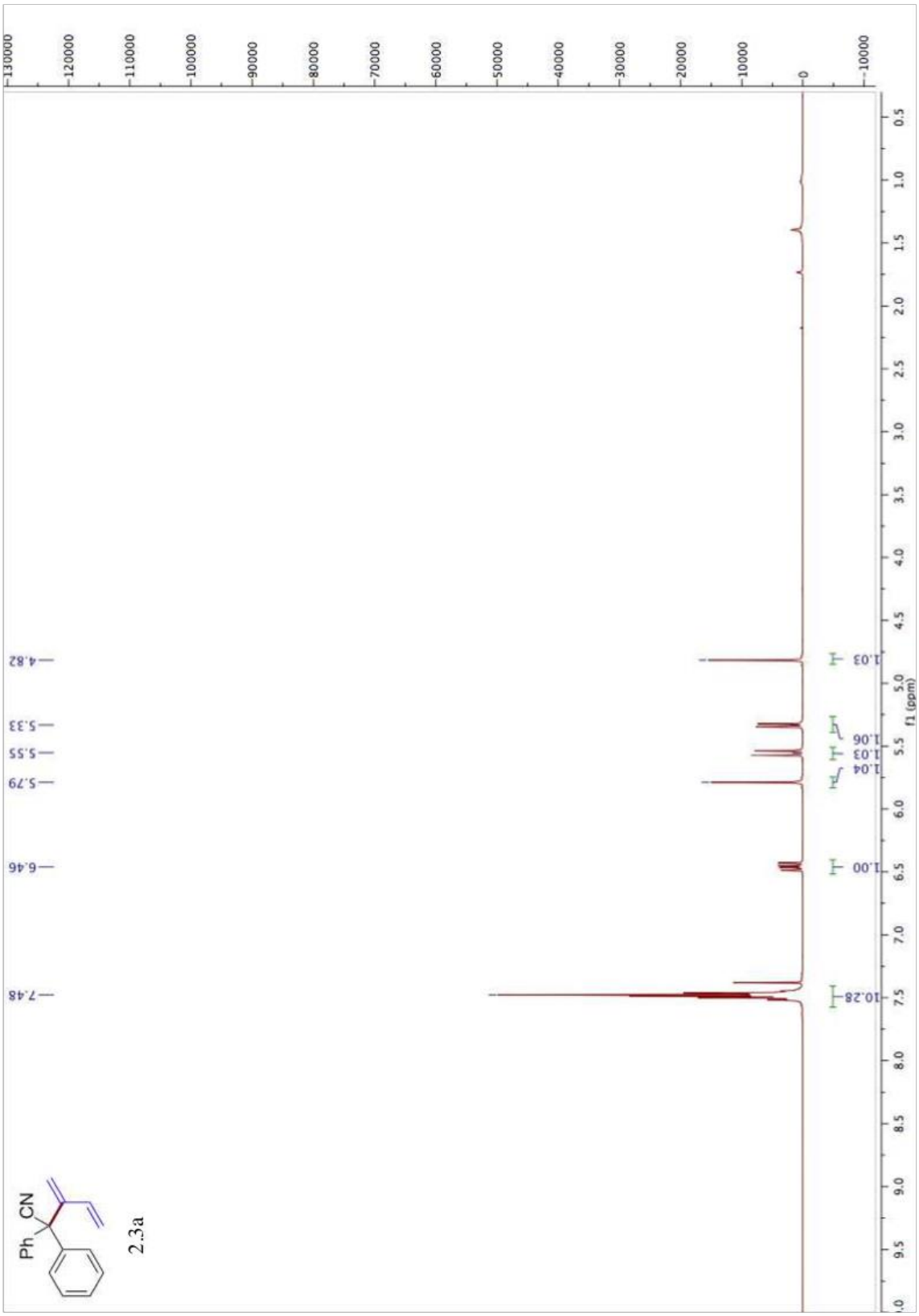
4.82
5.33
5.55
5.79
6.46
7.48
1.03
1.06
1.03
1.04
1.00
10.28
f1 (ppm)
Ph
CN
2.3a

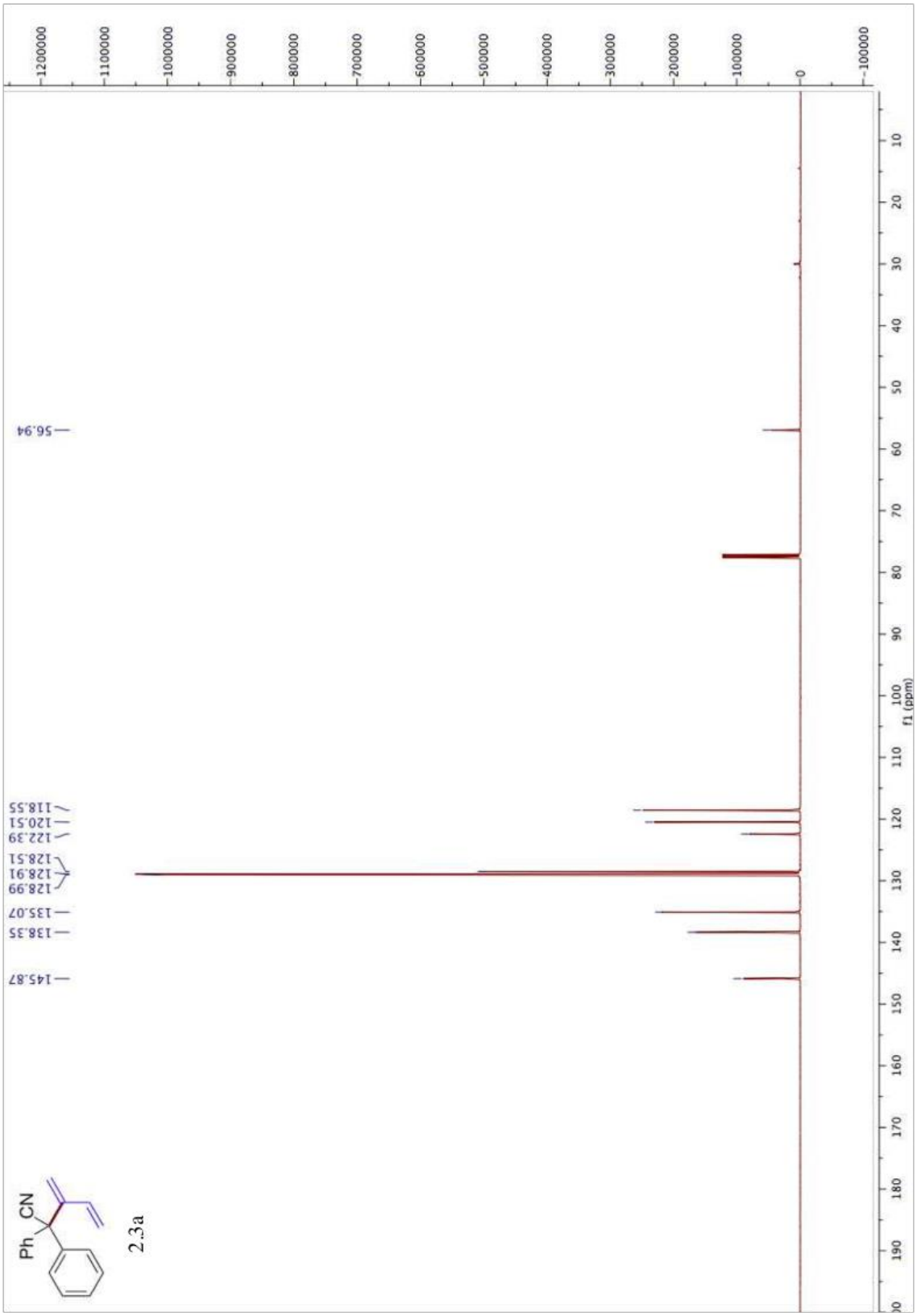
56.94
118.55
120.51
122.39
128.51
128.91
128.99
135.07
138.35
145.87
f1 (ppm)
Ph
CN
2.3a

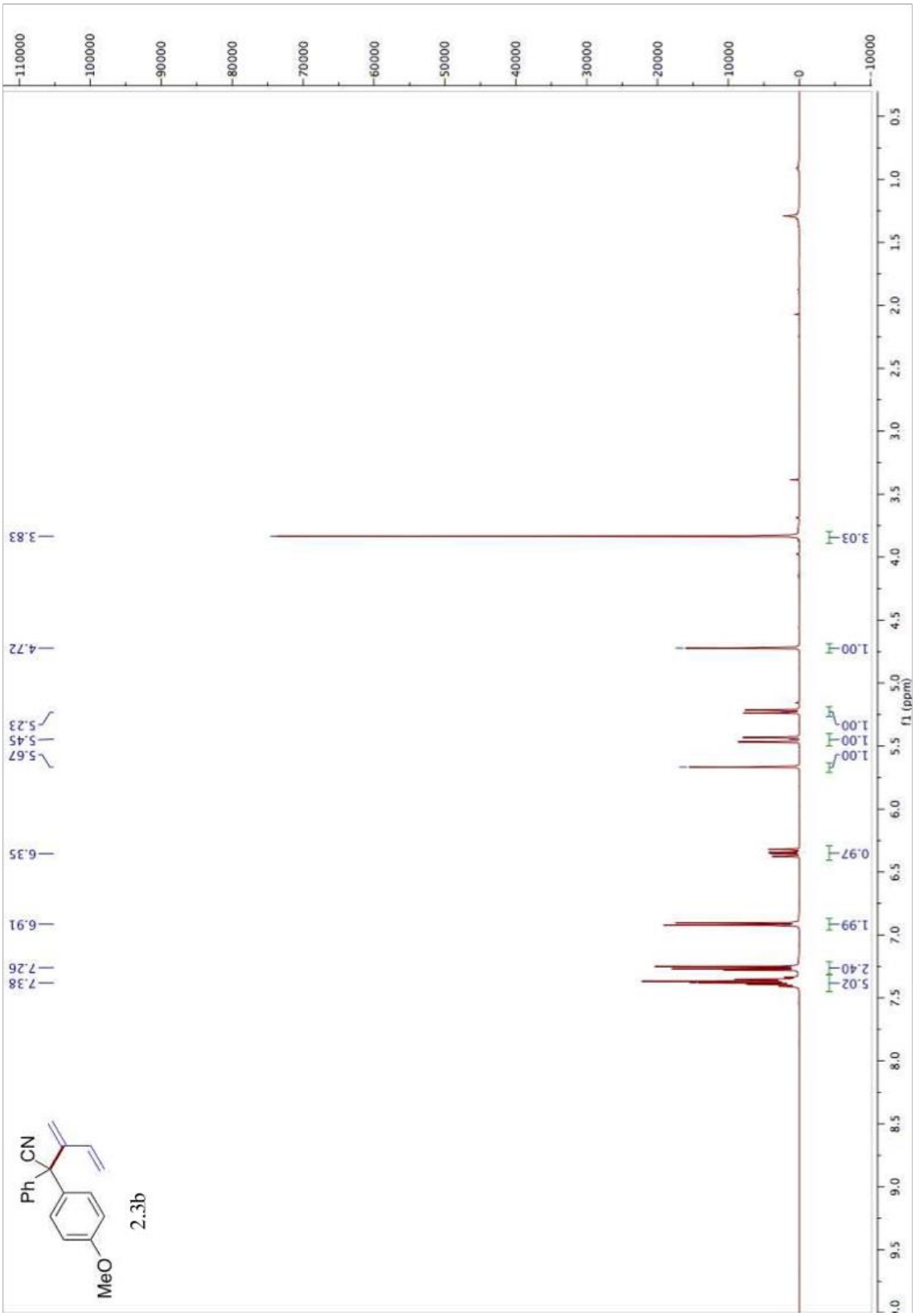
3.83
4.72
5.23
5.45
5.67
6.35
6.91
7.26
7.38
3.03
1.00
1.00
1.00
1.00
0.97
1.99
2.40
5.02
f1 (ppm)
Ph
CN
MeO
2.3b

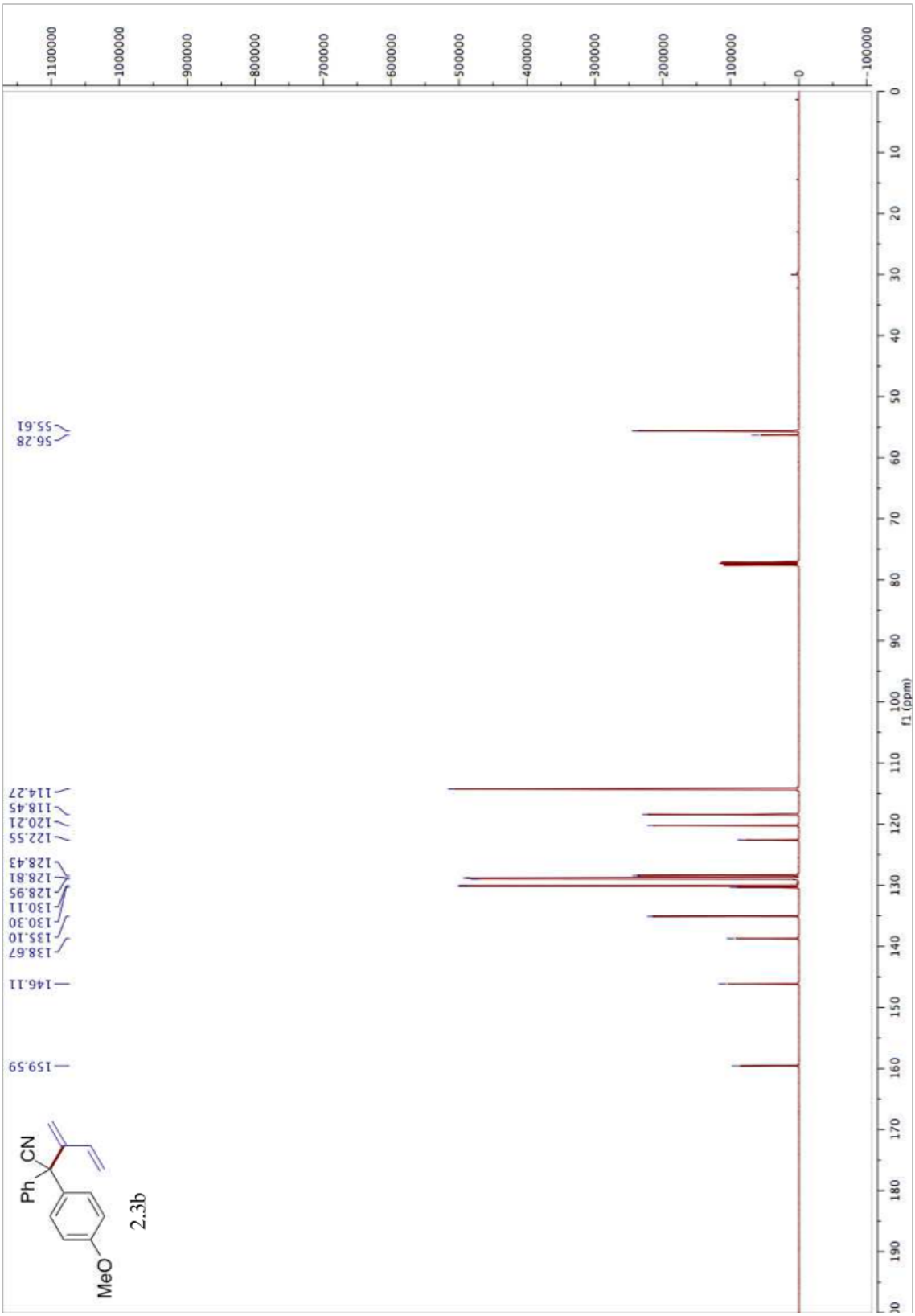
159.59
146.11
138.67
135.10
130.30
130.11
128.95
128.81
128.43
122.55
120.21
118.45
114.27
56.28
55.61
f1 (ppm)
Ph
CN
MeO
2.3b

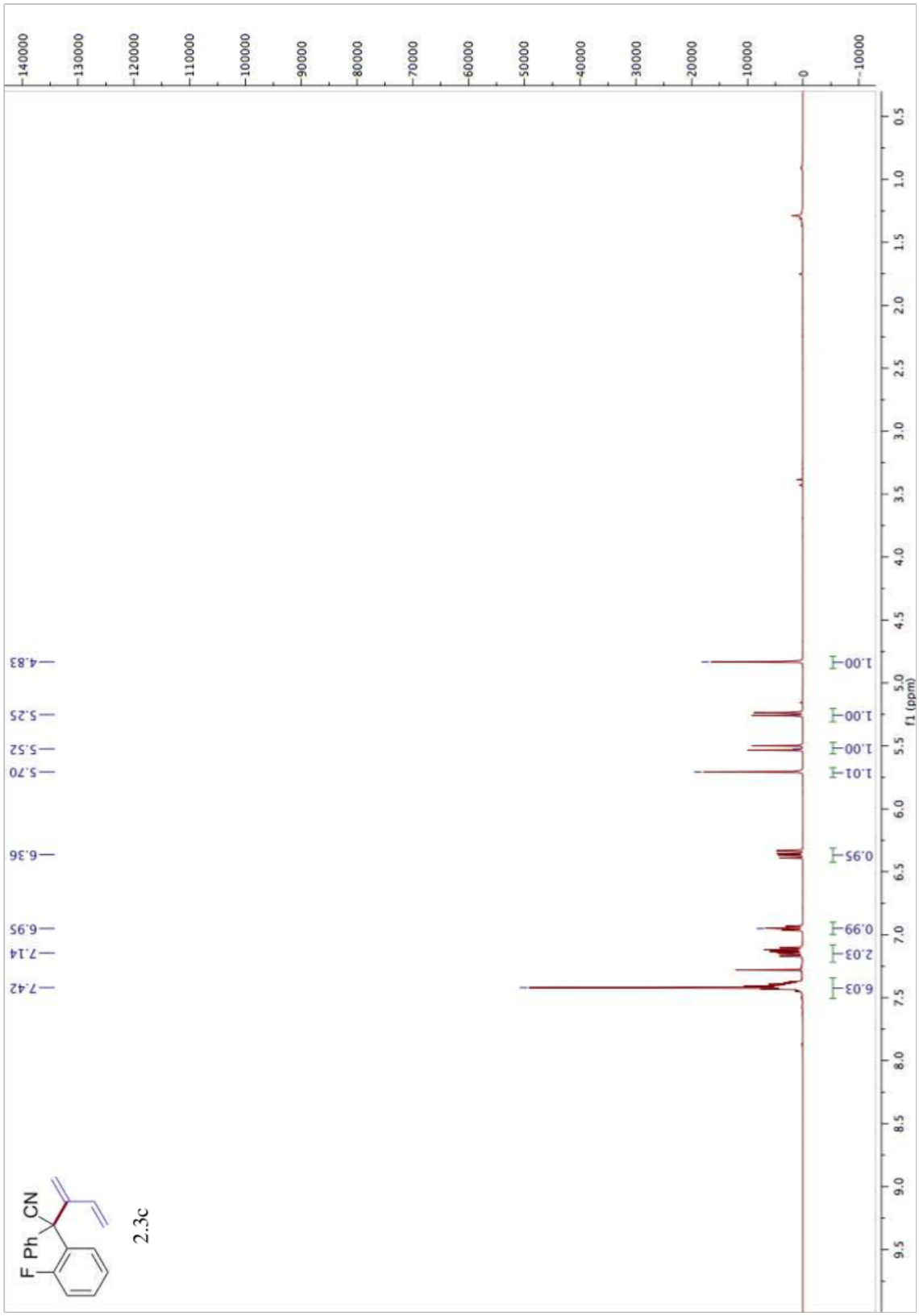
4.83
5.25
5.52
5.70
6.36
6.95
7.14
7.42
1.00
1.00
1.00
1.01
0.95
0.99
2.03
6.03
f1 (ppm)
F Ph CN
2.3c

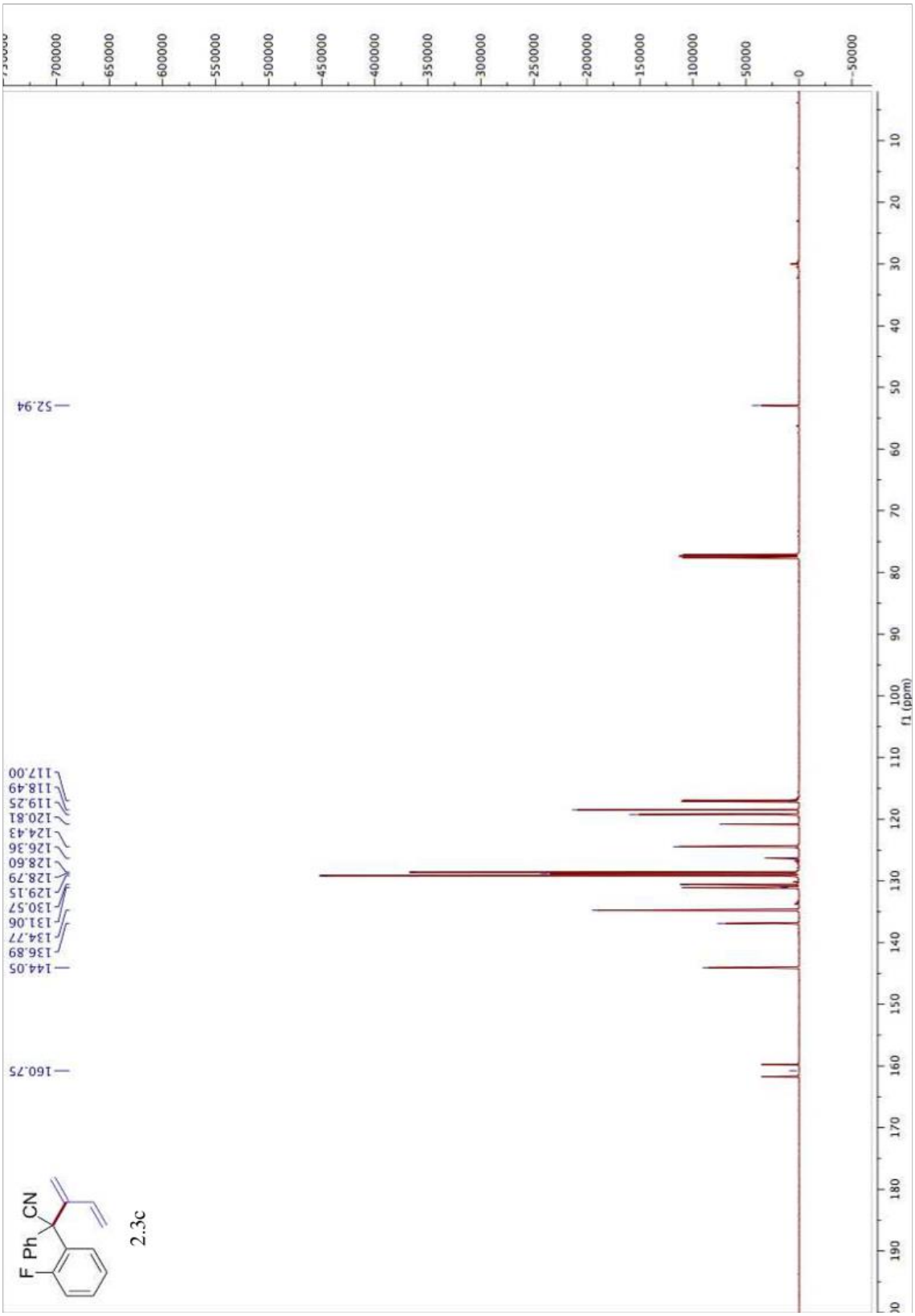
52.94
160.75
144.05
136.89
134.77
131.06
130.57
129.15
128.79
128.60
126.36
124.43
120.81
119.25
118.49
117.00
f1 (ppm)
F
Ph
CN
2.3c

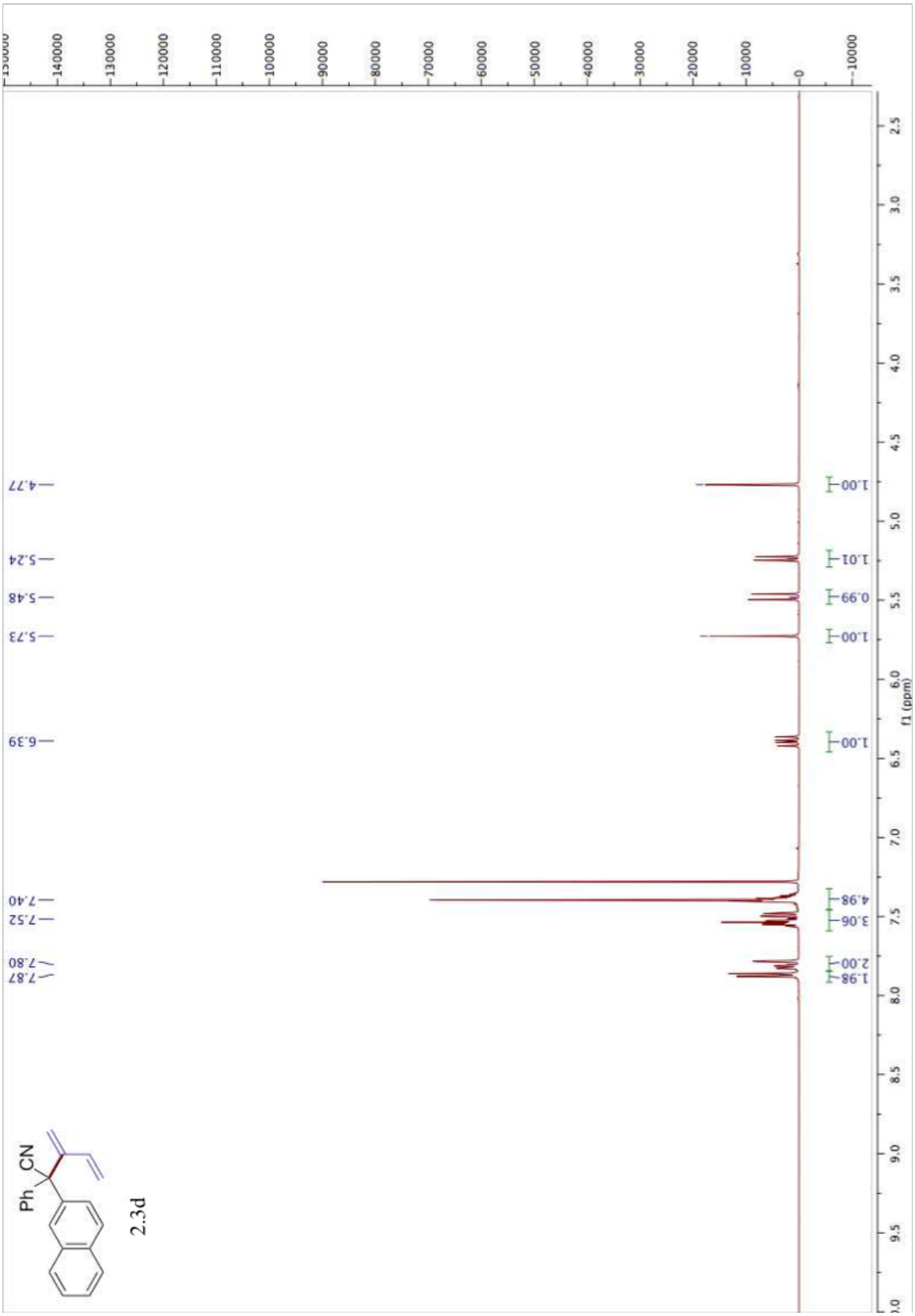
4.77
5.24
5.48
5.73
6.39
7.40
7.52
7.80
7.87
1.00
1.01
0.99
1.00
1.00
4.98
3.06
2.00
1.98
f1 (ppm)
Ph
CN
2.3d

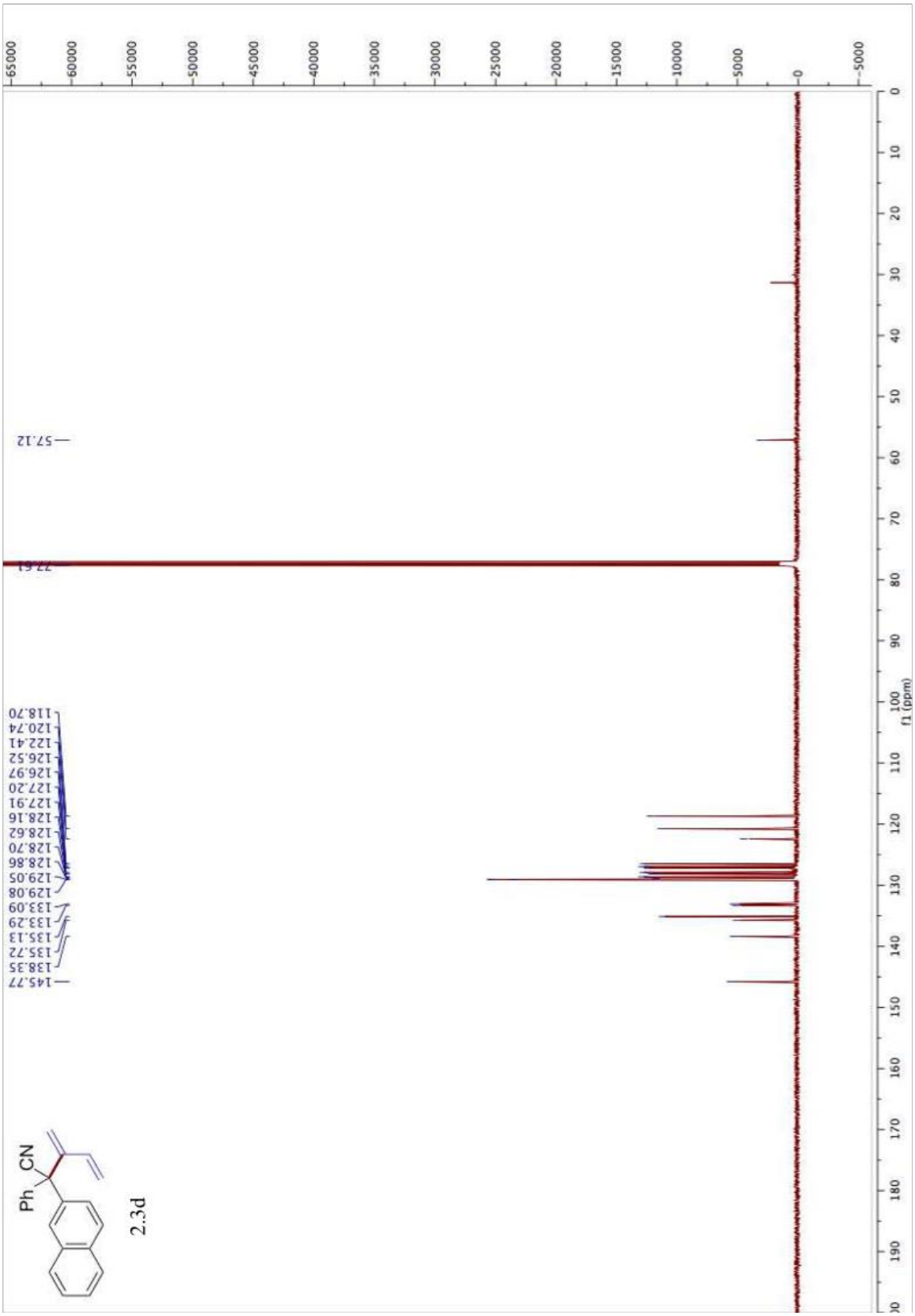
Ph
CN
2.3d
145.77
138.35
135.72
135.13
133.29
133.09
129.08
129.05
128.86
128.70
128.62
128.16
127.91
127.20
126.97
126.52
122.41
120.74
118.70
77.61
57.12
f1 (ppm)

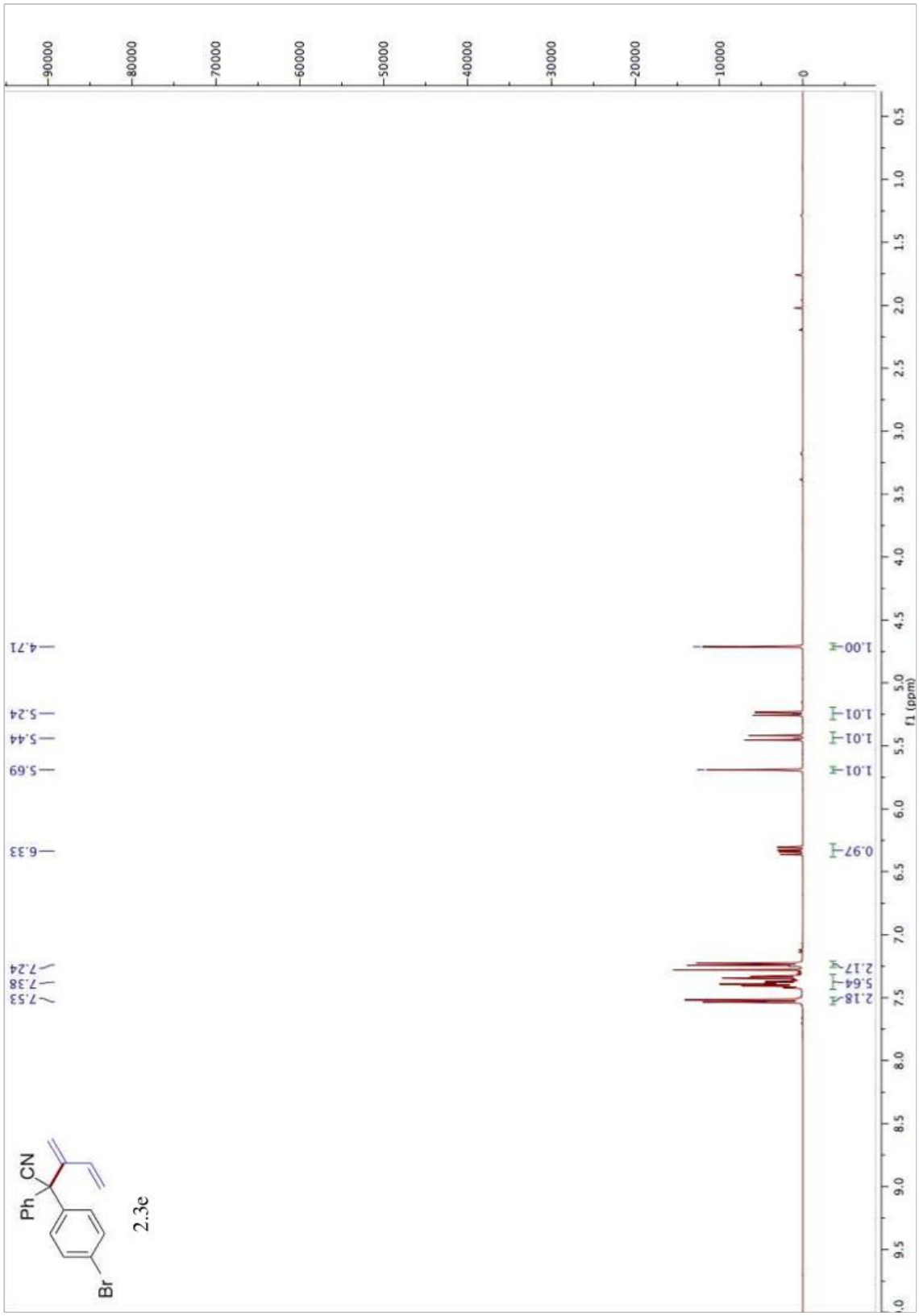
4.71
5.24
5.44
5.69
6.33
7.24
7.38
7.53
1.00
1.01
1.01
1.01
0.97
2.17
5.64
2.18
f1 (ppm)
Ph
CN
Br
2.3e

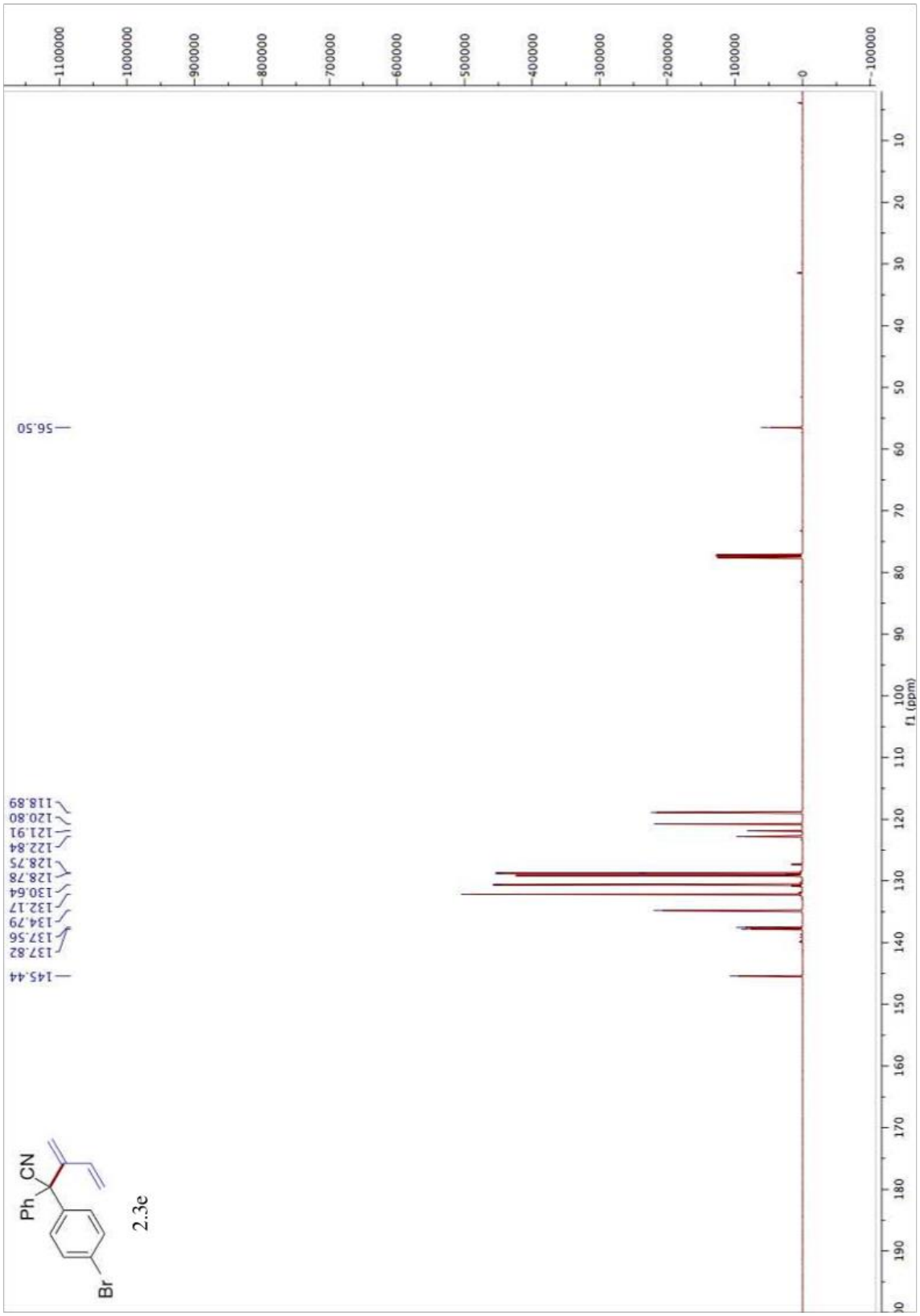
56.50
118.89
120.80
121.91
122.84
128.75
128.78
130.64
132.17
134.79
137.56
137.82
145.44
f1 (ppm)
Ph
CN
Br
2.3e

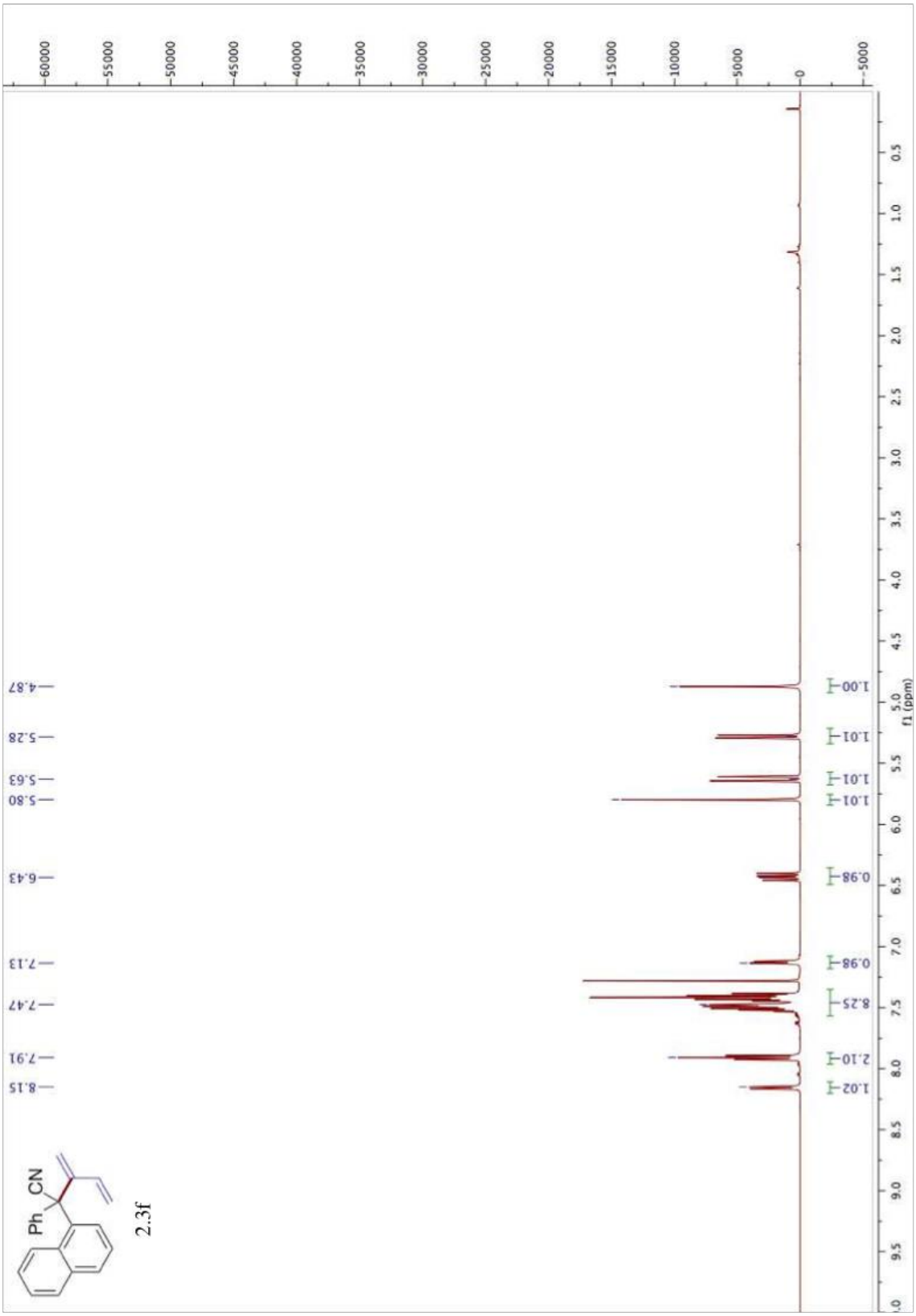
8.15
7.91
7.47
7.13
6.43
5.80
5.63
5.28
4.87
1.00
1.01
1.01
1.01
0.98
0.98
8.25
2.10
1.02
f1 (ppm)
Ph
CN
2.3f

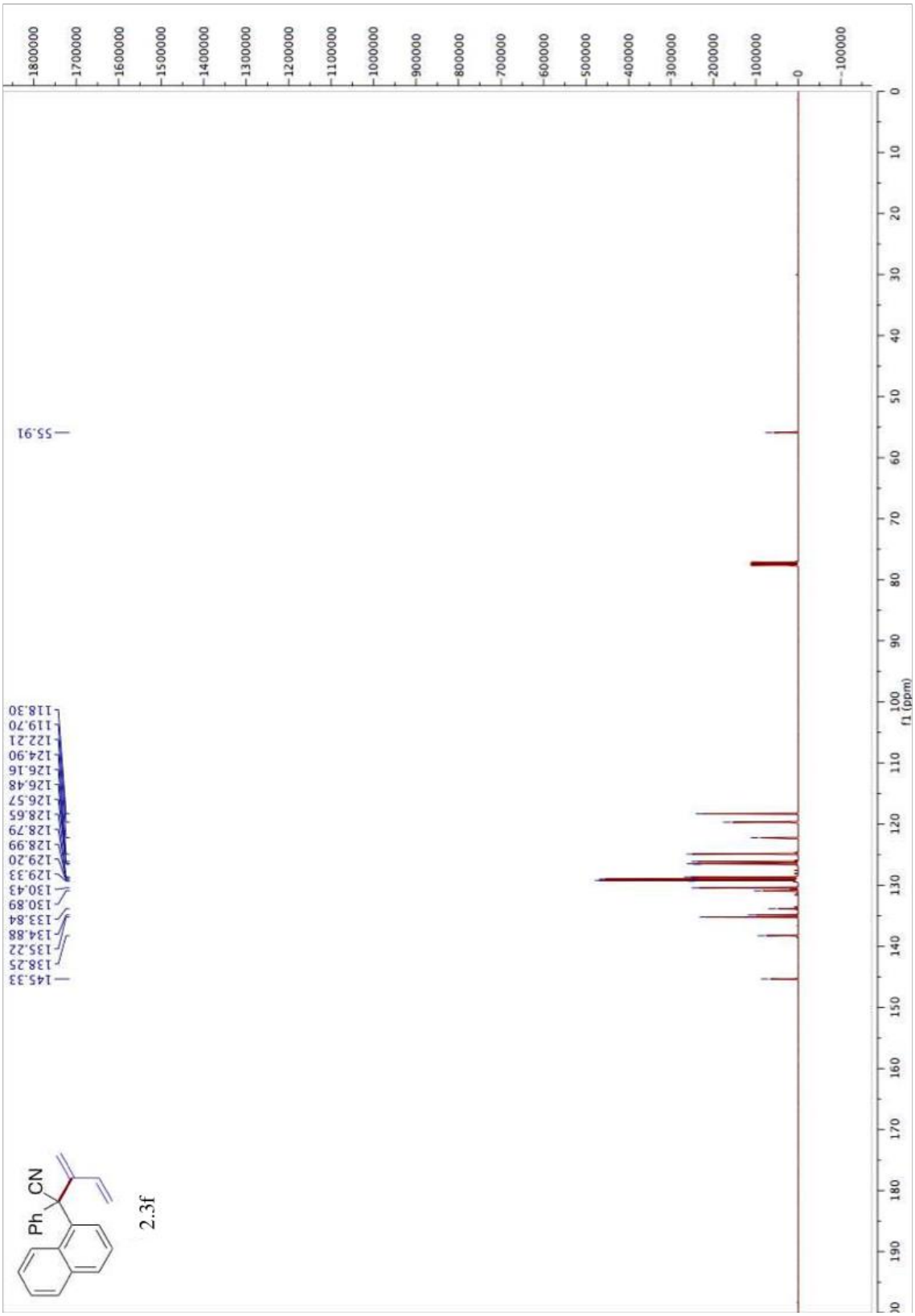
55.91
145.33
138.25
135.22
134.88
133.84
130.89
130.43
129.33
129.20
128.99
128.79
128.65
126.57
126.48
126.16
124.90
122.21
119.70
118.30
Ph
CN
2.3f
f1 (ppm)

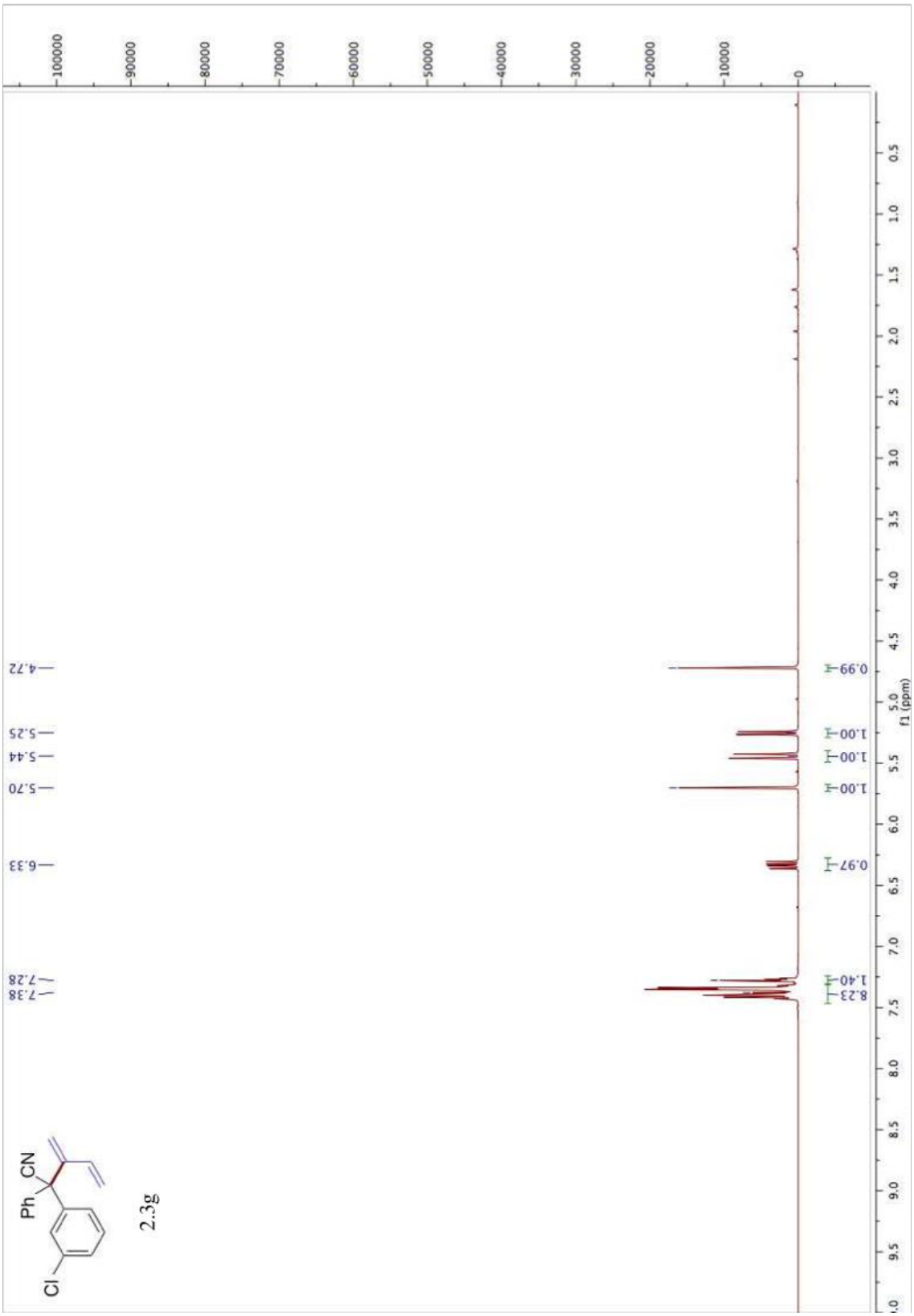
4.72
5.25
5.44
5.70
6.33
7.28
7.38
0.99
1.00
1.00
1.00
0.97
1.40
8.23
f1 (ppm)
Ph
CN
Cl
2.3g

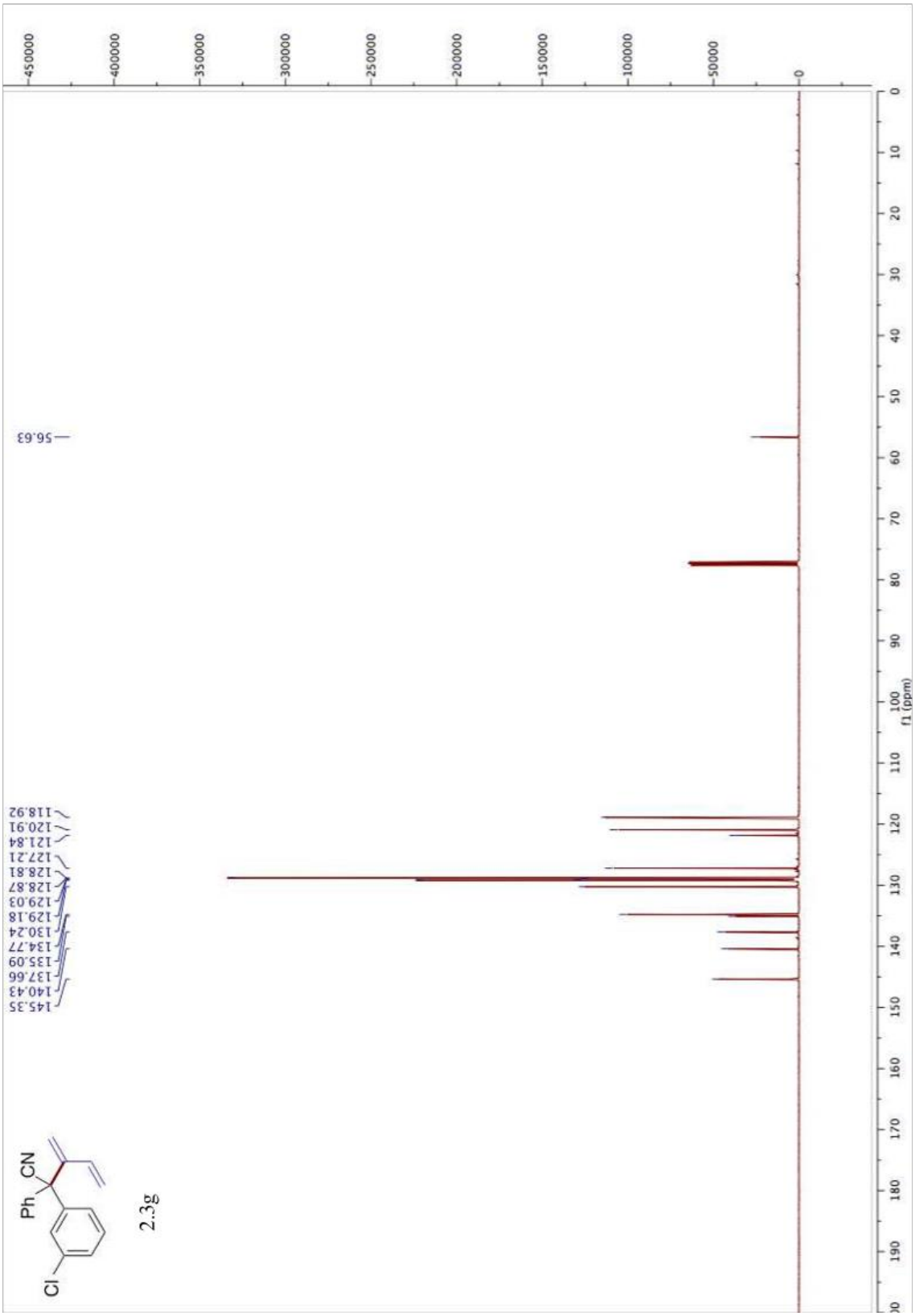
56.63
118.92
120.91
121.84
127.21
128.81
128.87
129.03
129.18
130.24
134.77
135.09
137.66
140.43
145.35
Ph
CN
Cl
2.3g
f1 (ppm)

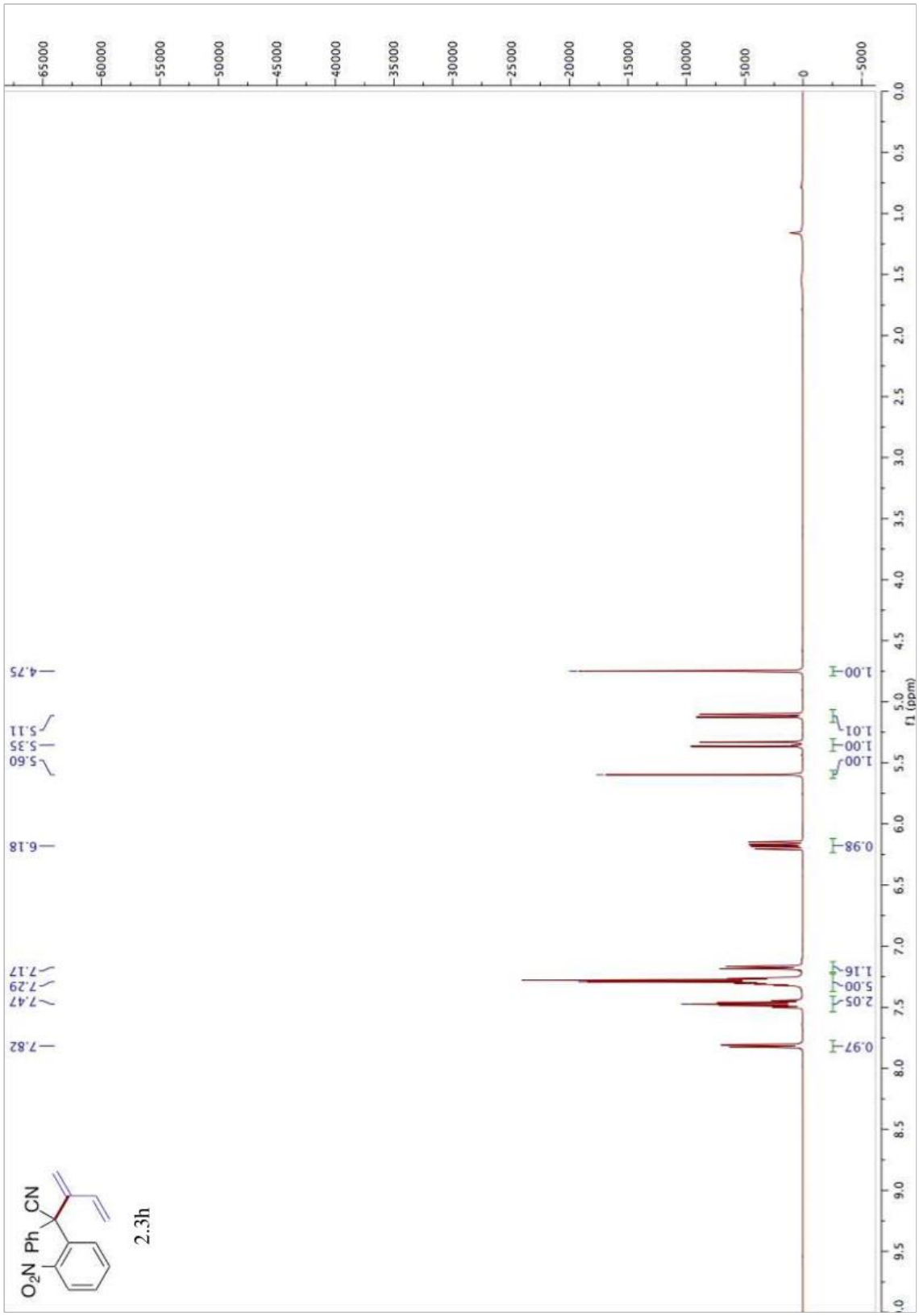
4.75
5.11
5.35
5.60
6.18
7.17
7.29
7.47
7.82
1.00
1.01
1.00
1.00
0.98
1.16
5.00
2.05
0.97
f1 (ppm)
O2N Ph CN
2.3h

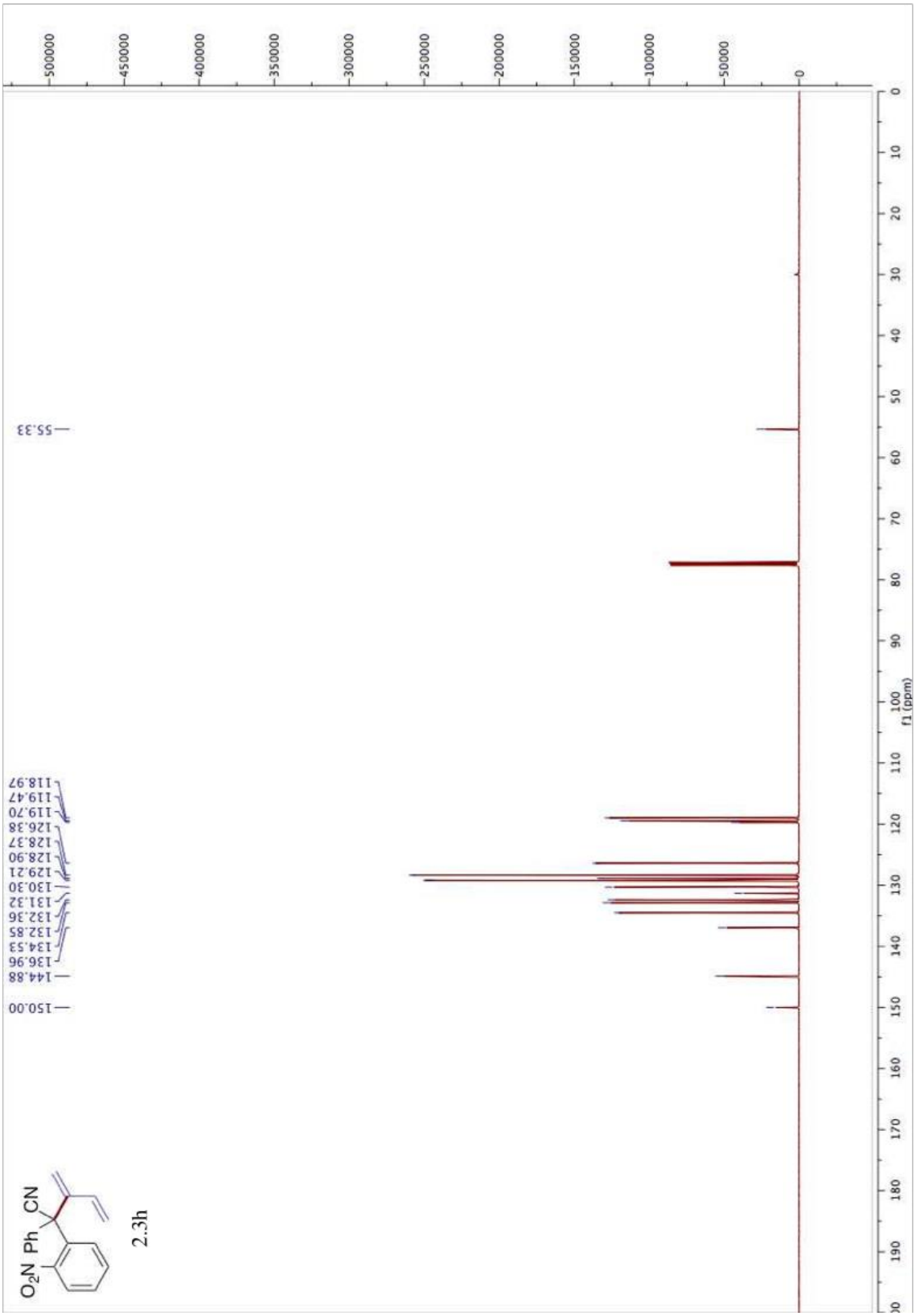
55.33
150.00
144.88
136.96
134.53
132.85
132.36
131.32
130.30
129.21
128.90
128.37
126.38
119.70
119.47
118.97
f1 (ppm)
O2N Ph CN
2.3h

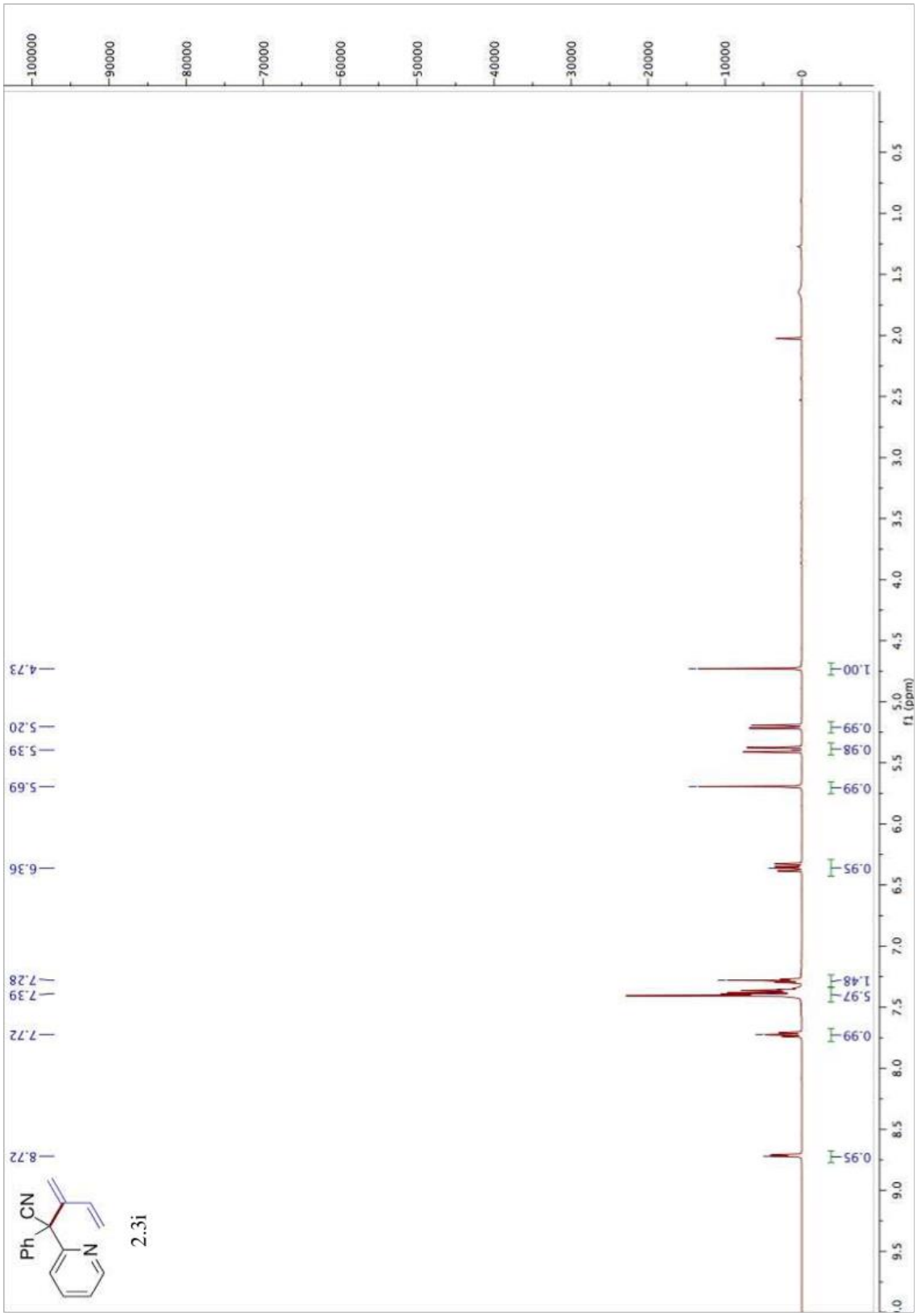
8.72
7.72
7.39
7.28
6.36
5.69
5.39
5.20
4.73
0.95
0.99
1.48
5.97
0.99
0.98
0.99
1.00
f1 (ppm)
Ph
CN
N
2.3i

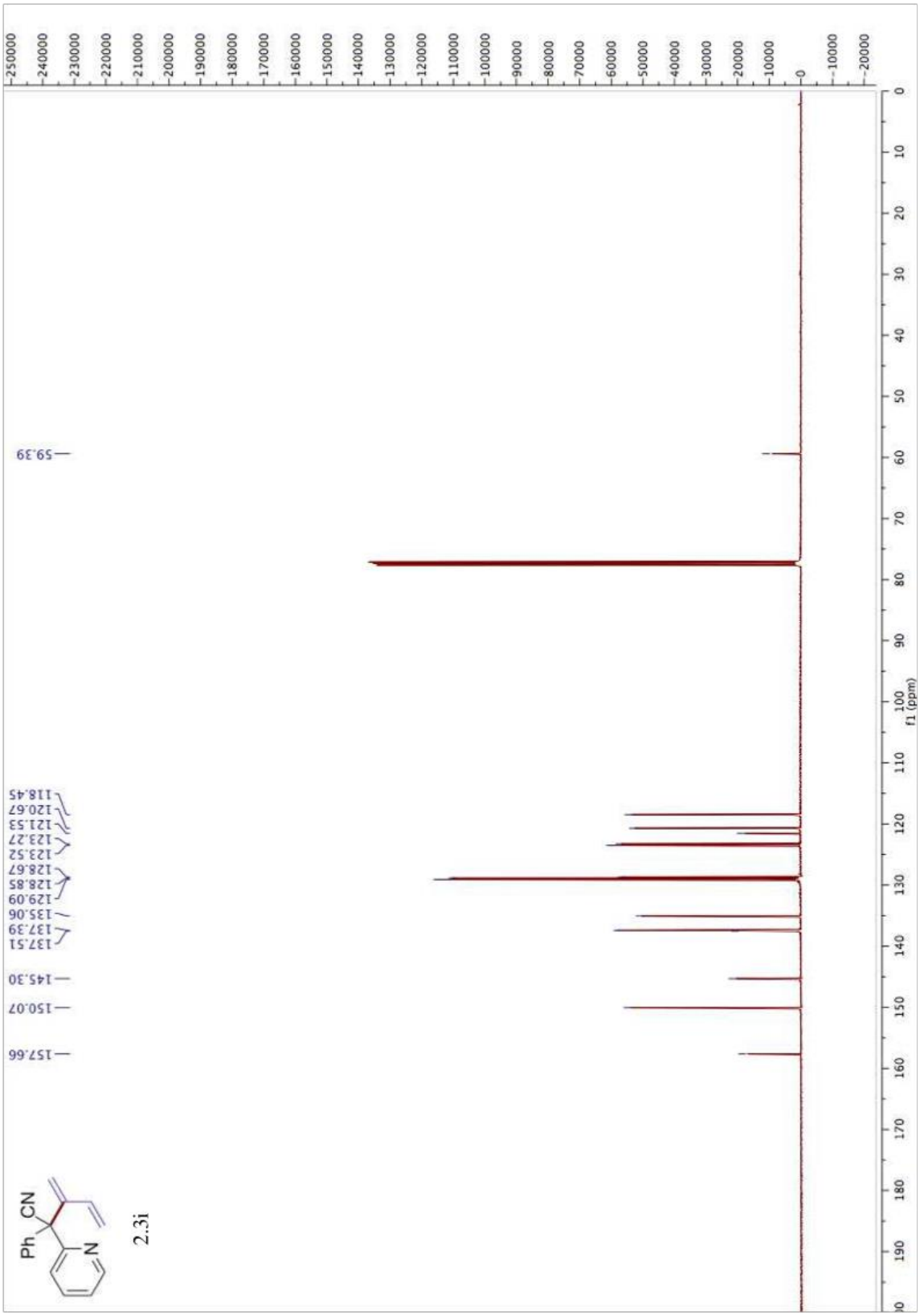
59.39
118.45
120.67
121.53
123.27
123.52
128.67
128.85
129.09
135.06
137.39
137.51
145.30
150.07
157.66
Ph
CN
N
2.3i
f1 (ppm)

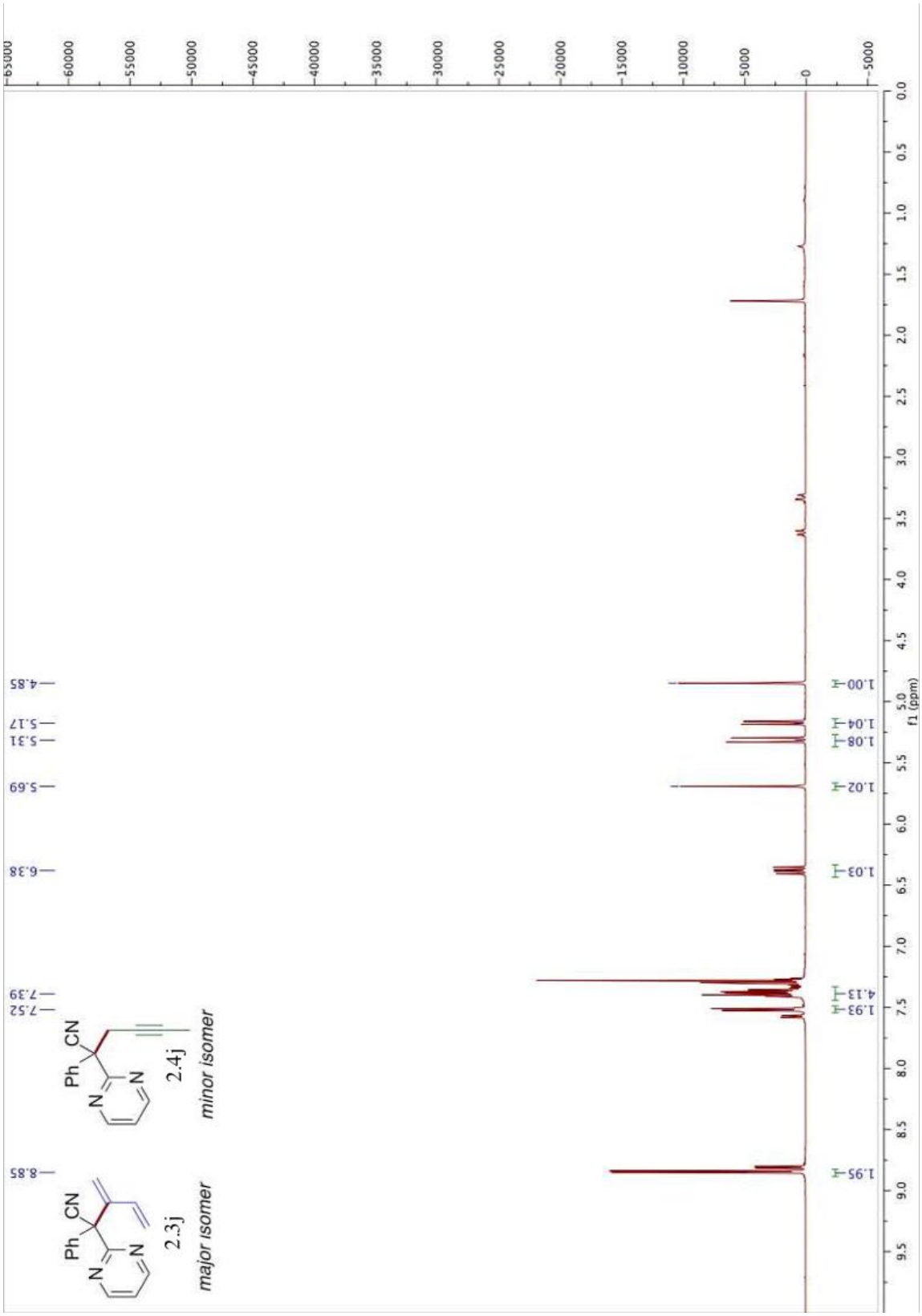
8.85
7.52
7.39
6.38
5.69
5.31
5.17
4.85
1.95
4.13
1.93
1.03
1.02
1.08
1.04
1.00
f1 (ppm)
Ph
CN
N
N
2.3j
major isomer
2.4j
minor isomer

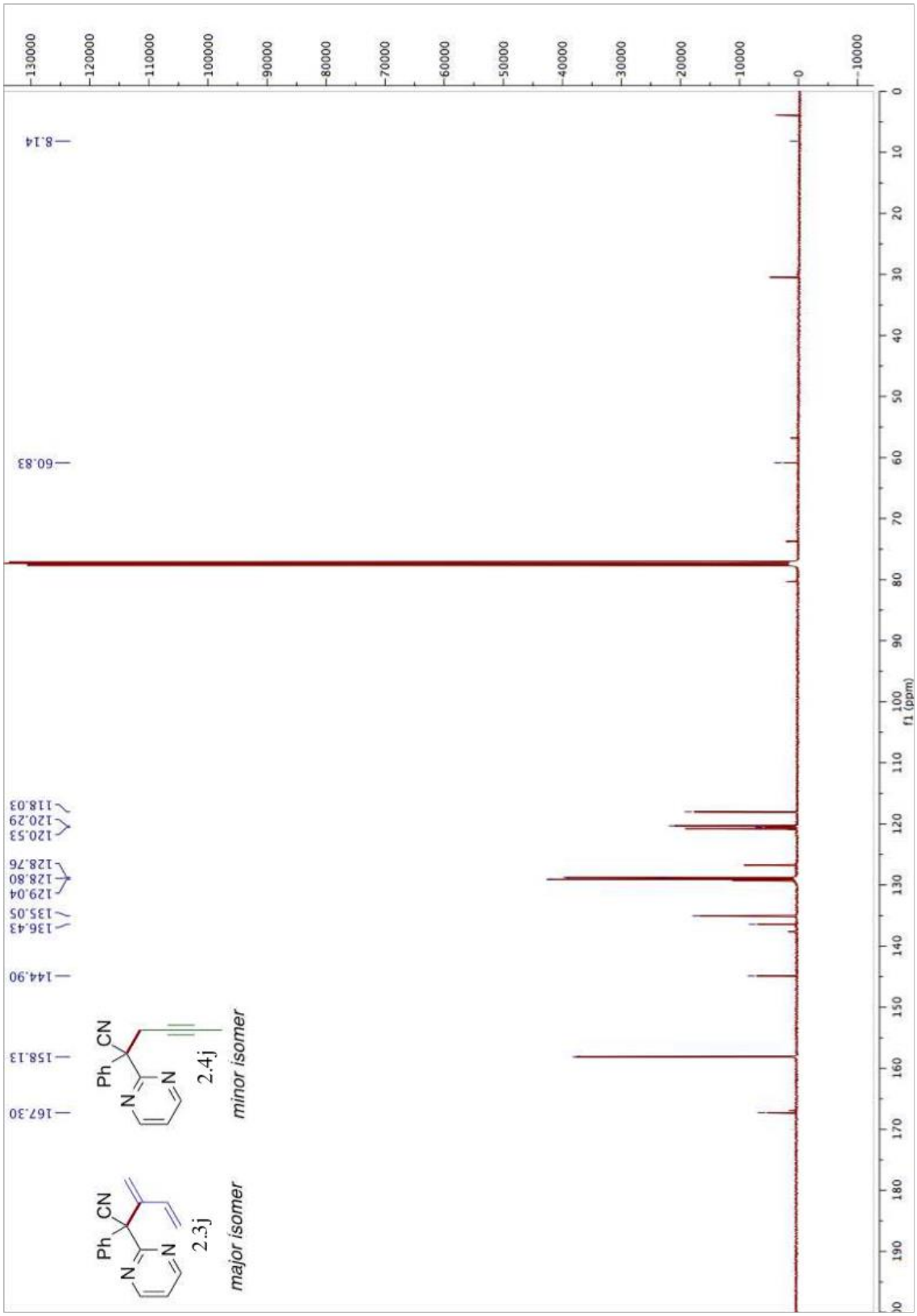
8.14
60.83
118.03
120.53
120.29
128.76
128.80
129.04
135.05
136.43
144.90
158.13
167.30
Ph
CN
N
N
2.3j
major isomer
2.4j
minor isomer
f1 (ppm)

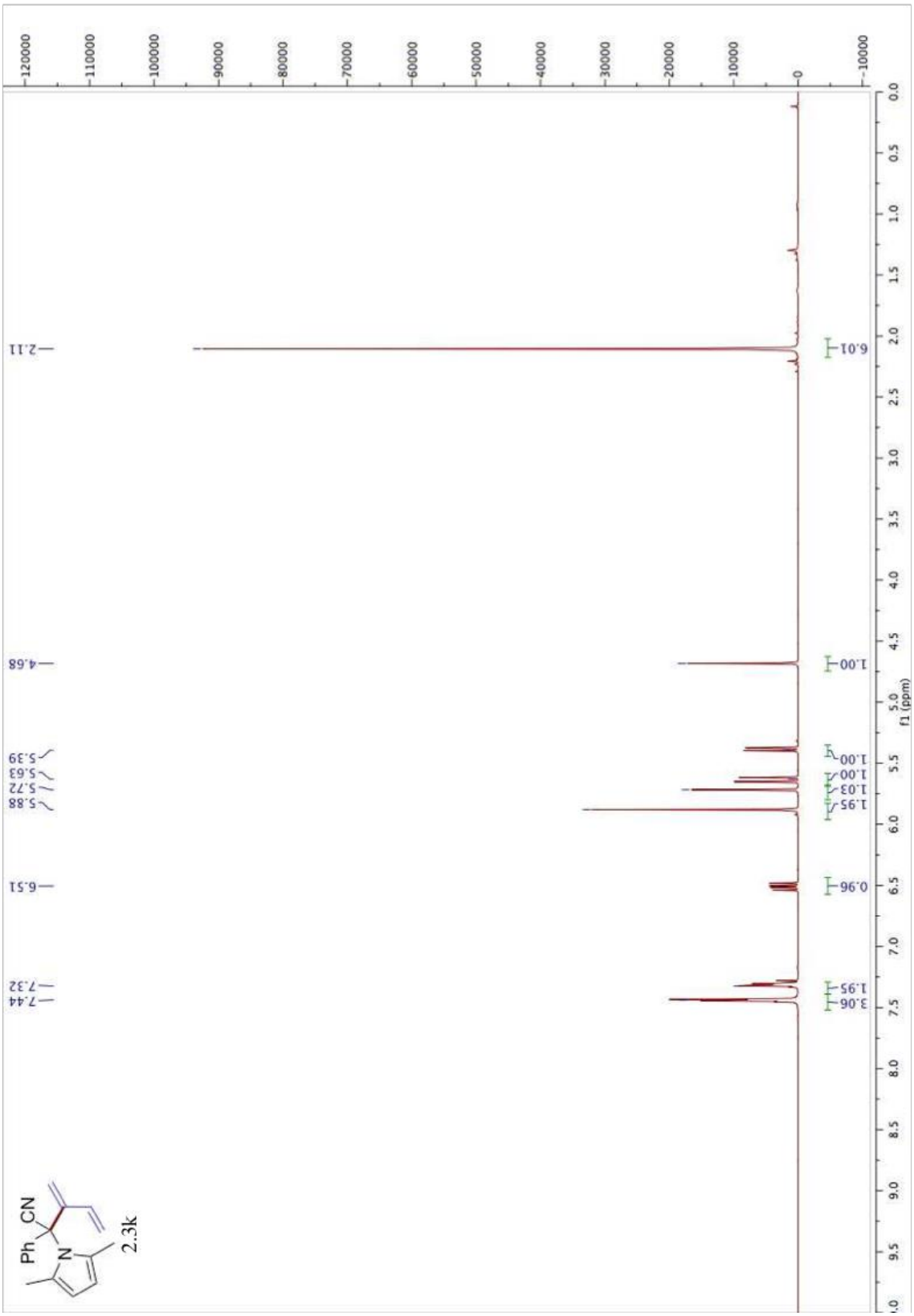
2.11
4.68
5.39
5.63
5.72
5.88
6.51
7.32
7.44
6.01
1.00
1.00
1.00
1.03
1.95
0.96
1.95
3.06
f1 (ppm)
Ph
CN
N
2.3k

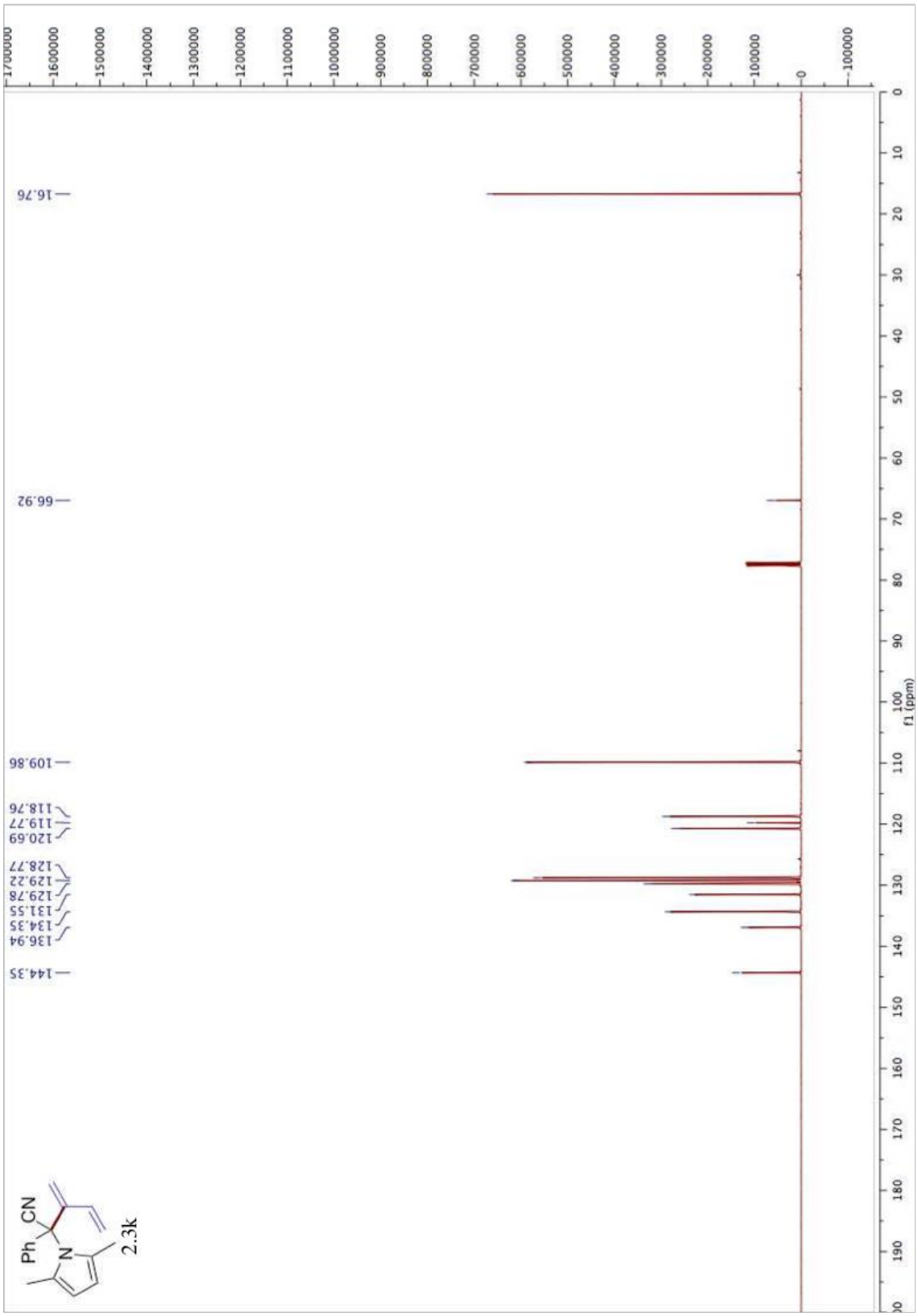
16.76
66.92
109.86
118.76
119.77
120.69
128.77
129.22
129.78
131.55
134.35
136.94
144.35
Ph
CN
N
2.3k
f1 (ppm)

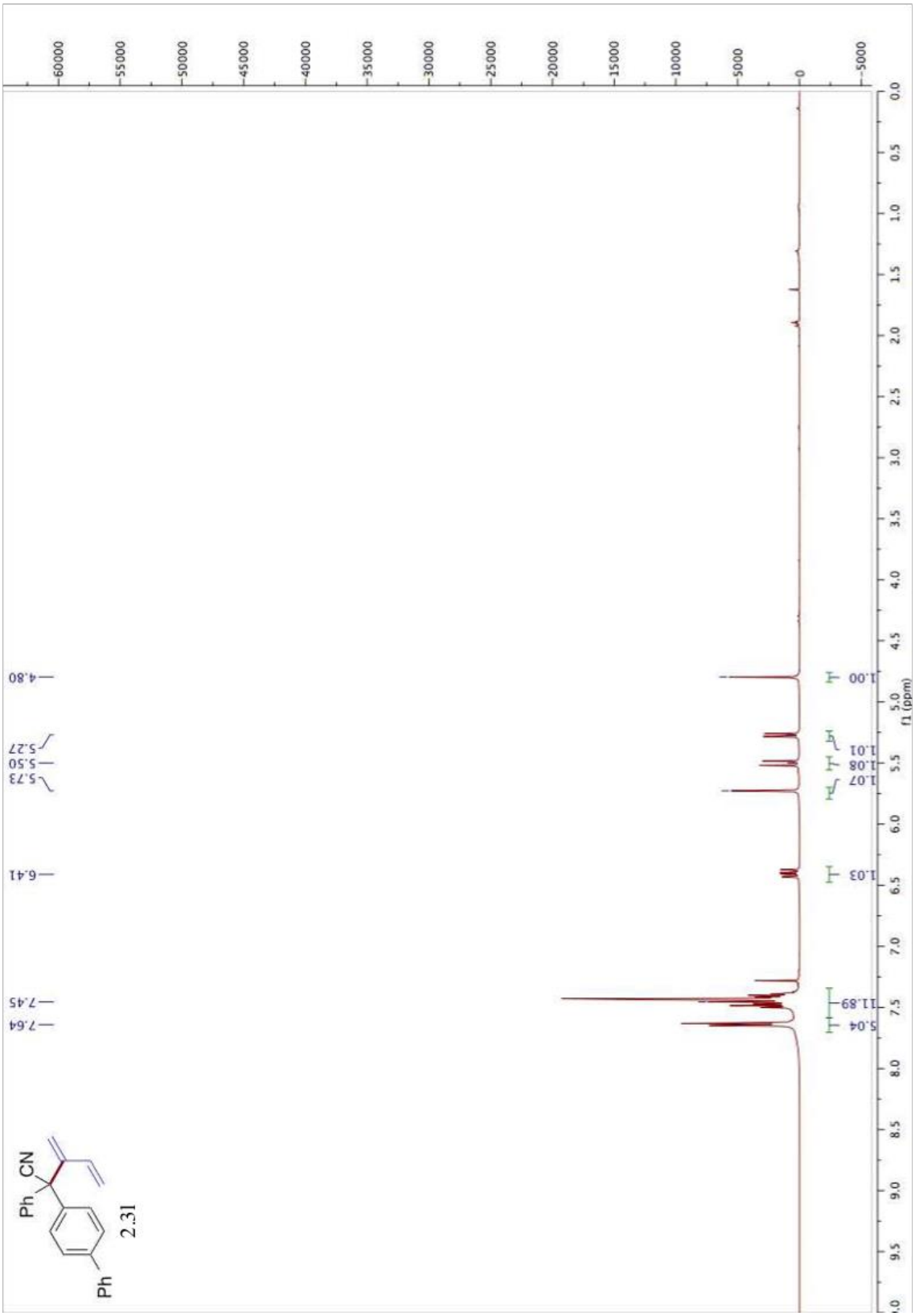
Ph
CN
Ph
2.31
7.64
7.45
6.41
5.73
5.50
5.27
4.80
5.04
11.89
1.03
1.07
1.08
1.01
1.00
f1 (ppm)

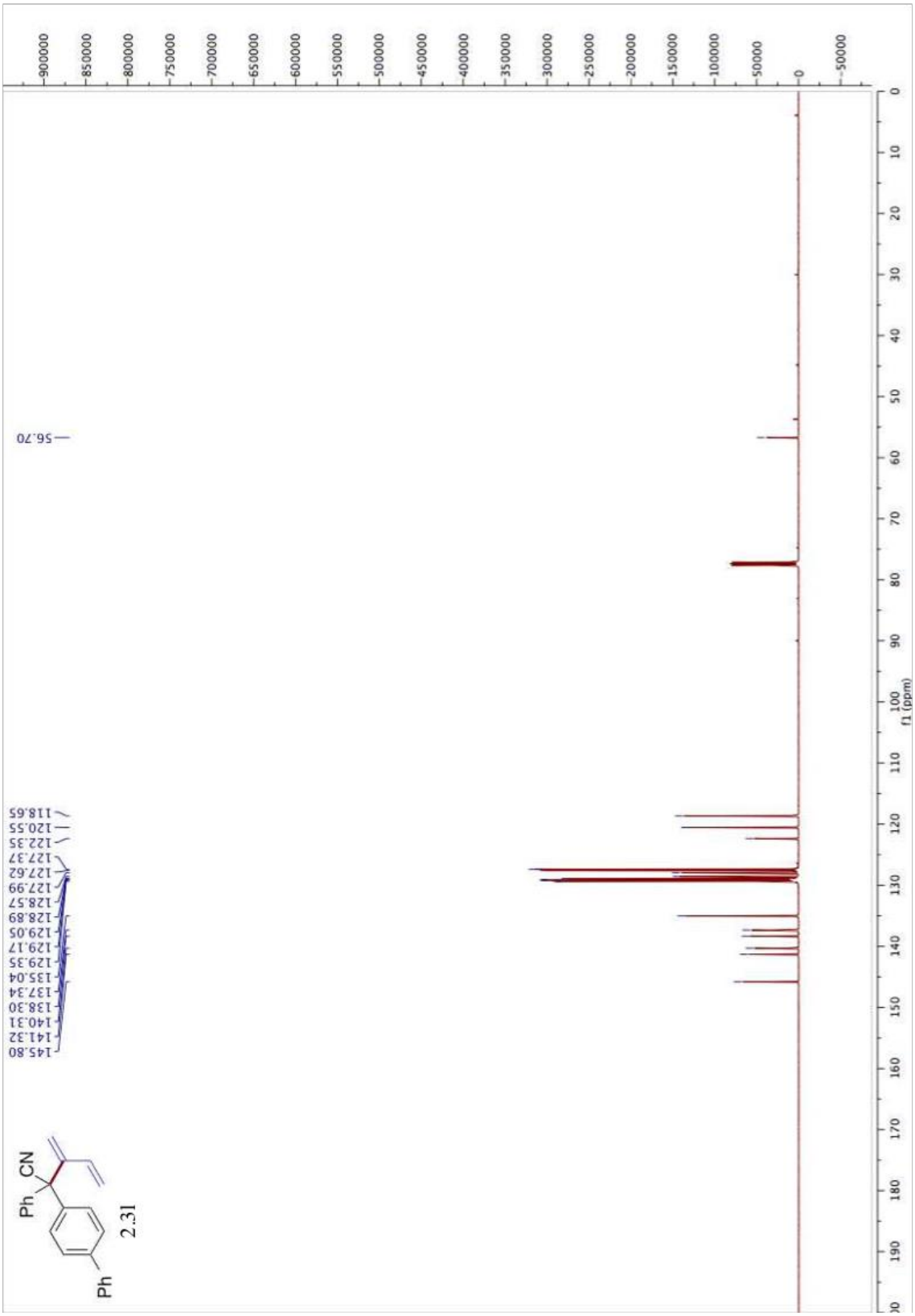
56.70
118.65
120.55
122.35
127.37
127.62
127.99
128.57
128.89
129.05
129.17
129.35
135.04
137.34
138.30
140.31
141.32
145.80
Ph
CN
Ph
2.31
f1 (ppm)

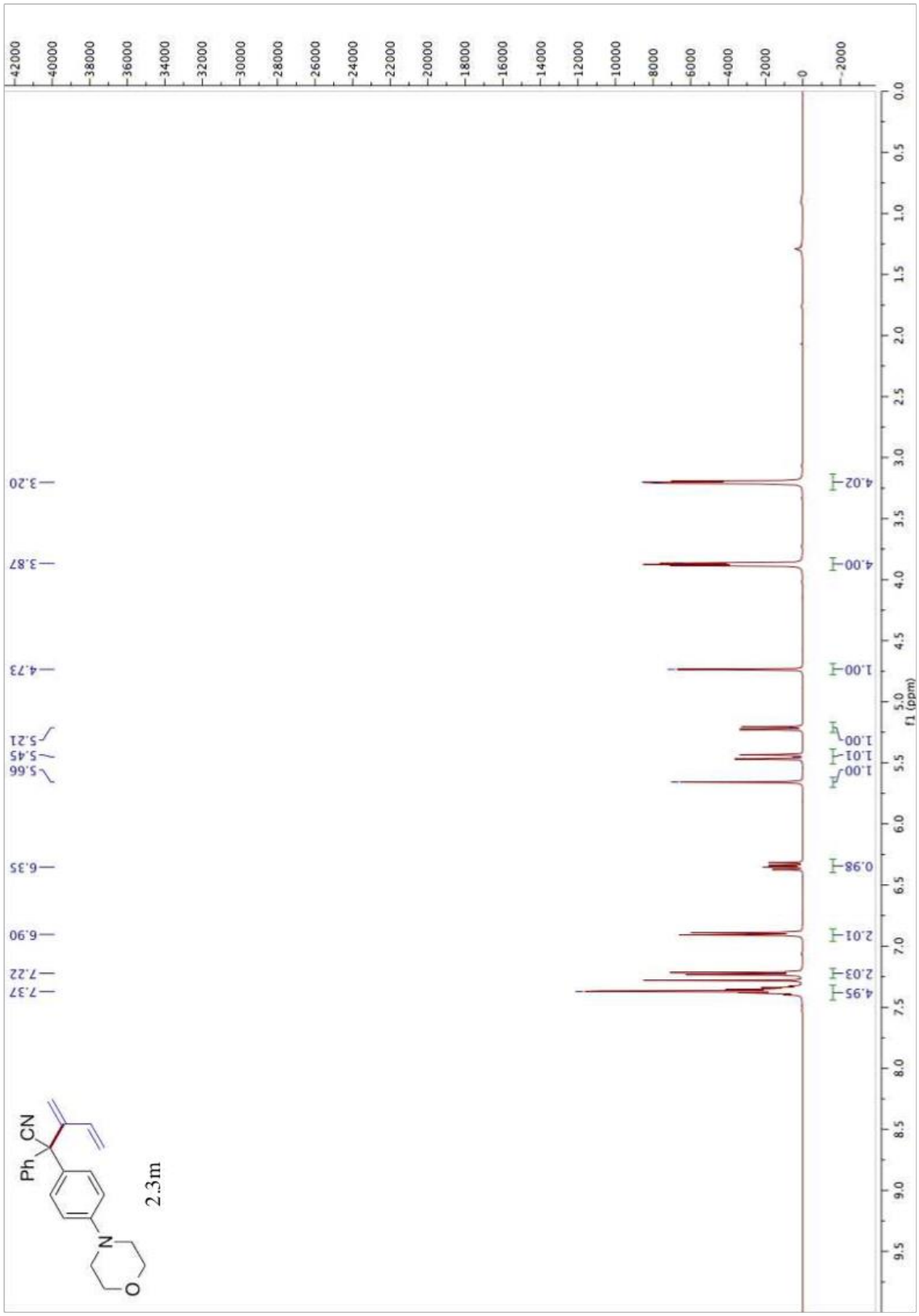
3.20
3.87
4.73
5.21
5.45
5.66
6.35
6.90
7.22
7.37
4.02
4.00
1.00
1.00
1.01
1.00
0.98
2.01
2.03
4.95
f1 (ppm)
Ph
CN
N
O
2.3m

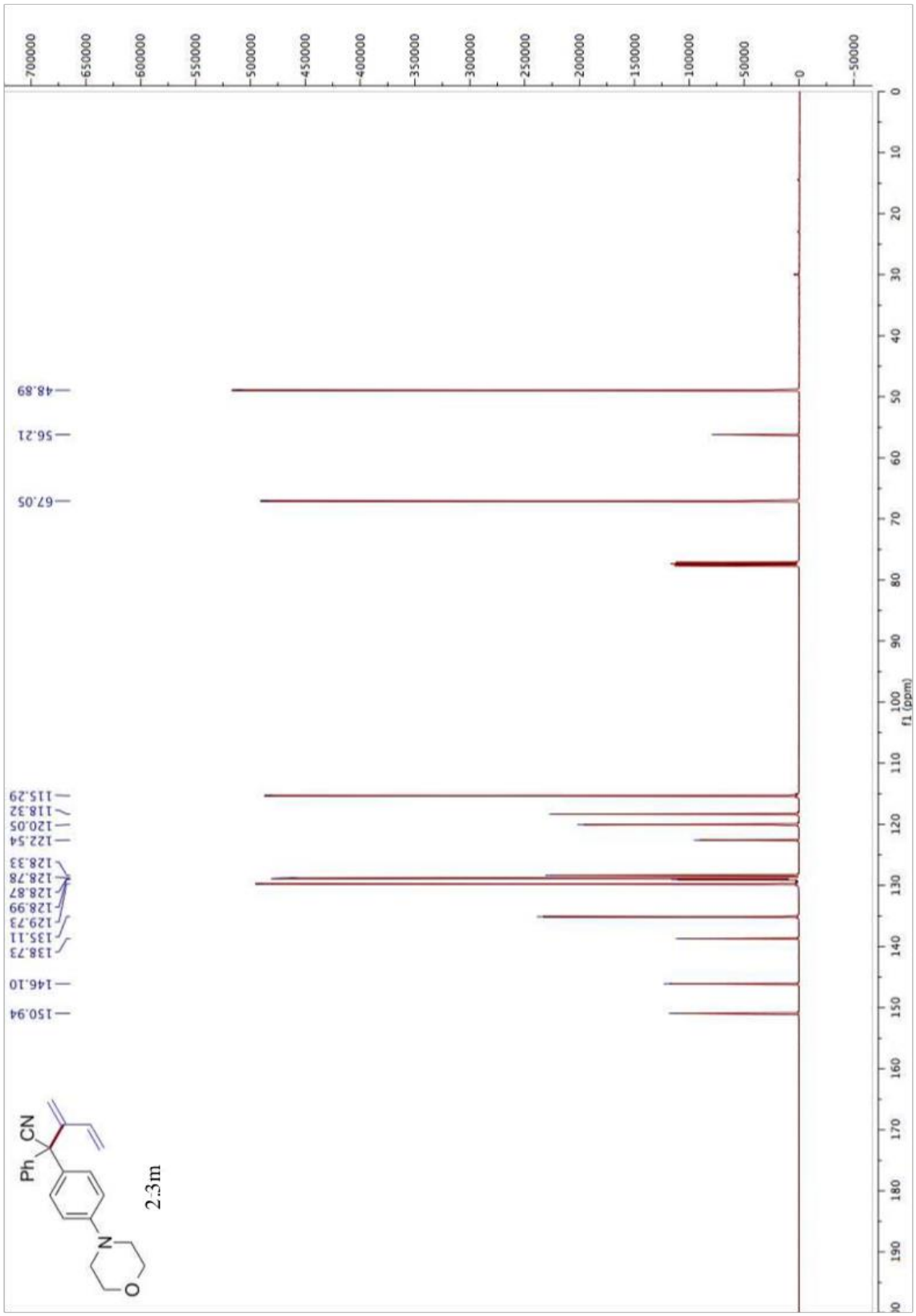
48.89
56.21
67.05
115.29
118.32
120.05
122.54
128.33
128.78
128.87
128.99
129.73
135.11
138.73
146.10
150.94
f1 (ppm)
Ph
CN
N
O
2.3m

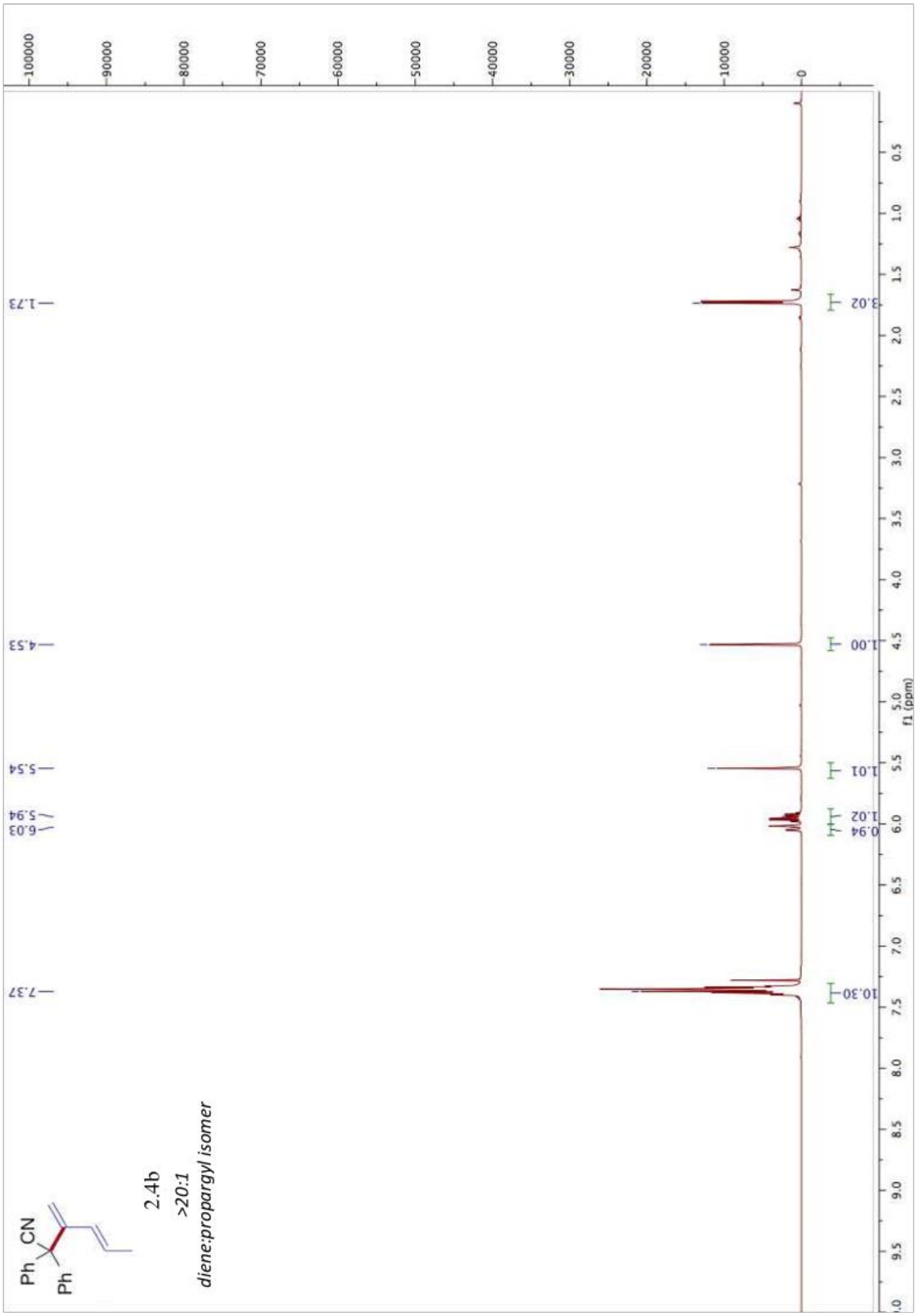
Ph
CN
Ph
2.4b
>20:1
diene:propargyl isomer
7.37
5.94
6.03
5.54
4.53
1.73
10.30
0.94
1.02
1.01
1.00
3.02
f1 (ppm)

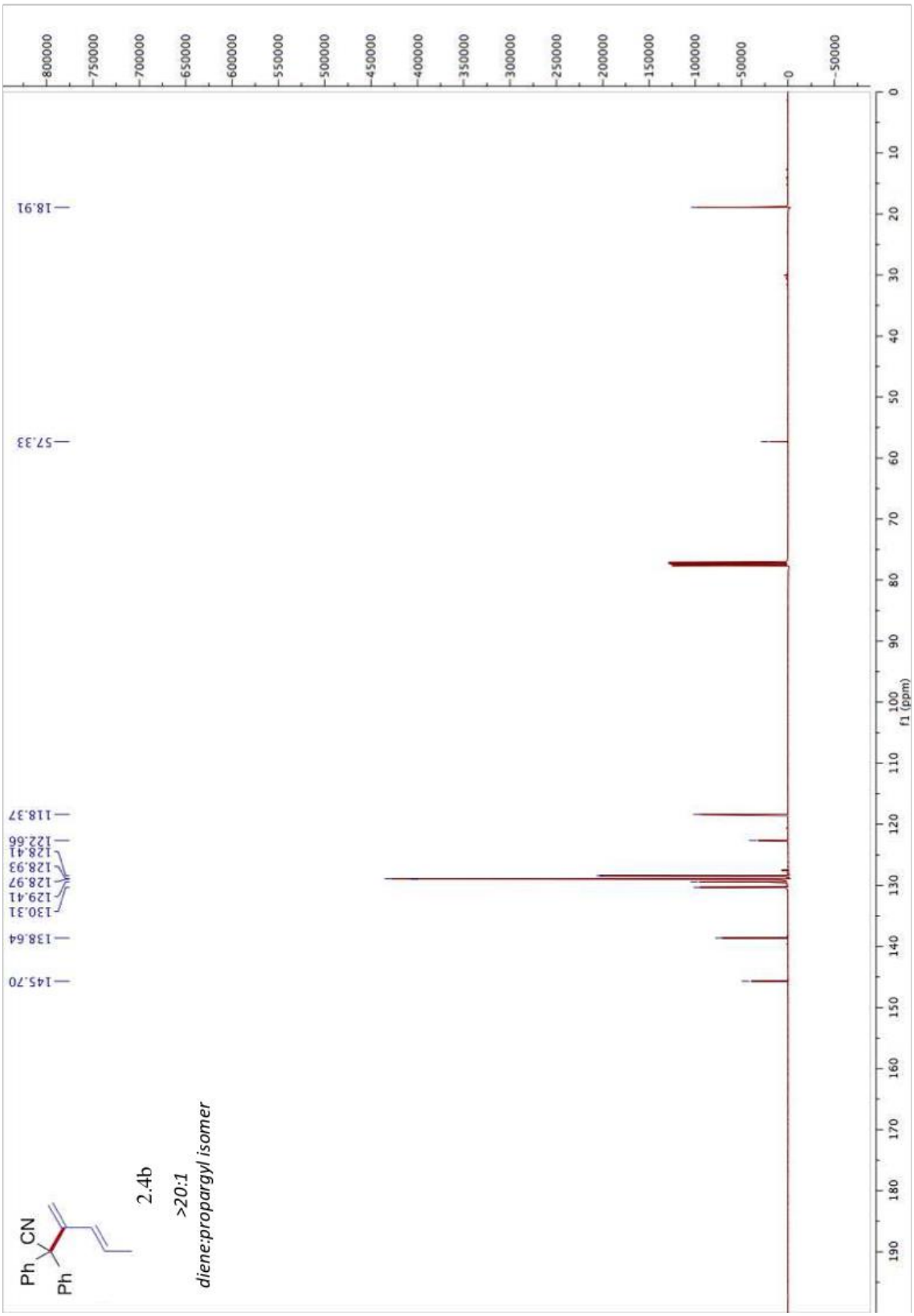
18.91
57.33
118.37
122.66
128.41
128.93
128.97
129.41
130.31
138.64
145.70
f1 (ppm)
Ph
CN
Ph
2.4b
>20:1
diene:propargyl isomer

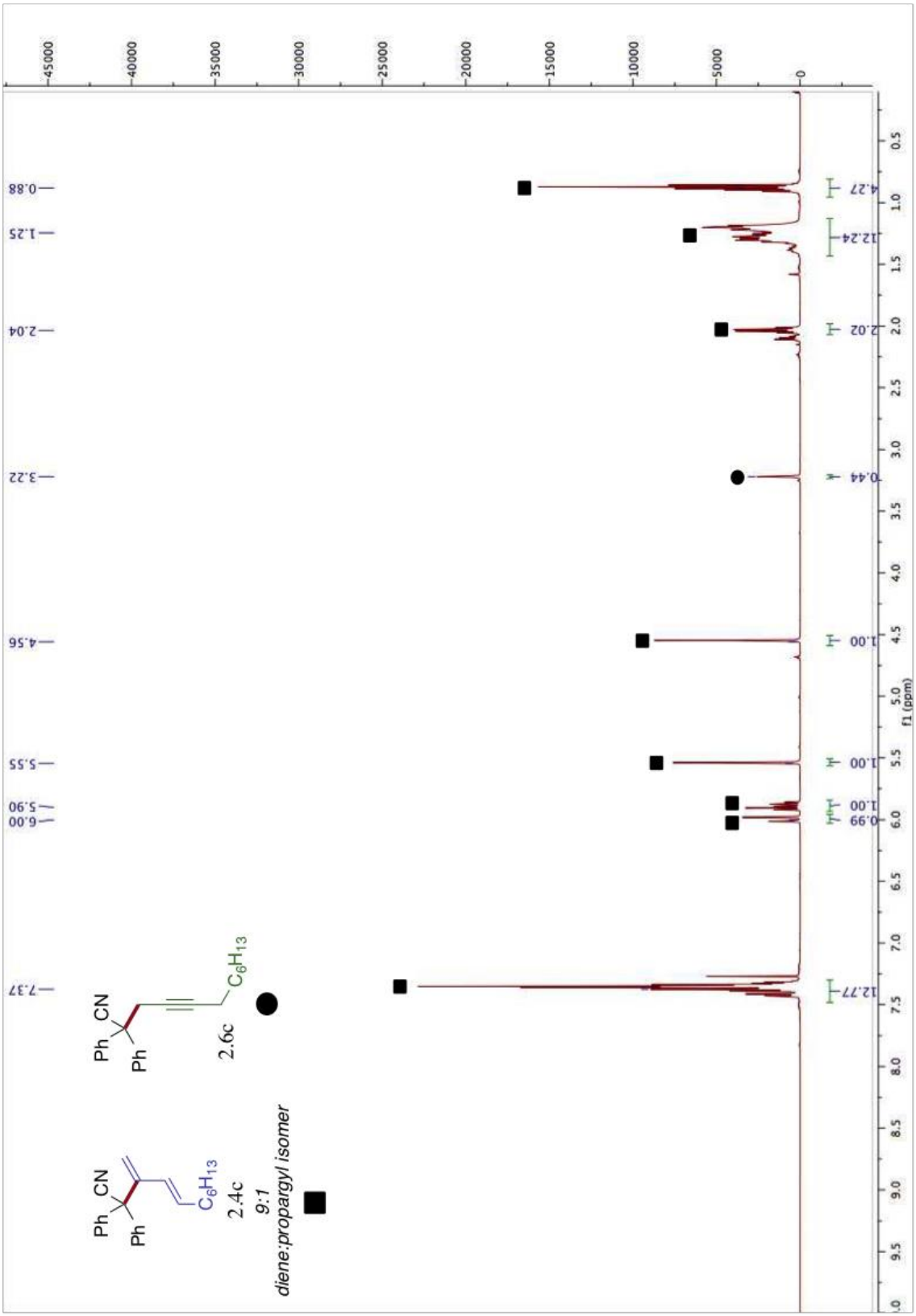
0.88
1.25
2.04
3.22
4.56
5.55
5.90
6.00
7.37
4.27
12.24
2.02
0.44
1.00
1.00
1.00
0.99
12.77
f1 (ppm)
Ph
CN
Ph
C6H13
2.6c
Ph
CN
Ph
C6H13
2.4c
9:1
diene:propargyl isomer

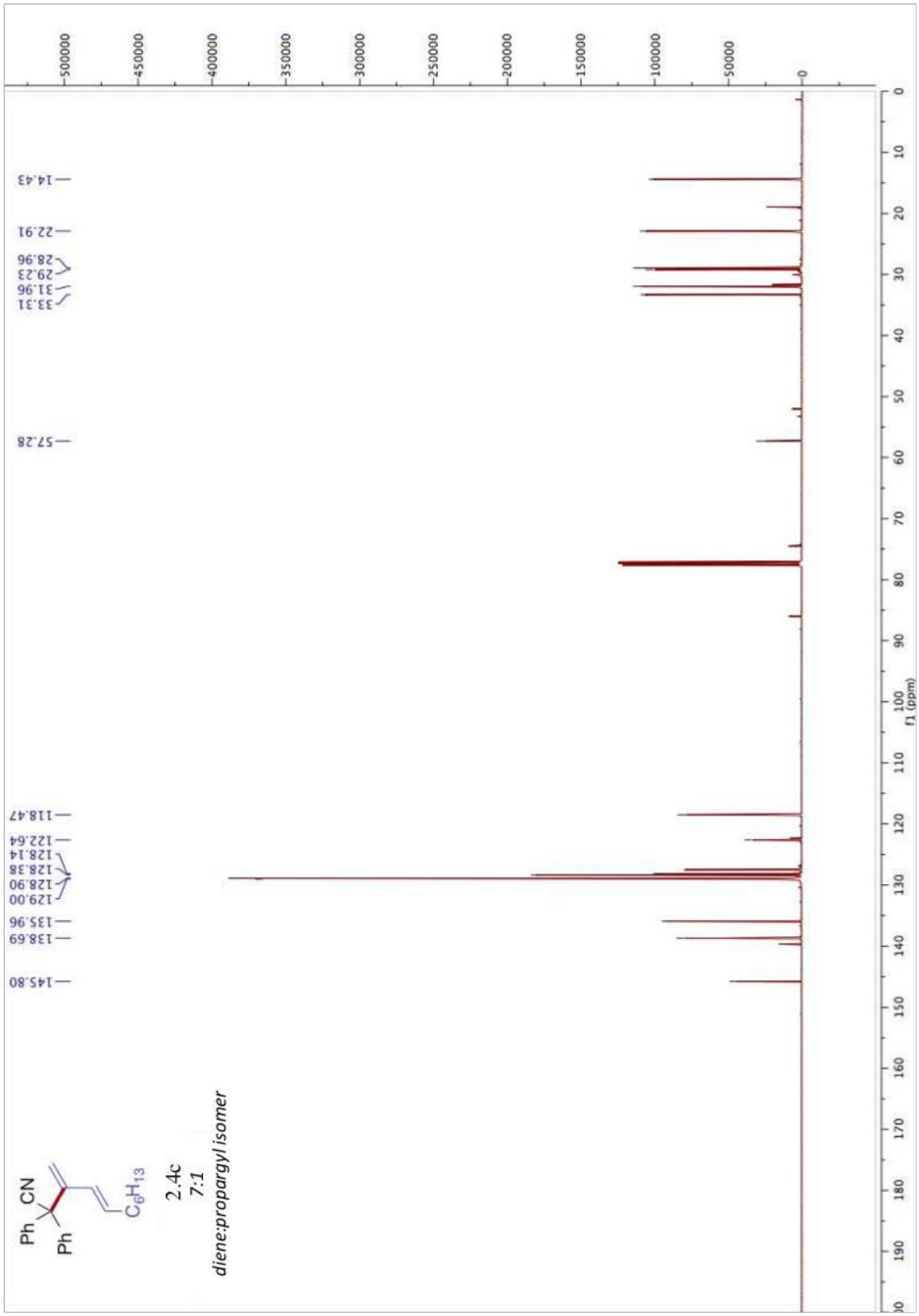
14.43
22.91
28.96
29.23
31.96
33.31
57.28
118.47
122.64
128.14
128.38
128.90
129.00
135.96
138.69
145.80
Ph
CN
Ph
C_6H_{13}
2.4c
7:1
diene:propargyl isomer
f1 (ppm)

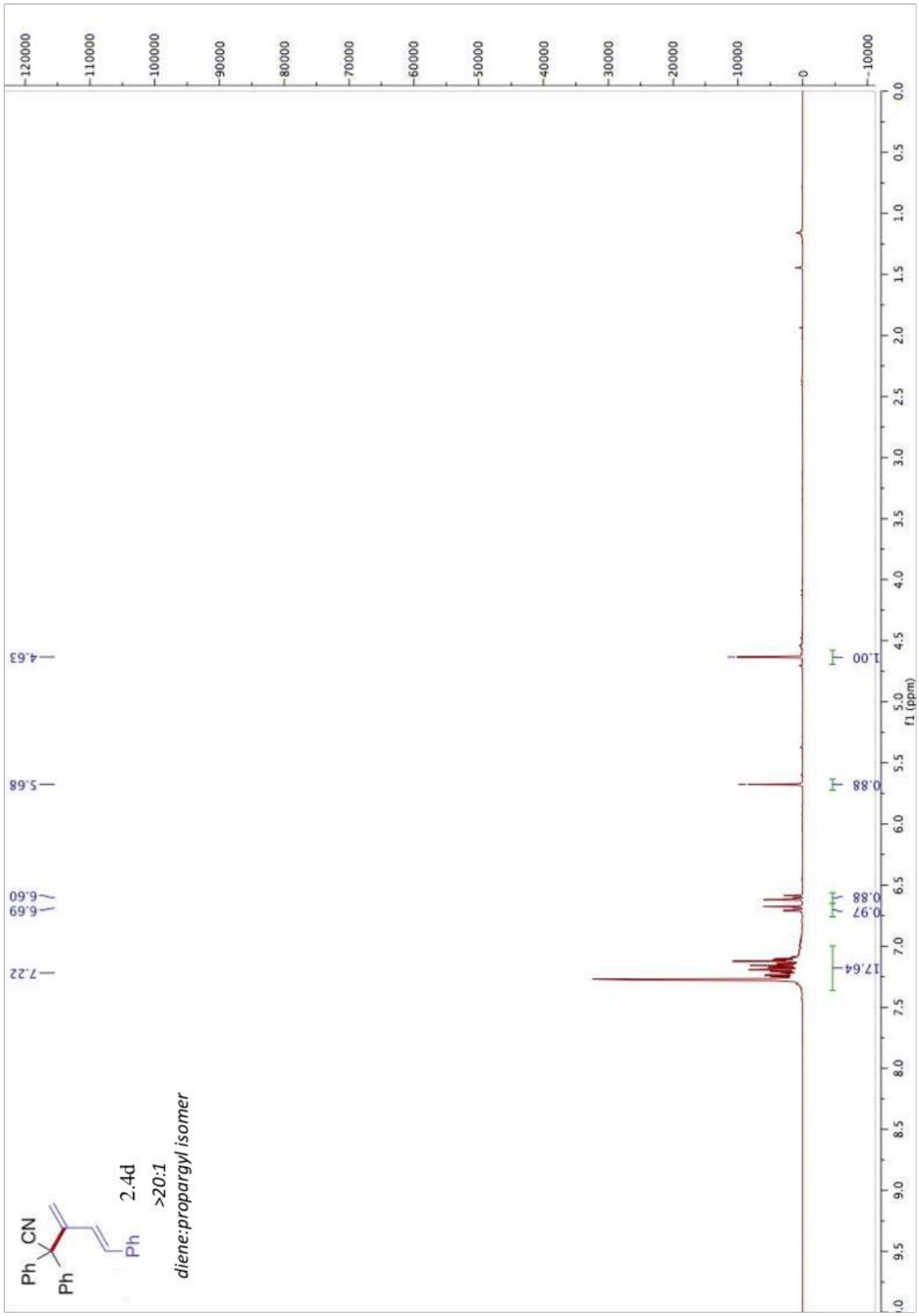
Ph
CN
Ph
Ph
2.4d
>20:1
diene:propargyl isomer
4.63
5.68
6.60
6.69
7.22
1.00
0.88
0.88
0.97
17.64
f1 (ppm)

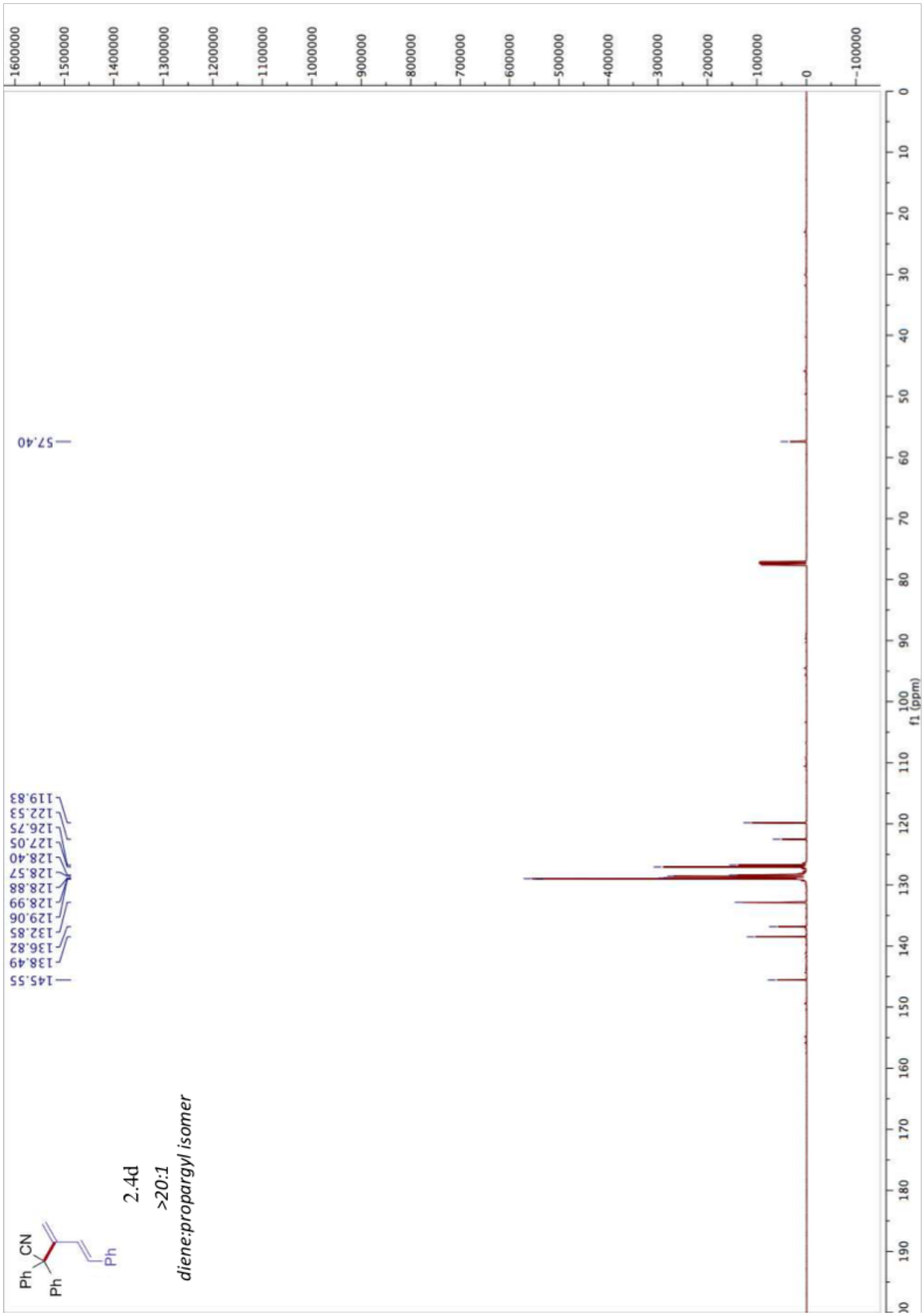
2.4d
>20:1
diene:propargyl isomer
Ph
CN
Ph
Ph
57.40
119.83
122.53
126.75
127.05
128.40
128.57
128.88
128.99
129.06
132.85
136.82
138.49
145.55
f1 (ppm)

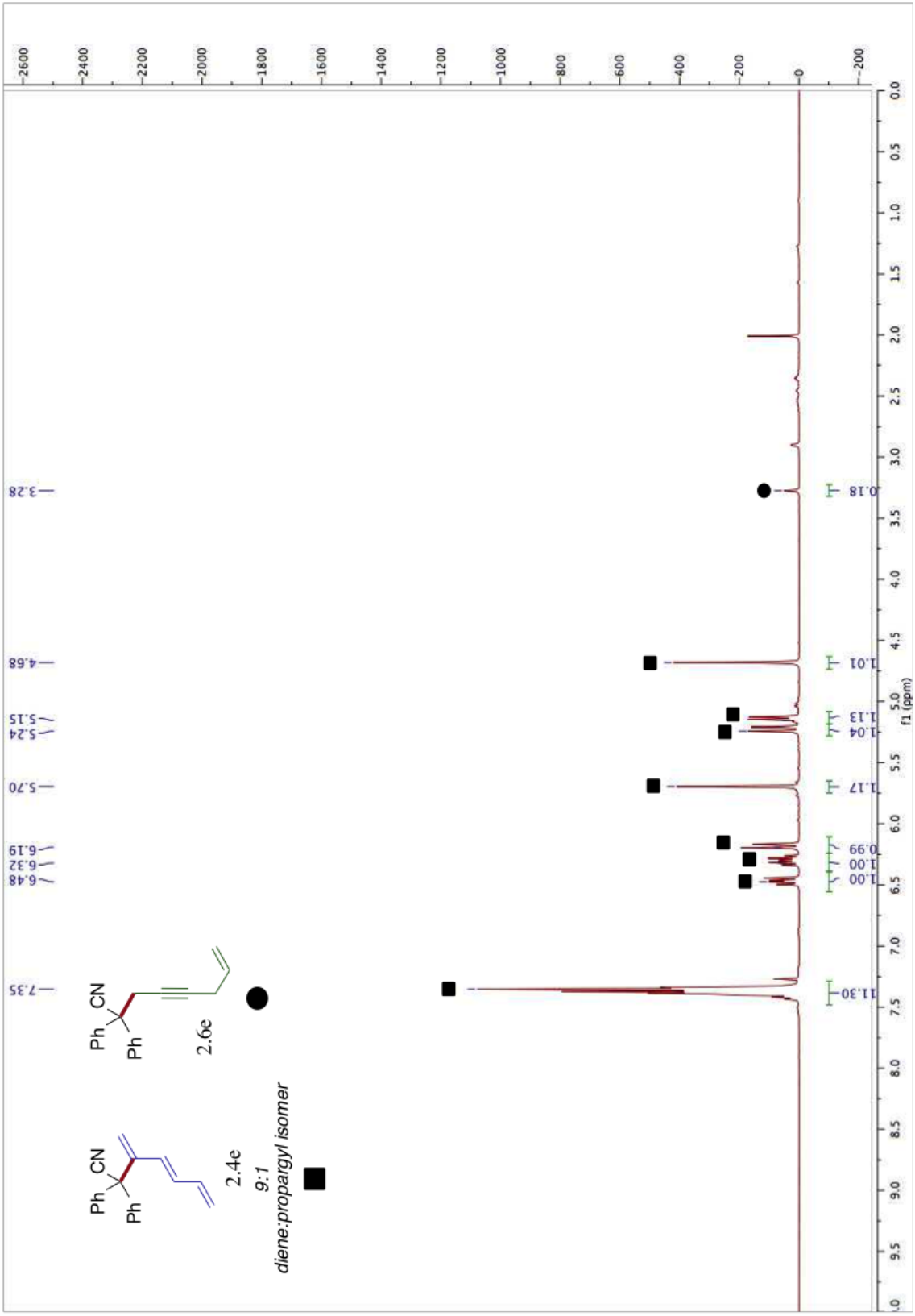
3.28
4.68
5.15
5.24
5.70
6.19
6.32
6.48
7.35
0.18
1.01
1.13
1.04
1.17
0.99
1.00
1.00
11.30
f1 (ppm)
Ph
CN
Ph
2.6e
2.4e
9:1
diene:propargyl isomer

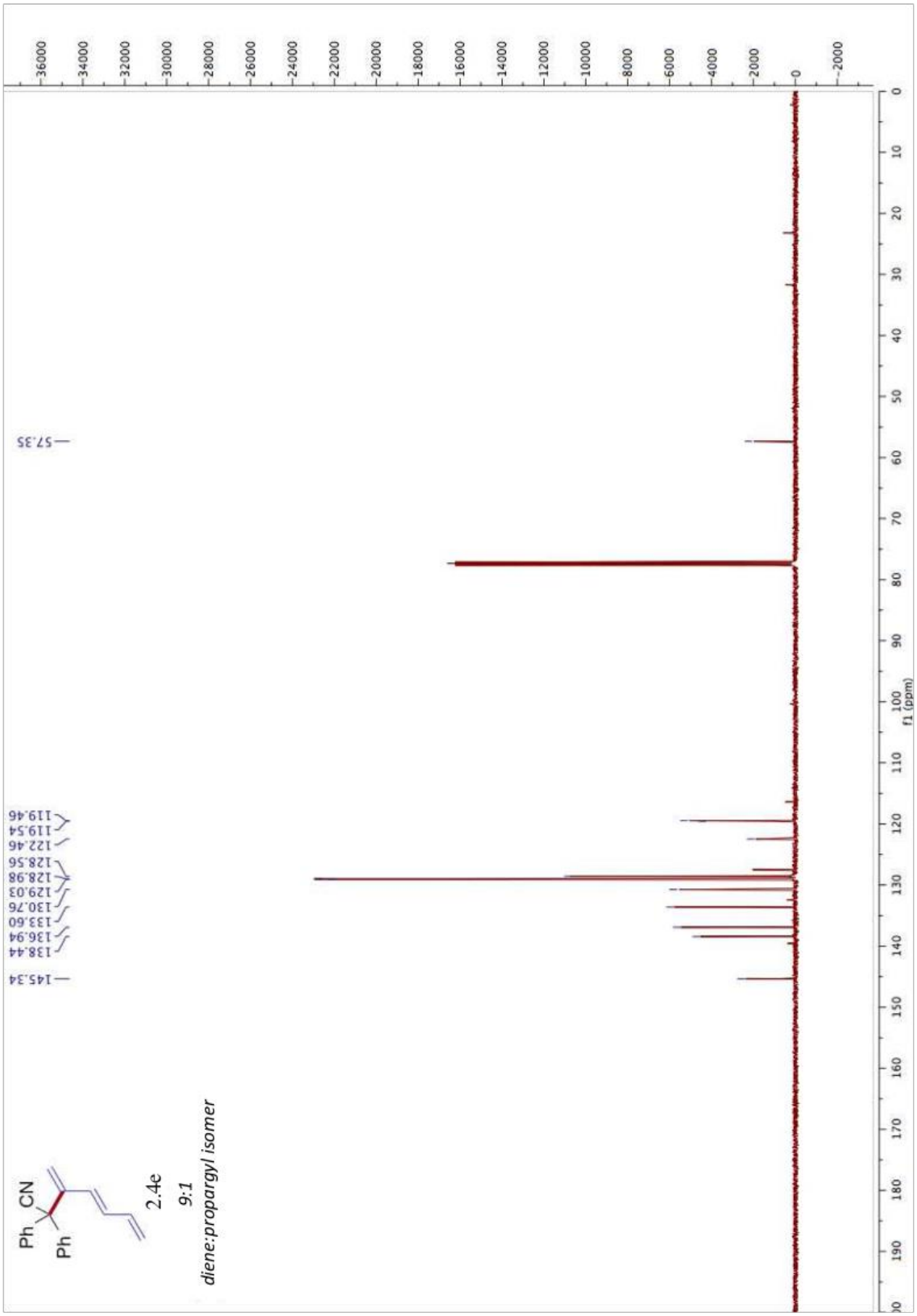
Ph
CN
Ph
2.4e
9:1
diene:propargyl isomer
145.34
138.44
136.94
133.60
130.76
129.03
128.98
128.56
122.46
119.54
119.46
57.35
f1 (ppm)

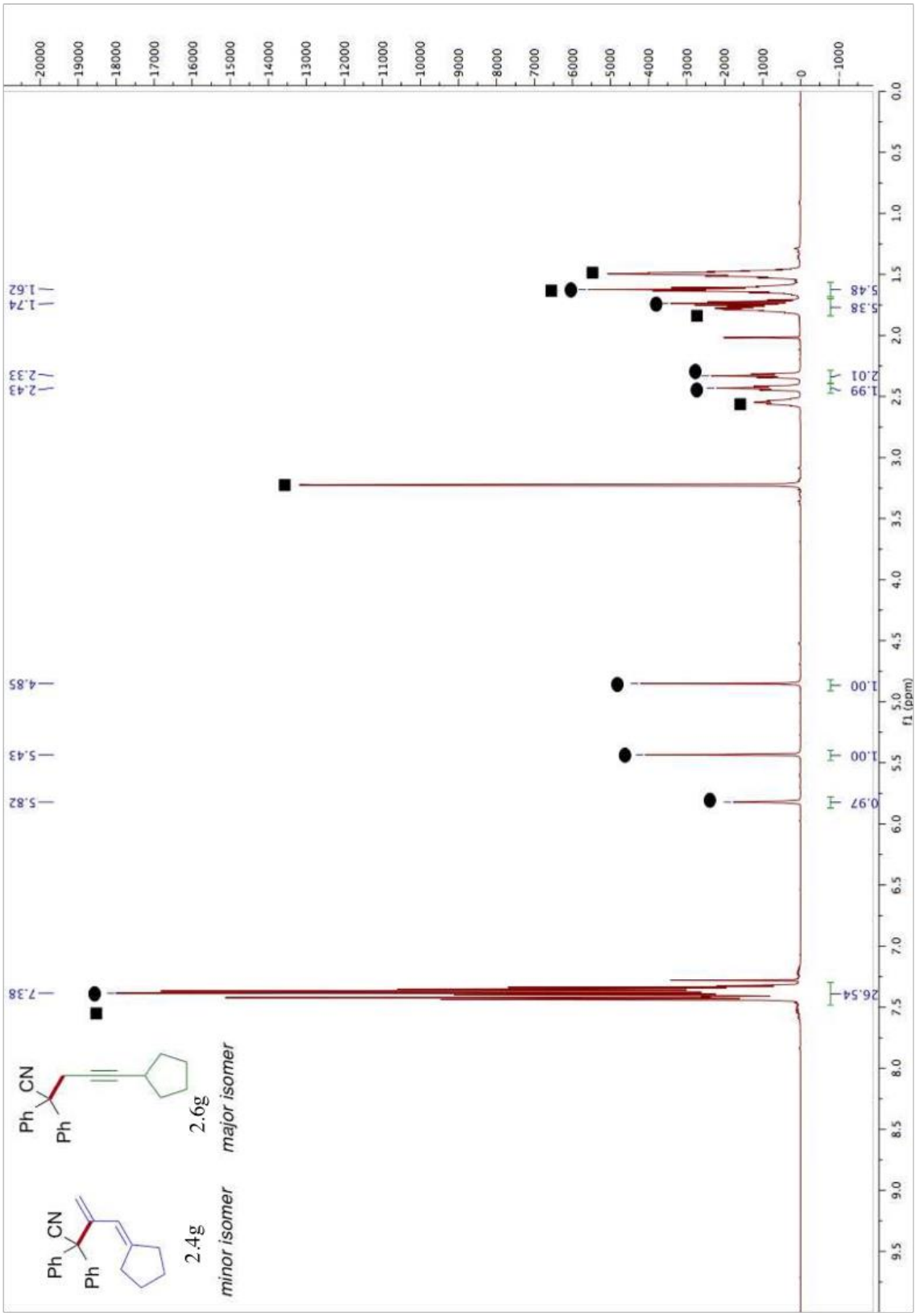
7.38
5.82
5.43
4.85
2.43
2.33
1.74
1.62
26.54
0.97
1.00
1.00
2.01
1.99
5.38
5.48
f1 (ppm)
Ph
CN
Ph
2.6g
major isomer
Ph
CN
Ph
2.4g
minor isomer

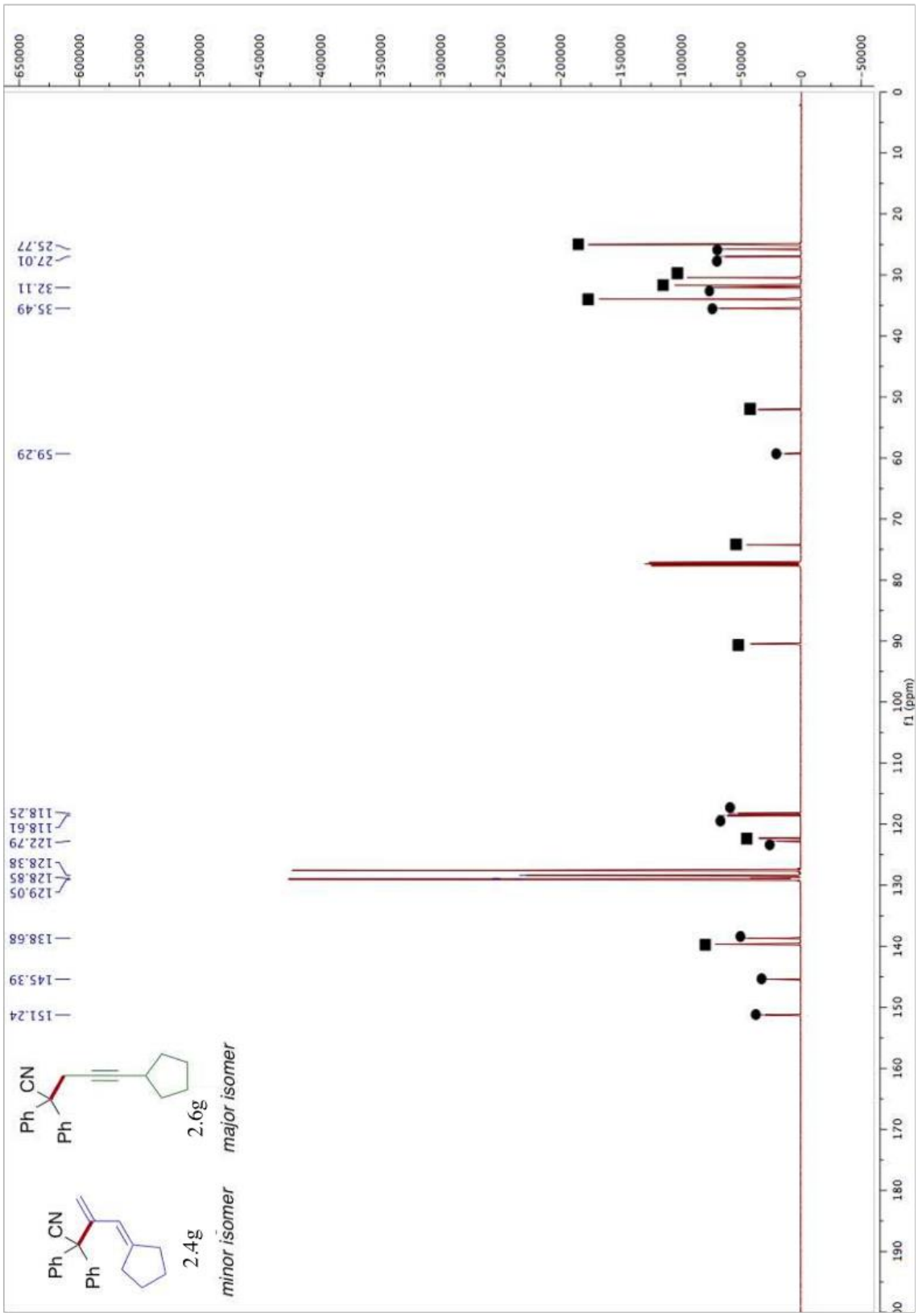
151.24
145.39
138.68
129.05
128.85
128.38
122.79
118.61
118.25
59.29
35.49
32.11
27.01
25.77
Ph
CN
Ph
2.6g
major isomer
Ph
CN
Ph
2.4g
minor isomer
f1 (ppm)

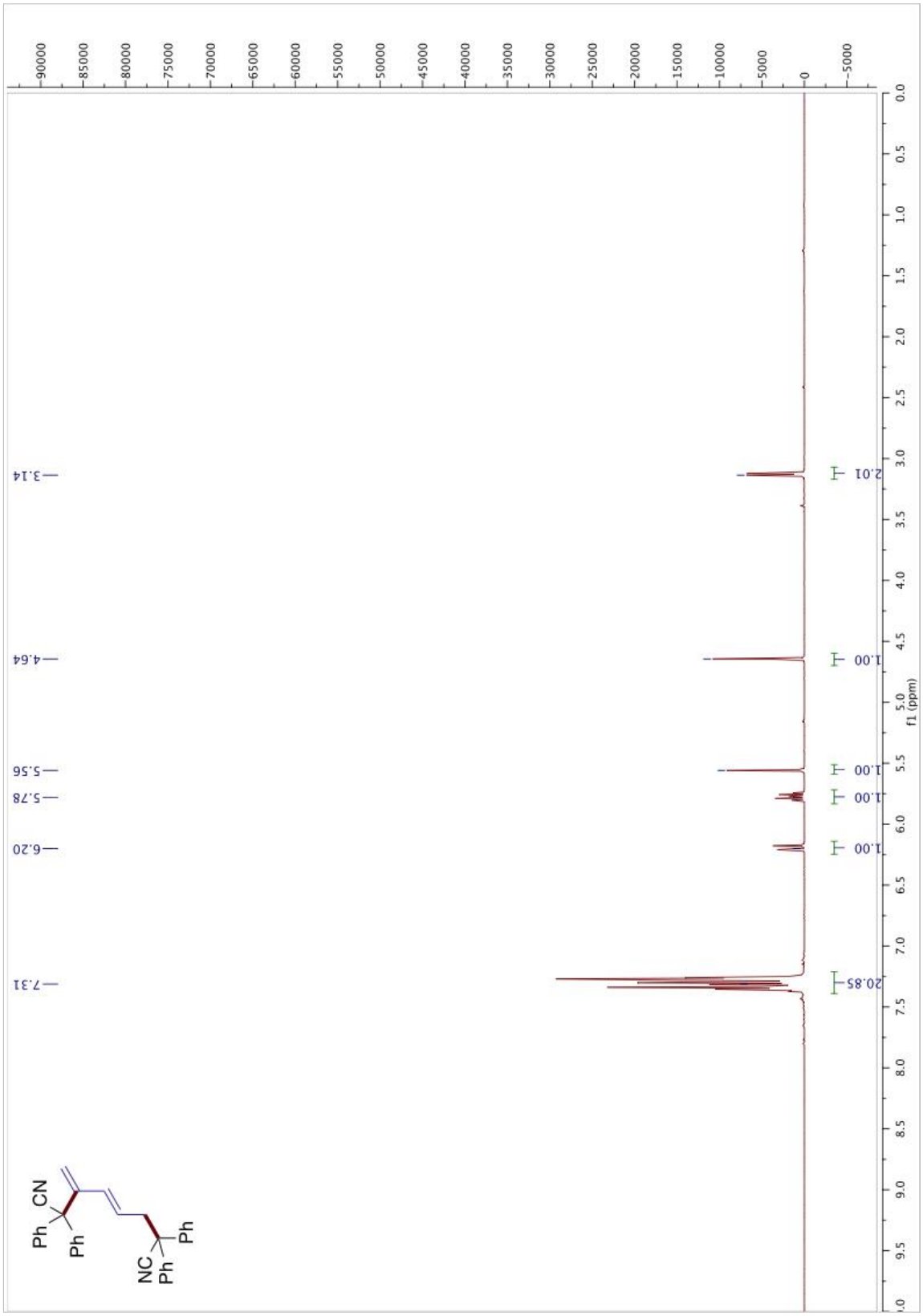
3.14
4.64
5.56
5.78
6.20
7.31
2.01
1.00
1.00
1.00
20.85
f1 (ppm)
Ph
CN
Ph
NC
Ph
Ph

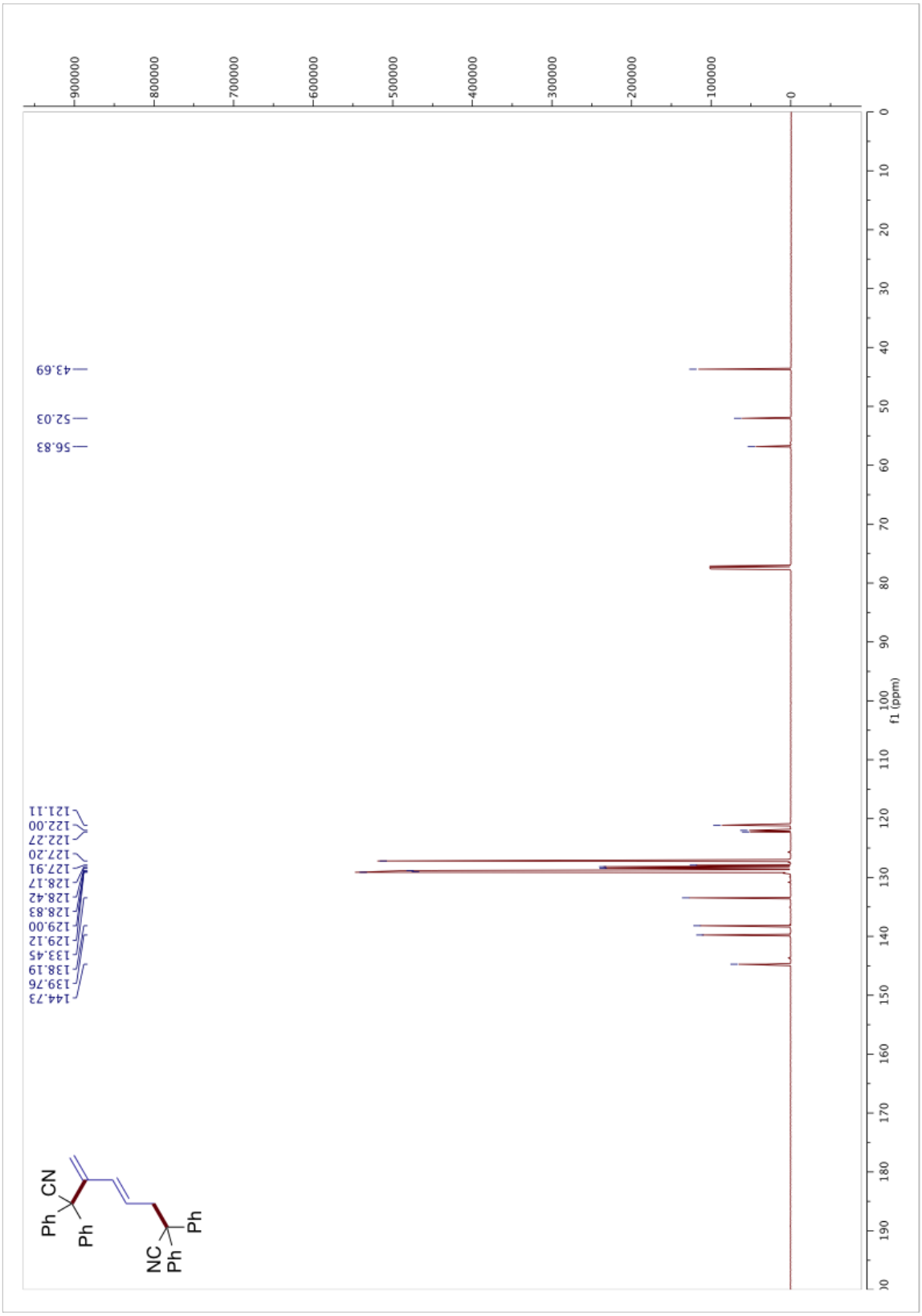
900000
800000
700000
600000
500000
400000
300000
200000
100000
0
43.69
52.03
56.83
121.11
122.00
122.27
127.20
127.91
128.17
128.42
128.83
129.00
129.12
133.45
138.19
139.76
144.73
0
10
20
30
40
50
60
70
80
90
100
110
120
130
140
150
160
170
180
190
f1 (ppm)
Ph
CN
Ph
NC
Ph
Ph

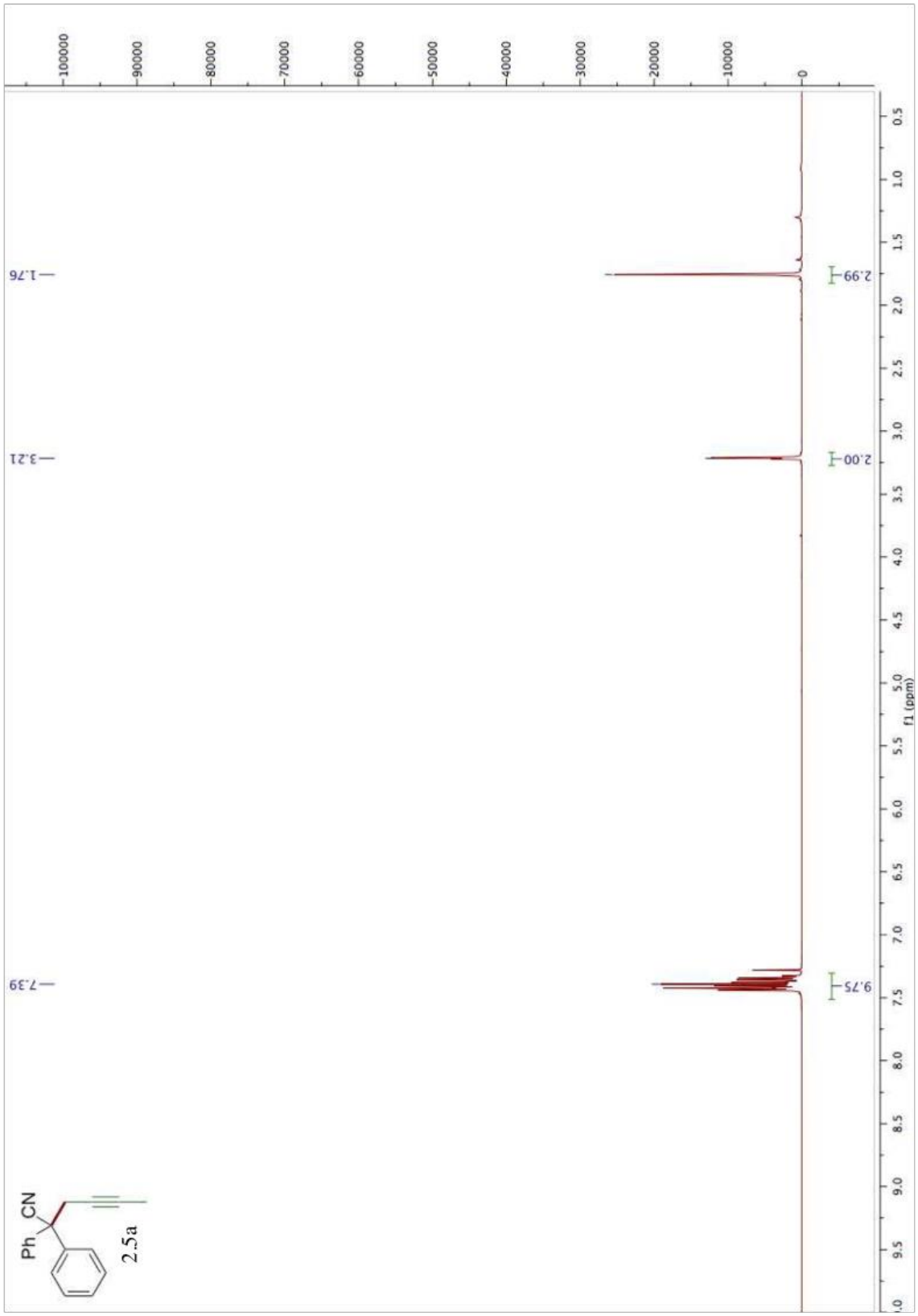
1.76
3.21
7.39
2.99
2.00
9.75
f1 (ppm)
Ph
CN
2.5a

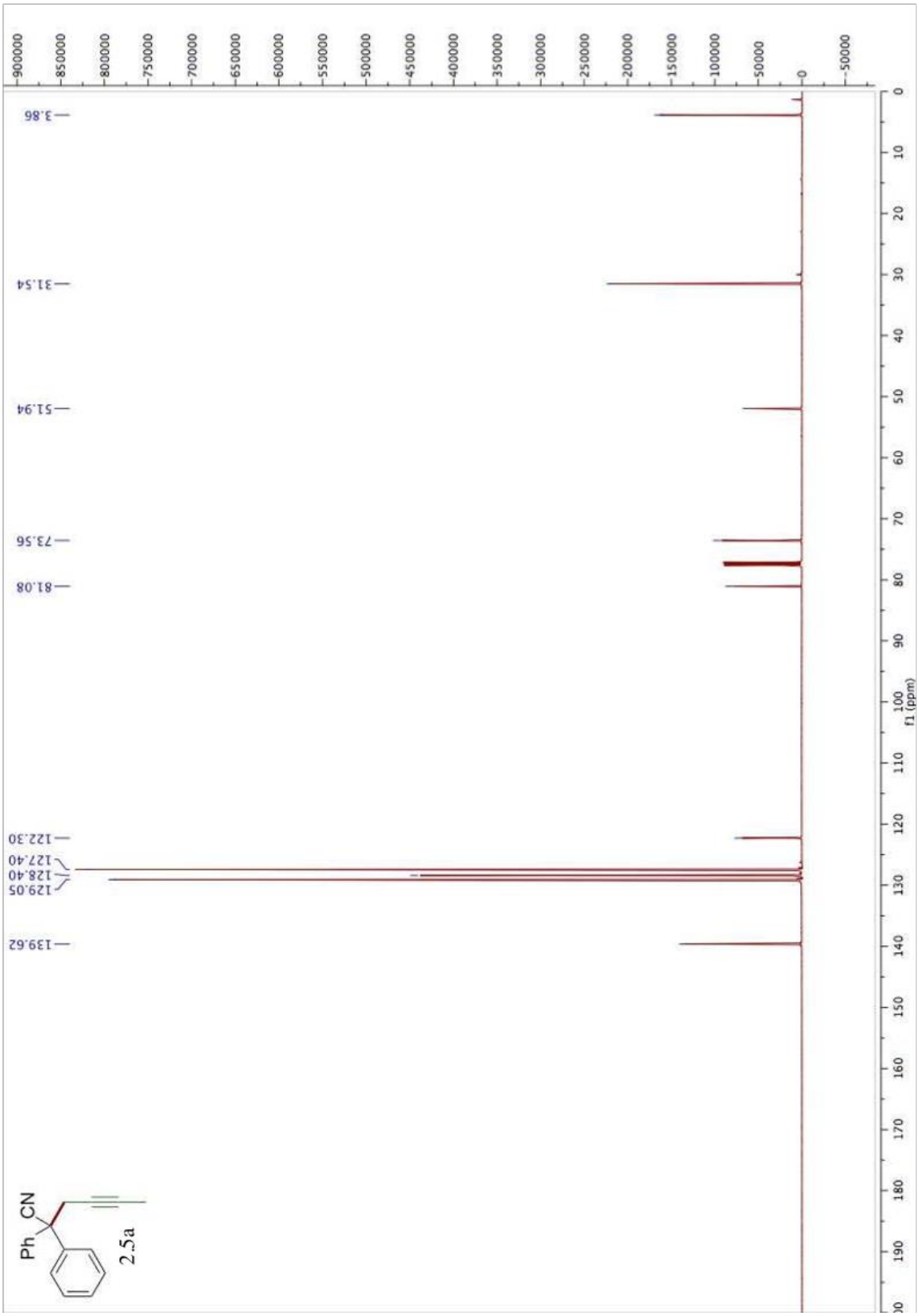
3.86
31.54
51.94
73.56
81.08
122.30
127.40
128.40
129.05
139.62
Ph
CN
2.5a
f1 (ppm)

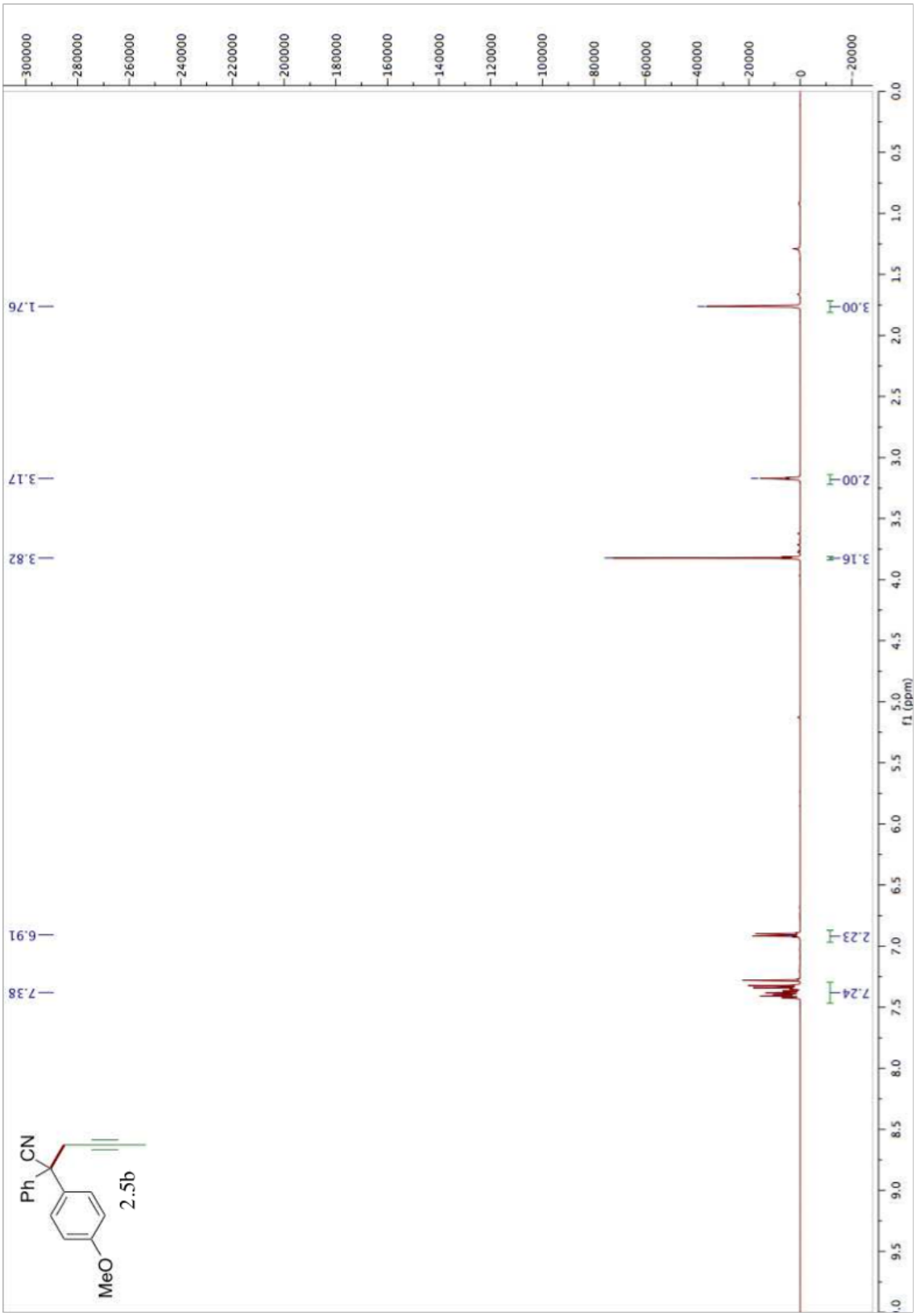
1.76
3.17
3.82
6.91
7.38
3.00
2.00
3.16
2.23
7.24
f1 (ppm)
Ph
CN
MeO
2.5b

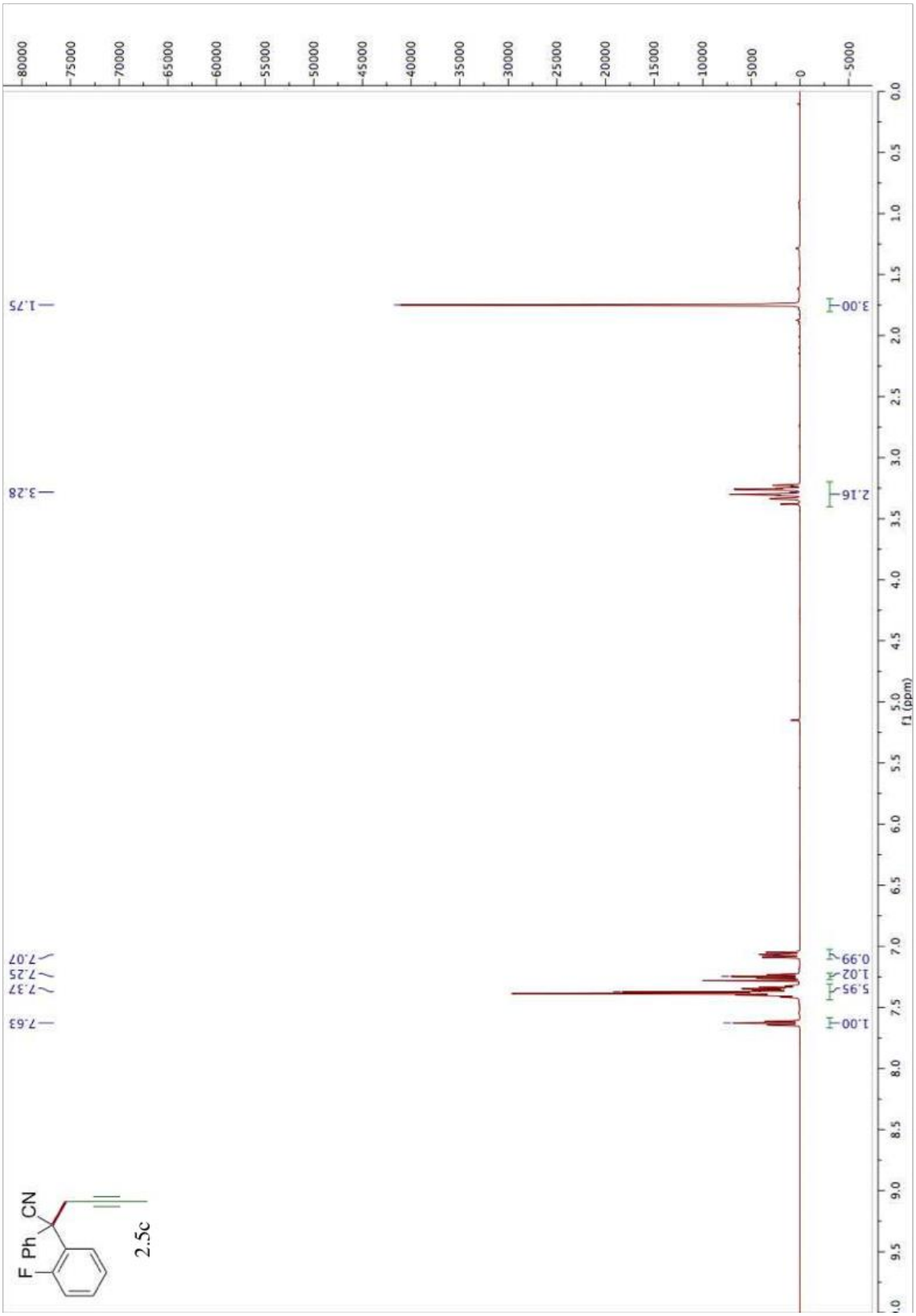
1.75
3.28
7.63
7.37
7.25
7.07
3.00
2.16
1.00
5.95
1.02
0.99
f1 (ppm)
F
Ph
CN
2.5c

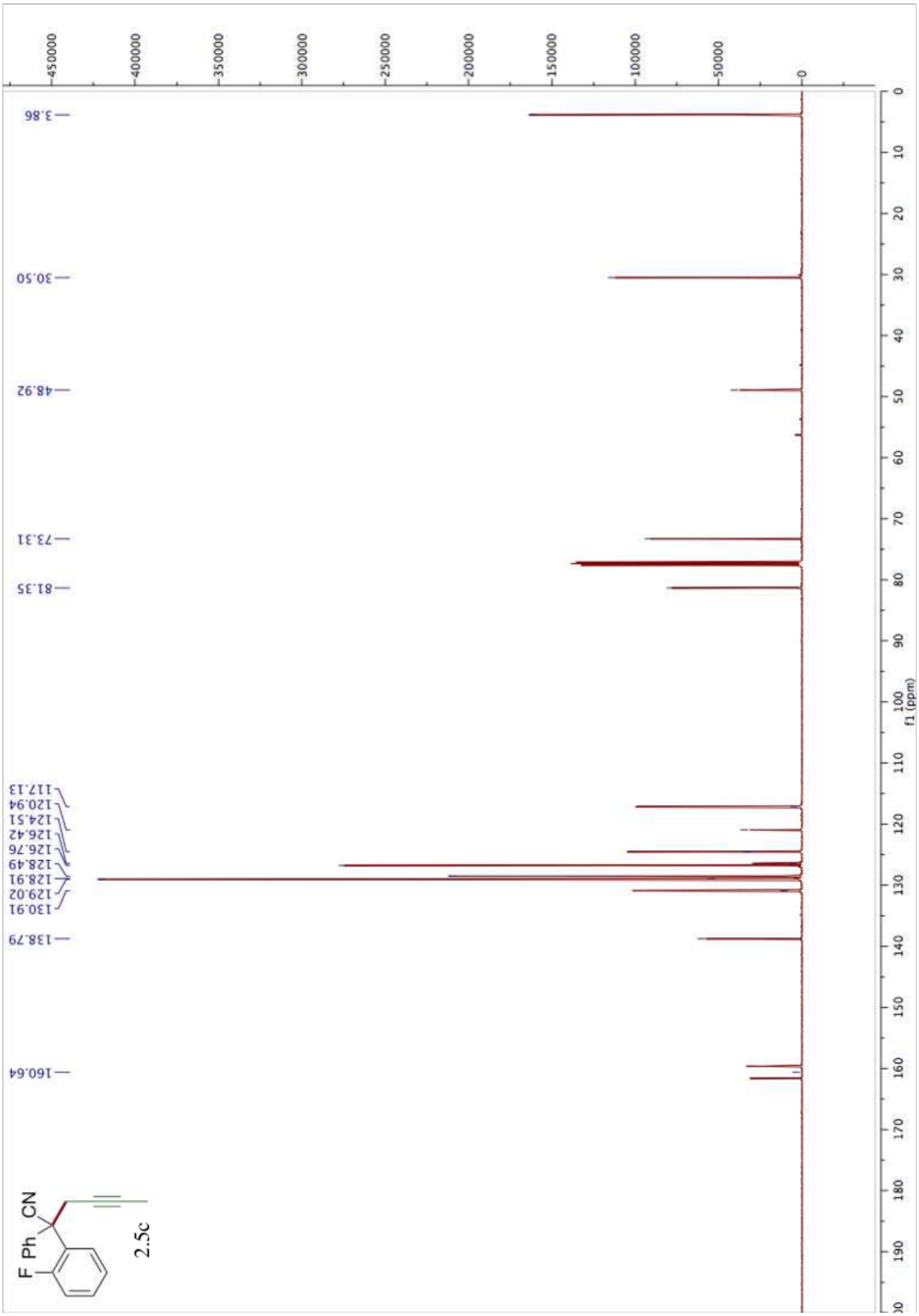
3.86
30.50
48.92
73.31
81.35
117.13
120.94
124.51
126.42
126.76
128.49
128.91
129.02
130.91
138.79
160.64
F
Ph
CN
2.5c
f1 (ppm)

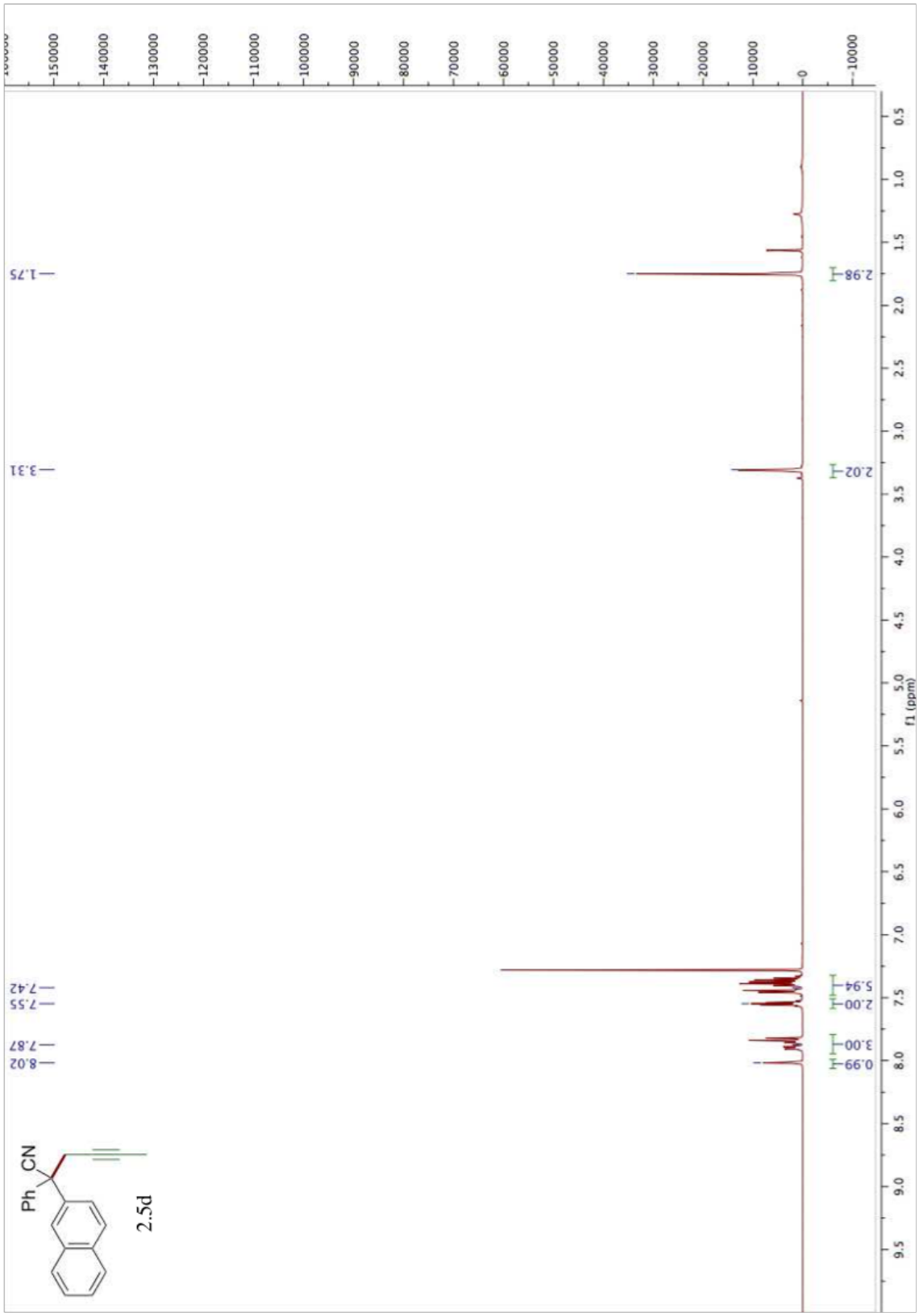
1.75
3.31
7.42
7.55
7.87
8.02
2.98
2.02
5.94
2.00
3.00
0.99
f1 (ppm)
Ph
CN
2.5d

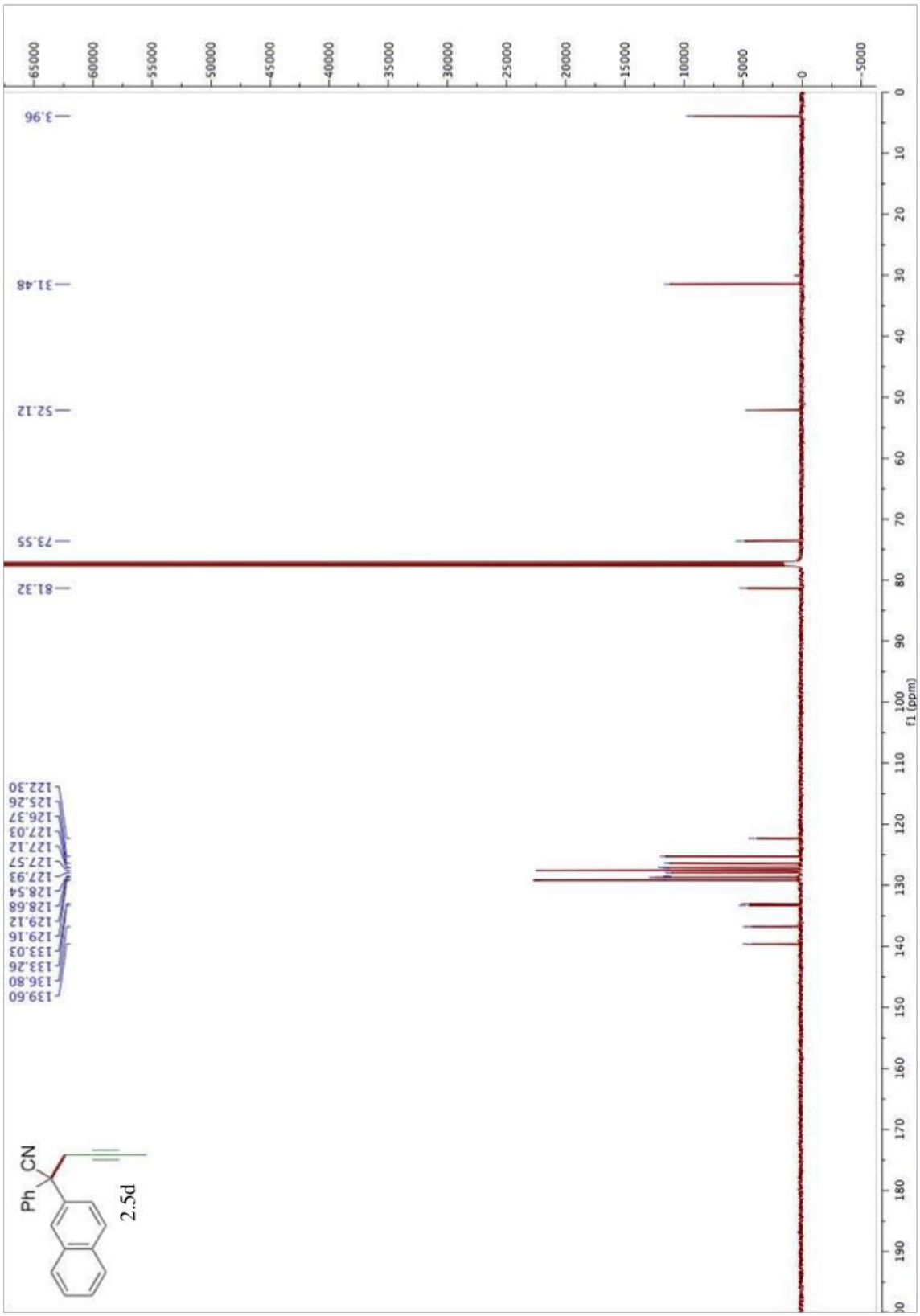
3.96
31.48
52.12
73.55
81.32
122.30
125.26
126.37
127.03
127.12
127.57
127.93
128.54
128.68
129.12
129.16
133.03
133.26
136.80
139.60
Ph
CN
2.5d
f1 (ppm)

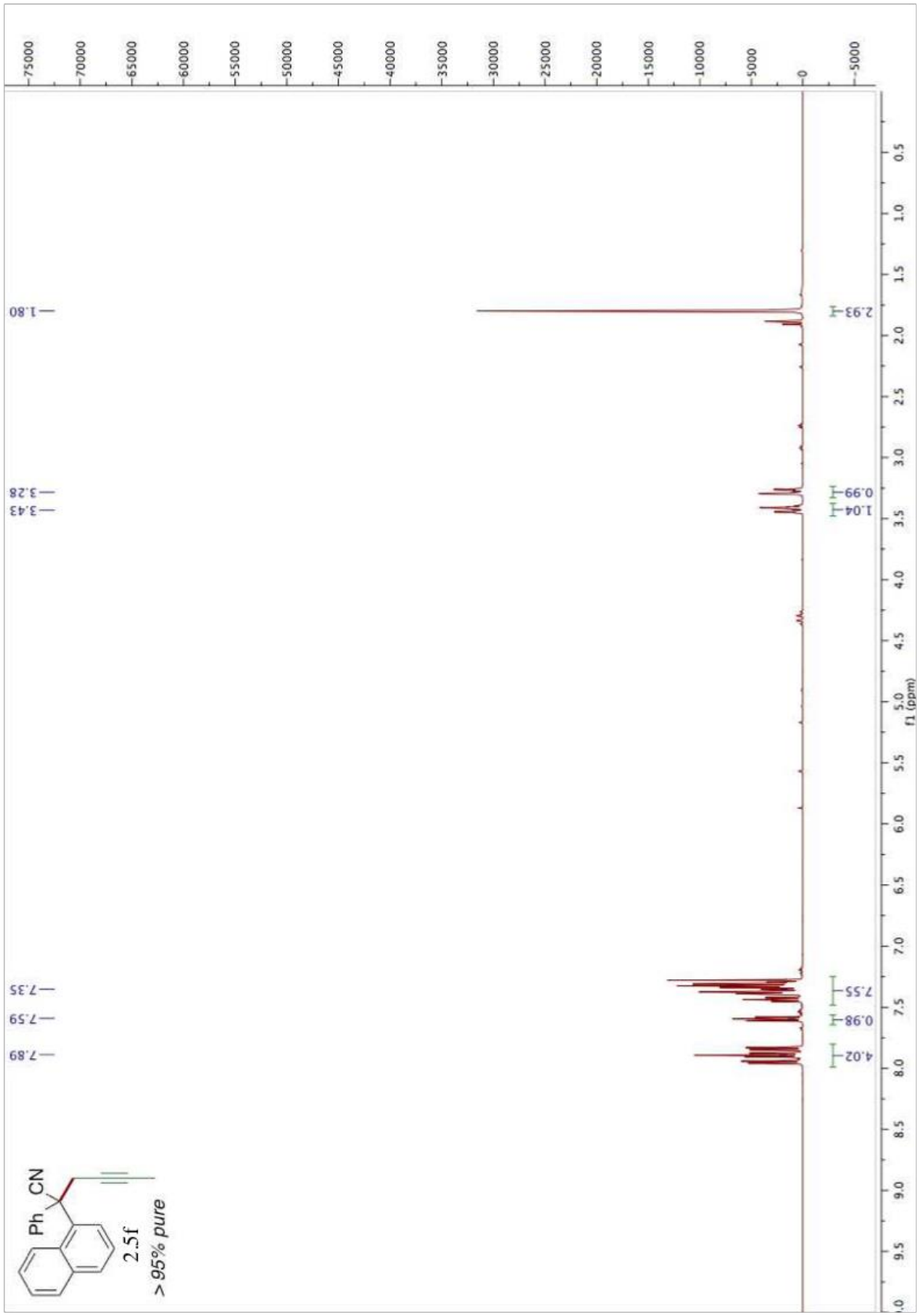
1.80
3.28
3.43
7.35
7.59
7.89
2.93
0.99
1.04
7.55
0.98
4.02
f1 (ppm)
Ph
CN
2.5f
> 95% pure

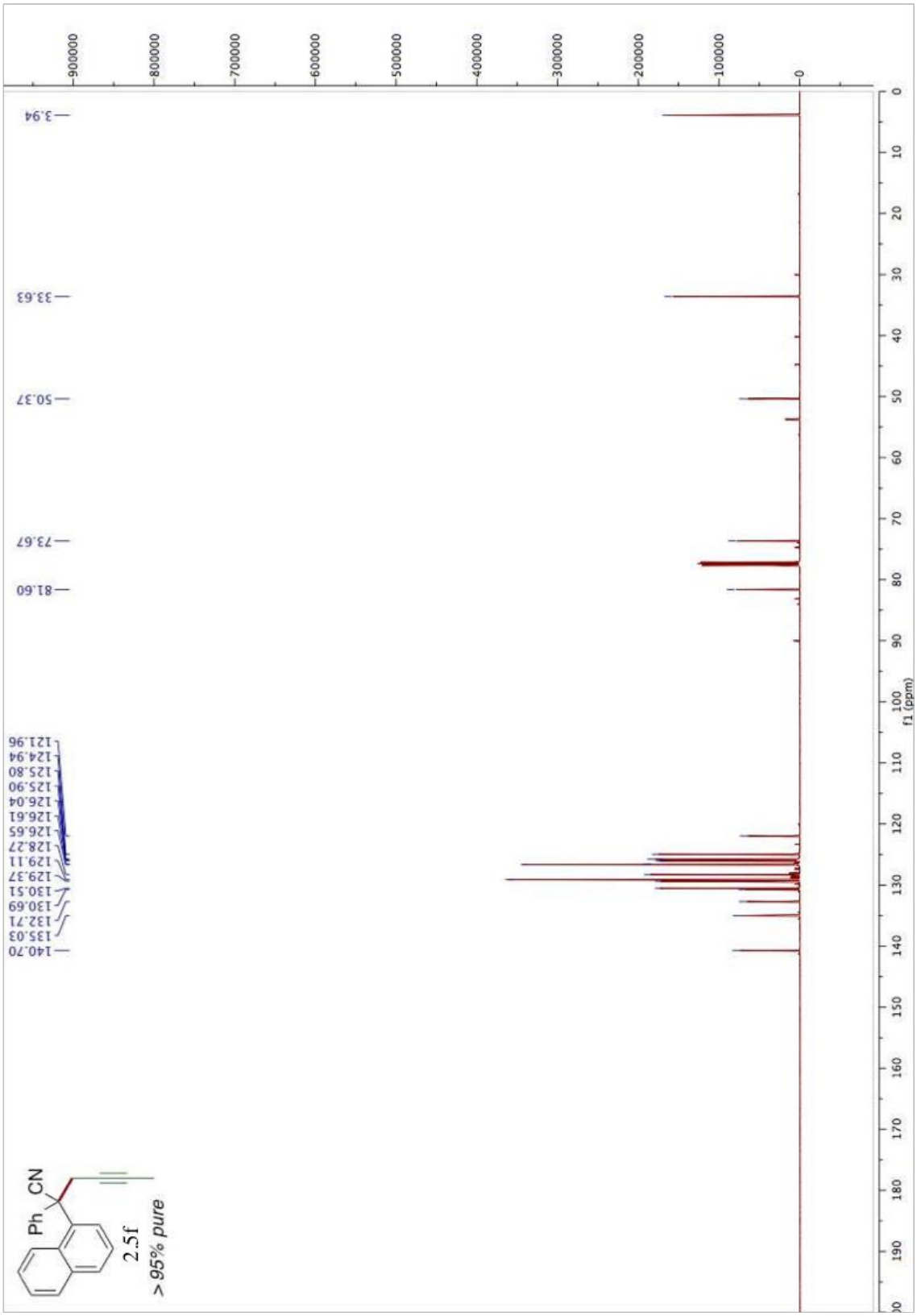
3.94
33.63
50.37
73.67
81.60
121.96
124.94
125.80
125.90
126.04
126.61
126.65
128.27
129.11
129.37
130.51
130.69
132.71
135.03
140.70
f1 (ppm)
Ph
CN
2.5f
> 95% pure

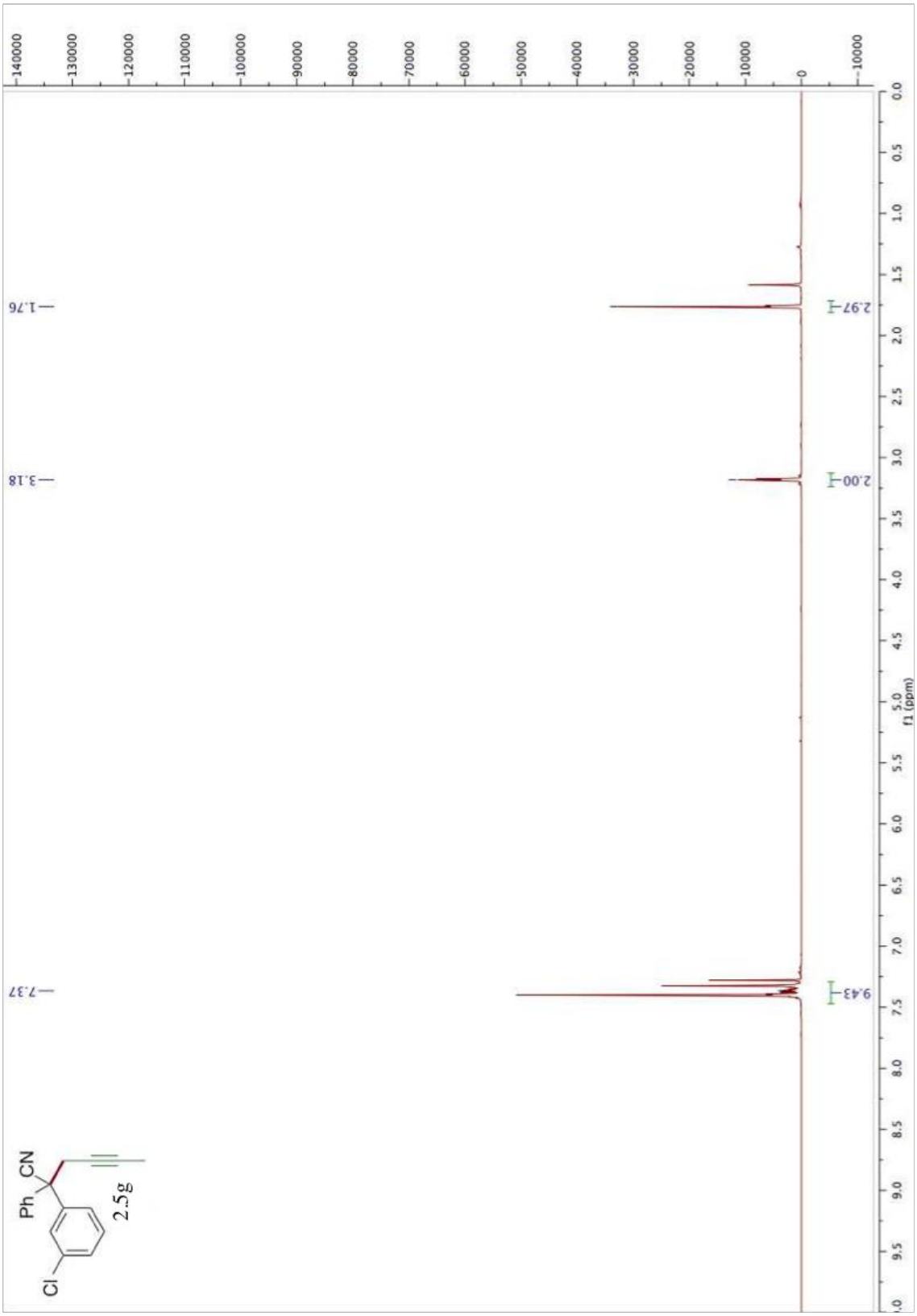
1.76
3.18
7.37
2.97
2.00
9.43
f1 (ppm)
Ph
CN
Cl
2.5g

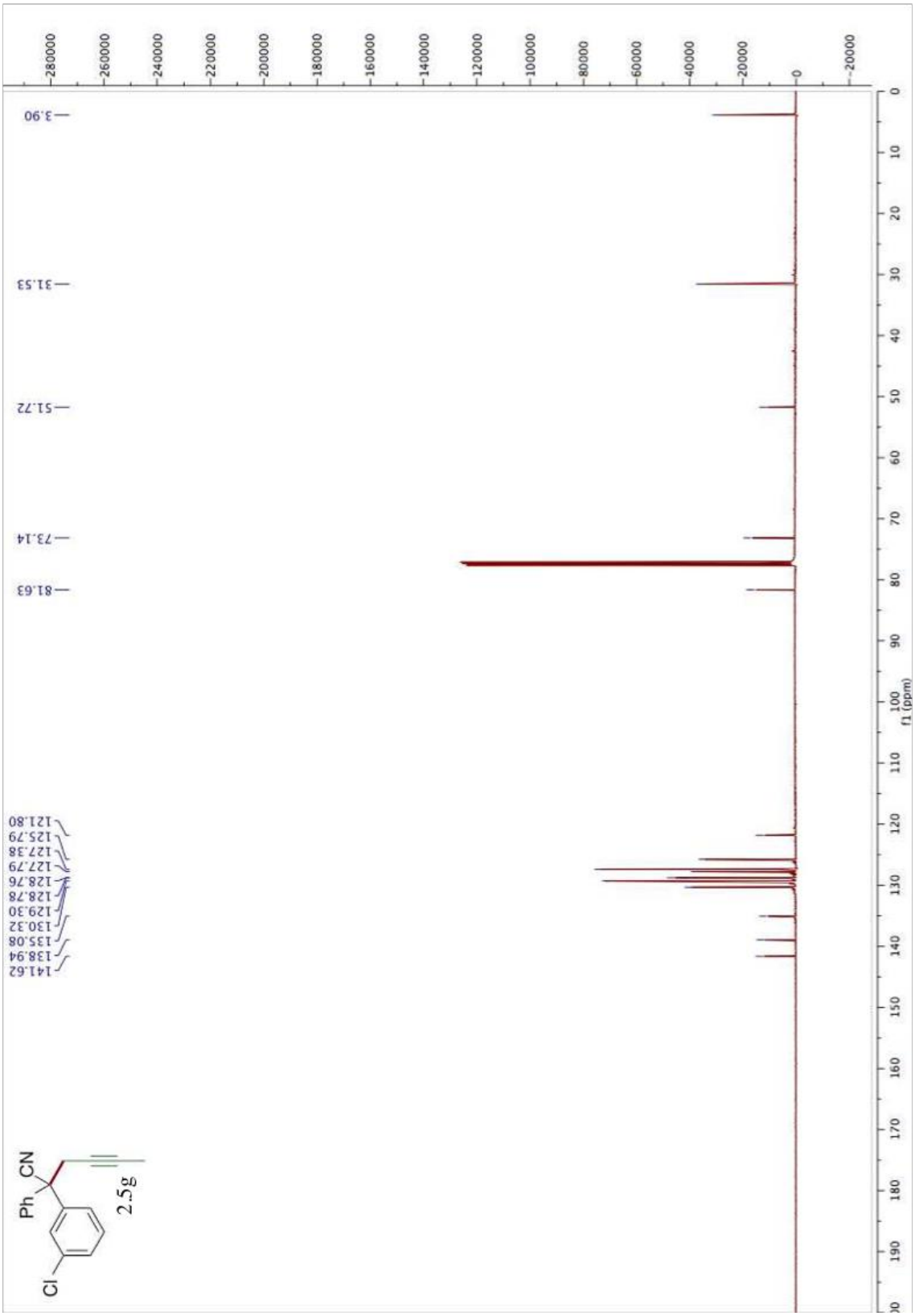
3.90
31.53
51.72
73.14
81.63
121.80
125.79
127.38
127.79
128.76
128.78
129.30
130.32
135.08
138.94
141.62
Ph
CN
Cl
2.5g
f1 (ppm)

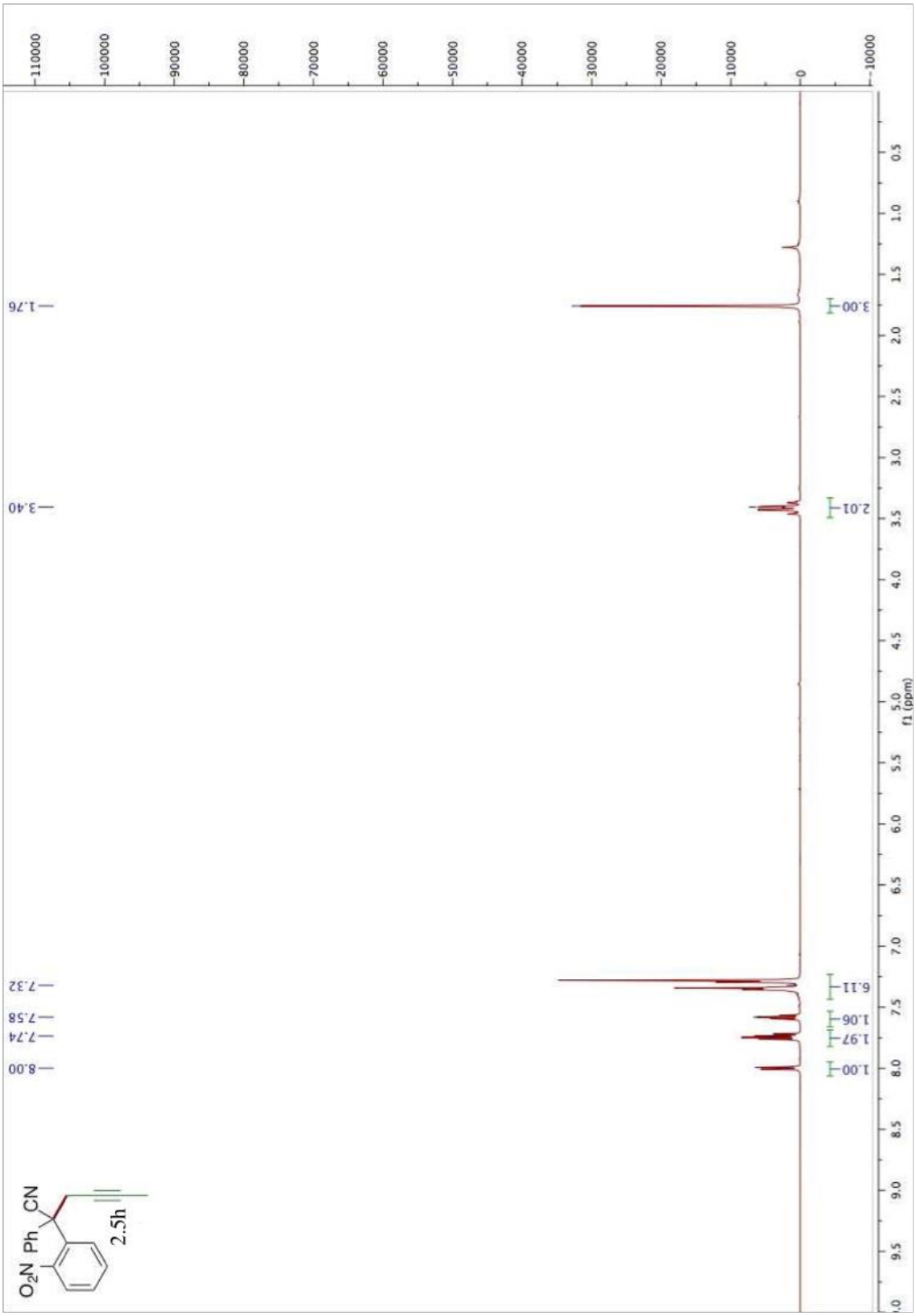
1.76
3.40
7.32
7.58
7.74
8.00
3.00
2.01
6.11
1.06
1.97
1.00
f1 (ppm)
O2N
Ph
CN
2.5h

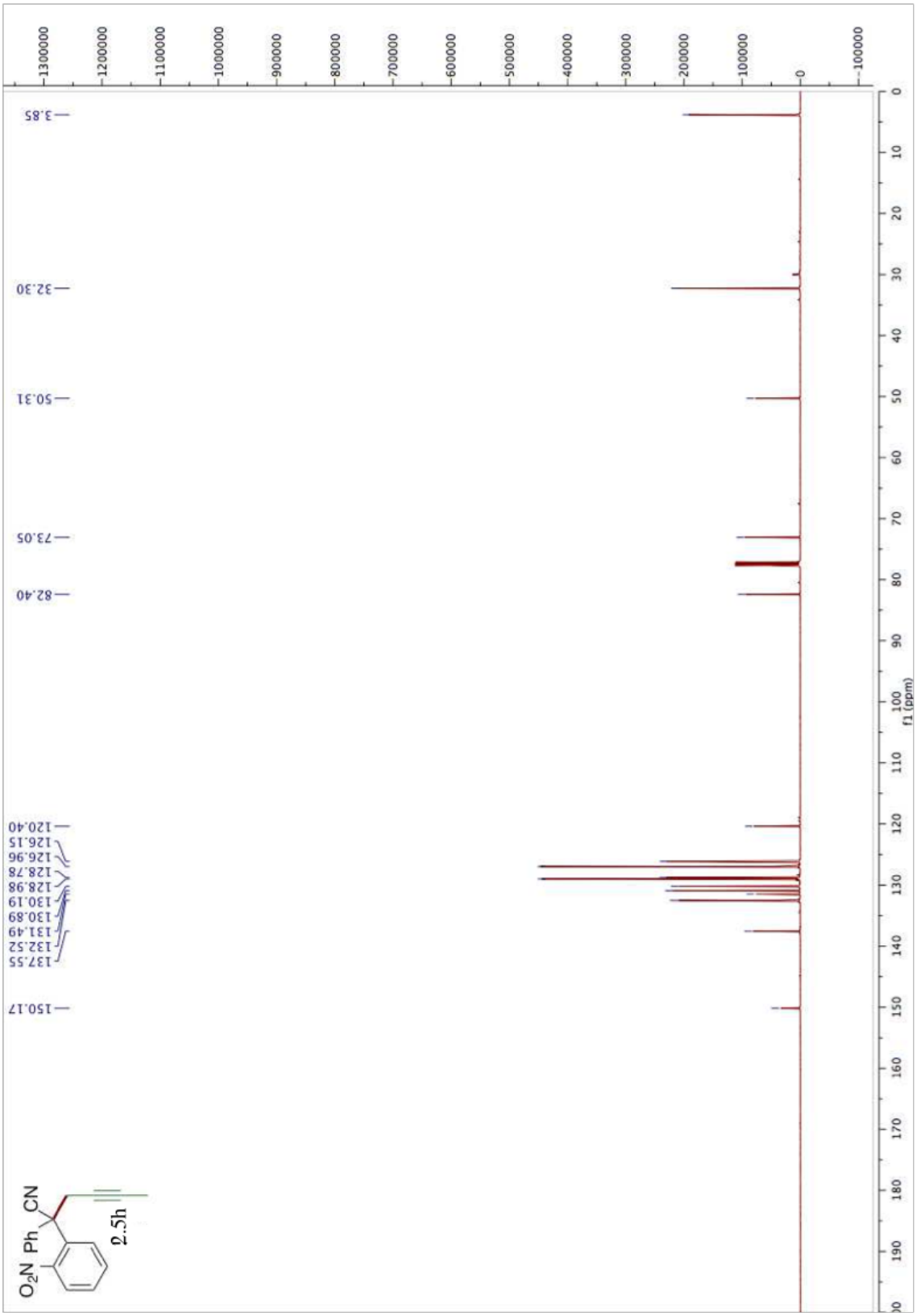
3.85
32.30
50.31
73.05
82.40
120.40
126.15
126.96
128.78
128.98
130.19
130.89
131.49
132.52
137.55
150.17
f1 (ppm)
O2N Ph CN
2.5h

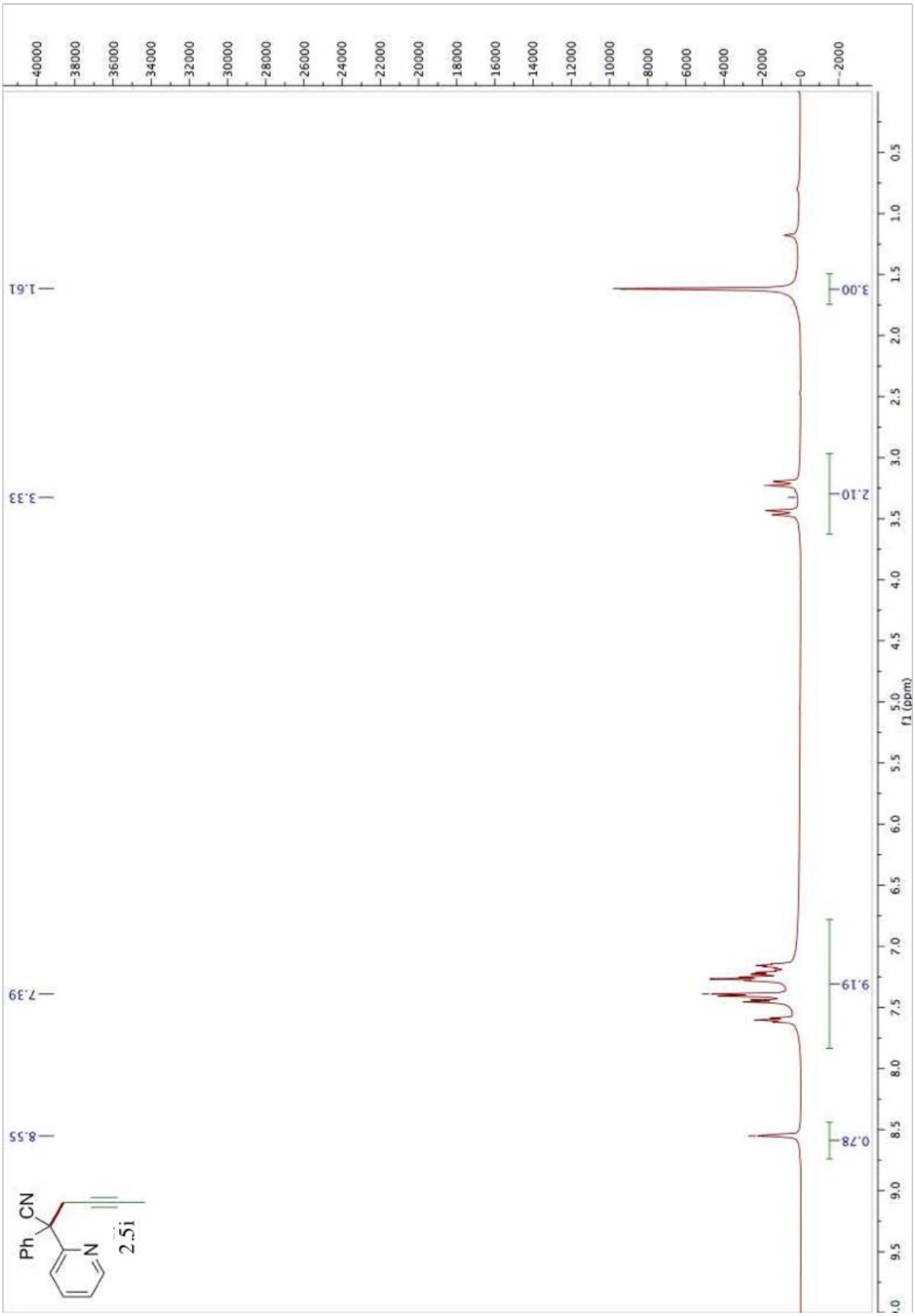
1.61
3.33
7.39
8.55
3.00
2.10
9.19
0.78
f1 (ppm)
Ph
CN
N
2.5i

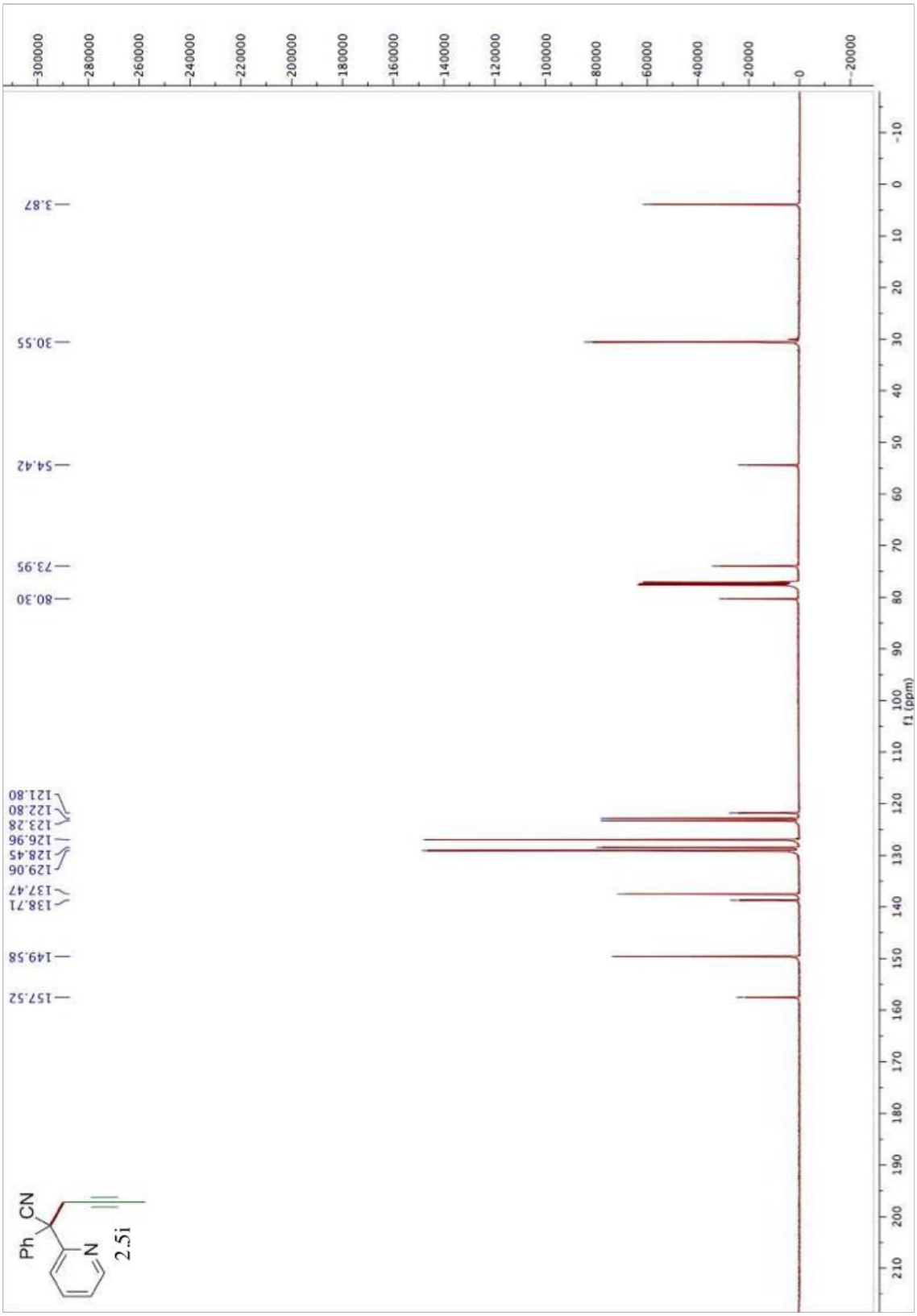
3.87
30.55
54.42
73.95
80.30
121.80
122.80
123.28
126.96
128.45
129.06
137.47
138.71
149.58
157.52
Ph
CN
N
2.5i
f1 (ppm)

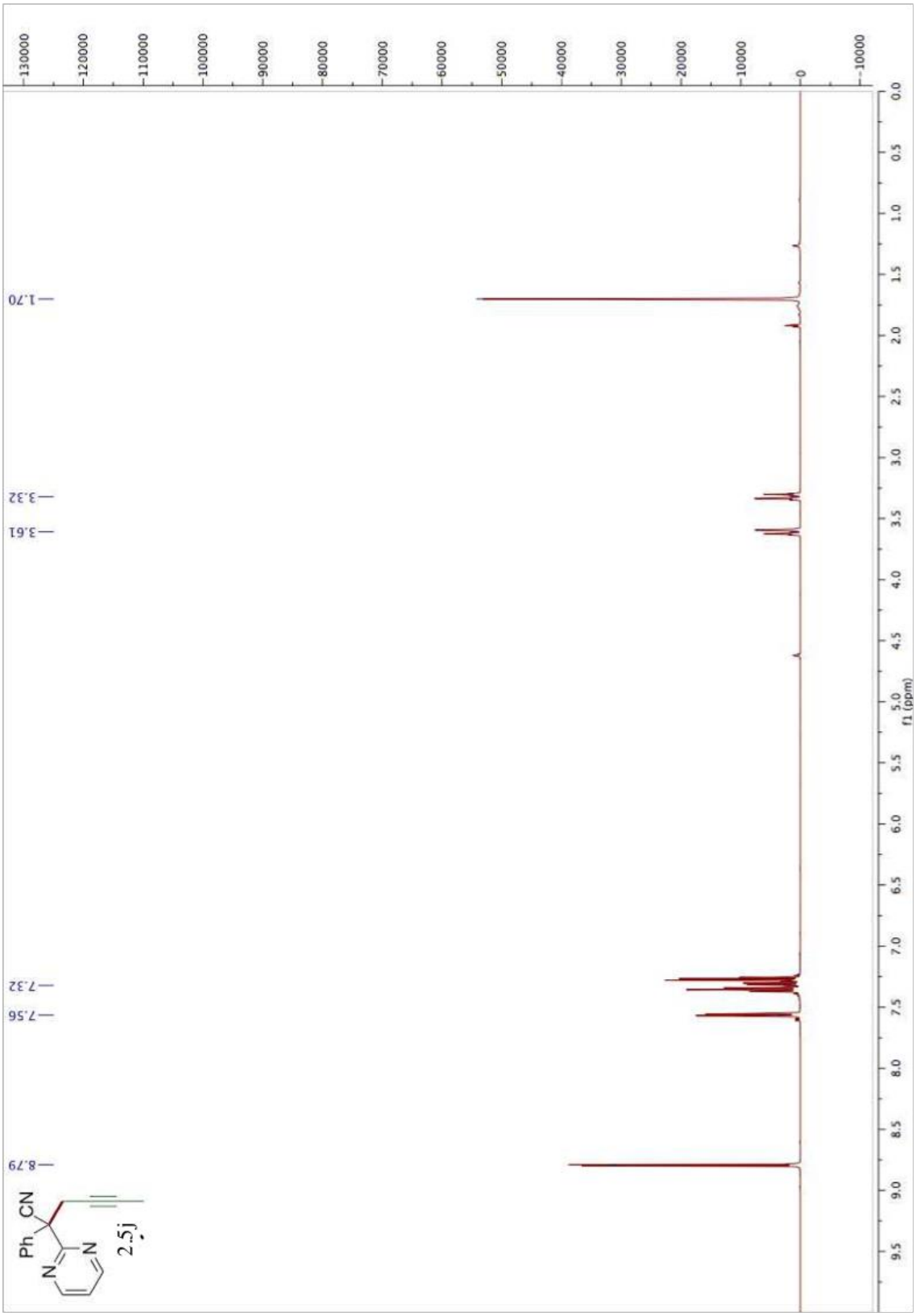
1.70
3.32
3.61
7.32
7.56
8.79
f1 (ppm)
Ph
CN
N
N
2.5j

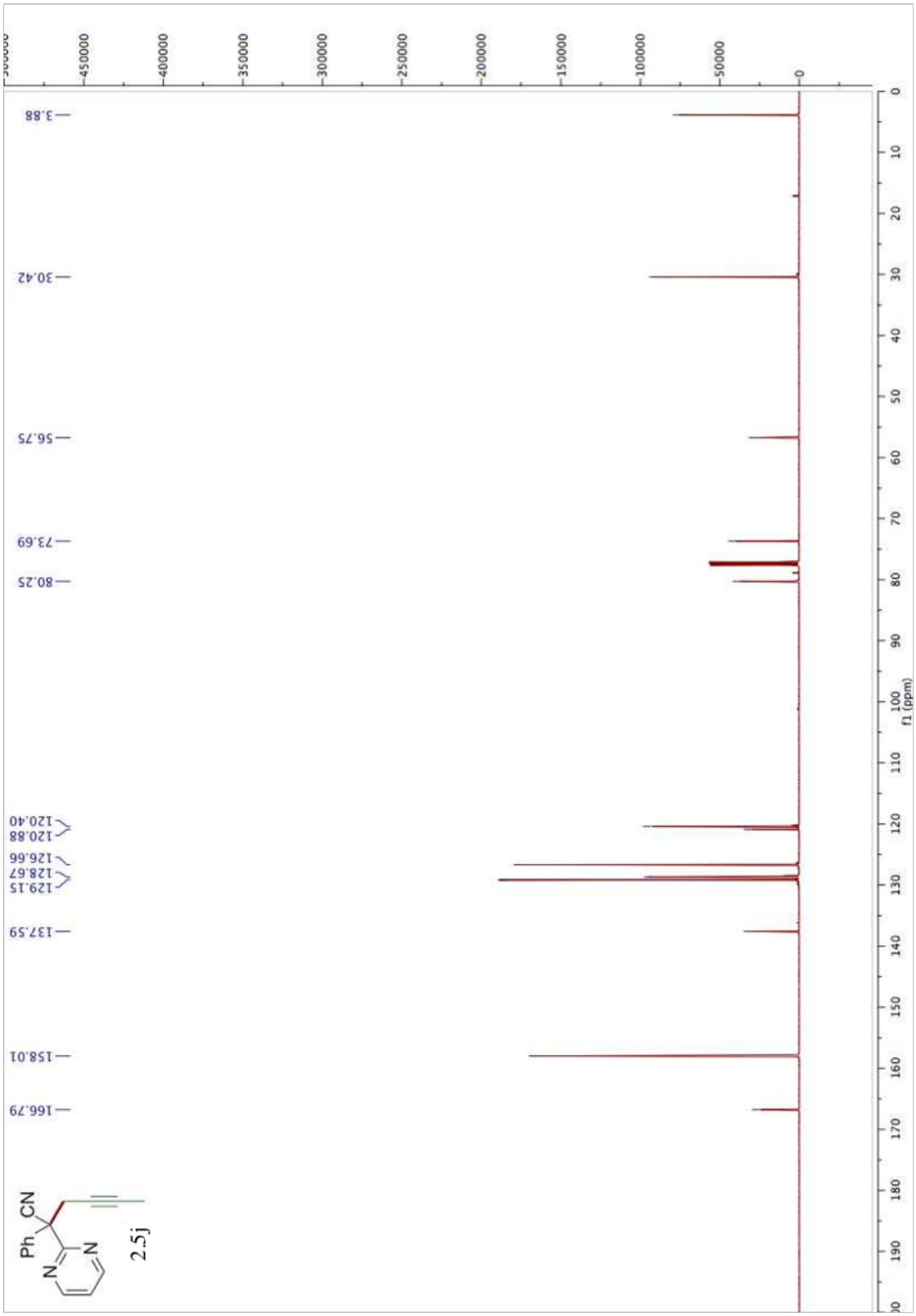
3.88
30.42
56.75
73.69
80.25
120.40
120.88
126.66
128.67
129.15
137.59
158.01
166.79
f1 (ppm)
Ph
CN
N
N
2.5j

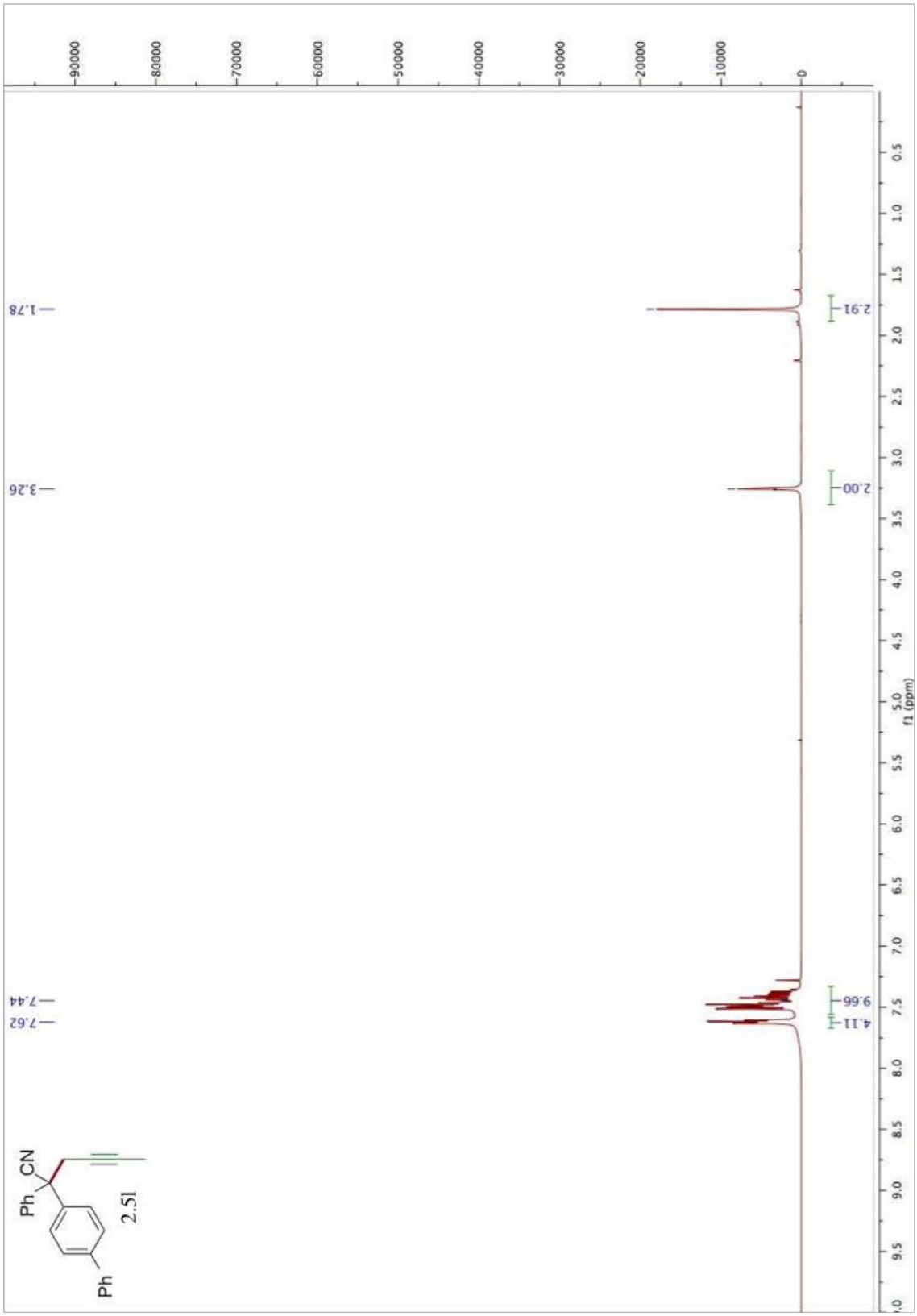
1.78
3.26
7.44
7.62
2.91
2.00
9.66
4.11
f1 (ppm)
Ph
CN
Ph
2.51

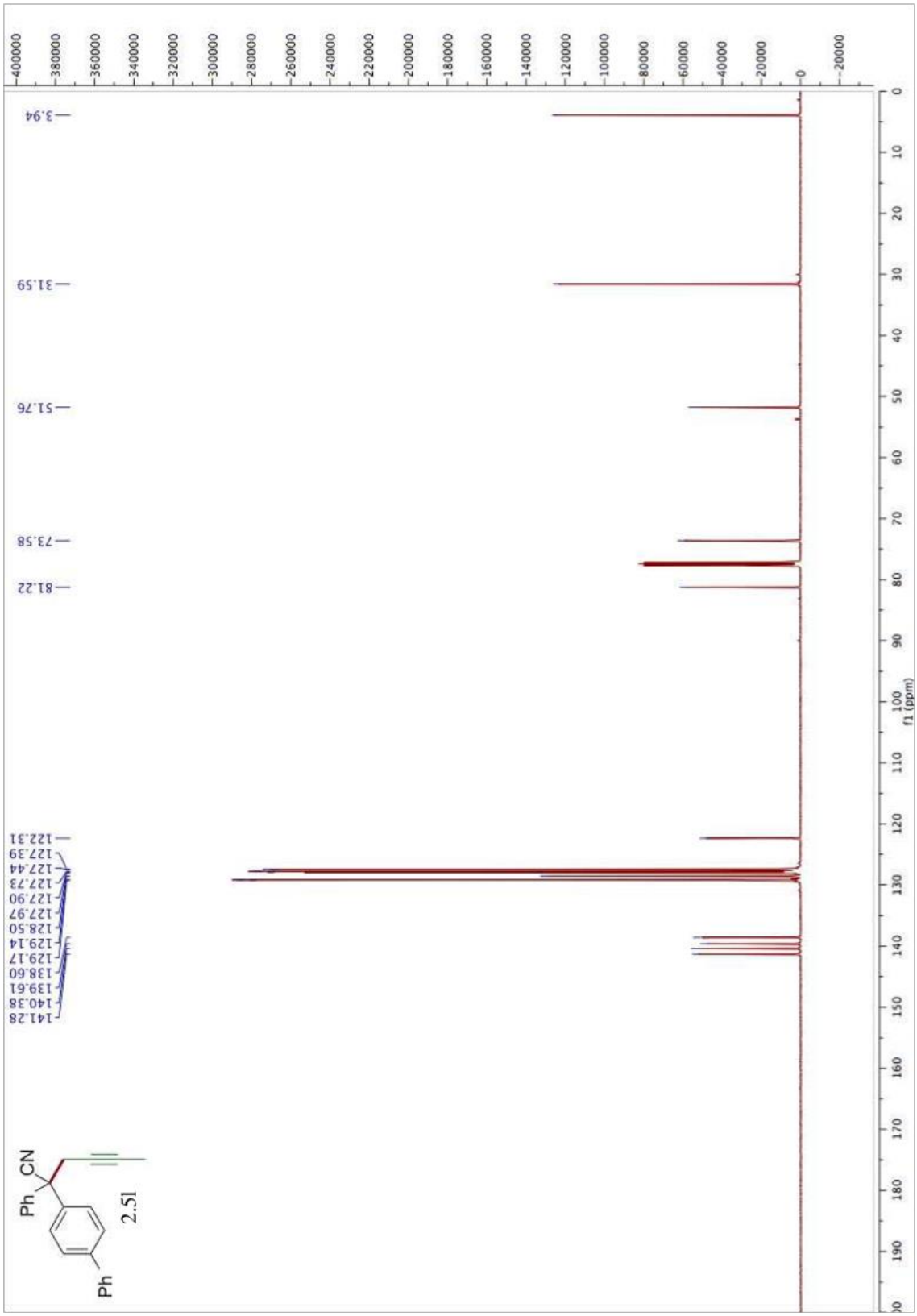
3.94
31.59
51.76
73.58
81.22
122.31
127.39
127.44
127.73
127.90
127.97
128.50
129.14
129.17
138.60
139.61
140.38
141.28
Ph
CN
Ph
2.51
f1 (ppm)

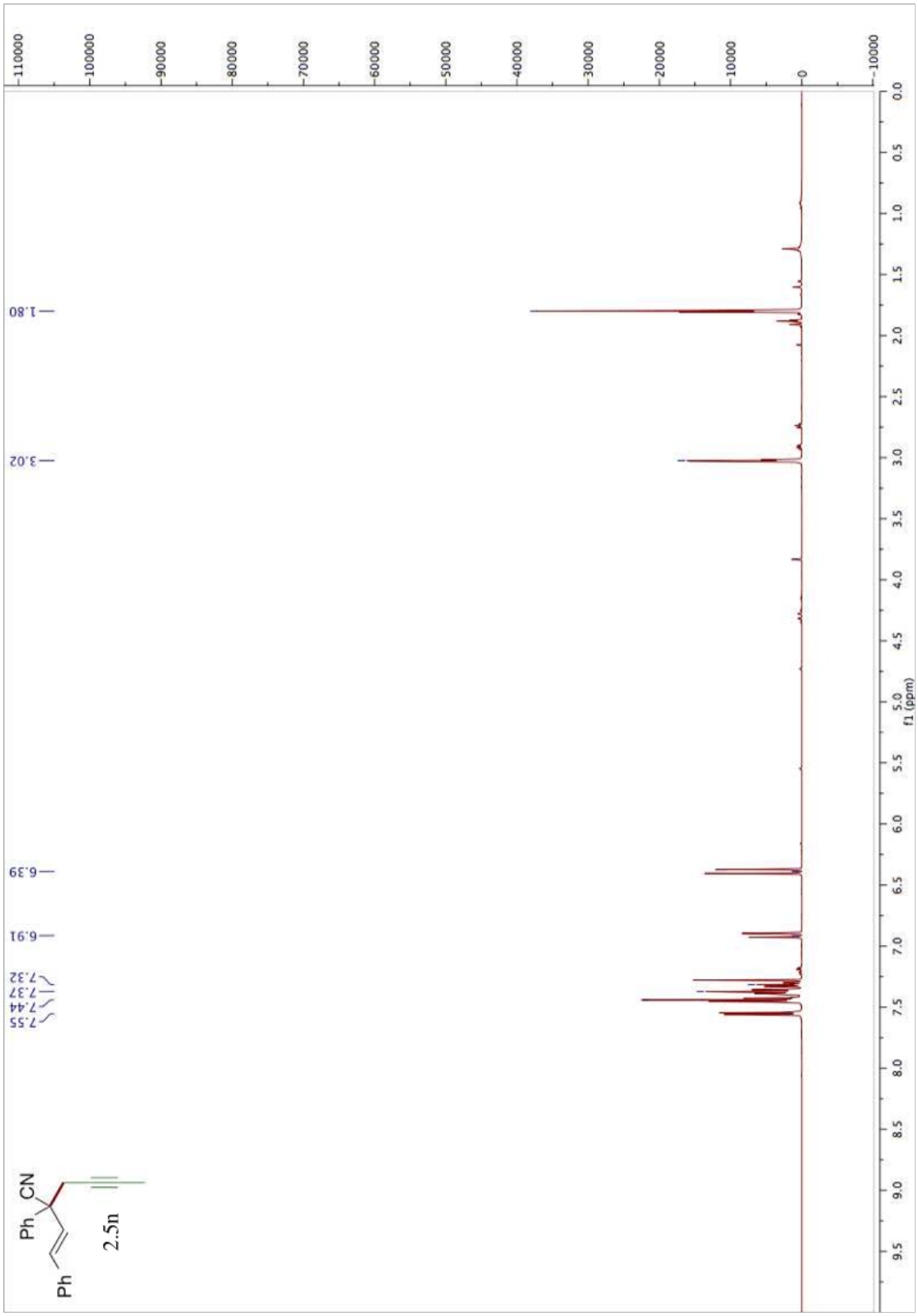
1.80
3.02
6.39
6.91
7.32
7.37
7.44
7.55
Ph
CN
Ph
2.5n
f1 (ppm)

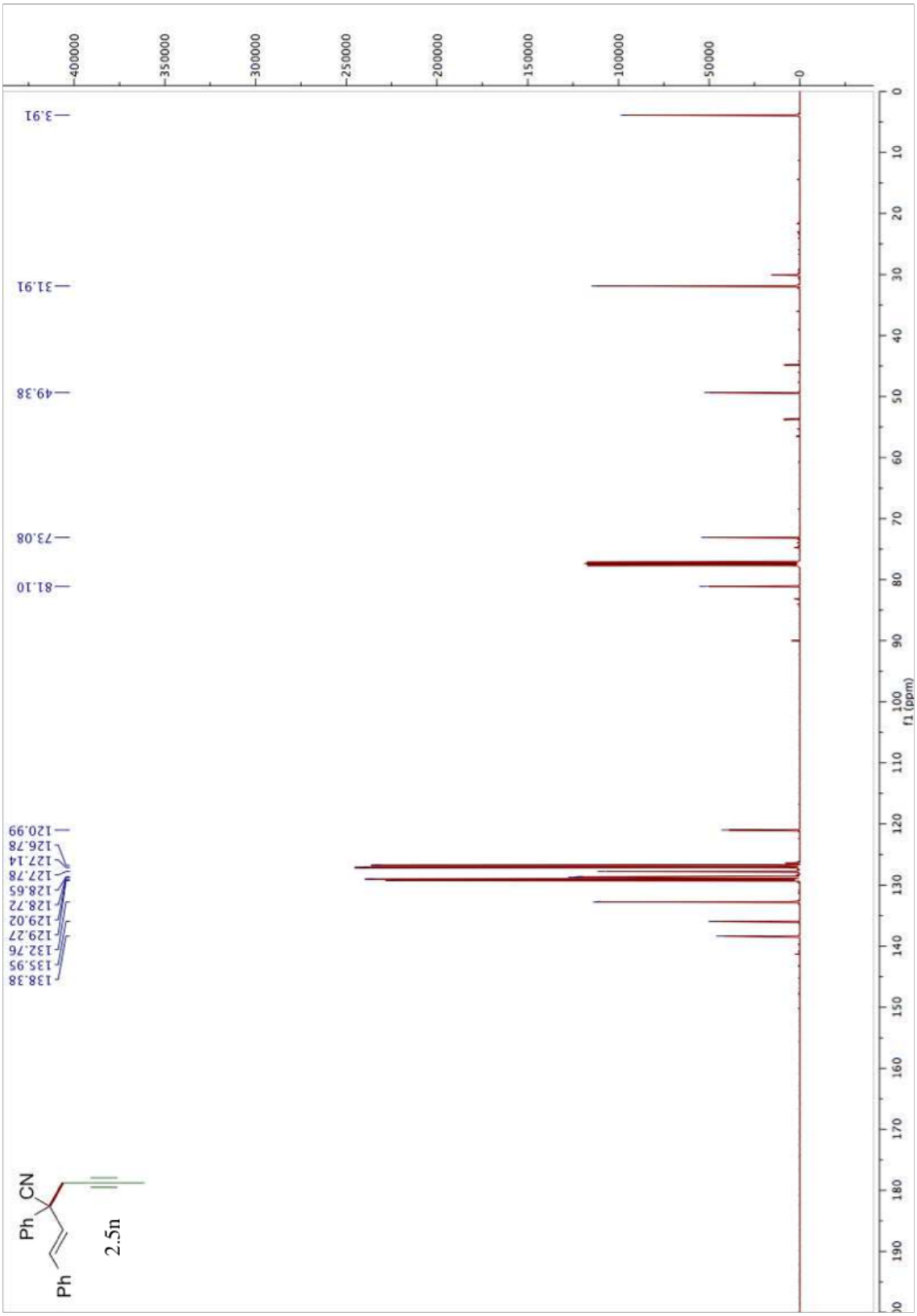
3.91
31.91
49.38
73.08
81.10
120.99
126.78
127.14
127.78
128.65
128.72
129.02
129.27
132.76
135.95
138.38
CN
Ph
Ph
2.5n
f1 (ppm)

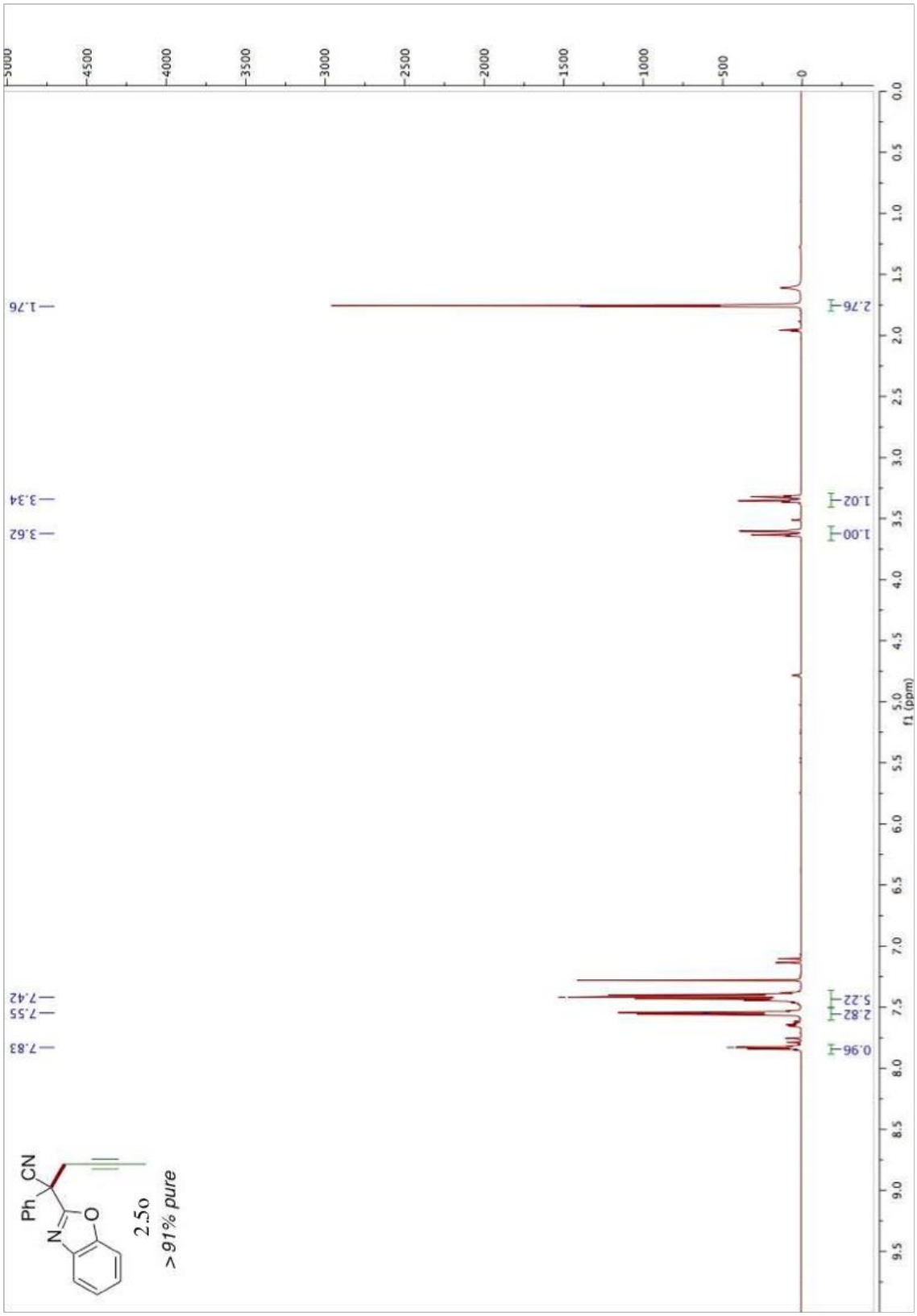
1.76
3.34
3.62
7.42
7.55
7.83
2.76
1.02
1.00
5.22
2.82
0.96
f1 (ppm)
Ph
CN
N
O
2.5o
>91% pure

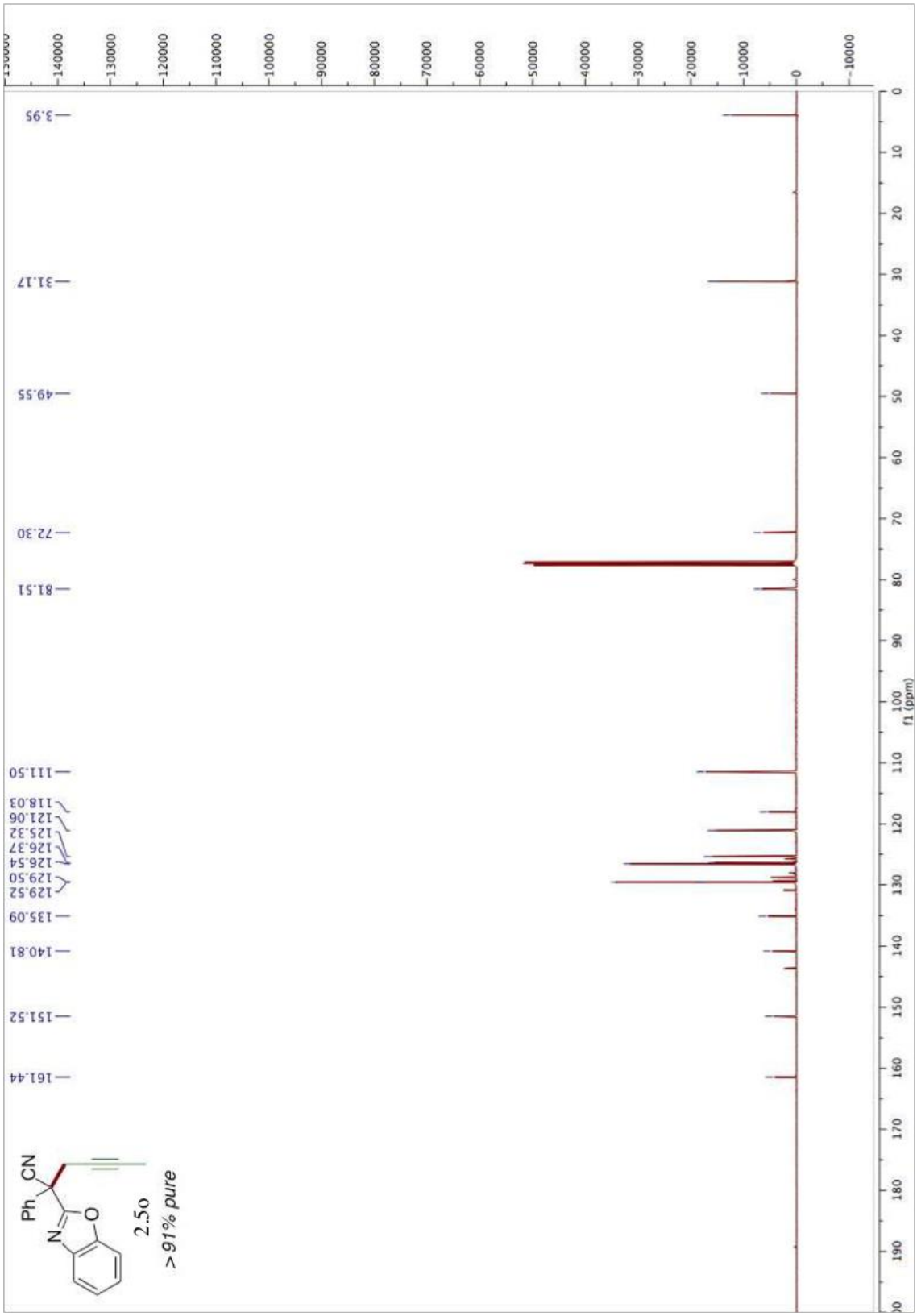
3.95
31.17
49.55
72.30
81.51
111.50
118.03
121.06
125.32
126.37
126.54
129.50
129.52
135.09
140.81
151.52
161.44
f1 (ppm)
Ph
CN
O
N
2.5o
>91% pure

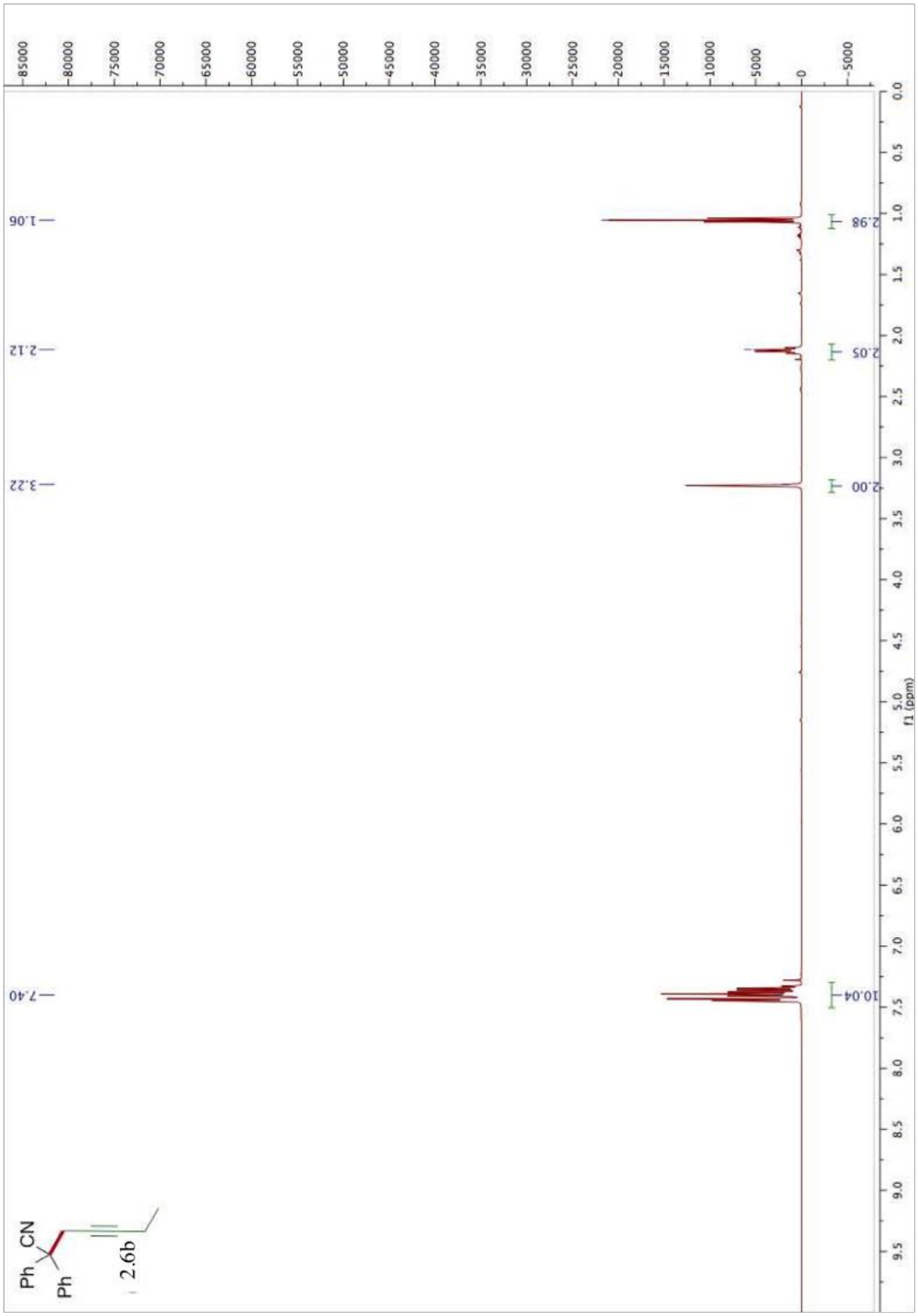
1.06
2.12
3.22
7.40
2.98
2.05
2.00
10.04
f1 (ppm)
Ph
CN
Ph
2.6b

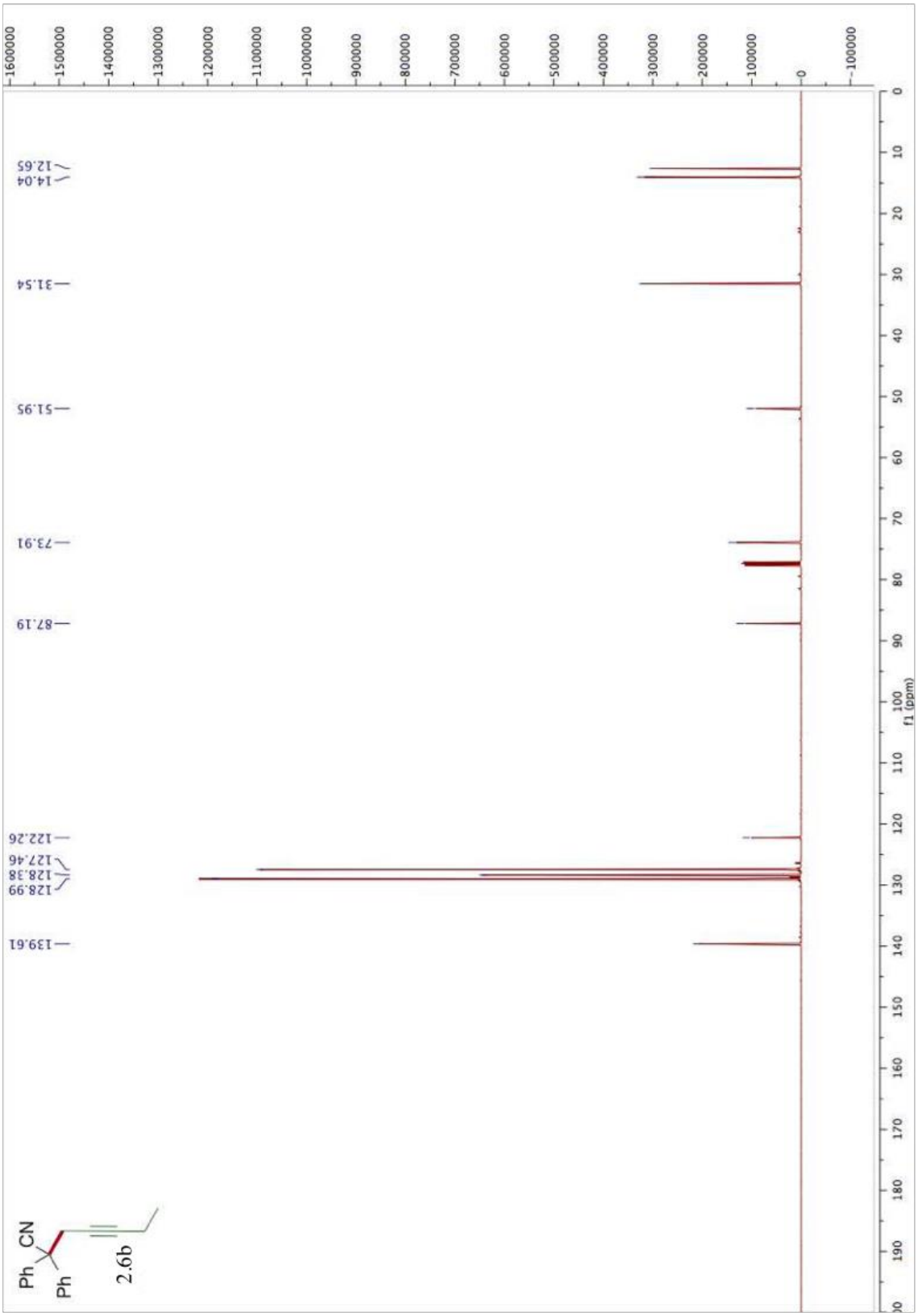
12.65
14.04
31.54
51.95
73.91
87.19
122.26
127.46
128.38
128.99
139.61
Ph
CN
Ph
2.6b
f1 (ppm)

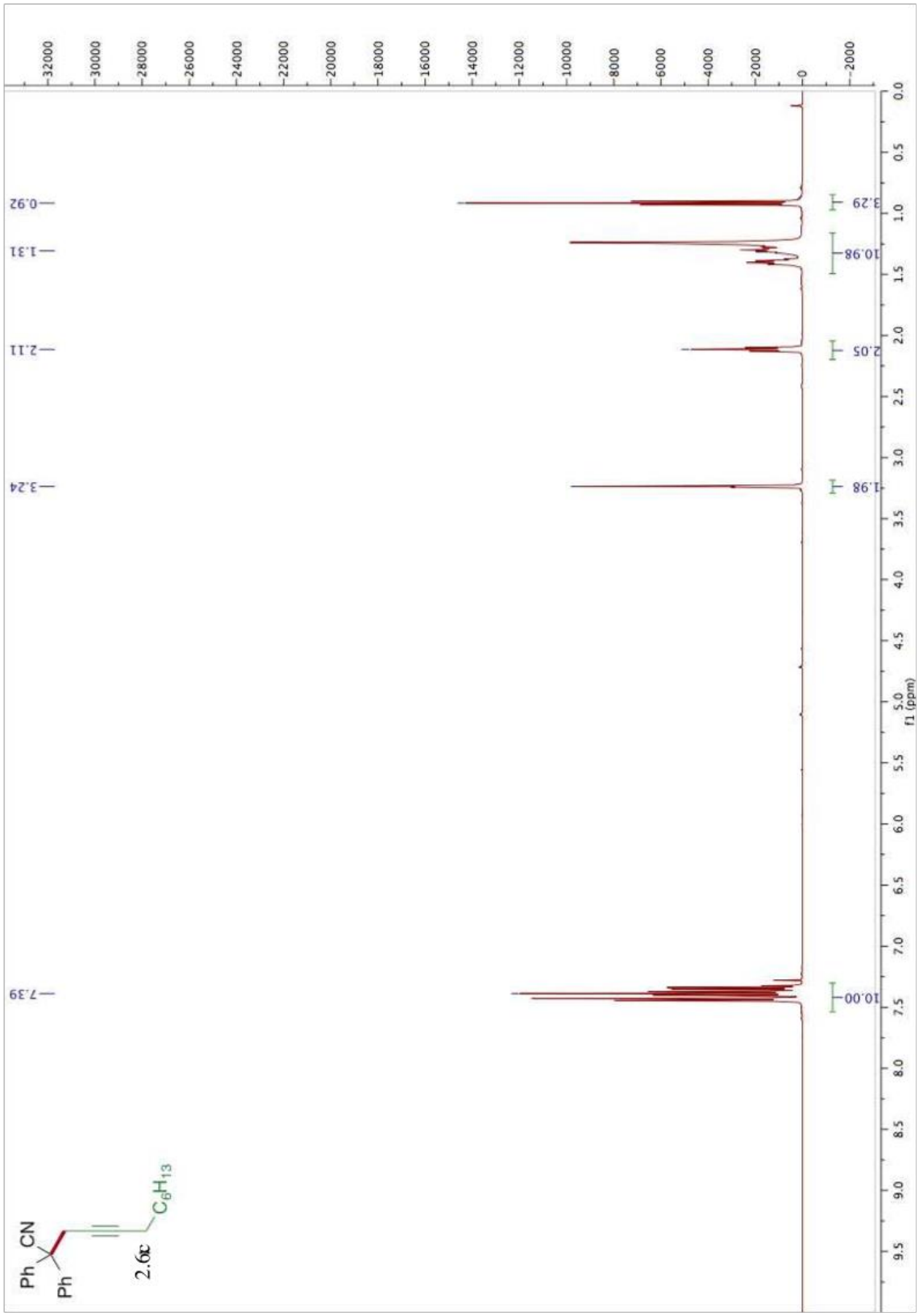
0.92
1.31
2.11
3.24
7.39
3.29
10.98
2.05
1.98
10.00
f1 (ppm)
Ph
CN
Ph
C_6H_{13}
2.6œ

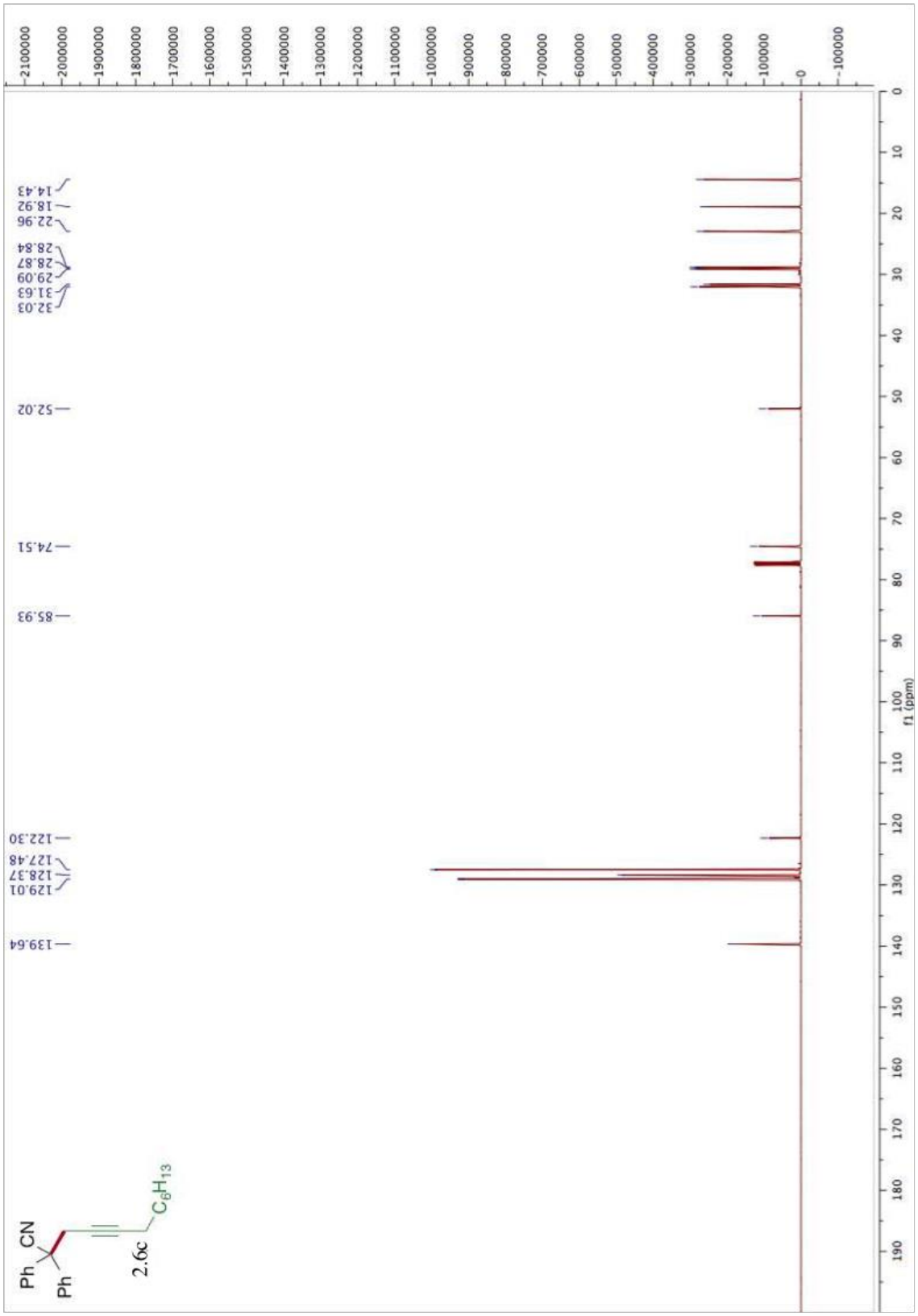
14.43
18.92
22.96
28.84
28.87
29.09
31.63
32.03
52.02
74.51
85.93
122.30
127.48
128.37
129.01
139.64
Ph
CN
Ph
2.6c
C_6H_{13}
f1 (ppm)

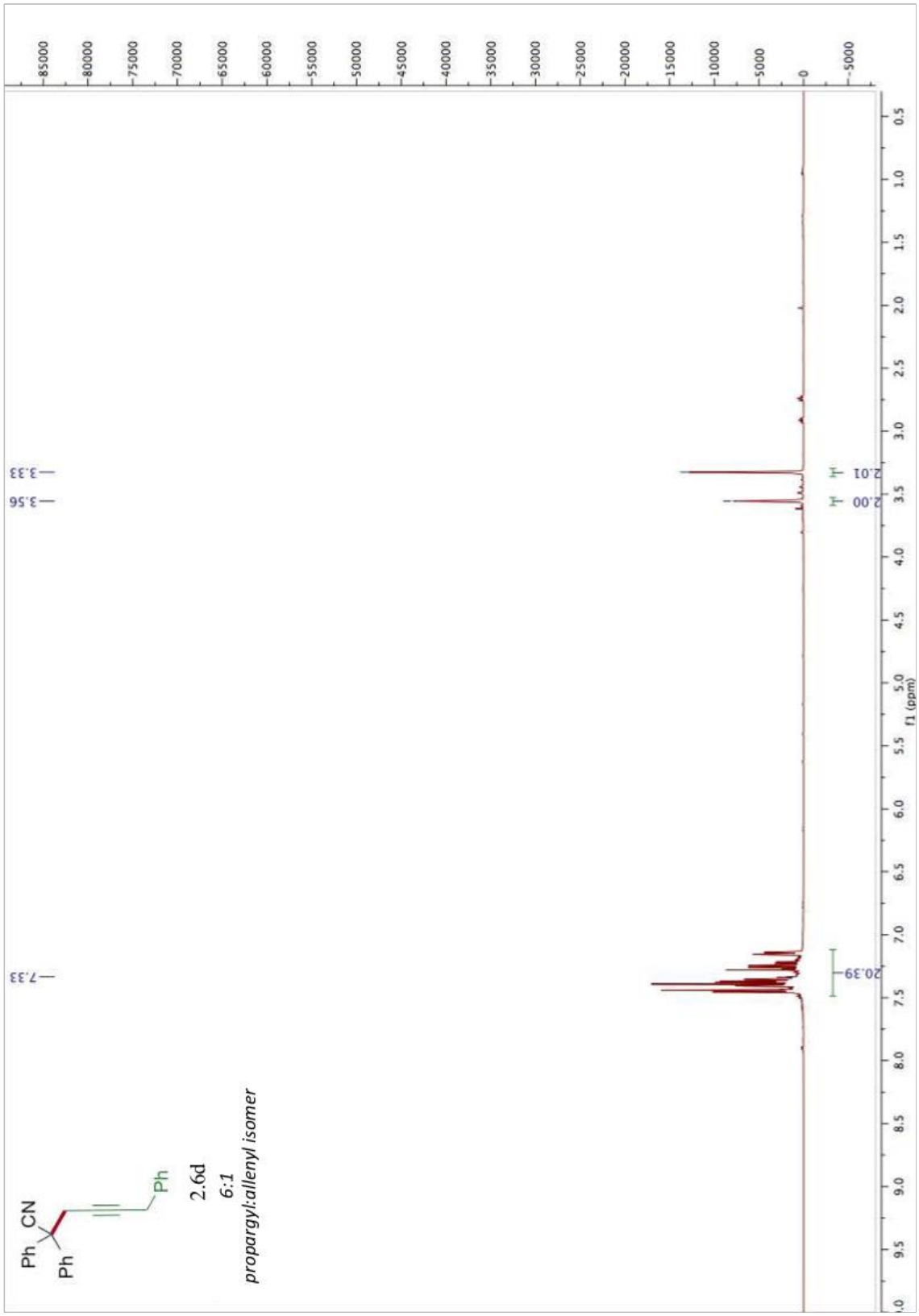
Ph
CN
Ph
Ph
2.6d
6:1
propargyl:allenyl isomer
7.33
3.56
3.33
20.39
2.00
2.01
f1 (ppm)

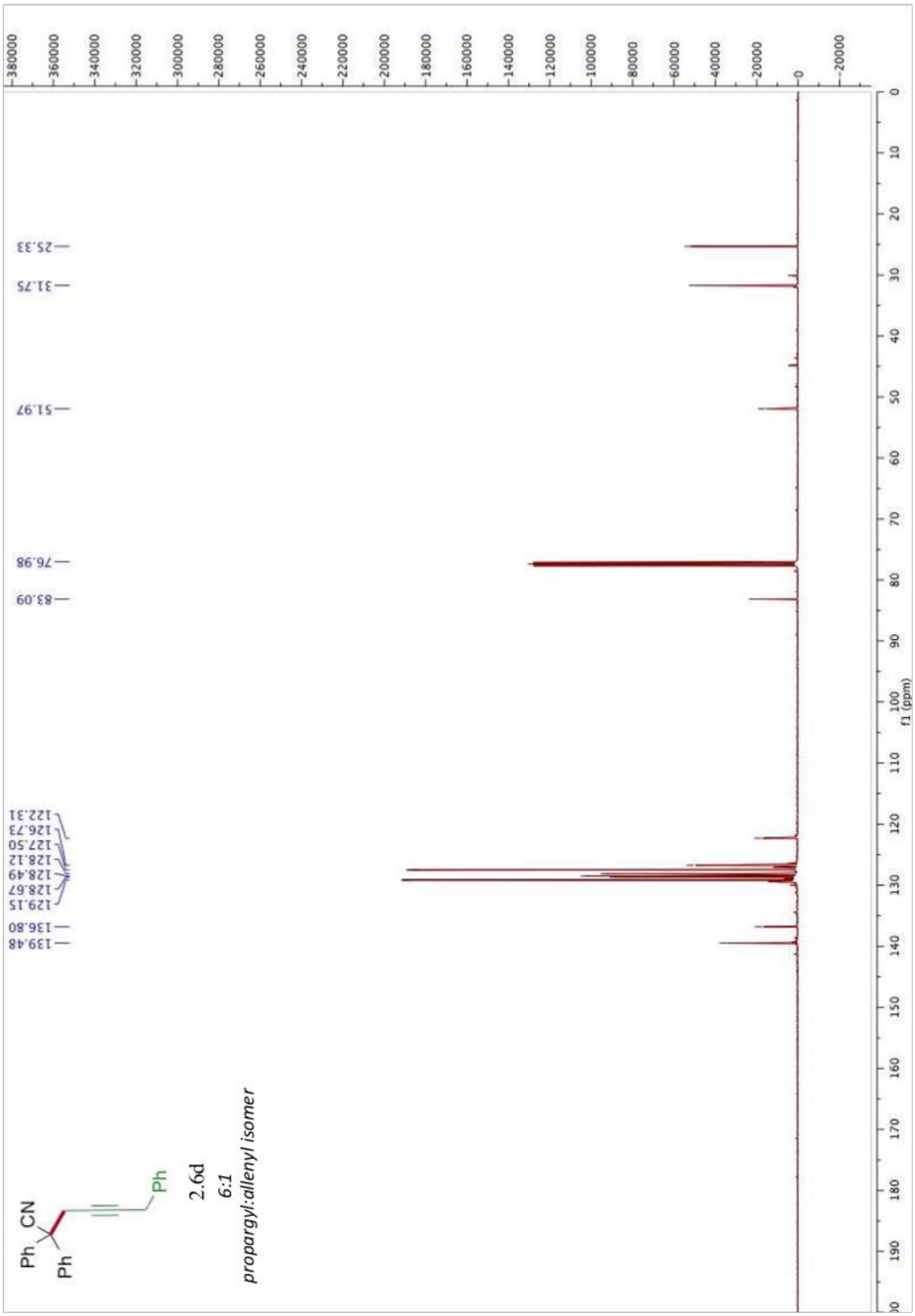
Ph
CN
Ph
Ph
2.6d
6:1
propargyl:allenyl isomer
139.48
136.80
129.15
128.67
128.49
128.12
127.50
126.73
122.31
83.09
76.98
51.97
31.75
25.33
f1 (ppm)

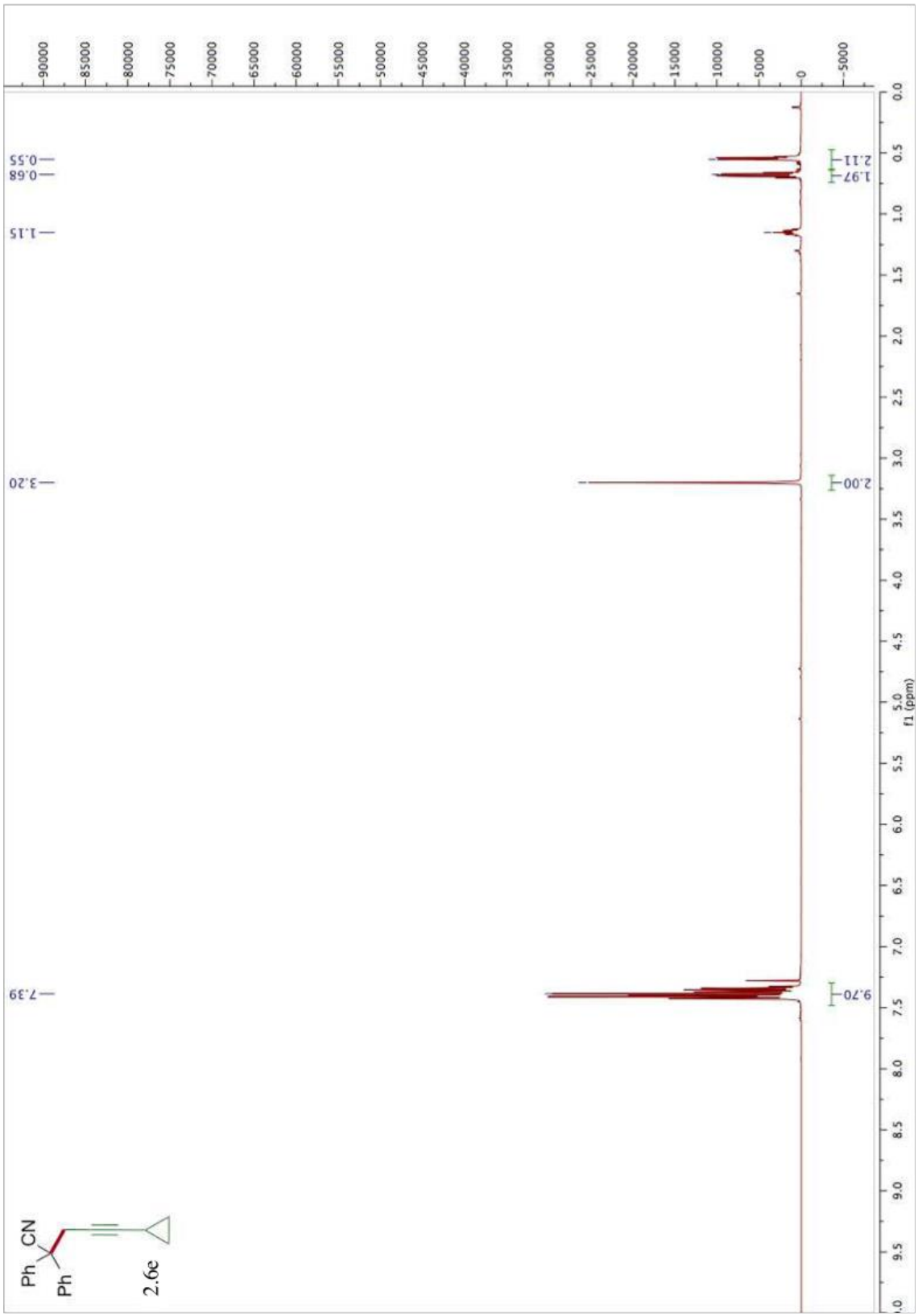
0.55
0.68
1.15
3.20
7.39
2.11
1.97
2.00
9.70
f1 (ppm)
Ph
CN
Ph
2.6e

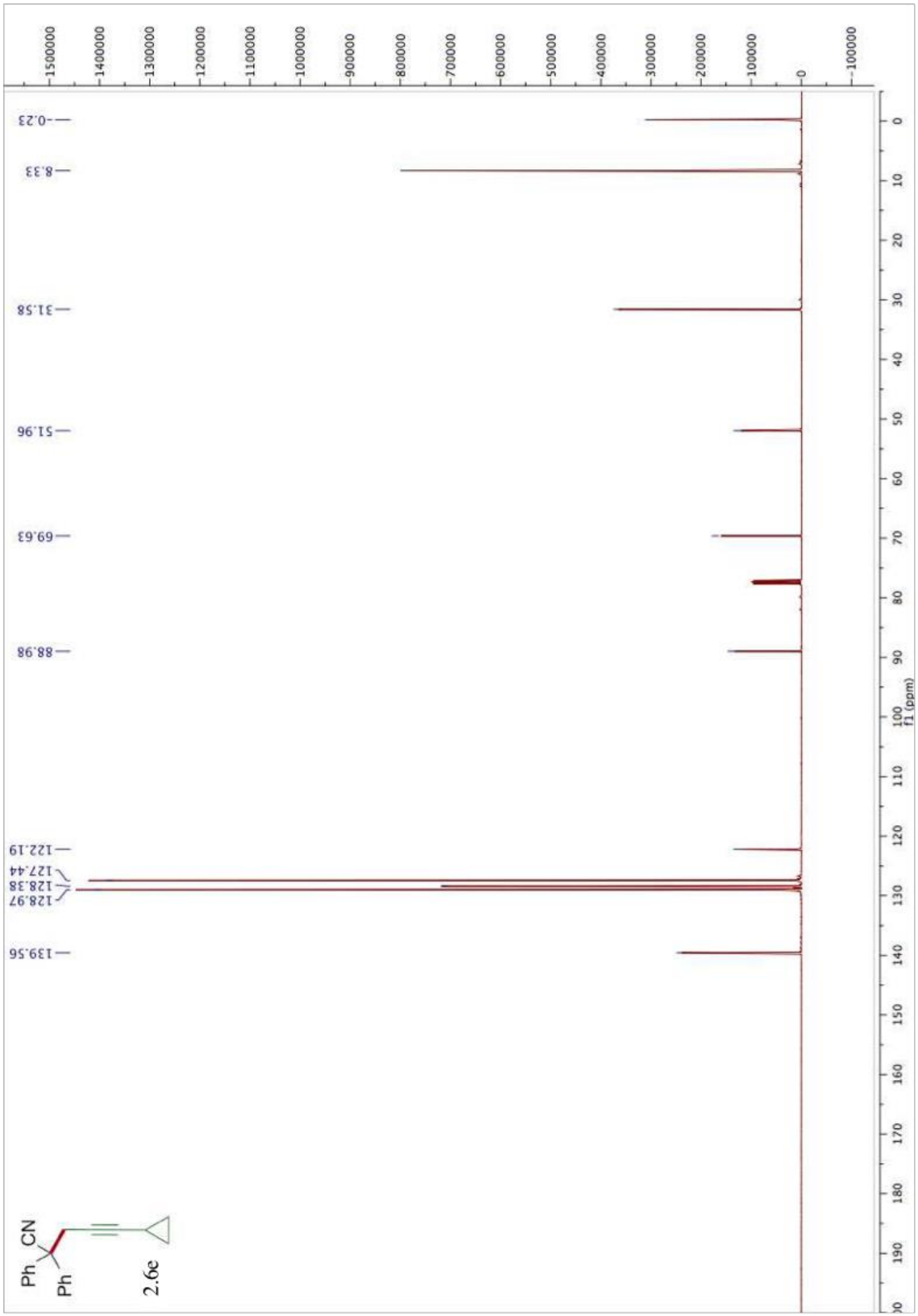
-0.23
8.33
31.58
51.96
69.63
88.98
122.19
127.44
128.38
128.97
139.56
Ph
CN
Ph
2.6e
f1 (ppm)

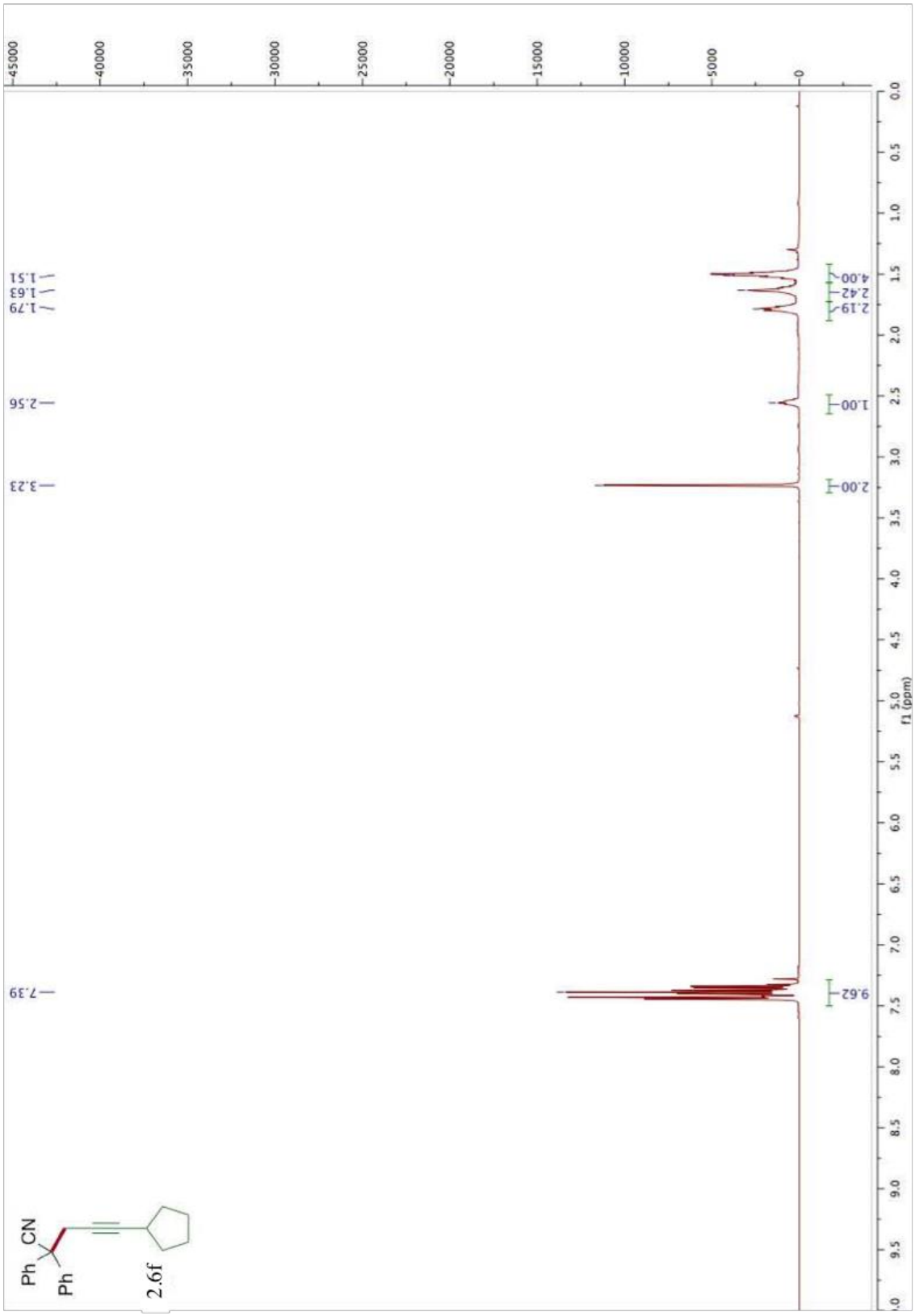
7.39
3.23
2.56
1.79
1.63
1.51
9.62
2.00
1.00
2.19
2.42
4.00
f1 (ppm)
Ph
CN
Ph
2.6f

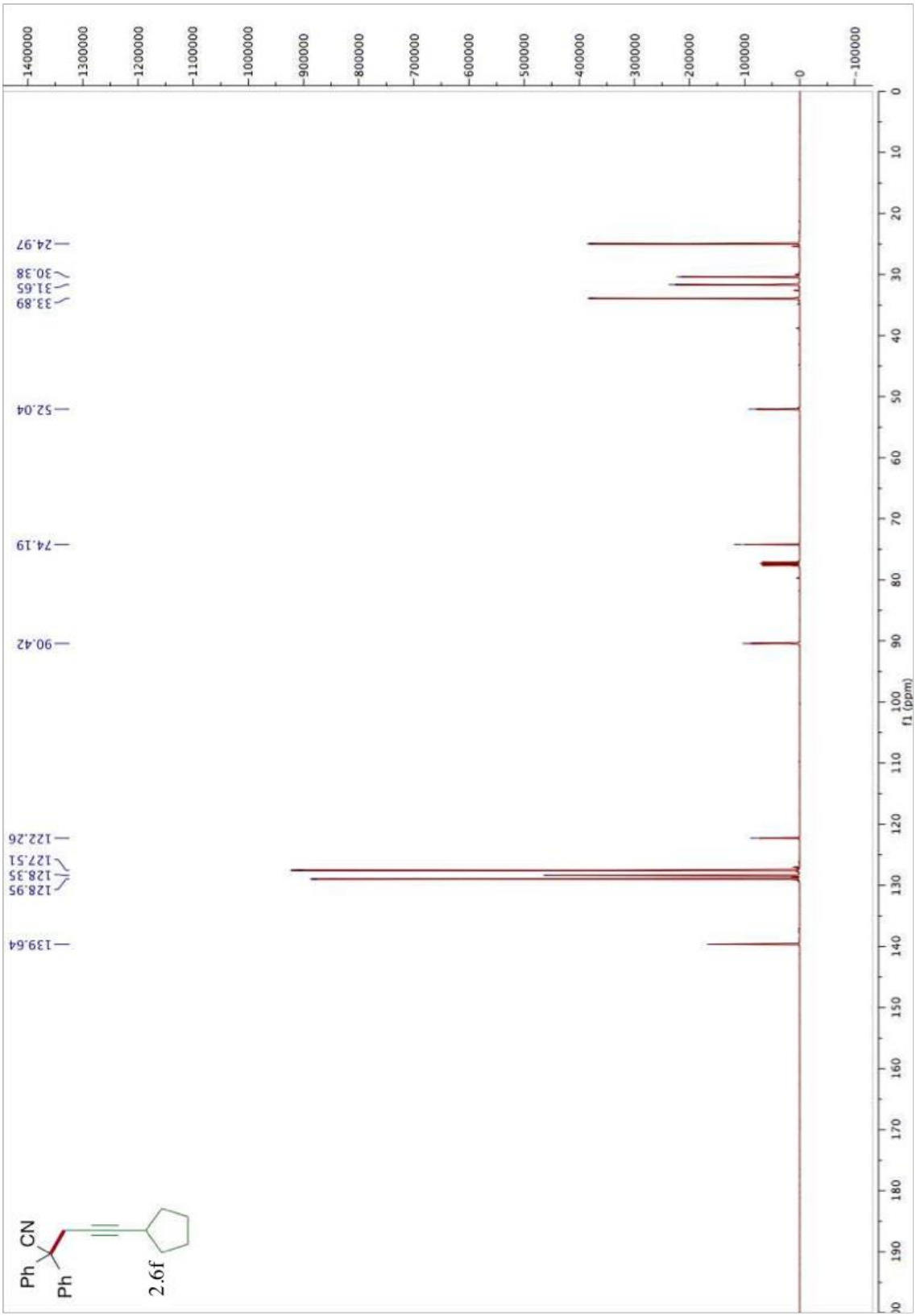
24.97
30.38
31.65
33.89
52.04
74.19
90.42
122.26
127.51
128.35
128.95
139.64
Ph
CN
Ph
2.6f
f1 (ppm)

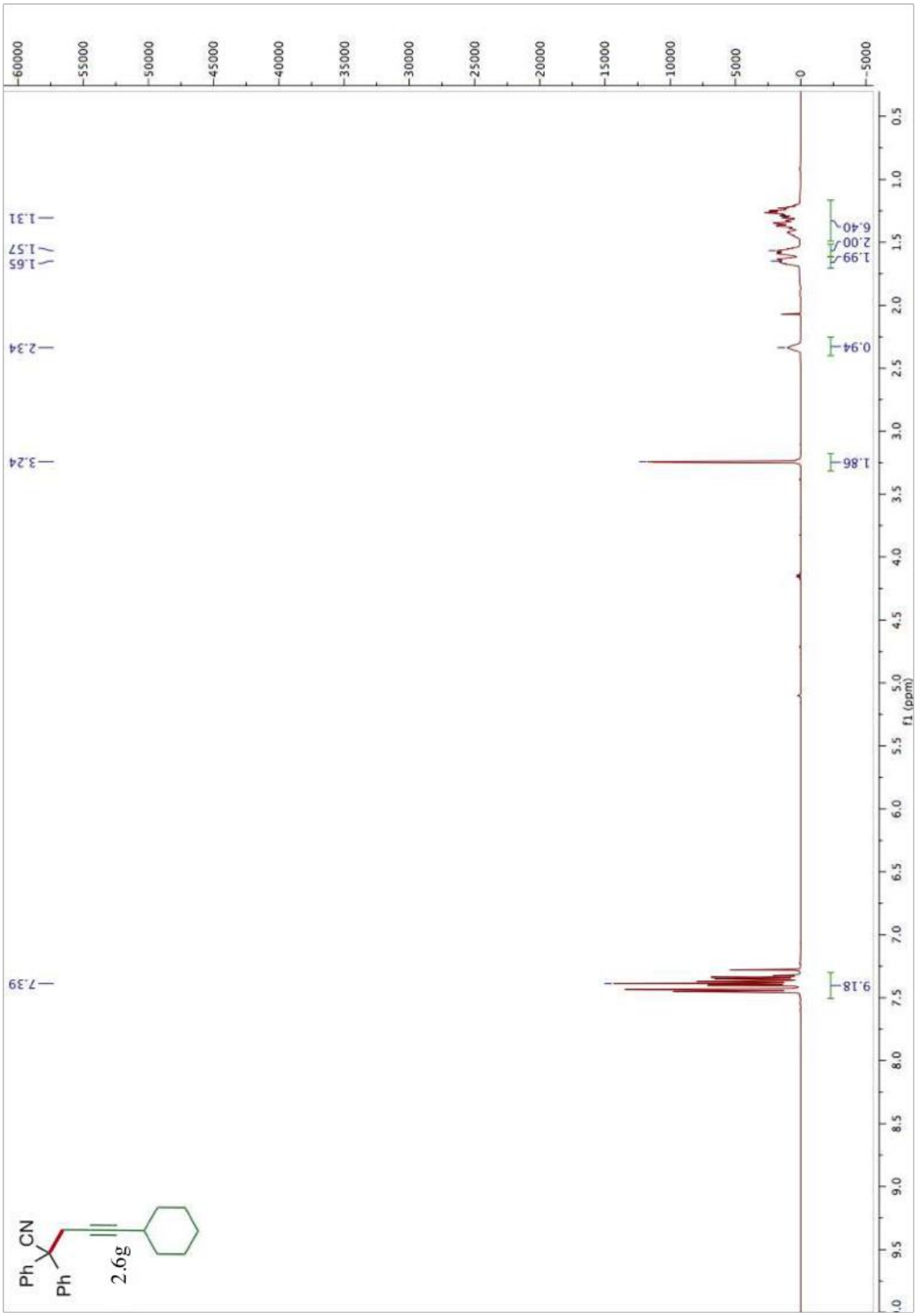
Ph
CN
Ph
2.6g
7.39
3.24
2.34
1.65
1.57
1.31
9.18
1.86
0.94
1.99
2.00
6.40
f1 (ppm)

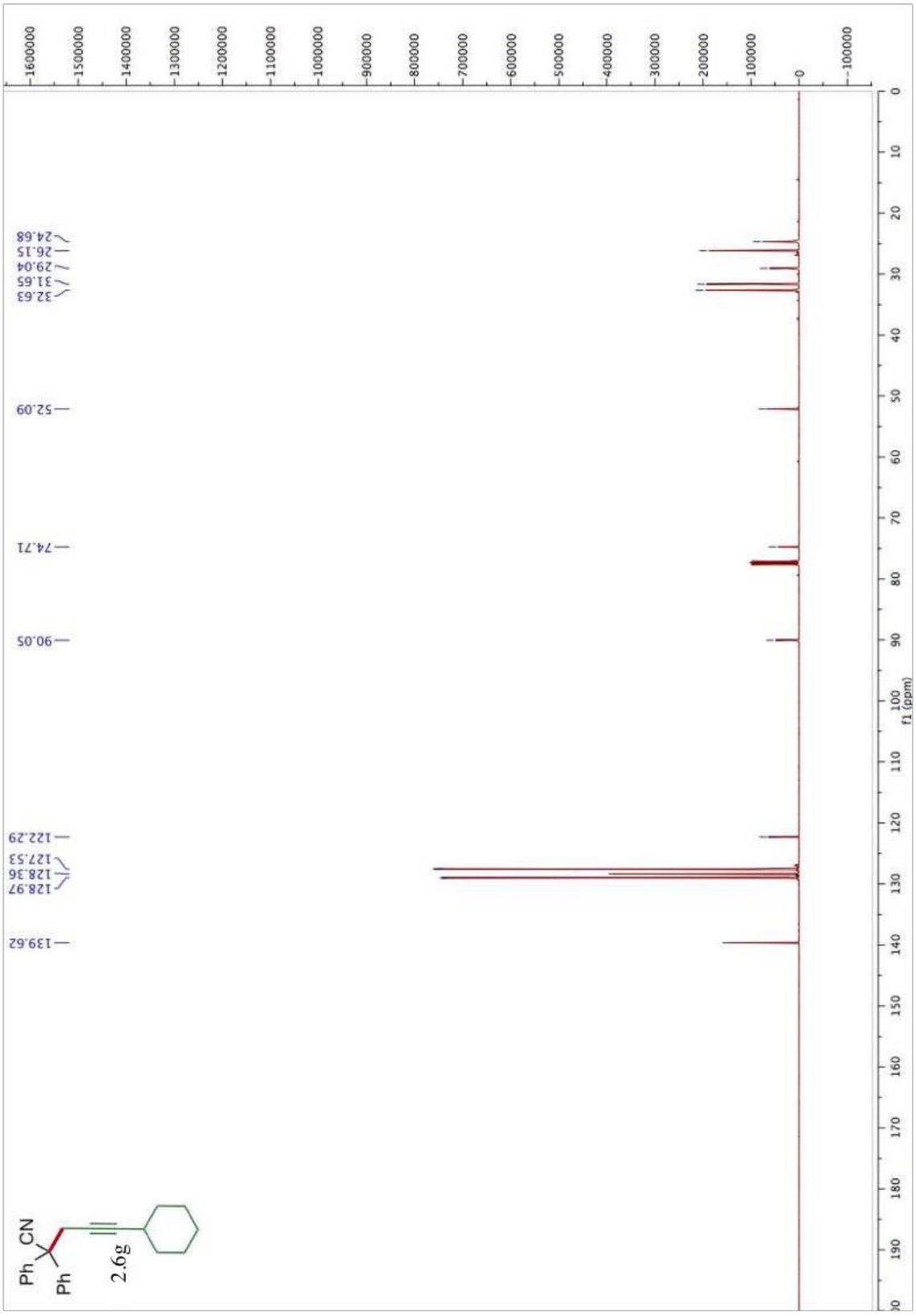
139.62
128.97
128.36
127.53
122.29
90.05
74.71
52.09
32.63
31.65
29.04
26.15
24.68
f1 (ppm)
Ph
CN
Ph
2.6g

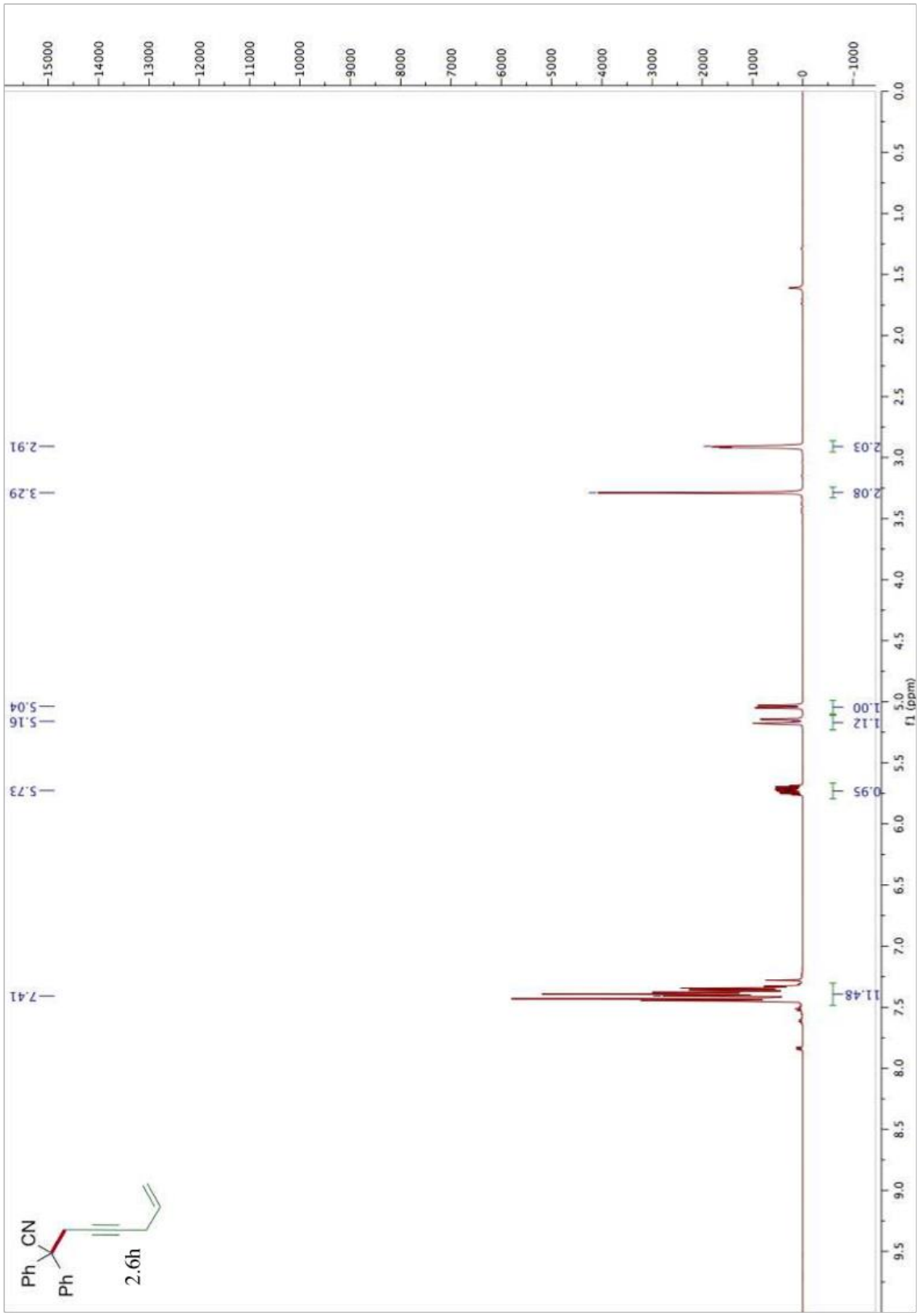
7.41
5.73
5.16
5.04
3.29
2.91
11.48
0.95
1.12
1.00
2.08
2.03
f1 (ppm)
Ph
CN
Ph
2.6h

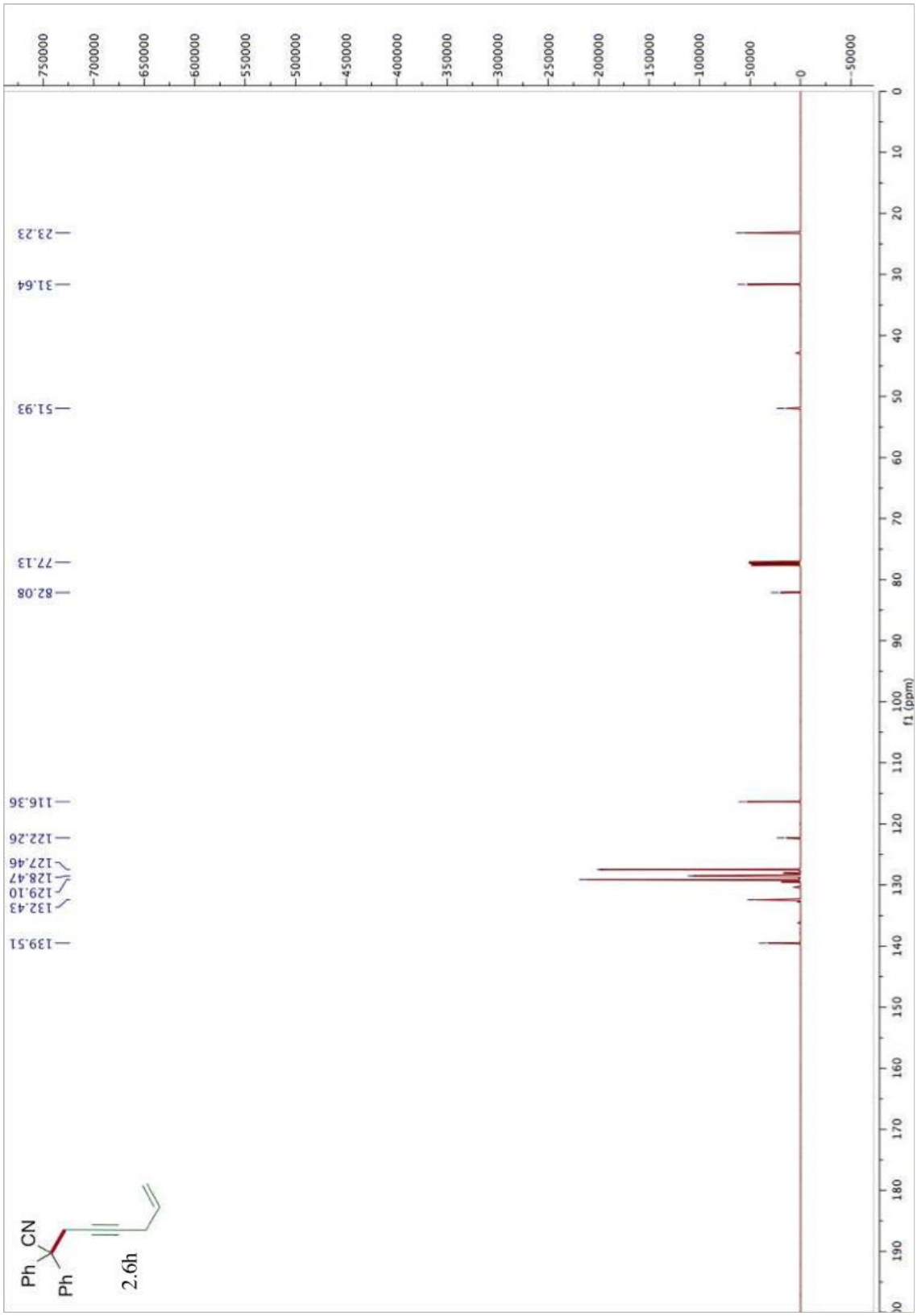
23.23
31.64
51.93
77.13
82.08
116.36
122.26
127.46
128.47
129.10
132.43
139.51
Ph
CN
Ph
2.6h
f1 (ppm)

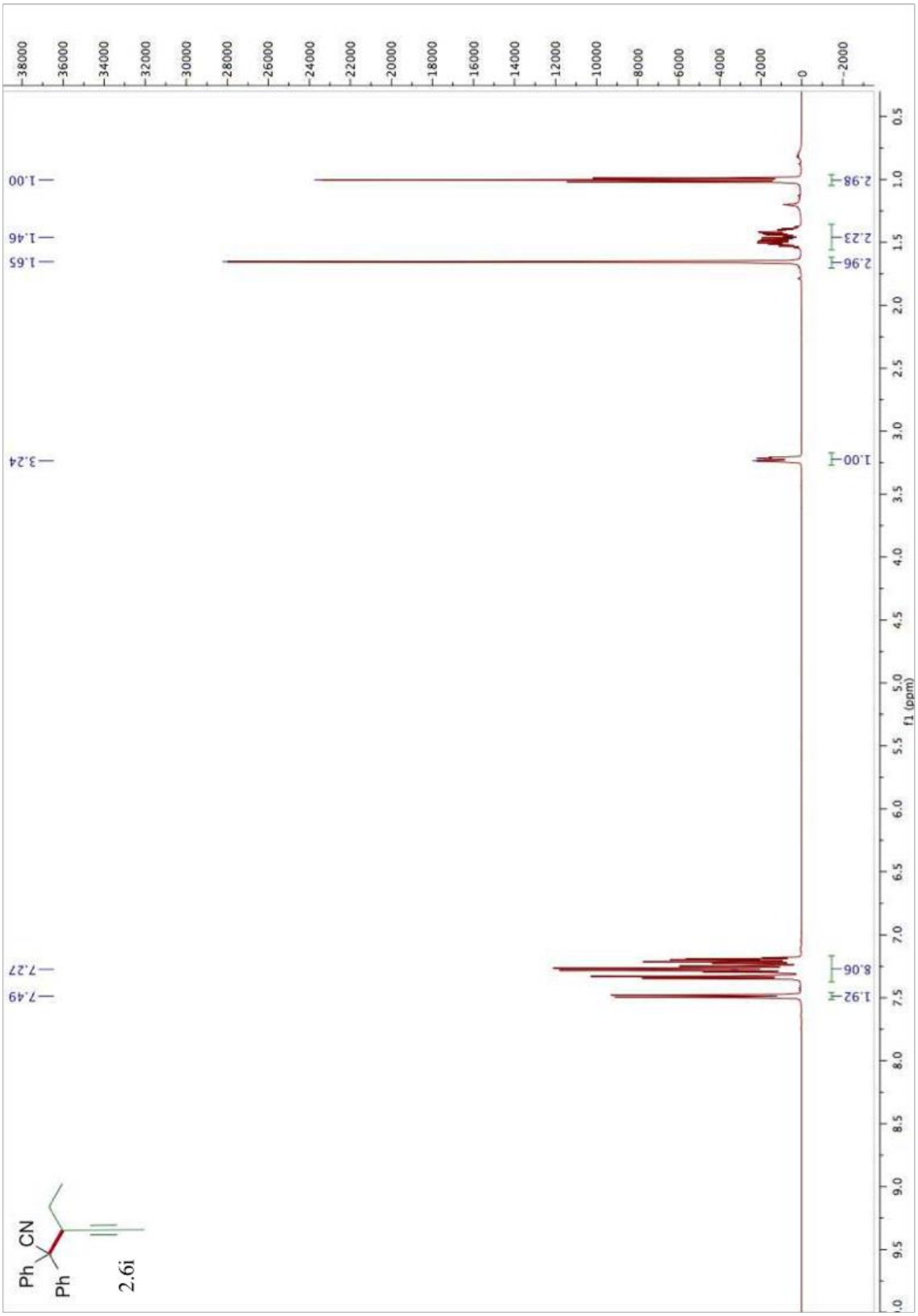
7.49
7.27
3.24
1.65
1.46
1.00
1.92
8.06
1.00
2.96
2.23
2.98
f1 (ppm)
Ph
CN
Ph
2.6i

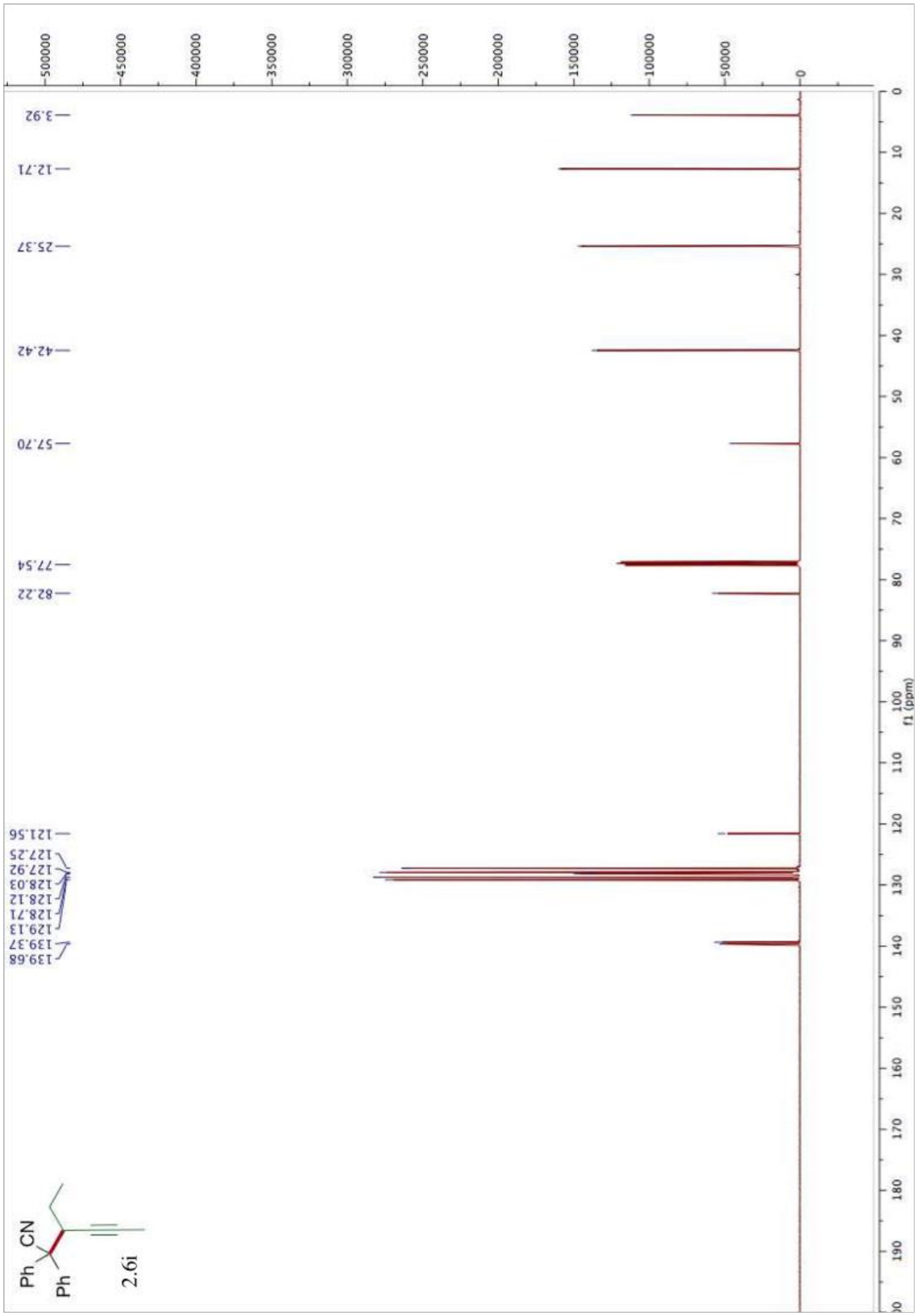
3.92
12.71
25.37
42.42
57.70
77.54
82.22
121.56
127.25
127.92
128.03
128.12
128.71
129.13
139.37
139.68
f1 (ppm)
Ph
CN
Ph
2.6i

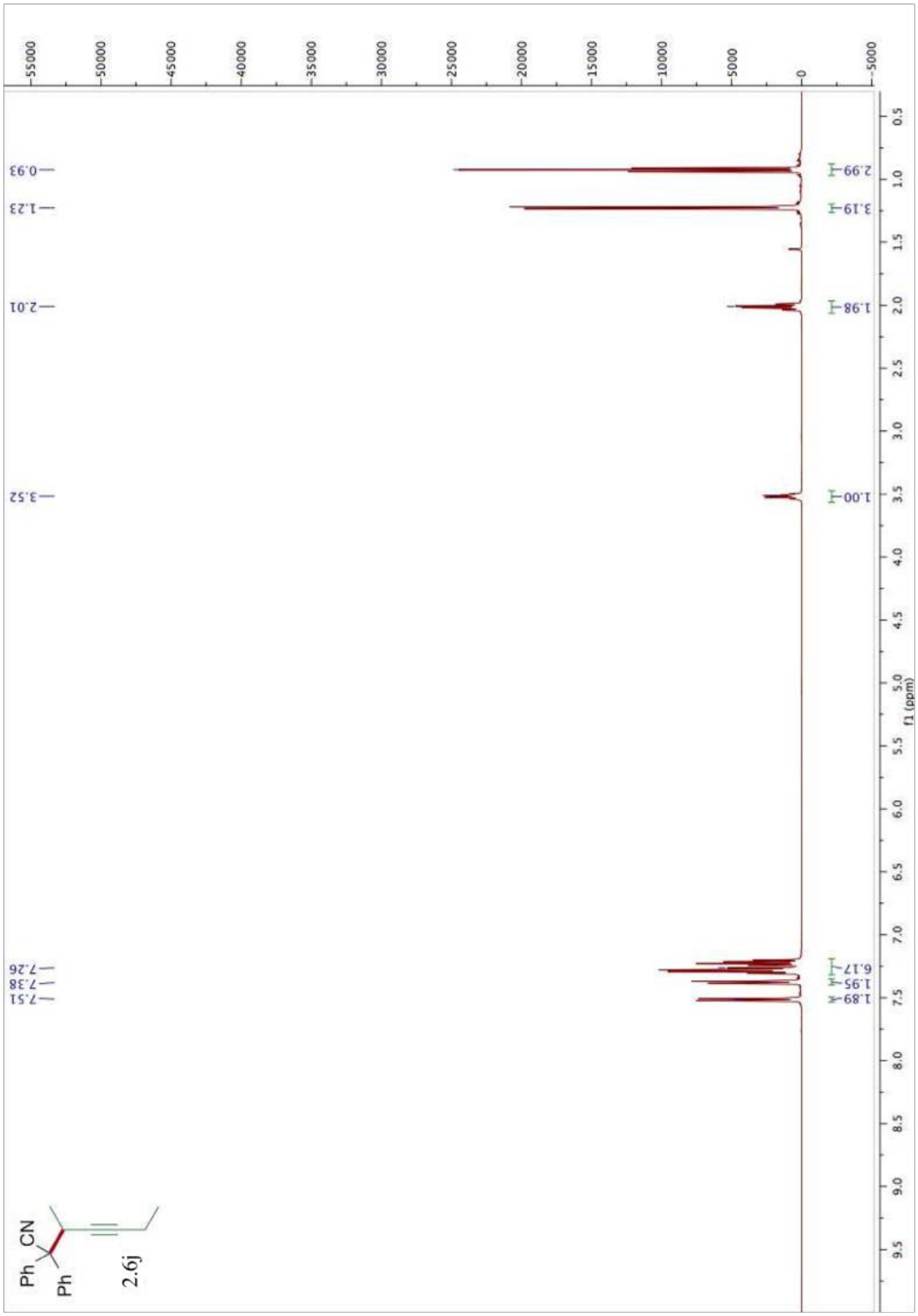
0.93
1.23
2.01
3.52
7.26
7.38
7.51
2.99
3.19
1.98
1.00
6.17
1.95
1.89
f1 (ppm)
Ph
CN
Ph
2.6j

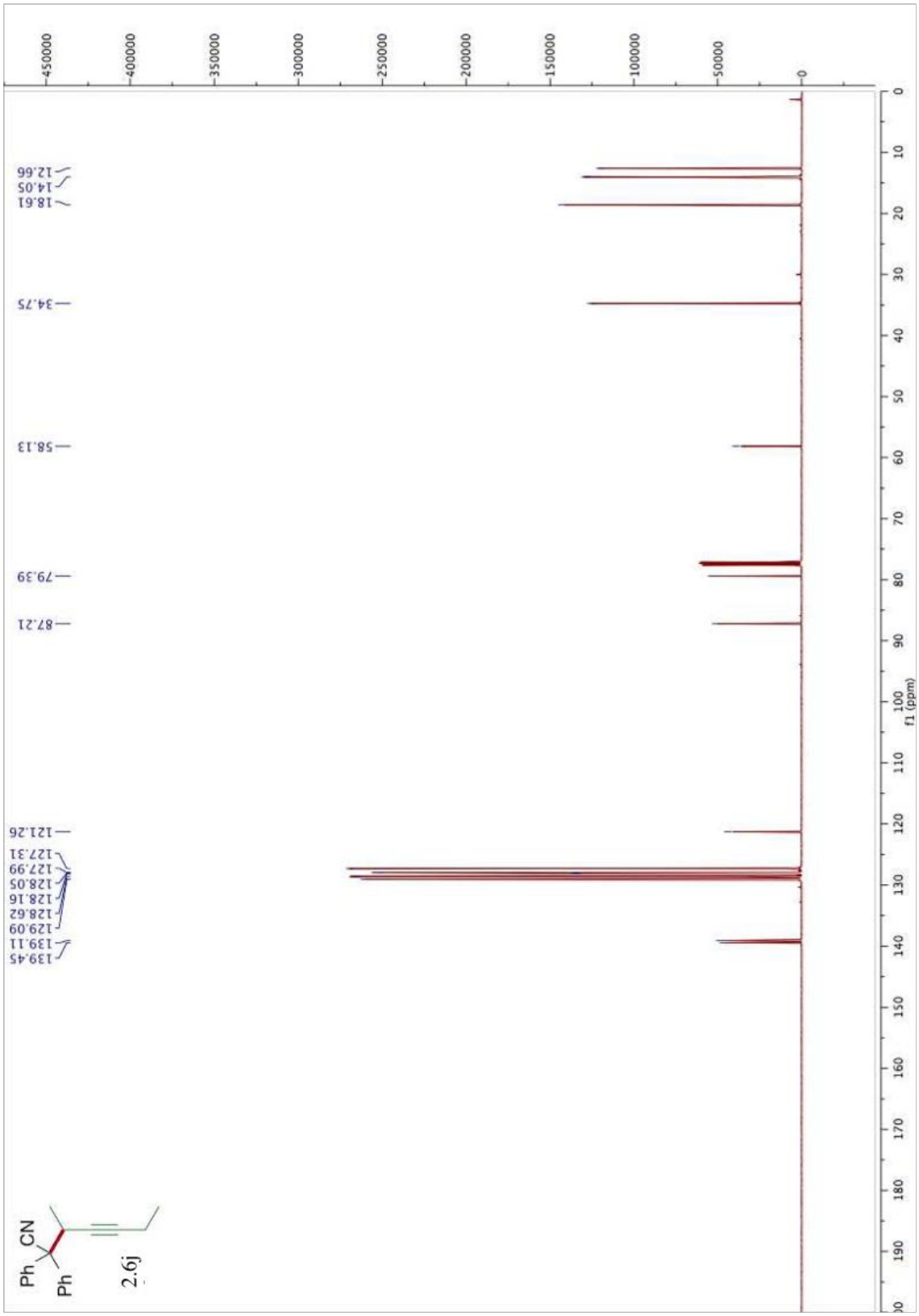
12.66
14.05
18.61
34.75
58.13
79.39
87.21
121.26
127.31
127.99
128.05
128.16
128.62
129.09
139.11
139.45
f1 (ppm)
CN
Ph
Ph
2.6j

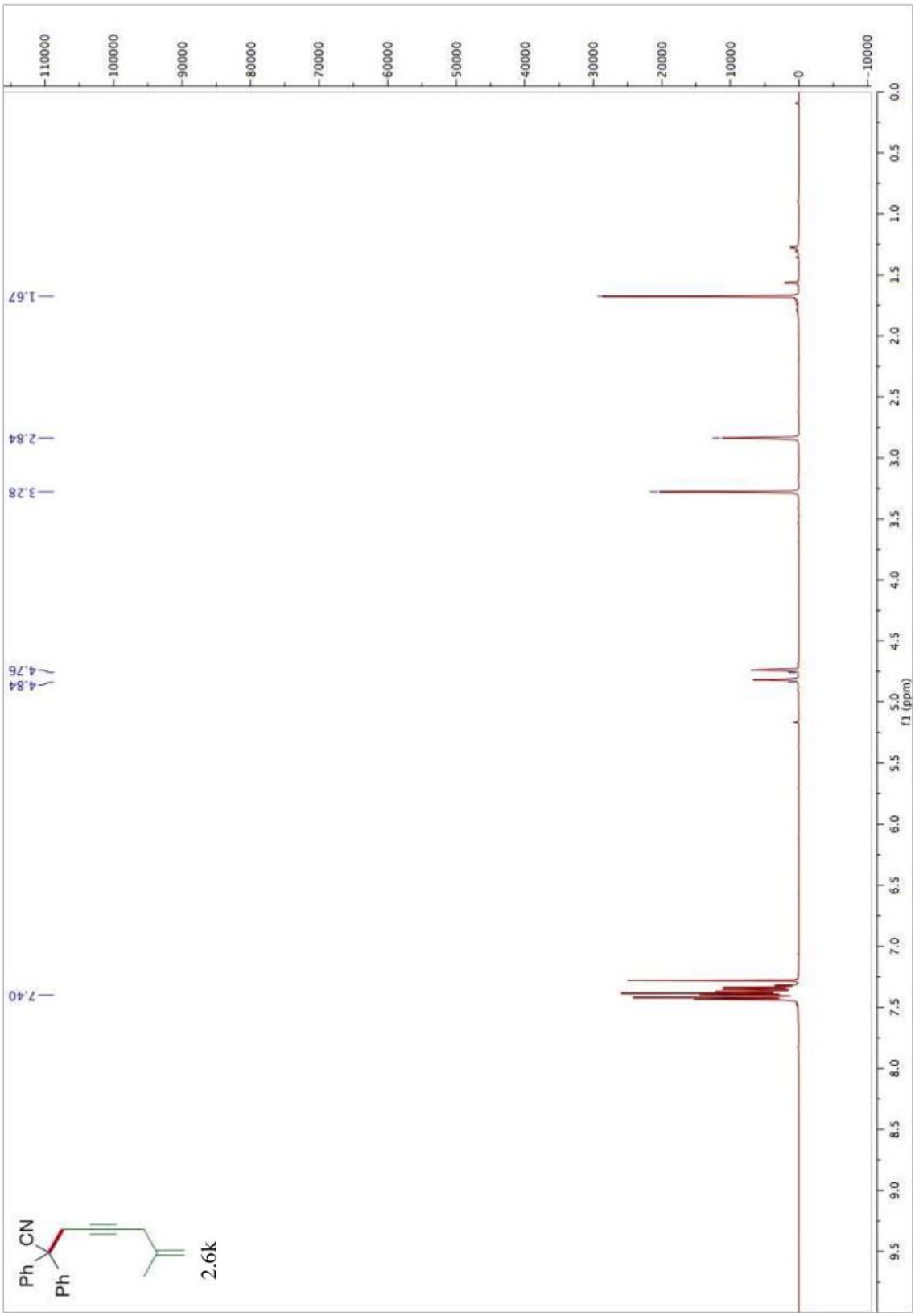
1.67
2.84
3.28
4.76
4.84
7.40
f1 (ppm)
Ph
CN
Ph
2.6k

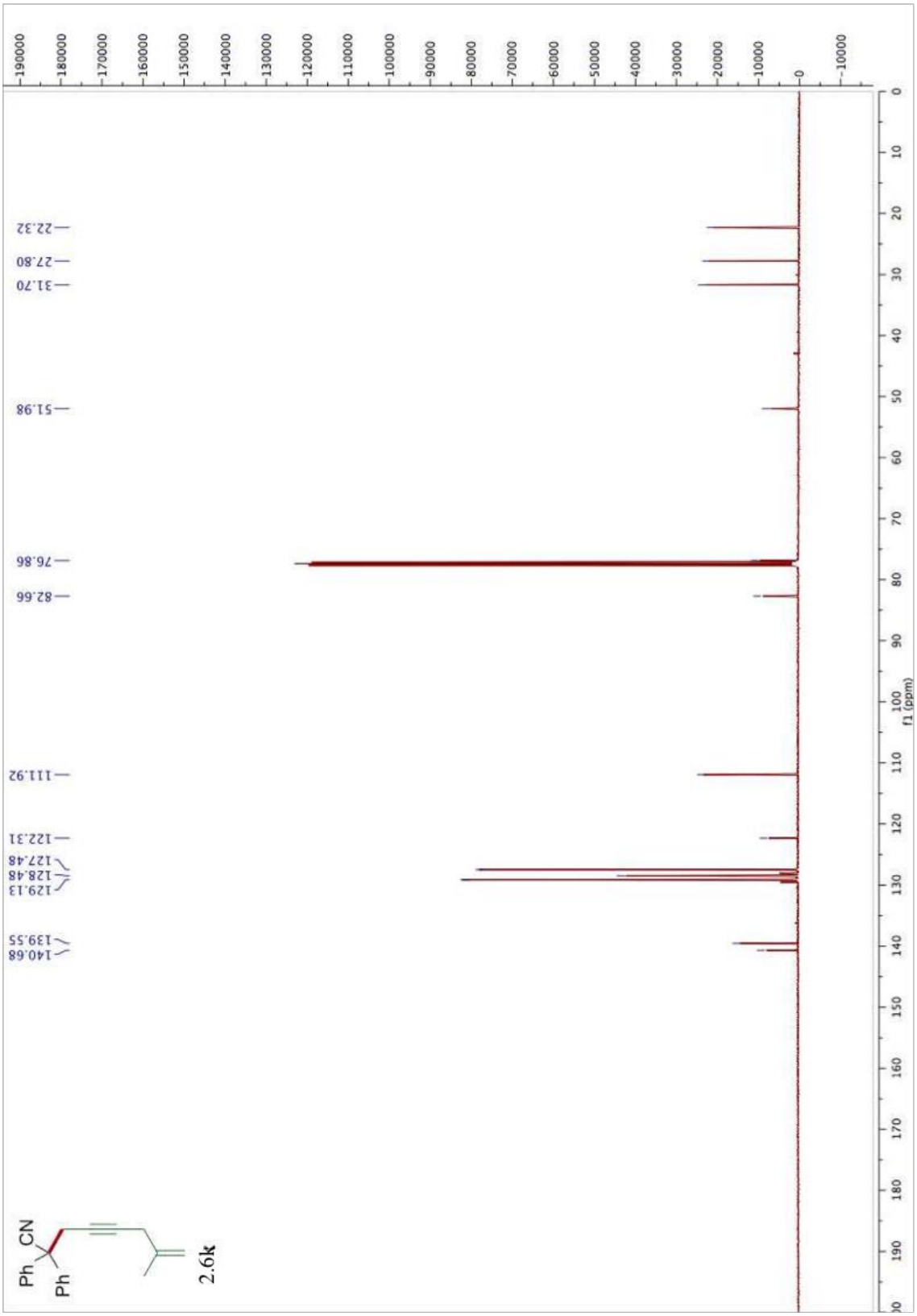
22.32
27.80
31.70
51.98
76.86
82.66
111.92
122.31
127.48
128.48
129.13
139.55
140.68
Ph
CN
Ph
2.6k
f1 (ppm)

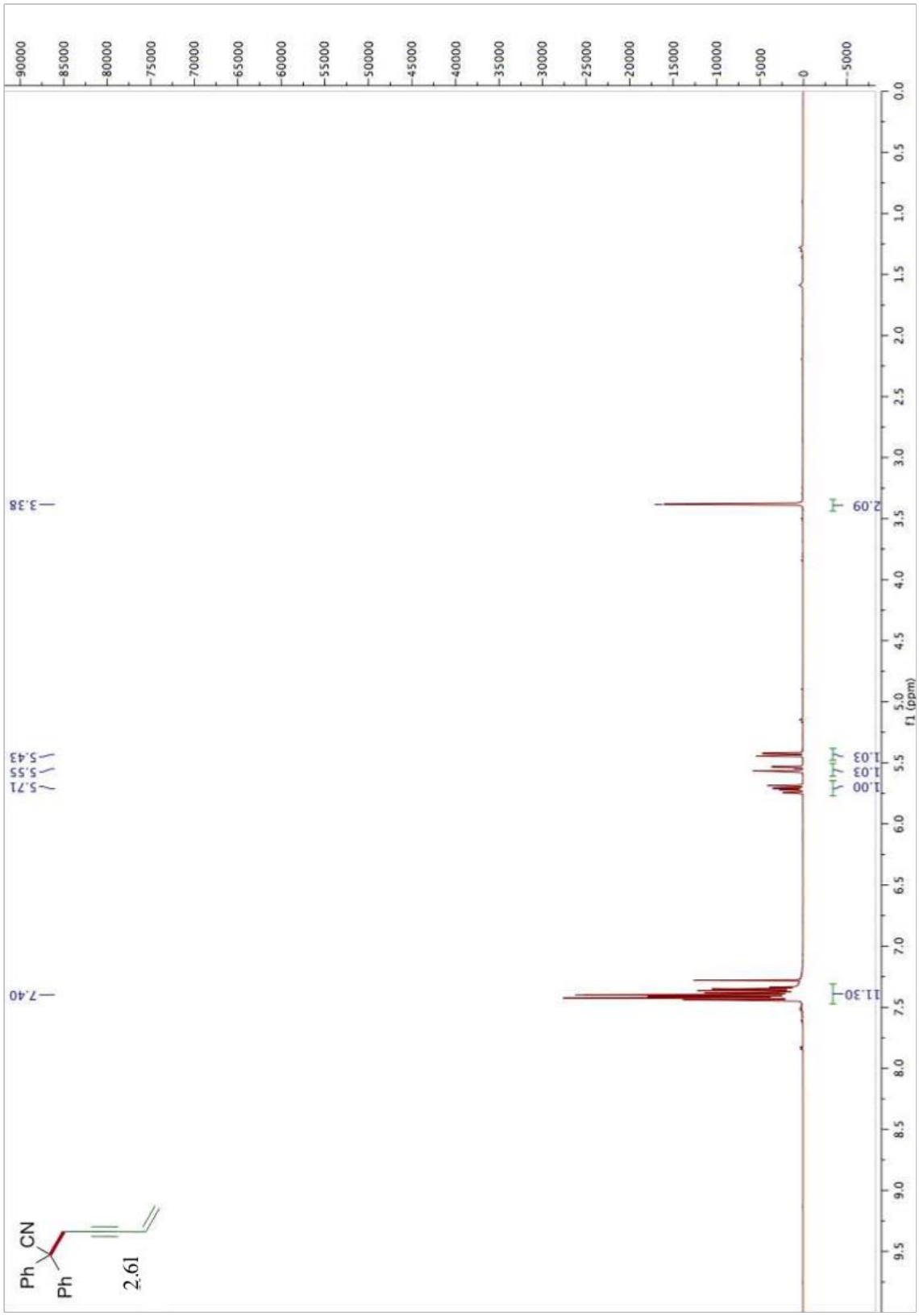
3.38
5.71
5.55
5.43
7.40
2.09
1.00
1.03
1.03
11.30
f1 (ppm)
Ph
CN
Ph
2.61

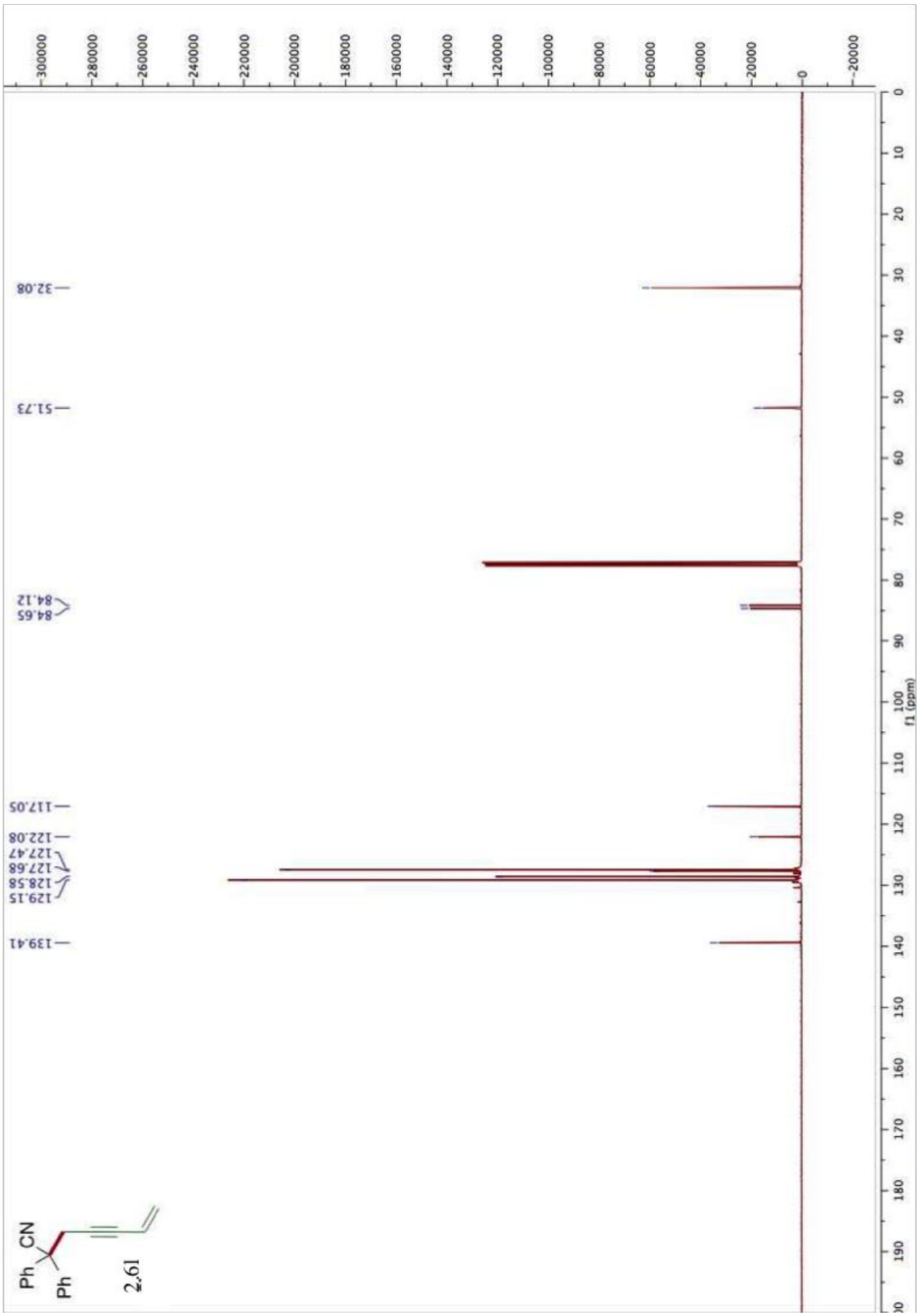
32.08
51.73
84.65
84.12
117.05
122.08
127.47
127.68
128.58
129.15
139.41
f1 (ppm)
Ph
CN
Ph
2.61

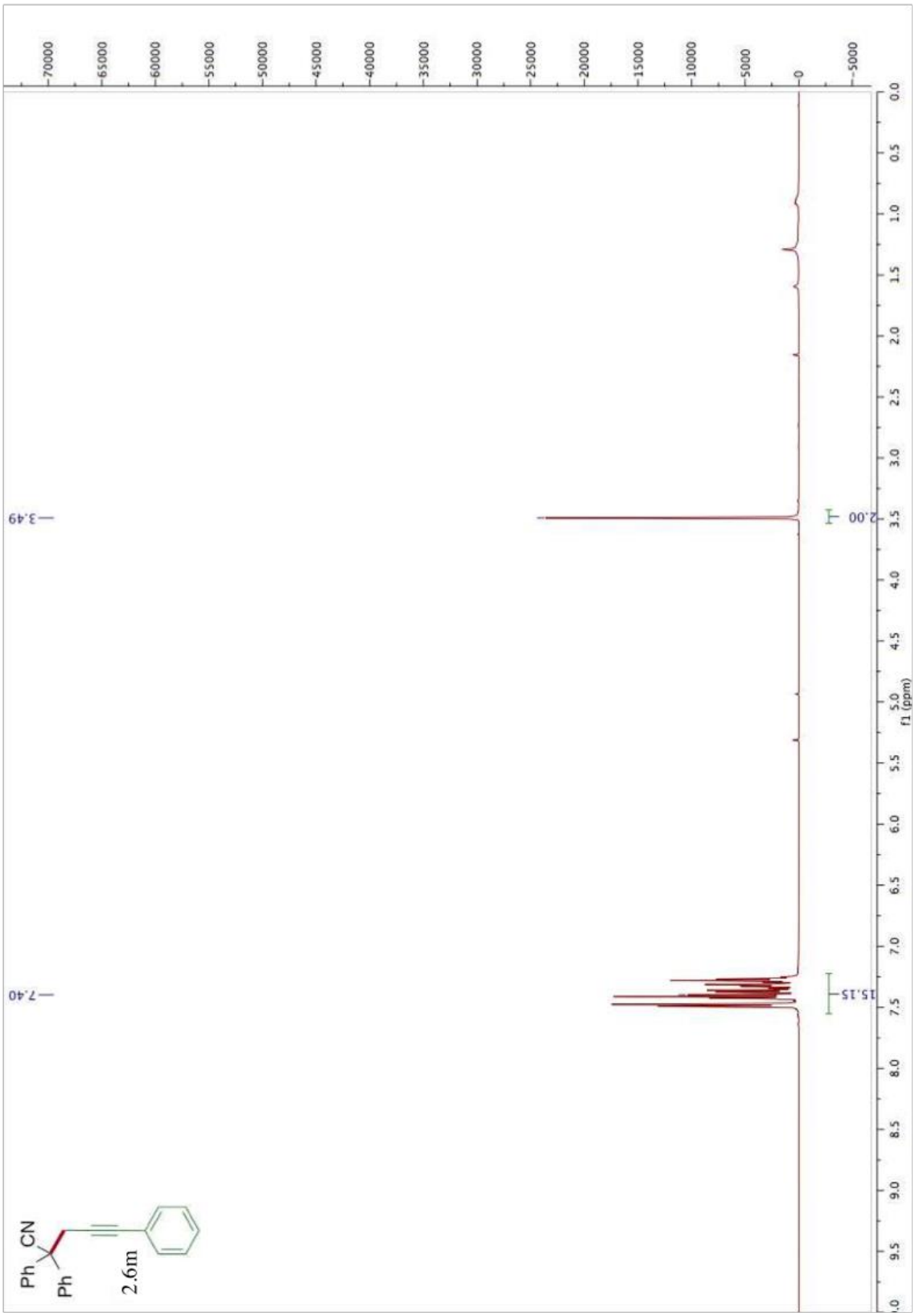
3.49
7.40
2.00
15.15
f1 (ppm)
Ph
CN
Ph
2.6m

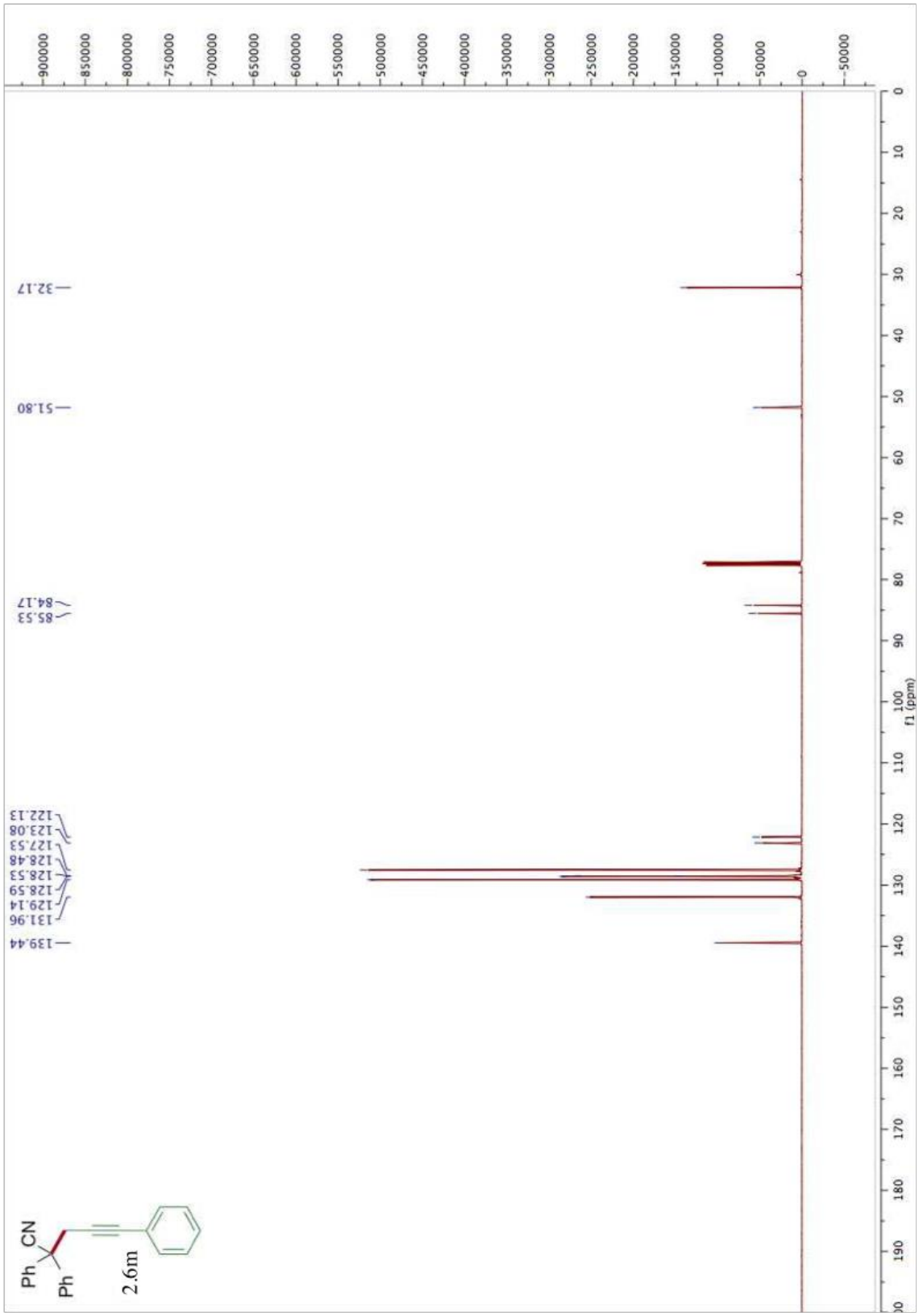
32.17
51.80
84.17
85.53
122.13
123.08
127.53
128.48
128.53
128.59
129.14
131.96
139.44
Ph
CN
Ph
2.6m
f1 (ppm)

Chapter 3. Palladium-Catalyzed Decarboxylative Propargylation and 1,3-Dienylation

3.1 Introduction to Metal-Catalyzed Decarboxylation

Chapter 2 of this dissertation presented methods developed for the intermolecular dienylation and propargylation of α,α-diaryl acetonitrile pronucleophiles (Scheme 3.1).[1] However, the substrate scope was limited to *weakly* stabilized α,α-diaryl acetonitriles with a pK_a similar to that of methanol (pK_a = ≤ 17). In order to expand the substrate scope to less stable nucleophiles (pK_a > 17) we envisioned the development of an intramolecular variant that would generate the activated nucleophile *in situ* via decarboxylation (Scheme 3.2).[2,3,4,5,6,7]

Scheme 3.1: Regiodivergent Substitution of Propargylic Carbonates.

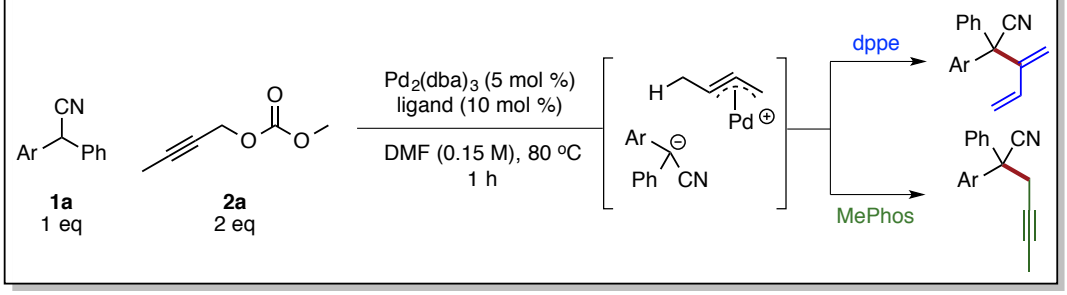

Scheme 3.2: Decarboxylative Dienylation and Propargylation

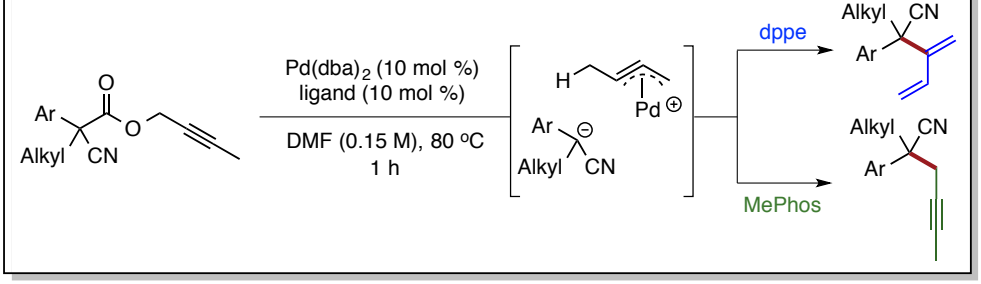

In standard transition metal-catalyzed cross-coupling methods both activation of the nucleophile and electrophile are required prior to bond formation (Scheme 3.3).[8] Activation is typically achieved using an external base or preformed organometallic species. The employed reagents are often expensive, toxic or highly basic. Further, a necessary result of these standard cross-coupling methods is the production of a stoichiometric amount of waste. Alternatively,

decarboxylative cross-coupling reactions possess significant advantages (Scheme 3.3).[8] For example, the required starting materials can be easily and efficiently synthesized from readily available reagents and irreversible decarboxylation can drive the formation of reactive intermediates while generating CO_2 as the only byproduct. Despite these significant advantages, only a handful of methods have been developed for decarboxylative propargylation, which will be presented in the following sections of this dissertation.

Scheme 3.3: Advantages of Decarboxylative Cross-Coupling

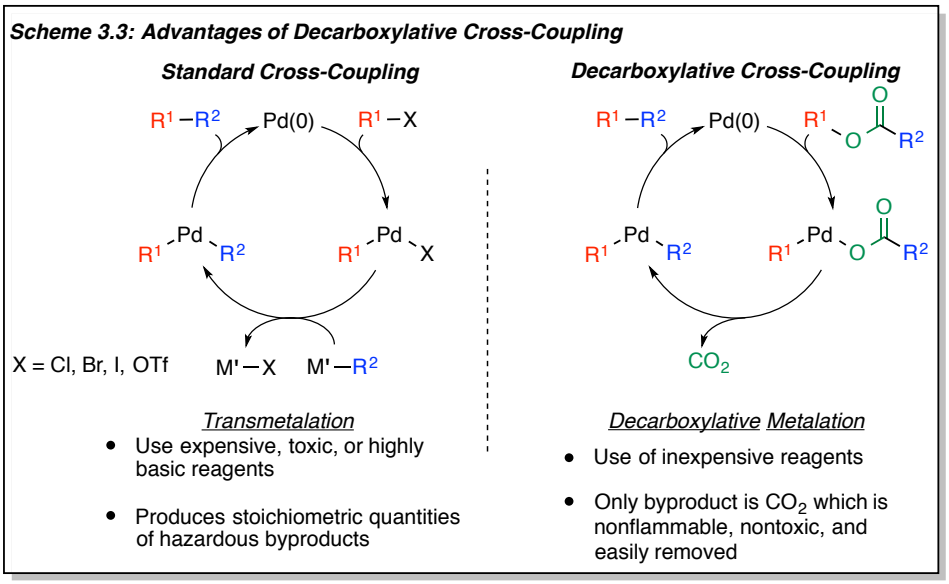

3.2 Decarboxylative Propargylation Methods

In 1994, Bienaymé reported that decarboxylative propargylation of substituted propargylic carbonates could be achieved using $Pd(PPh_3)_4$ (Scheme 3.4).[9] However, the method was not optimized for selective product formation and contamination by the allenyl isomer was frequently observed. Further, product ratios were largely affected by the substitution patterns on the starting carbonate. Specifically, terminal acetylene derivatives were found to favor the propargyl isomer while the addition of substituents, such as TMS or Ph, favored the allenyl isomer. The observed selectivity was suggested to arise from a change in the favored palladium-

bound intermediate from an η^1-propargylpalladium species to an η^1-allenylpalladium species which avoids unfavorable steric interactions with R^3 (Scheme 3.4). Lastly, in addition to the reported lack in selectivity, only poor to moderate yields of the product mixtures were obtained.

Scheme 3.4: Synthesis of Polyunsaturated Allenic Carbonyls.

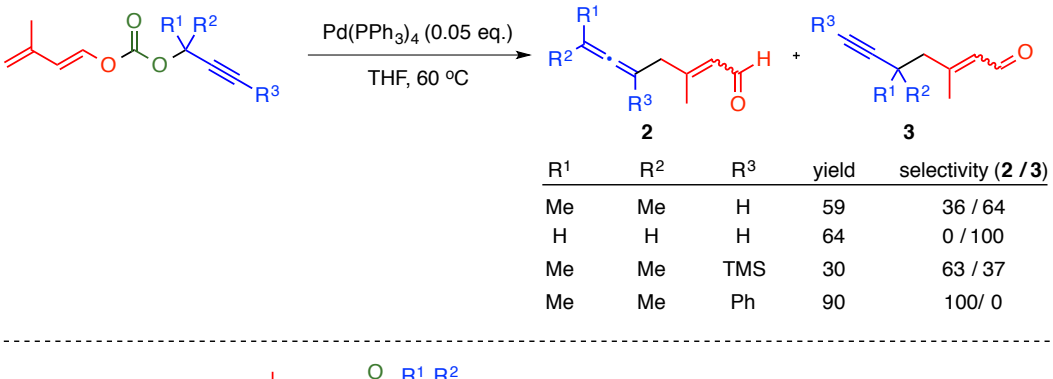

R^1	R^2	R^3	yield	selectivity (**2** / **3**)
Me	Me	H	59	36 / 64
H	H	H	64	0 / 100
Me	Me	TMS	30	63 / 37
Me	Me	Ph	90	100/ 0

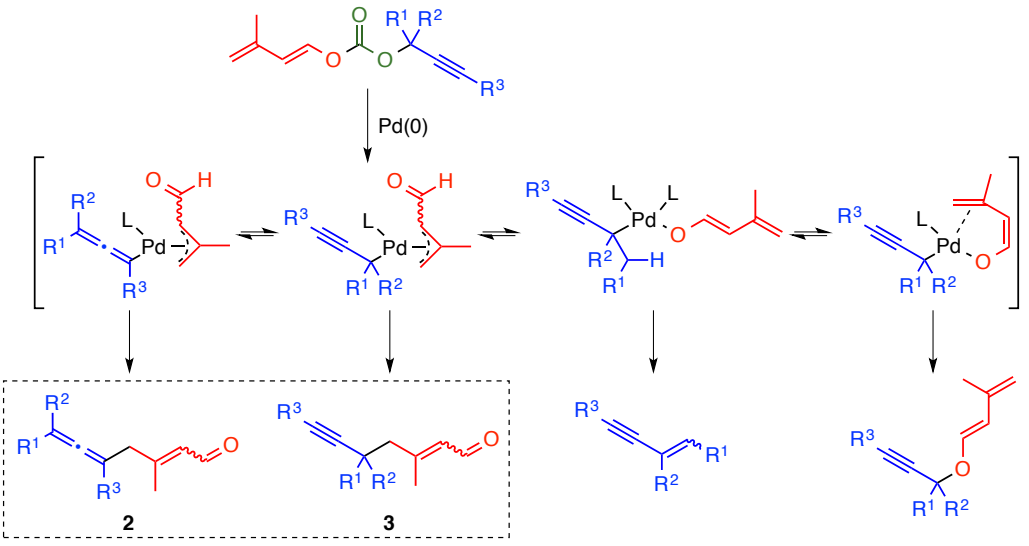

In 2011, Stoltz and coworkers reported a single example of the enantioselective decarboxylative propargylation of a cyclohexanone derivative (Scheme 3.5).[10] However, only a brief ligand screen was reported which resulted in poor enantiomeric excess and produced only moderate yields. Further, the reported product was not isolated and observed yields were determined by GC analysis with an internal standard.

Scheme 3.5: Enantioselective Propargylation

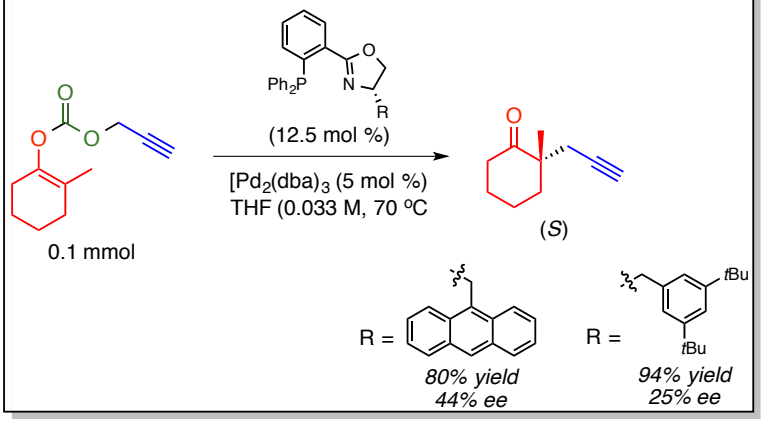

Later, in 2014, Altman and coworkers reported the copper-catalyzed decarboxylative trifluoromethylation of propargylic electrophiles to access substituted propargyl and allenyl products (Scheme 3.6).[11] However, like the method reported by Bienaymé, selective formation of the propargyl isomer was not obtained and reactions suffered from competitive formation of the allenyl isomer. Additionally, the propargyl products could not be successfully purified and were isolated in poor ratios with the allenyl isomer.

Scheme 3.6: Cu-Catalyzed Decarboxylative Trifluoromethylation

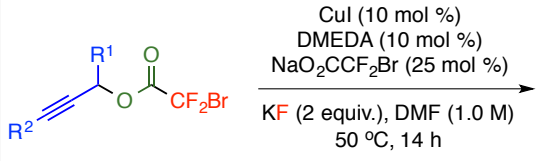

R¹	R²	% Yield	A : B	R¹	R²	% Yield	A : B
H	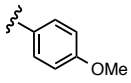	72	4.0 : 1	H	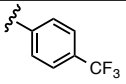	70	1.7 : 1
H	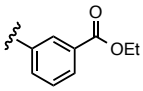	78	2.3 : 1	H		70	1.2 : 1
H	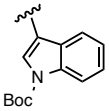	59	3.0 : 1	Me	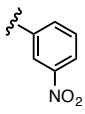	41	1.9 : 1

Through use of a cationic copper complex and chiral ligand, Xu[12] and Hu[13] were able to demonstrate the successful decarboxylative propargylation of ketone enolate equivalents, tertiary,

and secondary amines (Scheme 3.7). Overall, good yields and enantioselectivities were observed. However, the methods were restricted to 1-aryl propargylic carbonates and, as discussed previously in Chapter 1, limited to terminal acetylene derivatives that enable formation of the copper-acetylide and copper-allenylidene intermediates *in situ*.

Scheme 3.7: Copper-Catalyzed Decarboxylative Propargylic Alkylation

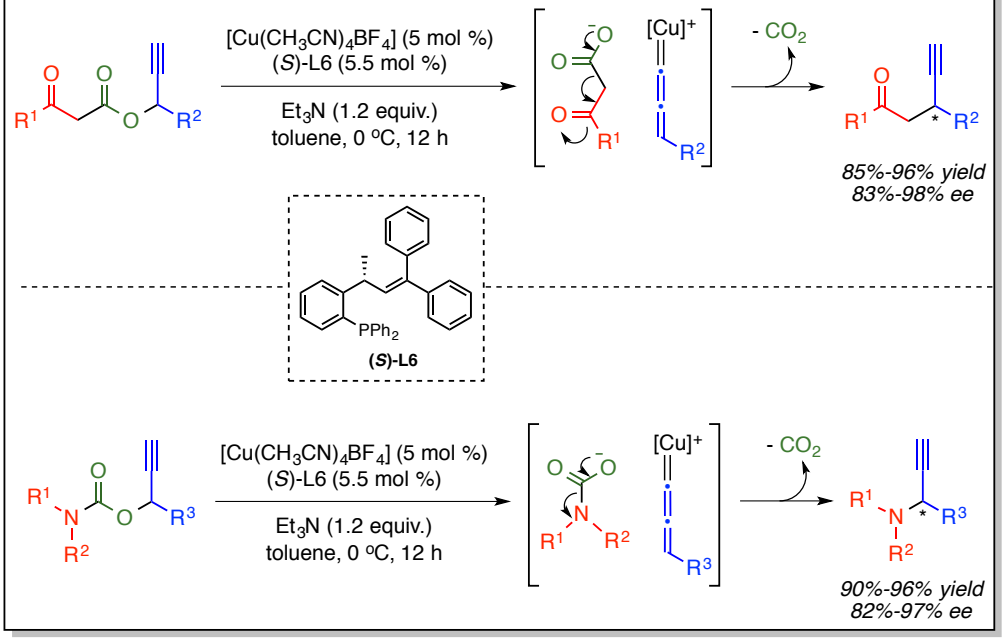

Lastly, Wu recently demonstrated the gold(I)-catalyzed decarboxylative propargylation of oxygen-centered nucleophiles (Scheme 3.8).[14] Substrates were once again limited to 1-aryl propargylic carbonates although 1,1-disubstituted propargylic carbonates were also tolerated and resulted in moderate isolated yields. Further, 3-substituted propargylic carbonates with either alkyl or aryl substituents resulted in low yields of the propargylated product, unless the aryl moiety was *ortho*-substituted. The *ortho*-substituent is proposed to perturb coordination of the gold catalyst to the π-bond and promote σ-activation resulting in the propargylated product (Scheme 3.8).

Scheme 3.8: Gold(I)-Catalyzed Decarboxylative Propargylation of Oxygen-Centered Nucleophiles.

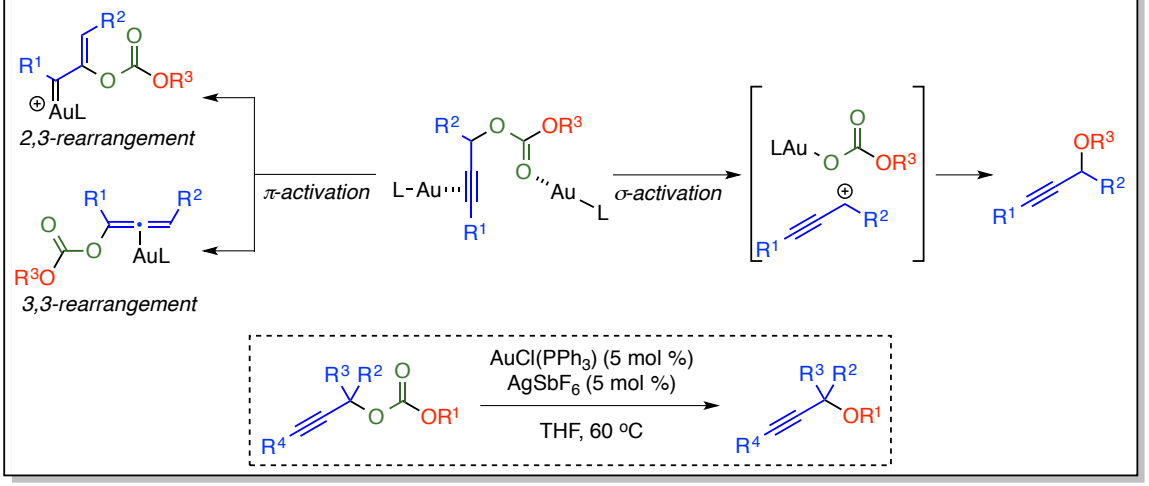

In the following, ongoing efforts to develop a generalized and selective method for the palladium-catalyzed decarboxylative propargylation and dienylation of acetonitrile derivatives will be presented. Development of such methods is necessary to provide facile, efficient, and selective access to propargyl and dienyl functionalities for application as synthetic intermediates in complex molecule synthesis.

3.3 Decarboxylative Propargylation and Dienylation of Acetonitrile Pronucleophiles

Decarboxylative cross-coupling minimizes the use of additives and provides efficient access to reactive intermediates via irreversible decarboxylation. As a result, these methods provide an environmentally friendly and atom-economic alternative to commonly employed coupling methods. Initially, we hypothesized that we could adopt decarboxylation as a way to expand on our previously developed methods for propargylation and dienylation of acetonitrile pronucleophiles in which substrates were limited to those with a pK_a of $\leq$ 17. We proposed that the source of this limitation was in pronucleophile activation by liberated methoxide, which would necessitate that the pronucleophile have a pK_a similar to that of methanol (Figure 3.1). Alternatively, if we employed a decarboxylation pathway starting from a propargylic ester, the

nucleophile would be generated *in situ*, after decarboxylation thus potentially providing access to a larger range of nucleophiles for coupling to the butadiene synthon (Scheme 3.9).

Figure 3.1: Proposed 1,3-Dienylation Pathway.

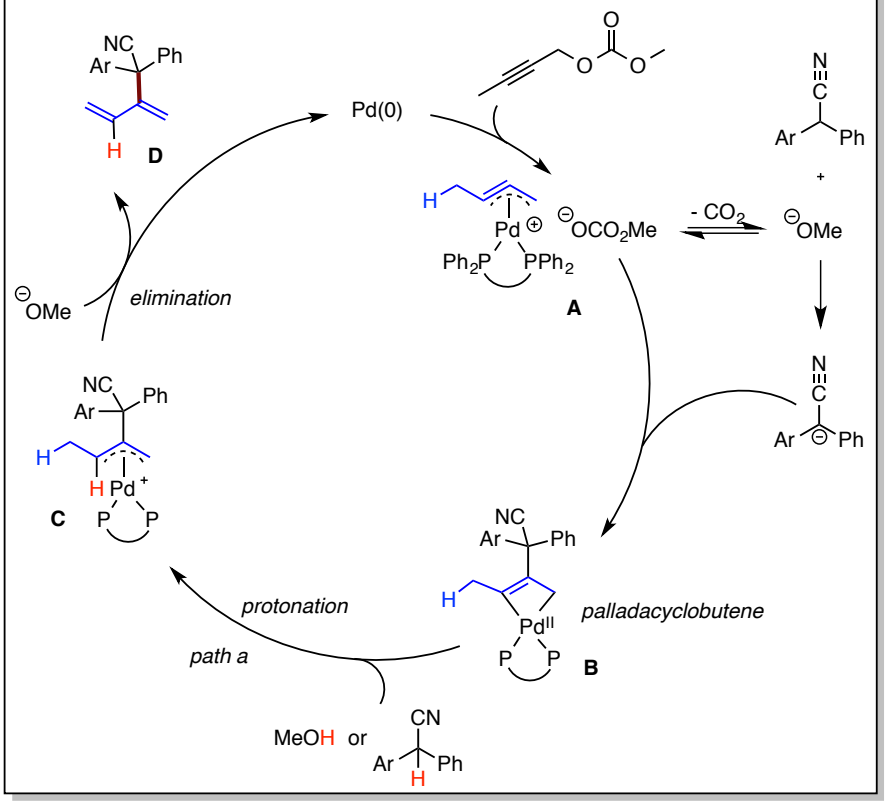

Scheme 3.9: Decarboxylative Activation of Pronucleophiles:

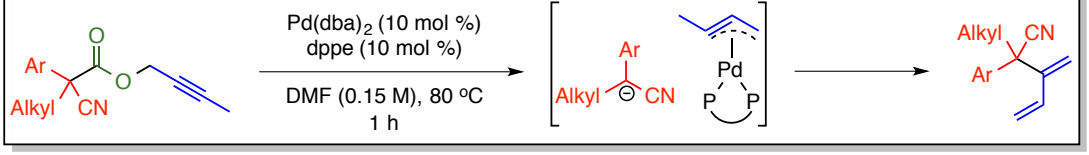

To begin, we subjected but-2-yl 2-cyano-2-phenylpropanoate to the reaction conditions developed for intermolecular dienylation of acetonitrile derivatives at elevated reaction temperatures (Table 3.1, entry 3).[1] Disappointingly, we observed only minimal reaction conversion in favor of the protonated product. Screening studies revealed that monomeric $Pd(dba)_2$ was a more efficient pre-catalyst as opposed to $Pd_2(dba)_3$ and conversion to product

could be increased after extended reaction times (Table 3.1 entry 4). However, only poor yields of the isolated product were obtained after purification via column chromatography.

Table 3.1:Optimization of Decarboxylative Dienylation

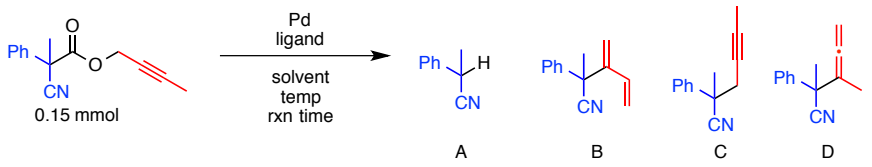

entry	cat.	mol %	ligand	mol %	additive	mol%	solvent	mL	temp	time	sm %	A%	B%	C% and D%
1	$Pd(dba)_2$	10	MePhos	10	---		DMF	0.5	40	1h	37	18	22	23
2	$Pd(dba)_2$	2.5	MePhos	2.5	---		DMF	0.5	80	1h	58	20	6	16
3	$Pd_2(dba)_3$	5	dppe	10	---		DMF	0.5	100	1h	83	15	3	0
4	$Pd(dba)_2$	10	dppe	10	---		DMF	0.5	100	6h	0	5	83	12
5	$Pd(dba)_2$	2.5	dppe	2.5	---		DMF	0.5	100	6h	88	11	1	0
6	$Pd(dba)_2$	10	dppe	10	---		DMF	1	150mw	10m	0	17	69	14
7	$Pd(dba)_2$	10	dppe	10	---		DMF	1	150mw	4m	0	15	71	14
8	$Pd(dba)_2$	10	dppe	10	---		DMF	1	150mw	1m	0	13	73	14
9	$Pd(dba)_2$	10	dppe	10	---		DMF	1	100mw	5m	72	11	16	2
10	$Pd(dba)_2$	10	dppe	10	---		DMF	1	120mw	1m	0	5	86	10
11	$Pd(dba)_2$	10	dppe	10	$NaHCO_3$	1	DMF	1	120mw	1m	23	7	62	8
12	$Pd(dba)_2$	10	dppe	10	---	--	DMF	0.25	120mw	1m	68	10	13	9
13	$Pd(dba)_2$	10	dppe	10	morpholine	1	DMF	1	100	4h	only	protonated		material
14	$Pd(dba)_2$	10	dppe	10	Bu_2NH	1	DMF	1	100	4h	0	77	23	0
15	$Pd(dba)_2$	10	dppe	10	Bn_2NH	1	DMF	1	100	4h	0	74	23	2
16	$Pd(dba)_2$	10	dppe	10	pyrrolidine	1	DMF	1	100	4h	0	61	39	0
17	$Pd(dba)_2$	10	dppe	10	azocane	1	DMF	1	100	4h	0	65	14	21
18	$Pd(dba)_2$	10	dppe	10	*i*-Pr_2NH	1	DMF	1	100	4h	0	8	92	0
19	$Pd(dba)_2$	10	dppe	10	TBD	1	DMF	1	100	4h	0	94	6	0
20	$Pd(dba)_2$	10	dppe	10	K_2HPO_4	1	DMF	1	100	4h	0	5	95	0
21	$Pd(dba)_2$	10	dppe	10	$NaHCO_3$	1	DMF	1	100	4h	0	11	89	0
22	$Pd(dba)_2$	10	dppe	10	mesitol	1	DMF	1	100	4h	0	40	60	0
23	$Pd(dba)_2$	10	dppe	10	2-nitroethanol	1	DMF	1	100	4h	62	38	0	0
24	$Pd(dba)_2$	10	dppe	10	2,2,2-trifluoroethanol	1	DMF	1	100	4h	very	Very	messy	
25	$Pd(dba)_2$	10	dppe	10	DBPC	1	DMF	1	100	4h	0	23	5	71
26	$Pd(dba)_2$	10	dppe	10	propofol	1	DMF	1	100	4h	0	35	5	60
27	$Pd(dba)_2$	10	dppe	10	benzoic acid	1	DMF	1	100	4h	48	47	0	5
28	$Pd(dba)_2$	10	dppe	10	MeOH	1	DMF	1	100	4h	0	22	54	14
29	$Pd(dba)_2$	10	dppe	10	H_2O	1	DMF	1	100	4h	0	61	39	0
30	$Pd(dba)_2$	10	dppe	10	*tert*-butanol	1	DMF	1	100	4h	0	8	92	0
31	$Pd(dba)_2$	10	dppe	10	*tert*-butanol	1	DMF	1	100	3h	0	50	50	0
32	$Pd(dba)_2$	10	dppe	10	K_2HPO_4	1	DMF	1	100	3h	59	19	22	0

Ratios were determined by GC/MS analysis.

Next, we evaluated the potential decarboxylative dienylation reaction pathway in order to optimize isolated yields of the dienylated product (Figure 3.2). Initially, we envisioned that palladium(0) would undergo oxidative addition to generate an η^3-propargylpalladium intermediate and activated nucleophile. As previously proposed, the activated nucleophile would then regioselectively attack the center carbon of the palladium complex to generate a pallada-cyclobutene.[15] However, unlike in the intermolecular variant, which could undergo protonation by

a molecule of methanol or substrate, neither is possible in the decarboxylation pathway since both compounds are absent from the reaction media. Therefore, we proposed that a proton source could be needed. Further, the proton source would also have to act as a competent base to deprotonate intermediate **C** (Scheme 3.2) for optimal product formation.

Figure 3.2: Proposed Decarboxylative 1,3-Dienylation Pathway.

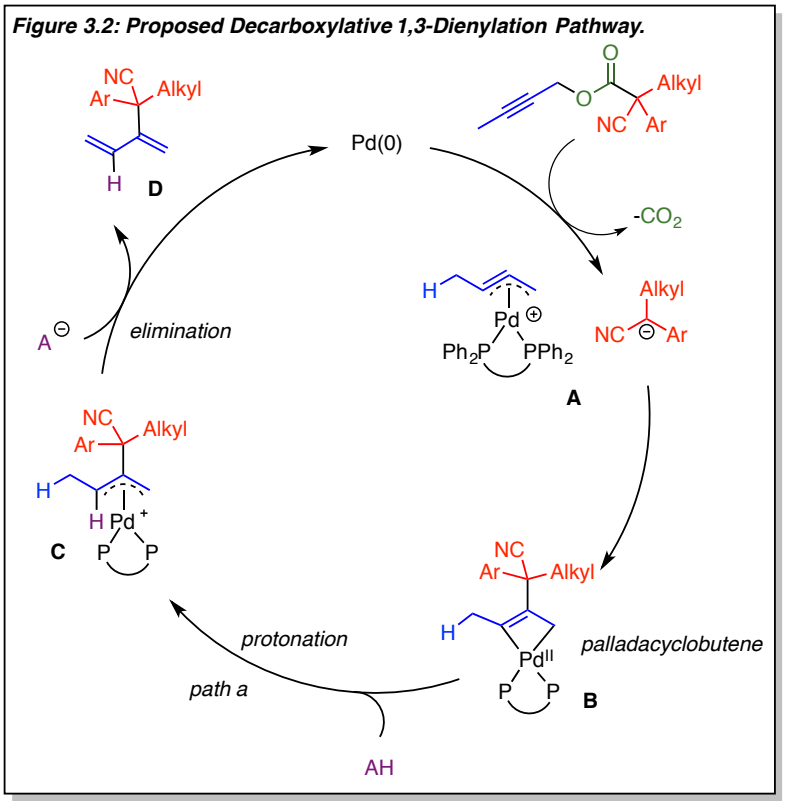

We next screened a variety of proton sources (Table 3.1) and found that K_2HPO_4 provided the optimal conversion to the diene product after 4 h. However, significantly decreased yields of the isolated product were still obtained compared to the suggested product formation by GC/MS analysis using mesitylene as an internal standard. It was next proposed that although acetonitrile derivatives are readily activated via decarboxylation in allylation-type chemistry,[8] activation utilizing propargylic esters might be more problematic. Further, if deprotonation of intermediate **C** (Scheme 3.10) occurred by the activated nitrile instead of the conjugate base of the additive, it could halt productive product formation. Therefore, we diverted our attention to

but-2-yn-1-yl-2-cyano-2-(4-nitrophenyl)propanoate which could stabilize the *in situ* generated anionic charge more efficiently and potentially lower the pK_a of the protonated product enough for reintroduction back into the catalytic cycle for dienylation. Gratifyingly, decarboxylative dienylation occurred using 10 mol % of $Pd(dba)_2$, 9.5 mol % dppe, in DMF at 80 °C after 1 h and moderate yields of the isolated product were obtained (Scheme 3.10, **2.1b**). We then screened other electron-deficient aryl substituents and found that a *para*-carbomethoxy derivative could be obtained in similar yield (**2.1c**). However, when *meta*-substituted electron-deficient aryl moieties were screened, a decrease in yield was observed (**2.1d**, **2.1e**, **2.1f**). Similarly, the reaction was tolerant of a *para*-chloro pyridine derivative (**2.1g**), and increased steric bulk of the α-substituted alkyl group (**2.1h**). Unfortunately, a further decrease in isolated yield of the diene product was observed when an ethyl group was incorporated at the 3-position of the propargylic substituent (**2.1i**) and with electron-donating substituents on the aryl moiety (**2.1j**).

Scheme 3.10: Scope of Decarboxylative Dienylation.[a]

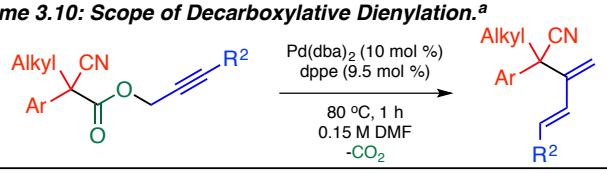

2.1a
47%[b]

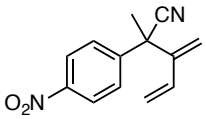

2.1b
75%[c]

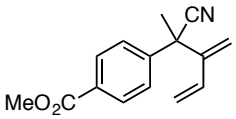

2.1c
78%[c]

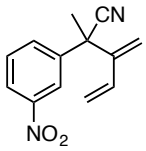

2.1d
50%[c]

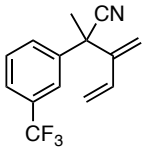

2.1e
51%[c]

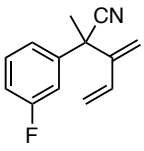

2.1f
40%

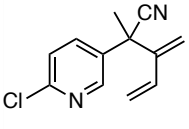

2.1g
41%

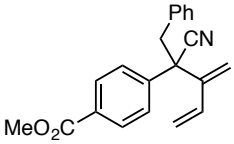

2.1h
53%[c]

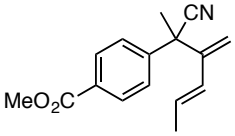

2.1i
25%[b]

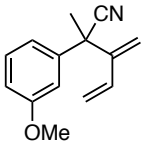

2.1j
17%

[a] propargyl ester (0.3 mmol), $Pd(dba)_2$ (10 mol %), dppe (9.5 mol %), DMF (2 mL), 80 °C, 1 h, isolated yields are reported.
[b] run with K_2HPO_4 (2.1 mmol).
[c] $Pd(dmdba)_2$ (10 mol %) used.

In addition to the successfully isolated products obtained from decarboxylative dienylation, we have also encountered limitations to the developed method (Scheme 3.11). When an allyl functionality was incorporated into the starting material, mostly unreacted starting material was observed (Scheme 3.11, **2.2a**, **2.2b**). Such a result is expected if the formation of a palladium π-allyl intermediate out-competes the formation of η^3-propargylpalladium complex, thus preventing diene formation. Likewise, a similar result was observed when a *para*-bromo

substituted aryl moiety was subjected to the optimized reaction conditions (**2.2c**). In this case, we proposed that oxidative addition of the aryl–bromine bond occurs in lieu of oxidative addition of the propargylic ester, which would also halt desired product formation. Alternatively, when the aryl ring contained an *ortho*-chloro substituent, minor conversion to the diene product was observed (18% by GC/MS) (**2.2d**). However, a higher relative percentage of the protonated product was present at 24% with 58% remaining as starting material. Lastly, increased steric bulk at the 3-position of the propargyl functionality also perturbed diene formation; only a 26% conversion of starting material **2.2e** was observed by GC/MS.

Scheme 3.11: Unsuccessful Decarboxylative Dienylation Scope:

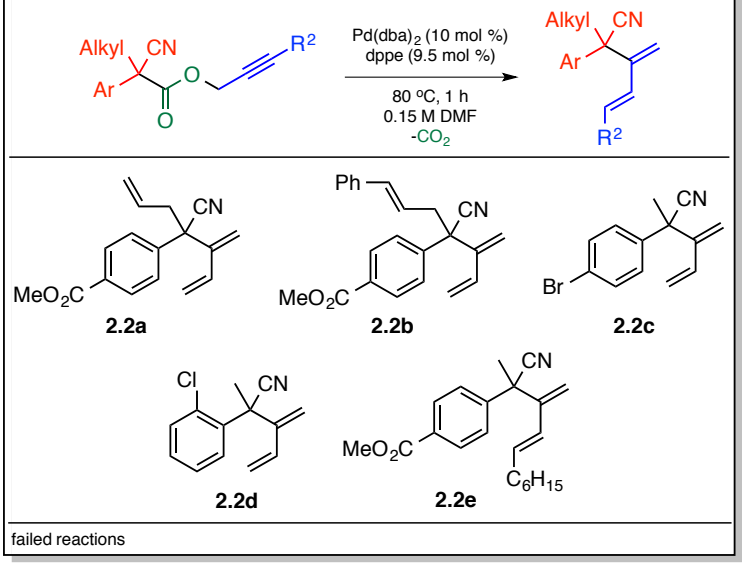

As previously presented, decarboxylative dienylation is currently restricted to electron-deficient aryl rings in order to obtain moderate yields. However, it should be mentioned that the developed method provides access to a broader range of nucleophiles than were previously successful in the palladium-catalyzed intermolecular dienylation using nitriles and propargyl carbonates (Scheme 3.12).

Scheme 3.12: Intermolecular Dienylation vs. Decarboxylative Dienylation

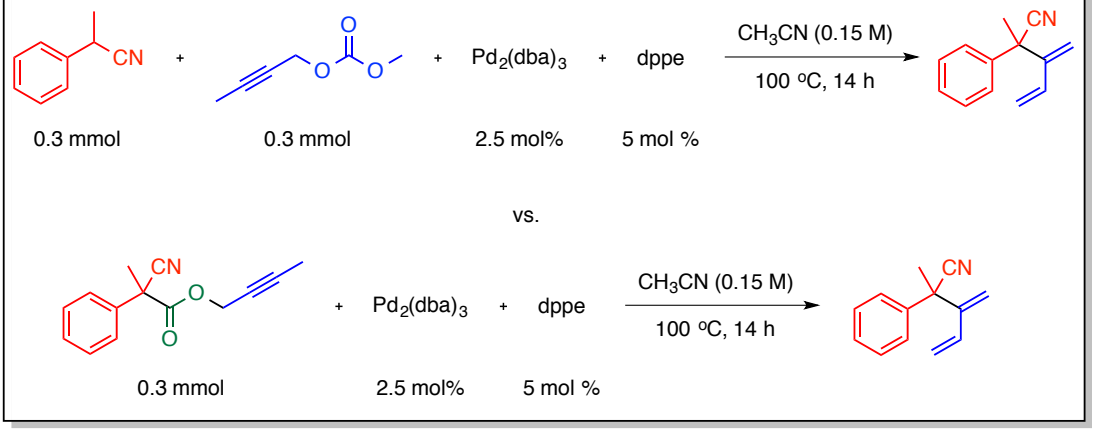

Due to the fact that the substrate scope of the decarboxylative dienylation reaction is somewhat limited, we aimed to expand the application of our method through a sequential dienylation/cyclization pathway to provide facile and efficient access to polycyclic cores.[16,17] A brief reaction optimization study evaluated the effects of temperature, additives, solvent, and reaction duration for the sequential reaction. Eventually, it was found that, after diene formation addition of 20 mol % $ZnBr_2$ and 2 equivalents of *N*-phenylmaleimide lead to the cyclized product in 47% isolated yield after 3 hours (Scheme 3.13).[18,19,20] Further, evaluation of the cyclized product by ^{1}H and ^{13}C NMR spectroscopies suggests that only one stereoisomer is formed of the Diels-Alder product, however, current efforts to obtain crystallographic information is ongoing in the laboratory. Additionally, efforts are also being put forth to further optimize the yield of the sequential reaction along with expanding the substrate scope of both diene and dienophile.

Scheme 3.13: One-Pot, Sequential Decarboxylative Dienylation and Diels-Alder Cyclization

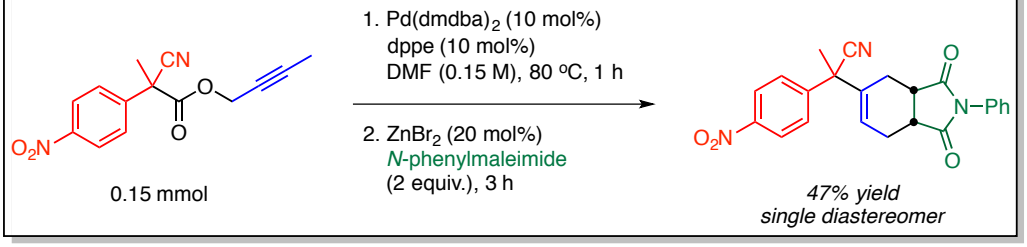

We next explored the capacity for the decarboxylative dienylation method to be diverted toward decarboxylative propargylation of acetonitrile derivatives from propargylic esters (Scheme 3.14). Beginning with methyl 4-(2-cyanohex-4-yn-2-yl)benzoate, which was an optimal substrate for the dienylation pathway, we once again changed the denticity of the coordinating ligand from bidentate (dppe) to monodentate (MePhos) and were able to obtain a 60% isolated yield of the propargylated product (Scheme 3.14, **2.5a**). Altering the *para*-carbomethoxy substituent to a *para*-nitro moiety also produced the propargylated product in moderate yield (**2.5b**). Interestingly, when steric bulk was increased at the 3-position of the propargylic substituent, an increase in yield was observed (**2.5d**, **2.5e**). However, when the arene contained a strongly electron-withdrawing substituent in the *meta*-position as opposed to the *para*-position, a significant decrease in yield was observed (**2.5c)**. Lastly, the reaction was tolerant of alkyl variation to either allyl (**2.5f**) or benzyl (**2.5g**) substituents, which resulted in moderate yields of the isolated product.

Scheme 3.14: Scope of Decarboxylative Propargyation.[a]

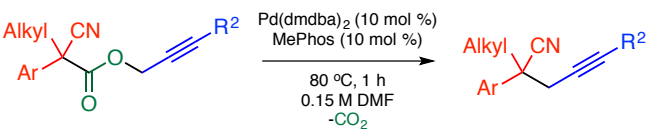

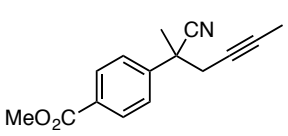

2.5a
60%

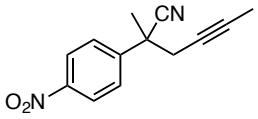

2.5b
60%

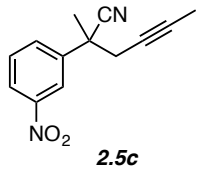

2.5c
35%

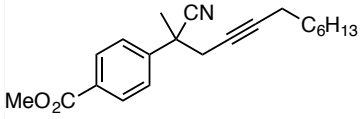

2.5d
72%

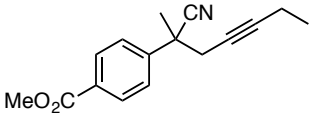

2.5e
81%

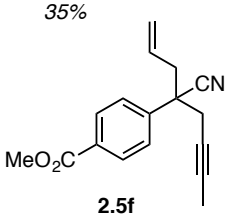

2.5f
45%

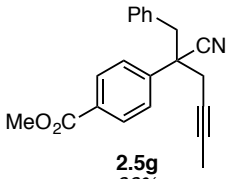

2.5g
66%

[a] propargyl ester (0.3 mmol), $Pd(dmdba)_2$ (10 mol %), dppe (9.5 mol %), DMF (2 mL), 80 °C, 1 h, isolated yields are reported.

Unfortunately, in addition to the substrates listed above that lead to successful isolation of the decarboxylative propargylic species, many substrates have been unsuccessful under the developed reaction conditions (Scheme 3.15). When a simple aryl substituent was employed, moderate reaction conversion to the propargylated product was observed by GC/MS but efforts to isolate the pure product have been unsuccessful (**2.6a**). Instead, the product has been obtained with significant contamination by the unreacted starting material. Further, when the aryl moiety contained a *para*-bromo (**2.6b**) or *ortho*-chloro (**2.6d**) substituent, only minor reaction conversion was observed. Again, this is potentially due to competitive oxidative addition of the aryl—halogen bond or unfavorable steric interactions by the *ortho*-substituted derivative. In general, when *meta*-substituted aryl functionalities were employed, predominate formation of the protonation product was observed over the propargyl isomer along with both the allenyl and

dienyl isomers (**2.6c**, **2.6e**, **2.6f**). Alternatively, when heteroaryl moieties were employed, equal formation of protonation and propargylation products along with unreacted starting material was observed by GC/MS (**2.6g**). Lastly, despite the moderate yield of the propargylated product obtained from a simple allyl substituent, incorporation of a cinnamyl substituent stopped reactivity (**2.6h**).

Scheme 3.15 Unsuccessful Decarboxylative Propargylation Scope.[a]

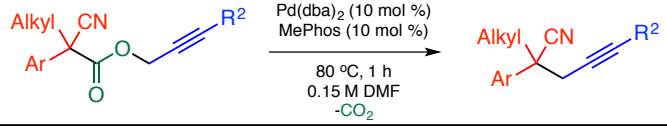

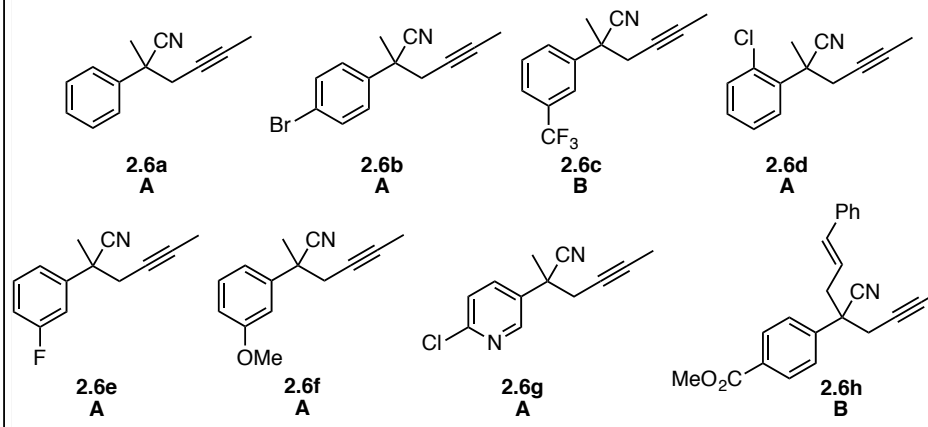

[a] Failed reactions
Method A: propargyl ester (0.3 mmol), $Pd(dba)_2$ (10 mol %), MePhos (9.5 mol %), DMF (2 mL), 80 °C, 1 h.
Method B: propargyl ester (0.3 mmol), $Pd(dmdba)_2$ (10 mol %), MePhos (9.5 mol %), DMF (2 mL), 80 °C, 1 h.

Given the apparent limitation of decarboxylative propargylation to *para*-substituted electron-withdrawing aryl substituents, we next aimed to develop a potential rational for this observation. Initially, we envision that oxidation addition of the propargylic ester to palladium(0) would occur to generate a palladium-bound intermediate (Figure 3.3). As initially proposed in chapter 2 for the intermolecular variant (Figure 3.4), propargylation is proposed to arise from inner-sphere nucleophilic attack of the η^1-allenylpalladium species over other palladium-bound intermediates.[21,22,23,24] Rational for this intermediate is twofold: 1) our observations of an increase in yield of the propargyl product with an increase in steric bulk at the 3-position of the propargyl

substituent and 2) the known coordination of *weakly* stabilized nitrile intermediates to palladium.[25,26]

Figure 3.3: Decarboxylative Propargylation

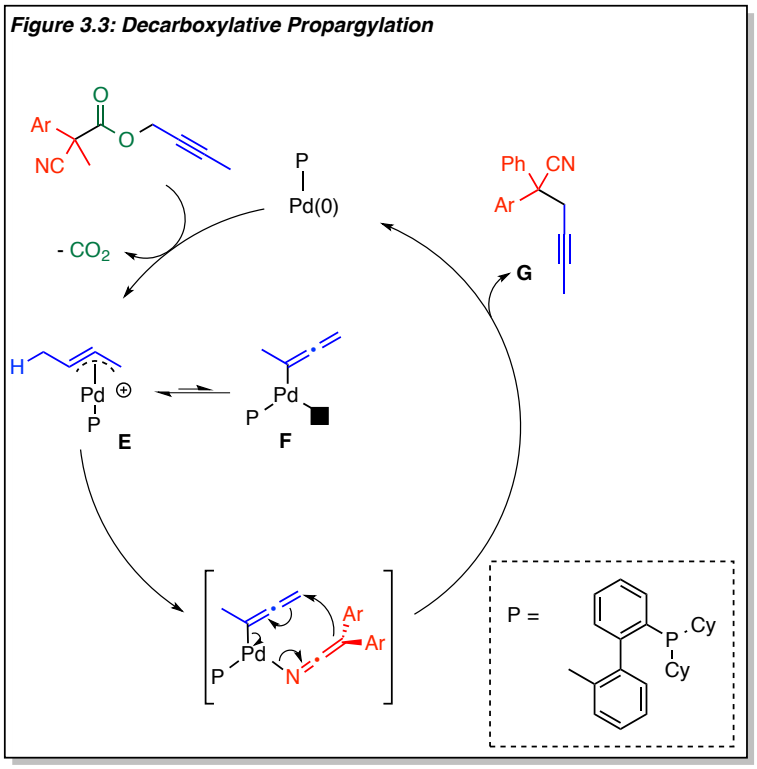

FIgure 3.4: Intermolecular Propargylation of Diaryl Acetonitrile Derivatives

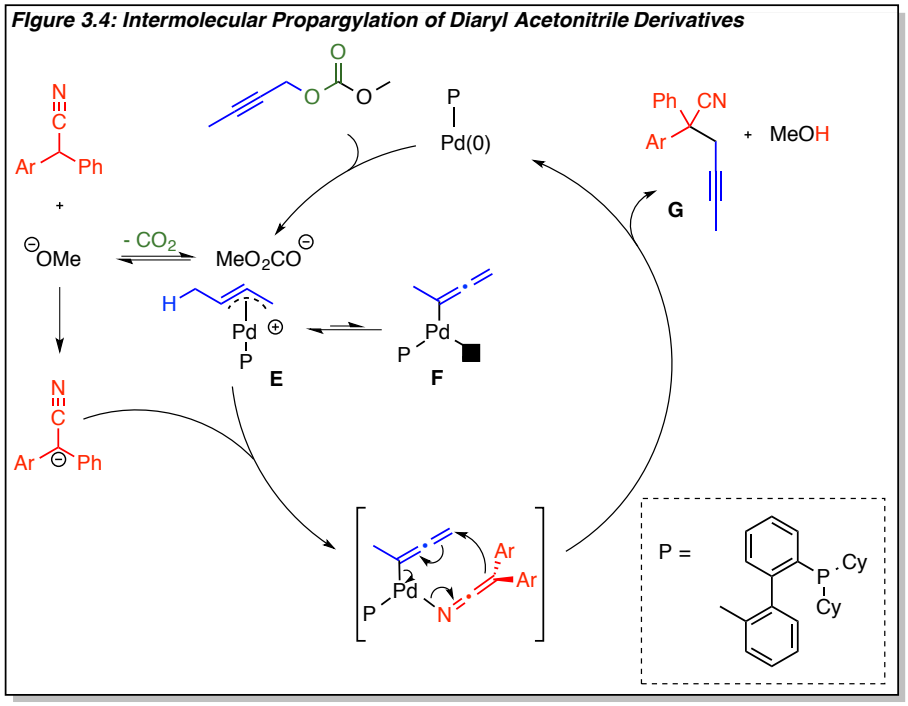

Alternatively, the rational for increased protonation and competitive product formation of *meta*-substituted derivatives is as follows. In contrast to the stabilizing effects of *para*-substituted electron-withdrawing aryl moieties, it is proposed that *meta*-substituted derivatives would be less efficient at anionic stabilization resulting in competitive formation of non-nitrile coordinated and nitrile coordinated palladium intermediates (Scheme 3.16). Lack of intermediate preference could then account for a mix of allenyl (**1.4G**), dienyl (**1.4E**), and propargyl (**1.4F**) isomers, however, the proton source that gives rise to protonated nitrile is currently unknown.

Scheme 3.16: Proposed Source of Competitive Product Formation with Meta-Substituted α-Aryl Nitriles.

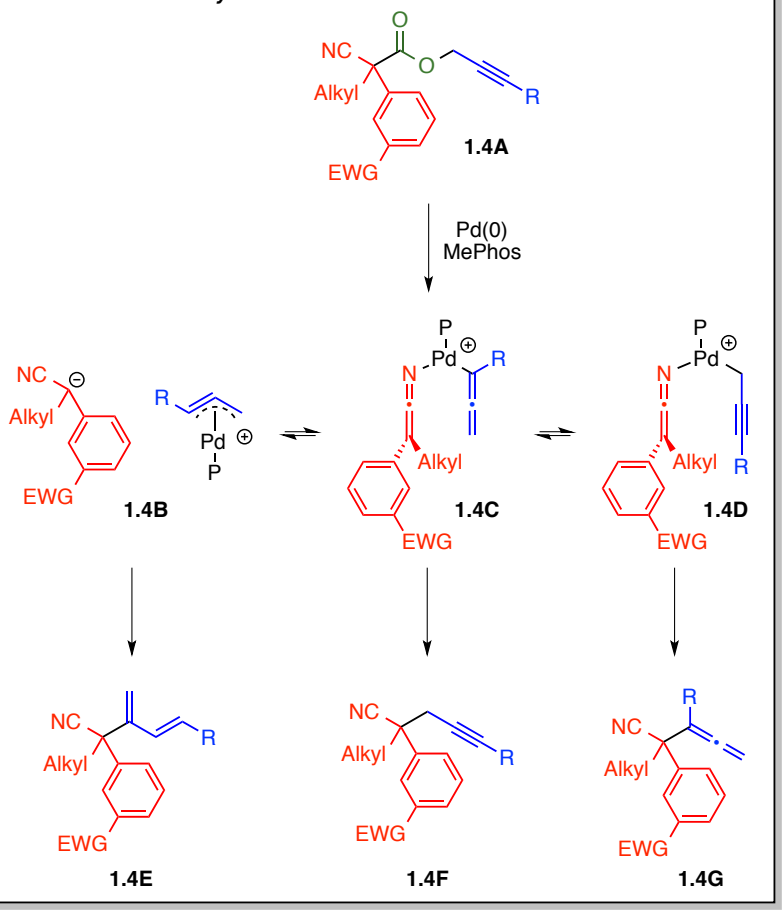

3.4 Conclusion:

In chapter 3 of this dissertation a regiodivergent method for decarboxylative dienylation and propargylation of acetonitrile pronucleophiles was presented. By generating the nucleophile

in situ, we have been able to expand the substrate scope to compounds that were previously unsuccessful for the intermolecular variant present in chapter 2. Additionally, although we are aware of limitations in both the dienylation and propargylation method, further studies are currently underway to expand the reaction scopes and provide support for the respective mechanistic pathways. Future direction will focus on the evaluation of diverse electron-withdrawing functional groups beyond nitriles and electron-deficient arenes and substitution effects at both the 1-position and 3-position of the propargylic moiety. Lastly, it would be beneficial to extend the application of the developed dienylation and propargylation methods to both inter- and intramolecular one-pot cyclization protocols to efficiently access polycyclic cores. In particular, further studies should focus on cyclization reactions that generate a single stereoisomer as eluted to previously in chapter 3.

3.5 References for Chapter 3:

[1] Locascio, T. M.; Tunge, J. A. "Palladium-Catalyzed Regiodivergent Substitution of Propargylic Carbonates." *manuscript submitted*

For group publications on decarboxylative coupling see:

[2] Mendis, S. N.; Tunge, J. A. "Decarboxylative dearomatization and mono-α-arylation of ketones." *Chem Commun*. **2016**, *52*, 7695-7698

[3] Mendis, S. N.; Tunge, J. A. "Palladium-Catalyzed Stereospecific Decarboxylative Benzylation of Alkynes." *Org. Lett*. **2015**, *17*, 5164-5167.

[4] Lang, S. B.; O'Nele, K. M.; Tunge, J. A. "Decarboxylative Allylation of Amino Alkanoic Acids and Esters via Dual Catalysis." *J. Am. Chem. Soc*. **2014**, *136*, 13606-13609.

[5] Recio III, A.; Heinzman, J. D.; Tunge. J. A. "Decarboxylative Benzylation and Arylation of Nitriles." *Chem. Commun*. **2012**, *48*, 4494-4497.

[6] Weaver, J. D.; Ka, B. J.; Morris, D. K.; Thompson, W.; Tunge, J. A. "Stereospecific Decarboxylative Allylation of Sulfones." *J. Am. Chem. Soc*. **2010**, *132*, 12179-12181.

[7] Grenning, A. J.; Tunge, J. A. "Rapid Decarboxylative Allylation of Nitroalkanes." *Org. Lett.* **2010**, *12*, 740-742.

[8] Weaver, J. D.; Recio, A.; Grenning, A. J.; Tunge, J. A. "Transition Metal-Catalyzed Decarboxylative Allylation and Benzylation Reations." *Chem. Rev.* **2011**, *111*, 1846-1913.

[9] Bienaymé, H. "A New Synthesis of Polyunsaturated Allenic Carbonyls." *Tetrahedron Lett.* **1994**, *35*, 7387-7390.

[10] Behenna, Justin T. Mohr, Nathaniel H. Sherden, Smaranda C. Marinescu, Andrew M. Harned, Kousuke Tani, Masaki Seto, Sandy Ma, Zoltán Novák, Michael R. Krout, Ryan M. McFadden, Jennifer L. Roizen, John A. Enquist Jr., David E. White, Samantha R. Levine, Krastina V. Petrova, Akihiko Iwashita, Scott C. Virgil, Brian M. Stoltz. "Enantioselective Decarboxylative Alkylation Reactions: Catalyst Development, Substrate Scope, and Mechanistic Studies." *Chem. – Eur. J.* **2011**, *17*, 14199-14223.

[11] Ambler, B. R.; Peddi, S.; Altman, R. A. "Copper-Catalyzed Decarboxylative Trifluoromethylation of Propargyl Bromodifluoroacetates. *Synthesis*. **2014**, *46*, 1938-1946.

[12] Zhu, F.-L.; Zou, Y.; Zhang, D.-Y.; Wang, Y.-H.; Hu, X.-H.; Chen, S.; Xu, J.; Hu, X.-P. "Enantioselective Copper-Catalyzed Decarboxylative Propargylic Alkylation of Propargyl β-Ketoesters with Chiral Ketimine." *Angew. Chem. Int. Ed.* **2014**, *53*, 1410-1414.

[13] Zou, Y.; Zhu, F.-L.; Duan, Z.-C.; Wang, Y.-H.; Zhang, D.-Y.; Cao, Z.; Zheng, Z.; Hu, X.-P. "Enantioselective Cu-catalyzed decarboxylative propargylic amination of propargylic carbonates." *Tetrahedron Lett.* **2014**, *55*, 2033-2036.

[14] Shen, R.; Yang, J.; Zhu, S.; Chen, C.; Wu, L. "Gold(I)-Catalyzed Decarboxylation of Propargyl Carbonates: Reactivity Reversal of the Gold Catalyst from π-Lewis Acidity to σ-Lewis Acidity." *Adv. Synth. Catal.* **2015**, *357*, 1259-1269.

[15] (a) Casey, C. P.; Nash, J. R.; Yi, C. S.; Selmeczy, A. D.; Chung, S.; Powell, D. R.; Hayashi, R. K. "Kinetic Addition of Nucleophiles to η3-Propargyl Rhenium Complexes Occurs at the Central Carbon to Produce Rhenacyclobutenes." *J. Am. Chem. Soc.* **1998**, *120*, 722-733. (b) Labrosse, J-R.; Lhoste, P.; Delbecq, F.; Sinou, D. "Palladium-Catalyzed Annulation of Aryl-1,2-diols and Propargylic Carbonates. Theoretical Study of the Observed Regioselectivities." *Eur. J. Org. Chem.* **2003**, 2813-2822.

[16] Kozikowski, A. P.; Kitigawa, Y. "Studies Directed Toward the Total Synthesis of the Rubradirin Antibiotics. 5. A Convenient Preparation of Functionalized Isoprene Units for the Diels-Alder Reaction." *Tetrahedron Lett.* **1982**, *23*, 2087-2090.

[17] Meyer, F. E.; Ang, K. H.; Steinig, A. G.; de Meijere, A. "Sequential Heck and Diels-Alder Reactions: Facile Construction of Bicyclic Systems in a Single Synthetic Operation." *Synlett*. **1994**, 191-193.

[18] Carreño, M. C.; Ruano, J. L. G.; Remor, C. Z.; Urbano, A. "Regio- and stereoselectivity in Diels–Alder reactions of 1,2-disubstituted dienes with enantiopure (SS)-(p-tolylsulfinyl)-1,4-benzoquinones." *Tetrahedron: Asymmetry*. **2000**, *11*, 4279-4296.

[19] Kosior, M.; Malinowska, M.; Jóźwik, J.; Caille, J.-C.; Jurczak, J. "Highly diastereoselective hetero-Diels–Alder reaction of buta-1,3-diene with N-glyoxyloyl-(2R)-bornane-10,2-sultam: an efficient synthesis of homochiral (S)-3-[2-{(methylsulfonyl)oxy}ethoxy]-4-(triphenylmethoxy)- 1-butanol methanesulfonate." *Tetrahedron: Asymmetry*. **2003**, *14*, 239-244.

[20] Zhu, L.; Zhou, C.; Yang, W.; He, S.; Cheng, G.-J.; Zhang, X. "Formal Syntheses of (±)-Platensimycin and (±)-Platencin via a DualMode Lewis Acid Induced Cascade Cyclization Approach." *J. Org. Chem*. **2013**, *78*, 7912-7929.

[21] Tsutsumi, K.; Kawase, T.; Kakiuchi, K.; Ogoshi, S.; Okada, Y.; Kurosawa, H. "Synthesis and Characterization of Some Cationic η3-Propargylpalladium Complexes." *Bull. Chem. Soc. Jpn*. **1999**, *72*, 2687-2692.

[22] Kalek, M.; Stawinski, J. "Novel, Stereoselective and Stereospecific Synthesis of Allenylphosphonates and Related Compounds *via* Palladium-Catalyzed Propargylic Substitution." *Adv. Synth. Catal*. **2011**, *353*, 1741-1755.

[23] Biermann, U.; Bornscheuer, U.; Meier, M. A. R.; Metzger, J. O.; Schaefer, H. J. "Oils and Fats as Renewable Raw Materials in Chemistry." *Angew. Chem. Int. Ed*. **2011**, *50*, 3854-3871.

[24] (a) Tsutsumi, K.; Yabukami, T.; Fujimoto, K.; Kawase, T.; Morimoto, T.; Kakiuchi, K. "Effects of a Bidentate Phosphine Ligand on Palladium-Catalyzed Nucleophilic Substitution Reactions of Propargyl and Allyl Halides with Thiol." *Organometallics*. **2003**, *22*, 2996-2999. (b) Tsutsumi, K.; Ogoshi, S.; Nishiguchi, S.; Kurosawa, H. "Synthesis, Structure, and Reactivity of Neutral η3-Propargylpalladium Complexes." *J. Am. Chem. Soc*. **1998**, *120*, 1938-1939. (c) Tsutsumi, K.; Kawase, K.; Kakiuchi, K.; Ogoshi, S.; Okada, Y.; Kurosawa, H. "Synthesis and Characterization of Some Cationic η3-Propargylpalladium Complexes." *Bull. Chem. Soc. Jpn*. **1999**, *72*, 2687-2692.

[25] Recio, A.; Tunge, J. A. "Regiospecific Decarboxylative Allylation of Nitriles." *Org. Lett*. **2009**, *11*, 5630-5633.

[26] Tsuji, J.; Mandai, T. "Palladium-Catalyzed Reactions of Propargylic Compounds in Organic Synthesis." *Angew. Chem. Int. Ed*. **1995**, *34*, 2589-2612.

Chapter 3 appendix

Experimental methods, spectral analysis and spectra for Ch. 3 compounds.

Table of Contents

General Information:

Purified compounds, unless otherwise stated, were obtained by column chromatography using 60 Å porosity, 230 x 400 mesh standard grade silica gel from Sorbent Technologies. TLC analysis was preformed on silica gel HL TLC plates w/UV254 from Sorbent Technologies. Gas chromatography/mass spectrometry data was obtained using a Shimadzu GCMS-QP2010 SE. NMR spectra were obtained on a Bruker Advance 500 DRX equipped with a QNP cryoprobe. ^{1}H and ^{13}C spectra were normalized using residual undeuterated solvent signals as a reference ($CDCl_3$ = 7.28 ppm for ^{1}H and 77.36 ppm for ^{13}C).[1] ^{19}F NMR spectra were referenced to α,α,α-trifluorotoluene (purchased from Sigma Aldrich) at -62.7 ppm.

N,*N*-Dimethylformamide (DMF) and nitromethane were purchased from Sigma Aldrich and stored in a glove box. Dichloromethane (DCM) and toluene were either purified by an Innovative Technology Pure Solv™ solvent purification system or purchased from Sigma Aldrich and stored in a glove box. Tetrahydrofuran (THF) was purified in a solvent still with sodium and benzophenone and obtained after relux. Bis(dibenzylideneacetone)palladium(0) ($Pd(dba)_2$) was purchased from Strem as were ethylenebis(diphenylphosphine) (dppe) and 2-dicyclohexylphosphino-2'-methylbiphenyl (MePhos). Bis(3,5,3',5'-dimethoxydibenzyli-deneactone)palladium(0) was obtained from Alfa Aesar. All were stored in a glove box. Acetonitrile derivatives were purchased from Sigma Aldrich, Alfa Aesar, VWR, and Acros Organics and used without further purification. N,N'-Carbonyldiimidazole (CDI) was purchased from Matrix Scientific and 2-Butyn-1-ol was purchased from Acros Organics. Both were used without further purification.

Synthesis of Starting Materials:

Synthesis of but-2-yn-1-yl 1H-imidazole-1-carboxylate.[1]

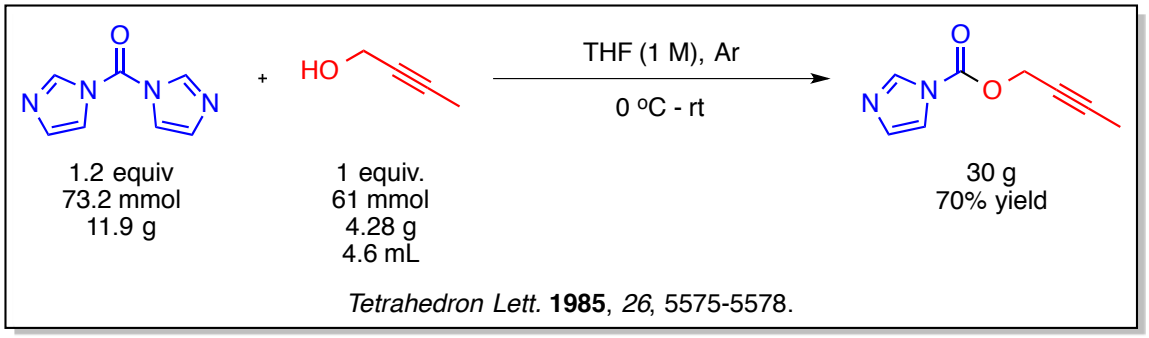

General procedure:

In a 500 mL flame-dried Schlenk flask under an atmosphere of argon, CDI was dissolved in dry THF and cooled to 0 °C. Next, 2-butyn-1-ol was added dropwise and the mixture was allowed to warm to room temperature and stirred overnight. Upon reaction completion, saturated ammonium chloride (75 mL) was added to quench the reaction and the mixture was diluted with distilled water (100 mL) and extracted with ethyl acetate (100 mL x 2) and washed with brine (50 mL). The organic layer was dried over sodium sulfate and concentrated before purification by column chromatography in a gradient of 2% - 5% -10% - 20% ethyl acetate in hexanes.

Synthesis of cyanopropanoate derivatives:[23]

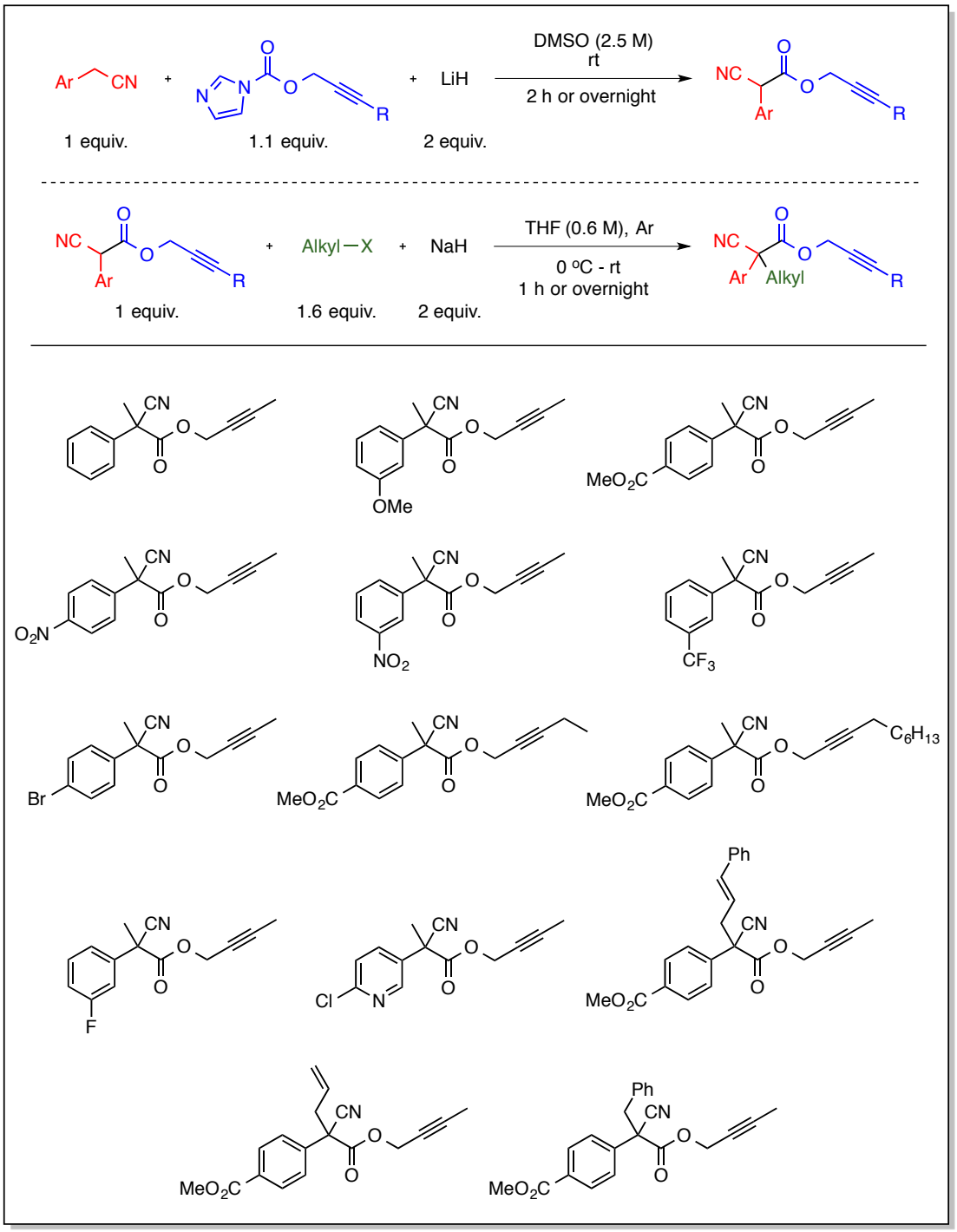

Characterization of cyanopropanoate derivatives:

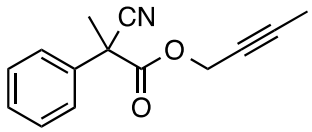

MLM-1-063

^{1}H NMR (500 MHz, $CDCl_3$): δ 7.58 – 7.52 (m, 2H), 7.46 – 7.37 (m, 3H), 4.73 (q, *J* = 2.2 Hz, 2H), 1.99 (s, 3H), 1.83 (t, *J* = 2.4 Hz, 3H).

^{13}C NMR (126 MHz, $CDCl_3$): δ 167.78, 135.71, 129.52, 129.26, 126.15, 119.54, 84.87, 72.09, 55.69, 48.57, 25.26, 4.00

HRMS TAPSI: [M+H] calcd for $C_{14}H_{14}NO_2$: 228.1025. Found: 228.1014.

IR: 3063, 2995, 2945, 2922, 2245, 1747, 1599, 1585, 1492, 1448, 1381, 1224, 1155, 1099, 1078, 1030, 947, 559, 476, 455, 420.

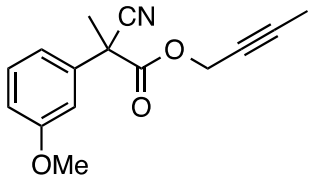

MLM-1-056

^{1}H NMR (500 MHz, $CDCl_3$): δ 7.34 (t, *J* = 8.1 Hz, 1H), 7.11 (ddd, *J* = 7.8, 1.9, 0.8 Hz, 1H), 7.06 (t, *J* = 2.2 Hz, 1H), 6.92 (ddd, *J* = 8.3, 2.5, 0.9 Hz, 1H), 4.73 (q, *J* = 2.4 Hz, 2H), 3.84 (s, 3H), 1.97 (s, 3H), 1.83 (t, *J* = 2.4 Hz, 3H).

^{13}C NMR (126 MHz, $CDCl_3$): δ 167.66, 160.38, 137.14, 130.55, 119.49, 118.30, 114.57, 112.16, 84.88, 72.12, 55.72, 48.53, 25.26, 3.99.

HRMS TAPSI: [M+H] calcd for $C_{15}H_{16}NO_3$: 258.1130. Found: 258.1135.

IR: 3001, 2943, 2922, 2839, 2245, 1755, 1747, 1602, 1585, 1492, 1454, 1435, 1381, 1369, 1319, 1294, 1261, 1224, 1155, 1105, 1091, 1066, 1043, 949, 561, 474, 430, 418.

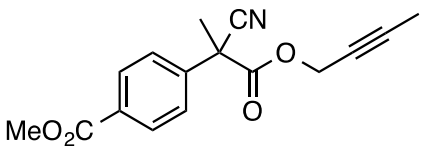

TL5-246

^{1}H NMR (500 MHz, $CDCl_3$): δ 8.11 – 8.07 (m, 2H), 7.65 – 7.61 (m, 2H), 4.74 (qd, *J* = 2.4, 0.9 Hz, 2H), 3.94 (s, 3H), 2.00 (s, 3H), 1.82 (t, *J* = 2.4 Hz, 3H).

^{13}C NMR (126 MHz, $CDCl_3$): δ 167.21, 166.53, 140.31, 131.14, 130.75, 126.36, 119.01, 85.12, 71.89, 55.94, 52.73, 48.63, 25.24, 3.99.

HRMS TAPSI: [M+H] calcd for $C_{16}H_{16}NO_4$: 286.1079. Found: 286.1067.

IR: 2999, 2953, 2924, 2848, 2245, 1755, 1749, 1726, 1610, 1510, 1454, 1435, 1411, 1381, 1371, 1317, 1282, 1224, 1192, 1157, 1112, 1097, 1018, 947, 862, 750, 584, 545, 526, 501, 457, 424.

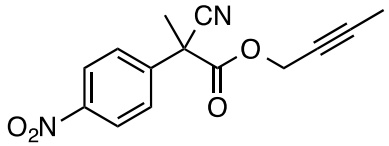

TL5-245

^{1}H NMR (500 MHz, $CDCl_3$): δ 8.28 (d, *J* = 8.5 Hz, 2H), 7.75 (d, *J* = 8.9 Hz, 2H), 4.95 – 4.58 (m, 2H), 2.02 (s, 3H), 1.87 – 1.65 (m, 3H).

^{13}C NMR (126 MHz, $CDCl_3$): δ 166.62, 148.42, 142.23, 127.52, 124.61, 118.41, 85.30, 71.66, 56.17, 48.47, 25.20, 3.91.

HRMS TAPSI: [M+H] calcd for $C_{14}H_{13}N_2O_4$: 273.0875. Found: 273.0869.

IR: 3115, 3084, 2999, 2949, 2924, 2858, 2245, 1766, 1755, 1747, 1732, 1714, 1608, 1599, 1519, 1494, 1446, 1435, 1411, 1384, 1367, 1348, 1323, 1296, 1222, 1157, 1118, 1095, 1064, 1014, 947, 864, 549, 520, 501, 437, 401.

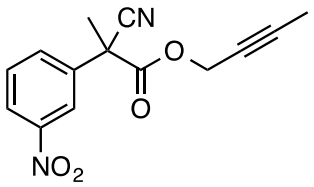

TL7-116

^{1}H NMR (500 MHz, $CDCl_3$): δ 8.40 (t, *J* = 2.0 Hz, 1H), 8.28 (ddd, *J* = 8.2, 2.1, 1.0 Hz, 1H), 7.95 (ddd, *J* = 7.9, 2.0, 1.0 Hz, 1H), 7.66 (t, *J* = 8.0 Hz, 1H), 4.77 (qq, *J* = 15.0, 7.3, 2.4 Hz, 2H), 2.05 (s, 3H), 1.83 (t, *J* = 2.4 Hz, 3H).

^{13}C NMR (126 MHz, $CDCl_3$): δ 166.80, 148.98, 137.82, 132.58, 130.69, 124.42, 121.52, 118.52, 85.48, 71.67, 56.23, 48.28, 25.22, 3.97.

HRMS TAPSI: [M+H] calcd for $C_{14}H_{13}N_2O_4$: 273.0875. Found: 273.0871.

IR: 3090. 2997, 2951, 2924, 2852, 2245, 1747, 1693, 1614, 1531, 1504, 1479, 1435, 1381, 1352, 1311, 1292, 1222, 1155, 1109, 1085, 949, 904, 547, 472, 435.

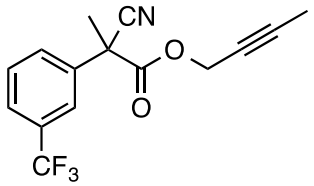

TL6-270

^{1}H NMR (500 MHz, $CDCl_3$): δ 7.81 – 7.75 (m, 2H), 7.70 – 7.65 (m, 1H), 7.63 – 7.53 (m, 1H), 4.76 (qq, *J* = 15.1, 10.1, 2.3 Hz, 2H), 2.01 (s, 3H), 1.82 (td, *J* = 2.4, 1.0 Hz, 3H).

^{13}C NMR (126 MHz, $CDCl_3$): δ 167.12, 136.83, 130.18, 129.82, 126.29 (q, *J* = 3.7 Hz), 123.08 (q, *J* = 3.8 Hz), 118.86, 85.20, 71.77, 55.98, 48.41, 25.31, 3.88.

HRMS TAPSI: [M+H] calcd for $C_{15}H_{13}F_3NO_2$: 296.0898. Found: 296.0889.

IR: 3070. 2997, 2949, 2926, 2858, 2245, 1747, 1616, 1597, 1492, 1440, 1383, 1369, 1329, 1288, 1224, 1170, 1130, 1080, 1016, 1003, 949, 927, 900, 869, 536, 491, 430.

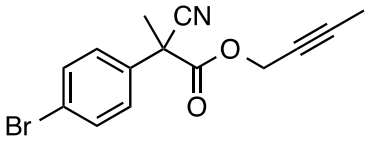

TL6-174

^{1}H NMR (500 MHz, $CDCl_3$): δ 7.59 – 7.51 (m, 2H), 7.46 – 7.40 (m, 2H), 4.73 (q, *J* = 2.3 Hz, 2H), 1.97 (s, 3H), 1.83 (t, *J* = 2.4 Hz, 3H).

^{13}C NMR (126 MHz, $CDCl_3$): δ 167.35, 134.74, 132.66, 128.77, 127.95, 123.63, 119.08, 85.09, 71.93, 55.89, 48.18, 25.12, 4.01.

HRMS TAPSI: [M+H] calcd for $C_{14}H_{13}NO_2Br$: 306.0130. Found: 306.0128.

IR: 2993, 2945, 2922, 2852, 2243, 1747, 1589, 1489, 1454, 1400, 1381, 1369, 1224, 1157, 1095, 1080, 1010, 945, 794, 750, 553, 501, 472, 437, 401.

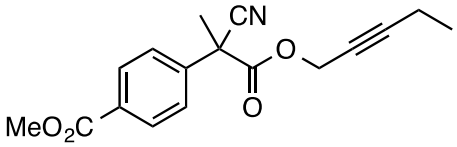

TL6-273

^{1}H NMR (500 MHz, $CDCl_3$): δ 8.17 – 8.03 (m, 2H), 7.70 – 7.59 (m, 2H), 4.75 (qt, *J* = 15.1, 5.4, 2.2 Hz, 2H), 3.94 (s, 3H), 2.19 (qt, *J* = 7.5, 2.2 Hz, 2H), 2.00 (s, 3H), 1.10 (t, *J* = 7.5 Hz, 3H).

^{13}C NMR (126 MHz, $CDCl_3$): δ 167.18, 166.52, 140.35, 131.13, 130.74, 126.36, 119.02, 90.77, 72.05, 55.94, 52.74, 48.62, 25.24, 13.74, 12.73.

HRMS TAPSI: [M+H] calcd for $C_{17}H_{18}NO_4$: 300.1236. Found: 300.1215.

IR: 2980, 2953, 2879, 2845, 2243, 1753, 1724, 1610, 1437, 1410, 1369, 1317, 1282, 1222, 1192, 1151, 1112, 1097, 1018, 964, 943, 750, 547, 501, 472, 437.

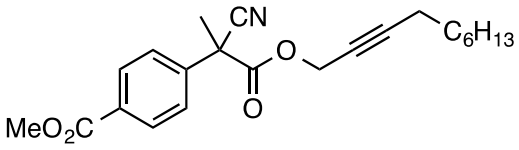

TL6-272

^{1}H NMR (500 MHz, $CDCl_3$): δ 8.11 – 8.07 (m, 2H), 7.65 – 7.60 (m, 2H), 4.76 (qt, *J* = 15.1, 7.9, 2.2 Hz, 2H), 3.94 (s, 3H), 2.17 (tt, *J* = 7.1, 2.2 Hz, 2H), 2.00 (s, 3H), 1.50 – 1.40 (m, 2H), 1.37 – 1.19 (m, 8H), 0.89 (t, *J* = 7.0 Hz, 3H).

^{13}C NMR (126 MHz, $CDCl_3$): δ 166.83, 166.17, 140.03, 130.79, 130.41, 126.03, 118.69, 89.29, 72.33, 55.65, 52.38, 48.30, 31.70, 28.74, 28.24, 24.91, 22.63, 18.68, 14.10.

HRMS TAPSI: [M-H] calcd for $C_{22}H_{28}NO_4$: 370.2018. Found: 370.1997.

IR: 2953, 2929, 2856, 2241, 1749, 1728, 1610, 1435, 1411, 1379, 1369, 1317, 1282, 1222, 1192, 1149, 1112, 1097, 1018, 947, 860.

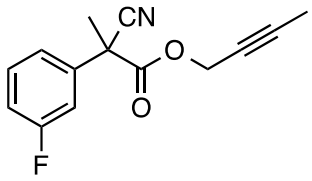

TL6-280

^{1}H NMR (500 MHz, $CDCl_3$): δ 7.45 – 7.38 (m, 1H), 7.35 (ddd, *J* = 7.9, 1.9, 1.0 Hz, 1H), 7.25 (dt, *J* = 9.8, 2.1 Hz, 1H), 7.10 (tdd, *J* = 8.2, 2.5, 1.0 Hz, 1H), 4.74 (qd, *J* = 2.4, 1.7 Hz, 2H), 1.98 (s, 3H), 1.83 (t, *J* = 2.4 Hz, 3H).

^{13}C NMR (126 MHz, $CDCl_3$): δ 167.28, 163.25 (d, *J* = 248.1 Hz), 137.98 (d, *J* = 7.5 Hz), 131.15 (d, *J* = 8.5 Hz), 121.99 (d, *J* = 3.2 Hz), 119.06, 116.43 (d, *J* = 21.2 Hz), 113.74 (d, *J* = 24.0 Hz), 85.12, 71.92, 55.90, 48.29 (d, *J* = 1.9 Hz), 25.21, 3.96.

HRMS TAPSI: [M+H] calcd for $C_{14}H_{13}FNO_2$: 246.0930. Found: 246.0922.

IR: 3078, 2997, 2947, 2924, 2856, 2359, 2339, 2245, 1764, 1755, 1747, 1614, 1593, 1489, 1442, 1381, 1371, 1224, 1180, 1155, 1139, 1101, 949, 887, 783, 667, 518, 484, 470, 422, 418.

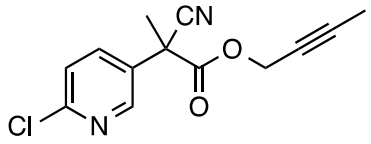

TL6-224

^{1}H NMR (500 MHz, $CDCl_3$): δ 8.60 (dd, *J* = 2.8, 0.7 Hz, 1H), 7.85 (dd, *J* = 8.4, 2.8 Hz, 1H), 7.42 (dd, *J* = 8.5, 0.7 Hz, 1H), 4.80 – 4.72 (m, 2H), 2.02 (s, 3H), 1.84 (t, *J* = 2.4 Hz, 3H).

^{13}C NMR (126 MHz, $CDCl_3$): δ 166.75, 152.72, 147.74, 137.01, 130.70, 124.93, 118.12, 85.51, 71.67, 56.29, 46.34, 25.04, 4.01.

HRMS TAPSI: [M+H] calcd for $C_{13}H_{12}ClN_2O_2$: 263.0587. Found: 263.0580.

IR: 3093, 3063, 2997, 2949, 2922, 2877, 2856, 2324, 2245, 1747, 1732, 1714, 1697, 1680, 1668, 1583, 1564, 1454, 1446, 1433, 1417, 1373, 1217, 1298, 1222, 1155, 1112, 1068, 1016, 947, 412.

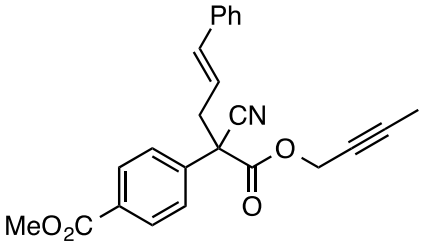

TL7-083

^{1}H NMR (500 MHz, $CDCl_3$): δ 8.13 – 8.08 (m, 2H), 7.71 – 7.66 (m, 2H), 7.35 – 7.22 (m, 5H), 6.60 (d, *J* = 15.8 Hz, 1H), 6.11 (dt, *J* = 15.7, 7.4 Hz, 1H), 4.75 (p, *J* = 2.3 Hz, 2H), 3.94 (s, 3H), 3.32 (ddd, *J* = 14.0, 7.7, 1.2 Hz, 1H), 3.03 (ddd, *J* = 13.9, 7.1, 1.3 Hz, 1H), 1.76 (t, *J* = 2.3 Hz, 3H).

^{13}C NMR (126 MHz, $CDCl_3$): δ 166.53, 166.48, 138.64, 136.95, 136.63, 131.24, 130.73, 128.88, 128.33, 126.87, 126.81, 121.26, 117.65, 85.14, 71.91, 55.91, 54.77, 52.74, 42.20, 3.91.

HRMS TAPSI: [M+H] calcd for $C_{24}H_{22}NO_4$: 388.1549. Found: 388.1543.

IR: 3082, 3061, 3028, 3003, 2953, 2922, 2850, 2243, 1747, 1728 1716, 1610, 1575, 1496, 1435, 1410, 1371, 1317, 1282, 1246, 1211, 1161, 1112, 1072, 1020, 968, 933, 547, 536, 489, 472, 424.

Dienylation Reaction Optimization:

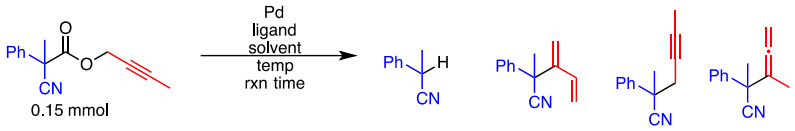

cat.	mol %	ligand	mol %	additive	mol%	solvent	mL	temp	time	sm %	A%	B%	C% and D%	
$Pd(dba)_2$	10	MePhos	10	---		DMF	0.5	40	1h	37	18	22	23	
$Pd(dba)_2$	2.5	MePhos	2.5	---		DMF	0.5	80	1h	58	20	6	16	
$Pd_2(dba)_3$	5	Dppe	10	---		DMF	0.5	100	1h	83	15	3	0	
$Pd(dba)_2$	10	Dppe	10	---		DMF	0.5	100	6h	0	5	83	12	
$Pd(dba)_2$	2.5	Dppe	2.5	---		DMF	0.5	100	6h	88	11	1	0	
$Pd(dba)_2$	10	dppe	10	---		DMF	1	150mw	10m	0	17	69	14	37% yield
$Pd(dba)_2$	10	dppe	10	---		DMF	1	150mw	4m	0	15	71	14	30% GC/MS yield w xylene
$Pd(dba)_2$	10	dppe	10	---		DMF	1	150mw	1m	0	13	73	14	40% isolated yield
$Pd(dba)_2$	10	dppe	10	---		DMF	1	100mw	5m	72	11	16	2	
$Pd(dba)_2$	10	dppe	10	---		DMF	1	120mw	1m	0	5	86	10	40% by GC/MS yield w xylene
$Pd(dba)_2$	10	dppe	10	$NaHCO_3$	1	DMF	1	120mw	1m	23	7	62	8	
$Pd(dba)_2$	10	dppe	10	---	--	DMF	0.25	120mw	1m	68	10	13	9	
$Pd(dba)_2$	10	dppe	10	morphiline	1	DMF	1	100	4h	only	protonated		material	
$Pd(dba)_2$	10	dppe	10	Bu_2NH	1	DMF	1	100	4h	0	77	23	0	
$Pd(dba)_2$	10	dppe	10	Bz_2NH	1	DMF	1	100	4h	0	74	23	2	
$Pd(dba)_2$	10	dppe	10	pyrrolidine	1	DMF	1	100	4h	0	61	39	0	
$Pd(dba)_2$	10	dppe	10	Azocane	1	DMF	1	100	4h	0	65	14	21	
$Pd(dba)_2$	10	dppe	10	iPr_2NH	1	DMF	1	100	4h	0	8	92	0	
$Pd(dba)_2$	10	dppe	10	TBD	1	DMF	1	100	4h	0	94	6	0	
$Pd(dba)_2$	10	dppe	10	K_2HPO_4	1	DMF	1	100	4h	0	5	95	0	
$Pd(dba)_2$	10	dppe	10	$NaHCO_3$	1	DMF	1	100	4h	0	11	89	0	
$Pd(dba)_2$	10	dppe	10	2,4,6trimephol	1	DMF	1	100	4h	0	40	60%	pdt w mass of 188	
$Pd(dba)_2$	10	dppe	10	2nitroethanol	1	DMF	1	100	4h	62	38	0	0	
$Pd(dba)_2$	10	dppe	10	triFethanol	1	DMF	1	100	4h	very	Very	messy		
$Pd(dba)_2$	10	dppe	10	2,6tbu4mephol	1	DMF	1	100	4h	0	23	5	71	
$Pd(dba)_2$	10	dppe	10	2,6iPrphenol	1	DMF	1	100	4h	0	35	5	60	
$Pd(dba)_2$	10	dppe	10	benzoic acid	1	DMF	1	100	4h	48	47	0	5	
$Pd(dba)_2$	10	dppe	10	MeOH	1	DMF	1	100	4h	0	22	54	14	
$Pd(dba)_2$	10	dppe	10	H_2O	1	DMF	1	100	4h	0	61	39	0	
$Pd(dba)_2$	10	dppe	10	tbutanol	1	DMF	1	100	4h	0	8	92	0	
$Pd(dba)_2$	10	dppe	10	tbutanol	1	DMF	1	100	3h	0	50	50	0	
$Pd(dba)_2$	10	dppe	10	K_2HPO_4	1	DMF	1	100	3h	59	19	22	0	GC/MS internal std 1:1 std:pdts/sm

determined by GC/MS analysis

Experimental procedure for the dienylation and propargylation of cyanopropanoate derivatives:

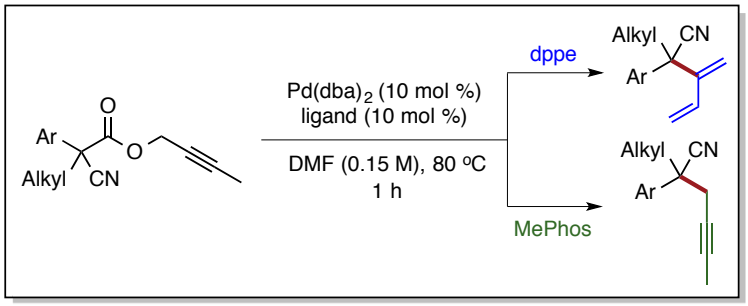

In an oven or flamed dried Biotage microwave reaction vial (part no. 354624) equipped with a magnetic stir bar, catalyst (10 mol % $Pd(dba)_2$), ligand (10 mol % dppe or 10 mol % MePhos) were added under an argon atmosphere in a glovebox. The solid mixture was dissolved in 2 mL anhydrous DMF followed by addition of cyanopropanoate (0.3 mmol). The vessel was sealed, removed from the glovebox, and placed in a preheated oil bath at 80 °C for 1 hr. After reaction completion, the vessel was unsealed and the crude product was placed directly on silica gel for purification via column chromatography in 1%-10% EtOAc:Hexane.

Characterization of dienylated and propargylated tertiary nitriles:

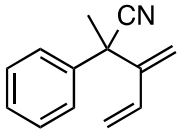

TL7-091

^{1}H NMR (500 MHz, $CDCl_3$): δ 7.46 – 7.30 (m, 5H), 6.09 (dd, *J* = 17.5, 11.2 Hz, 1H), 5.56 (s, 1H), 5.46 (s, 1H), 5.33 (d, *J* = 17.0 Hz, 1H), 5.11 (d, *J* = 11.1 Hz, 1H), 1.86 (s, 3H).

^{13}C NMR (126 MHz, $CDCl_3$): δ 145.59, 139.59, 134.32, 129.31, 128.31, 126.34, 122.64, 118.41, 115.58, 77.11, 45.81, 27.60.

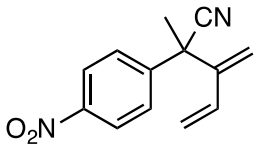

TL6-019

^{1}H NMR (500 MHz, $CDCl_3$): δ 8.27 – 8.22 (m, 2H), 7.66 – 7.59 (m, 2H), 6.09 (dd, *J* = 17.5, 11.2 Hz, 1H), 5.64 (s, 1H), 5.52 (s, 1H), 5.26 (d, *J* = 17.5 Hz, 1H), 5.14 (d, *J* = 11.2 Hz, 1H), 1.89 (s, 3H).

^{13}C NMR (126 MHz, $CDCl_3$): δ 147.86, 146.86, 144.26, 133.82, 127.44, 124.58, 121.43, 119.16, 117.17, 45.62, 27.67.

HRMS: $[M+H]^+$ calcd for $C_{13}H_{13}N_2O_2$: 229.0977. Found: 229.0977.

IR: 3109, 3082, 2991, 2943, 2858, 2237, 1633, 1604, 1595, 1531, 1519, 1494, 1462, 1454, 1427, 1410, 1392, 1346, 1317, 1296, 1209, 1188, 1153, 1112, 1085, 1066, 1014, 989, 923, 862, 559, 420.

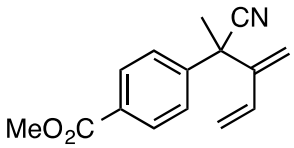

TL6-018

^{1}H NMR (500 MHz, $CDCl_3$): δ 8.10 – 8.00 (m, 2H), 7.56 – 7.46 (m, 2H), 6.07 (dd, *J* = 17.7, 11.0 Hz, 1H), 5.58 (s, 1H), 5.47 (s, 1H), 5.27 (d, *J* = 17.5 Hz, 1H), 5.10 (d, *J* = 11.2 Hz, 1H), 3.92 (s, 3H), 1.86 (s, 3H).

^{13}C NMR (126 MHz, $CDCl_3$): δ 166.66, 144.86, 144.58, 134.05, 130.21, 126.38, 121.98, 118.71, 116.38, 52.55, 45.71, 27.54.

HRMS: $[M+H]^+$ calcd for $C_{15}H_{15}NO_2$: 242.1181. Found: 242.1162.

IR: 3095, 2991, 2953, 2926, 2848, 2237, 1728, 1714, 1633, 1608, 1597, 1575, 1454, 1435, 1410, 1392, 1373, 1313, 1282, 1190, 1151, 1114, 1087, 1018, 989, 966, 920, 476, 432, 420.

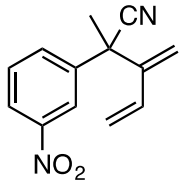

TL6-247

^{1}H NMR (500 MHz, $CDCl_3$): δ 8.24 (t, *J* = 2.0 Hz, 1H), 8.21 (ddd, *J* = 8.1, 2.2, 1.0 Hz, 1H), 7.85 (ddd, *J* = 7.8, 2.0, 1.0 Hz, 1H), 7.61 (t, *J* = 8.0 Hz, 1H), 6.09 (dd, *J* = 17.5, 11.2 1H), 5.65 (s, 1H), 5.54 (s, 1H), 5.30 (d, *J* = 17.5 Hz, 1H), 5.15 (d, *J* = 11.2 Hz, 1H), 1.92 (s, 3H).

^{13}C NMR (126 MHz, $CDCl_3$): δ 149.01, 144.32, 142.04, 133.70, 132.66, 130.50, 123.55, 121.52, 121.40, 119.24, 117.12, 45.53, 27.53.

HRMS TAPSI: [M+H] calcd for $C_{13}H_{13}N_2O_2$: 229.0977. Found: 229.0972.

IR: 3091, 3076, 2989, 2928, 2874, 2237, 1631, 1612, 1593, 1583, 1531, 1479, 1456, 1433, 1352, 1309, 1290, 1211, 1107, 989, 920, 671, 632, 611, 592, 567, 545, 489, 420.

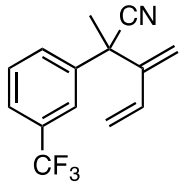

TL6-052

^{1}H NMR (500 MHz, $CDCl_3$): δ 7.69 – 7.63 (m, 2H), 7.62 – 7.57 (m, 1H), 7.53 (tt, *J* = 7.7, 0.8 Hz, 1H), 6.08 (dd, *J* = 17.5, 11.1 Hz, 1H), 5.62 (s, 1H), 5.50 (s, 1H), 5.30 (d, *J* = 17.4 Hz, 1H), 5.14 (d, *J* = 11.1 Hz, 1H), 1.89 (s, 3H).

^{13}C NMR (126 MHz, $CDCl_3$): δ 144.80, 140.85, 133.92, 131.82 (q, *J* = 32.6 Hz), 129.96, 129.93 (d, *J* = 1.4 Hz), 125.37 (q, *J* = 3.8 Hz), 124.08 (q, *J* = 273.0 Hz), 123.12 (q, *J* = 3.8 Hz), 121.91, 118.95, 116.54, 45.66, 27.62.

HRMS: $[M+H]^+$ calcd for $C_{15}H_{13}F_3NO_2$: 296.0898. Found: 296.0868.

IR: 3102, 2990, 2936, 2851, 2500, 2241, 1599, 1493, 1441, 1329, 1287, 1202, 1169, 1128, 1072, 914, 804, 706, 662.

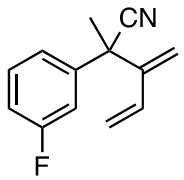

TL7-087

^{1}H NMR (500 MHz, $CDCl_3$): δ 7.37 (td, *J* = 8.0, 5.9 Hz, 1H), 7.28 – 7.24 (m, 1H), 7.11 (dt, *J* = 10.0, 2.2 Hz, 1H), 7.03 (tdd, *J* = 8.2, 2.5, 0.9 Hz, 1H), 6.09 (dd, *J* = 17.5, 11.2 Hz, 1H), 5.58 (s, 1H), 5.47 (s, 1H), 5.33 (d, *J* = 17.5 Hz, 1H), 5.13 (d, *J* = 11.2 Hz, 1H), 1.86 (s, 3H).

^{13}C NMR (126 MHz, $CDCl_3$): δ 163.02 (d, *J* = 247.5 Hz), 144.74, 141.89 (d, *J* = 7.2 Hz), 133.73, 130.60 (d, *J* = 8.3 Hz), 121.79, 121.77, 118.38, 115.76, 115.11 (d, 20.9 Hz), 113.37 (d, 23.5 Hz), 45.25, 27.20.

HRMS TAPSI: [M+H] calcd for $C_{13}H_{13}FN$: 202.1032. Found: 202.1024.

IR: 3091, 3063, 2989, 2926, 2852, 2237, 1614, 1591, 1487, 1440, 1392, 1379, 1273, 1251, 1172, 1159, 1145, 1093, 1074, 987, 923, 879, 750, 644, 501, 472, 457, 449, 428, 401.

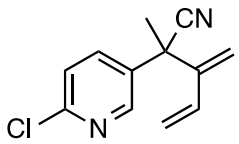

TL7-086

^{1}H NMR (500 MHz, $CDCl_3$): δ 8.45 (dd, *J* = 2.8, 0.7 Hz, 1H), 7.70 (dd, *J* = 8.4, 2.7 Hz, 1H), 7.36 (dd, *J* = 8.5, 0.8 Hz, 1H), 6.09 (dd, *J* = 17.3, 11.0 Hz, 1H), 5.62 (s, 1H), 5.49 (s, 1H), 5.32 (d, *J* = 17.5 Hz, 1H), 5.18 (d, *J* = 11.2 Hz, 1H), 1.89 (s, 3H).

^{13}C NMR (126 MHz, $CDCl_3$) δ 151.69, 147.91, 144.14, 137.13, 134.57, 133.56, 124.82, 121.20, 119.40, 116.87, 43.57, 27.37.

HRMS TAPSI: [M+H] calcd for $C_{12}H_{12}ClN$: 219.0684. Found: 219.0677.

IR: 3095, 3055, 2989, 2926, 2850, 2237, 1633, 1583, 1562, 1462, 1456, 1371, 1141, 1111, 1016, 987, 918, 553, 476, 455, 420, 403.

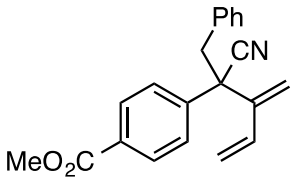

TL7-077

^{1}H NMR (500 MHz, $CDCl_3$): δ 8.00 – 7.96 (m, 2H), 7.34 – 7.29 (m, 2H), 7.25 – 7.14 (m, 3H), 6.92 – 6.87 (m, 2H), 6.09 (dd, *J* = 17.5, 11.2 Hz, 1H), 5.66 (s, 1H), 5.55 (s, 1H), 5.33 (d, *J* = 17.4 Hz, 1H), 5.12 (d, *J* = 11.2 Hz, 1H), 3.93 (s, 3H), 3.55 (d, *J* = 12.9 Hz, 1H), 3.28 (d, *J* = 12.9 Hz, 1H).

^{13}C NMR (126 MHz, $CDCl_3$): δ 166.77, 144.45, 142.42, 134.52, 134.18, 130.84, 130.24, 130.21, 128.30, 127.78, 127.43, 120.45, 118.81, 116.57, 52.58, 52.29, 44.23.

HRMS TAPSI: [M+H] calcd for $C_{21}H_{20}NO_2$: 318.1494. Found: 318.1479.

IR: 3063, 3032, 2951, 2359, 2341, 2239, 1732, 1714, 1681, 1633, 1608, 1573, 1496, 1454, 1435, 1410, 1313, 1284, 1240, 1188, 1159, 1112, 1085, 1020, 989, 964, 920, 667, 557, 439.

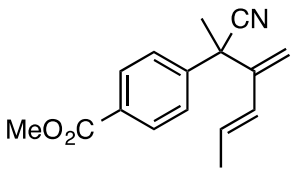

TL6-289

^{1}H NMR (500 MHz, $CDCl_3$): δ 8.08 – 8.02 (m, 2H), 7.54 – 7.48 (m, 2H), 5.85 – 5.71 (m, 2H), 5.46 (s, 1H), 5.33 (s, 1H), 3.93 (s, 3H), 1.85 (s, 3H), 1.64 (d, J = 5.5 Hz, 3H).

^{13}C NMR:

HRMS TAPSI: [M+H] calcd for $C_{16}H_{18}NO_2$: 256.1338. Found: 256.1328.

IR: 3059, 3989, 253, 2887, 2850, 2237, 1766, 1726, 1608, 1573, 1508, 1435, 1410, 1371, 1315, 1280, 1190, 1114, 1060, 1018, 964, 750, 551, 437, 424.

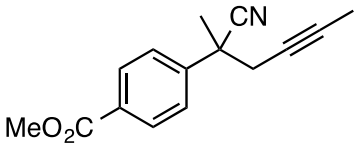

TL6-236

Impure with 23% methyl 4-acetylbenzoate

^{1}H NMR (500 MHz, $CDCl_3$): δ 8.09 – 8.04 (m, 2H), 7.61 – 7.53 (m, 2H), 3.93 (s, 3H), 2.75 (qq, J = 16.6, 7.6, 2.5 Hz, 2H), 1.83 (s, 3H), 1.78 (t, J = 2.5 Hz, 3H).

^{13}C NMR (126 MHz, $CDCl_3$): δ 166.74, 144.43, 130.41, 128.53, 126.14, 122.80, 80.97, 73.00, 52.61, 42.51, 33.18, 26.07, 3.82.

HRMS TAPSI: [M+H] calcd for $C_{15}H_{16}NO_2$: 242.1181. Found: 242.1172.

IR: 2989, 2953, 2922, 2850, 2239, 1728, 1716, 1693, 1612, 1573, 1435, 1410, 1315, 1282, 1192, 1114, 1018, 964, 750, 536, 437, 430, 412, 401.

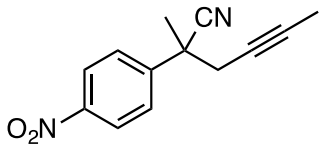

TL6-253

95% pure

^{1}H NMR (500 MHz, $CDCl_3$): δ 8.29 – 8.24 (m, 2H), 7.71 – 7.65 (m, 2H), 2.80 (q, *J* = 2.5 Hz, 2H), 1.85 (s, 3H), 1.77 (t, *J* = 2.5 Hz, 3H).

^{13}C NMR (126 MHz, $CDCl_3$): δ 147.95, 146.49, 127.30, 124.33, 122.25, 81.53, 72.49, 42.47, 33.13, 26.11, 3.79.

HRMS TAPSI: [M+H] calcd for $C_{13}H_{13}N_2O_2$: 229.0977. Found: 229.0967.

IR: 3082, 2987, 2939, 2922, 2856, 2239, 1693, 1604, 1599, 1519, 1496, 1454, 1435, 1410, 1379, 1346, 1319, 1298, 1273, 1190, 1112, 1093, 1062, 1014, 858.

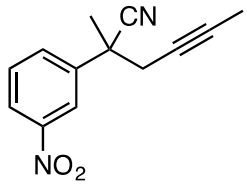

MLM-1-088

^{1}H NMR (500 MHz, $CDCl_3$): δ 8.36 (t, *J* = 2.0 Hz, 1H), 8.24 (ddd, *J* = 8.2, 2.2, 1.0 Hz, 1H), 7.90 (ddd, *J* = 7.9, 2.0, 1.0 Hz, 1H), 7.62 (t, *J* = 8.04 Hz, 1H), 2.81 (q, *J* = 2.5 Hz, 2H), 1.88 (s, 3H), 1.78 (t, *J* = 2.5 Hz, 3H).

^{13}C NMR (126 MHz, $CDCl_3$): δ 148.78, 141.66, 132.60, 130.26, 123.65, 122.34, 121.20, 81.75, 72.52, 42.13, 33.32, 25.96, 3.81.

GC/MS: calc: 228.3. Found 228.1.

IR: 3363, 3242, 3208, 3165, 3090, 2987, 2918, 2848, 2252, 2239, 1531, 1454, 1435, 1352, 1271, 1111, 912.

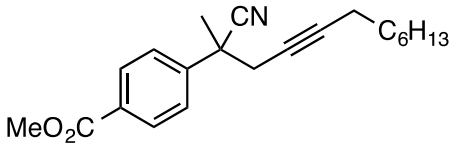

TL6-286

^{1}H NMR (500 MHz, $CDCl_3$): δ 8.09 – 8.03 (m, 2H), 7.59 – 7.53 (m, 2H), 3.92 (s, 3H), 2.78 (qt, *J* = 16.6, 3.0, 2.4 Hz, 2H), 2.11 (tt, *J* = 7.1, 2.4 Hz, 2H), 1.82 (s, 3H), 1.42 (p, *J* = 6.9 Hz, 2H), 1.34 – 1.17 (m, 8H), 0.88 (t, *J* = 7.1 Hz, 3H).

^{13}C NMR (126 MHz, $CDCl_3$): δ 166.69, 144.43, 130.34, 130.27, 126.17, 122.76, 85.74, 73.84, 52.56, 42.53, 33.19, 32.03, 29.08, 28.99, 28.92, 26.04, 22.93, 18.88, 14.39.

HRMS TAPSI: [M-H] calcd for $C_{21}H_{28}NO_2$: 326.2120. Found: 326.2104.

IR: 2953, 2929, 2856, 2239, 1732, 1714, 1681, 1612, 1575, 1512, 1454, 1435, 1410, 1379, 1315, 1284, 1246, 1192, 1112, 1064, 1018, 966, 856, 472, 406, 399.

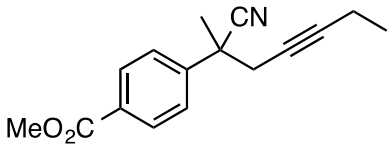

TL6-290

^{1}H NMR (500 MHz, $CDCl_3$): δ 8.12 – 7.99 (m, 2H), 7.62 – 7.52 (m, 2H), 3.93 (s, 3H), 2.76 (qt, *J* = 16.5, 4.6, 2.4 Hz, 2H), 2.14 (qt, *J* = 7.5, 2.4 Hz, 2H), 1.83 (s, 3H), 1.08 (t, *J* = 7.5 Hz, 3H).

^{13}C NMR (126 MHz, $CDCl_3$): δ 166.73, 144.41, 130.35, 130.30, 126.18, 122.76, 87.03, 73.27, 52.58, 42.51, 33.19, 25.94, 14.19, 12.63.

HRMS TAPSI: [M+H] calcd for $C_{16}H_{18}NO_2$: 256.1338. Found: 256.1326.

IR: 3061, 2980, 2953, 2939, 2918, 2879, 2847, 2239, 1934, 1805, 1732, 1714, 1612, 1575, 1552, 1512, 1454, 1435, 1410, 1379, 1317, 1284, 1192, 1114, 1062, 1018, 966, 943, 858, 547, 491, 449, 437.

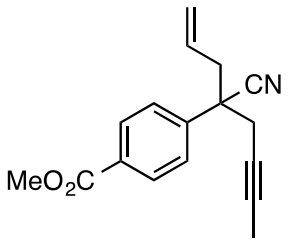

TL7-076

^{1}H NMR (500 MHz, $CDCl_3$): δ 8.11 – 8.04 (m, 2H), 7.60 – 7.51 (m, 2H), 5.65 (dddd, *J* = 17.1, 10.2, 7.5, 6.9 Hz, 1H), 5.25 – 5.10 (m, 2H), 3.93 (s, 3H), 2.96 – 2.69 (m, 4H), 1.76 (t, *J* = 2.5 Hz, 3H).

^{13}C NMR (126 MHz, $CDCl_3$): δ 166.75, 142.65, 131.28, 130.34, 130.32, 126.76, 121.45, 121.22, 81.20, 72.76, 52.60, 47.68, 43.17, 31.06, 3.83.

HRMS TAPSI: [M+H] calcd for $C_{17}H_{18}NO_2$: 268.1338. Found: 268.1330.

IR: 3080, 2953, 2922, 2852, 2239, 1728, 1714, 1643, 1612, 1435, 1410, 1317, 1284, 1247, 1193, 1112, 1020, 993, 964, 929, 750, 545, 472, 406.

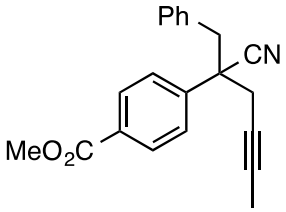

TL7-079

78% pure isolated with 22% protonated pdt

^{1}H NMR (500 MHz, $CDCl_3$): δ 8.07 – 8.02 (m, 2H), 7.49 – 7.44 (m, 2H), 7.26 – 7.20 (m, 3H), 7.06 – 7.01 (m, 2H), 3.95 (s, 3H), 3.42 (d, *J* = 13.5 Hz, 1H), 3.27 – 3.22 (m, 1H), 2.90 (qq, *J* = 16.6, 6.6, 2.6 Hz, 2H), 1.81 (t, *J* = 2.5 Hz, 3H).

^{13}C NMR (126 MHz, $CDCl_3$): δ 166.78, 142.60, 134.41, 130.62, 130.56, 130.15, 128.56, 127.89, 127.02,121.49, 81.43, 73.02, 52.59, 49.08, 45.33, 30.15, 3.89.

HRMS TAPSI: [M+H] calcd for $C_{21}H_{20}NO_2$: 318.1494. Found: 318.1489.

IR: 3063, 3032, 3005, 2953, 2922, 2854, 2241, 1722, 1716, 1610, 1573, 1496, 1454, 1454, 1435, 1410, 1317, 1282, 1192, 1112, 1087, 1020, 966, 856, 547, 516, 474, 461, 435, 412.

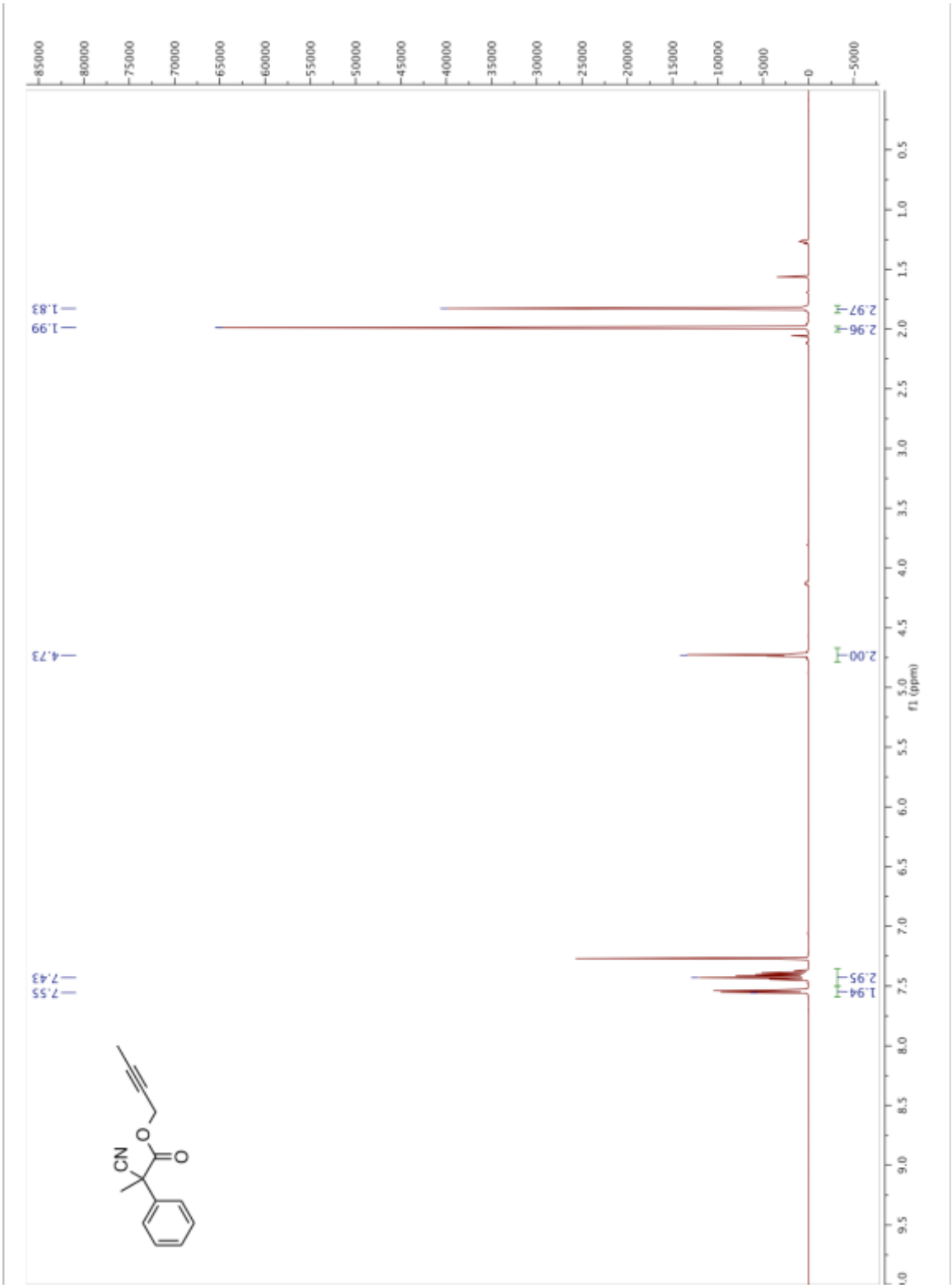
7.43
7.55
4.73
1.99
1.83
2.95
1.94
2.00
2.97
2.96
f1 (ppm)
CN
O
O

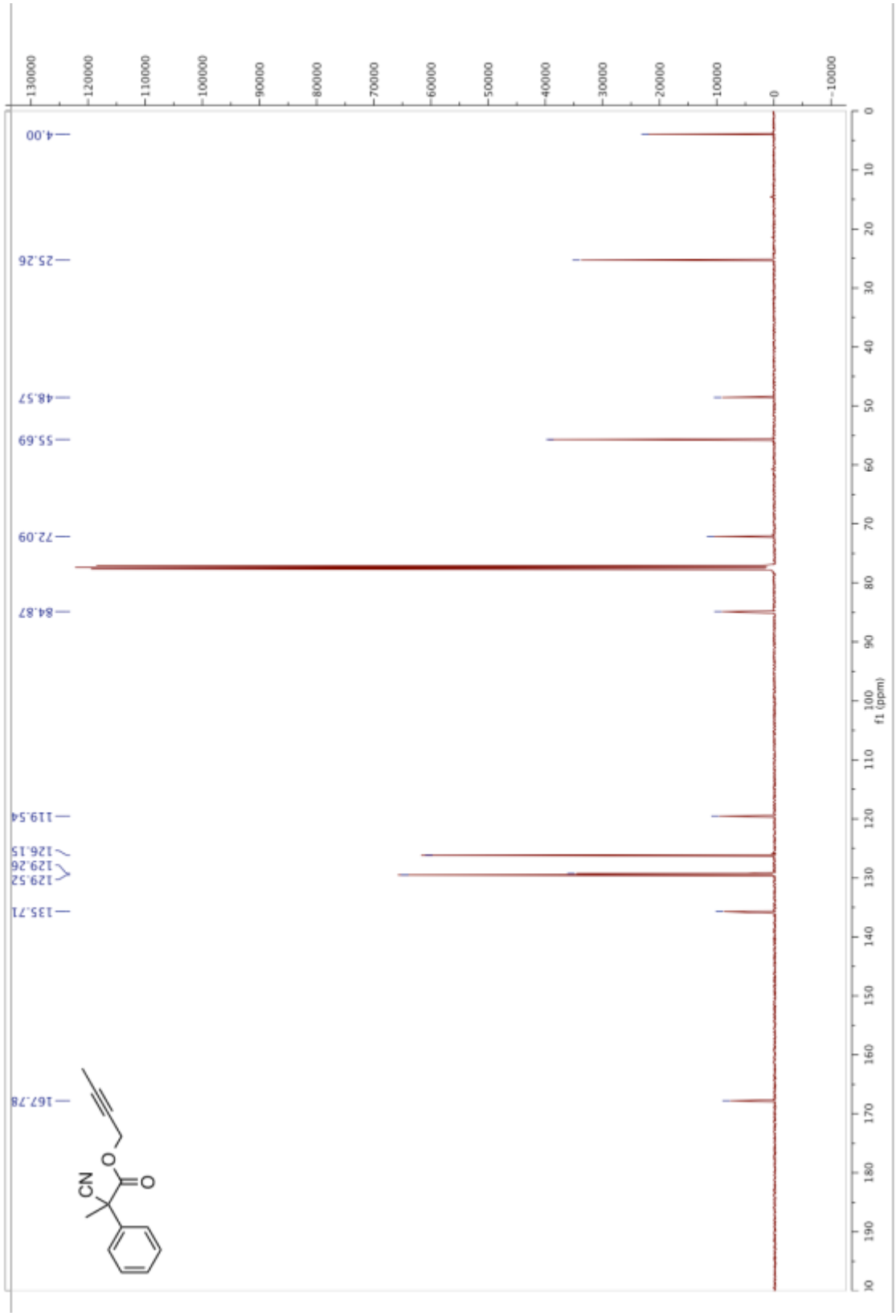
4.00
25.26
48.57
55.69
72.09
84.87
119.54
126.15
129.26
129.52
135.71
167.78
CN
O
O
f1 (ppm)

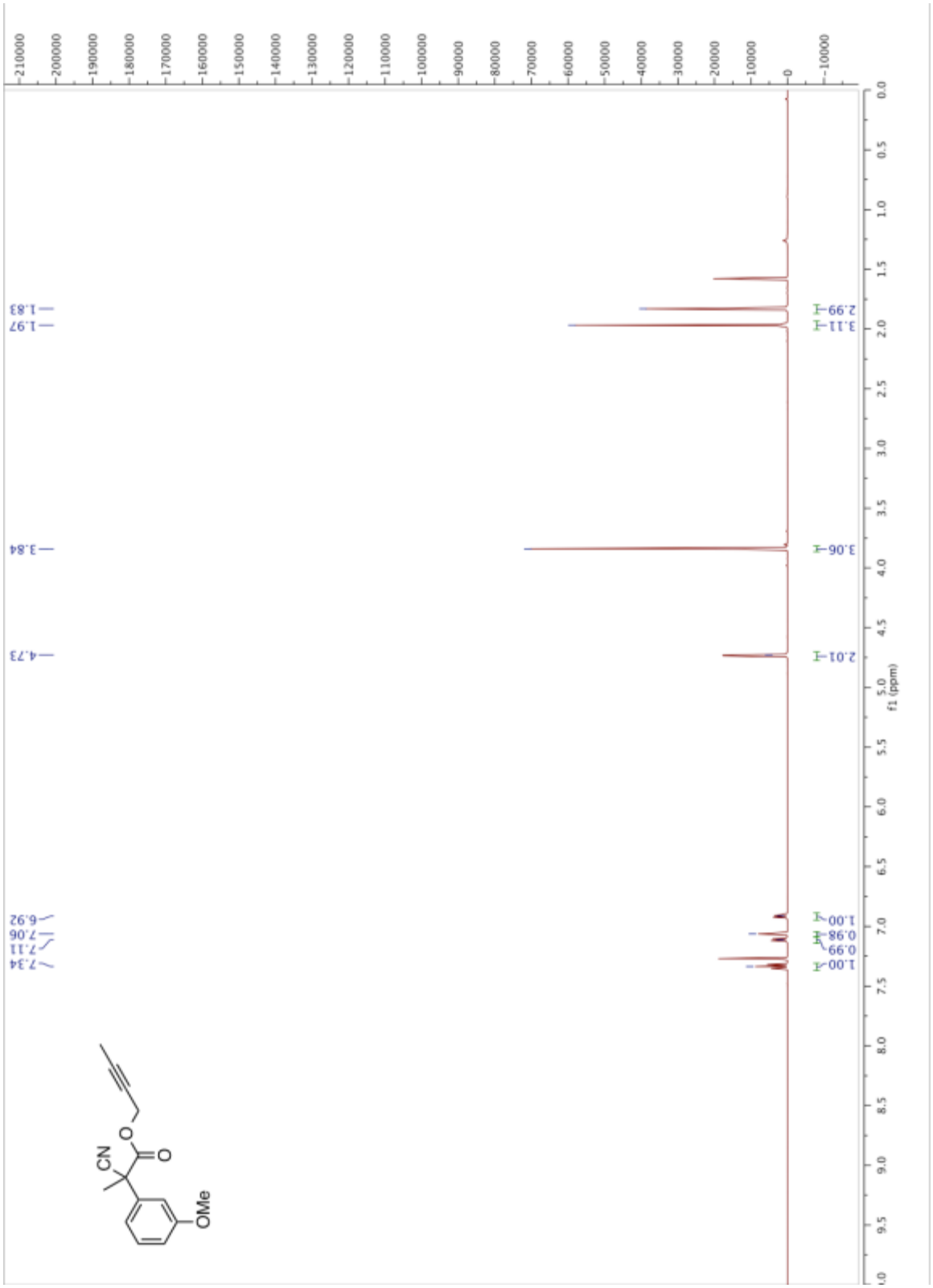
1.83
1.97
3.84
4.73
6.92
7.06
7.11
7.34
2.99
3.11
3.06
2.01
1.00
0.98
0.99
1.00
f1 (ppm)
CN
O
O
OMe

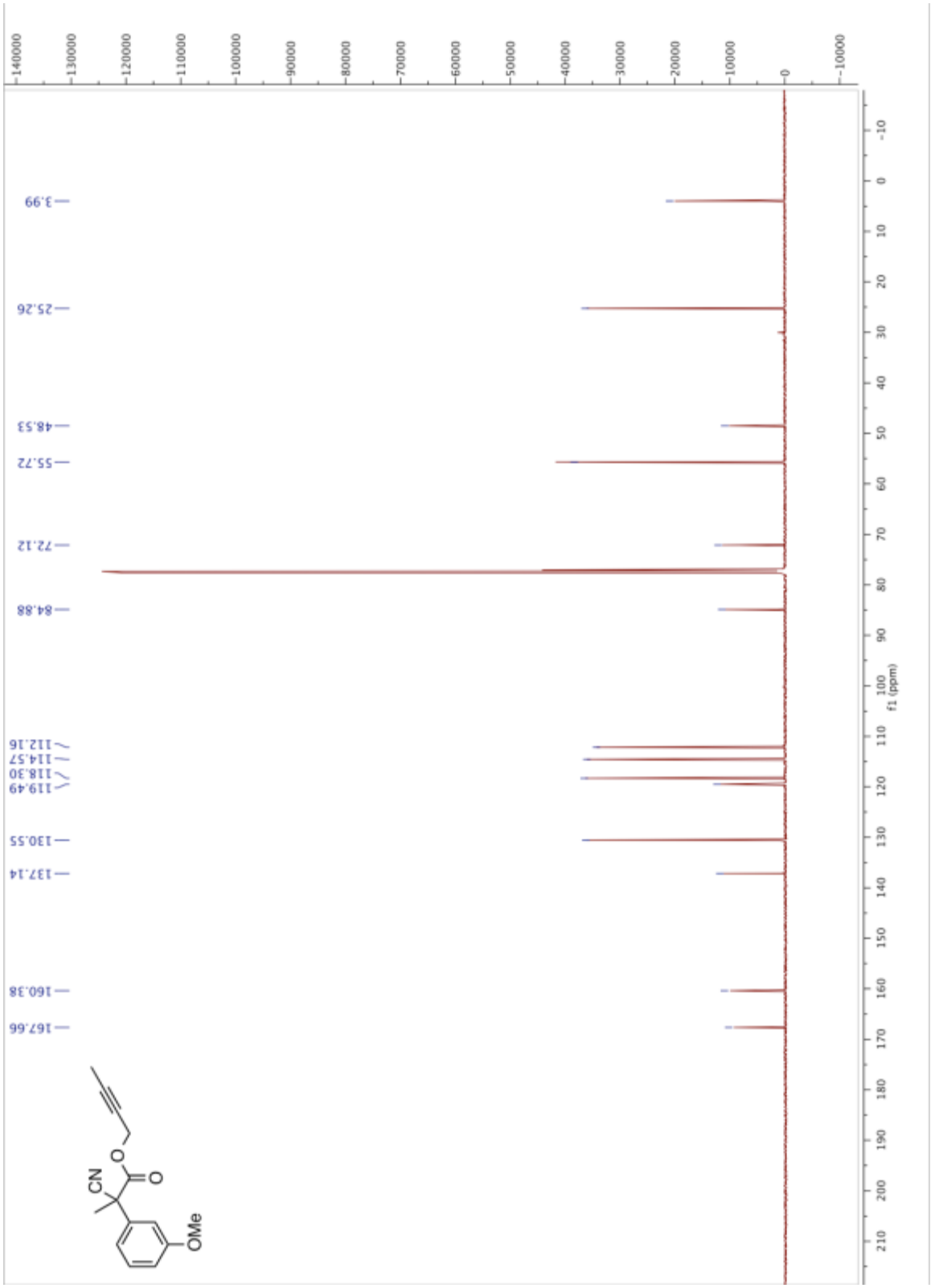
3.99
25.26
48.53
55.72
72.12
84.88
112.16
114.57
118.30
119.49
130.55
137.14
160.38
167.66
CN
O
O
OMe
f1 (ppm)

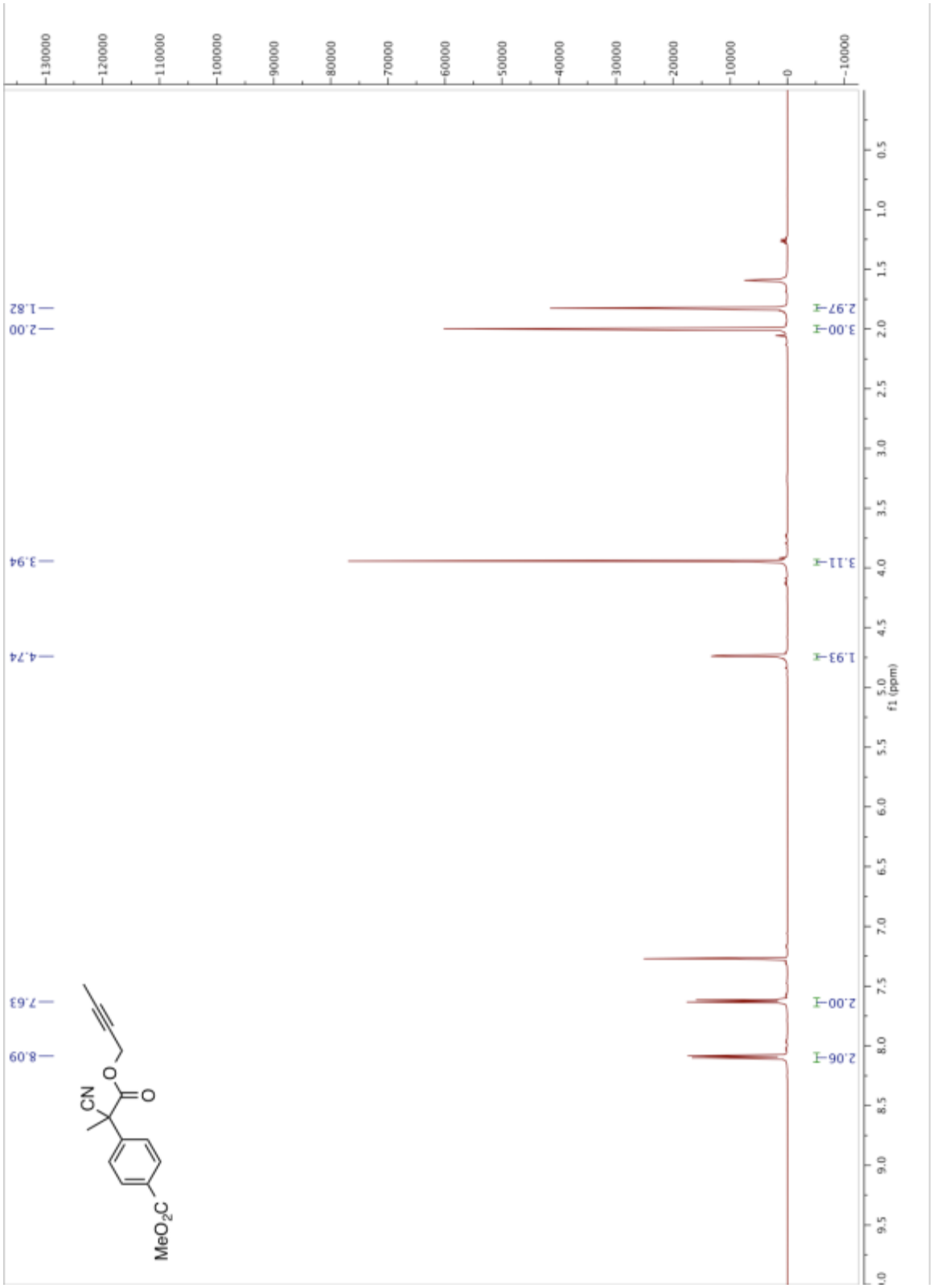
1.82
2.00
3.94
4.74
7.63
8.09
2.97
3.00
3.11
1.93
2.00
2.06
f1 (ppm)
CN
O
O
MeO2C

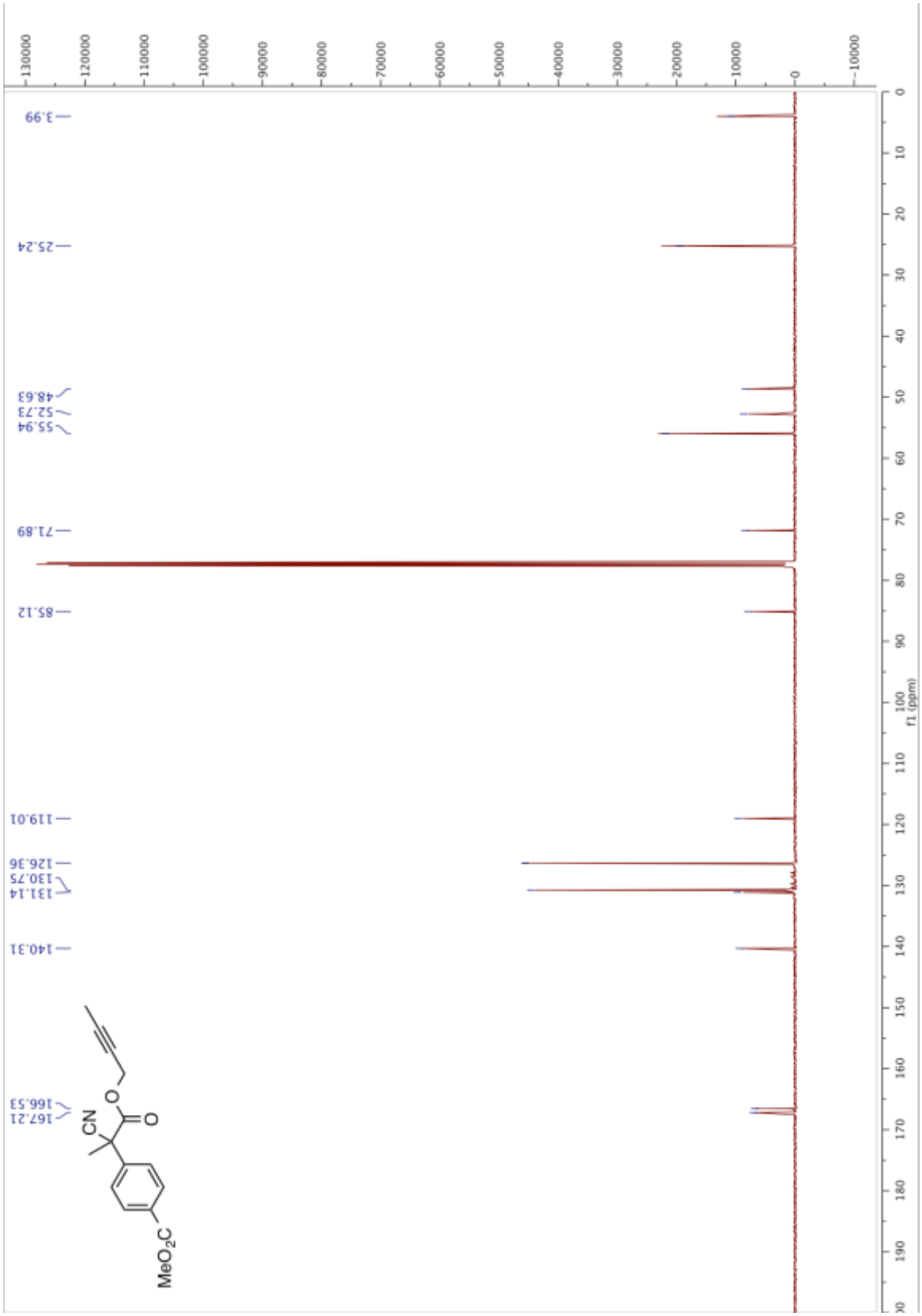
3.99
25.24
48.63
52.73
55.94
71.89
85.12
119.01
126.36
130.75
131.14
140.31
166.53
167.21
CN
O
O
MeO2C
f1 (ppm)

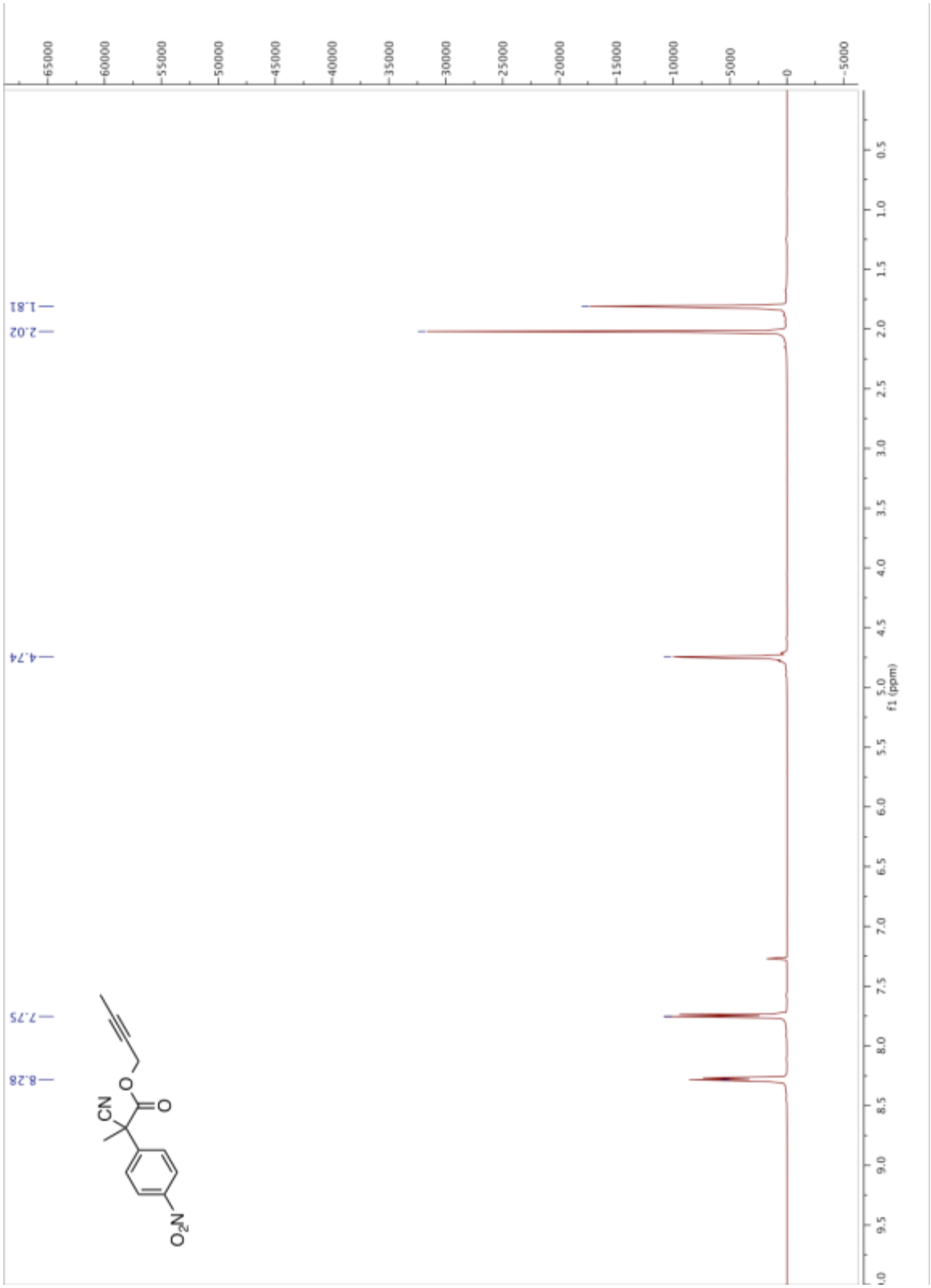
1.81
2.02
4.74
7.75
8.28
f1 (ppm)

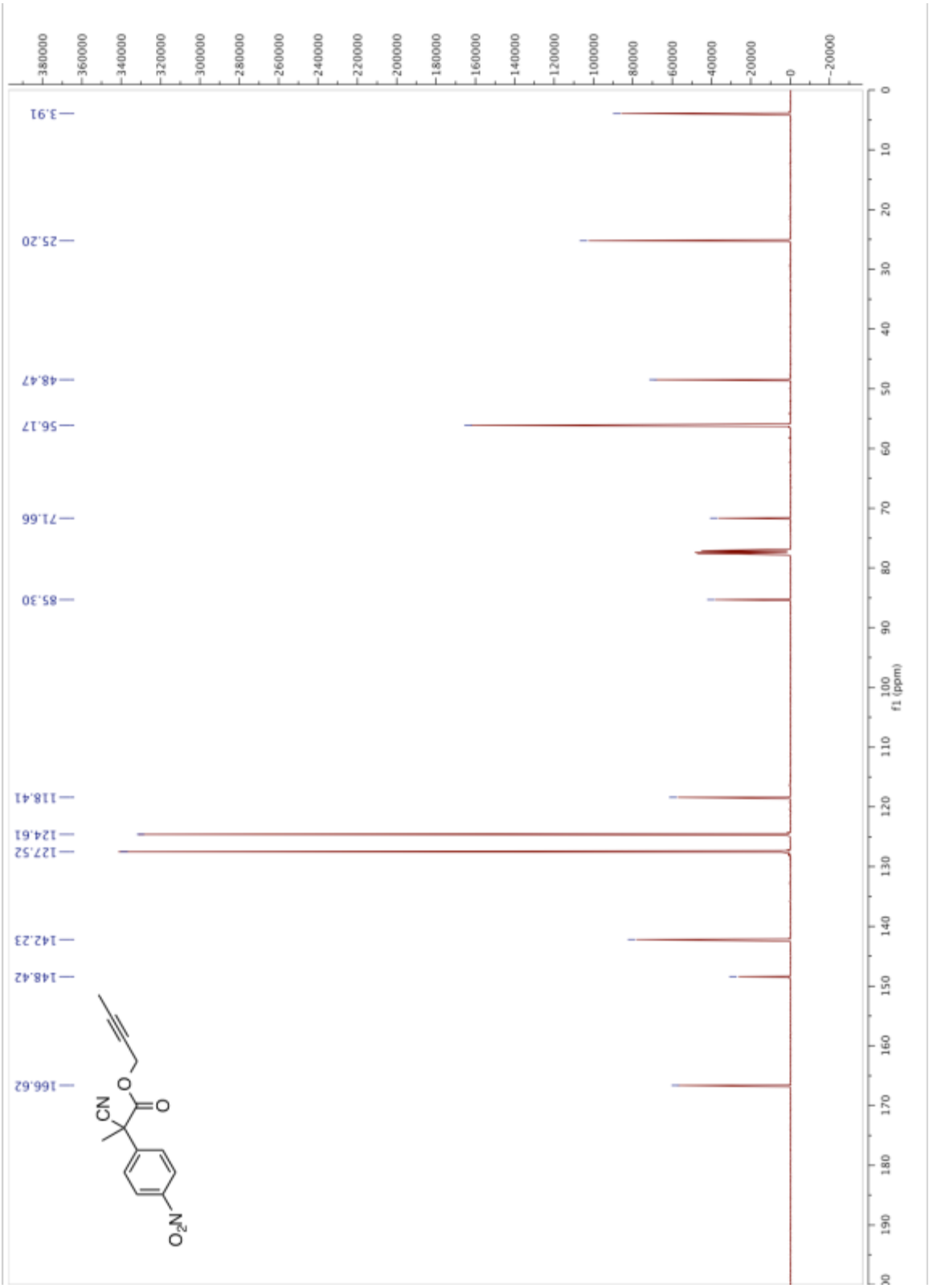
3.91
25.20
48.47
56.17
71.66
85.30
118.41
124.61
127.52
142.23
148.42
166.62
CN
O
O
O2N
f1 (ppm)

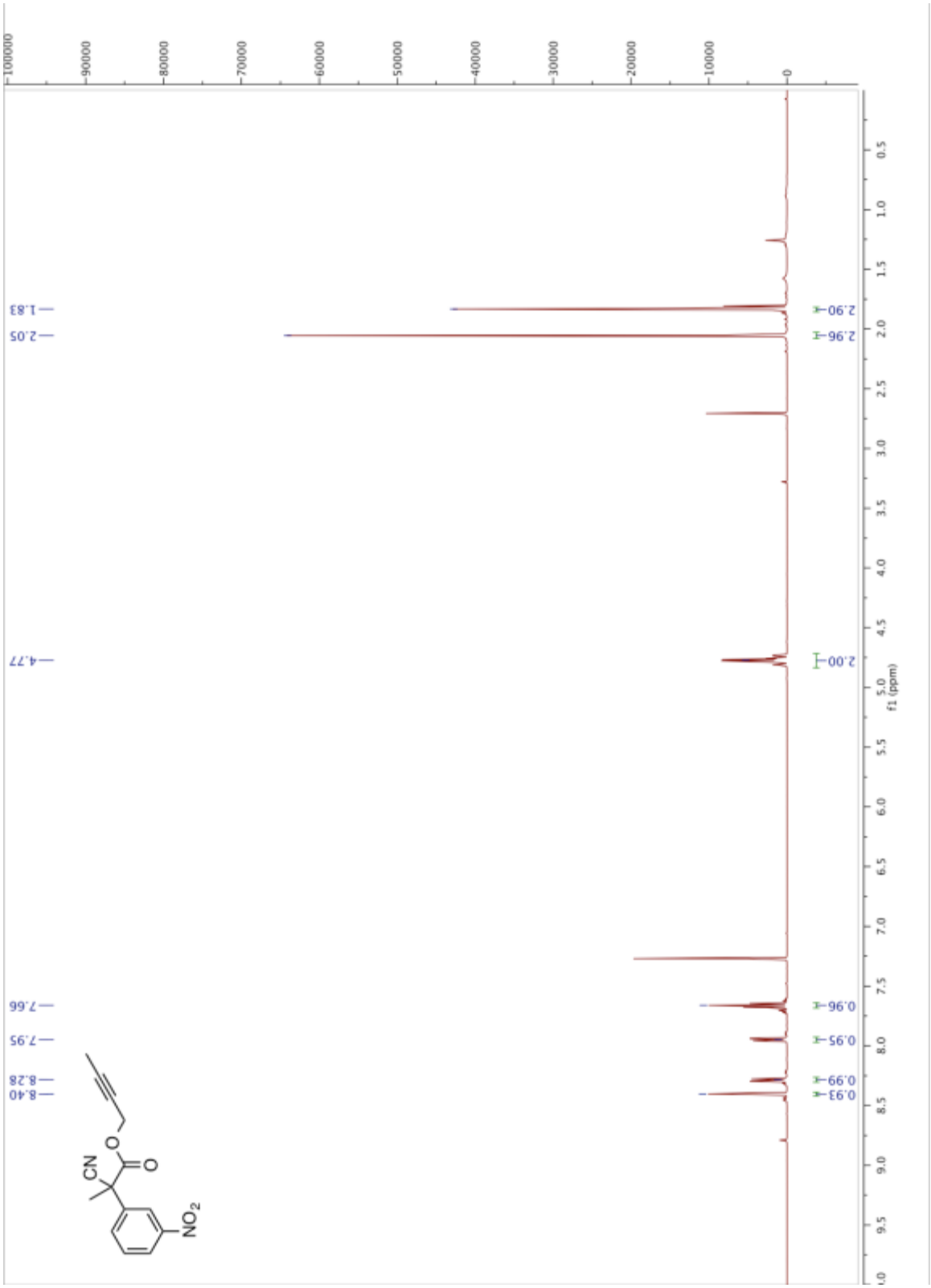
1.83
2.05
4.77
7.66
7.95
8.28
8.40
2.90
2.96
2.00
0.96
0.95
0.99
0.93
f1 (ppm)
CN
O
O
NO2

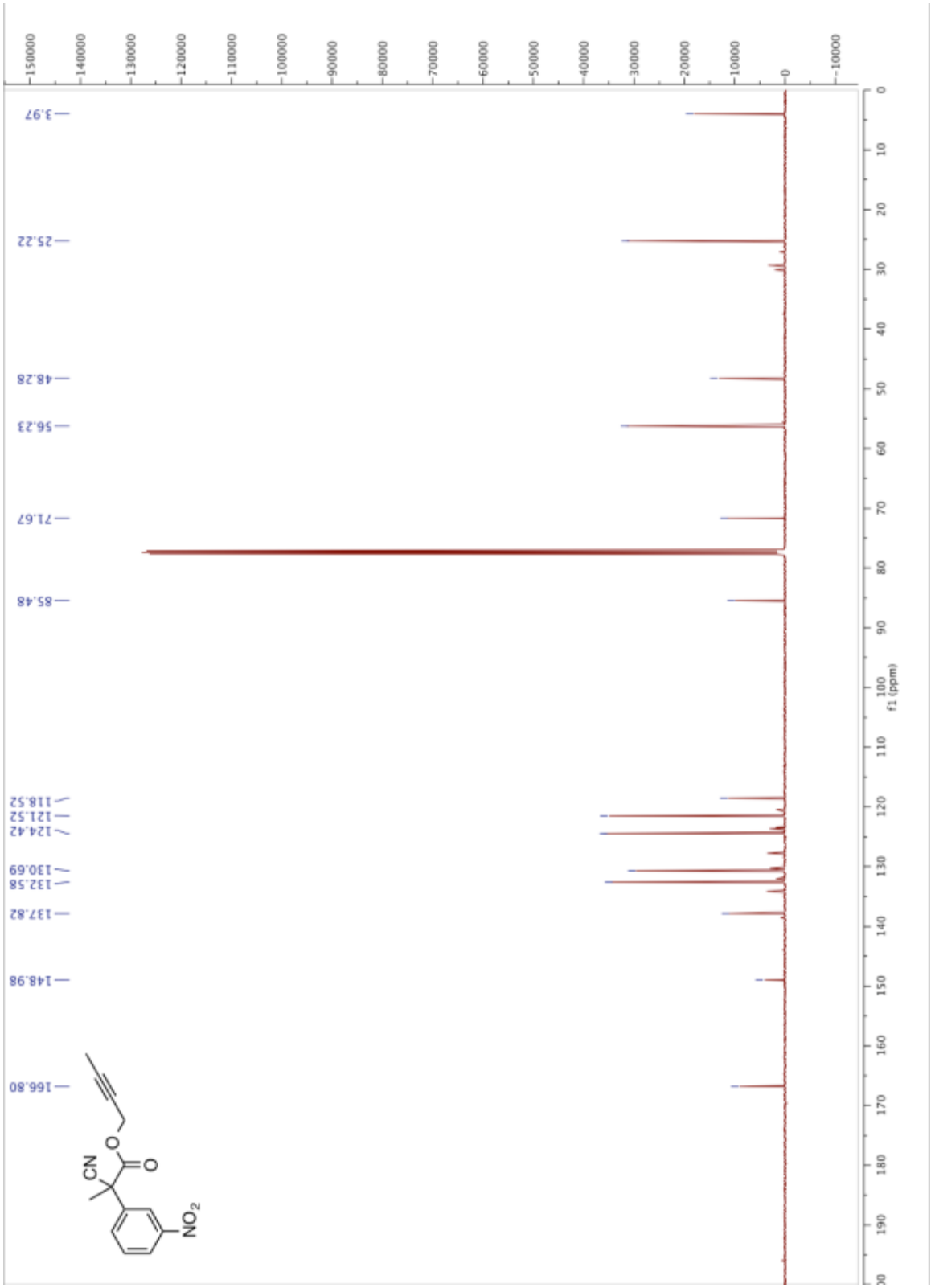
3.97
25.22
48.28
56.23
71.67
85.48
118.52
121.52
124.42
130.69
132.58
137.82
148.98
166.80
CN
O
O
NO2
f1 (ppm)

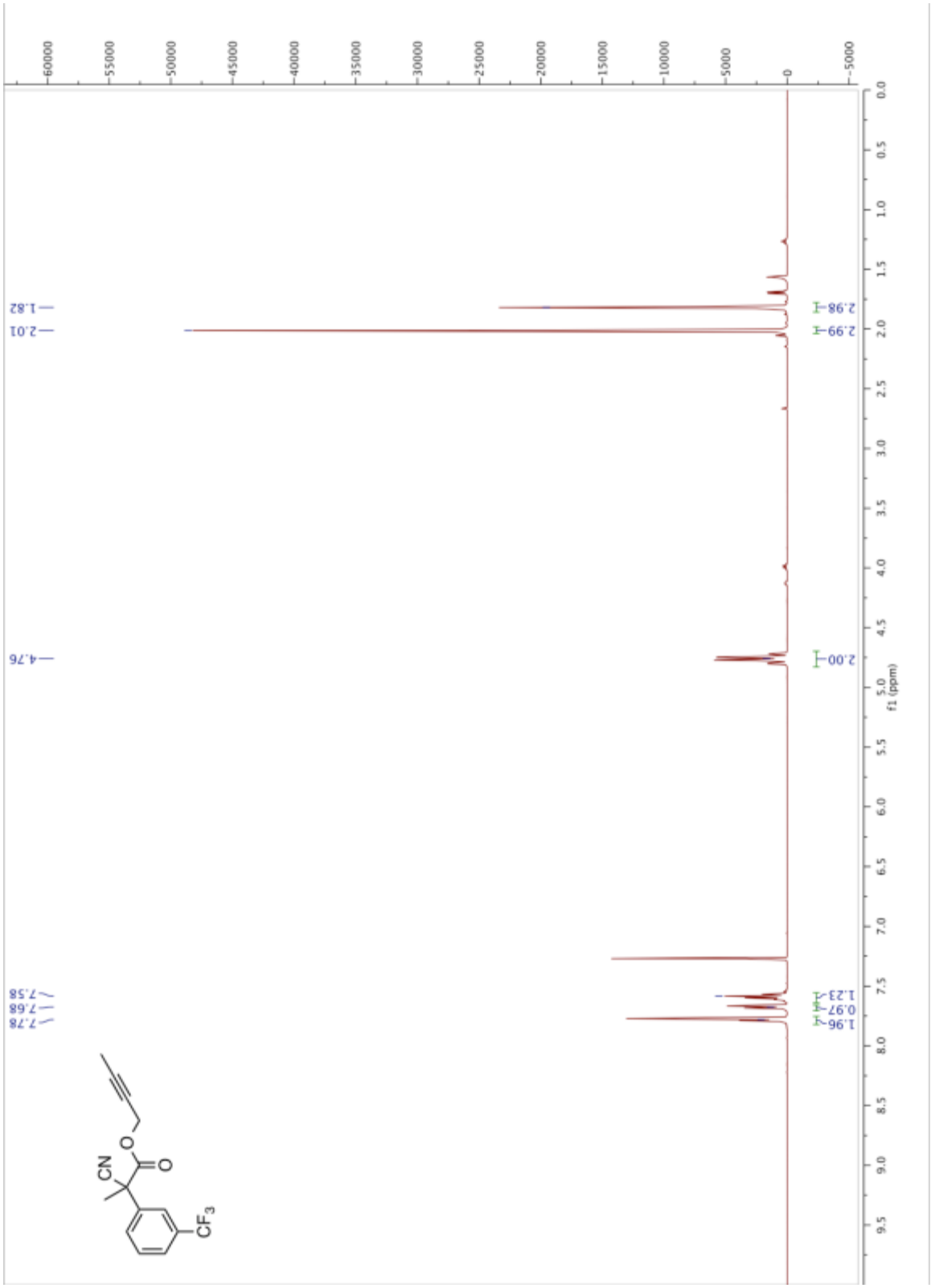
1.82
2.01
4.76
7.58
7.68
7.78
2.98
2.99
2.00
1.23
0.97
1.96
f1 (ppm)
CN
O
O
CF3

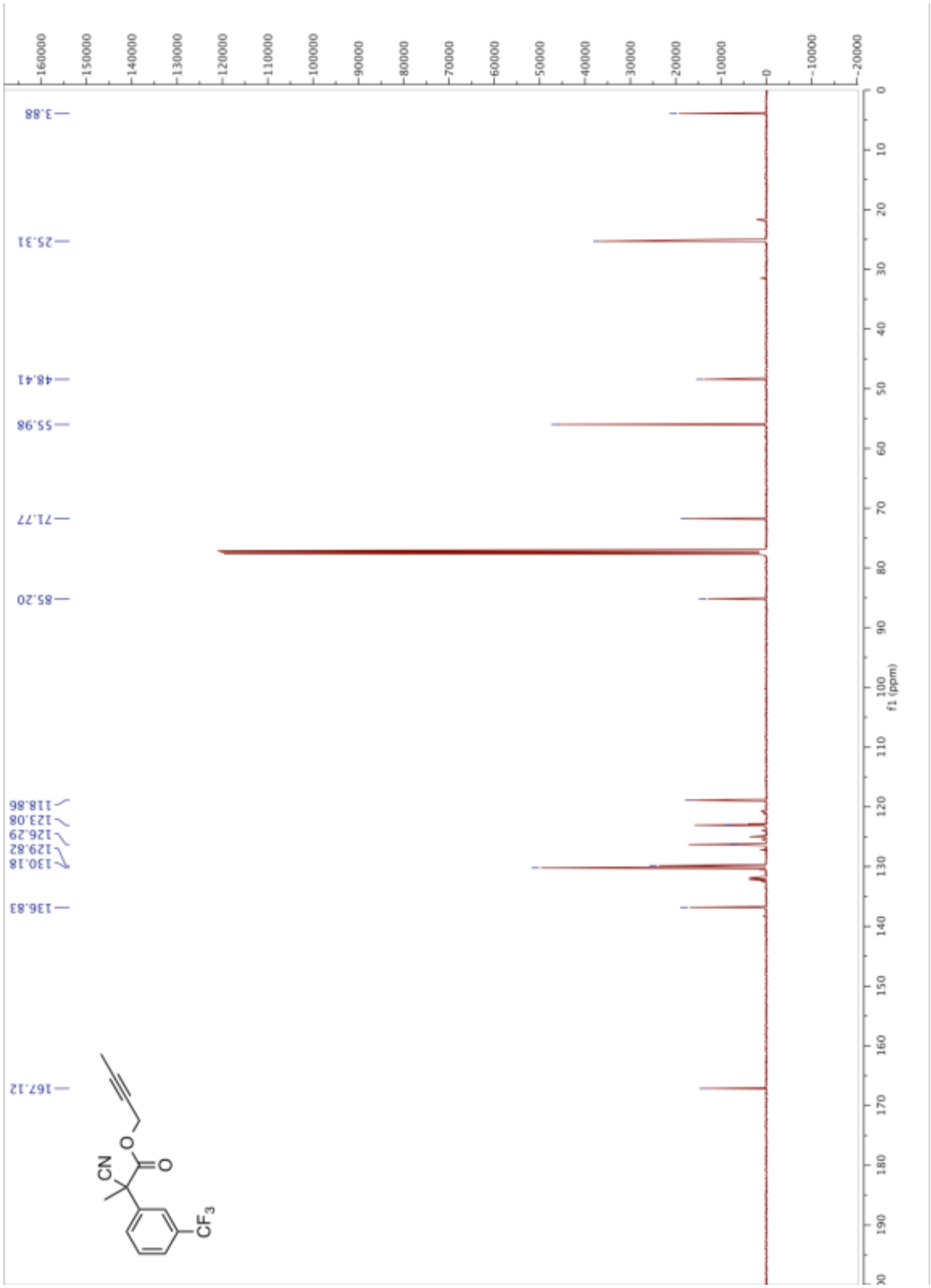
3.88
25.31
48.41
55.98
71.77
85.20
118.86
123.08
126.29
129.82
130.18
136.83
167.12
CN
O
O
CF3
f1 (ppm)

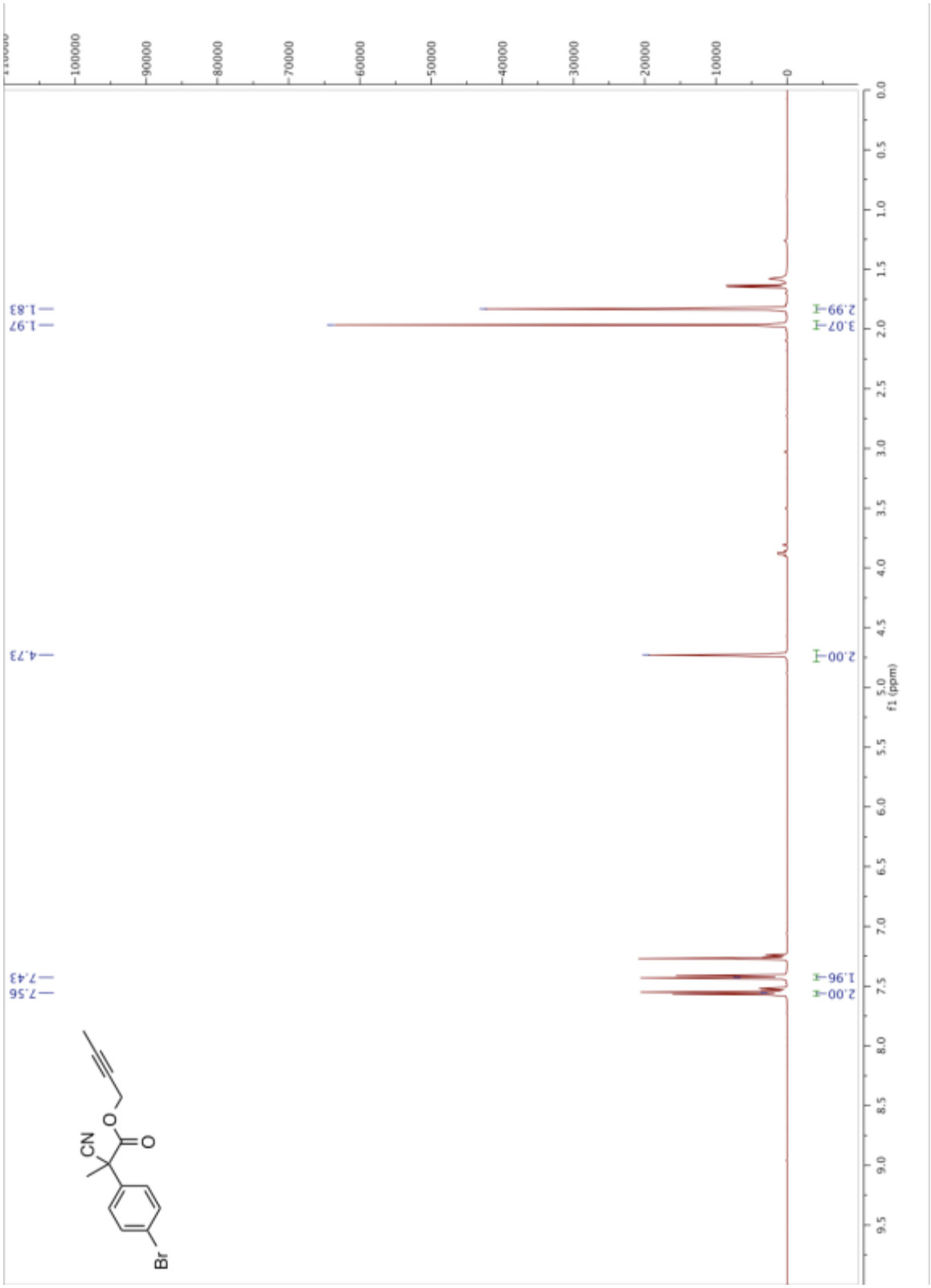
1.83
1.97
4.73
7.43
7.56
2.99
3.07
2.00
1.96
2.00
f1 (ppm)
CN
O
O
Br

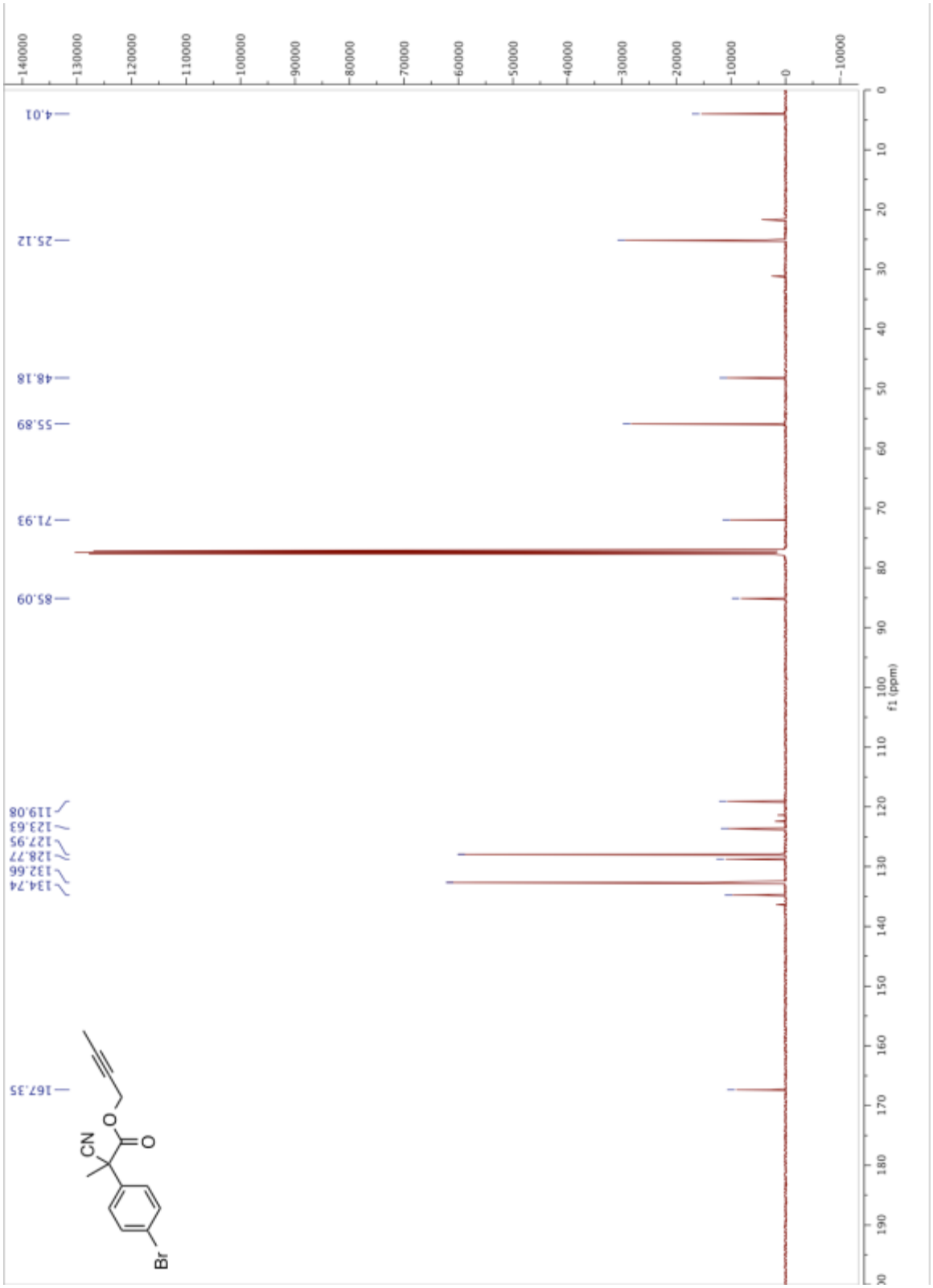
4.01
25.12
48.18
55.89
71.93
85.09
119.08
123.63
127.95
128.77
132.66
134.74
167.35
CN
O
O
Br
f1 (ppm)

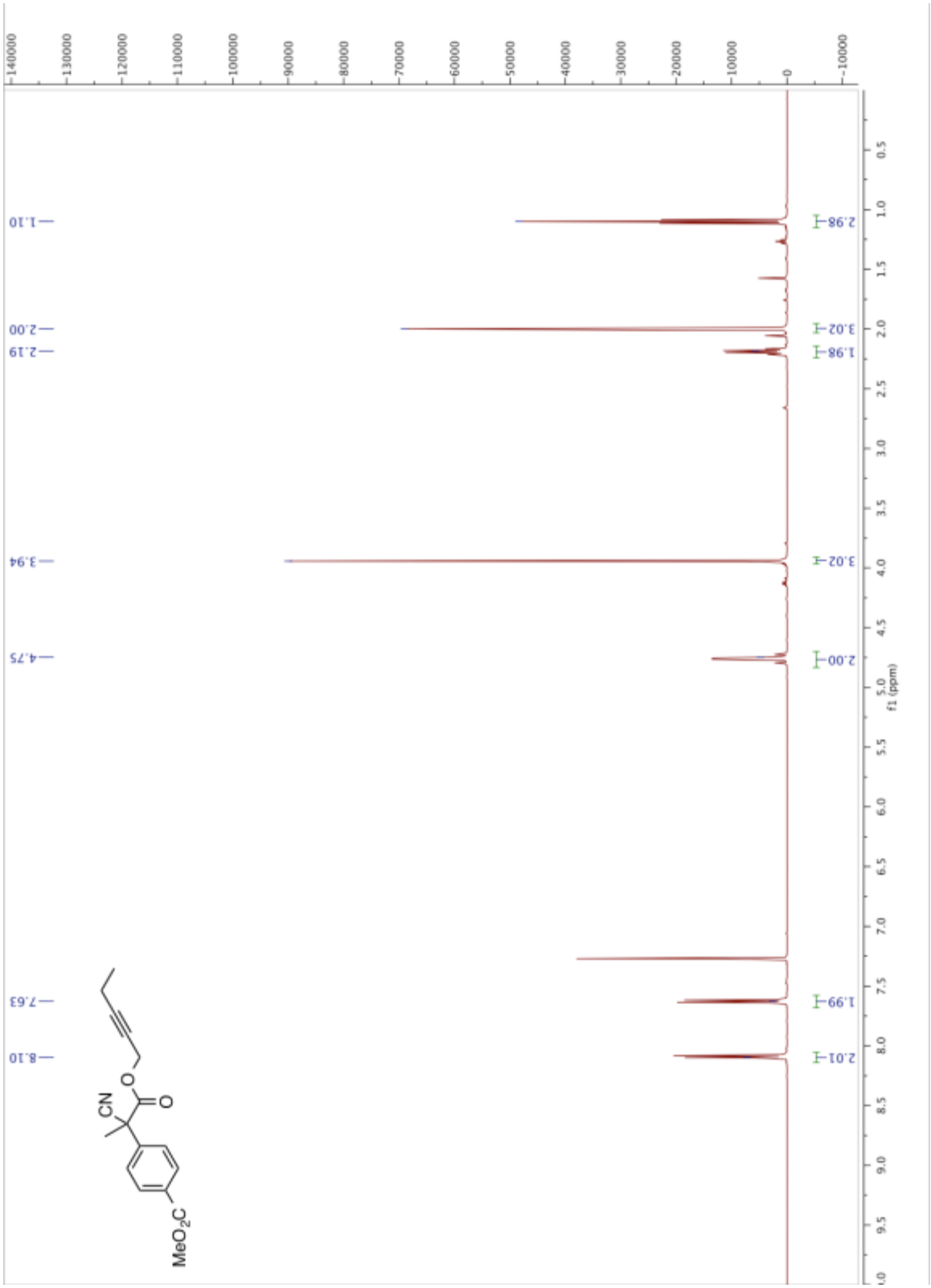
8.10
7.63
4.75
3.94
2.19
2.00
1.10
2.01
1.99
2.00
3.02
1.98
3.02
2.98
f1 (ppm)
CN
O
O
MeO2C

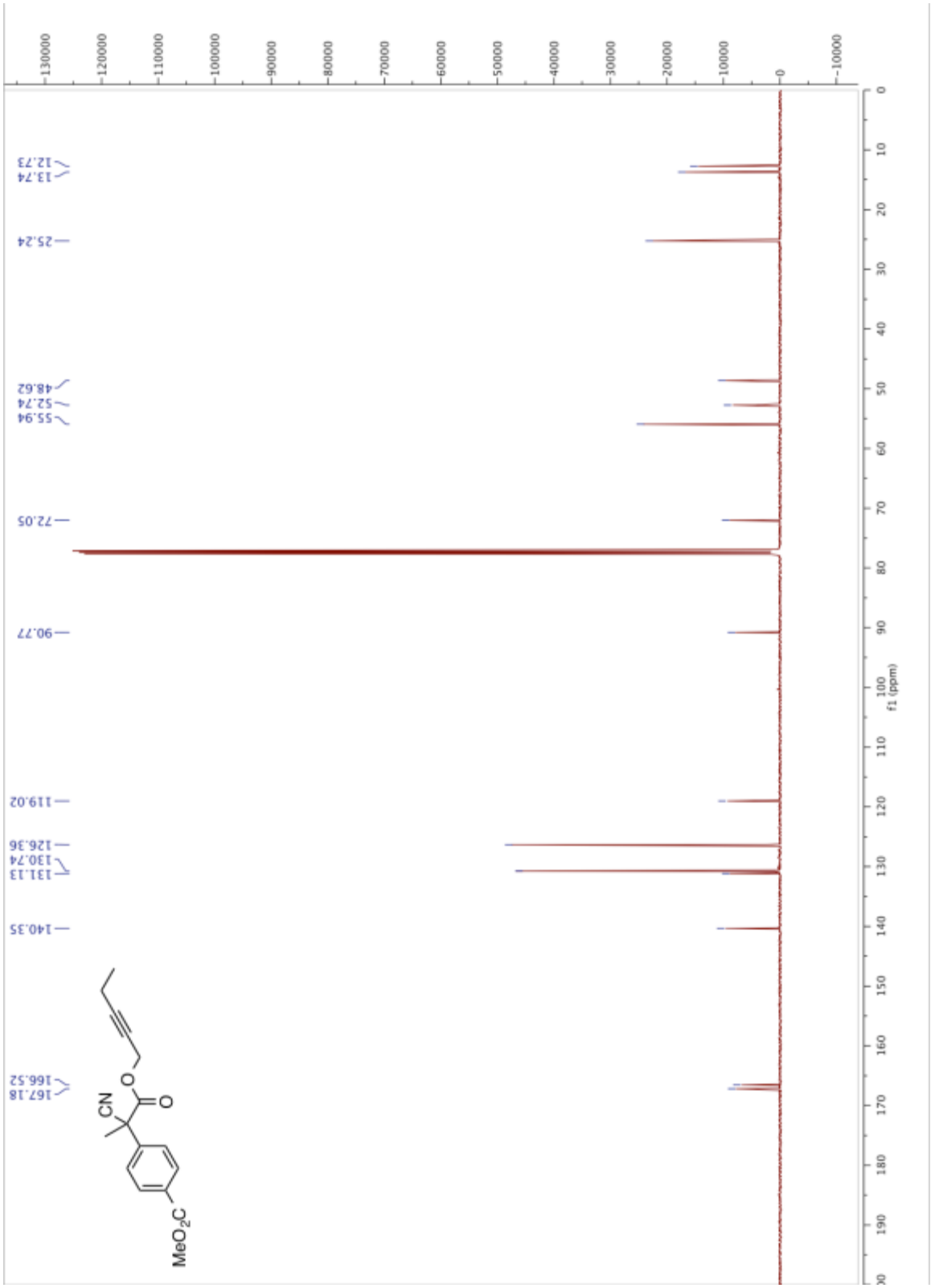
12.73
13.74
25.24
48.62
52.74
55.94
72.05
90.77
119.02
126.36
130.74
131.13
140.35
166.52
167.18
CN
O
O
MeO2C
f1 (ppm)

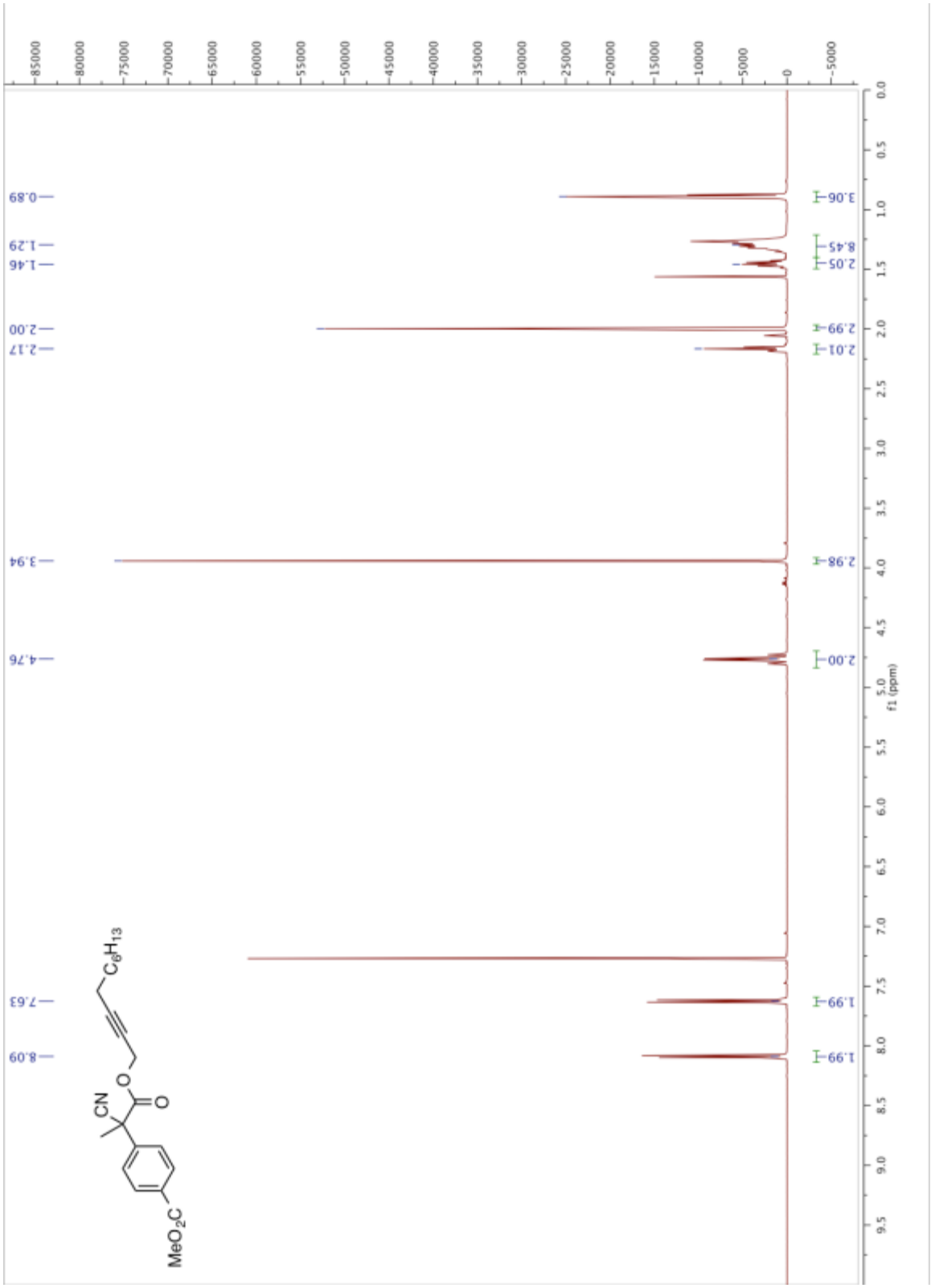
0.89
1.29
1.46
2.00
2.17
3.94
4.76
7.63
8.09
3.06
8.45
2.05
2.99
2.01
2.98
2.00
1.99
1.99
f1 (ppm)
CN
O
O
C_6H_{13}
MeO_2C

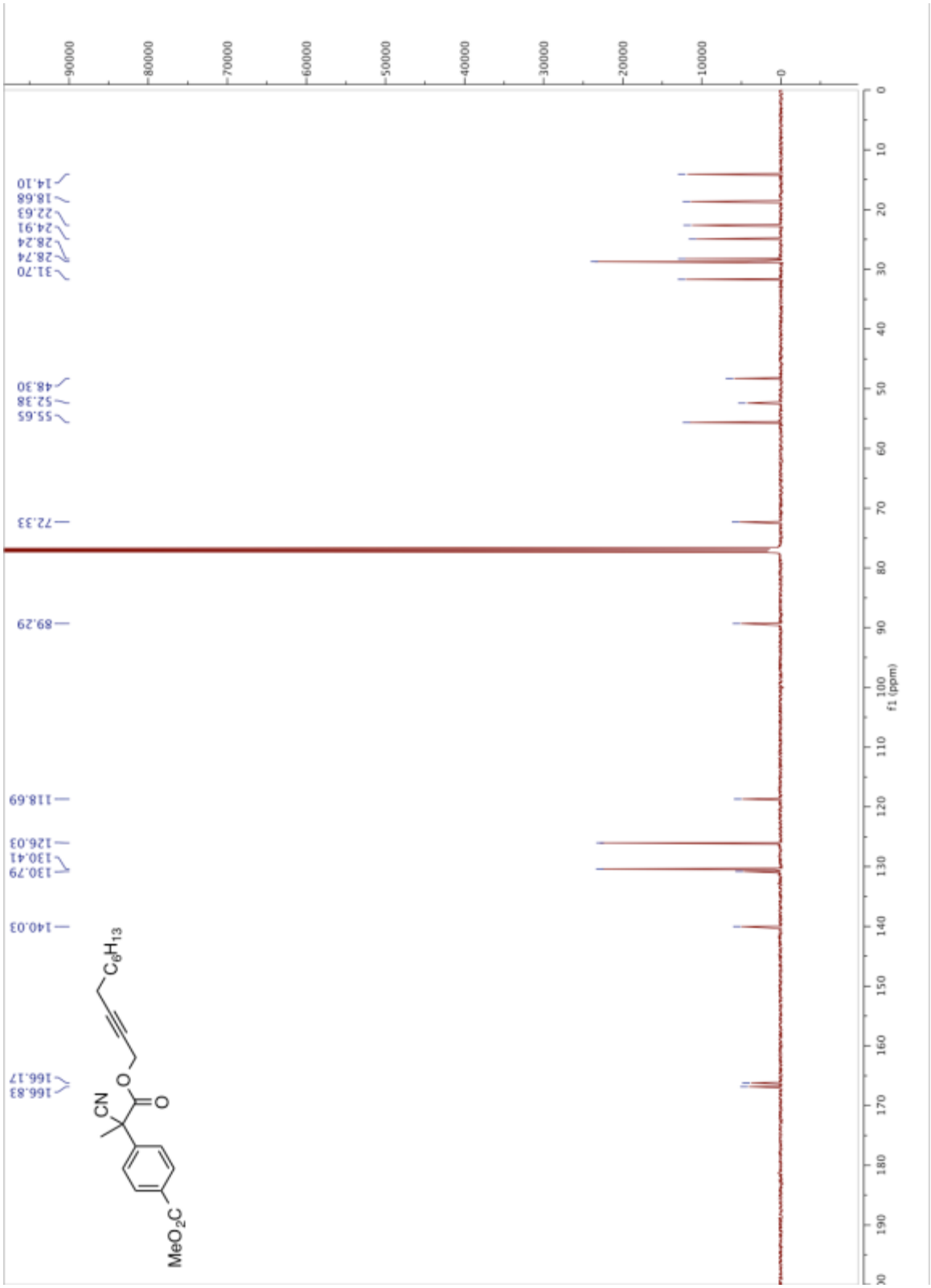
166.83
166.17
140.03
130.79
130.41
126.03
118.69
89.29
72.33
55.65
52.38
48.30
31.70
28.74
28.24
24.91
22.63
18.68
14.10
CN
O
O
C_6H_{13}
MeO_2C
f1 (ppm)

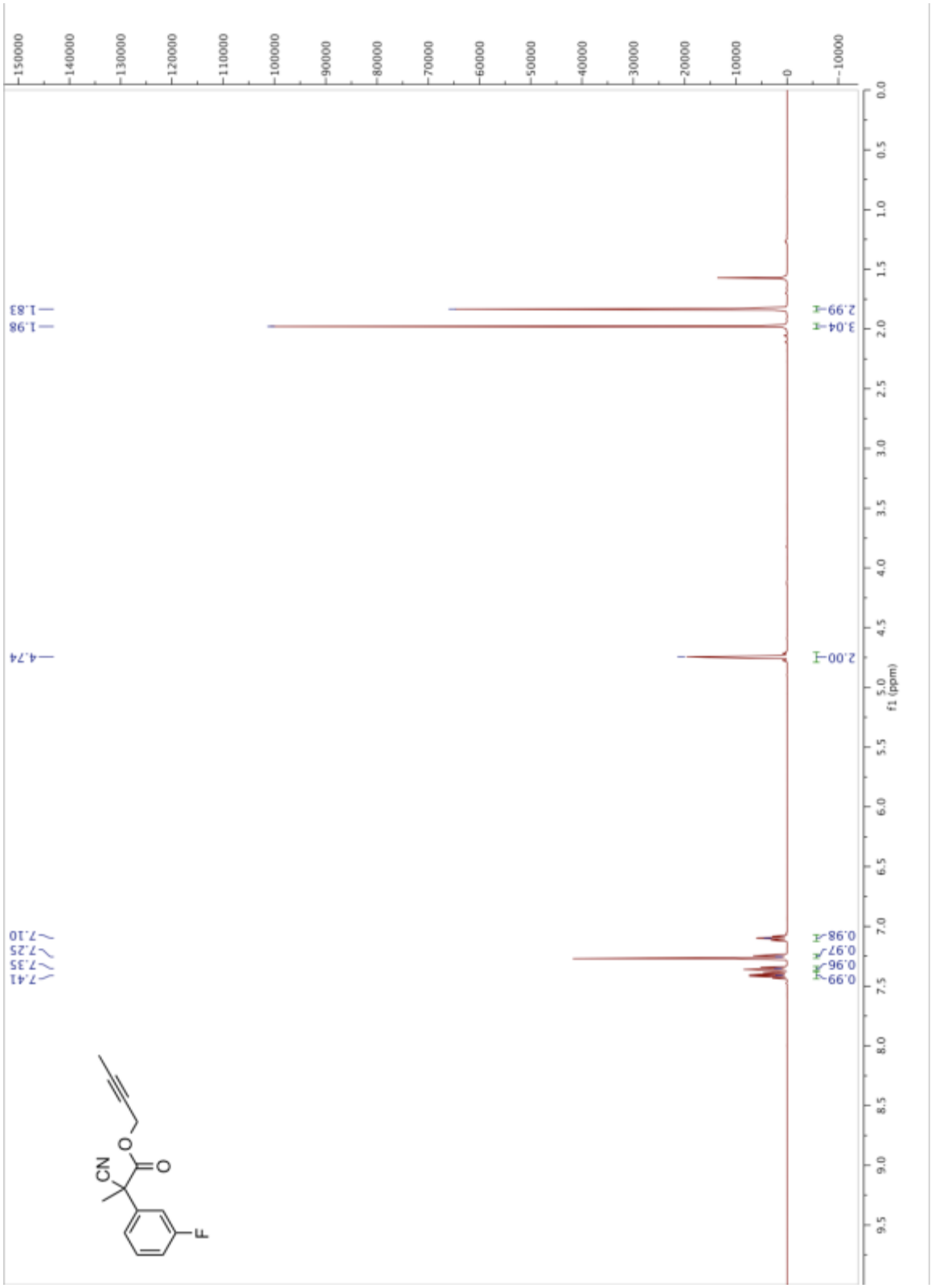
1.83
1.98
4.74
7.10
7.25
7.35
7.41
2.99
3.04
2.00
0.98
0.97
0.96
0.99
f1 (ppm)
CN
O
O
F

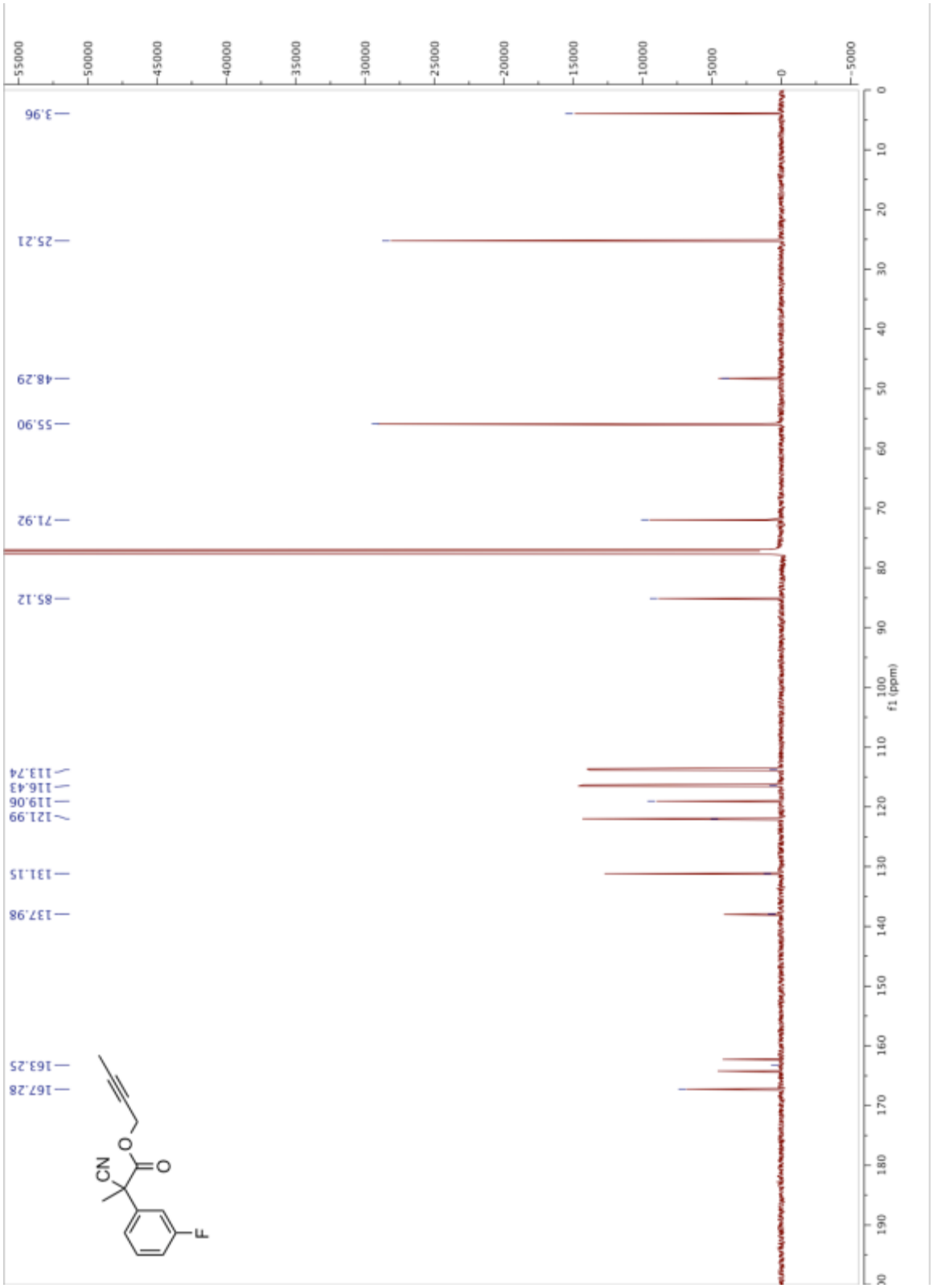
3.96
25.21
48.29
55.90
71.92
85.12
113.74
116.43
119.06
121.99
131.15
137.98
163.25
167.28
CN
O
O
F
f1 (ppm)

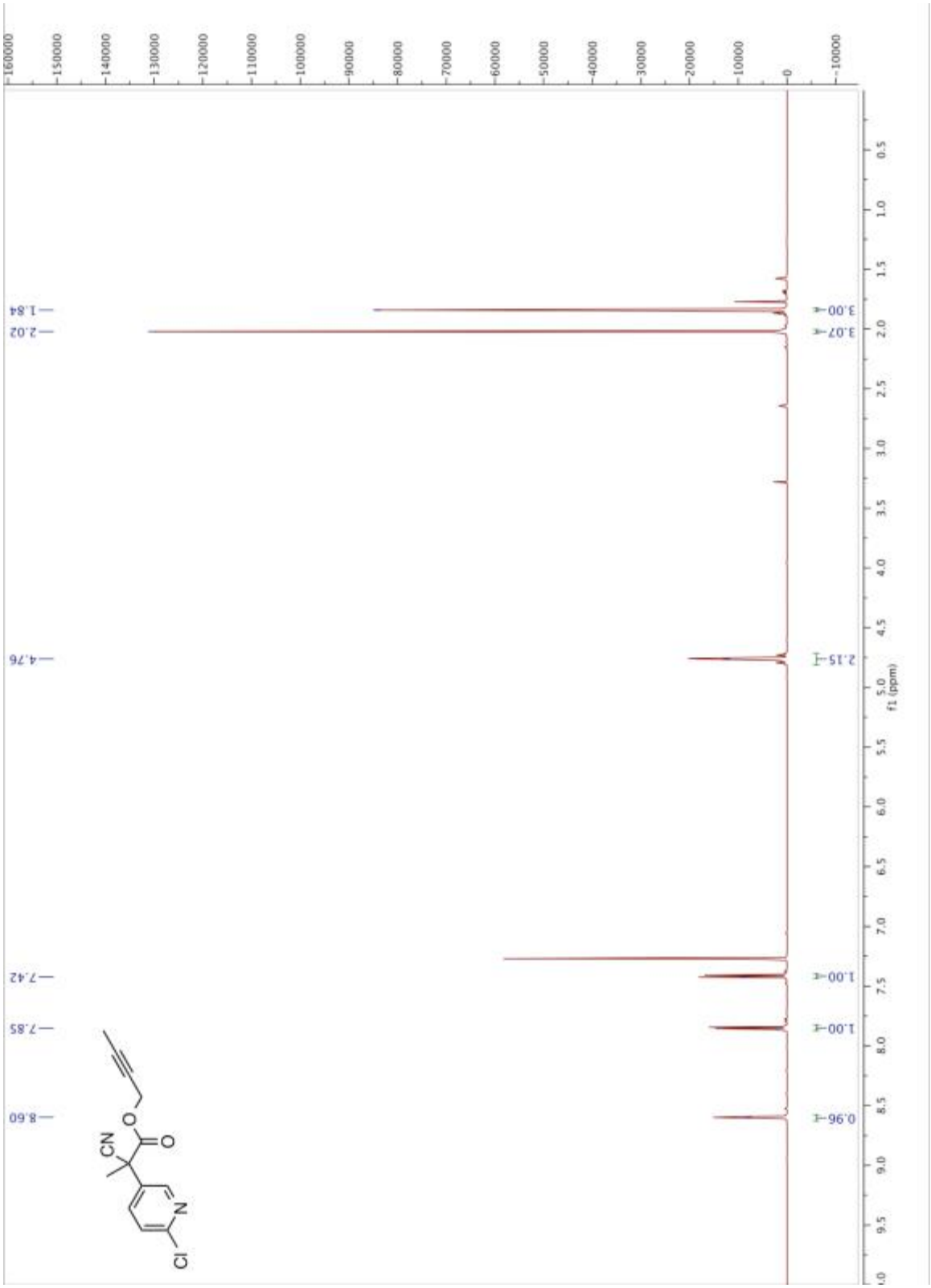
8.60
7.85
7.42
4.76
2.02
1.84
0.96
1.00
1.00
2.15
3.07
3.00
f1 (ppm)
CN
O
O
N
Cl

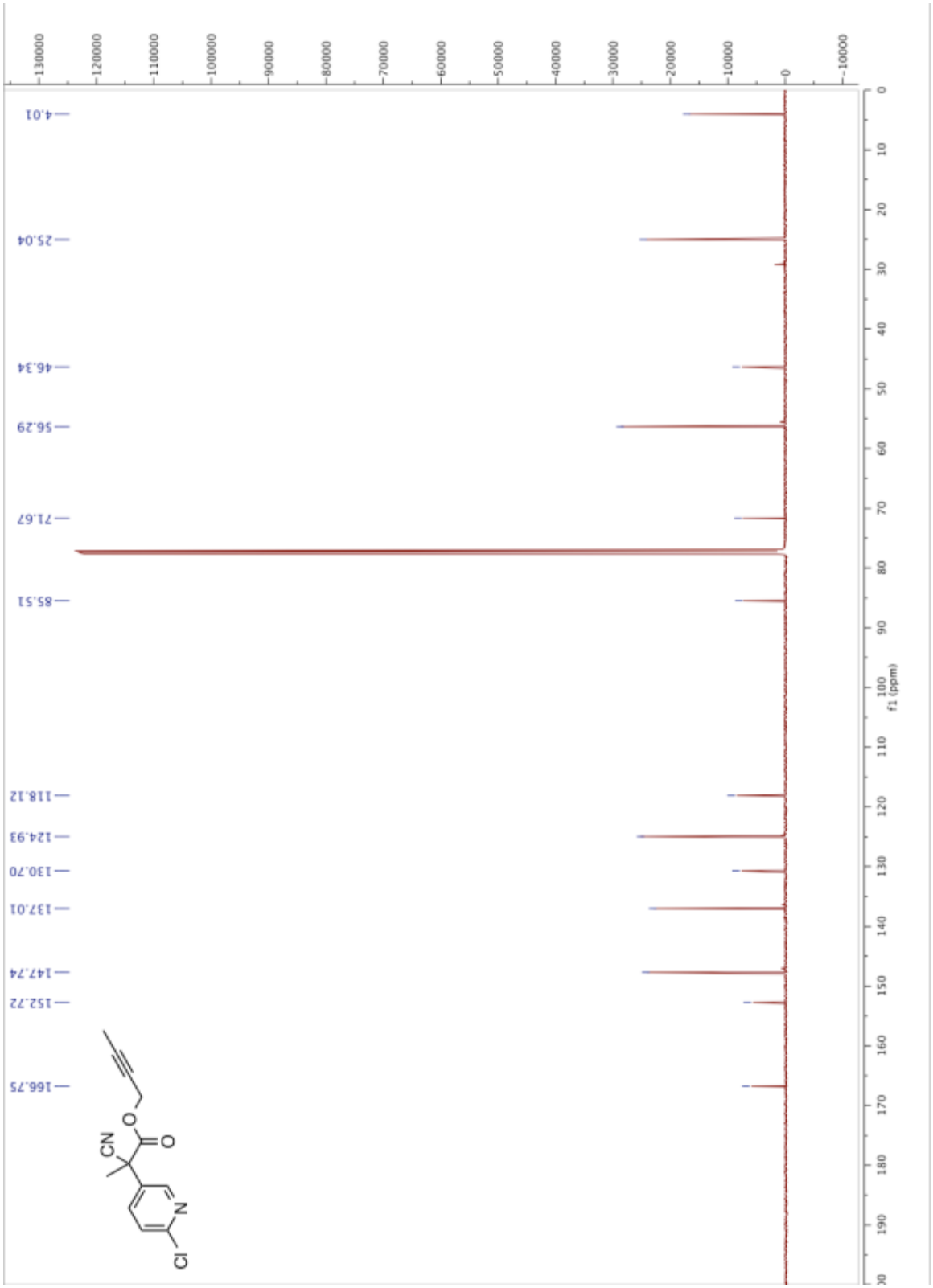
4.01
25.04
46.34
56.29
71.67
85.51
118.12
124.93
130.70
137.01
147.74
152.72
166.75
CN
O
O
N
Cl
f1 (ppm)

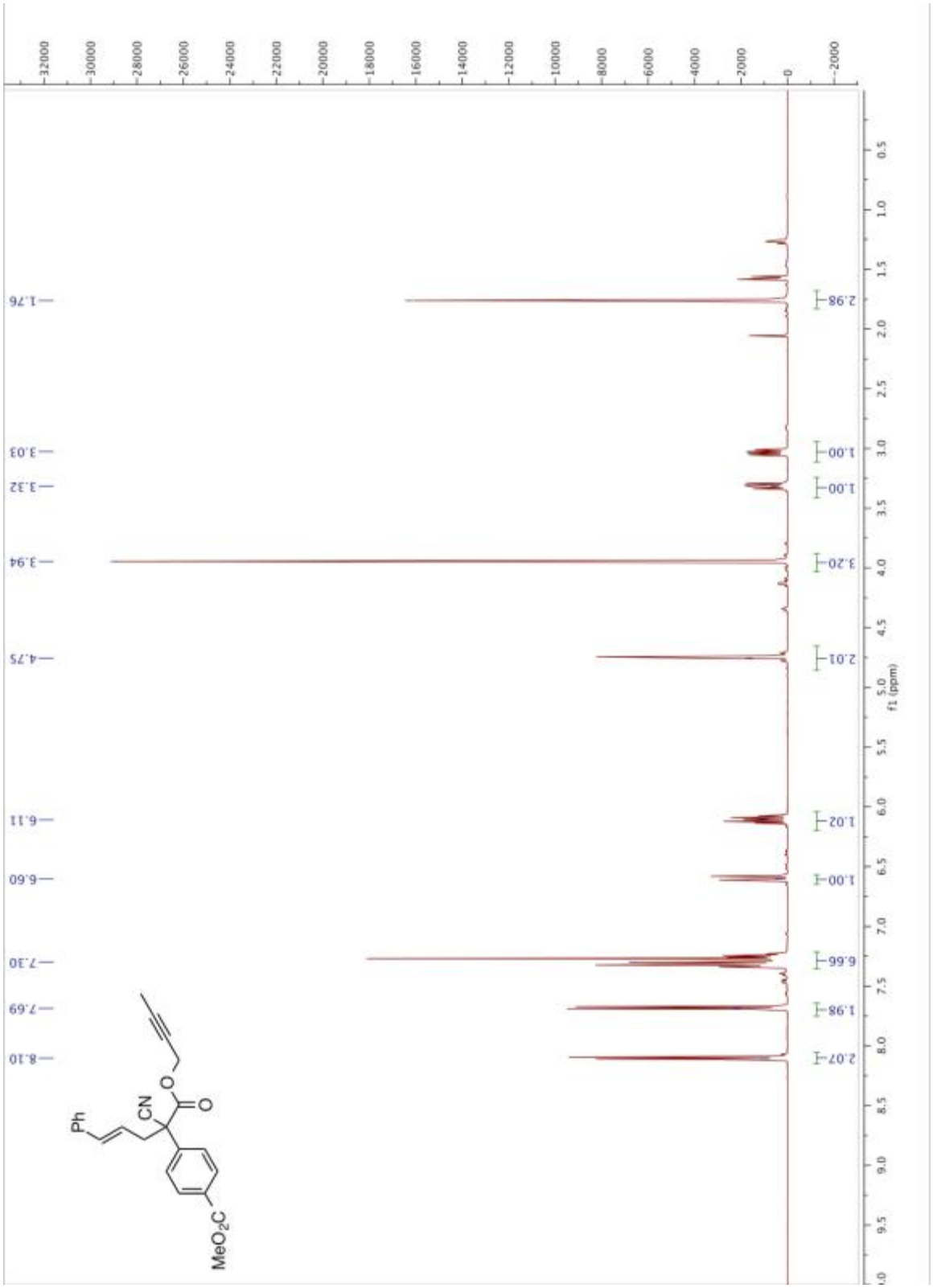
1.76
3.03
3.32
3.94
4.75
6.11
6.60
7.30
7.69
8.10
2.98
1.00
1.00
3.20
2.01
1.02
1.00
6.66
1.98
2.07
f1 (ppm)
Ph
CN
O
O
MeO2C

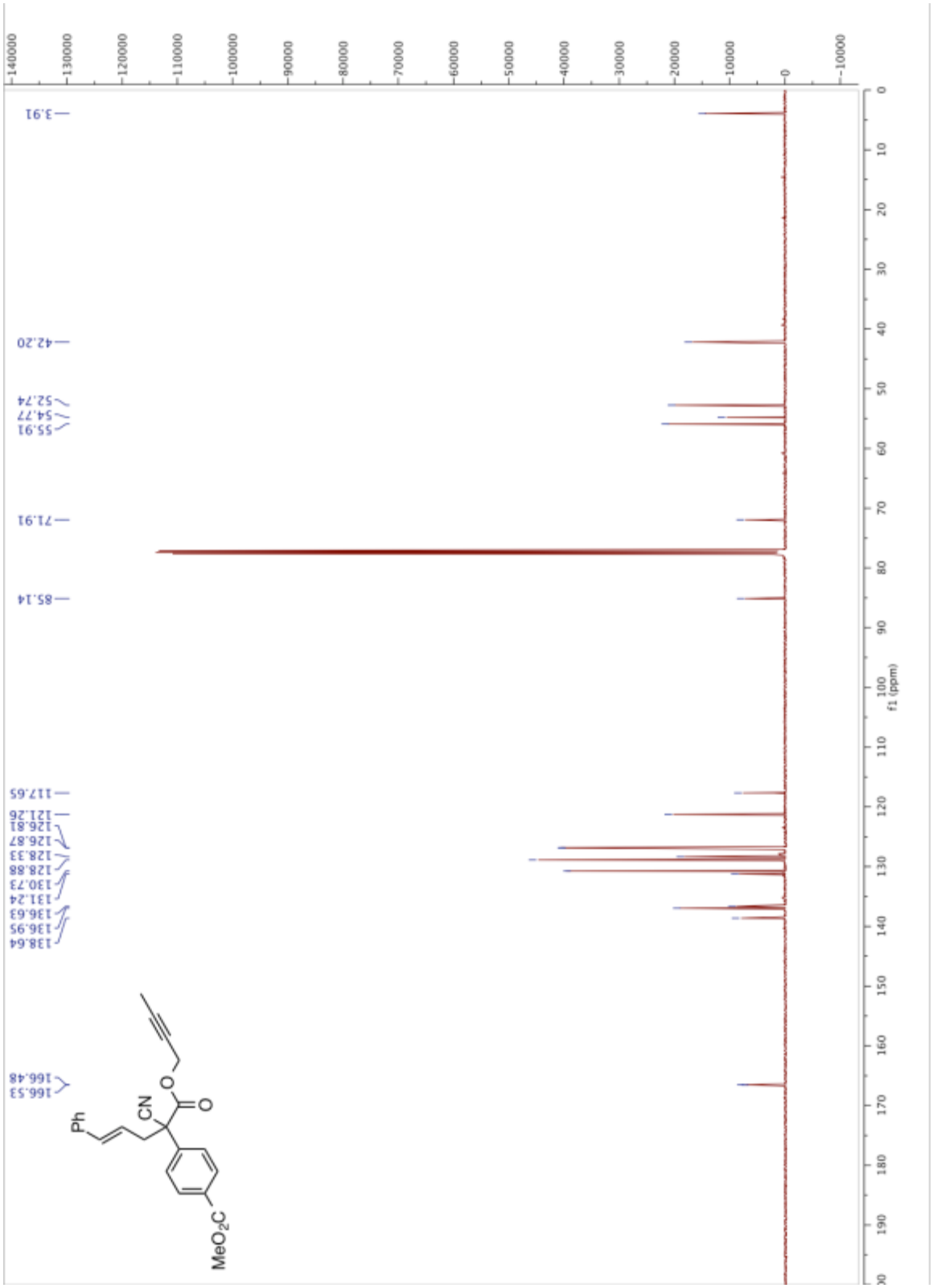
3.91
42.20
52.74
54.77
55.91
71.91
85.14
117.65
121.26
126.81
126.87
128.33
128.88
130.73
131.24
136.63
136.95
138.64
166.48
166.53
f1 (ppm)
Ph
CN
O
O
MeO2C

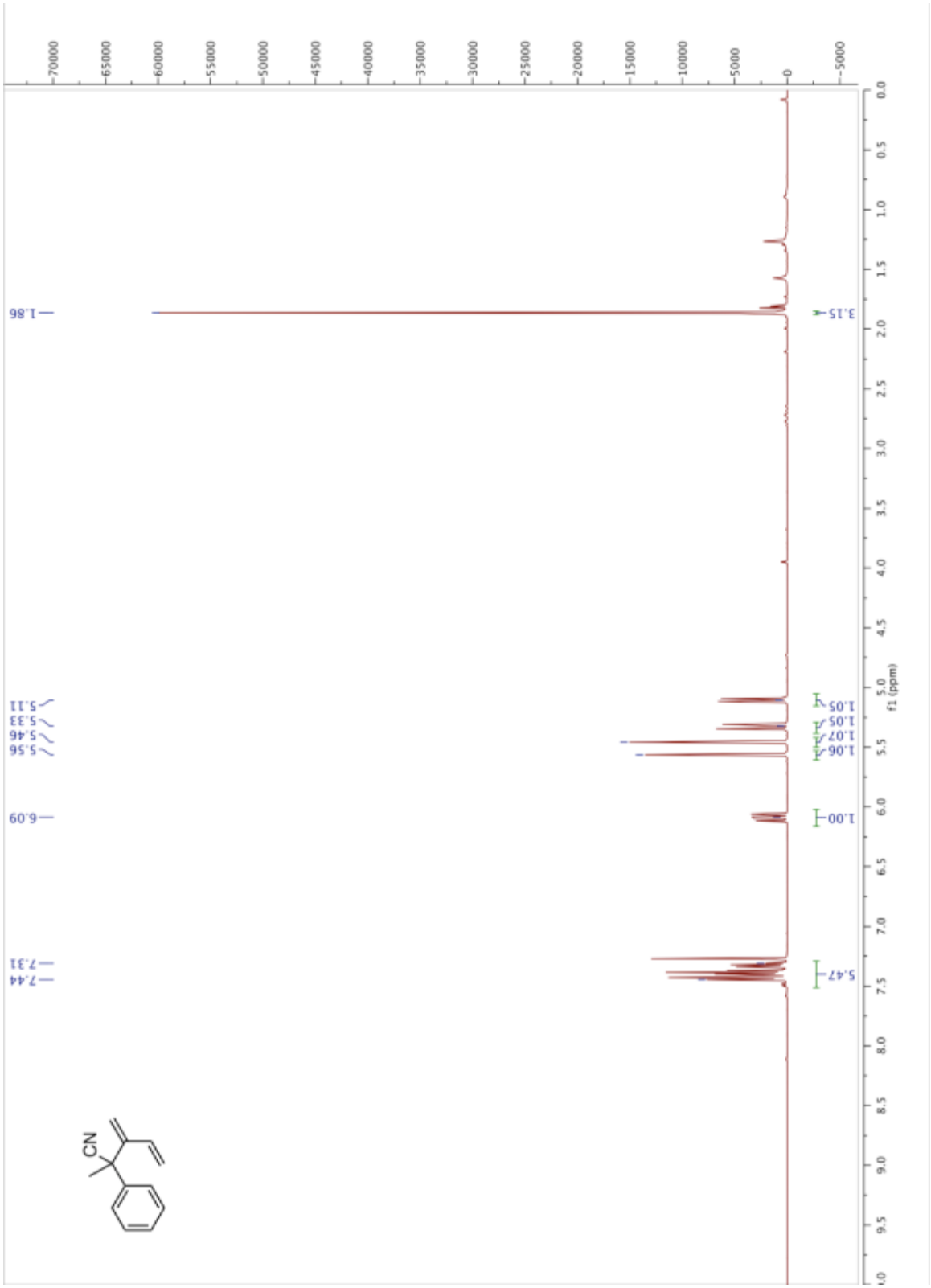
1.86
5.11
5.33
5.46
5.56
6.09
7.31
7.44
3.15
1.05
1.05
1.07
1.06
1.00
5.47
CN
f1 (ppm)

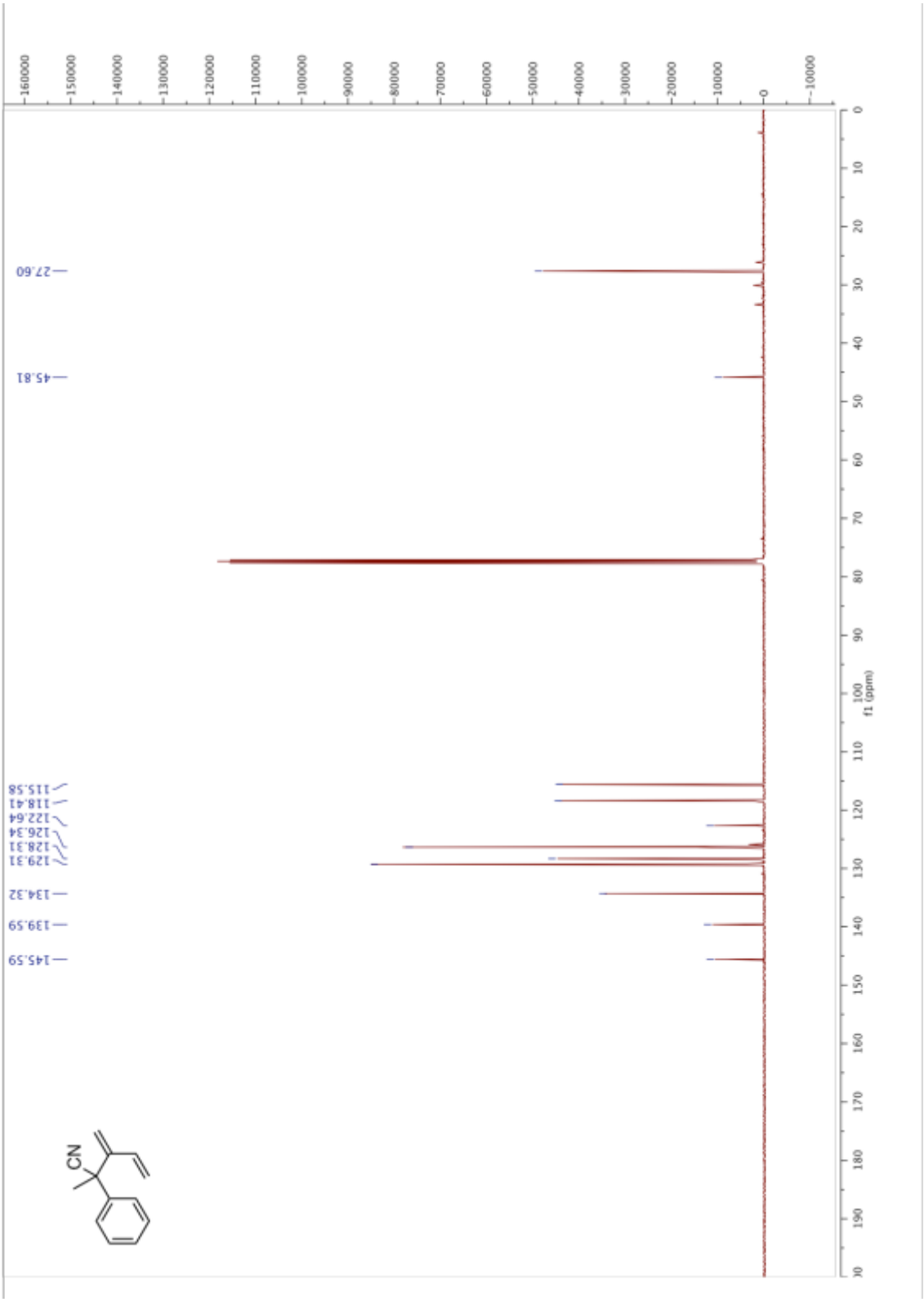
27.60
45.81
115.58
118.41
122.64
126.34
128.31
129.31
134.32
139.59
145.59
CN
f1 (ppm)

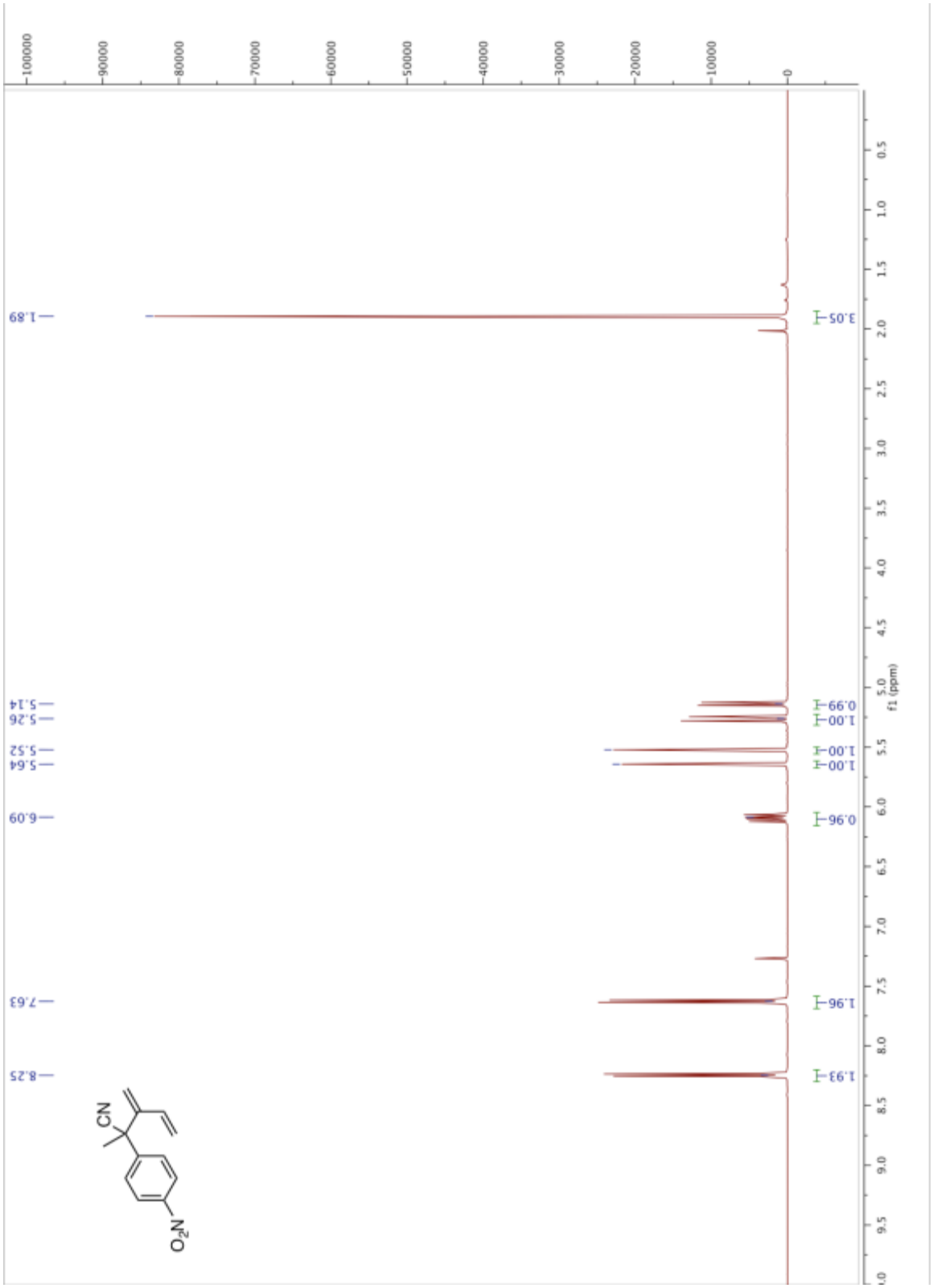
1.89
5.14
5.26
5.52
5.64
6.09
7.63
8.25
3.05
0.99
1.00
1.00
1.00
0.96
1.96
1.93
f1 (ppm)
CN
O2N

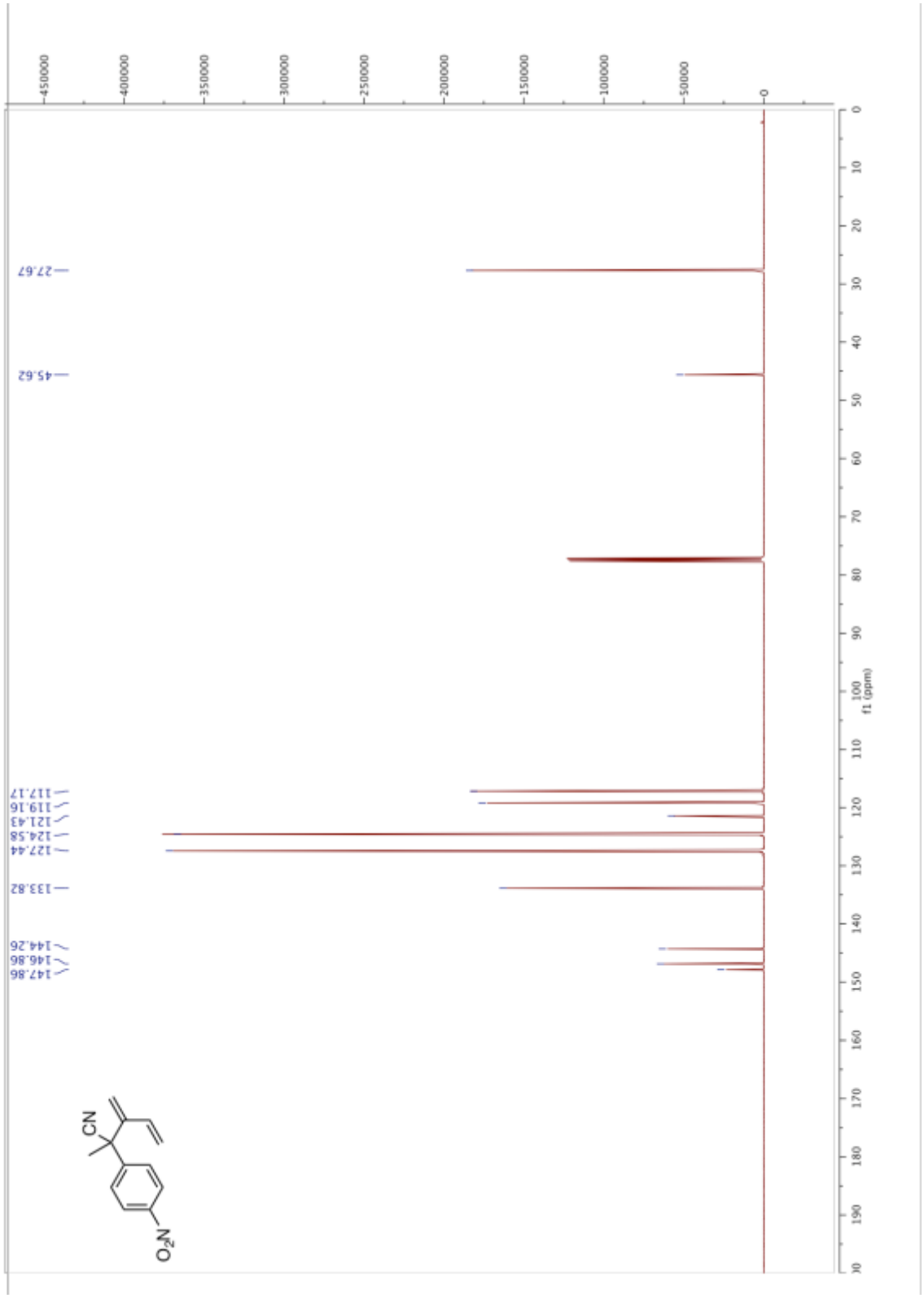
27.67
45.62
117.17
119.16
121.43
124.58
127.44
133.82
144.26
146.86
147.86
CN
O2N
f1 (ppm)

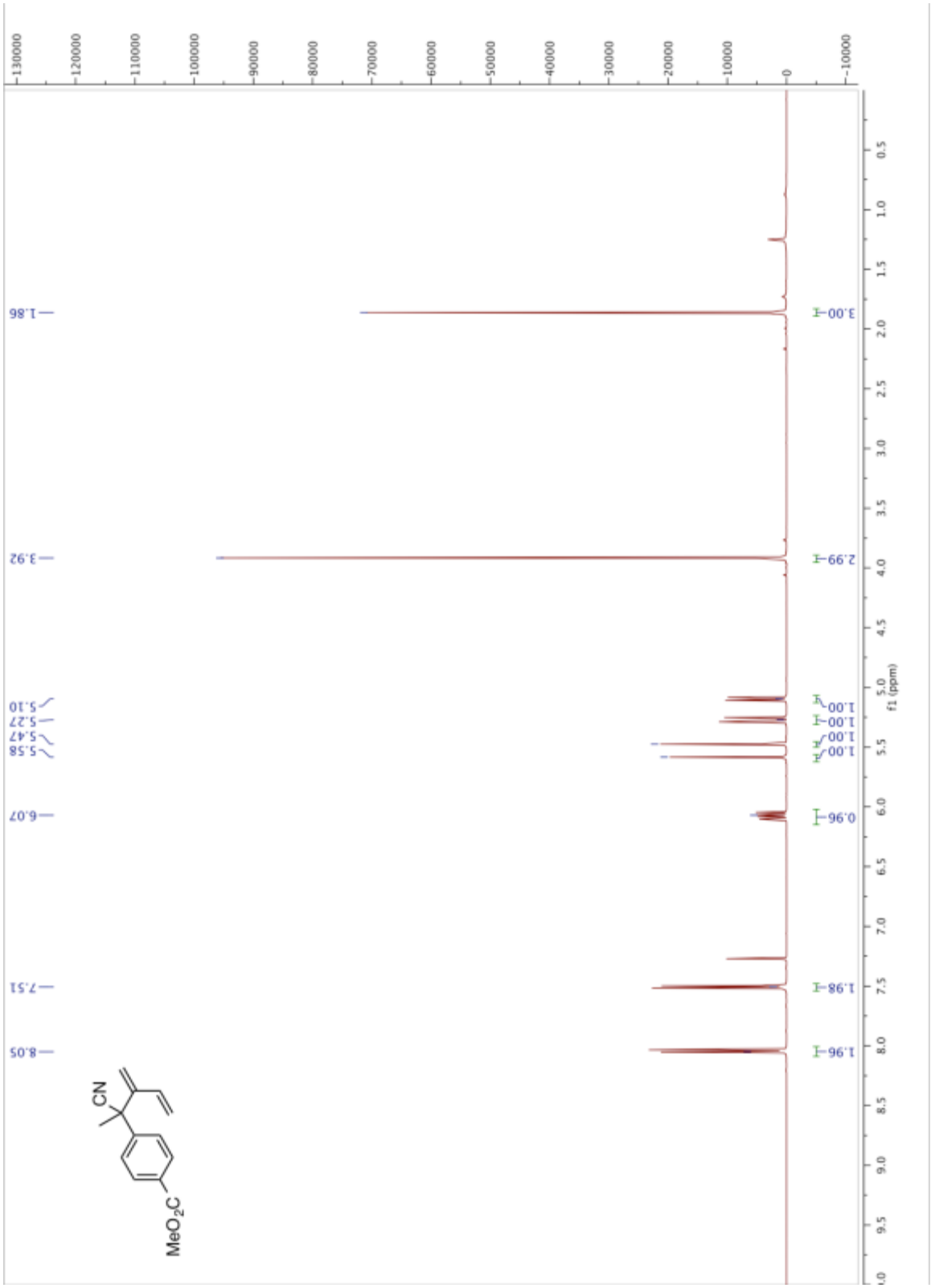
1.86
3.92
5.10
5.27
5.47
5.58
6.07
7.51
8.05
3.00
2.99
1.00
1.00
1.00
1.00
0.96
1.98
1.96
f1 (ppm)
CN
MeO2C

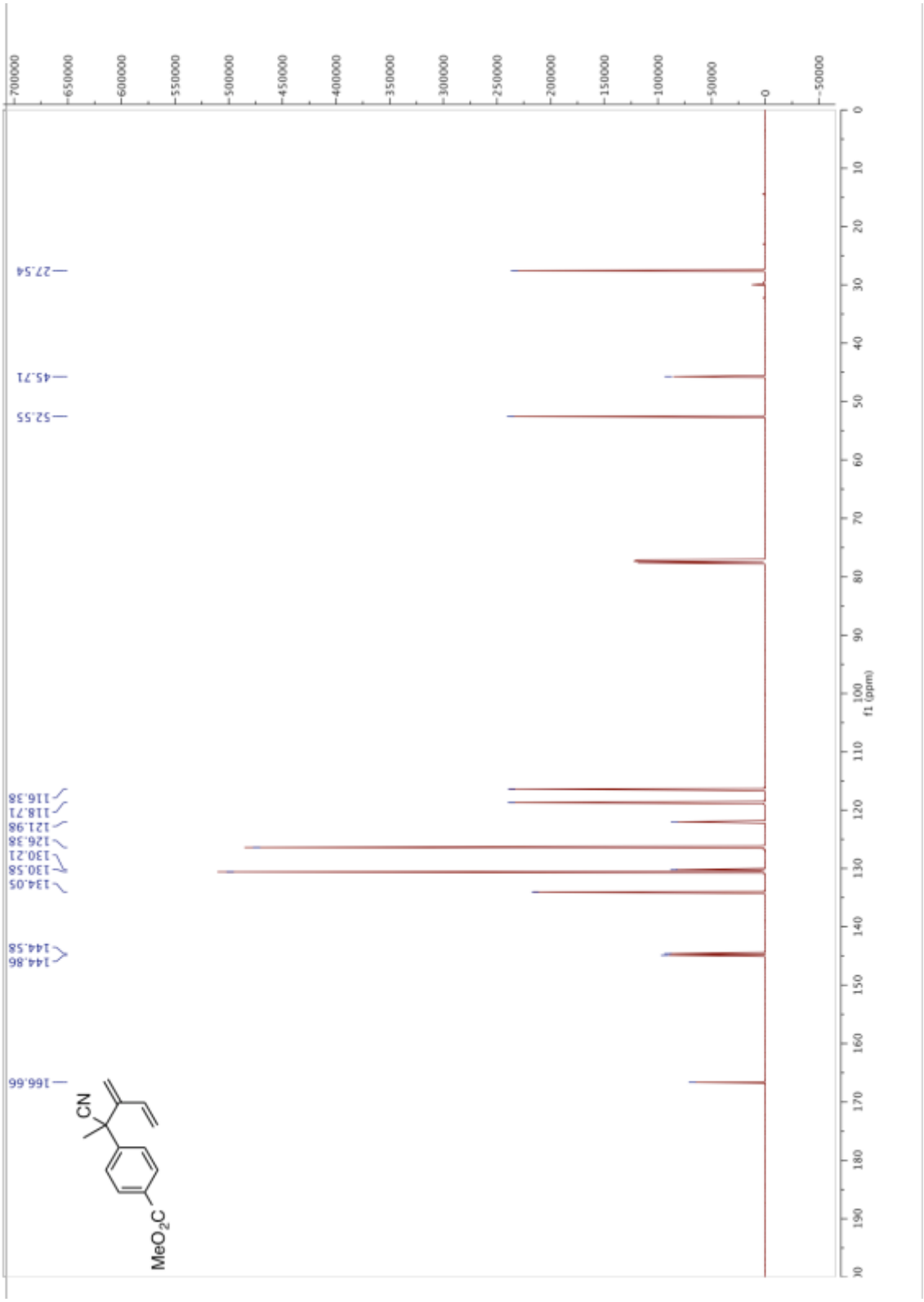
27.54
45.71
52.55
116.38
118.71
121.98
126.38
130.21
130.58
134.05
144.58
144.86
166.66
CN
MeO2C
f1 (ppm)

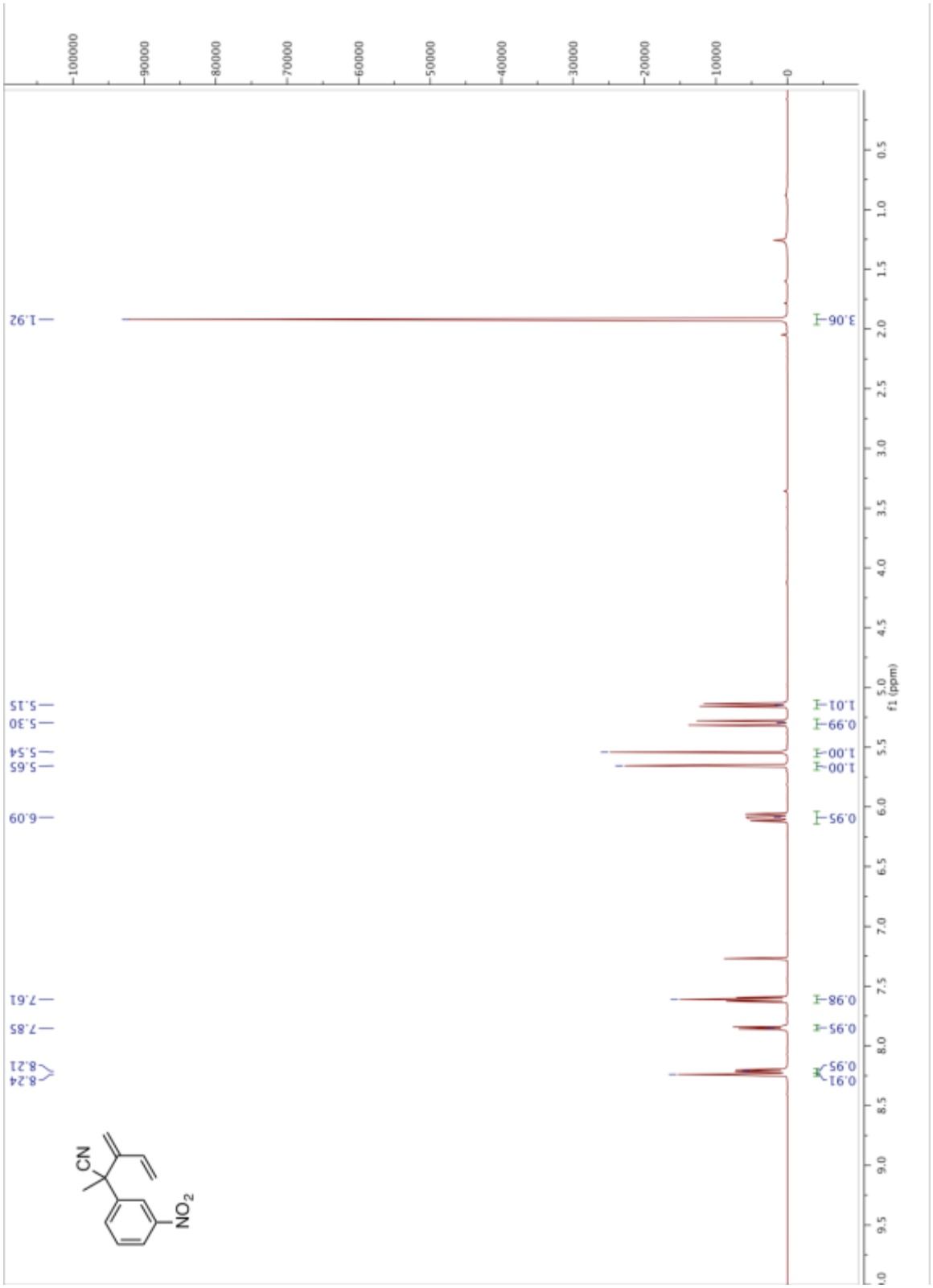
1.92
5.15
5.30
5.54
5.65
6.09
7.61
7.85
8.21
8.24
3.06
1.01
0.99
1.00
1.00
0.95
0.98
0.95
0.95
0.91
f1 (ppm)
CN
NO2

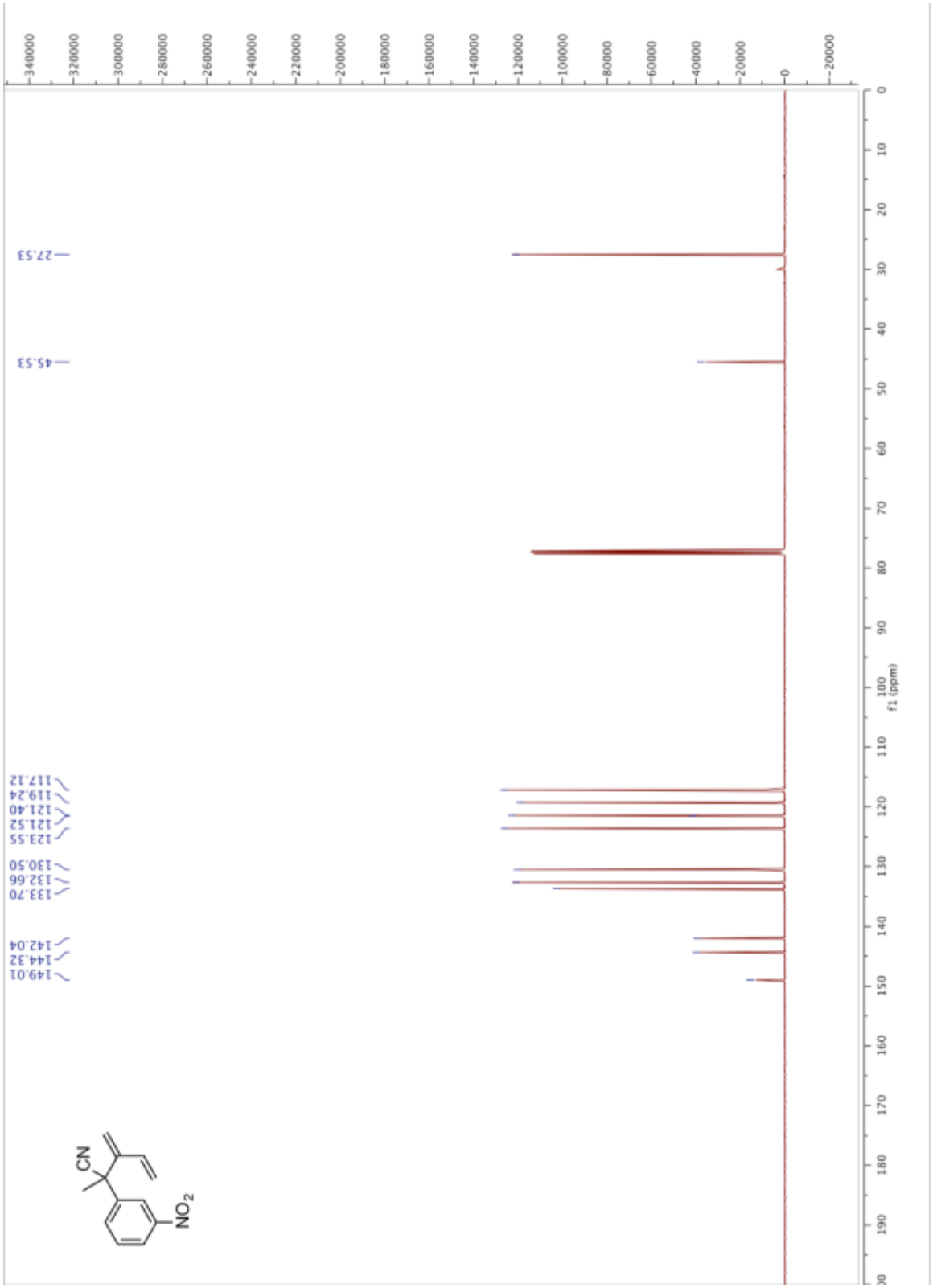
27.53
45.53
117.12
119.24
121.40
121.52
123.55
130.50
132.66
133.70
142.04
144.32
149.01
f1 (ppm)
CN
NO2

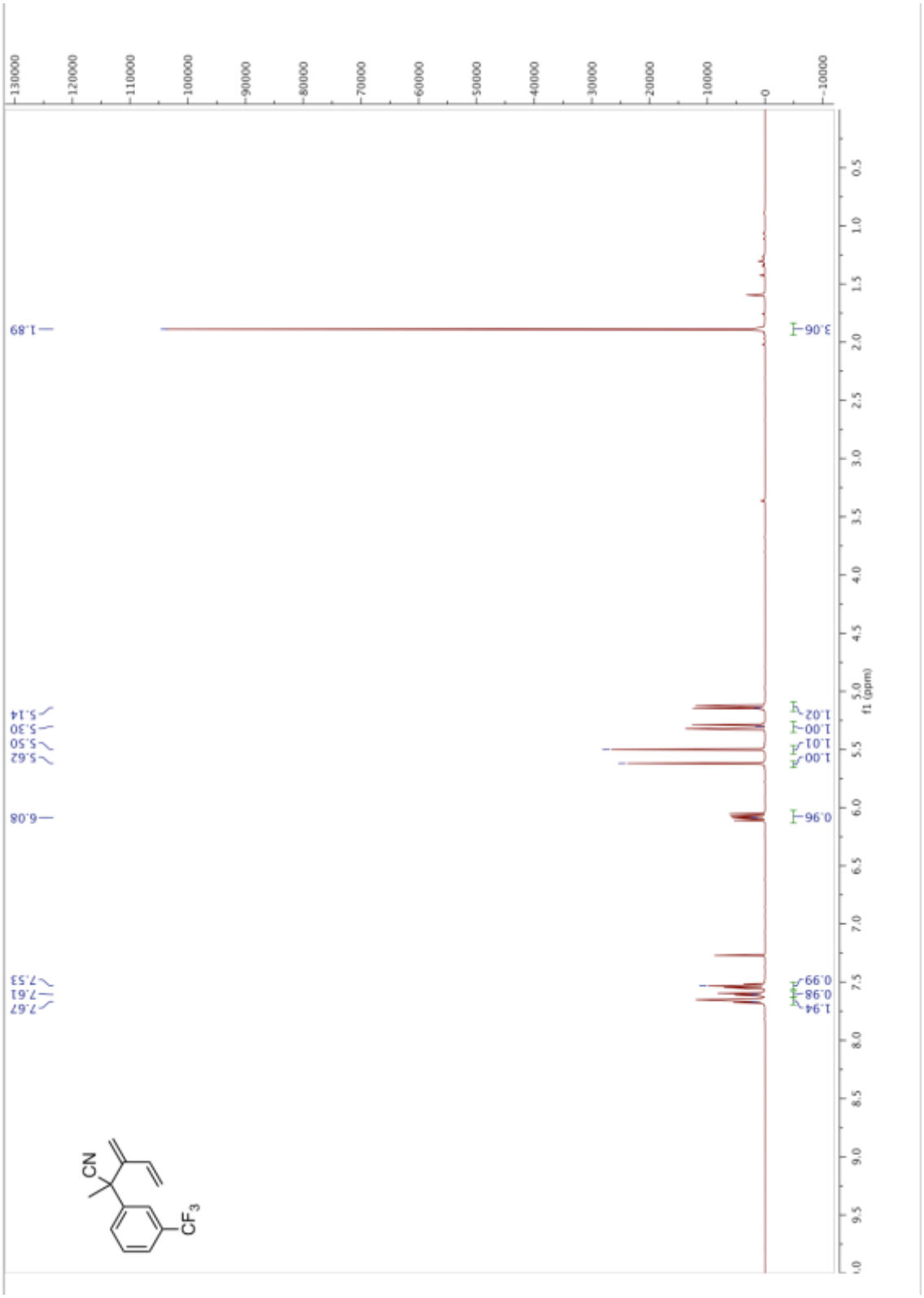
CN
CF3
1.89
6.08
5.62
5.50
5.30
5.14
7.67
7.61
7.53
3.06
1.02
1.00
1.01
1.00
0.96
0.99
0.98
1.94
f1 (ppm)

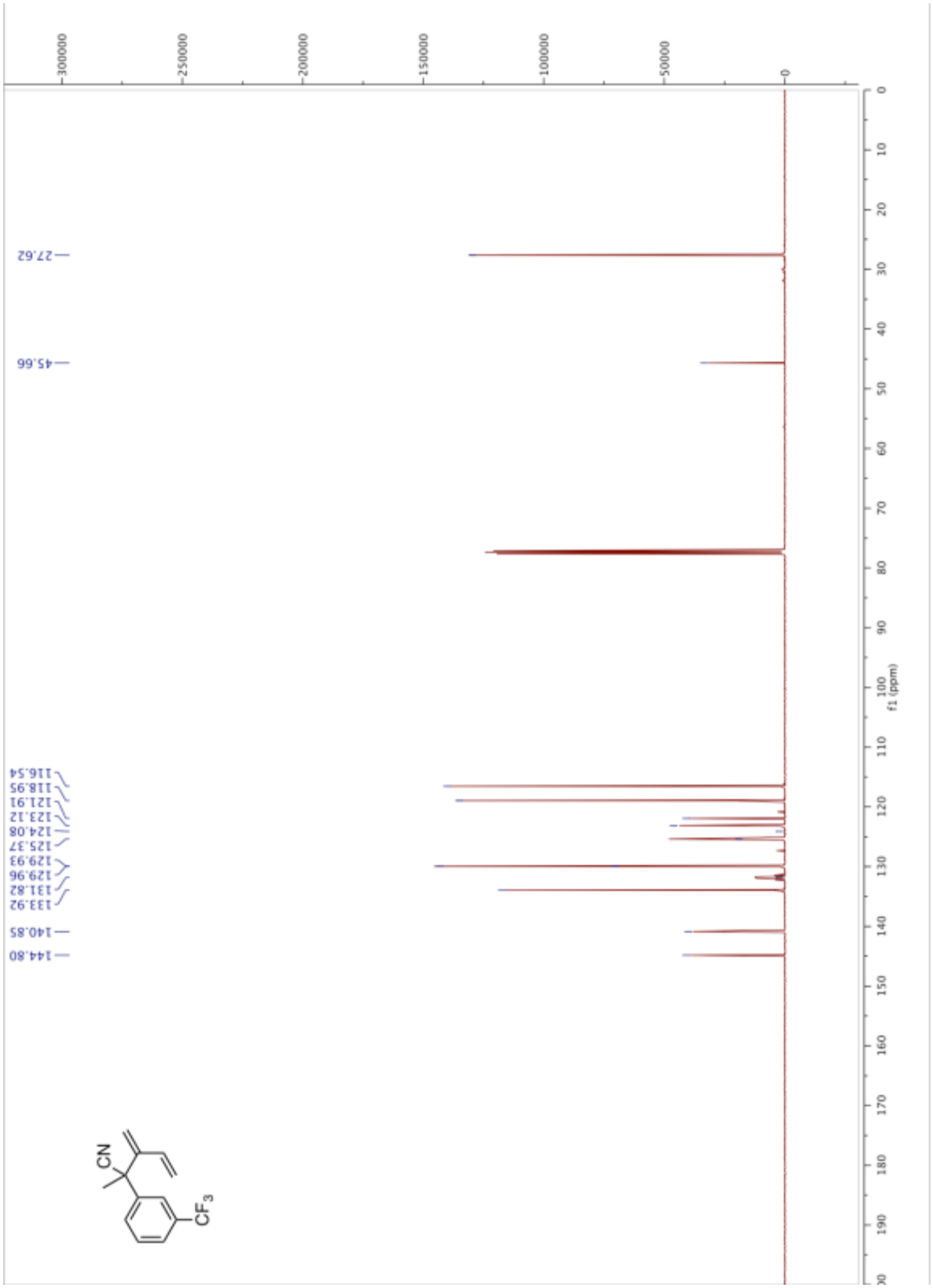
300000
250000
200000
150000
100000
50000
0
27.62
45.66
116.54
118.95
121.91
123.12
124.08
125.37
129.93
129.96
131.82
133.92
140.85
144.80
f1 (ppm)
CN
CF3

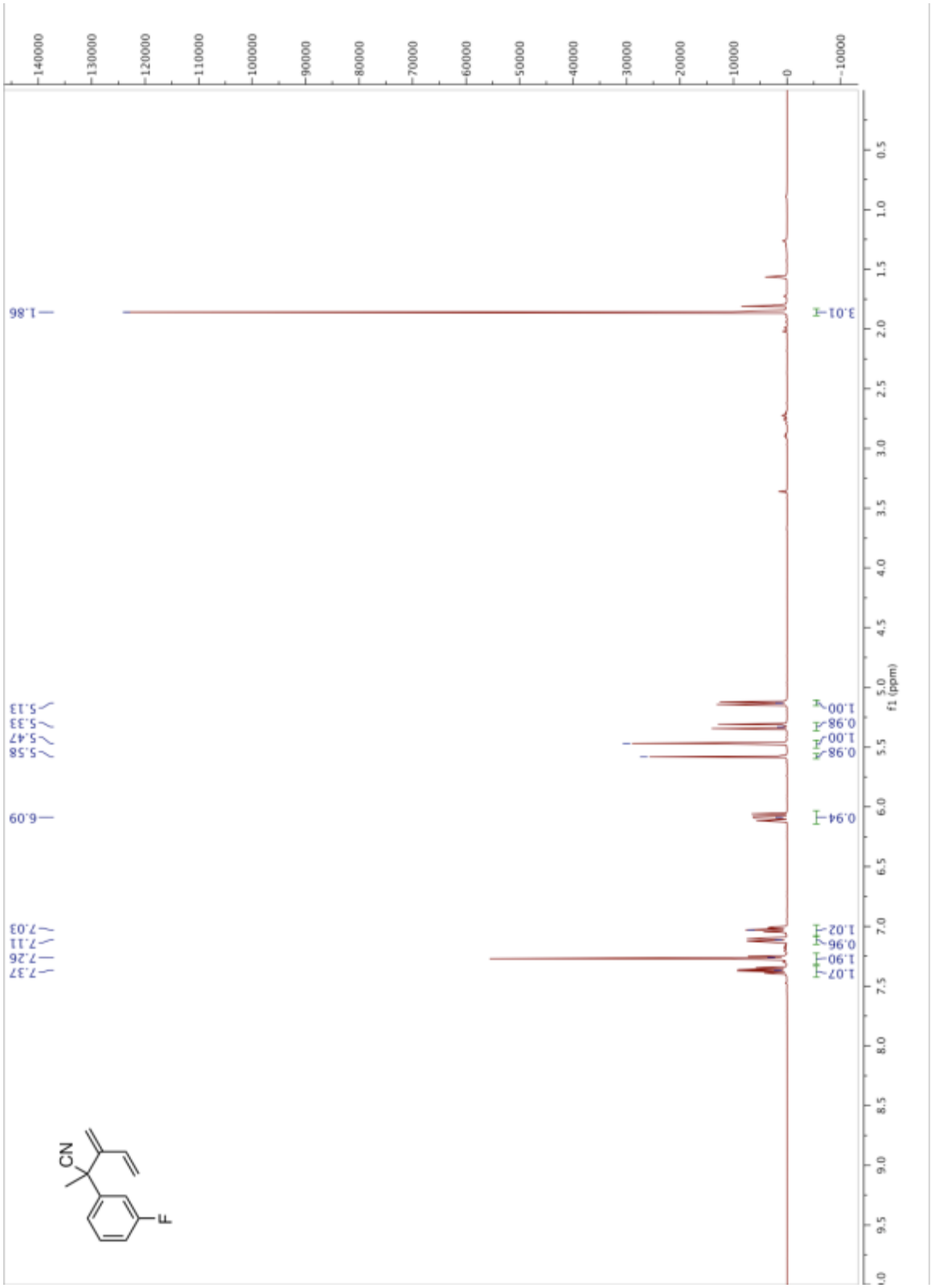
1.86
5.13
5.33
5.47
5.58
6.09
7.03
7.11
7.26
7.37
3.01
1.00
0.98
1.00
0.98
0.94
1.02
0.96
1.90
1.07
CN
F
f1 (ppm)

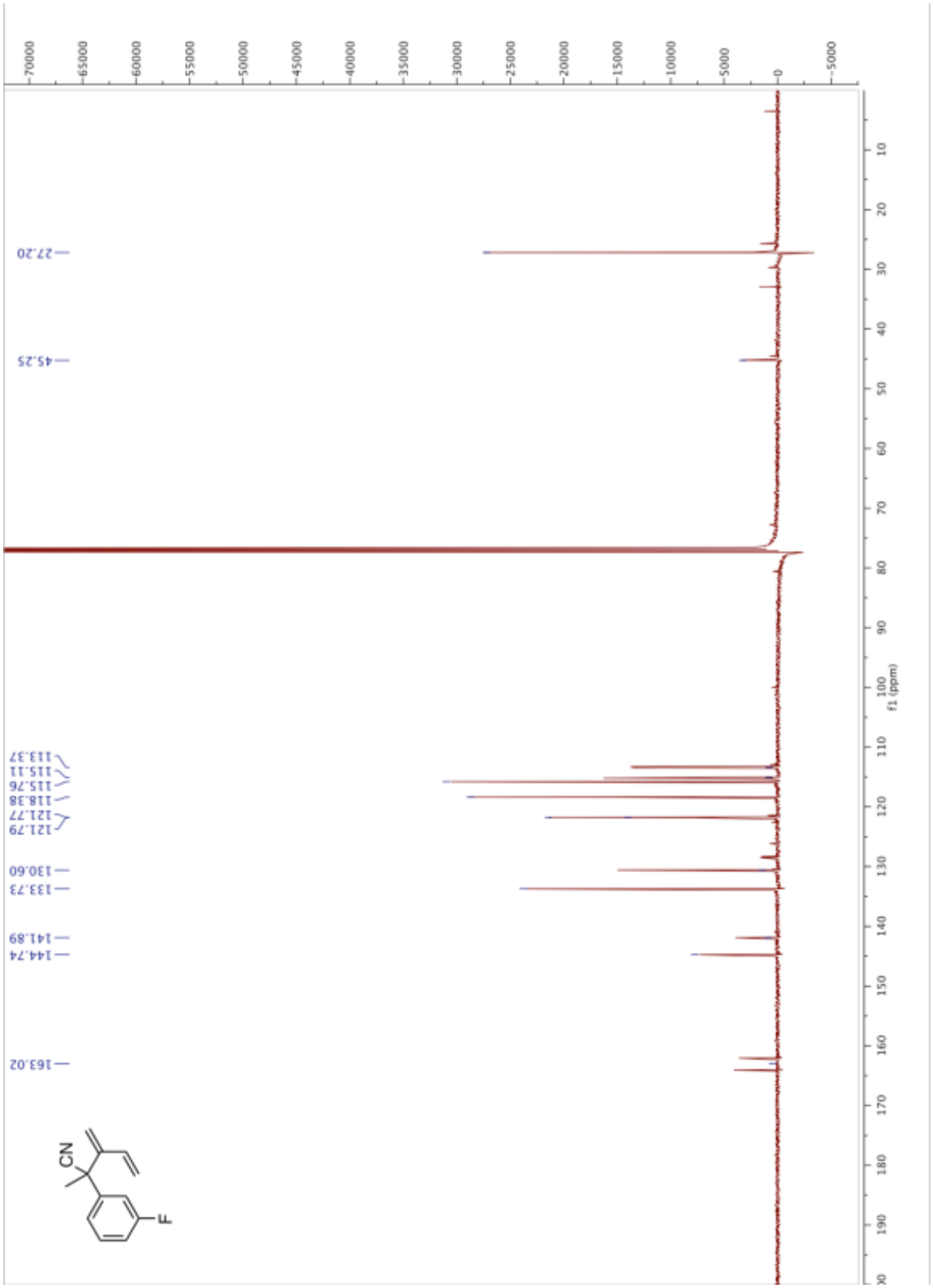
27.20
45.25
113.37
115.11
115.76
118.38
121.77
121.79
130.60
133.73
141.89
144.74
163.02
CN
F
f1 (ppm)

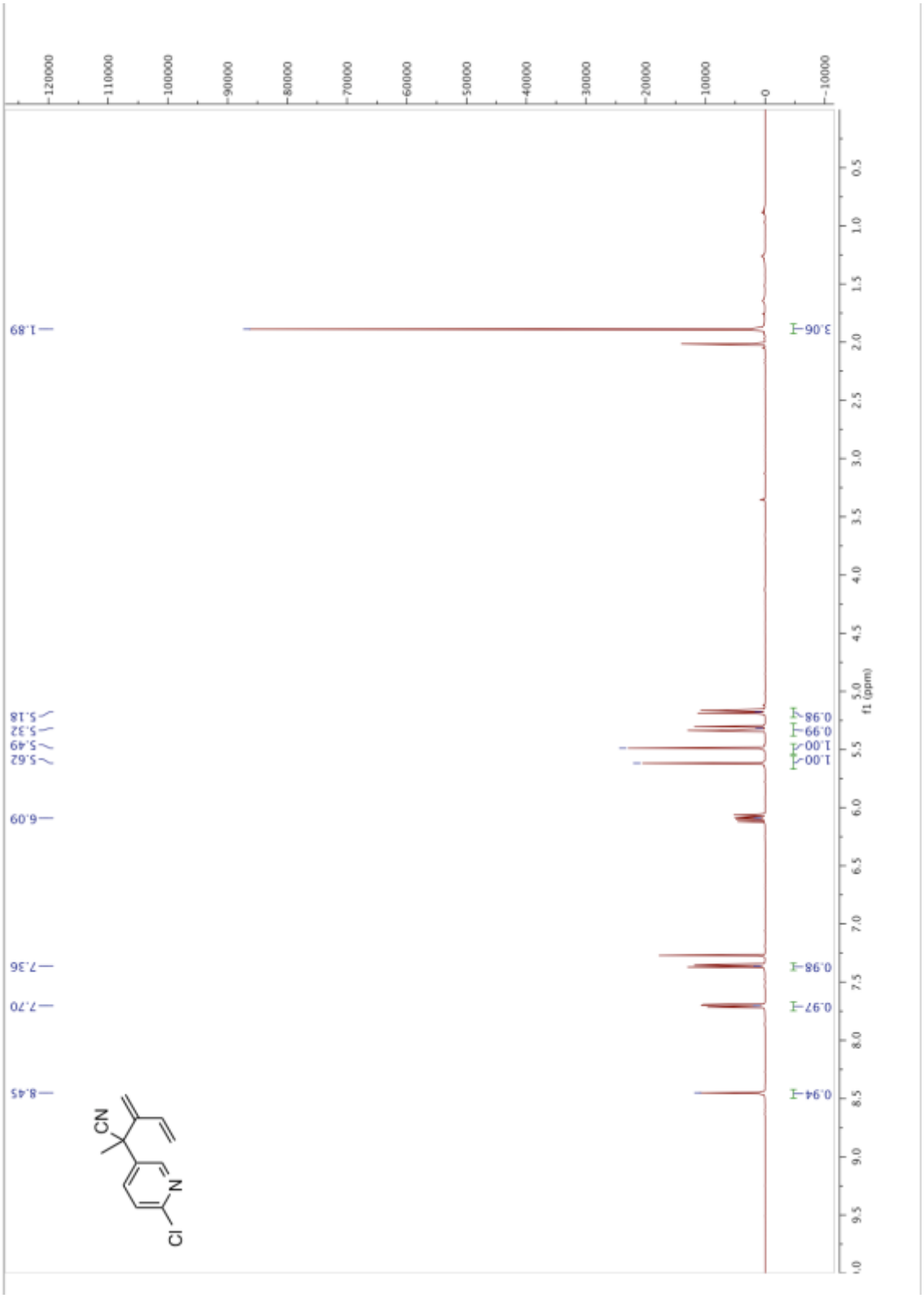
8.45
7.70
7.36
6.09
5.62
5.49
5.32
5.18
1.89
0.94
0.97
0.98
1.00
1.00
0.99
0.98
3.06
f1 (ppm)
CN
N
Cl

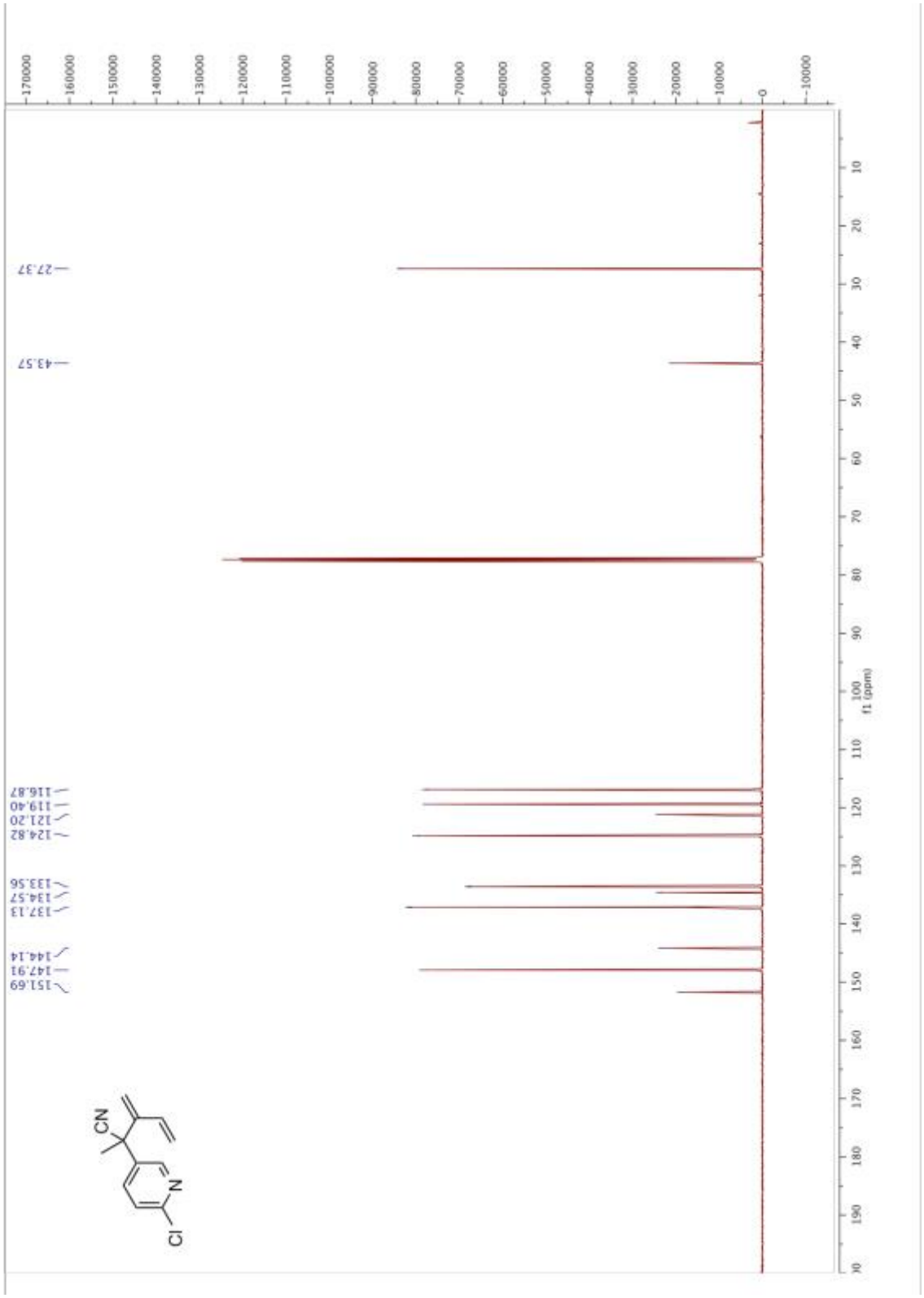
27.37
43.57
116.87
119.40
121.20
124.82
133.56
134.57
137.13
144.14
147.91
151.69
CN
N
Cl
f1 (ppm)

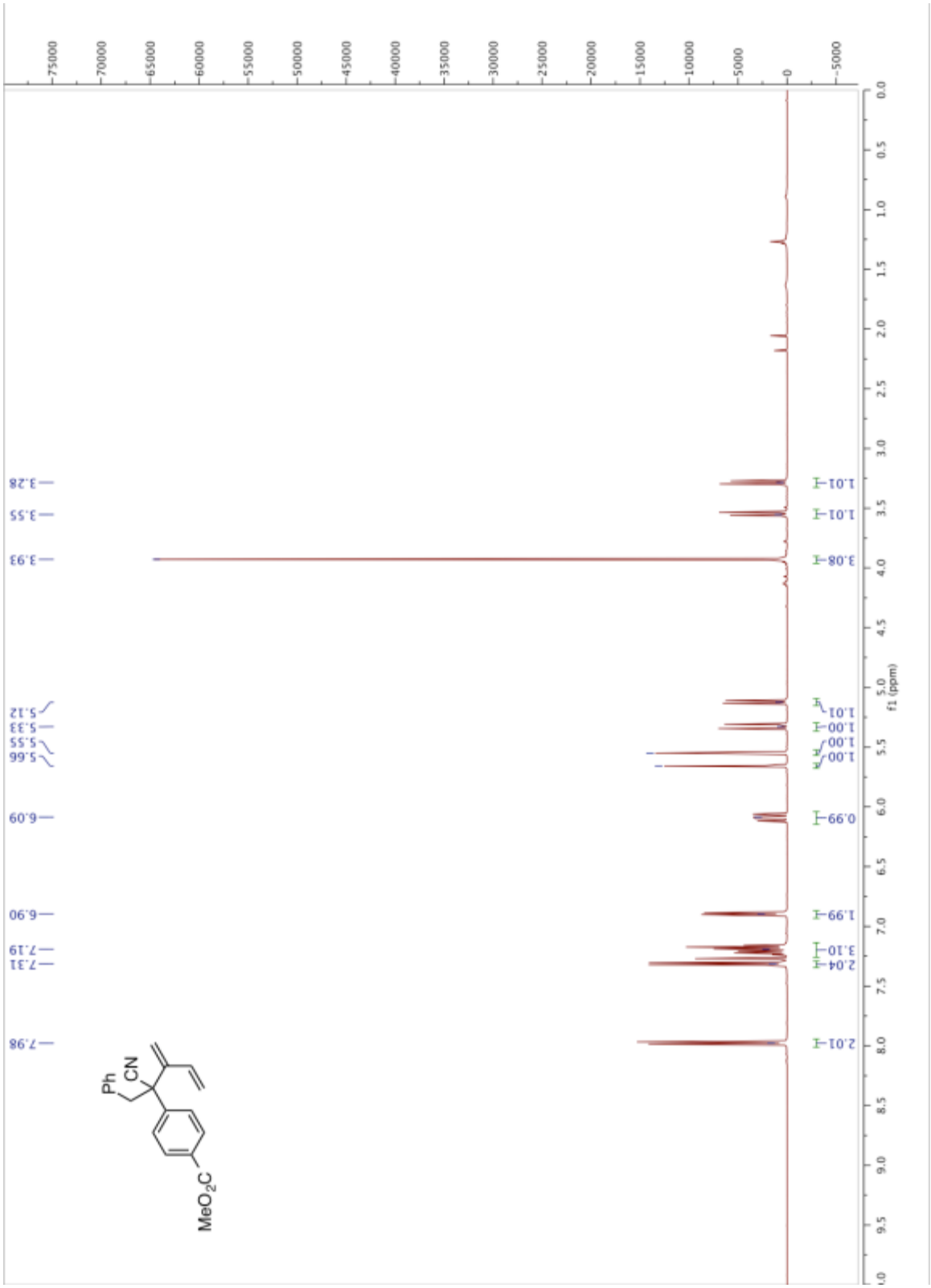
3.28
3.55
3.93
5.12
5.33
5.55
5.66
6.09
6.90
7.19
7.31
7.98
1.01
1.01
3.08
1.01
1.00
1.00
0.99
1.99
3.10
2.04
2.01
f1 (ppm)
Ph
CN
MeO2C

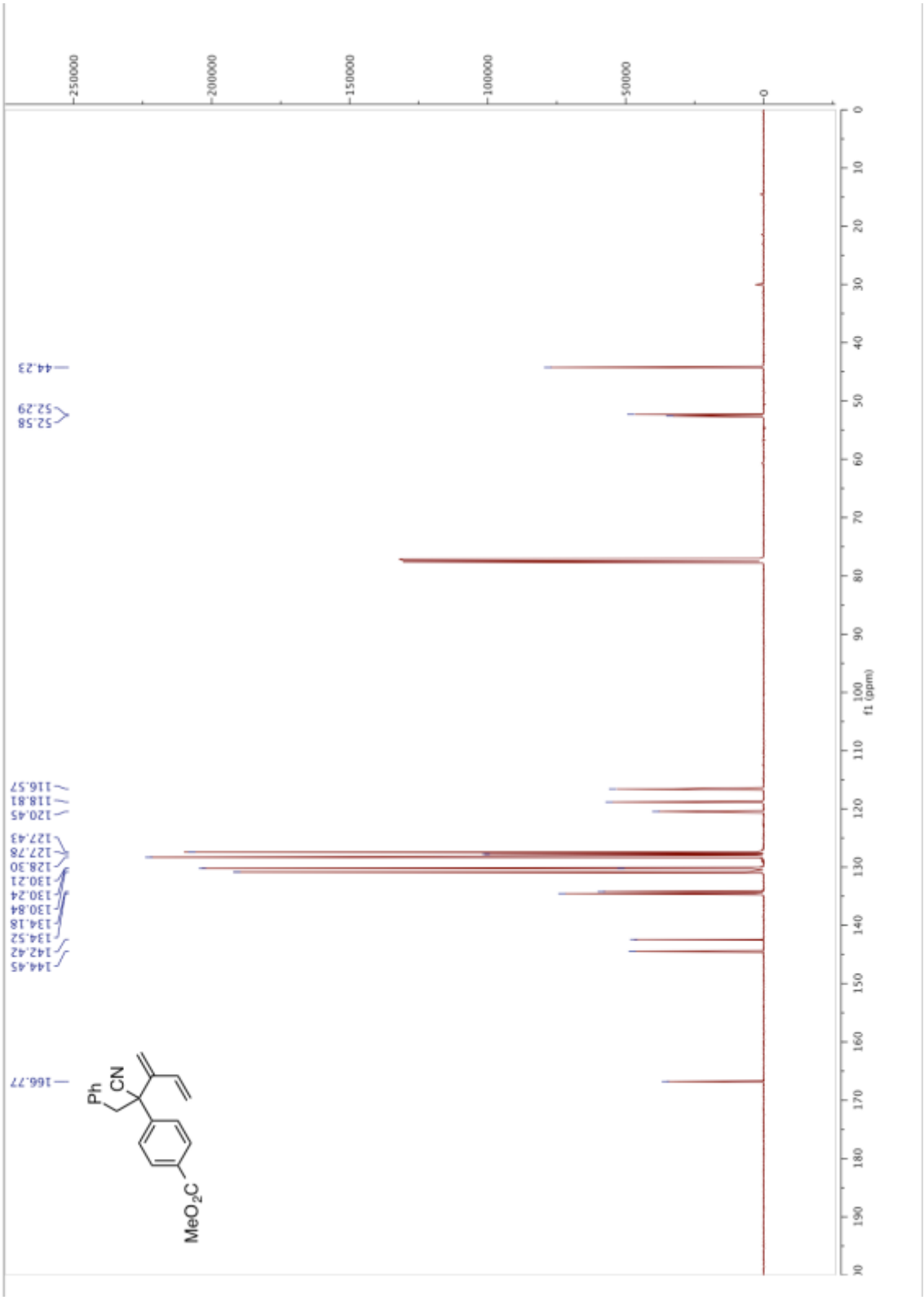
166.77
144.45
142.42
134.52
134.18
130.84
130.24
130.21
128.30
127.78
127.43
120.45
118.81
116.57
52.58
52.29
44.23
Ph
CN
MeO2C
f1 (ppm)

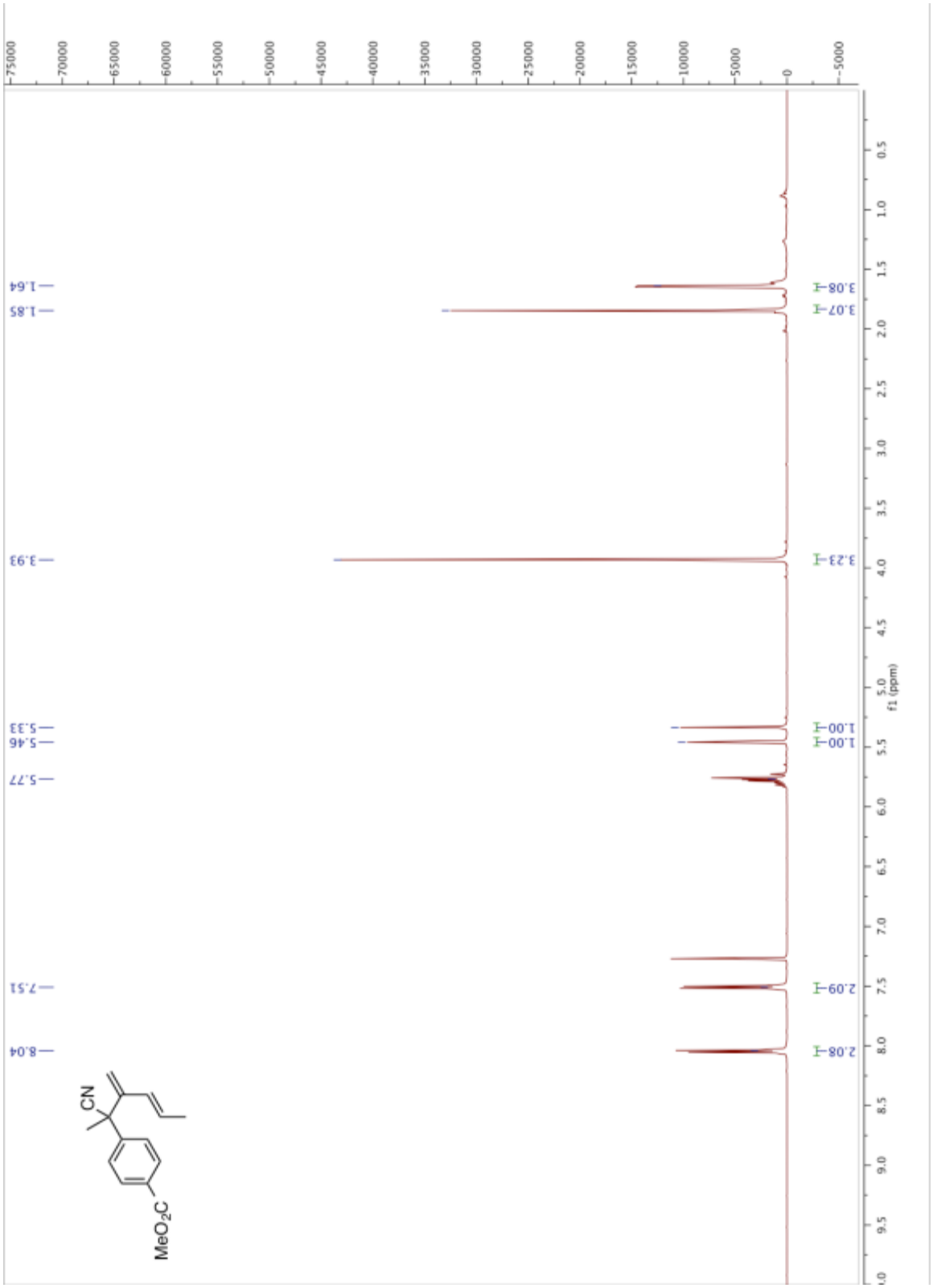
1.64
1.85
3.93
5.33
5.46
5.77
7.51
8.04
3.08
3.07
3.23
1.00
1.00
2.09
2.08
CN
MeO2C
f1 (ppm)

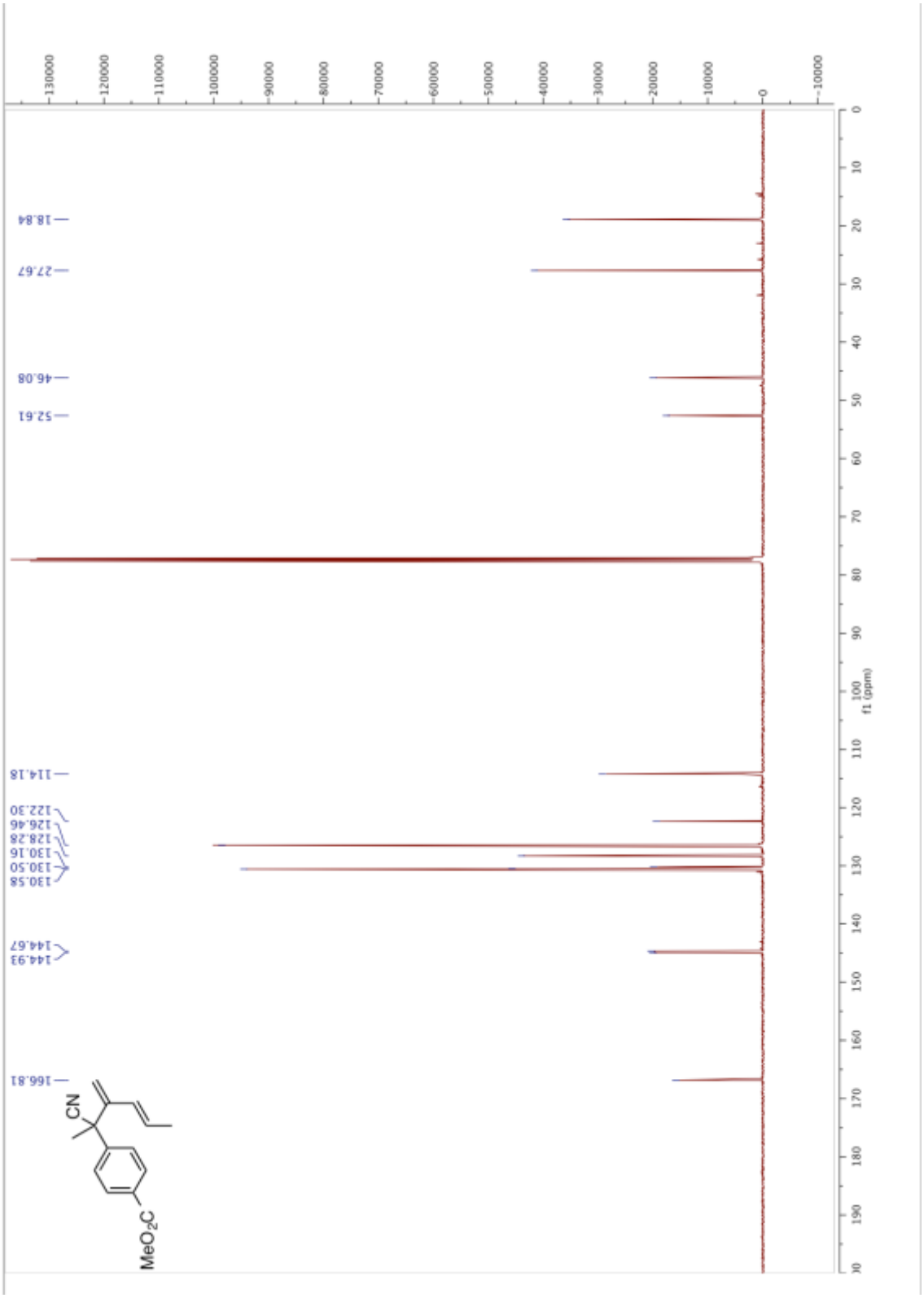
18.84
27.67
46.08
52.61
114.18
122.30
126.46
128.28
130.16
130.50
130.58
144.67
144.93
166.81
CN
MeO2C
f1 (ppm)

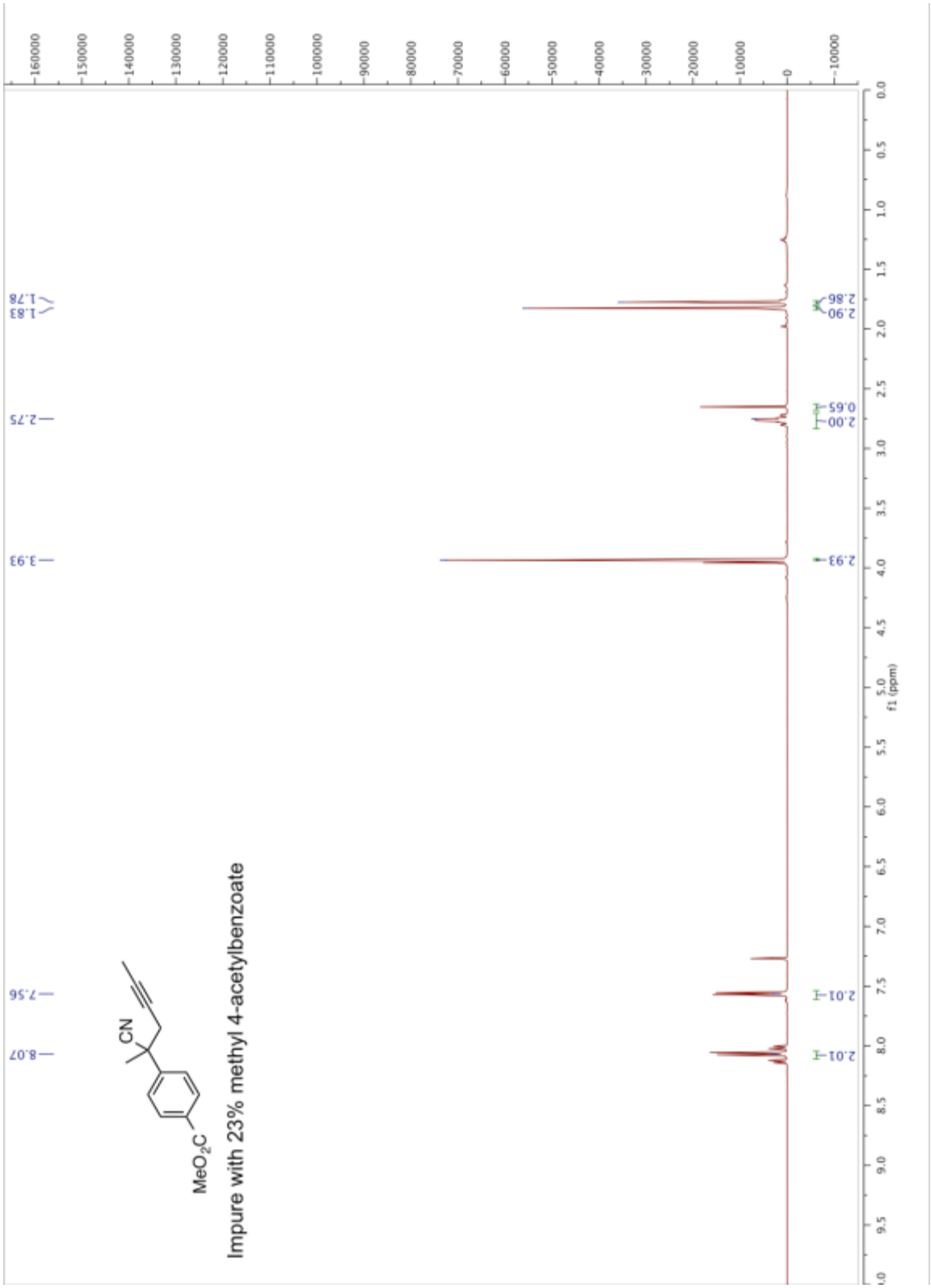
Impure with 23% methyl 4-acetylbenzoate
CN
MeO2C
8.07
7.56
3.93
2.75
1.83
1.78
2.01
2.01
2.93
0.65
2.00
2.90
2.86
f1 (ppm)

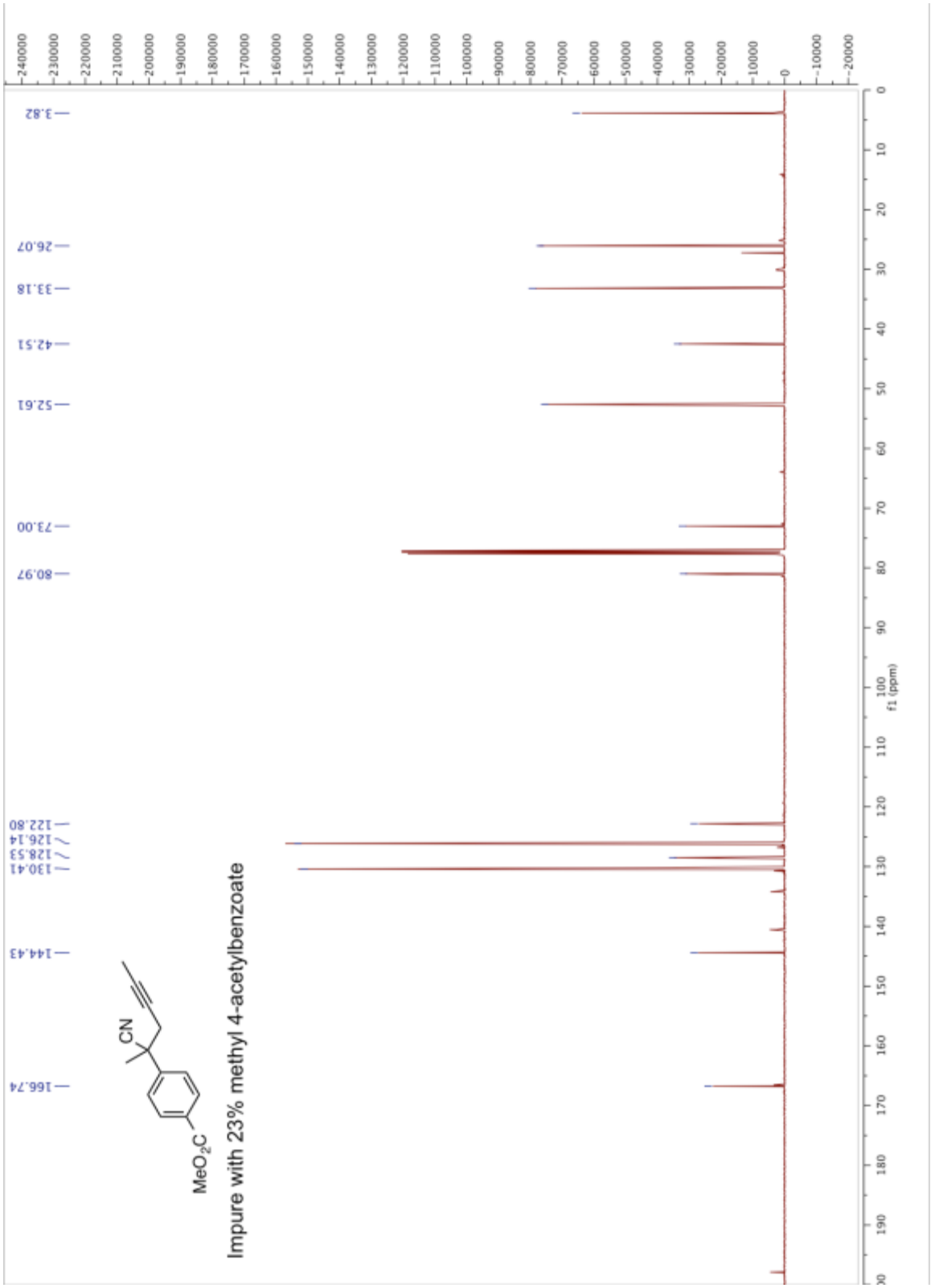
Impure with 23% methyl 4-acetylbenzoate
CN
MeO2C
166.74
144.43
130.41
128.53
126.14
122.80
80.97
73.00
52.61
42.51
33.18
26.07
3.82
f1 (ppm)

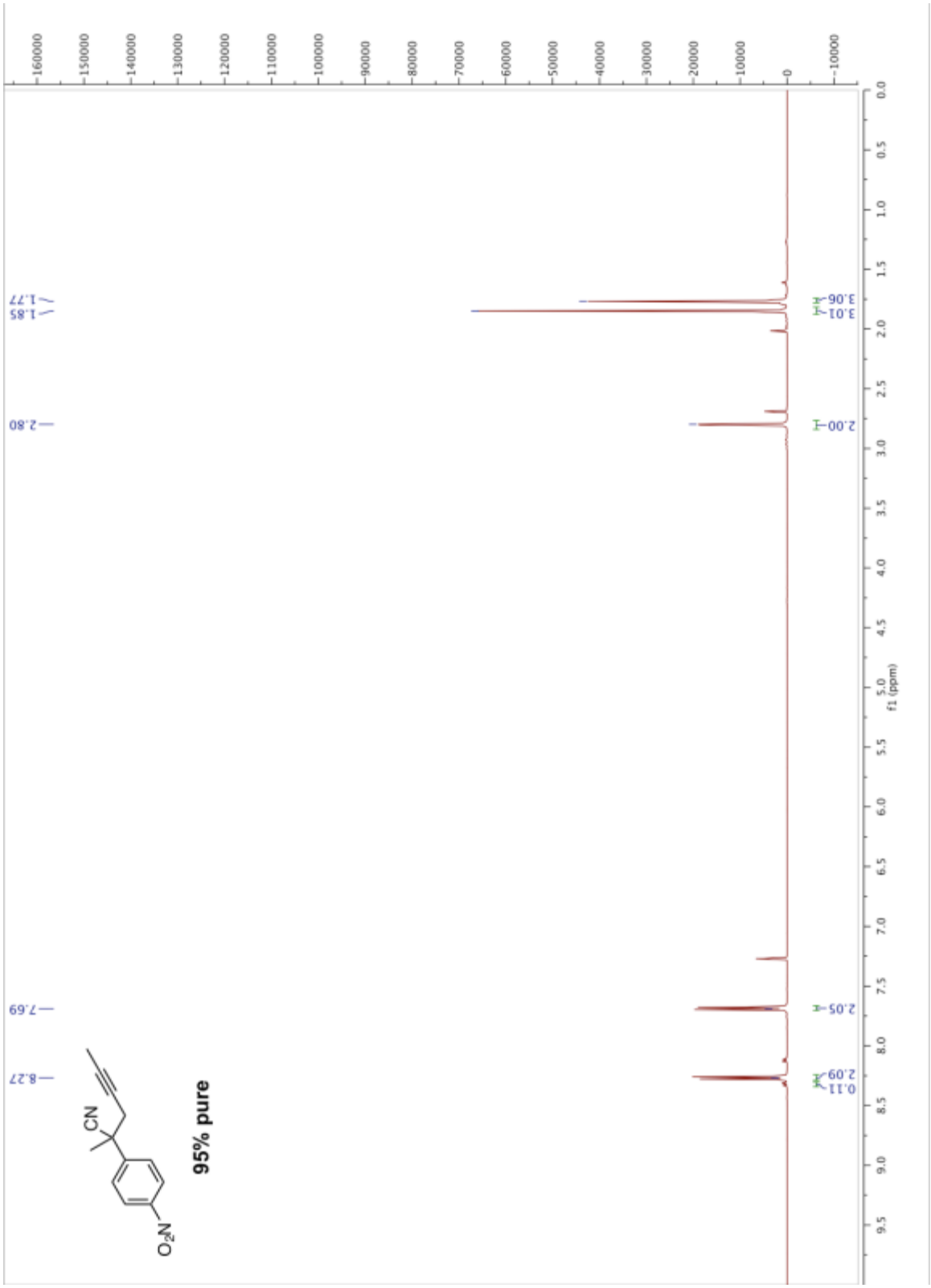
95% pure
CN
O2N
8.27
7.69
2.80
1.85
1.77
2.09
2.05
2.00
3.01
3.06
0.11
f1 (ppm)

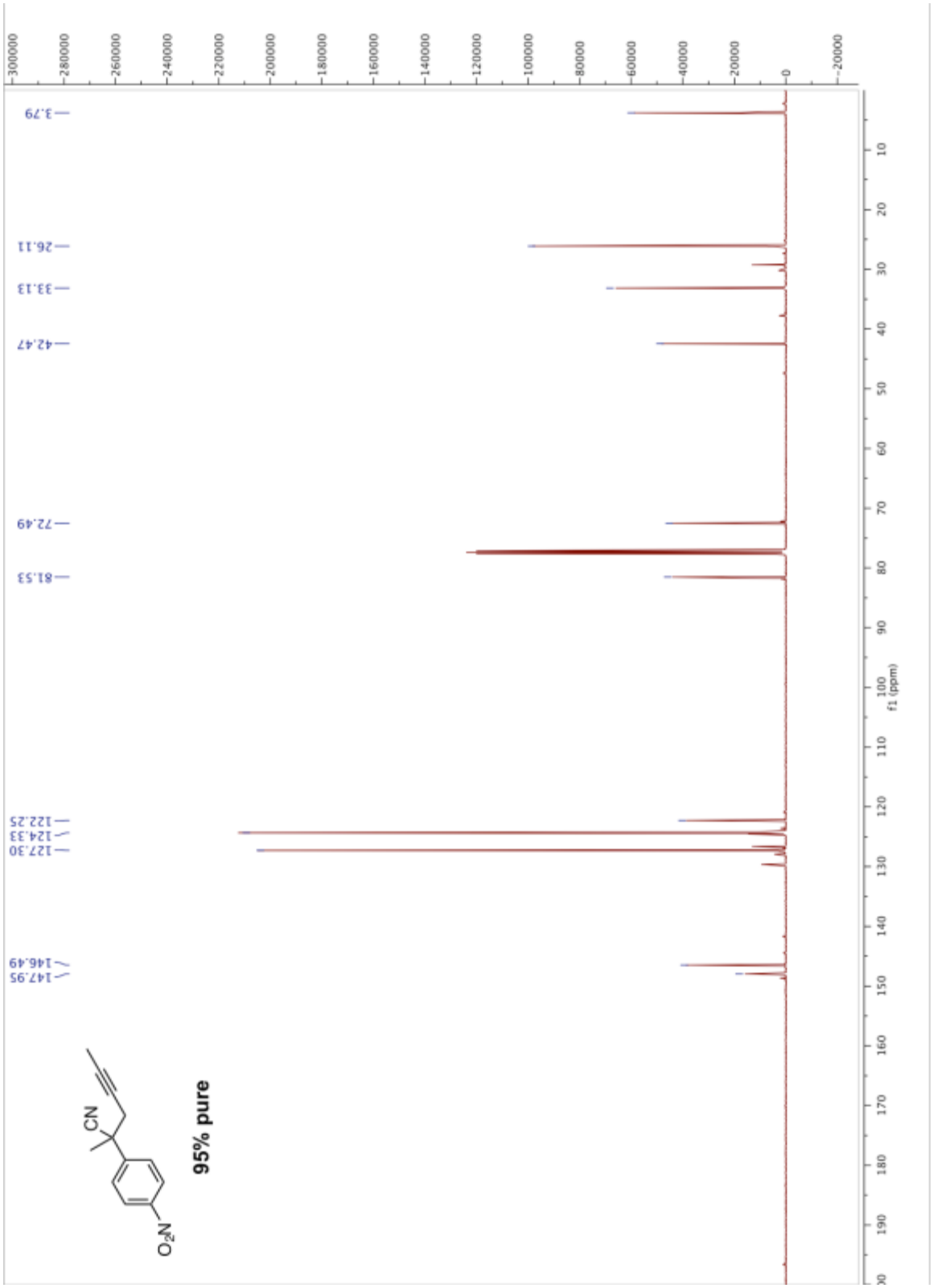
3.79
26.11
33.13
42.47
72.49
81.53
122.25
124.33
127.30
146.49
147.95
CN
O_2N
95% pure
f1 (ppm)

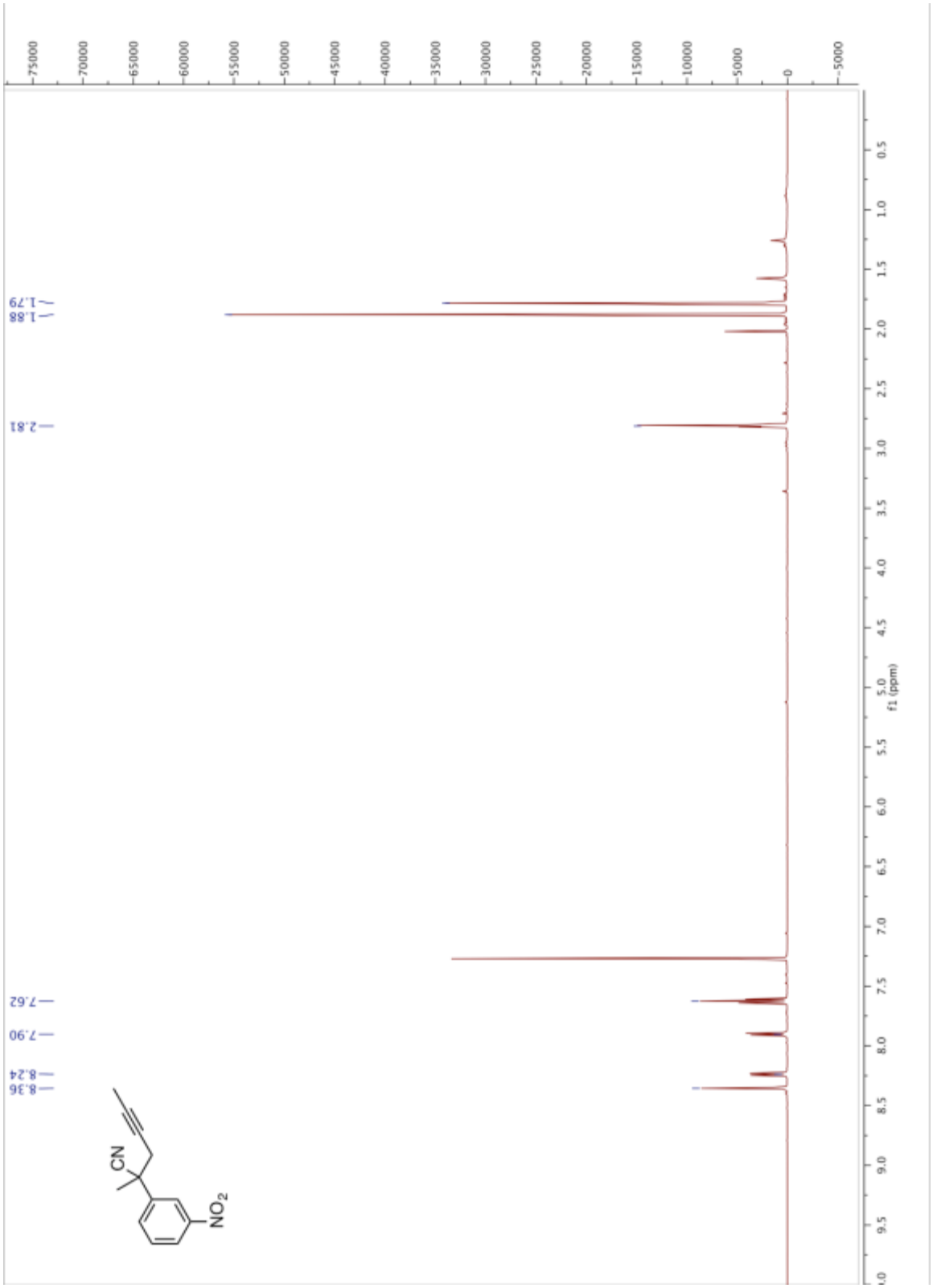
1.79
1.88
2.81
7.62
7.90
8.24
8.36
CN
NO2
f1 (ppm)

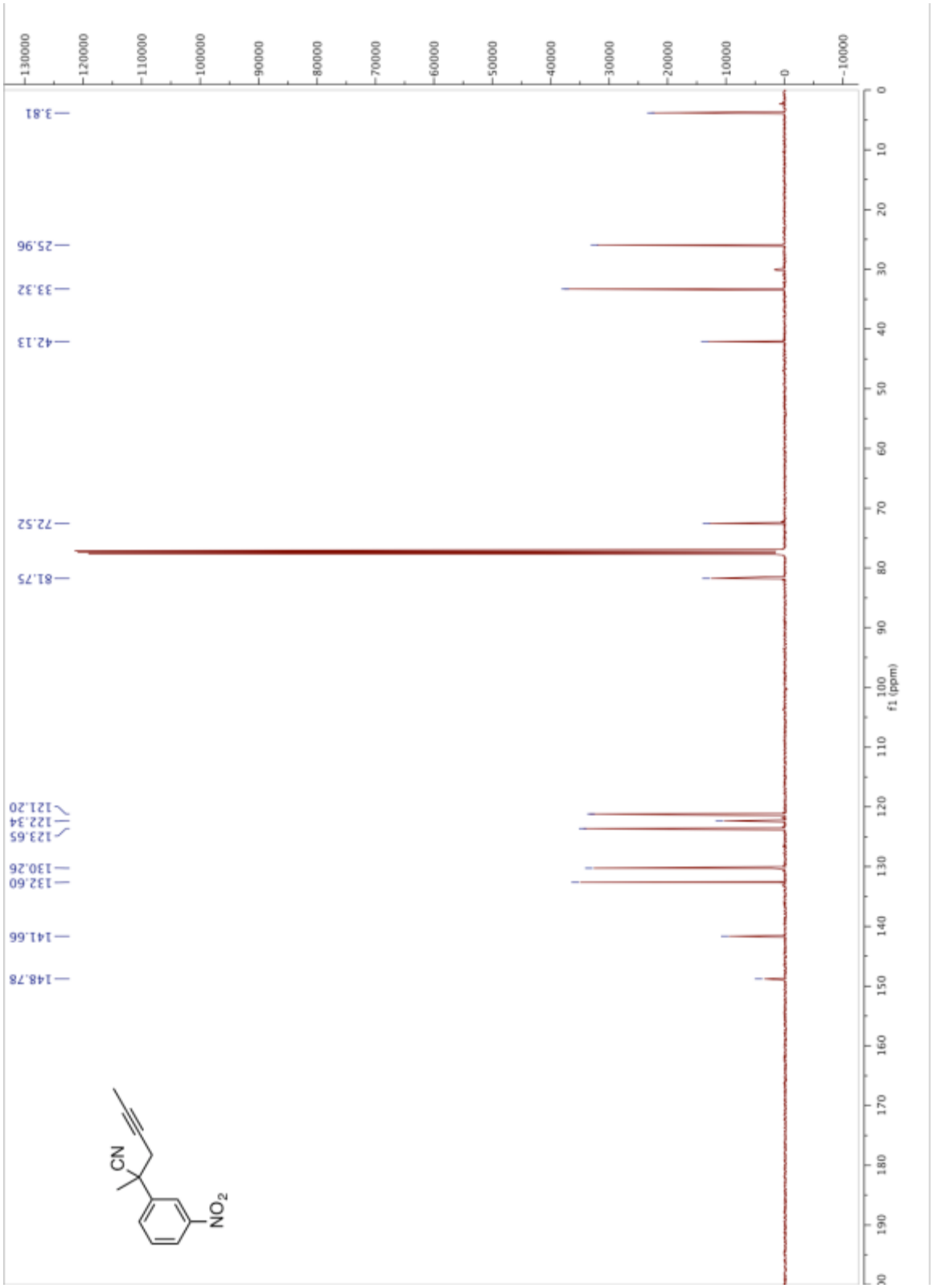
3.81
25.96
33.32
42.13
72.52
81.75
121.20
122.34
123.65
130.26
132.60
141.66
148.78
CN
NO2
f1 (ppm)

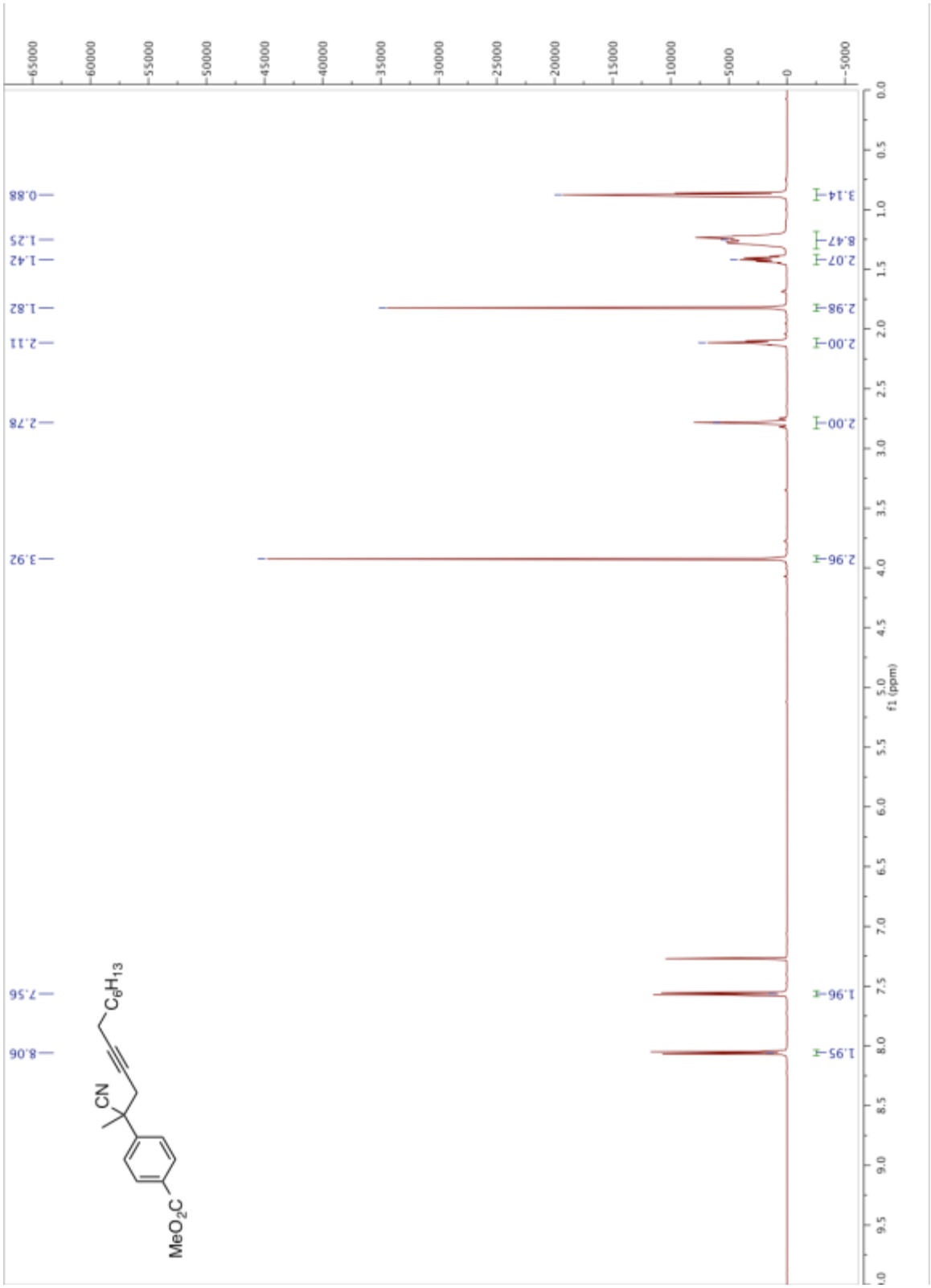
0.88
1.25
1.42
1.82
2.11
2.78
3.92
7.56
8.06
3.14
8.47
2.07
2.98
2.00
2.00
2.96
1.96
1.95
f1 (ppm)
CN
C6H13
MeO2C

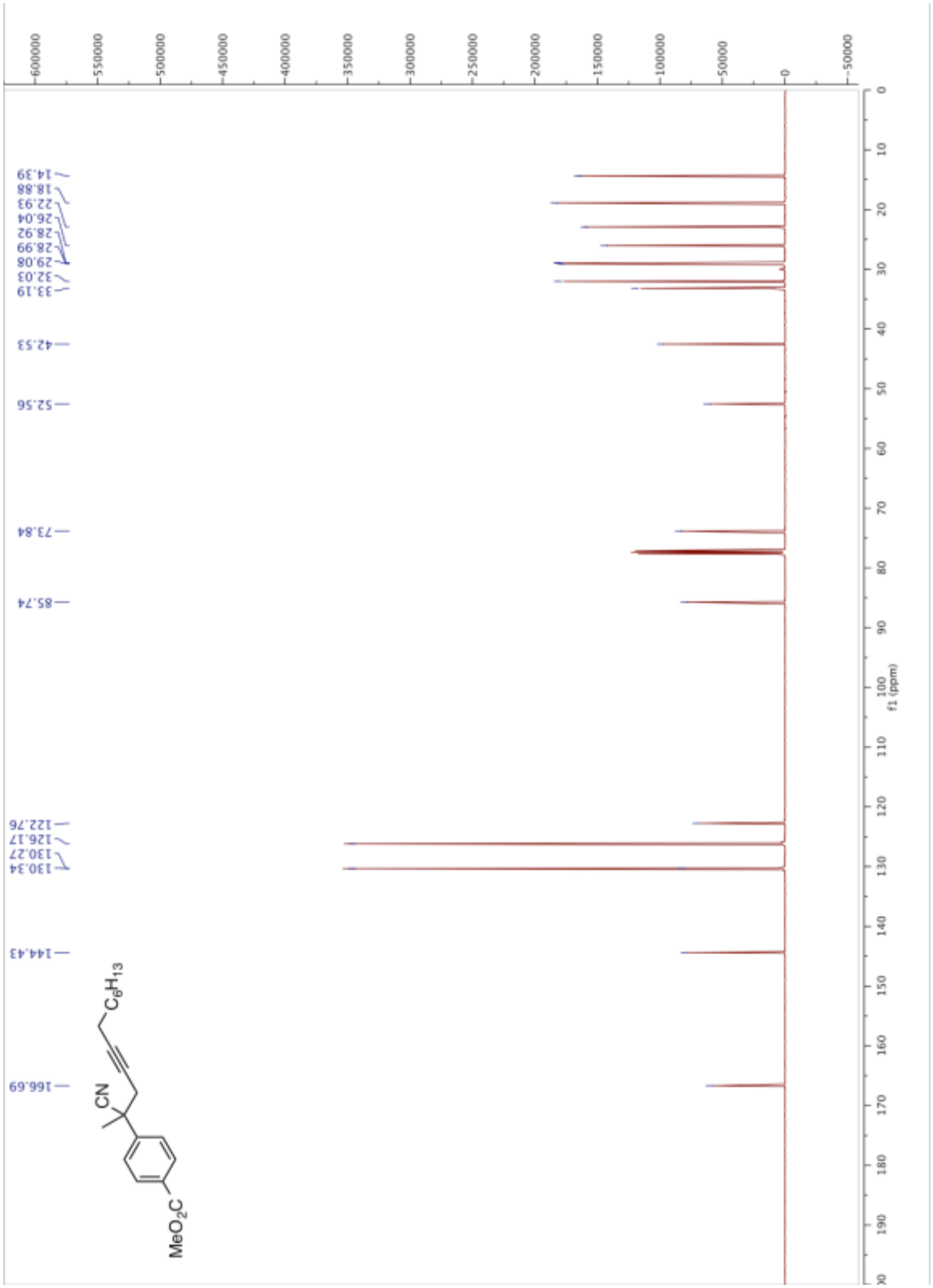
14.39
18.88
22.93
26.04
28.92
28.99
29.08
32.03
33.19
42.53
52.56
73.84
85.74
122.76
126.17
130.27
130.34
144.43
166.69
CN
C6H13
MeO2C
f1 (ppm)

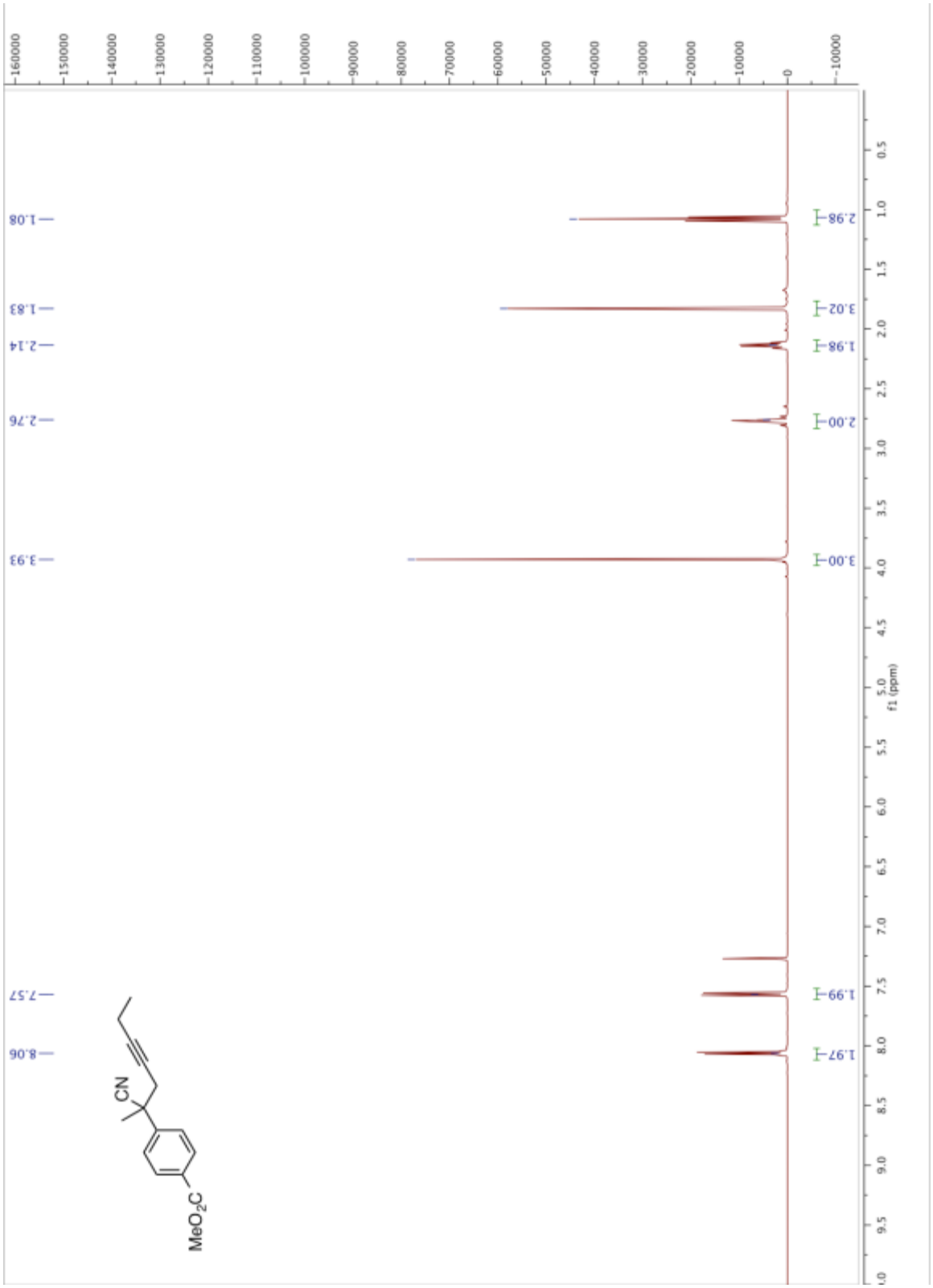
1.08
1.83
2.14
2.76
3.93
7.57
8.06
2.98
3.02
1.98
2.00
3.00
1.99
1.97
CN
MeO2C
f1 (ppm)

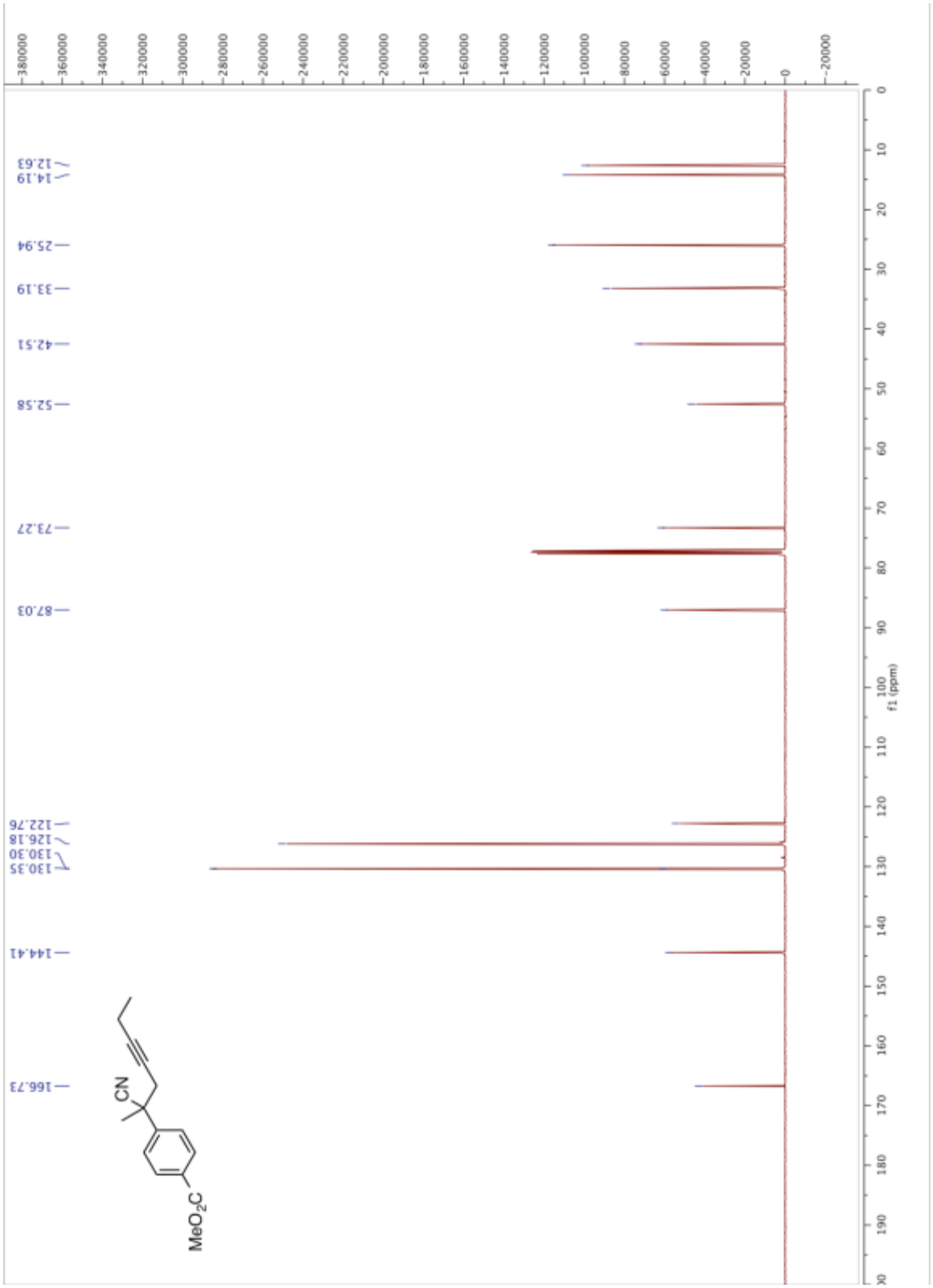
12.63
14.19
25.94
33.19
42.51
52.58
73.27
87.03
122.76
126.18
130.30
130.35
144.41
166.73
CN
MeO2C
f1 (ppm)

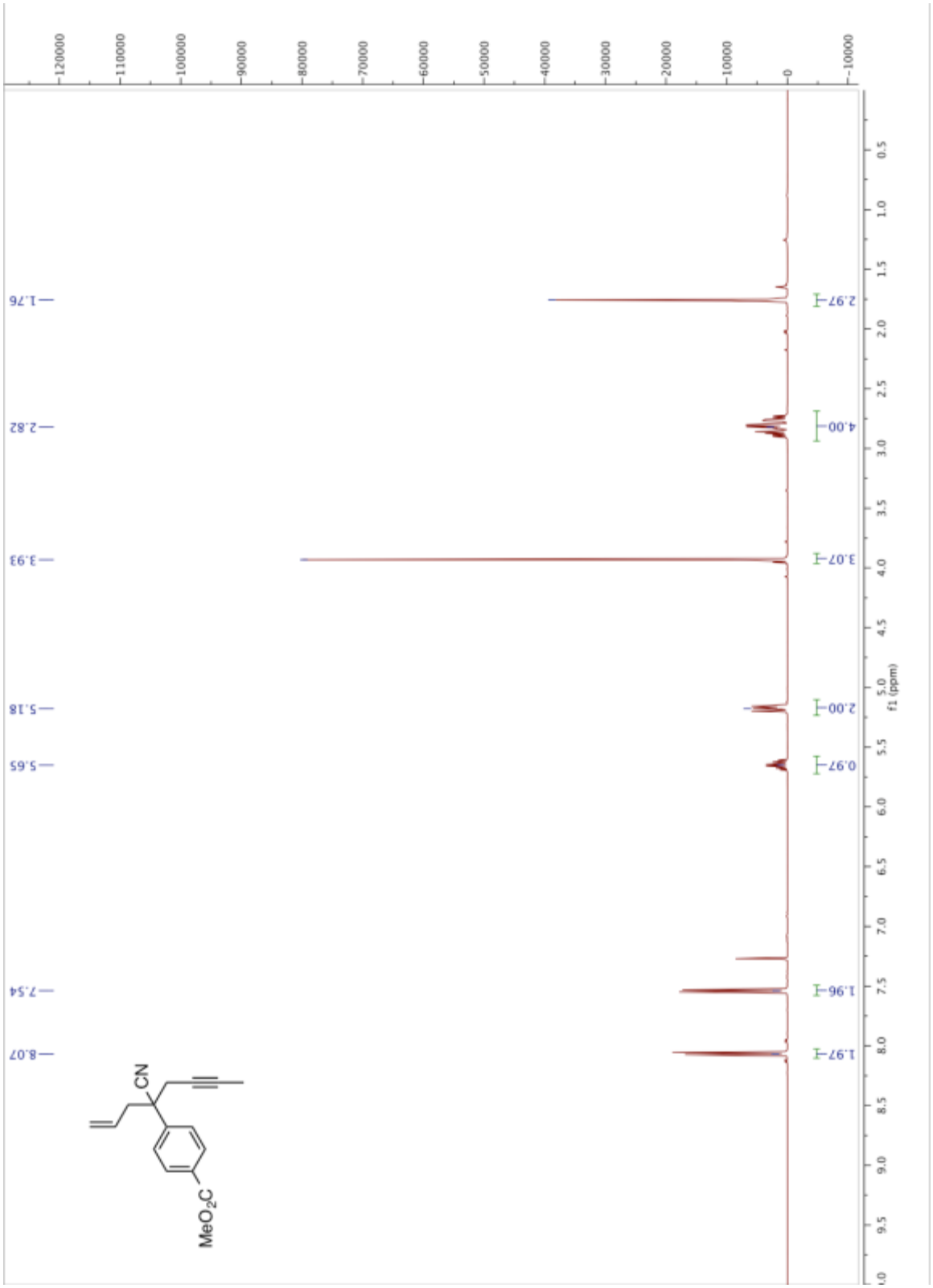
1.76
2.82
3.93
5.18
5.65
7.54
8.07
2.97
4.00
3.07
2.00
0.97
1.96
1.97
f1 (ppm)
CN
MeO2C

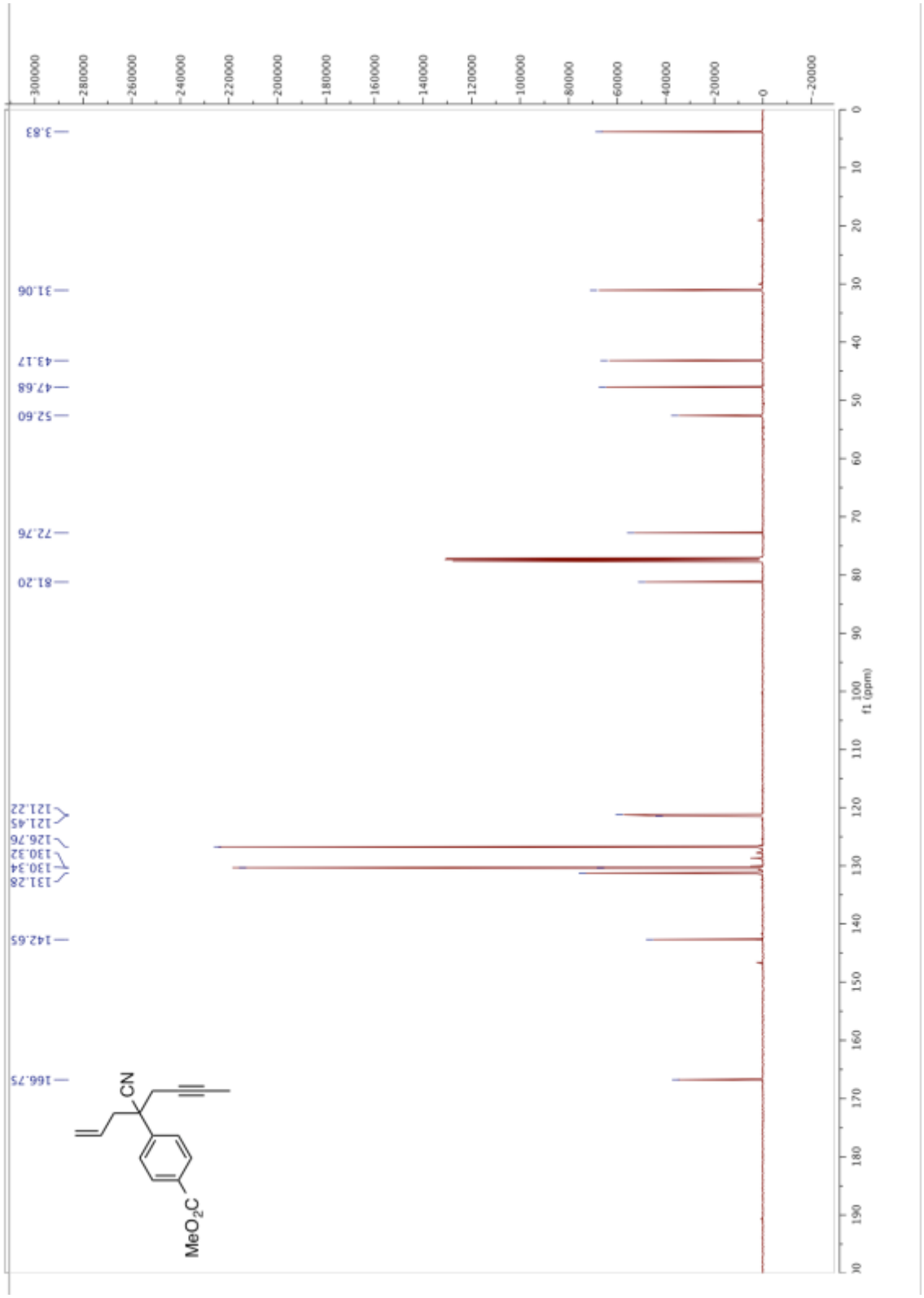
3.83
31.06
43.17
47.68
52.60
72.76
81.20
121.22
121.45
126.76
130.32
130.34
131.28
142.65
166.75
CN
MeO2C
f1 (ppm)

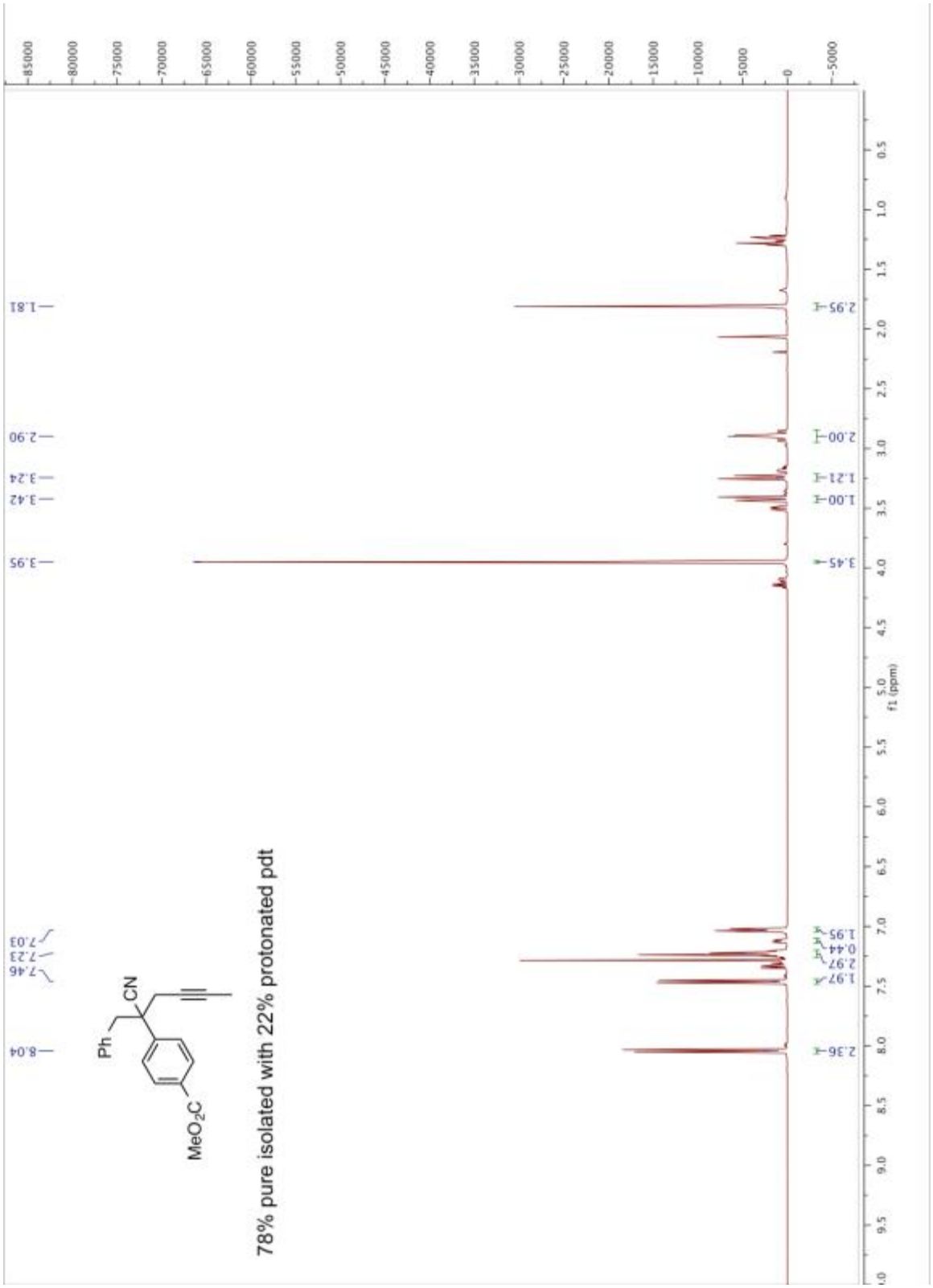
78% pure isolated with 22% protonated pdt
Ph
CN
MeO2C
f1 (ppm)

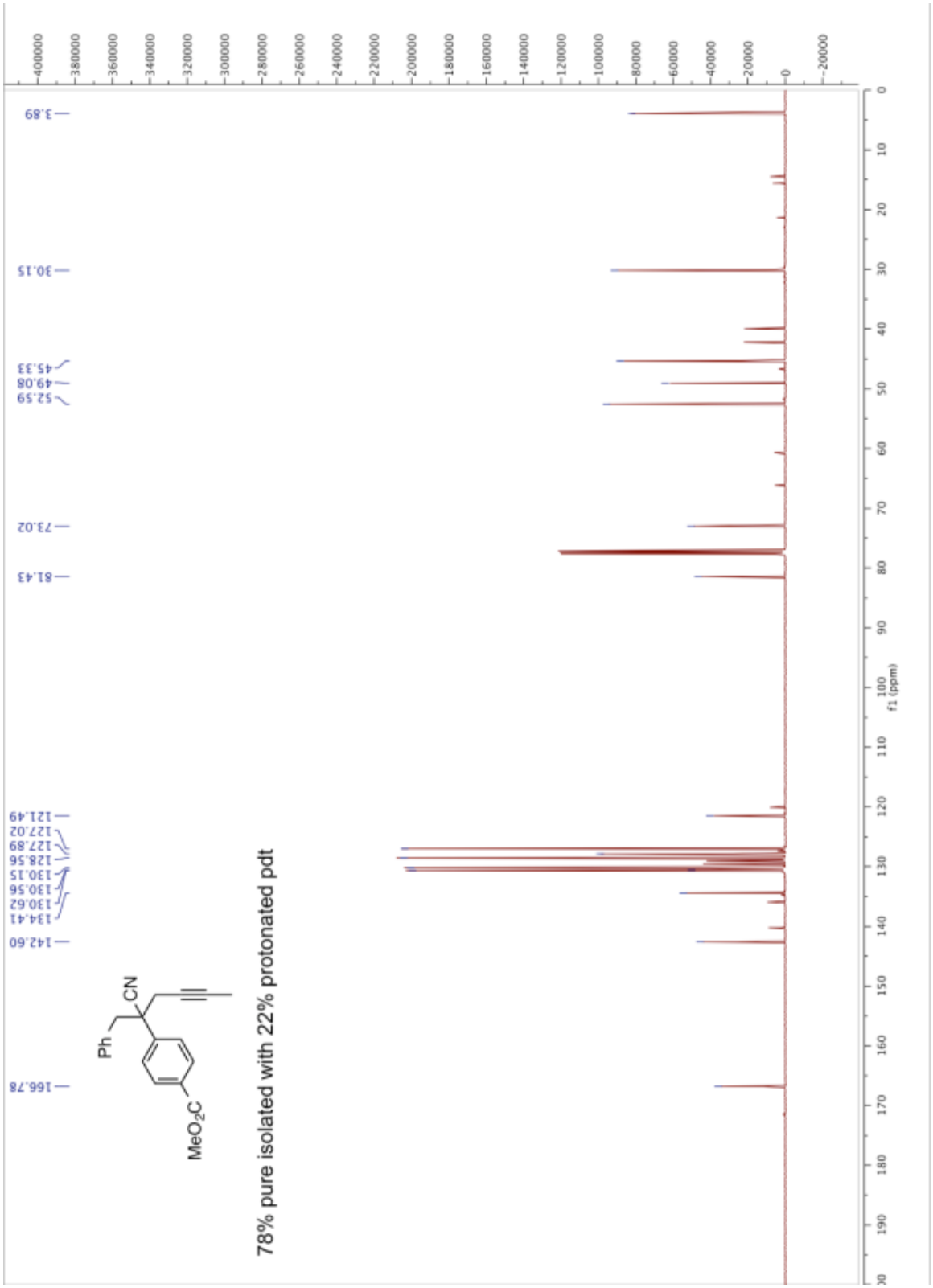
78% pure isolated with 22% protonated pdt
Ph
CN
MeO2C
166.78
142.60
134.41
130.62
130.56
130.15
128.56
127.89
127.02
121.49
81.43
73.02
52.59
49.08
45.33
30.15
3.89
f1 (ppm)

[1] Tanaka, T.; Okamura, N.; Bannai, K.; Hazato, A.; Sugiura, S.; Manabe, K.; Kurozumi, S. "Stereospecific Synthesis of (5E)-PGE2 by Palladium-Catalyzed Decarboxylative 2-Alkenylation of 2-Alkenyloxycarbonylated Cyclopentanone Derivative." *Tetrahedron Lett.* **1985**, *26*, 5575-5578.

[2] Crumbie, R. L.; Nimitz, J. S.; Mosher, H. S. "α-Nitro Ketones and Esters from Acylimidazoles." *J. Org. Chem.* **1982**, *47*, 4040-4045.

[3[Grenning, A. J.; Tunge, J. A. "Deacylative Allylation: Allylic Alkylation via Retro-Claisen Activation." *J. Am. Chem. Soc.* **2011**, *133*, 14785-14794.

Chapter 4. Activation of Alcohols with Carbon Dioxide: Intermolecular Allylation of Weakly Acidic Pronucleophiles[1]

4.1 Introduction to Allylation:

As mentioned in chapters 1-3 of this dissertation, incorporation of allylic moieties consisting of a three-carbon subunit (C–C=C) have been the subject of extensive research over the past four decades.[2-9] One potential reason for such extensive research lies in the ability of alkenes to serve as diverse functional handles for other chemoselective transformations.[10] Further, unlike asymmetric reactions involving a prochiral olefin or carbonyl moieties where asymmetric induction relies on facial differentiation, asymmetric allylic alkylations can arise from numerous methods of asymmetric induction.[7] Specifically, incorporation of chiral elements can occur about the nucleophile, electrophile, or both. Lastly, allylic alkylations can also form numerous types of bonds making them attractive considerations in total synthesis.[7]

In general, allylic substituents can be incorporated into synthetic intermediates as nucleophiles (allylic anion)[11-14] or as most commonly is observed, electrophiles (allyl cation).[2-9,15] The most highly utilized method for catalytic electrophilic allylic alkylation, known as the Tsuji-Trost reaction, involves the use of palladium, activated allylic electrophile (allyl acetate or allyl carbonate), and a stabilized nucleophile. In contrast to simple substitution reactions with allylic halides, the Tsuji-Trost reaction uses more readily available alcohols and the use of palladium can control the regio- and stereochemical outcome of product formation.

4.2 Development and Application of the Tsuji-Trost Reaction.

First reported in 1965 by Tsuji and coworkers, the ability for palladium to promote allylic alkylation of carbon-centered nucleophiles was accomplished in the presence of sodium ethoxide (Scheme 4.1).[16] Although a mixture of allylated and diallylated products was observed using

stoichiometric palladium(allyl)chloride dimer, Tsuji and coworkers revealed the importance of palladium π-allyl intermediates for successful allylic alkylation.

Scheme 4.1: Tsuji's First Report of the Allylation of Carbon-centered Nucleophiles with Palladium *p*-Allyl Species.

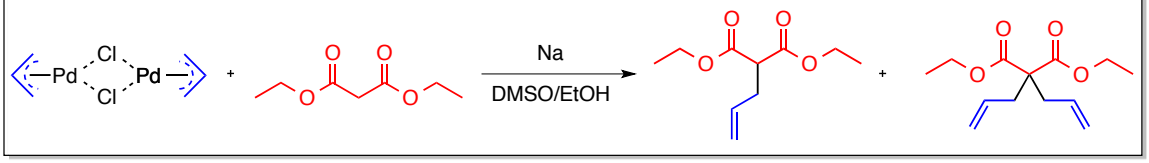

Over the next couple of years, it was revealed that not only could palladium π-allyl intermediates be generated from allylic electrophiles equipped with a good leaving group in the presence of a palladium(0) catalyst, but also that the amount of palladium could be reduced and used catalytically (Scheme 4.2).[17] In general, the mechanism of the Tsuji-Trost allylation reaction begins with coordination of an allylic electrophile to palladium(0) (Scheme 4.3).[7] Then, ionization occurs via oxidative addition to palladium to form a cationic palladium π-allyl intermediate. Lastly, nucleophilic substitution by an activated nucleophile will yield the allylated species along with regeneration of the active palladium(0) catalyst.[7]

Scheme 4.2: Catalytic Allylic Alkylation of Carbon-centered Nucleophiles

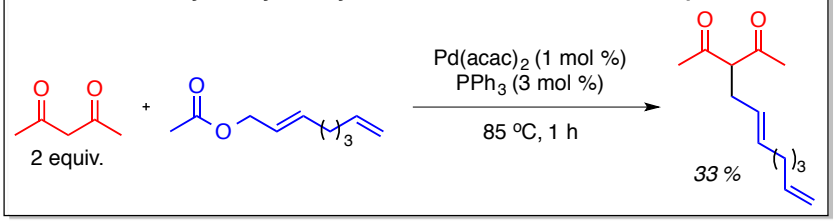

Scheme 4.3: Tsuji-Trost Allylic Alkylation Mechanism.

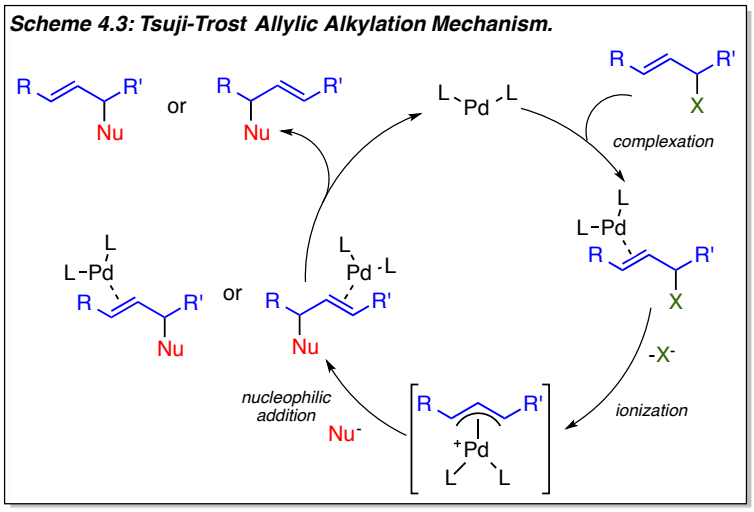

As it pertains to material that will be presented later in the chapter, in 1980 Tsuji[18] and Saegusa[19] expanded the scope of allylic alkylation methods to include the *in situ* generation of enolate nucleophiles from the palladium(0)-catalyzed decarboxylation of β-ketocarboxylates. Although Nesmeyanov and coworkers had previously demonstrated that metal β-ketocarboxylates readily undergo decarboxylation to generate metal enolates,[20] application in the Tsuji-Trost reaction, as presented by Tsuji and Saegusa, allowed for both activation of the electrophile and nucleophile *in situ*. Specifically, *in situ* activation of various nucleophiles could bypass the previously existing pK_a limits of the reaction and significantly expand the functional group compatibility.[9] Importantly, a single example demonstrated by Saegusa and coworkers revealed that an acetonitrile derivative was also a compatible starting material for the decarboxylative allylation reaction despite minor contamination with the diallylated species (Scheme 4.4).[19] Subsequent studies conducted by Tunge and coworker in 2009 further revealed that the decarboxylative allylation of nitriles was regiospecific when conducted in the presence of much more acidic α-protons (Scheme 4.5).[21] Their studies demonstrated the application of decarboxylative allylation methods as opposed to base-mediated nucleophilic activation.[21]

Scheme 4.4: Decarboxylative Allylation of Acetonitrile Derivatives.

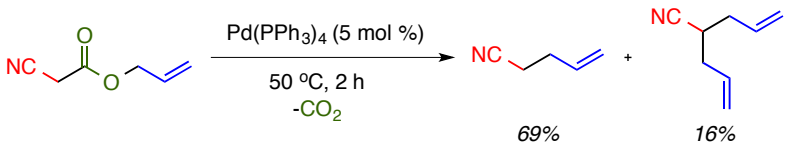

Scheme 4.5: Regioselective Decarboxylative Allylation of Nitriles.

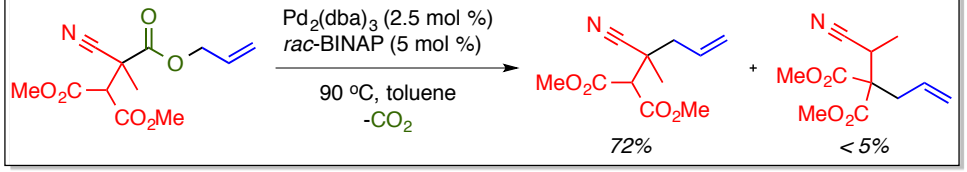

In addition to the decarboxylative activation of nitriles for allylic substitution, it is also necessary to briefly discuss advances in the decarboxylative allylation of nitroalkanes. Along with providing additional examples of the decarboxylative allylation of nitriles (in which allylation was observed in competition with protonation), in 1987 Tsuji and coworkers reported that nitroalkanes were viable substrates for decarboxylative allylic coupling to form a new C—C bond (Scheme 4.6).[22] However, the reaction was significantly effected by competing *O*-allylation even at reduced reactions temperatures (Scheme 4.6).

Scheme 4.6: Competitive C- vs. O-Allylation of Nitroalkanes.

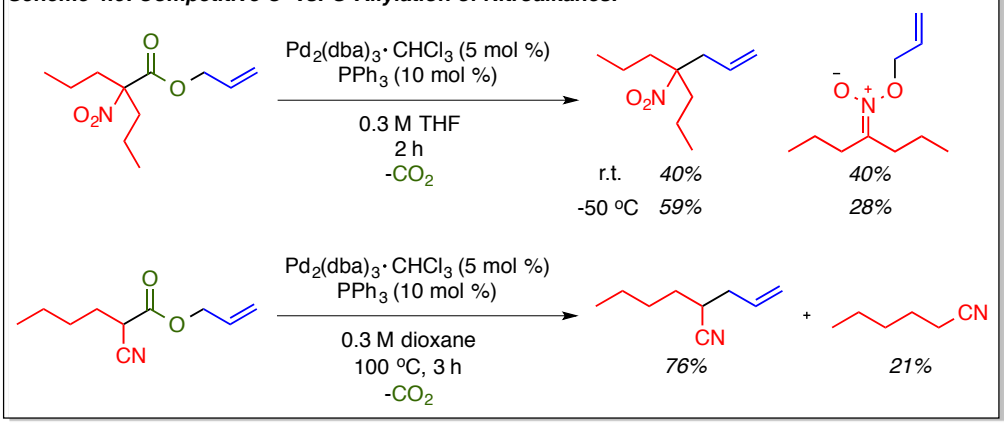

To expand the scope of decarboxylative allylation to nitroalkanes, in 2010 Tunge and coworker optimized reaction conditions that resulted in predominately *C*-allylation (Scheme 4.7).[23] Further, it was determined that *O*-allylation is fast and reversible as opposed to *C*-

allylation, which was irreversible. Therefore, in cases where aldehyde products (presumably formed as a result of elimination of *O*-allylation products) were formed competitively with *C*-allylation products, reactions could be conducted under more concentrated conditions to facilitate higher yields of *C*-allylation products.

Scheme 4.7. Rapid Decarboxylative Allylation of Nitroalkanes.

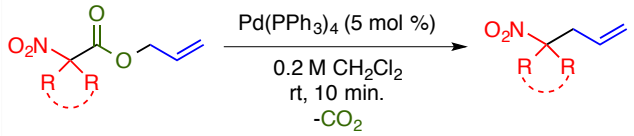

4.3 Regioselectivity of the Tsuji-Trost Allylic Alkylation.

In addition to the development of various methods for nucleophilic activation, substantial research has been conducted on the mode of nucleophilic attack once generated (Scheme 4.8).[24-26] Starting from a chiral allylic acetate or carbonate, palladium(0) will undergo oxidative addition of the allylic electrophile to generate a palladium π-allyl intermediate with inversion of stereochemistry. For soft, stabilized nucleophiles like malonates (pK_a = <18), nucleophilic attack will occur with inversion at the π-allyl ligand to displace palladium resulting in a formal retention of stereochemistry. Alternatively, hard nucleophiles (pK_a = >25), will first undergo transmetalation at the palladium center followed by reductive elimination to yield retention of stereochemistry and an overall inversion product.

Scheme 4.8. Regioselectivity and Stereoselectivity of the Tsuji-Trost Reaction.

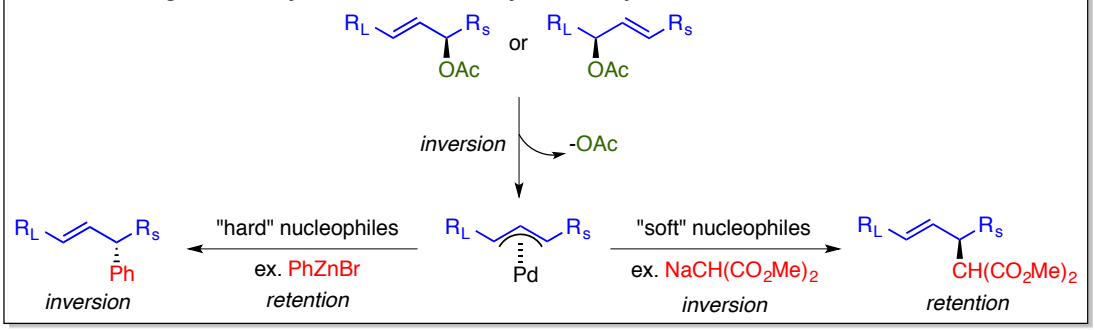

4.4 Activation of Allylic Alcohols for the Allylation of Carbon-Centered Nucleophiles.

The Tsuji-Trost reaction is an extremely valuable method for allylic incorporation into molecular scaffolds as demonstrated by its prevalent use over the last four decades. However, application of this method requires preactivation of alcohols, which possess a poor leaving group to form a better leaving group (typically converting the allylic alcohol to an allylic acetate or carbonate). Therefore, a logical improvement of the Tsuji-Trost reaction would be to develop methods that utilize allylic alcohols directly for the allylation of carbon-centered nucleophiles. Development of such a method would significantly increase the atom economy and efficiency of allylation reactions.

Scheme 4.9: Carbonylation with Palladium Chloride.

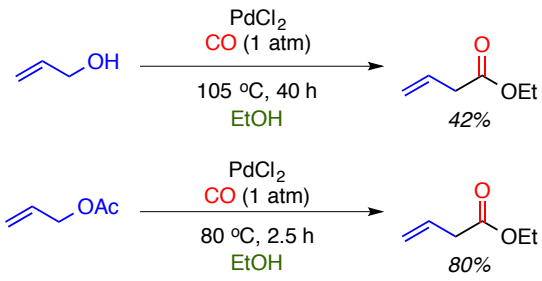

In 1964, Tsuji and coworkers demonstrated that allylic alcohols could be esterified using 1 atm of carbon monoxide in ethanol in the presence of palladium chloride (Scheme 4.9).[27,28] However, compared to allylic acetate derivatives, allylic alcohols required extended reaction times, higher temperatures, and resulted in lower overall yields. Fifteen years later, in 1979, Commereuc and coworkers reported that a single substrate, diethyl acetamidomalonate, could be allylated in the presence of allyl alcohol, $Pd(OAc)_2$, PPh_3 and PhONa (Scheme 4.10).[29] Further, under similar reaction conditions Sas[30] and Bergbreiter[31] reported the allylation of nitroalkanes (Scheme 4.11),[30] nitriles (Scheme 4.12),[31] and β-ketoesters (Scheme 4.13),[31] however, the reported methods suffered from extended reaction times, high temperatures, or lacked product selectivity when compared to Tsuji-Trost reaction alternatives.

Scheme 4.10. Allylation of Diethyl Acetamidomalonate.

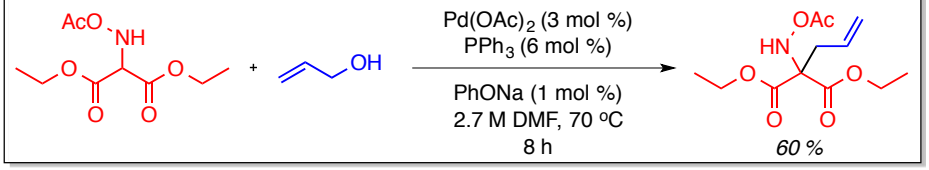

Scheme 4.11. Allylation of Nitroalkanes with Allylic Alcohols.

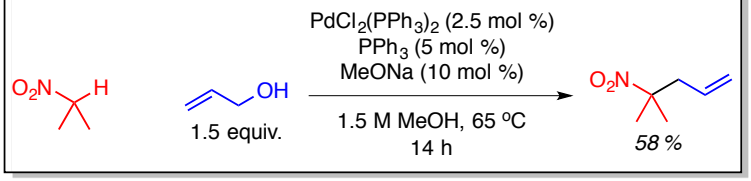

Scheme 4.12. Allylation of Nitriles with Allyl Alcohol.

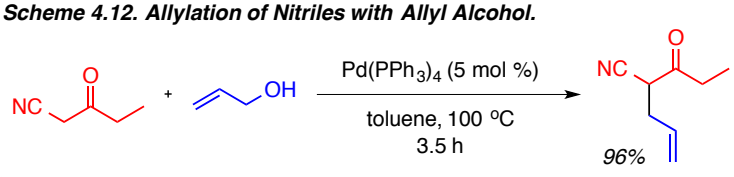

Scheme 4.13. Allylation of b-Ketoesters with Allylic Alcohols.

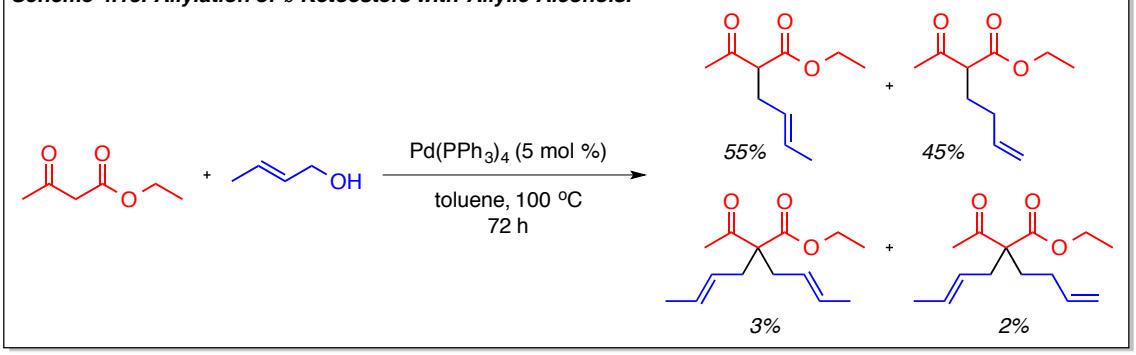

In 2011, Tunge and coworker reported that allylic alcohols could be activated *in situ* by ketone pronucleophiles for successful *C*-allylation (Scheme 4.14).[32] The mechanism proceeds via deacylative allylation where a retro-Claisen rearrangement occurs to generate allyl acetate *in situ* along with an activated nucleophile. Allyl acetate would then undergo activation by palladium(0) to ultimately generate the allylated product. In contrast to palladium-catalyzed reactions that attempted to couple allylic alcohols directly, Tunge and coworker demonstrated that their method was highly advantageous resulting in good yields for both stabilized and weakly stabilized carbon

nucleophiles. The retro-Claisen allylation was also applicable to a diverse range of substituted allylic alcohols.

Scheme 4.14. Deacylative Allylation: Allylic Alkylation via Retro-Claisen Activation.

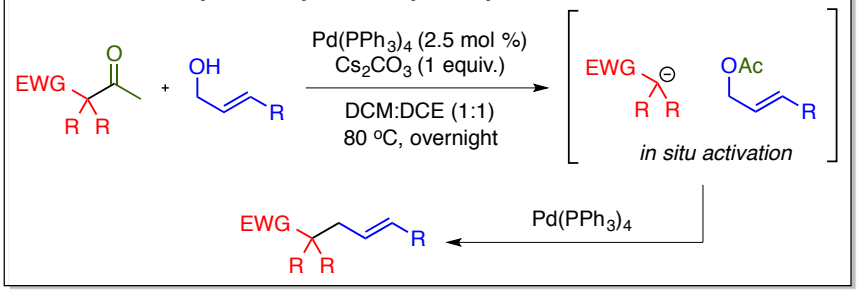

In addition to deacylative allylation as developed by Tunge and coworkers, numerous other methods have been developed toward the activation of allylic alcohols for allylic alkylation of carbon nucleophiles. A brief review of allylation methods utilizing catalysts such as Lewis and Brønsted acids, hydrogen-bond donors, and catalysts based on ligand design will be presented in the following sections.

4.5 Lewis Acid-Catalyzed Allylic Alcohol Activation.

A common method for the activation of allylic alcohols is through the employment of Lewis acids that coordinate to the alcohol functionality and weaken the C—O bond *in situ,* rather than proceeding through a prior functional group manipulation. In 1993, Kočovsky and coworkers reported the first use of BPh_3 to activate allyl alcohol in the palladium(0) catalyzed allylation of lithium diethylmalonate (Scheme 4.15).[33] The reaction was tolerant of several substituted allylic alcohols, but the scope of the nucleophile was not examined. Further, refluxing conditions, along with an excess of the starting nucleophile, were required to prevent dialkylation.

Scheme 4.15. BPh_3-Catalyzed Activation of Allylic Alcohols.

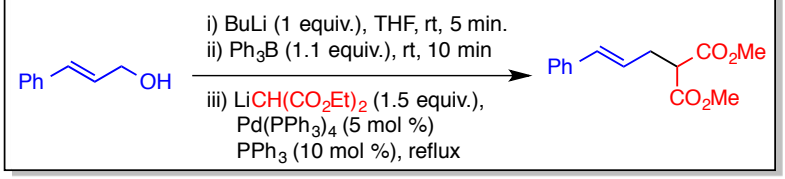

Subsequent reports beginning in 2000 by Tamaru and coworkers began to further investigate alkylboranes as a source of *in situ* allylic alcohol activation (Scheme 4.16).[4,34,35] After reaction optimization, Tamaru and coworkers reported that Et_3B activated various allylic alcohol for successful allylic alkylation of active methylene compounds in moderate yields. However, the reaction required superstoichiometric Et_3B, NaH and extended reaction times when more sterically encumbered allylic alcohols were used.

Scheme 4.16: Et_3B Promoted Allylic Alcohol Activation.

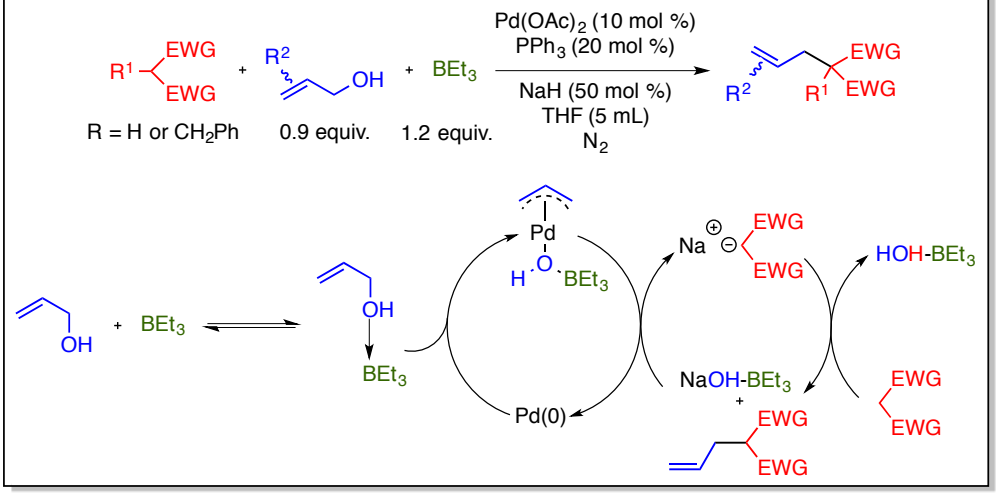

4.6 Brønsted Acid-Catalyzed Activation of Allylic Alcohols.

In addition to trialkylborane Lewis acids, As_2O_3,[36] $Ti(OiPr)_3$,[37] $SnCl_2$,[38] and B_2O_3,[39] have also been employed most often in stoichiometric quantities. As an alternative, Brønsted acid-catalysis has been developed to minimize the production of waste by reducing the amount of catalysts employed. In 2003, Kobayashi and coworker reported that palladium tetrakis with 10

mol% of 1-adamantanecarboxylic acid efficiently catalyzed the allylation of various nucleophiles equipped with two electron-withdrawing groups (EWG's) (Scheme 4.17).[40] Despite the fact that the reaction could be conducted in water absent of any organic solvents or stoichiometric additives, refluxing reaction conditions are a significant limitation along with the narrow substrate scope for substituted allylic alcohols.

Scheme 4.17: Carboxylic Acid-Assisted Allylation with Allylic Alcohols in Water.

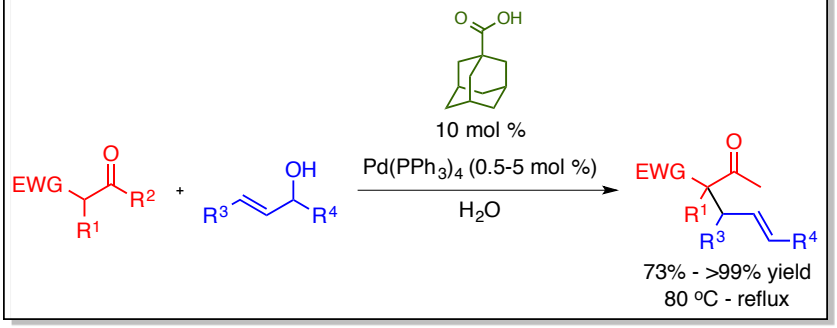

In 2011, List and coworkers employed the use of $Pd(PPh_3)_4$ with chiral Brønsted acid and benzhydryl amine to facilitate both allylic alcohol activation and chiral induction in the asymmetric allylation of aldehyde derivatives (Scheme 4.18).[41] Although the developed method produced adequate yields and high ee's, the substrate scope was limited to carbonyl functionalities that could generate an imine *in situ*. Further, the use of transition metal, Brønsted acid, and amine catalysts deviates from the overall objective to develop an atom-economical alternative to the Tsuji-Trost allylation method.

Scheme 4.18. Chiral Bronsted Acid-Catalyed Allylic Alkylation.

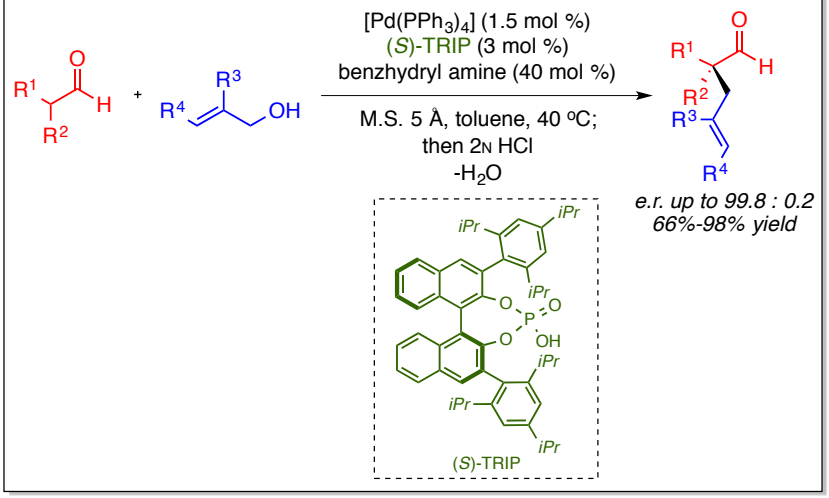

In attempt to minimize the number of requisite additives and expand the substrate scope of asymmetric allylic alkylations, in 2013 Gong and coworkers reported the use of palladium(0) with chiral phosphoric acid and a chiral phosphoramidite ligand in the asymmetric allylation of pyrazol-5-ones (Scheme 4.19).[42] The method was found to be functional group tolerant and resulted in high yields and ee's. However, chiral induction is largely based on the presence of hydrogen bonding in the transition-state, which limits the scope of the nucleophile.

Scheme 4.19. Palladium-Catalyzed Asymmetric Allylic Alkylation of Pyrazol-5-ones.

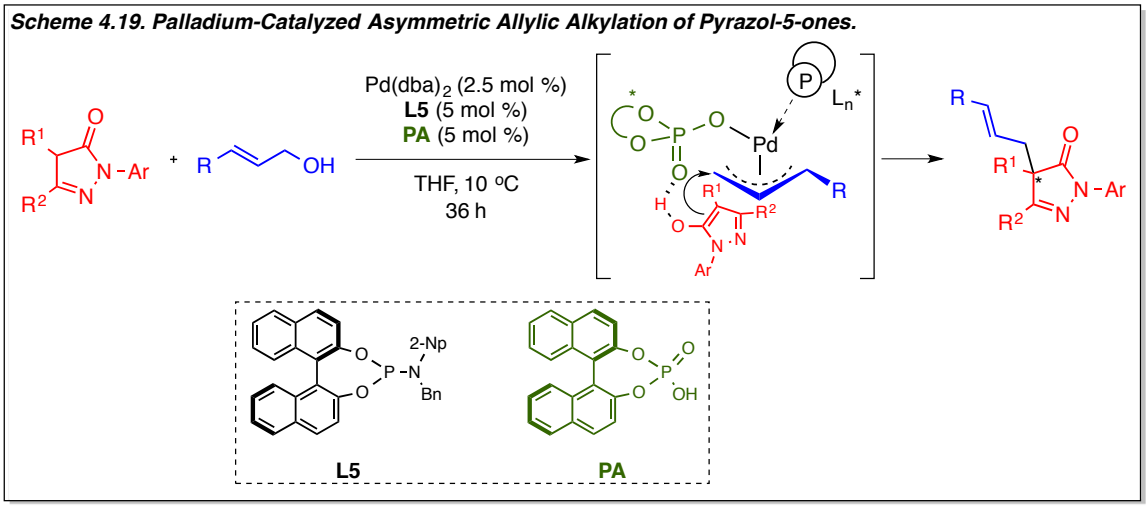

4.7 Hydrogen-Bond Donor (HBD) Activation of Allylic Alcohols.

In effort to further minimize the amount of additives required for the *in situ* activation of allylic alcohols, Reek and coworkers reported that simple diethylurea could be utilized as a HBD catalyst in only 3 mol % for allylic alkylation of carbon nucleophiles (Scheme 4.20).[43] However, the developed method was only successful for simple allyl alcohol. When substituted derivatives were employed, significantly decreased yields were observed or the allylation reaction was shut down completely. Lastly, the scope of the nucleophile appeared to be limited to indole-type derivatives.

Scheme 4.20. HBD-Assisted Allylic Alcohol Activation.

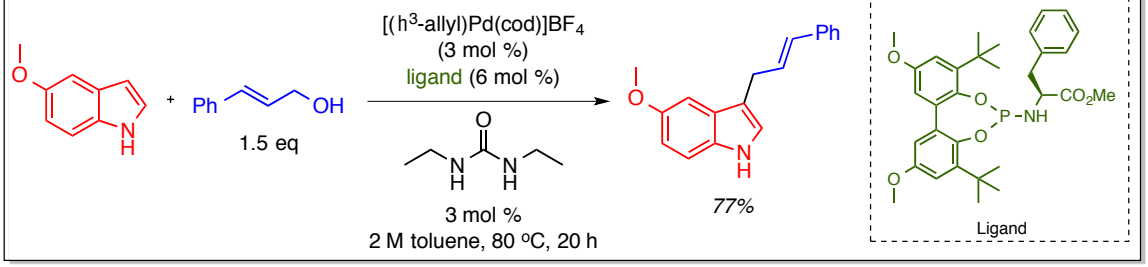

4.8 Allylic Alcohol Activation via Ligand Design.

One last method of allylic alcohol activation was demonstrated by Ozawa and workers in 2002 through the use of sp^2-hydridized phosphorous ligands (Scheme 4.21).[44] Unlike the methods presented previously, allylic alcohol activation occurred absent of any additional additives beyond catalytic palladium and ligand. The active catalytic species is proposed to be a palladium-hydride intermediate which will facilitate a proton transfer to generate a palladium(0) intermediate and activated allylic species for nucleophilic attack.[44] However, both the scope of the nucleophile and allylic alcohol were extremely limited. Further, a large excess of the starting nucleophile was required to access the reported yields.

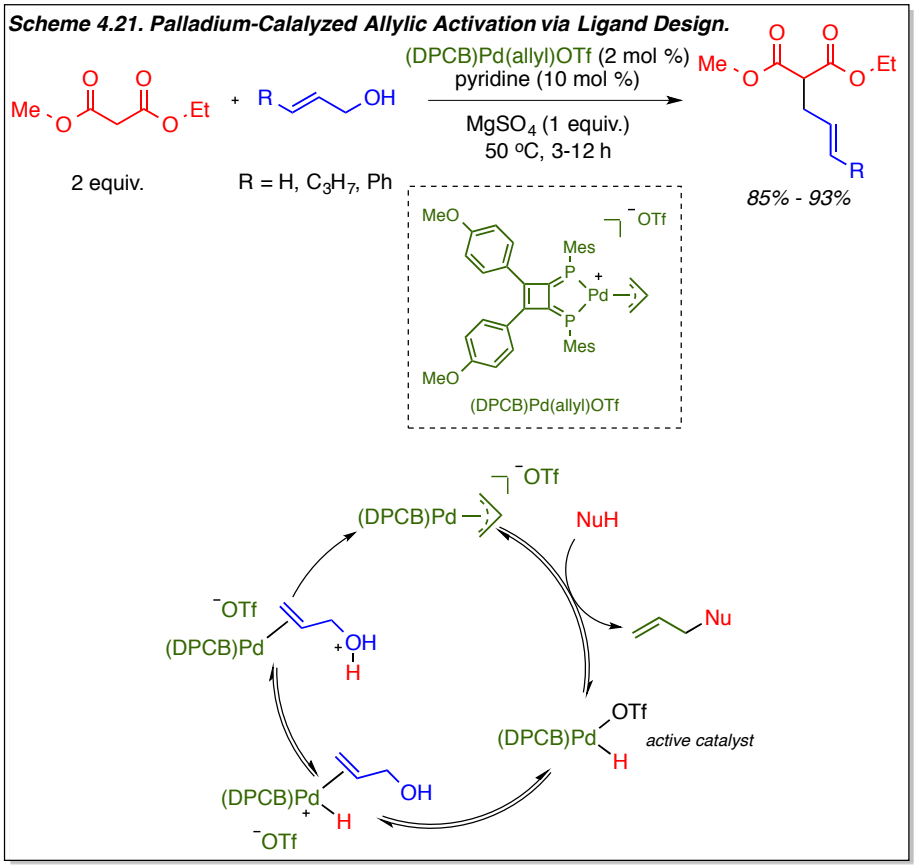

4.9 Activation of Allylic Alcohols with CO_2.

As demonstrated in sections 1.4 – 1.8 of chapter 4, a variety of methods have been developed for the *in situ* activation of allylic alcohols using various additives or specifically designed ligands. However, the developed methods are limited to non- or weakly basic nucleophiles. More strongly basic nucleophiles would be incompatible under Brønsted or Lewis Acid catalysis. Additionally, these methods often suffer from diminished yields or failed reactions when substituted allylic alcohols are employed. The use of additives also deviates from the goal of achieving an atom-economical alternative to the Tsuji-Trost allylic alkylation reaction since the additives require removal upon reaction completion. In lieu of these drawbacks, we were

inspired to develop an environmentally benign method to activate both allylic alcohols and a large class of nucleophiles *in situ* for allylic alkylation of carbon-centered nucleophiles.

In 1995, Yamamoto and coworkers reported that CO_2 could be used at high pressure to catalyze the allylation of acidic β-dicarbonyl compounds in the presence of allylic alcohols (Scheme 4.22).[45] At the time, it was initially proposed that CO_2 reversibly inserts into allylic alcohols to form allyl carbonic acids *in situ* which then undergo activation by palladium. Then in 2001,[46] and in subsequent reports,[47-48] Eckert and coworkers demonstrated that alkylcarbonic acids form *in situ* from the addition of CO_2 to alcohols (Scheme 4.23). Based on these initial reports, we sought to expand the application of CO_2 activation of allylic alcohols to a broader substrate class beyond highly stabilized malonate-type derivatives as reported Yamamoto (Scheme 4.22).[45]

Scheme 4.22. CO_2-Catalyzed Allylation of Carbon Nucleophiles at High Pressures

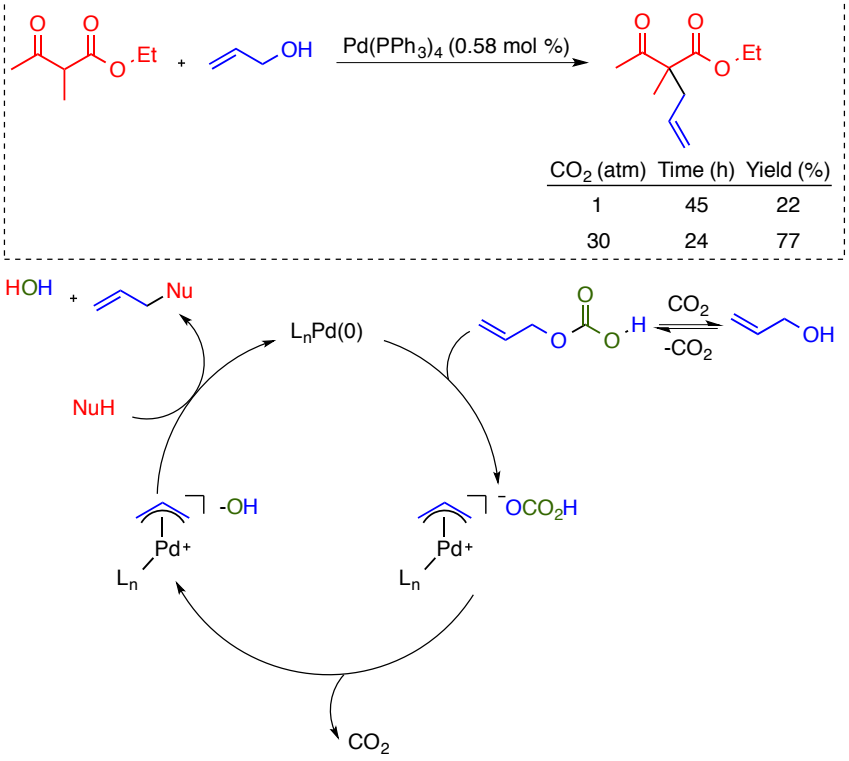

Scheme 4.23. CO_2-Activation of Alcohols

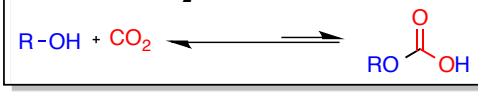

By employing CO_2 as an *in situ* activator of allylic alcohols, we envisioned expanding the known method to *weakly* acidic pronucleophiles, such as nitroalkanes, nitriles, and aldehydes (Scheme 4.24). Beginning with nucleophilic attack of allyl alcohol on CO_2, allylic carbonate would be generated *in situ* and sufficiently activated for oxidative addition by palladium(0) to yield a palladium π-allyl intermediate along with bicarbonate. Subsequent decarboxylation of bicarbonate could then form a strong hydroxide base (pK_a = 30 in DMSO) necessary for pronucleophile activation and generate water as the only stoichiometric by-product. Lastly, nucleophilic attack on the palladium π-allyl intermediate would occur to yield the allylated product and regenerate the active palladium(0) catalyst.

Scheme 2.24. CO_2-Activation of Alcohols for Intermolecular Allylation.

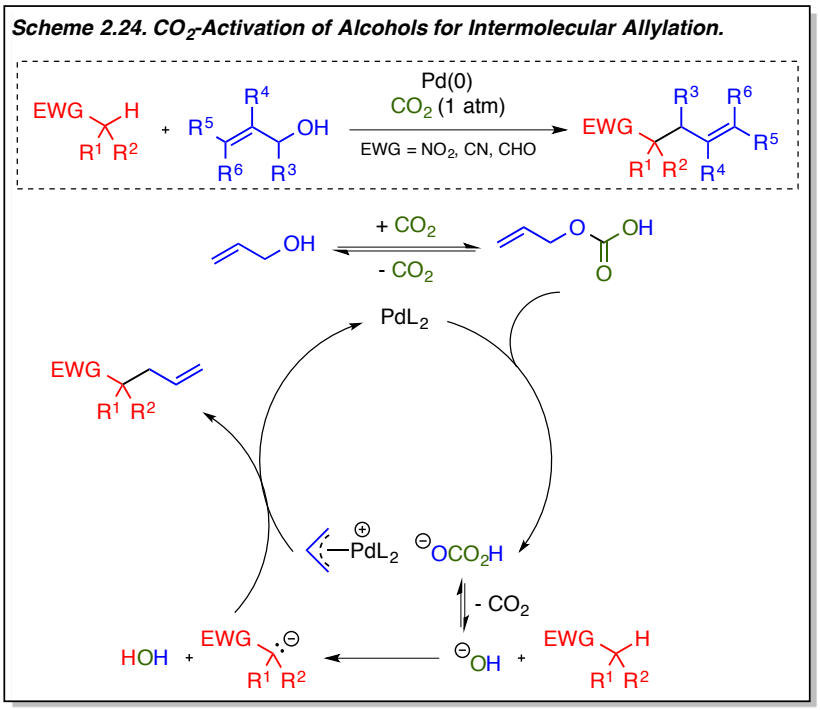

Initial studies were conducted by Simon Lang using relatively acidic nitroalkane derivatives (pK_a = 17 in DMSO). It was found that high yields of the allylated product were

obtained when a sealed vial containing nitroalkane, allyl alcohol, and $Pd(PPh_3)_4$ in DMSO under 1 atm of CO_2 was heated at 80 °C overnight (Scheme 2.25). Further, when argon replaced CO_2, ^1H NMR spectroscopy of the crude reaction mixture indicated that no appreciable amount of allylated product formed (Scheme 2.25).

Scheme 2.25. Optimized Reaction Conditions.

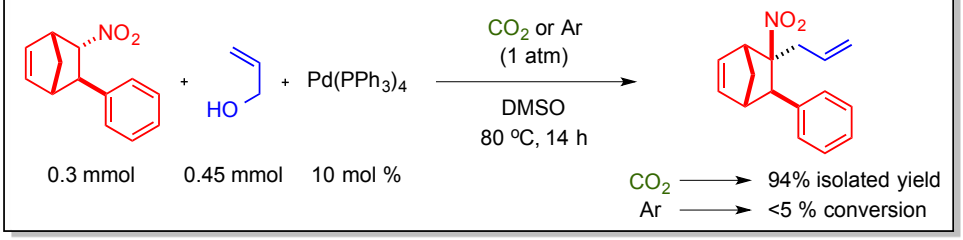

Next, Simon examined the scope of nitroalkanes using the developed allylation reaction in which he found that both cyclic and acyclic nitroalkanes were well tolerated (Scheme 2.26). Further, upon examination of the functional group tolerance of the reaction, it was found that olefins (**1a**, **1c**, **1h**), α,β-unsaturated esters (**1l**), ethers (**1e, 1f**), and indole (**1d**) were well tolerated. Additionally, β-methallyl alcohol also lead to a high isolated yield of the allylated nitroalkane (**1j**). However, prenyl and crotyl alcohols were unsuccessful under the optimized reaction conditions. Lastly, successful allylation of nitroalkane derivatives could also occur under microwave conditions in just 20 min at 160 °C.

Scheme 2.26. CO_2-Catalyzed Allylation of Nitroalkanes.

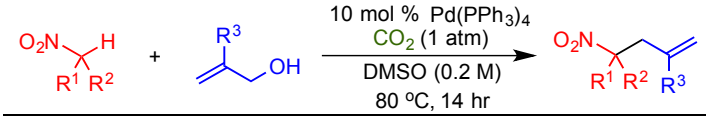

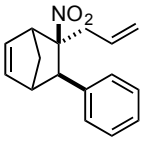

1a
94 %[a] (<5 %)[c]
95 : 5 dr

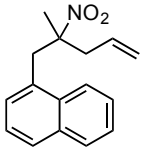

1b
83%[a] (7 %)[c]

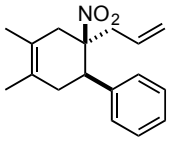

1c
88 %[a]
>95 : 5 dr

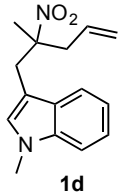

1d
86 %[a]

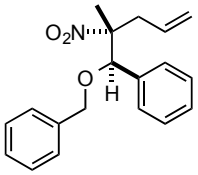

1e
93 %[a]
88 : 12 dr

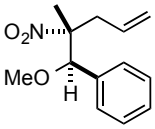

1f
96 %[a]
88 : 12 dr

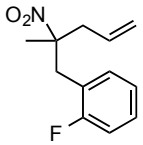

1g
92 %[a]

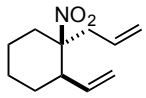

1h
90 %[a]
85 : 15 dr

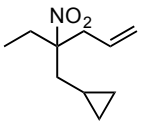

1i
71 %[a]

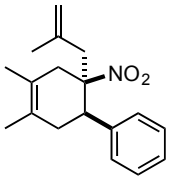

1j
97 %[a]
90 : 10 dr

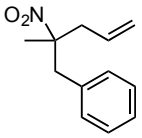

1k
89 %[a]
85 %[d] (7 %)[d,c]

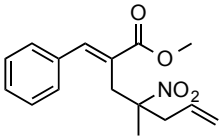

1l
91 %[a]

a) Nitroalkane (0.3 mmol) and allyl alcohol (0.45 mmol) in 1.75 mL DMSO under 1 atm CO_2. b) Isolated yields. c) Ar replaced CO_2 (% conversion via crude 1H NMR). d) Allyl alcohol (0.9 mmol), 160 °C, 20 min. in a microwave reactor.

Next, Simon evaluated the ability of various aldehyde derivatives to undergo CO_2-catalyzed allylic alkylation from allylic alcohols despite the fact that aldehydes can be prone dimerization (Scheme 2.27). Gratifyingly, under the standard reaction conditions developed for

nitroalkanes, both cyclic (**2a-2g, 2j-3l**) and acylic (**2h-2i**) aldehyde derivatives were successfully allylated in good to high overall yields. In regards to α-aryl aldehydes, both electron-withdrawing (**2c, 2e**) and electron-donating functionalities (**2b**, **2d**) were tolerated on the aryl ring along with 2-napthyl and biaryl motifs (**2f**, **2g**). Further, aldehydes containing a protected amino aldehyde (**2j**) and benzyl substituents (**2k**, **2l**) also resulted in good to high yields of the allylated products.

Scheme 2.27. Scope of the Allylation of Aldehydes[a,b]

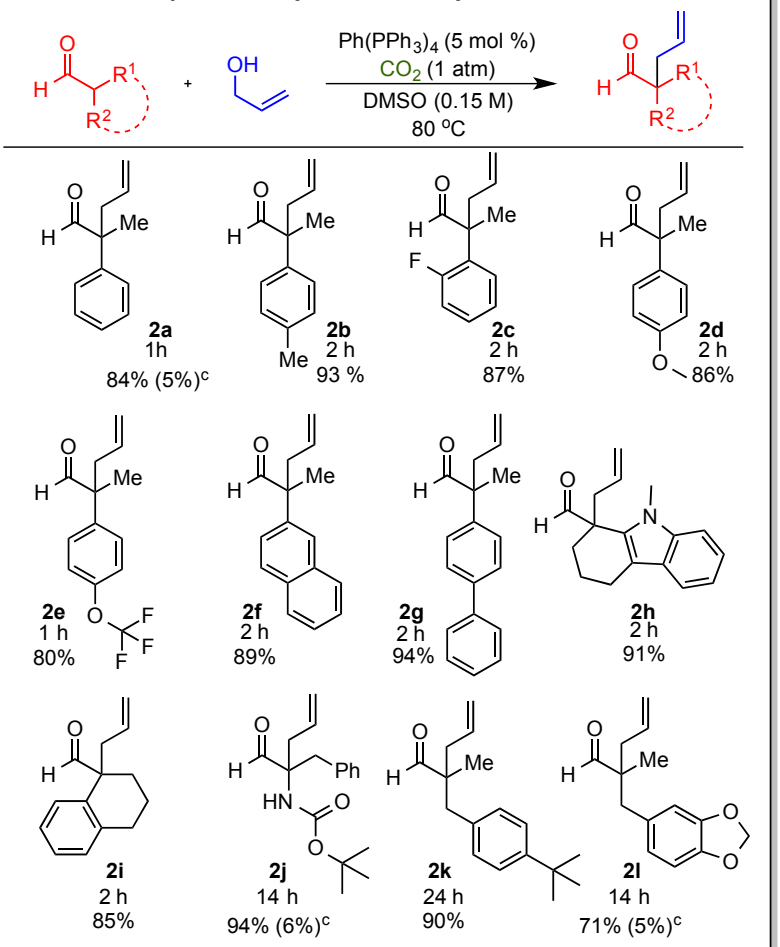

a) Aldehyde (0.30 mmol) and alcohol (0.45 mmol) in 2.0 mL DMSO under 1 atm of CO_2. b) Isolated yields. c) Ar replaced CO_2 (% conversion via GC/MS).

In order to probe to identity of the *in situ* generated base and examine how weakly acidic the nucleophile coupling partner could be, we next extended the nucleophile scope beyond nitroalkanes (pK_a = 17 in DMSO) to tertiary nitriles (pK_a = 22-25 in DMSO) (Scheme 2.28). In

slight contrast to the method developed for the allylation of aldehydes and nitroalkanes, optimized reaction conditions for the allylation of nitriles resulted in lowered catalyst loading, more concentrated solutions, and slightly elevated reaction temperatures. However, as found with both nitroalkanes and aldehydes, the CO_2-catalyzed allylation of nitriles resulted in good to high yields of the allylated products. This result suggests that pronucleophile activation occurs from a hydroxide/carbonate mixture generated *in situ* instead of bicarbonate which is not a sufficient base for nitrile activation.

Upon examining the substrate scope of the nitrile coupling partner, it was found that the reaction was tolerant of halogens (**3b-3c**), aryl ether (**3d**), ketone (**3f**), and indole substituents (**3h**). However, allylation of a sterically congested ortho-disubstituted nitrile was unsuccessful under the optimized reaction conditions. Further, yields of the allylated products were significantly higher than when the same reactions conducted under argon. Presumably, since nitriles are known to undergo hydrolysis to form carboxylic acids, the observed minor reaction conversion to the allylated product in the absence of CO_2 could be acid catalyzed as reported by Kobayashi.

Scheme 2.28. Scope of the Allylation of nitriles.[a,b]

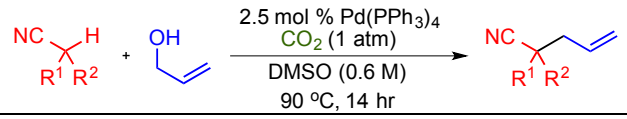

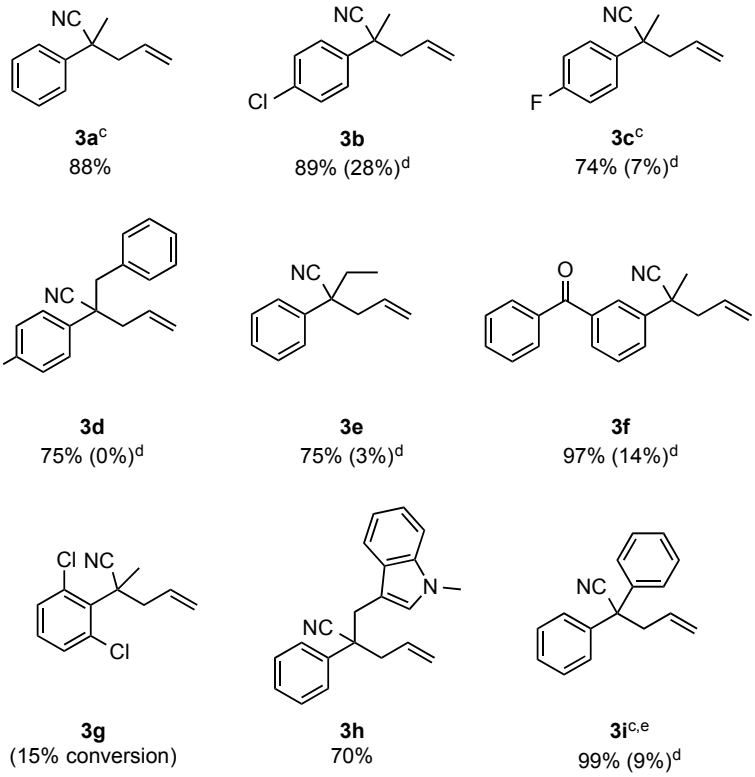

3a[c] 88%

3b 89% (28%)[d]

3c[c] 74% (7%)[d]

3d 75% (0%)[d]

3e 75% (3%)[d]

3f 97% (14%)[d]

3g (15% conversion)

3h 70%

3i[c,e] 99% (9%)[d]

a) Nitrile (0.3 mmol) and allyl alcohol (0.6 mmol) in 0.5 mL DMSO under
b) Isolated yields c) 2 mL of DMSO used d) Ar replaced CO_2 e) 80°C

Lastly, we examined the scope of the reaction utilizing substituted allylic alcohols with tertiary nitriles and aldehydes (Scheme 2.29). In general, comparable yields were observed as those resulting from allylation reactions with simple allyl alcohol (**4a-4o**). Both 2-methyl and 2-phenyl-2-propen-1-ol were well tolerated by both nitriles and aldehydes resulting in good to high isolated yields of the allylated product (**4a**, **4b**, **4j**). Further, as typically observed in palladium-catalyzed allylation reactions, the linear regioisomer was predominately favored over the branched isomer. For nitrile derivatives a trend was observed where the ratio of the linear:branched isomers increased with an increase in steric bulk on the substituted allylic alcohol

(**4c**-**4f**). Selectivity is proposed to arise from an outer-sphere C-allylation mechanism.[48,49] When comparing cinnamyl alcohol and α-vinylbenzyl alcohol, which result in the same palladium π-allyl intermediate *in situ*, comparable selectivity was observed, resulting in a >95:5 linear:branched ratio (**4f**, **4g**). However, the overall isolated yield of the allylated products was slightly lower using the cinnamyl reactant (**4f**, **4g**). Unfortunately, employment of prenyl alcohol failed to produce any of the desired product, presumably due to the increased steric hindrance at the terminal position of the allylic alcohol (**4i**). Lastly, for aldehyde derivatives, ether and substituted aryl moieties were well tolerated on the allylic alcohol resulting in good yields and high regioselectivity for the linear isomer (**4k**-**4o**).

Scheme 2.29. Scope of allyl alcohols[a,b]

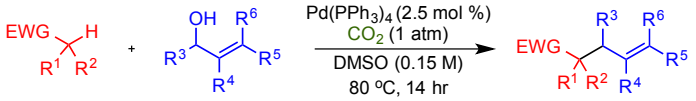

Substrate	Alcohol	Product	Yield	l:b
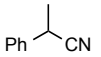	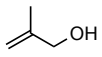	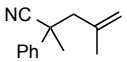 **4a**[b]	94%	--
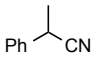	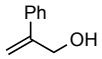	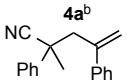 **4b**[b]	79%	--
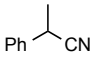	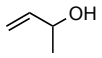	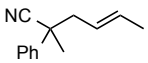 **4c**[b,c]	73%	2:1
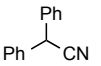	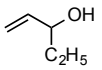	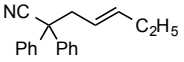 **4d**	99%	10.5:1
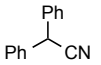	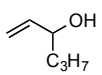	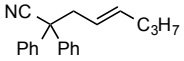 **4e**[d]	99%	11.2:1
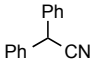	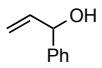	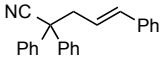 **4f**	94%	>95:5
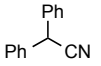	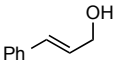	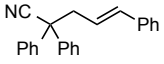 **4g**	79%	>95:5
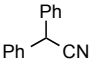	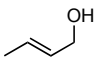	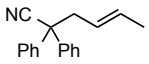 **4h**[e]	99%	1.4:1
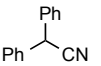	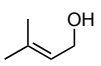	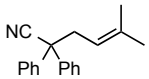 **4i**[f]	0%	--
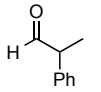	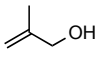	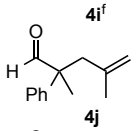 **4j**	77%	--
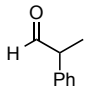	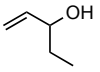	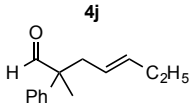 **4k**	79%	93:7
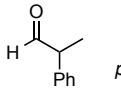	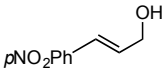	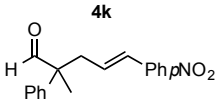 **4l**	79%	86:14
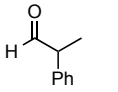	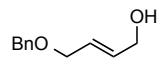	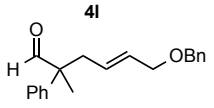 **4m**[g]	73%	>95:5
		4n[h]	70%	>95:5
		4o[i]	79%	>95:5

4.10 Conclusion

The development of a CO_2-catalyzed method for the *in situ* activation of allylic alcohols enabled the allylation of *weakly* acidic nitroalkanes, nitriles, and aldehydes under mild conditions with water as the only stoichiometric byproduct. Further, the presented method provides an atom-economic alternative to the Tsuji-Trost allylic alkylation absent of stoichiometric or catalytic additives that require removal upon reaction completion.

4.11 References for Chapter 4:

[1] Lang, S. B.; Locascio, T. M.; Tunge, J. A. "Activation of Alcohols with Carbon Dioxide: Intermolecular Allylation of Weakly Acidic Pronucleophiles." *Org. Lett.* **2014**, *16*, 4308.

[2] Trost, B. M.; Van Vranken, D. L. "Asymmetric Transition Metal-Catalyzed Allyli Alkylations." *Chem. Rev.* **1996**, *96*, 395-422.

[3] Sundararaju, B.; Achard, M.; Bruneau, C. "Transition metal catalyzed nucleophilic allylic substitution: activation of allylic alcohols *via* π-allylic species." *Chem. Soc. Rev.* **2012**, *41*, 4467-4483.

[4] Tamaru, Y. "Activation of Allyl Alcohols as Allyl Cations, Allyl Anions, and Amphiphilic Allylic Species by Palladium." *Eur. J. Org. Chem.* **2005**, 2647-2656.

[5] Muzart, J. "Palladium-catalysed reactions of alcohols. Part B: Formation of C—C, and C—N bonds from unsaturated alcohols." *Tetrahedron*. **2005**, *61*, 4179-4212.

[6] Lu, Z.; Ma, S. "Metal-Catalyzed Enantioselective Allylation in Asymmetric Synthesis." *Angew. Chem. Int. Ed.* **2008**, *47*, 258-297.

[7] Trost, B. M.; Crawley, M. L. "Asymmetric Transition-Metal-Catalyzed Allylic Alkylations: Applications in Total Synthesis." *Chem. Rev.* **2003**, *103*, 2921-2943.

[8] Butt, N. A.; Zhang, W. "Transition metal-catalyzed allylic substitution reactions with unactivated allylic substrates." *Chem. Rev.* **2015**, *44*, 7929-7967.

[9] Weaver, J. D.; Recio III, A.; Grenning, A. J.; Tunge, J. A. "Transition Metal-Catalyzed Decarboxylative Allylation and Benzylation Reactions." *Chem. Rev.* **2011**, *111*, 1846-1913.

[10] Yus, M.; González-Gómez, J. C.; Foubelo, F. "Diastereoselective Allylation of Carbonyl Compounds and Imines: Application to the Synthesis of Natural Products." *Chem. Rev.* **2013**, *113*, 5595-5698.

[11] Puentes, C. O.; Kouznetsov, V. "Recent advancements in the homoallylamine chemistry." *J. Heterocycl. Chem.* **2002**, *39*, 595-614.

[12] Katritzky, A. R.; Piffl, M.; Lang, H.; Anders, E. "Regioselectivity of the Reactions of Heteroatom-Stabilized Allyl Anions with Electrophiles." *Chem. Rev.* **1999**, *99*, 665-722.

[13] Silverio, D. L.; Torker, S.; Pilugina, T.; Vieira, E. M.; Snapper, M. L.; Haeffner, F.; Hoveyda, A. H. "Simple organic molecules as catalysts for enantioselective synthesis of amines and alcohols." *Nature*. **2013**, *494*, 216-221.

[14] Gandhi, S.; List, B. "Catalytic Asymmetric Three-Component Synthesis of Homoallylic Amines." *Angew. Chem. Int. Ed.* **2013**, *52*, 2573-2576.

[15] Trost, B. M. "Pd- and Mo-Catalyzed Asymmetric Allylic Alkylation." *Org. ProcessRes. Dev.* **2012**, *16*, 185-194.

[16] Tsuji, J.; Takahashi, H.; Morikawa, M. "Organic Syntheses by Means of Nobel Metal Compounds XVII. Reaction of π-Allylpalladium Chloride with Nucleophiles." *Tetrahedron Lett.* **1965**, *49*, 4387-4388.

[17] Atkins, K. E.; Walker, W. E., Manyik, R. M. "Palladium Catalyzed Transfer of Allylic Groups." *Tetrahedron Lett.* **1970**, *43*, 3821-3824.

[18] Shimizu, I.; Yamada, T; Tsuji, J. "Palladium-Catalyzed Rearrangement of Allylic Esters of Acetoacetic Acid to give γ,δ-Unsaturated Methyl Ketones." *Tetrahedron Lett.* **1980**, *21*, 3199-3202.

[19] Tsuda, T.; Chujo, Y.; Nishi, S-i.; Tawara, T.; Saegusa, T. "Facile Generation of a Reactive Palladium(II) Enolate Intermediate by the Decarboxylation of Palladium(II) β-Ketocarboxylate and Its Utilization in Allylic Acylation." *J. Am. Chem. Soc.* **1980**, *102*, 6381-6384.

[20] Nesmeyanov, A. N.; Lutsenko, I. F.; Ananchenko, S. N. *Org. Khim.* **1950**, *132*, 136.

[21] Recio III, A.; Tunge, J. A. "Regiospecific Decarboxylative Allylation of Nitriles." *Org. Lett.* **2009**, *11*, 5630-5633.

[22] Tsuji, J.; Yamada, T.; Minami, I.; Yuhara, M.; Nisar, M.; Shimizu, I. "Palladium-Catalyzed Decarboxylation-Allylation of Allylic Esters of α-Substituted β-Keto Carboxylic , Malonic, Cyanoacetic, and Nitroacetic Acids." *J. Org. Chem.* **1987**, *52*, 2988-2995.

[23] Grenning, A. J.; Tunge, J. A. "Rapid Decarboxylative Allylation of Nitroalkanes." *Org. Lett.* **2010**, *12*, 740-742.

[24] Hayashi, T.; Yamamoto, A.; Hagihara, T. "Stereo- and Regiochemistry in Palladium-Catalyzed Nucleophilic Substitution of Optically Active (*E*)- and (*Z*)-Allyl Acetates." *J. Org. Chem.* **1986**, *51*, 723-727.

[25] Keinan, E.; Sahai, M. "Regioselectivity in Organo-transition-metal Chemistry. A Remarkable Steric Effect in π-Allyl Palladium Chemsitry." *J. Chem. Soc. Chem. Commun*. **1984**, 648-650.

[26] Acemoglu, L.; Williams, J. M. J. "Remarkable Ligand Effects in Regioselective Palladium-Catalysed Allylic Substitution Reactions." *Adv. Synth. Catal.* **2001**, *343*, 75-77.

[27] Tsuji, J.; Kiji, J.; Imamura, S.; Morikawa, M.; "Organic Synthesis by Means of Noble Metal Compounds. VIII. Catalytic Carbonylation of Allylic Compounds with Palladium Chloride." *J. Am. Chem. Soc*. **1964**, 4350-4353.

[28] Friedrich, W.; Bernhauer, K. "Vitamin B_{12}-Analoga des Belebtschlammes." *Angew. Chem.* **1959**, *71*, 284.

[29] Haudegond, J-P.; Chauvin, Y.; Commereuc, D. "Synthesis of α-Amino Acids by Alkylation of Diethyl Acetamidomalonate in the Presence of Palladium Complexes." *J. Org. Chem.* **1979**, *44*, 3063-3065.

[30] Aleksandrowicz, P.; Piotrowska, H.; Sas, W. "Palladium Catalyzed C-Allylation of Nitroalkanes." *Tetrahedron*. **1982**, *38*, 1321-1327.

[31] Bergbreiter, D. E.; Weatherford, D. A. "Alkylation of Active Methylene Compounds by Allylic Alcohols using Tetrakis(triphenylphosphine)palladium(0)." *J. Chem. Soc. Chem. Commun*. **1989**, 883-884.

[32] Grenning, A. J.; Tunge, J. A. "Deacylative Allylation: Allylic Alkylation via Retro-Claisen Activation." *J. Am. Chem. Soc*. **2011**, *133*, 14785-14794.

[33] Starý, I.; Stará, I. G.; Kočovsky, P. "Allylic Alcohols as Substrates for the Palladium(0)-Catalyzed Allylic Substitution." *Tetrahedron Lett.* **1993**, *34*, 179-182.

[34] Tamaru, Y.; Harino, Y.; Araki, M.; Tanaka, S.; Kimura, M. "Et_3B-promoted, Pd(0)-catalyzed allylation of active methylene compounds with allylic alcohols." *Tetrahedron Lett.* **2000**, *41*, 5705-5709.

[35] Kimura, M.; Mukai, R.; Tanigawa, N.; Tanaka, S.; Tamaru, Y. "Triethylborane as an efficient promoter for palladium-catalyzed allylation of active methylene compounds with allylic alcohols." *Tetrahedron.* **2003**, *59*, 7767-7777.

[36] Lu, X.; Lu, L.; Sun, J. "Palladium and Arsenic(III) Oxide-Catalyzed Allylic Alkylation by Allylic Alcohols Under Neutral Conditions." *J. Mol. Catal.* **1987**, *41*, 245-251.

[37] Satah, T.; Ikeda, M.; Nomura, M. "*J. Org. Chem.* **1997**, *62*, 4877-4879.

[38] Masuyama, Y.; Takahara, J. P.; Kurusu, Y.; *J. Am. Chem. Soc.* **1988**, *110*, 4473-4474.

[39] Lu, X.; Jiang, X.; Tao, X. "Palladium-catalyzed allylic alkylation of carbonucleophiles with allylic borates or allylic alcohols and boron oxide under neutral conditions." *J. Organomet. Chem.* **1988**, *344*, 109-118.

[40] Manabe, K.; Kobayashi, S. "Palladium-Catalyzed, Carboxylic Acid-Assisted Allylic Substitution of Carbon Nucleophiles with Allyl Alcohols as Allylating Agents in Water." *Org. Lett.* **2003**, *5*, 3241-3244.

[41] Jiang, G.; List, B. "Direct Asymmetric α-Allylation of Aldehydes with Simple Allylic Alcohols Enabled by the Concerted Action of Three Different Catalysts." *Angew. Chem. Int. Ed.* **2011**, *50*, 9471-9474.

[42] Tao, Z-L.; Zhang, W-Q.; Chen, D-F.; Adele, A.; Gong, L-Z. "Pd-Catalyzed Asymmetric Allylic Alkylation of Pyrazol-5-ones with Allylic Alcohols: The Role of the Chiral Phosphoric Acid in C–O Bond Cleavage and Stereocontrol." *J. Am. Chem. Soc.* **2013**, *135*, 9255-9258.

[43] Gumrukcu, Y.; De Bruin, B.; Reek, J. N. H. "Hydrogen-Bond-Assisted Activation of Allylic Alcohols for Palladium-Catalyzed Coupling Reactions." *ChemSusChem*, **2014**, *7*, 890-896.

[44] Sakamoto, M.; Shimizu, I.; Yamamoto, A. "Activation of C–O and C–N Bonds in Allylic Alcohols and Amines by Palladium Complexes Promoted by CO_2. Synthetic Applications to Allylation of Nucleophiles, Carbonylation, and Allylamine Disproportionation." *Bull. Chem. Soc. Jpn.* **1996**, *69*, 1065-1078.

[45] West, K. N.; Wheeler, C.; McCarney, J. P.; Griffith, K. N.; Bush, D.; Liotta, C. L.; Eckert, C. A. "Formation of Alkylcarbonic Acids with CO_2." *J. Phys. Chem. A.* **2001**, *105*, 3947-3948.

[46] Weikel, R. R.; Hallett, J. P.; Liotta, C. L.; Eckert, C. A. "Self-Neutralizing in Situ Acid Catalysts from CO_2." *Top. Catal.* **2005**, *37*, 75.

[47] Weikel, R. R.; Hallett, J. P.; Liotta, C. L.; Eckert, C. A. "Self-Neutralizing in Situ Acid Catalysis for Single-Pot Synthesis of Iodobenzene and Methyl Yellow in CO_2-Expanded Methanol." *Ind. Eng. Chem. Res.* **2007**, *46*, 5252-5257.

[48] Kazmaier, U.; Zumpe, F. L. "Palladium-Catalyzed Allylic Alkylations without Isomerization–Dream or Reality." *Angew. Chem. Int. Ed.* **2000**, *39*, 802-804.

[49] Consiglio, G.; Waymouth, R. M. "Enantioselective Homogeneous Catalysis Involving Transition-Metal-Allyl Intermediates." *Chem. Rev.* **1989**, *89*, 257-276.

Chapter 4. Appendix

Experimental Methods and Spectral Analysis for Chapter 4 Compounds

Table of Contents:

General Information:

All reactions were run in oven or flame dried 2.0 – 5.0 mL microwave vials from Biotage. DMSO was purchased from Sigma Aldrich and stored in a glove box. Allyl alcohol was purchased from Sigma Aldrich and stored over 3 Å mol sieves. 2-Phenylprop-2-en-1-ol was prepared according to a literature procedure.[1] Palladium tetrakis(triphenylphosphine) was purchased from Strem, stored in a glovebox, and used as received. CO_2 was dispensed through a Matheson 3040 series regulator attached to a cylinder purchased from Lindweld.

TLC analysis was performed with silica gel HL TLC plates w/UV254 from Sorbent Technologies. 60 Å porosity, 230 x 400 mesh standard grade silica gel from Sorbent Technologies was used for column chromatography. GC/MS data was obtained using a Shimadzu GCMS-QP2010 SE. Microwave experiments were run in a Biotage Initiator. ^{1}H, ^{13}C, and ^{19}F NMR spectra were obtained on a Bruker Advance 500 DRX equipped with a QNP cryoprobe or a Bruker Advance 400. ^{19}F NMR spectra were referenced to trifluoromethyltoluene while ^{1}H and ^{13}C NMR spectra were referenced to residual protio solvent signals.

Nitroalkanes were prepared according to literature procedures:

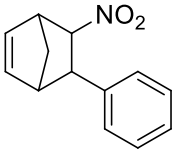

ref. 2

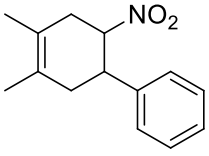

ref. 2

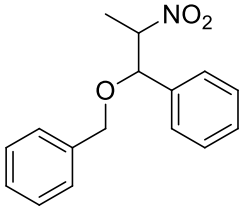

ref. 3

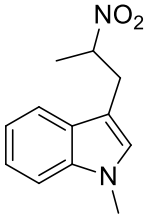

ref. 4

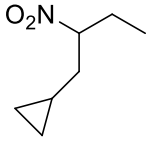

ref. 5

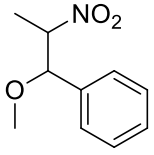

ref. 6

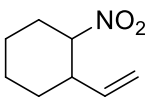

ref. 7

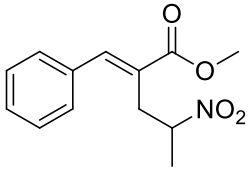

ref. 8

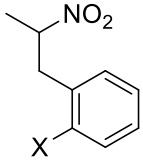

ref. 9
X = H, F

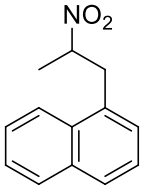

ref. 10

Procedure A (synthesis of 2-(4-chlorophenyl)propanenitrile, 2-(4-fluorophenyl)-propanenitrile):[11]

To a glass sleeve, the respective phenylacetonitrile (16.5 mmol) was added with dimethyl carbonate (25 mL, 16 equiv.), and K_2CO_3 (4.5 g, 2 equiv.). The sleeve was placed in a stainless steel Parr reactor, sealed, heated to 160 °C and stirred for 3 hr. The reaction was then quenched by turning off the heating source and allowing the apparatus to cool to room temperature. After removal of the glass sleeve, the contents were subjected to a water workup (200 mL), extracted with EtOAc (100 mL), and purified by flash chromatography over silica in 2% EtOAc:Hexanes.

Procedure B (synthesis of 2-(4-methoxyphenyl)-3-phenylpropanenitrile):[12]

In a 100 mL flame-dried Schlenk flask under Ar dry THF (13 mL) was added. The solvent was then place in a dry ice/acetone bath and cooled to -78 °C. *n*-BuLi (8.0 mL, solution 1.6 M/Hex from Aldrich) was added dropwise and the solution was stirred for 10 min. The solution was then warmed to room temperature, stirred for 5 minutes then cooled to -78 °C. Next, commercially available 4-methoxyphenylacetonitrile (1.85 g, 12.6 mmol) was added dropwise over 10 minutes. The solution was stirred for 1 hr before benzyl bromide (2.15 g ,1 equiv) was added dropwise. The resulting solution was stirred for 30 min., warmed to room temperature, and stirred overnight. The reaction was quenched with aq. NH_4Cl (20 mL), subjected to a water workup (2 x 50 mL), and extracted with EtOAc (50 mL) and dried over $MgSO_4$. The solution was then filtered and concentrated via rotary evaporation to yield a light yellow oil that solidified upon standing. The solid was then purified via recrystallization by heating the solid in 50 mL EtOH until dissolved then placed in the freezer. The product was collected via vacuum filtration as an off-white solid.

Procedure C (synthesis of substrate 3-(1-methyl-1*H*-indol-3-yl)-2-phenylpropanenitrile):[13]

A 100 mL round bottom flask was charged with benzyl cyanide (.94 g, 8.0 mmol), 1-methylindole-3-carboxaldehyde (1.27 g, 8 mmol), sodium methoxide (0.04 g, 0.8 mmol) and EtOH (12 mL) and stirred at room temperature overnight. The reaction mixture was then concentrated *in vacuo* followed by an aqueous workup in water (2 x 50 mL), extracted with EtOAc (100 mL), and dried over $MgSO_4$. After concentration via rotary evaporation, the crude product was heated until dissolved in 20 mL EtOH to yield 4-(1-methyl-1*H*-indol-3-yl)-2-phenylbut-3-enenitrile as an orange solid (1.25 g, 4.8 mmol). The solid was then dissolved in THF (5 mL) and cooled to 0 ^oC followed by the addition of $NaBH_4$ (0.2 g, 4.8 mmol). The solution was allowed to warm to room temperature and stirred overnight followed by quenching with NH_4Cl (10 mL), aqueous workup (3 x 20 mL), extraction with EtOAc (20 mL), and purification via column chromatography in 2% EtOAc:Hexane.

Aldehyde starting materials:

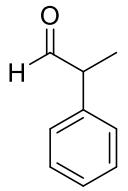

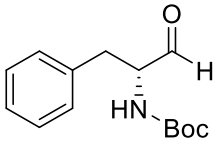

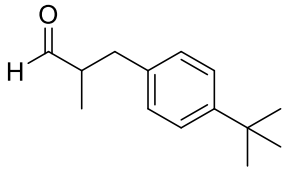

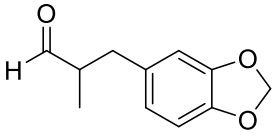

commercially available

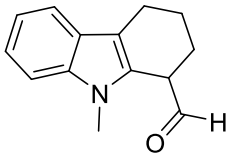

ref 14

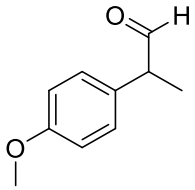

ref 15

The remaining aldehydes were synthesized according to the two step procedure outlined in:

Baumann, T.; Vogt, H.; Bräse. *Eur. J. Org. Chem.* **2007**, 266.

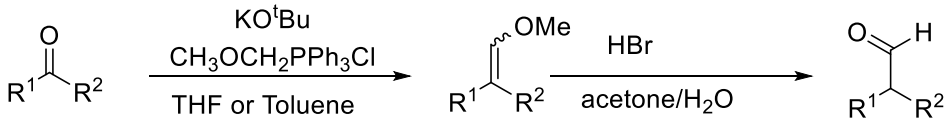

References:

[1] Duan et al. *J. Org. Chem.* **2009**, *74*, 9191-9194.

[2] Gates et al. *J. Org. Chem.* **1943**, *8*, 373-379.

[3] Kamimura et al. *J. Org. Chem.* **1990**, *55*, 2437-2442.

[4] Szmuszkovicz et al. *J. Org. Chem.* **1960**, *25*, 1548-1558. See ref. 9 method B for reduction conditions (1 eq $NaBH_4$ used).

[5] B. Quiclet-Sire and S. Z. Zard. *Synthesis*. **2005**, *19*, 3319-3326. See ref 9 method B for reduction conditions of the nitroalkene (2 eq $NaBH_4$ used).

[6] M. Osorio-Olivares et al. *Bioorg. Med. Chem.* **2004**, *12*, 4055-4066.

[7] H. Estreicher and E. J. Corey. *J. Am. Chem. Soc.* **1978**, *100*, 6294-6295.

[8] J. S. Rao and D. Basavaiah. *Tetrahedron Letters*. **2004**, *45*, 1621-1625.

[9] Kabalka et al. *Tetrahedron*. **1990**, *46*, 7443-7457. (Method B was used).

[10] Vilvhes- Herrea et al. *Bioorg. Med. Chem.* **2009**, *17*, 2452-2460. See ref 9 method B for reduction conditions of the nitroalkene (2 eq $NaBH_4$ used).

[11] A.J. Grenning and J.A. Tunge. *Org. Lett.* **2010**, *12*, 740-742.

[12] Tundo, P. *Pure Appl. Chem.* **2000**, *72*, 1793.

[13] Fleming, F. F.; Liu, W.; Ghosh, S.; Steward, O. W. *J. Org. Chem.* **2008**, *73*, 2803.

[14] Downie, I. M.; Earie, M. J.; Heaney, H.; Shuhaibar, K. F. Tetrahedron. 1993, 4015.

[15] Havare, Z.; Plattner, D. A. Org. Lett. 2012, 5078.

[16] Martin, S. F.; Phillips, G. W. *J. Org. Chem.* **1978**, *43*, 3792-3794.

[17] Srikrishna, A.; Sunderbabu, G. *Tetrahedron Lett.* **1989**, *30*, 3561-3562.

[18] Jiang, G.; List, B. *Adv. Syn. Catal.* **2011**, *353*, 1667-1670.

[19] Takeda, T.; Kazuo, A.; Mamada, A.; Tooru, F. *Chem. Lett.* **1985**, 1149-1152.

[20] Kimura, Y.; Kirszensztejn, P.; Regen, S. L. *J. Org. Chem.* **1983**, *48*, 385-386.

[21] Schultz, E. M.; Robb, C. M.; Sprague, J. M. *J. Am. Chem. Soc.* **1947**, *69*, 2454-2459.

[22] Recio, A.; Tunge, J. A. *Org. Lett.* **2009**, *11*, 5630-5633.

[23] Gaudin, J.-M.; Millet, P. *Chem. Comm.* **2008**, 588-590.

[24] Grenning, A. J.; Tunge, J. A. *J. Am. Chem. Soc.* **2011**, *133*, 14785-14794.

[25] Ciganek, E.; Read, J. M.; Calabrese, J. C. *J. Org. Chem.* **1995**, *60*, 5795-5802.

[26] Murahashi, S.; Makabe, Y. *Tetrahedron Lett.* **1985**, *26*, 5563-5566.

[27] Murahashi, S.; Makabe, Y.; Kunita, K. *J. Org. Chem.* **1988**, *53*, 4489-4495.

Representative procedure for the CO_2 catalyzed activation of allyl alcohol towards allylation of nitroalkanes:

A 2.0 – 5.0 mL microwave vial (Biotage #351521) dried in an oven is charged with a stir bar and taken into a glove box. $Pd(PPh_3)_4$ (10 mol %, 0.035 g) is added along with DMSO (2.0 mL) and the vial is capped using a vial cap (Biotage #352298) and a manual cap crimper (Biotage #353671). The vial is removed from the glovebox and substrate (0.30 mmol) and allyl alcohol (0.45 mmol, 0.026 g) are added sequentially via syringe. CO_2 is then bubbled through the solvent using a 20G needle connected to a balloon and a separate 25.5G needle to vent. After 6 mins the vent needle was removed followed by the CO_2 needle and the top of the vial is wrapped in parafilm "M". The vial was then placed in an oil bath at room temperature and heated/stirred at 80 ^oC for 14 hours.

After 14 hours the vial is removed from the bath, and allowed to cool to room temperature. The contents were taken up in EtOAc (10 mL) and transferred to a separatory funnel and were washed with 30 mL DI water 3x. The organic layer was dried over $MgSO_4$, filtered, and the solvent evaporated *in vacuo* followed by purification via silica gel column chromatography using 1:20 EtOAc:Pentanes as an eluent.

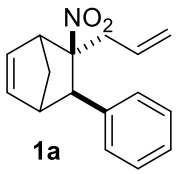

1a

dr = 95:5 ; Stereochemistry assigned by inference. See Ref. 11.

^{1}H NMR Spectra (500 MHz, $CDCl_3$):

(major diastereomer) δ 7.47 (d, *J* = 7.43 Hz, 2H), 7.37 (t, *J* = 7.40 Hz, 2H), 7.30 (m, 1H), 6.54 (dd, *J* = 5.66, 3.22 Hz, 1H), 6.26 (dd, *J* = 5.67, 2.82 Hz, 1H), 5.57 (m, 1H), 5.04 (dt, *J* = 10.2, 0.95 Hz 1H), 4.90 (dq, *J* = 16.9 Hz, 1.50 Hz, 1H), 3.52 (d, *J* = 2.63 Hz, 1H), 3.41 (s, 1H), 3.12 (s, 1H), 2.29 (ddt, *J* = 15.0, 6.97, 1.20 Hz, 1H), 2.05 (d, *J* = 9.60 Hz, 1H), 1.95 (dd, *J* = 15.0, 7.60 Hz, 1H), 1.85 (dq, *J* = 9.56, 2.07 Hz, 1H).

^{13}C NMR (126 MHz, $CDCl_3$):

(major diastereomer) δ 139.79, 138.18, 135.82, 130.21, 127.45, 126.06, 118.66, 100.40, 52.03, 47.13, 45.67, 44.58, 42.14.

GC/MS Data: 255.1 (M^+, 1 %), 66.1, base peak.

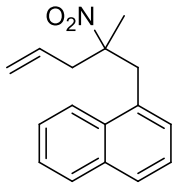

1b

^{1}H NMR Spectra (500 MHz, $CDCl_3$):

δ 7.99 (d, *J* = 8.66 Hz, 1H), 7.87 (d, *J* = 8.08 Hz, 1H), 7.80 (d, *J* = 8.40 Hz, 1H), 7.44 (m, 2H), 7.51 (t, *J* = 7.65 Hz, 1H), 7.26 (d, *J* = 6.22 Hz, 1H), 5.71 (m, 1H), 5.21 (m, 2H), 3.78 (d, *J* = 14.7 Hz, 1H), 3.71 (d, *J* = 14.6 Hz, 1H), 3.02 (dd, *J* = 14.2, 6.86 Hz, 1H), 2.57 (dd, *J* = 14.2, 7.76 Hz, 1H), 1.43 (s, 3H).

^{13}C NMR (126 MHz, $CDCl_3$):

δ 133.91, 132.66, 131.15, 130.92, 129.01, 128.47, 128.38, 126.27, 125.67, 125.38, 123.63, 120.93, 92.43, 44.36, 41.09, 21.31.

GC/MS data: 255.1 (M^+, 8 %), 141.1, base peak.

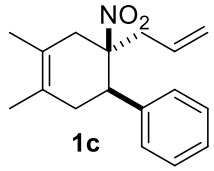

1c

dr > 95:5; Stereochemistry assigned by inference. See Ref. 11.

^{1}H NMR Spectra (500 MHz, $CDCl_3$):

δ 7.23 (m, 3H), 7.11 (m, 2H), 5.63 (m, 1H), 5.14 (m, 2H), 3.47 (d, *J* = 6.82 Hz, 1H), 2.85 (dd, *J* = 14.1, 6.81 Hz, 1H), 2.64 (m, 3H), 2.34 (m, 2H), 1.75 (d, *J* = 10.9 Hz, 6H).

^{13}C NMR (126 MHz, $CDCl_3$):

δ 140.27, 130.99, 128.47, 128.27, 127.53, 124.40, 123.72, 120.64, 92.98, 46.8, 41.80, 36.6, 33.35, 19.36, 18.30.

GC/MS data: 225.2 ($M - NO_2$, 8%), 183.1, base peak.

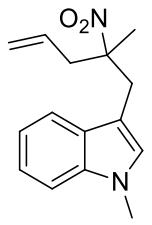

1d

^{1}H NMR Spectra (500 MHz, $CDCl_3$):

δ 7.53 (dt, *J* = 7.97, 0.92 Hz, 1H), 7.30 (dt, *J* = 8.31, 0.91 Hz, 1H), 7.23 (ddd, *J* = 8.18, 6.99, 1.11 Hz, 1H), 7.13 (ddd, *J* = 7.99, 6.94, 1.08 Hz, 1H), 6.84 (s, 1H), 5.74 (m, 1H), 5.19 (m, 2H), 3.75 (s, 3H), 3.49 (d, *J* = 14.8 Hz, 1H), 3.24 (d, *J* = 14.8 Hz, 1H), 2.92 (dd, *J* = 14.2, 7.05 Hz, 1H), 2.57 (dd, *J* = 14.1, 7.62 Hz, 1H), 1.51 (s, 3H).

^{13}C NMR (126 MHz, $CDCl_3$):

δ 136.62, 131.19, 128.48, 128.45, 121.69, 120.50, 119.32, 118.74, 109.37, 107.48, 92.63, 44.04, 35.61, 32.78, 21.50.

GC/MS data: 258.1 (M^+, 14%) 144.1, base peak.

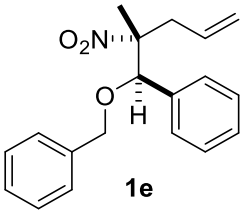

1e

dr = 88:12; Relative stereomchemistry assigned via x-ray structure of corresponding amine salt.

^{1}H NMR Spectra (500 MHz, $CDCl_3$):

(major diastereomer) δ 7.30 (m, 8H), 7.18 (m, 2H), 5.62 (m, 1H), 5.04 (m, 2H), 4.86 (s, 1H), 4.44 (d, *J* = 11.5 Hz, 1H), 4.20 (d, *J* = 11.5, 1H), 3.01 (dd, *J* = 14.5, 6.63 Hz, 1H), 2.53 (dd, *J* = 14.6, 7.89 Hz, 1H), 1.33 (s, 3H).

^{13}C NMR (126 MHz, $CDCl_3$):

(major diastereomer) δ 136.19, 134.15, 130.31, 127.82, 127.43, 127.40, 127.33, 126.88, 119.34, 93.20, 83.66, 70.43, 39.01, 16.74.

GC/MS data: 221.1 (M – toluene, 1%), 91.1, base peak.

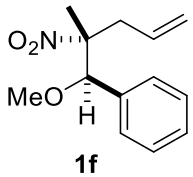

1f

dr = 88:12; Relative stereochemistry assigned based on the x-ray structure of the 1e salt.

^{1}H NMR Spectra (500 MHz, $CDCl_3$):

(major diastereomer) δ 7.35 (m, 3H), 7.27 (m, 2H), 5.71 (m, 1H), 5.13 (m, 2H), 4.73 (s, 1H), 3.26 (s, 3H), 3.09 (dd, *J* = 14.1, 6.75 Hz, 1H), 2.56 (dd, *J* = 14.5, 7.90 Hz, 1H), 1.38 (s, 3H).

^{13}C NMR (126 MHz, $CDCl_3$):

(major diastereomer) δ 135.17, 131.41, 128.75, 128.37, 128.22, 120.32, 94.18, 87.23, 57.84, 39.83, 17.85.

GC/MS data: 121.1 base peak.

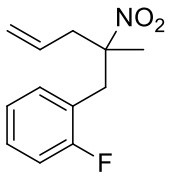

1g

^{1}H NMR Spectra (500 MHz, $CDCl_3$):

δ 7.27 (m, 1H), 7.07 (m, 3H), 5.70 (m, 1H), 5.20 (m, 2H), 3.33 (d, *J* = 14.3 Hz, 1H), 3.25 (d, *J* = 14.2 Hz, 1H), 2.89 (dd, *J* = 14.1, 6.93 Hz, 1H), 2.53 (dd, *J* = 14.2, 7.68 Hz, 1H), 1.48 (s, 3H).

^{13}C NMR (126 MHz, $CDCl_3$):

δ 161.27 (d, J_{CF} = 246 Hz), 131.82 (d, J_{CF} = 3.91 Hz), 130.74, 129.47 (d, J_{CF} = 8.32 Hz), 124.41 (d, J_{CF} = 3.60 Hz), 121.89 (d, J_{CF} = 15.7 Hz), 120.87, 115.44 (d, J_{CF} = 22.7 Hz), 91.65, 43.95, 38.19, 20.78.

^{19}FNMR (376 MHz, $CDCl_3$):

δ -116.75.

GC/MS data: 223.05 (M^+ 0.1 %), 109.1, base peak.

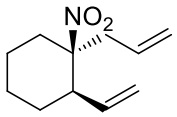

1h

dr = 85:15; Stereochemistry assigned by inference. See Ref. 11.

^{1}H NMR Spectra (500 MHz, $CDCl_3$):

(major diastereomer) δ 5.98 (m, 1H), 5.62 (m, 1H), 5.13 (m, 4H), 2.80 (dd, *J* = 15.1 Hz, 7.08 Hz, 1H), 2.69 (dd, *J* = 14.1, 7.60 Hz, 1H), 2.55 (m, 1H), 2.23 (ddd, *J* = 13.8, 8.62, 3.78 Hz, 1H), 1.60 (m, 8H).

^{13}C NMR (126 MHz, $CDCl_3$):

(major diastereomer) δ 136.18, 130.72, 120.40, 118.15, 93.55, 48.66, 41.56, 29.62, 28.48, 22.09.

GC/MS data: 149.2 ($M - NO_2$, 5%), 81.1 (base peak).

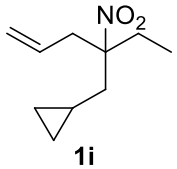

1i

^{1}H NMR Spectra (500 MHz, $CDCl_3$):

δ 5.63 (ddt, *J* = 17.3, 10.1, 7.30 Hz, 1H), 5.17 (m, 2H), 2.77 (dt, *J* = 7.30, 1.24 Hz, 2H), 2.01 (m, 2H), 1.84 (dd, *J* = 6.8, 1.46 Hz, 2H), 0.87 (t, *J* = 7.45 Hz, 3H), 0.61 (m, 1H), 0.46 (m, 2H), 0.10 (m, 2H).

^{13}C NMR (126 MHz, $CDCl_3$):

δ 130.28, 118.98, 93.78, 39.02, 37.73, 28.68, 7.03, 4.61, 2.85, 2.78.

GC/MS data: 154.1 (M – ethyl, 0.4 %), 55.1, base peak.

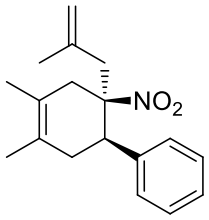

1j

dr = 90:10; Stereochemistry assigned by inference. See Ref. 11.

^{1}H NMR Spectra (500 MHz, $CDCl_3$):

δ 7.23 (m, 3H), 7.10 (m, 2H), 4.90 (t, *J* = 1.70 Hz, 1H), 4.65 (d, *J* = 1.05 Hz, 1H), 3.44 (d, *J* = 7.17 Hz, 1H), 2.93 (d, *J* = 14.0 Hz, 1H), 2.69 (m, 3H), 2.36 (m, 2H), 1.75 (d, *J* = 13.6 Hz, 6H), 1.63 (s, 3H).

^{13}C NMR (126 MHz, $CDCl_3$):

δ 140.34, 139.64, 128.44, 128.32, 127.52, 124.27, 123.91, 116.68, 92.85, 47.33, 44.73, 37.19, 32.61, 23.19, 19.35, 18.25.

GC/MS data: 239.2 (M – NO_2), 197.1 183.1, base peak.

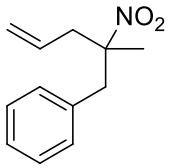

1k

^{1}H NMR Spectra (500 MHz, $CDCl_3$):

δ 7.30 (m, 3H), 7.02 (dd, *J* = 7.52, 1.90 Hz, 2H), 5.63 (dddd, *J* = 17.1, 10.2, 7.61, 6.96 Hz, 1H), 5.12 (m, 2H), 3.29 (d, *J* = 13.9 Hz, 1H), 2.98 (d, *J* = 13.9 Hz, 1H), 2.79 (dd, *J* = 14.2, 6.97 Hz, 1H), 2.43 (dt, *J* = 14.2, 7.68, 1.07 Hz, 1H), 1.39 (s, 3H).

^{13}C NMR (126 MHz, $CDCl_3$):

δ 134.60, 130.88, 130.10, 128.54, 127.52, 120.80, 91.51, 45.62, 43.82, 21.29.

GC/MS data: 159.1 (M- NO_2, 4%), 91.1, base peak

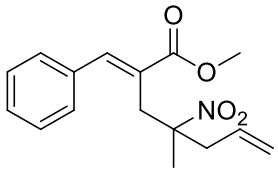

1l

^{1}H NMR Spectra (500 MHz, $CDCl_3$):

δ 7.90 (s, 1H), 7.39 (m, 3H), 7.28 (m, 2H), 5.47 (m, 1H), 5.06 (m, 2H), 3.79 (s, 3H), 3.37 (d, *J* = 16.5 Hz, 1H), 3.26 (d, *J* = 14.6 Hz, 1H), 2.73 (dd, *J* = 14.1, 6.78 Hz, 1H), 2.26 (dd, *J* = 14.2, 8.00 Hz, 1H), 1.34 (s, 3H).

^{13}C NMR (126 MHz, $CDCl_3$):

δ 168.22, 143.67, 135.05, 130.78, 128.75, 128.67, 128.54, 127.88, 120.73, 90.46, 52.21, 43.85, 35.50, 21.17.

GC/MS data: 289.1 (M^+, 1%), 115.1, base peak.

Representative procedure for the CO_2 catalyzed activation of allyl alcohol towards allylation of aldehydes:

A 2.0 – 5.0 mL microwave vial (Biotage #351521) dried in an oven is charged with a stir bar and taken into a glove box. $Pd(PPh_3)_4$ (5 mol %, 0.014 g) is added along with DMSO (2.0 mL) and the vial is capped using a vial cap (Biotage #352298) and a manual cap crimper (Biotage #353671). The vial is removed from the glovebox and substrate (0.30 mmol) and allyl alcohol (0.45 mmol, 0.026 g) are added sequentially via syringe. CO_2 is then bubbled through the solvent using a 20G needle connected to a balloon and a separate 25.5G needle to vent. After 6 mins the vent needle was removed followed by the CO_2 needle and the top of the vial is wrapped in parafilm "M". The vial was then placed in an oil bath at room temperature and heated/stirred at 80 °C until the reaction was complete as shown by GC/MS. The reaction mixture was dry loaded onto silica gel and purified by flash chromatography.

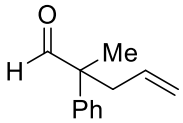

2a

ref. 16

^{1}H NMR Spectra (500 MHz, $CDCl_3$):

δ 9.52 (s, 1H), 7.39 (m, 2H), 7.30 (m, 1H), 7.26 (m, 2H), 5.55 (m, 1H), 5.04 (m, 2H), 2.70 (ddt, *J* = 14.2, 6.93, 1.32 Hz, 1H), 2.63 (ddt, *J* = 14.1, 7.72, 1.19 Hz, 1H), 1.45 (s, 3H).

^{13}C NMR (126 MHz, $CDCl_3$):

δ 201.97, 139.43, 133.17, 128.86, 127.34, 127.17, 118.61, 53.63, 40.60, 18.83.

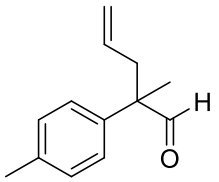

2b

ref. 17

^{1}H NMR Spectra (500 MHz, $CDCl_3$):

δ 9.49 (s, 1H), 7.20 (m, 2H), 7.14 (m, 2H), 5.56 (m, 1H), 5.04 (m, 2H), 2.68 (ddt, *J* = 14.1, 6.91, 1.13 Hz, 1H), 2.61 (ddt, *J* = 14.1, 7.67, 1.13 Hz, 1H), 2.35 (s, 3H), 1.43 (s, 3H).

^{13}C NMR (126 MHz, $CDCl_3$):

δ 202.02, 137.07, 136.31, 133.31, 129.57, 127.07, 118.49, 53.26, 40.52, 20.97, 18.83.

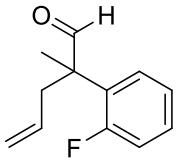

2c

ref. 18

^{1}H NMR Spectra (500 MHz, $CDCl_3$):

δ 9.68 (d, *J* = 4.97 Hz, 1H), 7.30 (m, 2H), 7.18 (td, *J* = 7.58, 7.53, 1.35 Hz, 1H), 7.08 (ddd, *J* = 11.8, 8.18, 1.33 Hz, 1H), 5.53 (m, 1H), 5.02 (m ,2H), 2.75 (dd, *J* = 14.0, 6.99 Hz, 1H), 2.63 (dd, *J* = 14.1, 7.77 Hz, 1H), 1.42 (s, 3H).

^{13}C NMR (126 MHz, $CDCl_3$):

δ 201.87 (d, *J* = 2.32 Hz), 161.85, 159.89, 132.74, 129.42 (d, *J* = 8.57 Hz), 128.62 (d, *J* = 4.95 Hz), 127.87 (d, *J* = 13.1 Hz), 124.44 (d, *J* = 3.21 Hz), 118.84, 116.12 (d, *J* = 22.8 Hz), 51.85 (d, *J* = 3.15 Hz), 39.24 (d, *J* = 2.50 Hz), 19.16.

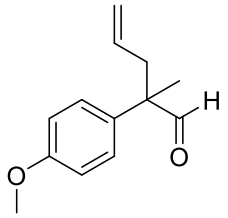

2d

ref. 18

^{1}H NMR Spectra (500 MHz, $CDCl_3$):

δ 9.46 (s, 1H), 7.17 (m, 2H), 6.92 (m, 2H), 5.55 (m, 1H), 5.04 (m, 2H), 3.80 (s, 3H), 2.66 (ddt, *J* = 14.1, 6.78, 1.37 Hz, 1H), 2.59 (dd, *J* = 14.2, 7.79, 1.21 Hz, 1H), 1.42 (s, 3H).

^{13}C NMR (126 MHz, $CDCl_3$):

δ 201.90, 158.75, 133.31, 131.14, 128.33, 118.49, 114.22, 55.27, 52.91, 40.54, 18.86.

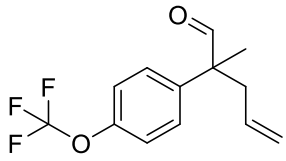

2e

^{1}H NMR Spectra (300 MHz, $CDCl_3$):

δ 9.51 (s, 1H), 7.28 (m, 2H), 7.23 (m, 2H), 5.52 (m, 1H), 5.06 (m, 2H), 2.67 (dd, *J* = 10.6, 6.93 Hz, 1H), 2.62 (dd, *J* = 10.8, 7.62 Hz, 1H), 1.45 (s, 3H).

^{13}C NMR (126 MHz, $CDCl_3$):

δ 201.41, 148.39 (d, J = 2.09 Hz), 138.14, 132.59, 128.68, 121.18, 120.5 (q, J = 257 Hz), 119.08, 53.30, 40.68, 18.98.

^{19}FNMR (376 MHz, $CDCl_3$):

δ -58.86

HRMS: [M+]: calc: 258.0868, found: 258.0872.

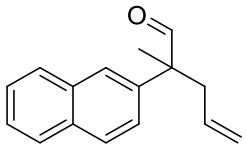

2f

^{1}H NMR Spectra (300 MHz, $CDCl_3$):

δ 9.60 (s, 1H), 7.85 (m, 3H), 7.72 (d, J = 1.95 Hz, 1H), 7.51 (m, 2H), 7.37 (dd, J = 8.60, 1.96 Hz, 1H), 5.57 (m, 1H), 5.06 (m, 2H), 2.83 (ddt, J = 14.2, 6.82, 1.29 Hz, 1H), 2.72 (ddt, J = 14.1, 7.74, 1.10 Hz, 1H), 1.56 (s, 3H).

^{13}C NMR (126 MHz, $CDCl_3$):

δ 201.98, 136.80, 133.3, 133.13, 132.41, 128.60, 128.03, 127.55, 126.40, 126.30, 126.29, 125.00, 118.70, 53.81, 40.52, 18.94.

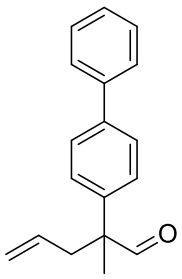

2g

ref. 18

^{1}H NMR Spectra (500 MHz, $CDCl_3$):

δ 9.56 (s, 1H), 7.61 (m, 4H), 7.45 (m, 2H), 7.35 (ddt, *J* = 16.9, 8.76, 1.71 Hz, 3H), 5.60 (m, 1H), 5.08 (m, 2H), 2.74 (ddt, *J* = 14.1, 6.87, 1.29 Hz, 1H), 2.67 (ddt, *J* = 14.1, 7.78, 1.16 Hz, 1H), 1.49 (s, 3H).

^{13}C NMR (126 MHz, $CDCl_3$):

δ 201.87, 140.38, 140.21, 138.41, 133.12, 128.83, 127.63, 127.53, 127.48, 127.06, 118.74, 53.45, 40.59, 18.90.

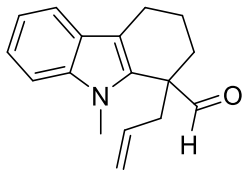

2h

^{1}H NMR Spectra (500 MHz, $CDCl_3$):

δ 9.63 (s, 1H), 7.54 (dt, *J* = 7.80, 0.99 Hz, 1H), 7.26 (m, 2H), 7.12 (ddd, *J* = 7.93, 6.77, 1.24 Hz, 1H), 5.61 (m, 1H), 5.12 (dq, *J* = 17.0. 1.61 Hz, 1H), 5.03 (ddt, *J* = 10.1, 2.07, 1.10 Hz, 1H), 3.63 (s, 3H), 2.90 (ddt, *J* = 14.7, 6.95, 1.41 Hz, 1H), 2.81 (t, *J* = 5.9 Hz, 2H), 2.69 (ddt, *J* = 14.8, 7.53, 1.19 Hz, 1H), 1.97 (m, 4H).

^{13}C NMR (126 MHz, $CDCl_3$):

δ 201.58, 137.85, 133.66, 131.42, 126.60, 122.07, 119.12, 118.44, 113.91, 108.94, 51.29, 38.09, 31.25, 30.64, 21.24, 19.41.

HRMS: [M+H] calc: 254.1545, found: 254.1535.

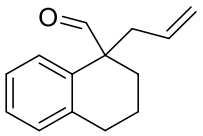

2i

^{1}H NMR Spectra (300 MHz, $CDCl_3$):

δ 9.55 (s, 1H), 7.18 (m, 4H), 5.60 (m ,1H), 5.05 (m, 2H), 2.78 (t, *J* = 5.65 Hz, 2H), 2.63 (dd, *J* = 7.22, 1.28 Hz, 2H), 2.09 (m, 1H), 1.83 (m, 3H).

^{13}C NMR (126 MHz, $CDCl_3$):

δ 200.09, 138.65, 134.00, 133.69, 129.88, 128.29, 127.02, 126.37, 118.47, 53.04, 41.13, 29.88, 27.84, 19.23.

HRMS: [M+Na] calc: 223.1099, found: 223.1103.

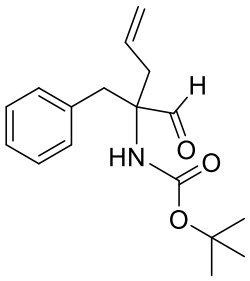

2j

^{1}H NMR Spectra (500 MHz, $CDCl_3$):

δ 9.40 (s, 1H), 7.18 (m, 3H), 6.99 (d, *J* = 7.08 Hz, 2H), 5.53 (m, 1H), 5.04 (m, 2H), 4.99 (s, 1H), 3.28 (d, *J* = 14.0 Hz, 1H), 3.0 (d, *J* = 14.0 Hz, 1H), 2.79 (dd, *J* = 14.5, 7.48 Hz, 1H), 2.45 (dd, *J* = 14.4, 7.32 Hz, 1H), 1.38 (s, 9H).

^{13}C NMR (126 MHz, $CDCl_3$):

δ 200.25, 154.54, 135.39, 131.19, 130.20, 128.34, 126.95, 119.89, 79.80, 66.01, 38.55, 37.75, 28.34.

HRMS: [M+Na] calc: 312.1576, found: 312.1542.

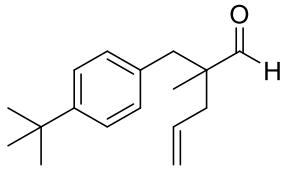

2k

ref. 18

^{1}H NMR Spectra (500 MHz, $CDCl_3$):

δ 9.60 (s, 1H), 7.28 (d, *J* = 8.28 Hz, 2H), 7.02 (d, *J* = 8.23 Hz, 2H), 5.74 (m, 1H), 5.11 (m, 2H), 2.85 (d, *J* = 13.8 Hz, 1H), 2.72 (d, *J* = 13.7 Hz, 1H), 2.36 (ddt, *J* = 14.2, 7.14, 1.28 Hz, 1H), 2.18 (dd, *J* = 14.2, 7.70, 1.25 Hz, 1H), 1.30 (s, 9H), 1.03 (s, 3H).

^{13}C NMR (126 MHz, $CDCl_3$):

δ 206.20, 149.40, 133.48, 133.13, 129.91, 125.12, 118.80, 50.18, 41.36, 39.91, 34.40, 31.36, 18.56.

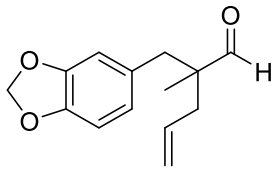

2l

^{1}H NMR Spectra (500 MHz, $CDCl_3$):

δ 9.57 (s, 1H), 6.71 (d, *J* = 7.90, 1H), 6.58 (d, *J* = 1.76 Hz, 1H), 6.54 (dd, *J* = 7.95, 1.76 Hz, 1H), 5.92 (s, 3H), 5.72 (m, 1H), 5.11 (m, 2H), 2.81 (d, *J* = 13.9 Hz, 1H), 2.66 (d, *J* = 13.9 Hz, 1H), 2.34 (ddt, *J* = 14.4, 7.32, 1.35 Hz, 1H) 2.17 (dd, *J* = 14.1, 7.73, 1.22 Hz, 1H), 1.02 (s, 3H).

^{13}C NMR (126 MHz, $CDCl_3$):

δ 206.00, 147.42, 146.26, 132.96, 130.25, 123.27, 118.92, 110.56, 108.03, 100.92, 50.18, 41.49, 39.92, 29.72, 18.57.

HRMS: [M+H] calc: 233.1178, found: 233.1189.

Representative procedure for the CO_2 catalyzed activation of allylic alcohol towards allylation of nitriles:

A 2.0 – 5.0 mL microwave vial (Biotage #351521) was flame dried and charged with the nitrile substrate (if solid, 0.3 mmol) and a stir bar. In the glove box, $Pd(PPh_3)_4$ (2.5 mol %, 0.009 g) was added along with DMSO (2 mL) and the vial was capped using a vial cap (Biotage #352298) and a manual cap crimper (Biotage #353671). The vial was then removed from the glove box and substrate (if liquid, 0.3 mmol) and allyl alcohol (0.6 mmol, 0.035 g) were added sequentially via syringe. CO_2 was then bubbled through the solvent using a 20G needle connected to a balloon

and a separate 25.5G needle to vent. After 5 minutes, the vent needle is removed followed by the CO_2 needle and the top of the vial was wrapped in parafilm. The vial was then placed in an oil bath at room temperature and heated/stirred at 90 °C for 14 hours.

After 14 hours the vial was removed from the bath, and allowed to cool to room temperature. An aliquot was then diluted in DCM and subjected to GC/MS analysis to determine conversion. The remaining solution was subjected to purification via silica gel column chromatography using 1:50 EtOAc:Pentanes as an eluent.

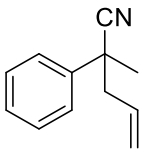

3a

ref. 19

^{1}H NMR Spectra (500 MHz, $CDCl_3$):

δ 7.44 (m, 2H), 7.38 (m, 2H), 7.30 (m, 1H), 5.70 (m, 1H), 5.15 (m, 2H), 2.67 (ddt, *J* = 13.9, 6.7, 1.3 Hz, 1H), 2.60 (ddt, *J* = 13.9, 7.8, 1.0 Hz, 1H), 1.7 (s, 3H).

^{13}C NMR Spectra (126 MHz, $CDCl_3$):

δ 140.02, 132.10, 129.09, 128.05, 125.79, 123.31, 120.37, 46.48, 42.37, 26.76.

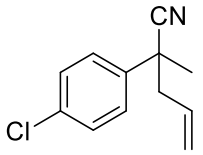

3b

^{1}H NMR Spectra (500 MHz, $CDCl_3$):

δ 7.38 (m, 4H), 5.69 (dddd, *J* = 17.0, 10.2, 7.6, 6.9 Hz, 1H), 5.17 (m, 2H), 2.62 (m, 2H), 1.71 (s, 3H).

^{13}C NMR Spectra (126 MHz, $CDCl_3$):

δ 138.64, 134.09, 131.75, 129.31, 127.38, 122.99, 120.84, 46.50, 42.09, 26.82.

GC/MS data: 205.1 (M^+), 164.1 (base peak).

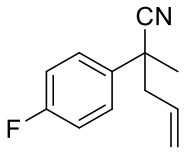

3c

^{1}H NMR Spectra (500 MHz, $CDCl_3$):

δ 7.42 (m, 2H), 7.09 (m, 2H), 5.70 (dddd, *J* = 17.0, 10.2, 7.6, 6.9 Hz, 1H), 5.18 (m, 2H), 2.63 (m, 2H), 1.71 (s, 3H).

^{13}C NMR Spectra (126 MHz, $CDCl_3$):

δ 163.44, 161.48, 135.94, 135.92, 131.92, 127.77, 127.70, 123.29, 120.77, 116.18, 116.01, 46.75, 41.96, 26.98.

GC/MS data: 189.1 (M^+), 148.1 (base peak).

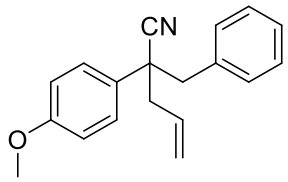

3d

^{1}H NMR Spectra (500 MHz, $CDCl_3$):

δ 7.13 (m, 5H), 6.89 (m, 2H), 6.78 (m, 2H), 5.61 (dddd, *J* = 16.9, 10.2, 7.6, 6.5 Hz, 1H), 5.07 (m, 2H), 3.72 (s, 3H), 3.12 (d, *J* = 13.5 Hz, 1H), 3.02 (d, *J* = 13.5 Hz, 1H), 2.68 (m, 2H).

^{13}C NMR Spectra (126 MHz, $CDCl_3$):

δ 159.30, 135.23, 132.24, 130.69, 129.59, 128.34, 128.02, 127.53, 122.07, 120.38, 114.24, 55.58, 48.91, 47.34, 43.95.

GC/MS data: 277.2 (M^+), 186.10 (base peak).

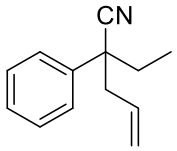

3e

ref. 20

^{1}H NMR Spectra (500 MHz, $CDCl_3$):

δ 7.40 (m, 4H), 7.32 (m, 1H), 5.66 (m, 1H), 5.13 (m, 2H), 2.69 (ddt, *J* = 7.0, 2.0, 1.1 Hz, 2H), 2.08 (m, 1H), 1.96 (m, 1H), 0.93 (t, *J* = 7.4 Hz, 3H).

^{13}C NMR Spectra (126 MHz, $CDCl_3$):

δ 138.14, 132.25, 129.15, 128.06, 126.52, 122.31, 120.19, 49.14, 45.34, 33.44, 9.92.

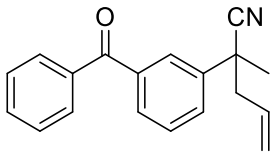

3f

^{1}H NMR Spectra (500 MHz, $CDCl_3$):

δ 7.87 (t, *J* = 1.9 Hz, 1H), 7.80 (m, 2H), 7.72 (m, 2H), 7.60 (m, 1H), 7.51 (m, 3H), 5.73 (ddt, *J* = 17.3, 10.3, 7.2 Hz, 1H), 5.18 (m, 2H), 2.68 (m, 2H), 1.75 (s, 3H).

^{13}C NMR Spectra (126 MHz, $CDCl_3$):

δ 196.29, 140.61, 138.46, 137.37, 133.03, 131.72, 130.28, 130.13, 129.91, 129.08, 128.66, 127.00, 122.91, 120.86, 46.35, 42.34, 26.68.

GC/MS data: 275.1 (M^+), 234.10 (base peak).

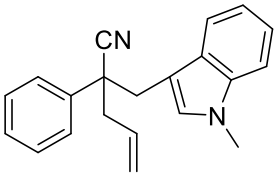

3h

^{1}H NMR Spectra (500 MHz, $CDCl_3$):

δ 7.45 (m, 2H), 7.36 (m, 2H), 7.29 (m, 3H), 7.19 (ddd, *J* = 8.2, 6.9, 1.1 Hz, 1H), 7.03 (ddd, *J* = 8.1, 6.9, 1.1 Hz, 1H), 6.85 (s, 1H), 5.68 (dddd, *J* = 17.1, 10.3, 7.6, 6.6 Hz, 1H), 5.12 (m, 2H), 3.73 (s, 3H), 3.44 (d, *J* = 14.7 Hz, 1H), 3.34 (d, *J* = 14.6 Hz, 1H), 2.82 (m, 2H).

^{13}C NMR Spectra (126 MHz, $CDCl_3$):

δ 138.66, 136.72, 132.47, 129.10, 129.05, 128.84, 128.12, 126.89, 122.82, 121.80, 120.23, 119.39, 119.00, 109.48, 108.26, 50.20, 43.47, 37.39, 33.12.

GC/MS data: 300.2 (M^+), 144.15 (base peak).

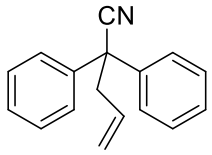

3i

ref. 21

^{1}H NMR Spectra (500 MHz, $CDCl_3$):

δ 7.45 (m, 4H), 7.39 (ddd, *J* = 7.8, 6.8, 1.3 Hz, 4H), 7.34 (m, 2H), 5.77 (ddt, *J* = 17.2, 10.2, 7.0 Hz, 1H), 5.23 (m, 2H), 3.19 (dt, *J* = 7.1, 1.2 Hz, 2H).

^{13}C NMR Spectra (126 MHz, $CDCl_3$):

δ 139.94, 132.00, 129.08, 128.17, 127.25, 122.19, 120.64, 51.94, 44.13.

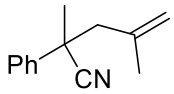

4a

ref. 22

^{1}H NMR Spectra (500 MHz, $CDCl_3$):

δ 7.48 (m, 2H), 7.39 (m, 2H), 7.33 (m, 1H), 4.92 (p, *J* = 1.6 Hz, 1H), 4.77 (dq, *J* = 1.8, 1.0 Hz, 1H), 2.64 (t, *J* = 1.0 Hz, 2H), 1.76 (s, 3H), 1.62 (m, 3H).

^{13}C NMR Spectra (126 MHz, $CDCl_3$):

δ 140.37, 140.27, 129.07, 128.05, 125.89, 123.88, 116.94, 50.08, 42.03, 27.83, 23.84.

GC/MS data: 185.1 (M^+), 130.1 (base peak).

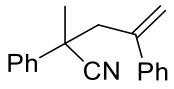

4b

^{1}H NMR Spectra (500 MHz, $CDCl_3$):

δ 7.41 (m, 2H), 7.28 (m, 3H), 5.39 (d, J = 1.1 Hz, 1H), 5.18 (q, J = 1.0 Hz, 1H), 3.12 (d, J = 1.0 Hz, 2H), 1.67 (s, 3H).

^{13}C NMR Spectra (126 MHz, $CDCl_3$):

δ 143.85, 141.74, 140.21, 128.98, 128.58, 128.04, 127.87, 126.81, 126.01, 123.33, 119.21, 47.46, 43.13, 27.28.

GC/MS data: 247.1 (M^+), 139.1 (base peak).

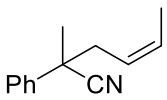

● linear Z diasteromer residues

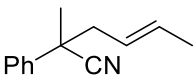

■ = linear E diastereomer residues

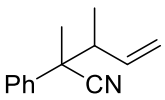

▲ = branched residues (both diastereomers)

4c (l : b, 2 : 1) (cis : trans, 1 : 2.5)

ref. 23

^{1}H NMR Spectra (500 MHz, $CDCl_3$):

δ 7.40 (m, 5H (Ph-H_{linear}), 5H (Ph-$H_{branched}$)), 5.89 (ddd, J = 16.6, 10.5, 8.8 Hz, 1H branched), 5.68 (m, 1H *cis*-linear), 5.59 (m, 1H (*trans*-linear), 1H (branched)), 5.36 (m, 1H (*cis*-linear), 1H

(*trans*-linear)), 5.20 (m, 2H, branched), 5.01 (m, 2H, branched), 2.59 (m, (2H *cis*-linear), (2H *trans*-linear), (1H branched)), 1.66 (d, J = 7.1 Hz, 3H, *trans*-linear), 1.57 (d, J = 7.1 Hz, 3H, *cis*-linear), 1.17 (d, J = 6.8 Hz, 3H, branched), 0.94 (d, J = 6.8 Hz, 2H, branched).

^{13}C NMR Spectra (126 MHz, $CDCl_3$):

δ 140.49, 140.36, 140.05, 139.26, 138.79, 138.16, 131.40, 129.23, 129.13, 128.85, 128.09, 128.04, 126.74, 126.22, 125.98, 125.95, 124.71, 123.93, 123.70, 123.07, 122.34, 117.99, 117.63, 48.69, 47.66, 47.04, 46.74, 45.60, 42.83, 42.59, 39.63, 26.77, 26.56, 24.57, 18.33, 17.21, 15.99, 13.38.

Isomers assigned by TOCSY NMR spectroscopy experiments

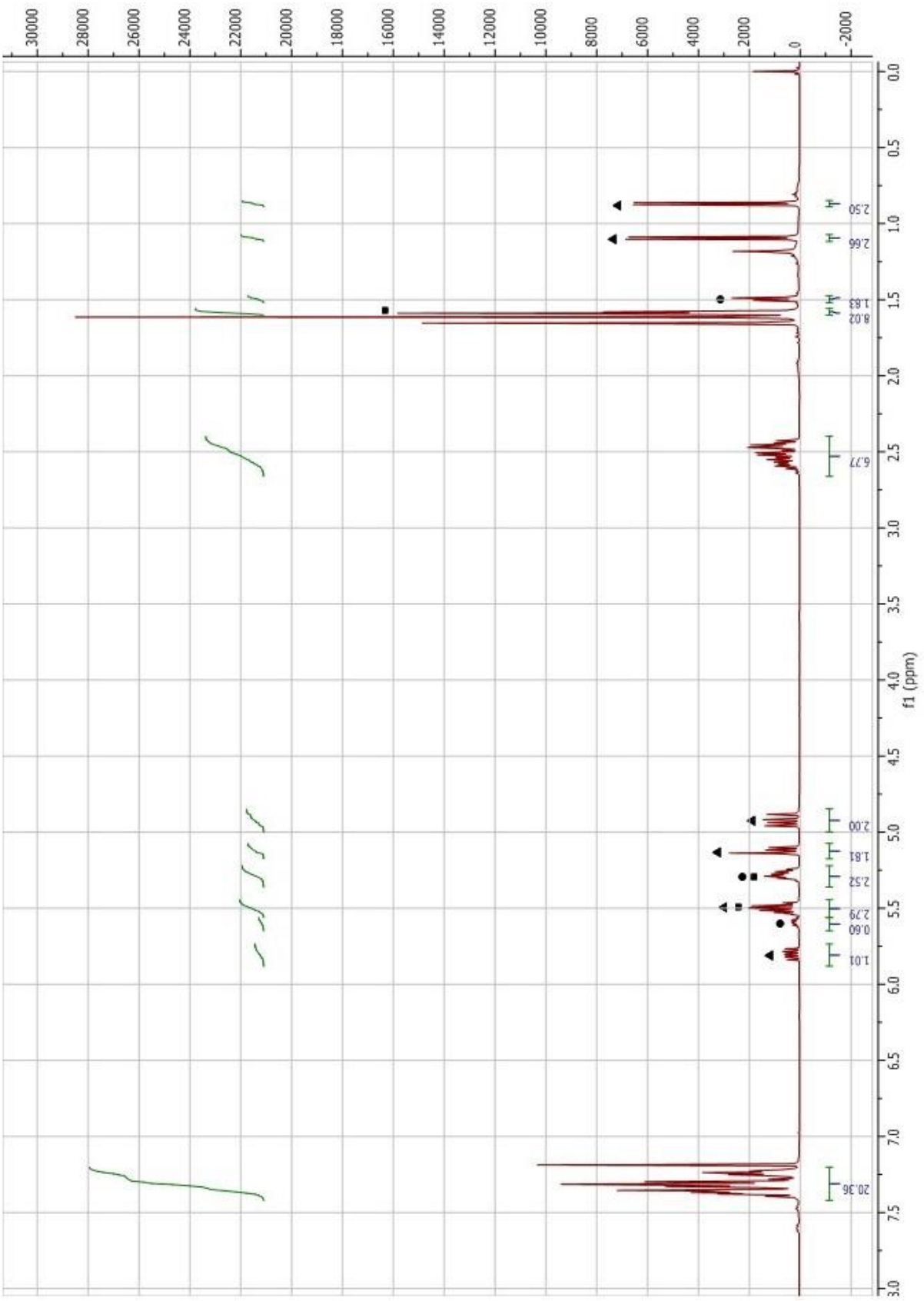
f1 (ppm)
20.36
6.77
8.02
1.83
2.50
2.66
2.00
1.81
2.52
0.60
2.79
1.01

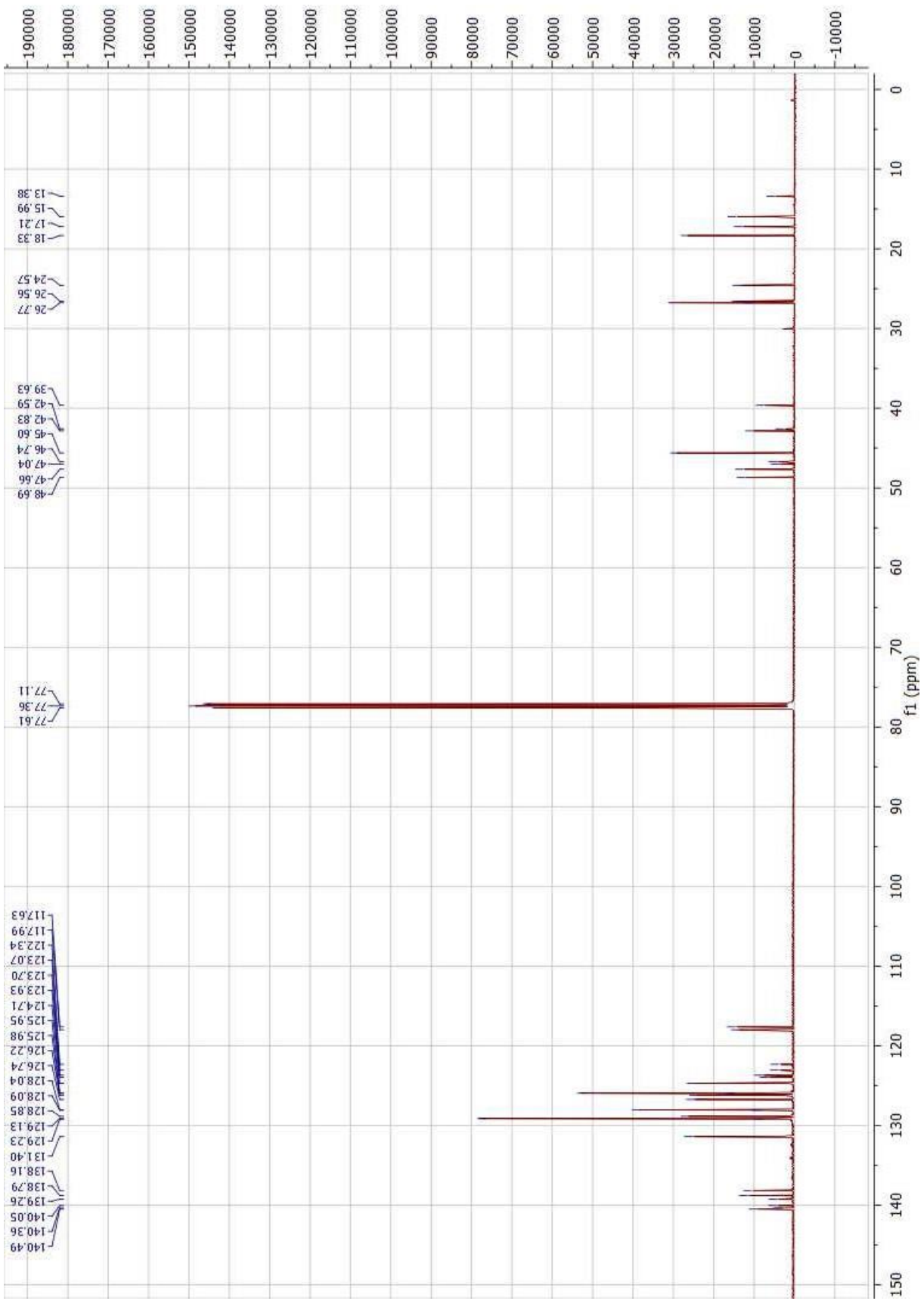
f1 (ppm)

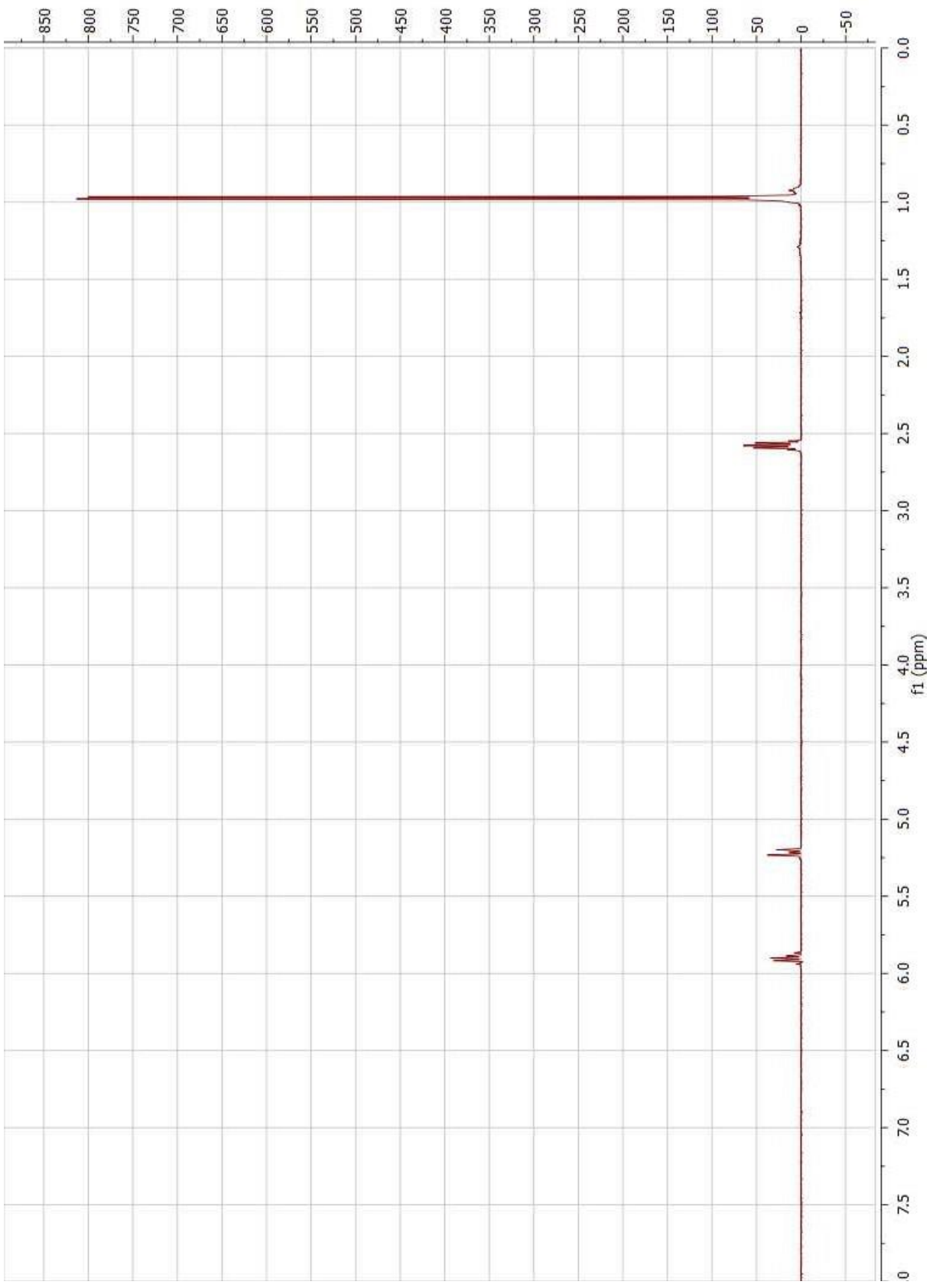
850
800
750
700
650
600
550
500
450
400
350
300
250
200
150
100
50
0
-50
0.0
0.5
1.0
1.5
2.0
2.5
3.0
3.5
4.0
4.5
5.0
5.5
6.0
6.5
7.0
7.5
0
f1 (ppm)

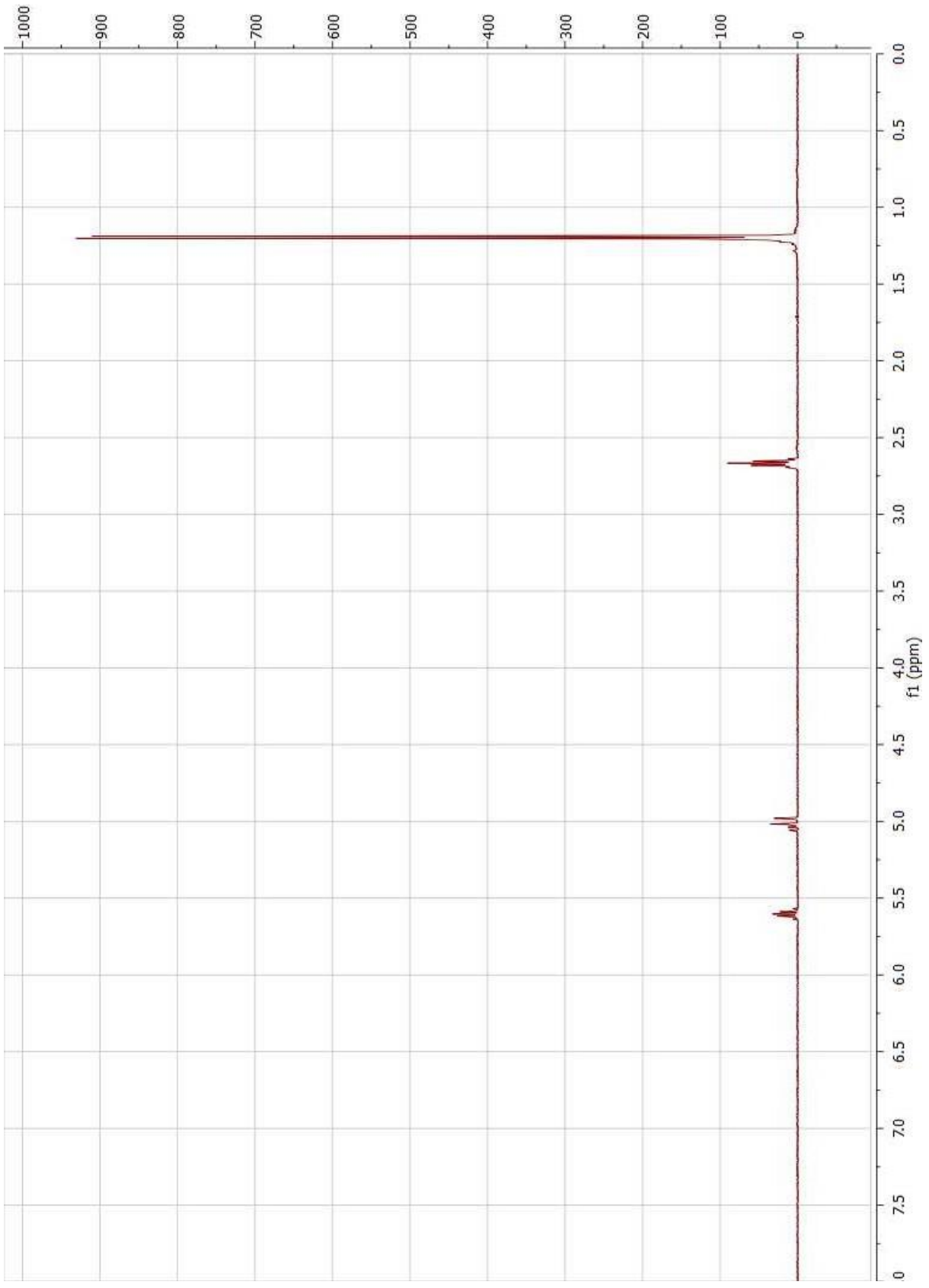
1000
900
800
700
600
500
400
300
200
100
0
0.0
0.5
1.0
1.5
2.0
2.5
3.0
3.5
4.0
4.5
5.0
5.5
6.0
6.5
7.0
7.5
0
f1 (ppm)

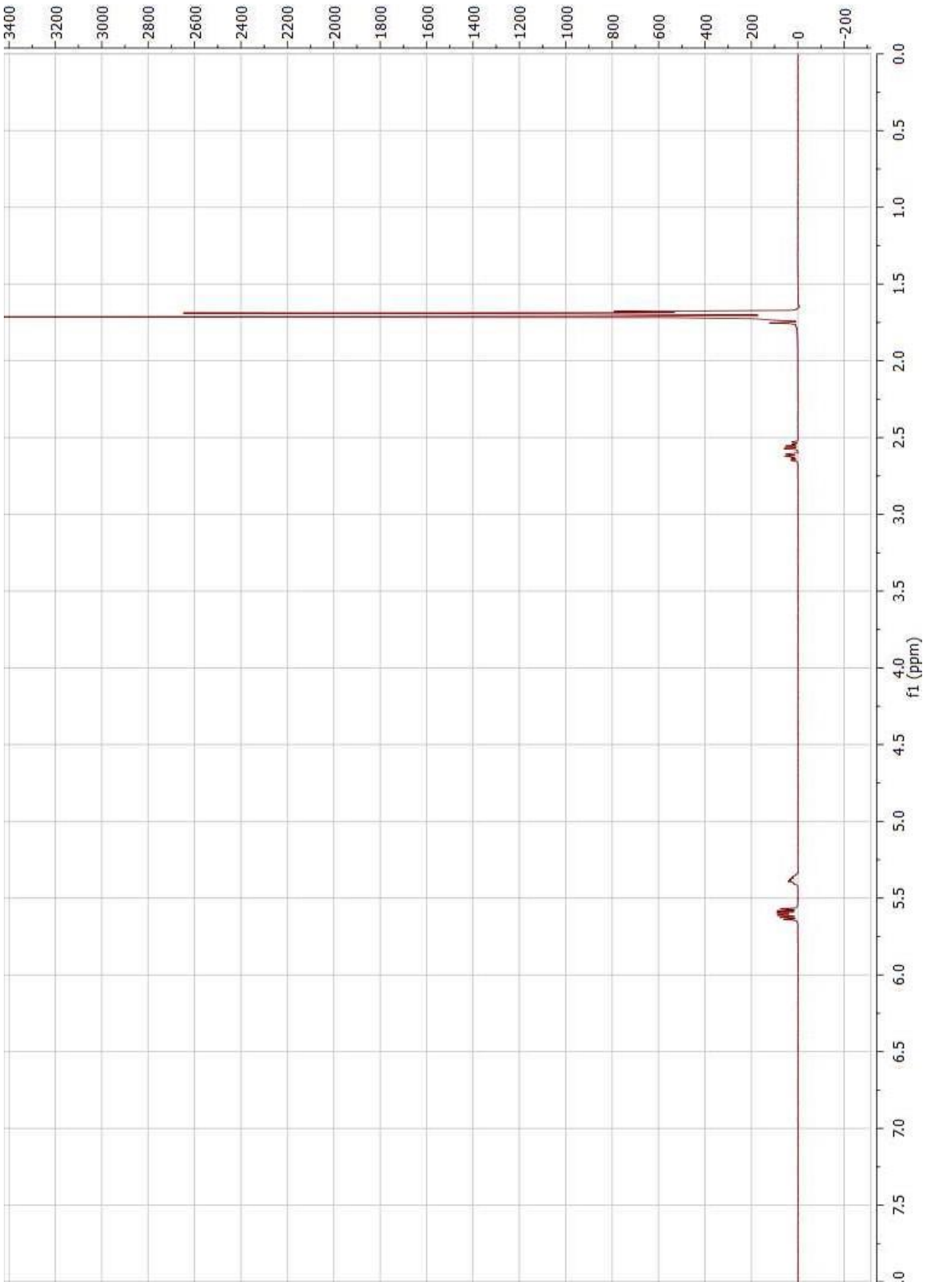
3400
3200
3000
2800
2600
2400
2200
2000
1800
1600
1400
1200
1000
800
600
400
200
0
-200
0.0
0.5
1.0
1.5
2.0
2.5
3.0
3.5
4.0
4.5
5.0
5.5
6.0
6.5
7.0
7.5
f1 (ppm)

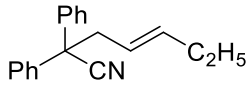

4d (l : b, 10.5 : 1)

^{1}H NMR Spectra (500 MHz, $CDCl_3$):

(Major linear diastereomer) δ 7.37 (m, 8H), 7.30 (m, 2H), 5.63 (dtt, *J* = 15.4, 6.5, 1.2 Hz, 1H), 5.31 (dtt, *J* = 15.5, 7.1, 1.6 Hz, 1H), 3.07 (dq, *J* = 7.2, 1.1 Hz, 2H), 1.98 (m, 2H), 0.90 (t, *J* = 7.5 Hz, 3H).

^{13}C NMR Spectra (126 MHz, $CDCl_3$):

(Major linear diasteromer) δ 140.33, 138.83, 129.08, 128.14, 127.47, 122.47, 122.32, 52.48, 43.18, 25.96, 13.89.

GC/MS data: 261.2 (M^+), 193.1 (base peak).

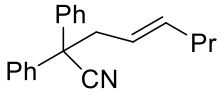

4e (l : b, 11.2 : 1) (cis : trans, 1 : 14.3)

ref. 23

^{1}H NMR Spectra (500 MHz, $CDCl_3$):

(Major linear diastereomer) δ 7.38 (m, 8H), 7.30 (m, 2H), 5.58 (dtt, *J* = 15.0, 6.8, 1.3 Hz, 1H), 5.32 (dtt, *J* = 15.4, 7.1, 1.4 Hz, 1H), 3.08 (dq, *J* = 7.1, 1.0 Hz, 2H), 1.94 (m, 2H), 1.31 (h, *J* = 7.3 Hz, 2H), 0.81 (t, *J* = 7.4 Hz, 3H).

^{13}C NMR Spectra (126 MHz, $CDCl_3$):

(Major linear diastereomer) δ 140.32, 137.14, 129.08, 128.13, 127.46, 123.47, 122.48, 52.46, 43.29, 34.91, 22.63, 13.83.

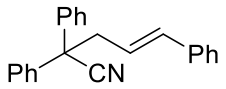

4f

^{1}H NMR Spectra (500 MHz, $CDCl_3$):

δ 7.37 (m, 15H), 6.54 (dt, *J* = 15.7, 1.4 Hz, 1H), 6.10 (dt, *J* = 15.7, 7.2 Hz, 1H), 3.31 (dd, *J* = 7.4, 1.3 Hz, 2H).

^{13}C NMR Spectra (126 MHz, $CDCl_3$):

δ 140.07, 137.05, 135.53, 129.20, 128.79, 128.31, 127.94, 127.41, 126.70, 123.39, 122.34, 52.36, 43.56.

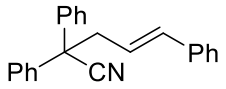

4g

ref. 25

^{1}H NMR Spectra (500 MHz, $CDCl_3$):

δ 7.37 (m, 15H), 6.54 (dt, *J* = 15.7, 1.4 Hz, 1H), 6.10 (dt, *J* = 15.7, 7.2 Hz, 1H), 3.31 (dd, *J* = 7.4, 1.3 Hz, 2H).

^{13}C NMR Spectra (126 MHz, $CDCl_3$):

δ 140.10, 137.08, 135.55, 129.23, 128.81, 128.33, 127.97, 127.44, 126.73, 123.42, 122.36, 52.39, 43.60.

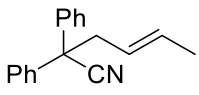

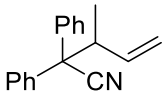

■ = Major linear ▲ = Branched residues

diastereomer residues

4h (l : b, 1.4 : 1) (cis : trans, 1 : 4.6)

^{1}H NMR Spectra (500 MHz, $CDCl_3$):

δ 7.38 (m, 10H (Ph-H_{linear}), 10H (Ph-$H_{branched}$)), 5.84 (ddd, J = 17.1, 10.5, 7.6 Hz, 1H, branched), 5.64 (m, 1H, linear), 5.34 (m, 1H, linear), 5.32 (m, 1H, linear diastereomer), 5.10 (m, 2H, branched), 3.45 (m, 1H, branched), 3.07 (dt, J = 7.3, 1.2 Hz, 2H, linear diatereomer) 2.98 (dt, J = 7.0, 1.2 Hz, 2H, linear), 1.64 (dq, J = 6.7, 1.2 Hz, 3H, linear), 1.50 (ddt, J = 6.9, 1.87, 0.94 Hz, 3H, linear diastereomer), 1.20 (d, J = 6.7 Hz, 3H, branched).

^{13}C NMR Spectra (126 MHz, $CDCl_3$):

δ 140.30, 139.63, 139.50, 138.53, 131.70, 129.24, 129.12, 129.10, 129.01, 128.20, 128.15, 128.04, 127.94, 127.49, 127.42, 127.13, 124.49, 123.95, 122.50, 121.12, 117.85, 58.19, 52.48, 51.88, 44.51, 43.25, 37.52, 18.37, 17.33, 13.48.

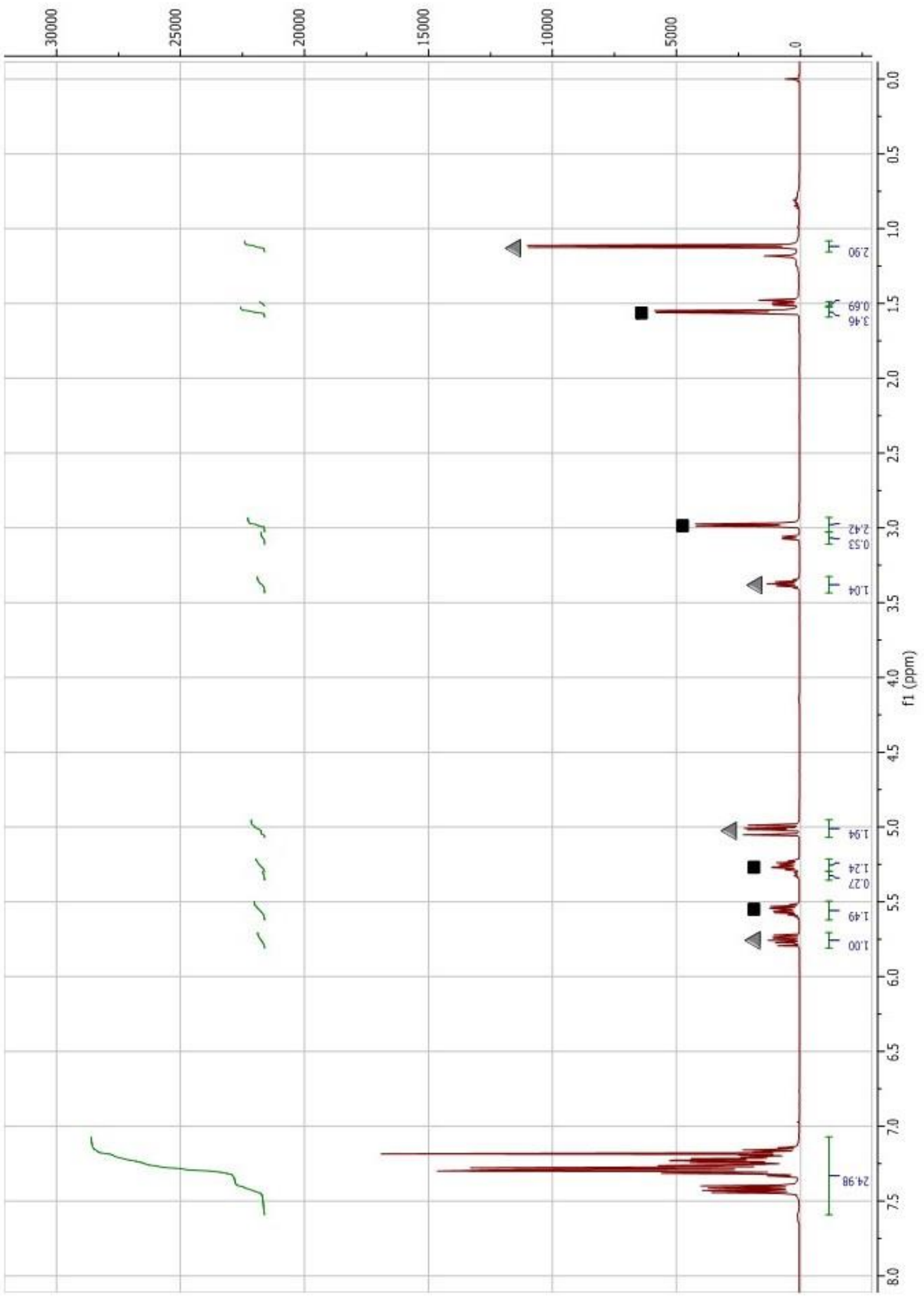
30000
25000
20000
15000
10000
5000
0
0.0
0.5
1.0
1.5
2.0
2.5
3.0
3.5
4.0
4.5
5.0
5.5
6.0
6.5
7.0
7.5
8.0
f1 (ppm)
2.90
3.46
0.69
0.53
2.42
1.04
1.94
0.27
1.24
1.49
1.00
24.98

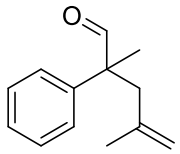

4j

ref. 26

^{1}H NMR Spectra (300 MHz, $CDCl_3$):

δ 9.54 (s, 1H), 7.38 (m, 2H), 7.29 (m, 3H), 4.81 (p, *J* = 1.57, 1.53 Hz, 1H), 4.62 (dq, *J* = 1.78, 0.89 Hz, 1H), 2.69 (q, *J* = 13.9 Hz, 2H), 1.47 (s, 3H), 1.40 (s, 3H).

^{13}C NMR (126 MHz, $CDCl_3$):

δ 201.96, 141.49, 139.77, 128.79, 127.33, 127.31, 115.43, 53.51, 44.20, 24.16, 18.56.

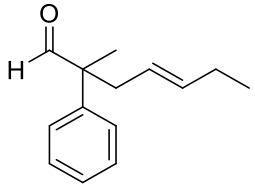

4k

93:7 linear:branched

linear product data reported

^{1}H NMR Spectra (500 MHz, $CDCl_3$):

δ 9.45 (s, 1H), 7.30 (m, 2H), 7.19 (m, 3H), 5.42 (m, 1H), 5.09 (m, 1H), 2.53 (dd, *J* = 7.32, 1.16 Hz, 2H), 1.87 (m, 2H), 1.34 (s, 3H), 0.83 (t, *J* = 7.46 Hz, 3H).

^{13}C NMR (126 MHz, $CDCl_3$):

δ 202.44, 139.87, 136.54, 128.75, 127.18, 127.15, 123.11, 53.89, 39.26, 25.62, 19.02, 13.81

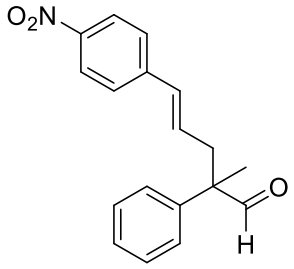

4l

86:14 linear to branched

linear data reported

^{1}H NMR Spectra (500 MHz, $CDCl_3$):

δ 9.55 (s, 1H), 8.11 (d, *J* = 8.76 Hz, 2H), 7.42 (dd, *J* = 8.24, 6.94 Hz, 2H), 7.35 (dd, *J* = 8.12, 6.89 Hz, 3H), 7.28 (m, 2H), 6.44 (d, *J* = 15.8 Hz, 1H), 6.13 (ddd, *J* = 15.8, 7.93, 7.00 Hz, 1H), 2.88 (ddd, *J* = 14.3, 7.01, 1.47 Hz, 1H), 2.81 (ddd, *J* = 14.3, 7.98, 1.28 Hz, 1H), 1.52 (s, 3H).

^{13}C NMR (126 MHz, $CDCl_3$):

δ 201.43, 146.68, 143.52, 138.86, 131.67, 130.60, 129.08, 127.69, 127.10, 126.57, 123.95, 54.08, 40.14, 18.86.

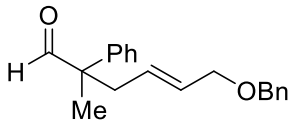

84:16 trans:cis

4m

^{1}H NMR Spectra (500 MHz, $CDCl_3$):

δ 9.52 (s, 1H), 7.39 (m, 2H), 7.31 (m, 6H), 7.25 (m, 2H), 5.63 (dtt, *J* = 15.1, 6.17, 1.37 Hz, 1H), 5.47 (dtt, *J* = 14.6, 7.43, 1.24 Hz, 1H), 4.40, (s, 2H), 3.91 (ddd, *J* = 6.27, 2.31, 1.23 Hz, 2H), 2.71 (ddd, *J* = 14.3, 6.96, 1.34 Hz, 1H), 2.64 (ddd, *J* = 14.2, 7.70, 1.17 Hz, 1H), 1.46 (s, 3H).

^{13}C NMR (126 MHz, $CDCl_3$):

δ 201.88, 139.32, 138.24, 130.63, 128.91, 128.63, 128.36, 127.77, 127.58, 127.40, 127.17, 71.75, 70.38, 53.76, 39.11, 18.93.

HRMS: [M+Na] calc: 317.1512, found: 317.1515.

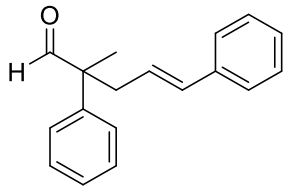

4n

96:4 linear:branched

linear product data reported

ref. 27

^{1}H NMR Spectra (300 MHz, $CDCl_3$):

δ 9.58 (s, 1H), 7.41 (m, 2H), 7.28 (m, 6H), 7.20 (m, 2H), 6.41 (dt, *J* = 15.7, 1.33 Hz, 1H), 5.94 (dt, *J* = 15.2, 7.44 Hz, 1H), 2.81 (m, 2H), 1.50 (s, 3H).

^{13}C NMR (126 MHz, $CDCl_3$):

δ 202.00, 139.41, 137.18, 133.58, 128.94, 128.48, 127.44, 127.26, 127.19, 126.11, 124.91, 54.13, 39.95, 18.95.

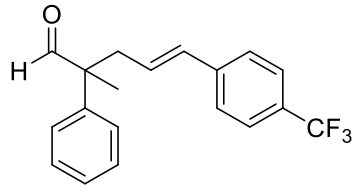

4o

^{1}H NMR Spectra (500 MHz, $CDCl_3$):

δ 9.56 (s, 1H), 7.50 (d, *J* = 8.12 Hz, 2H), 7.42 (dd, *J* = 8.21, 6.96 Hz, 2H), 7.33 (m, 3H), 7.28 (dd, *J* = 8.37, 1.30 Hz, 2H), 6.41 (d, *J* = 16.0 Hz, 1H), 6.04 (ddd, *J* = 15.4, 7.93, 7.07 Hz, 1H), 2.86 (ddd, *J* = 14.2, 7.06, 1.45 Hz, 1H), 2.79 (ddd, *J* = 14.2, 7.92, 1.27 Hz, 1H), 1.51 (s, 3H).

^{13}C NMR (126 MHz, $CDCl_3$):

δ 201.67, 140.58, 139.09, 132.30, 129.07 (q, J = 33.3 Hz), 129.02, 127.98, 127.58, 127.14, 126.23, 125.43 (q, J = 3.88 Hz), 124.18 (q, J = 271.82 Hz), 54.08, 39.99, 18.87.

Procedure for the reduction of compound 1e (Wurz, R. P.; Charette, A.B.; *J. Org. Chem.* **2004**, *69*. 1262-1269) and formation of the corresponding amine salt.

In a 50 mL round bottom flask equipped with a stir bar, compound **1e** (0.185g, 0.59 mmol) was dissolved in 12 mL isopropanol. To this solution 1.5 M HCl (6.0 mL) and zinc dust (0.740 g, 11.3 mmol) were added and the solution was stirred at 50 °C for 2 hours. Saturated aq K_2CO_3 (8.0 mL) was added after the solution cooled to rt. The reaction mixture was filtered though a pad of celite and extracted 3x with 25 mL $CHCl_3$ washes. The combined organic layers were washed with 20 mL brine and dried over $MgSO_4$.

The dried solution was filtered and concentrated *in vacuo* to afford the corresponding amine as a colorless oil (0.072 g, 43%). 2.0 M HCl in diethyl ether (5.0 mL) was added to the amine and the solvent removed *in vaccuo* to provide a white solid which was re-crystallized from EtOAc to provide suitable crystals of the HCl salt.

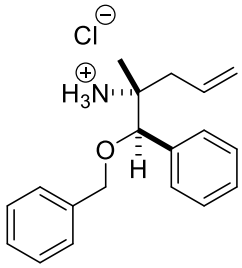

Major diastereomer shown.

^{1}H NMR Spectra (500 MHz, $CDCl_3$):

Major diastereomer δ 8.55 (s, 3H), 7.36 (m, 10H), 5.98 (ddt, *J* = 16.4, 11.4, 7.49 Hz, 1H), 5.19 (m, 2H), 4.90 (s, 1H), 4.62 (d, *J* = 11.4 Hz, 1H), 4.33 (d, *J* = 11.4 Hz, 1H), 2.69 (dd, *J* = 14.6, 7.02 Hz, 1H), 2.17 (dd, *J* = 14.6, 7.73 Hz, 1H), 1.31 (s, 3H).

^{13}C NMR (126 MHz, $CDCl_3$):

Major diasteromer δ 137.67, 135.26, 130.92, 128.68, 128.56, 128.36, 128.33, 128.06, 127.58, 127.46, 84.94, 71.25, 60.29, 37.61, 21.03.

HRMS:

[$C_{19}H_{24}NO$]: calc: 282.1858, found: 282.1855

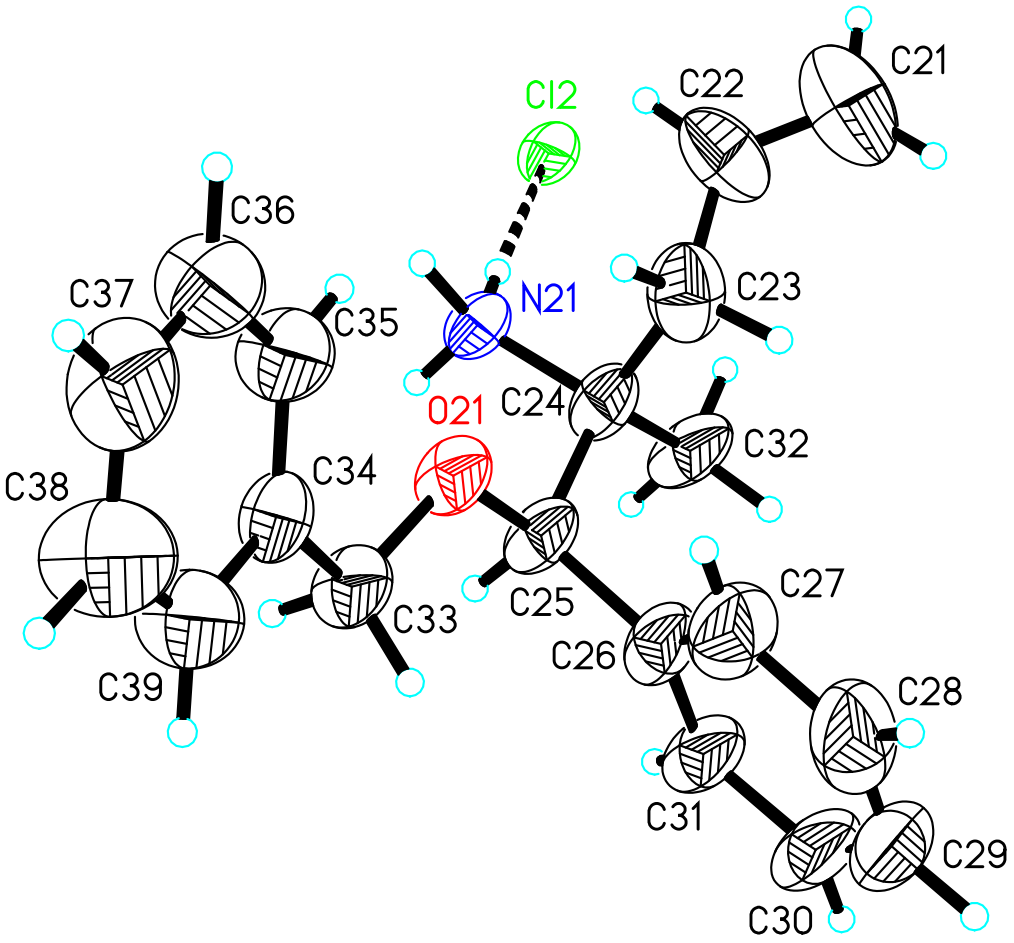

Detailed description of x-ray crystal structure determination for [C19H24NO][Cl] :

The alignment reflections for determining the preliminary unit cell for the crystal of [C19H24NO][Cl] (**1**) indexed quite well as a C-centered monoclinic lattice. The crystal was therefore believed to utilize a monoclinic space group and intensity data were collected accordingly. The monoclinic R_{sym} was 0.105 and the most probable space group appeared to be centrosymmetric C2/m. When the structure would not solve in C2/m, the intensity data were

further analyzed and this indicated the possible presence of a c-glide. The structure solved straightforwardly in the centrosymmetric space group C2/c with an asymmetric unit containing two [C19H24NO][Cl] cation/anion pairs. When this structure failed to refine below $R_1 = 0.153$, the possibility of it being a triclinic structure that was pseudomerohedrally twinned to look monoclinic was considered. This turned out to be the case and the final centrosymmetric triclinic asymmetric unit has four nearly identical, but crystallographically-independent [C19H24NO][Cl] cation/anion pairs, related by non-crystallographic pseudosymmetry. The crystals utilize the centro-symmetric triclinic space group $C\bar{1}$ [a nonstandard setting of $P\bar{1}$ – C_i^1 (No. 2)] with lattice constants at 100K of: $\boldsymbol{a}$ =26.96214(19)Å, $\boldsymbol{b}$ = 12.68483(10)Å, $\boldsymbol{c}$ = 21.88641(18)Å, $\boldsymbol{\alpha}$ = 90.4219(6)°, $\boldsymbol{\beta}$ = 104.5435(4)°, $\boldsymbol{\gamma}$ = 89.7970(4)°, V = 7245.3(1)Å^3 and Z = 16 [C19H24NO][Cl] moieties. The crystals are pseudomerohedrally (68%/32%) twinned with the two domains related by a 180° rotation about the $\boldsymbol{b}$ axis.

The final centrosymmetric triclinic asymmetric unit contains four cation/anion pairs. All nonhydrogen atoms were included in the structural model with variable anisotropic thermal parameters. All twelve hydrogens for the protonated amine groups were located from difference Fourier syntheses and incorporated into the structural model as individual isotropic atoms whose parameters were allowed to vary in least-squares refinement cycles. Mild restraints were applied to the anisotropic thermal parameters of two carbon atoms [C(78) and C(79)] and three of the ammonium hydrogens were fixed at values 1.2 times the equivalent isotropic thermal parameter of their nitrogen atom. The remainder of the hydrogen atoms were placed at idealized sp^2- or sp^3-hybridized positions with C-H bond lengths of 0.95 - 1.00 Å and isotropic thermal parameters fixed at values 1.20 (nonmethyl) or 1.50 (methyl) times the equivalent isotropic thermal parameter of the carbon atom to which they are bonded. Methyl groups were placed at idealized "staggered" positions. The terminal ethylene group for the first cation is 57%/43% disordered

between two conformations and both of these were restrained to have metrical parameters similar to that group in the fourth cation.

The final least-squares refinement cycles for **1** in space group $C\bar{1}$ utilized anisotropic thermal parameters for all nonhydrogen atoms, isotropic thermal parameters for all hydrogen atoms, 867 variables, 51 restraints and 11861 reflections having $2\theta(CuK\alpha) < 140.10°$. Final agreement factors at convergence for **1** are: R_1(unweighted, based on F) = 0.078 for 10457 independent absorption-corrected "observed" reflections having $2\theta(CuK\alpha) < 140.10°$ and $I>2\sigma(I)$; R_1(unweighted, based on F) = 0.086 and wR_2(weighted, based on F^2) = 0.213 for all 11861 independent absorption-corrected reflections having $2\theta(CuK\alpha) < 140.10°$. The largest shift/s.u. was 0.000 in the final refinement cycle. The final difference map had maxima and minima of 0.59 and -0.56 $e^-/Å^3$, respectively.